June 1999 • NREL/BK-210-25626

Technical Report

NCPV FY 1998 Annual Report

R.D. McConnell
PV Communications Leader

A. Hansen
Communications Coordinator

National Renewable Energy Laboratory

1617 Cole Boulevard
Golden, Colorado 80401-3393

NREL is a U.S. Department of Energy Laboratory
Operated by Midwest Research Institute • Battelle • Bechtel

Contract No. DE-AC36-98-GO10337

June 1999 • NREL/BK-210-25626

NCPV FY 1998 Annual Report

R.D. McConnell
PV Communications Leader

A. Hansen
Communications Coordinator

wable Energy Laboratory

1617 Cole Boulevard
Golden, Colorado 80401-3393

NREL is a U.S. Department of Energy Laboratory
Operated by Midwest Research Institute • Battelle • Bechtel

Contract No. DE-AC36-98-GO10337

NOTICE

Available to DOE and DOE contractors from:
Office of Scientific and Technical Information (OSTI)
P.O. Box 62
Oak Ridge, TN 37831
Prices available by calling 423-576-8401

Available to the public from:
National Technical Information Service (NTIS)
U.S. Department of Commerce
5285 Port Royal Road
Springfield, VA 22161
703-605-6000 or 800-553-6847
or
DOE Information Bridge
http://www.doe.gov/bridge/home.html

 Printed on paper containing at least 50% wastepaper, including 20% postconsumer waste

PREFACE

This report summarizes the in-house and subcontracted research and development (R&D) activities within the National Center for Photovoltaics (NCPV) from October 1, 1997, through September 30, 1998 (Fiscal Year 1998). The NCPV is part of the U.S. Department of Energy's (DOE's) National Photovoltaics Program, as described in the DOE *National Photovoltaics Program Plan for 1996-2000*. The mission of the DOE National Photovoltaics Program is to make PV a significant part of the domestic economy—as an industry and an energy resource. The two primary goals of the national program are to (1) maintain the U.S. Industry's world leadership in research and technology development, and (2) help the U.S. industry remain a major, profitable force in the world market. The NCPV provides leadership and support to the national program toward achieving its mission and goals.

The FY 1998 budget authority for carrying out the NCPV activities was $54.4 million in operating funds and $0.5 million in capital equipment funds. Subcontract activities represent a major part of the NCPV work, with $28.8 million (53% of PV funds) going to some 200 subcontractors. Cost sharing by industry added $16.5 million to the subcontract R&D activities with industry.

The activities of the NCPV are to: conduct basic, applied, and engineering research; manage subcontracted R&D projects; perform research complementary to subcontracted work; develop and maintain state-of-the-art measurement and device capabilities; develop PV manufacturing technology and modules; transfer results to industry; and evolve viable partnerships for PV systems and market development. The research activities under the program are summarized under the eleven project areas: PV Fundamental and Exploratory Research, PV Electronic Materials and Devices, Crystalline Silicon Cells, PV Measurements and Characterization, Thin-Film Technologies, Photovoltaic Manufacturing Technology, PV Engineering and Reliability, Balance of Systems, PV System Performance and Engineering, PV Domestic Applications and Markets, and PV International Applications and Markets.

(Note: Within the NREL organization is a group called the National Center for Photovoltaics. NREL's NCPV consists of three divisions—Electronic Materials and Devices, Measurements and Characterization, and Engineering and Reliability. In November of 1996, DOE formed its National Center for Photovoltaics, which is a virtual laboratory comprising NREL's three NCPV divisions, plus two departments at Sandia—PV System Applications and PV System Components.)

Lawrence Kazmerski
Director, National Center for Photovoltaics
National Renewable Energy Laboratory

Thomas Surek
Technology Manager,
NREL Photovoltaics Program

Christopher Cameron
Manager, PV System Applications Department
Sandia National Laboratories

James Gee
Manager, PV System Components Department
Sandia National Laboratories

TABLE OF CONTENTS

1.0 INTRODUCTION

This report summarizes the in-house and subcontracted research and development (R&D) activities within the National Center for Photovoltaics (NCPV) from October 1, 1997, through September 30, 1998 (FY 1998). The NCPV is part of the U.S. Department of Energy's (DOE's) National Photovoltaics Program, as described in the DOE *National Photovoltaics Program Plan for 1996-2000*. The FY 1998 budget authority for carrying out the NCPV activities was $54.4 million in operating funds and $0.5 million in capital equipment funds. Subcontract activities represent a major part of the NCPV work, with $28.8 million (53% of PV funds) going to some 200 subcontractors. Cost sharing by industry added more than $16.5 million to the subcontract R&D activities with industry.

1.1 Background

The NCPV is part of the DOE National Photovoltaics Program managed by the Office of Photovoltaic and Wind Technologies. This office is under the Office of Power Technologies in DOE's Office of Energy Efficiency and Renewable Energy. As background, within the NREL organization is a group called the National Center for Photovoltaics. NREL's NCPV consists of three divisions—Electronic Materials and Devices, Measurements and Characterization, and Engineering and Reliability. In November of 1996, DOE formed its National Center for Photovoltaics, which is a virtual laboratory comprising NREL's three NCPV divisions, plus two departments at Sandia—PV System Applications and PV System Components. DOE's NCPV implements projects funded by the DOE PV Program.

Major program thrusts in FY 1998 continued to be implemented based on DOE's *National Photovoltaics Program Plan for 1996-2000*. The program mission is to:

> Work in partnership with U.S. industry to develop and deploy photovoltaic technology for generating economically competitive electric power, making photovoltaics an important contributor to the nation's and the world's energy use and environmental improvement.

The two primary goals of the national program are to (1) maintain the U.S. industry's world leadership in research and technology development, and (2) help the U.S. industry remain a major, profitable force in the world market. The NCPV provides leadership and support to the national program toward achieving its mission and goals.

The DOE strategy over the next few years will be to lay the groundwork for a growing U.S. PV technology and industrial base, with increased emphasis on market and project development activities with industry. To accomplish this, the national program embraces three relatively equal-priority activities: (1) technology development and validation, (2) market conditioning, and (3) project venturing. This strategy continues a strong technology development program, but emphasizes R&D for the technologies and companies that are positioned to substantially penetrate the market, reduce prices, and scale up manufacturing. Program activities include continuing efforts to form partnerships with manufacturers and utilities (the ultimate benefactors and users), with universities, and with federal and state agencies.

Under the DOE National Photovoltaics Program, the NCPV supports long-term fundamental and mid-term applied R&D, near-term manufacturing development, and near-term systems and market development in PV energy technology. The activities also provide services to

industry, electric utilities, and other users, and provide overall programmatic support for the National Photovoltaics Program. The NCPV's subcontract program is responsible for most of the R&D, manufacturing technology development, and some of the systems and market development task areas under the National Photovoltaics Program. It is implemented via competitive public solicitations. One of the most important subcontracting mechanisms is government/industry partnership, with industry sharing the cost of research with DOE/NREL/SNL.

Closer work with industry, utilities, and other end users on PV manufacturing technology, systems, and market needs is being increasingly emphasized. Approaches for this emphasis include mitigating barriers to PV adoption in the utility and international marketplaces, and project venturing with decision-makers and organizations representing domestic and international market sectors for PV. As appropriate for the system and market development areas, the NCPV is supporting activities such as education; technical assistance and training; market, economic, and financial analysis; technology characterizations; regulatory, rate, and value analysis; codes and standards assessment and development; working with customers in project development activities; and co-financing demonstration projects. Under project venturing, DOE is placing particular emphasis on supporting and strengthening programs already in place, such as PV:BONUS (Photovoltaics Building Opportunities in the United States) and the Utility PhotoVoltaics Group (UPVG).

NCPV's activities include laboratory research and subcontract project management. The Center also provides technical support to efforts contracted from the DOE Golden Field Office (GO), such as PV:BONUS and UPVG. The primary research activities are conducted in advanced PV material technologies—including crystalline silicon and III-V alloys, amorphous silicon (a-Si) thin-film materials, and polycrystalline thin films, such as copper indium diselenide (CIS), cadmium telluride (CdTe), and their alloys. These activities are conducted in-house and through subcontracts with industry (mostly cost shared) and universities. The research activities are closely coordinated through several NREL/SNL/industry/university "team" efforts. Improving PV device manufacturing is vital. We are pursuing two complementary approaches:

- Government/industry partnerships, such as the PV Manufacturing Technology—or PVMaT—project (which focuses on improving manufacturing processes and products, accelerating manufacturing cost reduction, and laying the foundation for increased production capacity).
- Module development research to evaluate modules (and module performance) and suggest solutions to manufacturers' module problems.

System and market development rounds out the balanced approach pursued. The objective is to create an environment in which system technology, user acceptance, and the PV industry can accommodate the continued expansion of PV into large applications and markets. Subcontracts with NREL and SNL also support research on future-generation PV technologies for highly qualified research teams to expand the current limits of PV technology. Transferring research results into commercial products and applications in a timely and effective manner is another major activity of the NCPV.

Subcontracted R&D is a significant part of the NCPV work; typically, more than 50% of the DOE PV Program's budget is allocated yearly to subcontracts. Table 1.1-1 shows the history of distribution of both subcontract and in-house budgets. From FY 1978 through FY 1998, the NREL PV Program awarded more than 1400 subcontracts totaling $403 million out of the

total operating budget of $646 million. In FY 1998, the NREL/SNL PV programs awarded some 200 subcontracts with a total funding of $28.8 million. Cost sharing by industry subcontractors added more than $16.5 million to the almost $21.0 million in program funding to 100 industry subcontractors. NREL and SNL also subcontracted with 85 universities (not counting Sunrayce schools), with a total funding of $8.0 million. Figure 1.1-1 shows the industry-university-government distribution of subcontract funds by categories in DOE's *National Photovoltaics Program Plan for 1996-2000*. Table 1.1-2 shows the contacts for the various NCPV areas.

Table 1.1-1. PV Budget History

	NREL only	**NREL only**	**NREL only**	**NREL only**	**NREL + SNL**
Fiscal Year	**1978-1994 $M**	**1995 $M**	**1996 $M**	**1997 $M**	**1998 $M**
Task Area					
In-House R&D	141.2	18.8	17.6	17.5	25.6
Capital Equipment	26.2	0.8	0.3	0.4	0.5
Subtotal (in-house)	***167.4***	***19.6***	***17.9***	***17.9***	***26.1***
Subcontracted R&D					
Amorphous Silicon Thin Films	87.7	4.2	3.4	3.5	3.7
Polycrystalline Thin Films	67.2	8.2	6.6	6.6	8.0
High-Efficiency Concepts	38.3	0.3	0.4	0.5	0.1
Crystalline Silicon	27.1	1.0	0.9	0.9	0.8
New Ideas[1]	19.4	0.0	0.0	0.0	0.0
University Participation[2]	9.2	0.8	0.5	0.6	1.2
Subtotal (R&D subcontracts)	***249.0***	***14.5***	***11.8***	***12.1***	***13.8***
Manufacturing Technology Development and Systems and Market Development Subcontracts					
PVMaT Project	45.8	10.7	8.4	7.9	9.5
Module and System Performance and Engineering Project	3.2	0.6	0.3	0.1	1.5
PV Analysis and Applications Development Project	6.1	3.3	2.0	1.7	4.0
Subtotal (other subcontracts)	***55.1***	***14.6***	***10.7***	***9.7***	***15.0***
Subtotal (all subcontracts)[3]	**304.1**	**29.1**	**22.5**	**21.8**	**28.8**
TOTAL (NREL-only through FY 1997)	**471.5**	**48.7**	**40.4**	**39.7**	**54.9**

[1] Includes $9 million for photoelectrochemical cell research.
[2] In FY 1998, University Participation was combined with New Ideas, and it includes University Capital Equipment solicitation.
[3] Includes 15%-20% for technical program management, fees, etc., through FY 1997.

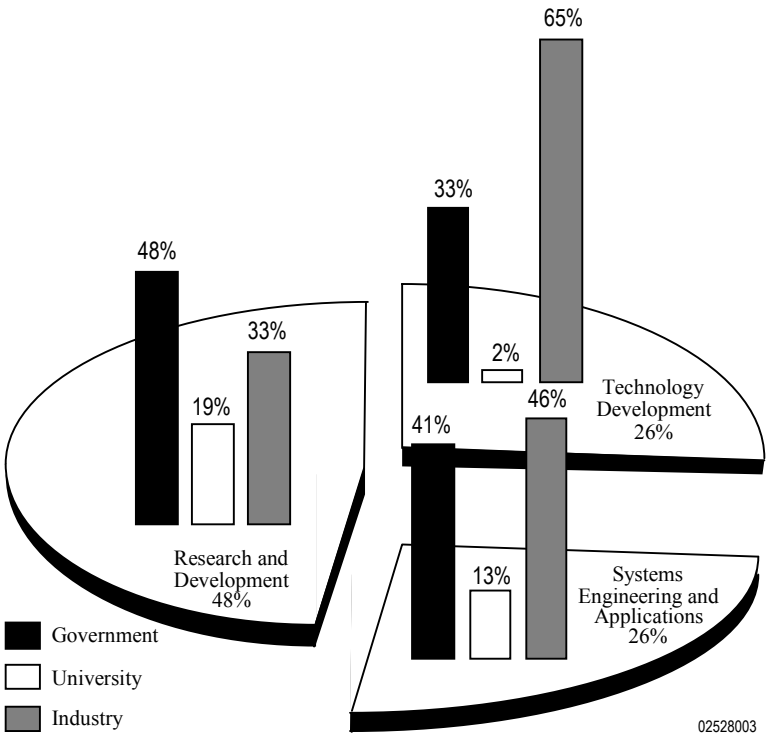

Figure 1.1-1. FY 1998 budget distribution for NCPV, with total funding of $54.9 million.

Table 1.1-2. NCPV Contacts by Project Area

Project	Leader	Telephone
PV Program Management	Thomas Surek	303-384-6471
PV Fundamental and Exploratory Research	Robert McConnell	303-384-6419
PV Measurements and Characterization	Lawrence Kazmerski	303-384-6600
Crystalline Silicon Cells	James Gee	505-844-7812
PV Electronic Materials and Devices	John Benner	303-384-6496
Thin Film PV Partnership	Ken Zweibel	303-384-6441
PVMaT	C. Edwin Witt	303-384-6402
Module/Array Performance and Reliability	Roland Hulstrom	303-384-6420
Balance of Systems	Russell Bonn	505-844-6710
PV System Performance and Engineering	Christopher Cameron	505-844-8161
PV Domestic Applications and Markets	John Thornton	303-384-6469
PV International Applications and Markets	Jack Stone	303-384-6470

1.2 Key FY 1998 Accomplishments

Table 1.2-1 describes some key achievements within the NCPV during FY 1998. The accomplishments are grouped according to eleven main project areas.

Table 1.2-1. Key Achievements

PV Fundamental and Exploratory Research Project

NREL	NREL's RFP entitled "University PV Research Equipment" closed on June 1, 1998. Awarded $1,061,135 for 17 university contracts during July and August.
NREL	Original HBCU contracts ended in 1998 and were assessed as a Program milestone.
NREL	NREL's RFP entitled "HBCU PV Research Associates Program" was issued to about 50 HBCUs. Received seven proposals, with awards to follow in early FY 1999 after review.
NREL	NREL's RFP entitled "University R&D for Future Generation PV Technologies" yielded 71 proposals for long-term research projects from many highly capable university researchers. Also 20 awards are planned in FY 1999.
NREL	Multilaboratory Next-Generation PV and Thin-Silicon-Based Teams held four workshops during FY 1998.
NREL	Won IEEE Electrotechnology Transfer Award by moving high-efficiency $GaInP_2/GaAs$ tandem solar cell to industrial production.
NREL	Demonstrated a 12%-efficient solar device to split water into hydrogen (a valuable fuel) and water.
NREL	Completed three years of projects with historically black colleges and universities and started new projects for another three years.

PV Measurements and Characterization Project

NREL	Initiated and maintained high-security data-transfer links to some 40 industry, university, and federal laboratories. Also provided more than 20 general data-transfer sites for routine and periodic collaborators.
NREL	Richard Ahrenkiel recognized through the Harold Hubbard Research Award for his pioneering work and instrument development in the minority-carrier lifetime spectroscopy area.
NREL	Performed more than 45,000 measurements in our laboratories on some 16,000 samples representing every PV technology.
NREL	Efforts in technique development addressed measurements specific to PV industry needs and the progress of manufacturing-environment methods.
NREL	Work written up in 80 journal, conference proceedings, and book publications, with some 70% of these with research collaborators from the internal and subcontractor communities.
NREL	New or improved analytical offerings include: temperature-controlled, large-area, continuous solar simulator; novel, minority-carrier lifetime spectrometer; and development and implementation of a defect evaluation procedure and instrumentation.

Crystalline-Silicon Project

NREL	Exceeded planning goal for 1999 by supporting development of 16.6%-efficient cell made of thin-layer crystalline silicon.
SNL	Fabricated and tested a 17.2%-efficient back-contact silicon solar cell using emitter wrap-through structure.
SNL	Demonstrated 33% reduction in reflectance using plasma-etch texturization, and filed for patent protection.
SNL	Demonstrated 0.8% absolute improvement in efficiency of screen-printed silicon solar cells using self-aligned selective-emitter cell structure.
SNL	Assembled modules using back-contact cells and low-temperature solder in a single step.

NREL	Examined effect of defect clusters and impurity precipitation in multicrystalline silicon. Results of work presented in two publications.
Georgia Institute of Technology	Published 17 journal articles, 17 conference papers, and received one patent. Demonstrated Al-alloyed back-surface field with surface recombination velocity <200 cm/s, screen-printed cells with fill factors of 0.78, new surface passivation treatments, and high-efficiency cells on commercial multicrystalline-silicon substrates.
NREL/GT Equipment Technol-ogies, Inc.	Grew a 20-mm-diameter Si tube 210 mm long.
NREL	Patented substrate formed by reacting metallurgical-grade silicon with boric oxide in air for thin-layer Si solar cells lattice-matched with Si within 0.05%.

PV Electronic Materials and Devices Project

NREL	American Physical Society News selected our work on vibrational properties of hot-wire chemical vapor deposition a-Si:H as a Physics Highlight.
NREL	Model proposed in 1997 that explained the metastability of a-Si passed peer review in the journals. Experiments in 1998 have provided evidence supporting the model.
NREL	Original work in analyzing junction formation in CdS/CIGS and the CdS/CdTe interface is attracting attention from important groups pursuing similar approaches.
NREL	Investigations of 1-eV nitrogen-bearing III-V alloys and solar cells appear to have stimulated a national adjustment of BES-funded PV research to place greater emphasis on developing the bottom cell of a high-efficiency stack.
NREL	Set new PV efficiency records for advanced processes such as high-deposition-rate HWCVD a-Si:H, electrochemically deposited CIS, CIS on flexible stainless steel, and CdTe devices on conventional and novel conducting oxides.
NREL	Investigation of nanostructured precursors for semiconductor deposition examined use of nanostructured Cu:HgTe for application in the graphite-based contact to CdTe devices.
NREL	Fabricated 15.4%-efficient CdTe device using process easy to duplicate.
NREL	Met two major planning milestones for CIS: Supporting debut of first commercial products; documenting their performance at 10% efficiency.
NREL	Incorporating small amount of H into hot-wire produced a-Si causes amorphous solid to behave more like a crystal.
NREL	Fabricated first cell entirely by hot-wire chemical vapor deposition with an a-Si i-layer and microcrystalline-Si-doped layers.

Thin Film PV Partnership Project

NREL	Awarded 34 new cost-shared, three-year subcontracts under the Thin Film PV Partnership Program.
NREL	Shared R&D 100 award with United Solar for triple-junction a-Si PV roofing module.
Siemens Solar Industries	Fabricated 11.8%-efficient, 3651-cm^2 CIGSS monolithic module.
Pennsylvania State University	Achieved cells with open-circuit voltages >0.90 V growing thin amorphous layers with high hydrogen dilution. Such layers act as buffers in n-i-buffer-p cell structures.
NREL with Cornell University	Observed a light-induced increase in the amount of molecular hydrogen in nanovoids of a-Si after light-soaking at room temperature.

United Solar Systems Corporation	For a-SiGe, a dual-junction cell with 14.4% initial, active-area efficiency; triple-junction cell with 15.2% initial, active area efficiency.
Solarex	Reduced silane gas flow during production by 50% without reducing performance of tandem-junction a-Si/a-SiGe:H modules.

PVMaT Project

NREL	Essentially completed five module manufacturing R&D subcontracts: ASE Americas; AstroPower, Inc.; Iowa Thin Films Technologies Inc.; Photovoltaics International , LLC; and Siemens Solar Industries.
NREL	Continued progress in 5 subcontracts that address issues in the general category of manufacturing improvements for PV system integration: Ascension Technology, Inc.; Evergreen Solar, Inc.; Solar Design Associates, Inc.; Solar Electric Specialties; and Utility Power Group, Inc.
NREL	Continued progress in 3 subcontracts that address manufacturing and product improvements: Advanced Energy Systems, Inc.; Omnion Power Engineering Corp.; and Trace Engineering.
NREL/SNL	Reduced module-manufacturing costs for the current PVMaT participants by 29% and increased their manufacturing capacity more than 5-fold since PVMaT was initiated.
NREL/SNL	Supported introduction of new products: ac PV modules, which were identified by *Popular Science* as among the "Best of What's New" for 1998; completed stand-alone PV products; integrated PV systems for utility applications and lower-cost inverters.
NREL/SNL	Extended support of PV system and component development and PV module manufacturing technology by issuing 14 additional, cost-shared, multi-year contracts to industrial partners.

Module and Array Performance and Reliability Project

NREL	Published 34 journal articles, conference papers, and technical reports on various topics of PV engineering and reliability.
NREL	Tested PV modules of various technologies both indoors under controlled conditions and outdoors under prevailing conditions to help industry determine their performance and stability characteristics.
NREL	Tested more than 30 modules both indoors and outdoors under accelerated environmental stress conditions to help industry determine their reliability/durability characteristics.
NREL	Completed a "users manual" for module reliability database. The database was developed with system users and covers anomalies, failure modes, and causes of failure in PV modules and systems.
NREL	Led the CdTe Reliability Team and completed a report on back-contact screening tests.
NREL	Planned and began implementing validation work on module energy ratings procedure. A detailed technical report on the modeling procedure will be written in FY 1999.
NREL	Expanded module energy ratings testbed (PERT 2 and 3). The testbed can now measure 45 individual modules.
NREL	Conducted materials/devices characterization, designed experiment conditions, and performed various Accelerated Environmental Testing studies and EVA/data analyses requested by six PV companies.
NREL	Developed an accelerated weathering test protocol that was submitted in a 40-page report.

NREL	Enhanced PV mini-module testing capabilities by acquiring a jar-mill for making NREL-developed EVA formulation, a PC-controlled electrochemical workstation and software.
SNL	A new method for comprehensive characterization of PV modules has been successfully demonstrated for virtually all PV technologies (crystalline silicon, thin film, and concentrator), and has been extended to characterization of large PV arrays. Extension of this method for estimating the annual energy production of PV systems has begun.
SNL	Developed new calibration and correction procedures for both thermopile-based (Eppley) pyranometers and the inexpensive but prolific silicon-photodiode-based pyranometers (LI-COR and Kipp & Zonen).
SNL	Provided analysis of modules experiencing abnormal glass fracture, and determined cause of fracture to airborne roof aggregate from high winds.
SNL	Performed metallographic analysis of solder bond joints for 3 PV manufacturers.
Florida Solar Energy Center	Examined adhesive forces in PV modules, and correlated adhesive force with surface analysis. Hosted a workshop on adhesion for PV.
SNL	Initiated Module Long-Term Exposure test, which will examine subtle degradation modes in commercial PV modules.

Balance-of-System Components Project

SNL	Tested commercial inverters using highly accelerated lifetime testing to identify latent failure modes.
SNL	Encouraged improvement of PV inverters with contracts supporting implementation of quality control procedures.
SNL	Identified conditions surrounding and developed strategies to deal with islanding of multiple PV systems connected to a single circuit of the utility grid.
SNL	Provided comprehensive characterization of a wide variety of inverters intended for PV applications.
SNL/Florida Solar Energy Center	Performed life-cycle testing on batteries from several manufacturers of different types. Began examination of optimal battery management in PV/hybrid systems.

PV System Performance and Engineering Project

NREL	Completed interim draft PV systems performance test procedure and published as an NREL technical report.
NREL	Conducted exploratory and outdoor performance testing of 8 PV systems currently installed at the NREL OTF and installed 6 new systems for test.
NREL	Announced the reorganization and expanded scope of the IEEE SCC21 to include Fuels Cells, Photovoltaics, Dispersed Generation, and Energy Storage.
NREL/SNL	Conducted the annual PV Performance and Reliability workshop sponsored by NREL and SNL, this year hosted by FSEC in November 1998 in Cocoa beach, Florida.
NREL	Enhanced PV system testing capabilities by completing the validation and calibration of the small-system flexible testbed and conducted small-system performance characterization tests by validating newly developed test procedures.
NREL	Reduced NREL spectral calibration uncertainty by 50%, improving NREL's ability to characterize spectral effects on PV devices and module performance.
NREL	Calibrated and characterized 49 radiometric sensors, systems, and light sources used to evaluate PV device, module, and system performances for NREL researchers and industrial partners.

NREL	Disseminated PV-related solar radiometric information in response to over 180 documented PV industry and internal NREL requests for measurements, data, sensors, solar simulator design, resource date, rating conditions, instrumentation calibration, and measurement techniques.
NREL	Continued work in using satellites for determining solar resources at any location on earth and produced a draft report on the activities.
NREL	Upgraded Renewable Resource Data Center (RReDC) Internet page to include spectral solar data, selected solar radiation and cloud cover maps, and Cooperative Network for Renewable Resource Measurements (CONFRRM) home page.
NREL	Augmented module testing facilities with test bed for small systems, high-voltage test bed, expanded outdoor test bed for energy ratings, and outdoor accelerated weathering tracking system.
NREL/SNL	Contributed to major new standards and certification applying to PV systems: IEEE-recommended practice for utility interface; PVGAP interim test methods for determining the performance of small systems; PowerMark Corporation accreditation of certification laboratories; and revisions to the National Electrical Code.
SNL	Assessed performance of PV installations owned by federal agencies.
SNL	Analyzed system performance data from several hundred SMUD and EPA PV residential systems. Estimate of operations and maintenance costs for these systems varied between $0.01 and 0.10/kWh.
SNL	Performed comprehensive performance and economic assessment of true system life-cycle cost for three large (>10 kW) hybrid systems. The overall net present value of the recurring costs (maintenance plus capital replacement) could be as high as 25%.

PV Domestic Applications and Markets Project

NREL	From March through May of 1998, a PV exhibit called "Rufus' Solar Neighborhood" was installed at the Walt Disney EPCOT Center near Orlando, Florida. According to EPCOT survey, more than 75,00 visitors stopped at the exhibit.
NREL	The "Under the Sun" exhibit opened in early July at the Smithsonian Institution's Cooper Hewitt National Design Museum in New York City. The 4-month long exhibit culminated in a Smithsonian-sponsored conference focused on raising the public's awareness of renewable energy.
NREL	Involved in other outreach activities, including a series of consumer workshops for potential homebuilders, and for farmers and ranchers.
NREL	Convened a meeting in July between CEOs of about 25 major insurance companies to introduce them to the possible uses of PV to reduce casualty losses from disasters.
NREL	Provided training to the Federal Emergency Management Agency in use of portable PV generator sets.
NREL	Project members continued extensive support to PV:BONUS, the Million Solar Roofs Initiative, utility deregulation, and upcoming Sunrayce '99.
NREL	Provided technical assistance to major demonstration projects—Million Solar Roofs, TEAM-UP, and PV Pioneer Project—by supporting training programs for installers, workshops for communities, and public information exhibits.
NREL	Continued PV:BONUS by selecting seven projects for product and business development.

PV International Applications and Markets Project

NREL	Important highlight of China activities include: a U.S./China workshop of small PV/wind technology applications for rural and remote development in China; completed the installation of 300 household and school lighting systems in Gansu Province; delivered equipment to Inner Mongolia for installation of over 200 PV/wind remote household stems; completed data collection for market and applications characterization surveys for rural electrification options in three key provinces; and completed background work for several reports characterizing PV business opportunities in China.
NREL	Activities in India continued to build on the successes of the rural electrification initiative which has been carried out as a cost-shared program for the past 5 years. Completed installations of U.S.-supplied PV systems in Sundarbans region of West Bengal. Tata Energy Research Institute did an extensive before-and-after social and economic impact study.
NREL	Continued data collection for two 50-kW hybrid power systems installed under auspices of the U.S.-Brazil cooperative program. U.S. industry continues to benefit from this past activity in the form of expanded business opportunities in the country.
NREL	Coordinated the PV International Activities with the NREL PV Program.
NREL	Village Power Conference detailed opportunities to expand PV into developing countries.
NREL	Three principal agencies—UNDP, World Bank, and USAID—continue to aggressively support renewable energy options around the world. This project continues to support these activities where appropriate.
NREL	Continued to support DOE and NREL with visitors from many foreign countries who arrive at NREL to learn more about renewable energy and commercially available options.
NREL	Provided technical assistance to many countries; met major milestones in India, China, Brazil, South Africa, and Mexico.
SNL	The Mexican program is exhibiting successful establishment of an infrastructure with increasing PV system sales after completion of demonstration projects.

1.3 Technology Transfer

Consistent with DOE policy, technology transfer within the NCPV is defined as collaborative R&D with industry to help industry commercialize products or services. An underlying theme of NCPV technology transfer activities is the joint work accomplished by industry and NCPV researchers focused on a common R&D objective. Among government laboratories, seven principal tools affect technology transfer: subcontracted R&D, cooperative R&D, industry-sponsored R&D, NCPV user facilities, technology licensees, researcher exchanges, and information dissemination. The NCPV conducts its technology transfer primarily through subcontracts, cooperative R&D, and information dissemination.

Subcontracts with Industry

Nearly one-half of the approximately 200 subcontracts placed in FY 1998 were with the U.S. PV industry. The DOE PV Program funding of $21.0 million to industry was supplemented by an additional $16.5 million (estimated) of cost sharing by the industry partners. The majority of industry funding (and cost sharing) was in the PVMaT project (see Figure 1.1-1). Technically knowledgeable research managers within the NCPV participate in defining, evaluating, awarding, and negotiating statements of work submitted by industry researchers in competitive solicitations. Following subcontract awards, NCPV subcontract managers direct and evaluate research progress by visiting subcontractor sites and evaluating subcontractor deliverables in the NCPV laboratories.

Cooperative R&D

NCPV in-house researchers frequently perform informal cooperative R&D with their industrial counterparts working under NREL and SNL subcontracts. These interactions have gone on since PV research started in 1977 at the Solar Energy Research Institute (now NREL) and since the mid-1970s at Sandia. Most involve performance measurements and materials analyses performed with NREL's large and unique set of capabilities for PV efficiency and materials analysis. Informal cooperative R&D, as distinguished from formal cooperative research and development agreements ((CRADAs), is a natural complement to DOE's subcontracted PV program. Informal cooperative R&D during FY 1998 included more than 45,000 measurements on some 16,000 PV material samples, devices, and modules on properties ranging from composition and microstructure to cell and module performance. More than 120 organizations from the worldwide PV community worked with NCPV researchers in this fashion.

We performed research under seven CRADAs during FY 1998: NREL and Energy Conversion Devices, Inc. (Upgrade and initial commercial operations of 2-MW Sovlux plant); NREL with Superconducting Core Tech., Inc. (Ferroelectric materials for advanced communications applications); NREL with Unisun (Improved processes for forming PV films); NREL with Lockheed Martin Astronautics (Development of large-area manufacturable lightweight CIS PV); NREL with ITN Energy Systems (Thin-film solid-state vanadium-oxide-based batteries; NREL with Paratek (Ferroelectric materials for advanced communications applications); and SNL with ASE Americas (Improvements in multicrystalline-silicon solar cells and modules using edge-defined film-fed growth silicon).

Information Dissemination

Effective traditional ways of transferring technology are to report R&D results to the technical community by publishing in scientific journals and by presenting at technical conferences and meetings. Section 12.0 contains a bibliography of FY 1998 publications, including subcontractor reports. During FY 1998, NCPV staff helped to organize several conferences and workshops, including the NCPV Photovoltaics Program Review, the Eighth Annual NREL Workshop on Silicon Defects and Impurities, the NREL/SNL Photovoltaic Performance and Reliability Workshop, and the NREL Photovoltaics Standards and Codes Forum. These gatherings provide important opportunities for industry researchers to exchange technical information with NCPV and university researchers.

NREL's program also distributes its quarterly newsletter, *NREL PV Working with Industry*, to about 1000 addresses. Sandia's program distributes its quarterly newsletter to about 2400 addresses. Adding to traditional information dissemination routes are several PV Web sites. These include:

- DOE PV Program (http://www.eren.doe.gov.pv)
- National Center for Photovoltaics (http://www.nrel.gov/ncpv)
- Sandia PV Program (http://www.sandia.gov/pv)
- Measurements and Characterization (http://www.nrel.gov/measurements)
- Basic Sciences and Materials (http://www.nrel.gov/basic_sciences)
- Renewable Resource Data Center(http://rredc.nrel.gov).
- Million Solar Roofs Initiative (http://www.MillionSolarRoofs.org).

1.4 Conclusions

This report reviews the in-house and subcontracted R&D activities within the NCPV in FY 1998. Major research thrusts during FY 1998 continued to be implemented based on DOE's *National Photovoltaics Program Plan for 1996-2000*.

In summary, the activities of the NCPV are to: conduct basic, applied, and engineering research; manage subcontracted R&D projects; perform research complementary to subcontracted work; develop and maintain state-of-the-art measurement and device capabilities; develop PV manufacturing technology and modules; transfer results to industry; and evolve viable partnerships for PV systems and market development.

This report describes the in-house and subcontracted R&D activities, many of which encompass close collaborations between NREL, SNL, and outside researchers.

The research activities performed or directed by NREL within the NCPV are summarized under eight project areas (Sections 2.0 to 9.0): PV Fundamental and Exploratory Research, PV Electronic Materials and Devices, PV Measurements and Characterization, Thin Film PV Partnership, PVMaT, PV Engineering and Reliability, PV Domestic Applications and Markets, and PV International Applications and Markets. The sections have, first, a brief overview that includes the objectives, approaches, and some key developments. Secondly, also included are technical summaries of the in-house and subcontract activities; the subcontract sections were provided directly by the subcontractors. Section 10.0 provides similar information, but specifically for SNL's activities. Finally, Section 11.0 lists the FY 1998 NREL subcontracts, and Section 12.0 is a FY 1998 bibliography of major research publications and subcontractor reports generated through NCPV activities.

2.0 PV Fundamental and Exploratory Research Project

2.0 PV FUNDAMENTAL AND EXPLORATORY RESEARCH PROJECT—Introduction

Robert McConnell

This project supports the fundamental and exploratory research needed for the advancement of PV technologies in the long-term, five to ten years and beyond. Today's belief within the PV community that thin-film PV technologies can meet ambitious cost and performance goals is the direct result of fundamental and exploratory research supported by the DOE PV Program more than ten years ago. NREL's first Conference on Future Generation Photovoltaic Technologies, held in FY 1997, provided clear evidence that PV innovation continues and can still lead to new PV technologies capable of meeting long-term DOE goals. However, as in the case of the early thin-film technologies, these new PV technologies typically have efficiencies well below 10%. At one extreme a PV device based on mixing CdSe nanocrystals with a conjugated polymer has efficiencies well below 1%. Yet conjugated polymers have the advantage of being easy to process to form large-area devices, and their energy gap and ionization potential can be readily tuned by chemical modification of the polymer chain. The possibility that conjugated polymer/nanocrystal composites may have the desired attributes of charge separation and transport justifies their exploratory research. Another device, the dye-sensitized photoelectrochemical cell has a charge separation process based more on a process common to photographic films than one occurring in conventional p-n junction solar cells. Yet it is an innovative PV concept with efficiencies of more than 10%. At the other extreme are the materials based on compounds from the third and fifth column of the periodic table. III-V compounds and their alloys make up the building blocks of multijunction solar cells with efficiencies higher than 30%, with a long-term potential of achieving 40% conversion efficiency. Such high-efficiency cells could be important for the future success of PV concentrator technologies to achieve long-term goals of $\$1/W_p$ for system costs with electricity costs of 5¢/kWh or less.

This project also supports liaison activities with DOE's Office of Energy Research (recently renamed the Office of Science) to leverage their funding of fundamental and exploratory research to support the long-term development of new PV technologies.

Within NREL, the Fundamental and Exploratory Research Project has seven tasks. These are:

- Physics of Photovoltaic Thin-Film Semiconductors
- Photochemical Solar Cell Development and Optimization
- Solid State Spectroscopy of Photovoltaic Materials
- University R&D for Future Generation PV Subcontracts
- Historically Black Colleges and Universities PV Research Associates Subcontracts
- Crystalline Silicon Materials Research
- Device Process Development

New Requests for Proposals and Subcontracts

NREL's Request For Proposal (RFP) entitled: " University PV Research Equipment" closed on June 1, 1998. The RFP's objective was to fund the acquisition of critical photovoltaic research and test equipment at universities participating in the NREL/DOE PV program to enhance their research capabilities as well as their research results. After reviewing and ranking the proposals, we awarded a total of $1,061,135 for 17 university subcontracts during July and August. The universities provided a total of $350,984 in "price participation" (called cost-sharing in the case of industry subcontracts) from other funding sources to supplement their awards. The funds for these subcontracts are accrued upon award since they pay for research equipment. These accruals helped NREL and DOE meet congressional requirements for not carrying over FY 1998 funds into FY 1999. The awards are listed below:

University	Award(+Price Participation)
Georgia Institute of Technology	$60,670 (+$20,300)
University of Utah	$49,280
Arizona State University	$66,932(+$13,431)
Colorado School of Mines	$83,000(+$48,000)
University of South Florida	$97,913
Syracuse University	$16,615
University of Delaware (IEC)	$100,000(+$37,250)
University of Toledo	$49,225(+$49,225)
Pennsylvania State University	$50,245(+$27,055)
Clemson University	$94,472(+$49,794)
California Institute of Technology	$23,875
University of South Florida	$50,000
University of Oregon	$45,787(+$17,929)
Washington State University	$49,156(+$12,000)
State University of New York-Buffalo	$32,935(+$19,000)
North Carolina State University	$100,000(+$57,000)
University of Florida	$91,000
TOTALS	$1,061,135(+$350,984)

These subcontract awards are expected to bolster university research equipment infrastructure by replacing or updating old equipment---10 to 15 years was not an unusual equipment age---thereby benefiting research on various PV research projects within the NREL/DOE PV program. In addition, helping meet congressional carryover requirements by making these awards so expeditiously maximized the benefits of appropriated FY 1998 DOE funding.

In 1995 the NREL/DOE National Photovoltaics Program first funded seven Historically Black Colleges and Universities (HBCUs) in its HBCU Photovoltaic Research Associates Program for a period of three years. The program's purpose has been to advance HBCU undergraduate knowledge of photovoltaics, primarily as a result of research

investigations performed, and encourage students to pursue careers in photovoltaics. These subcontracts were ending in 1998, coincident with a Five-Year Plan Milestone to assess the DOE/PV HBCU program. A poster presentation and publication for the NCPV Program Review Meeting proceedings reviewed results from a variety of HBCU PV projects ranging from fundamental research on PV materials to field projects of PV systems. The presentation and publication met the Five-Year Plan milestone.

Snapshots of the HBCU projects over the program's past three years include Central State's work on PV/wind water pumping systems, work with World Vision in Senegal, joint activities in a NASA-Lewis funded project called Consortium for the Advancement of Renewable Technologies (CARET), and creation of a five-day community outreach project to teach renewable energy to 25 local high school students. Clark Atlanta worked jointly with Vista University in South Africa on a project to assess the impact of aerosols (from coal cooking fires) on the solar resource and subsequently on PV system operation. HBCU interns from the Architecture Department at Hampton University did outstanding work in NREL's Buildings and Thermal Systems Center during the 1996 and 1997 summers. Mississippi Valley State University had a structured project for each undergraduate in their program, culminating in a PV symposium for others in the university in May 1998. Five Southern University undergraduates participated in the HBCU summer intern program at NREL where some of them did outstanding work on PV materials research projects. Texas Southern University (TSU) was highly successful in leveraging their DOE/NREL subcontract funds to obtain funding for a 4 kW PV system to be used as a teaching lab as well as for a Renewable Energy and Environmental Protection (REEP) summer academy conducted for three summers for some 60 minority high school students. The REEP Academy included trips to NREL, coordinated with NREL's Education Office, during the summers of 1997 and 1998. TSU obtained support from the DOE/NREL HBCU program for REEP trips to South Africa during the summers of 1997 and 1998, culminating in the hands-on PV installation of home lighting systems in a joint project with Port Elizabeth Technikon. Interns from Wilberforce and Central State also worked on the TSU/REEP projects in South Africa. Finally, Wilberforce University had one summer intern working with her professor in Ghana to obtain information on energy use in preparation for an NREL PV development proposal to the United Nations Development Program. Another Wilberforce intern worked summers at NASA-Lewis, at the Florida Solar Energy Center, and at the IEC at the University of Delaware.

Considering the relatively small funding for this program, approximately $400,000 annually, and that the PV Research Associates are undergraduates in the beginning of their careers the program has had some remarkable successes. These successes have benefited from the unique capabilities of the professors and students, as applied to their chosen PV projects, in the respective universities and departments participating in the program. Several of the students have indicated the DOE/NREL HBCU PV Research Associates program opened up new career possibilities for them in photovoltaics.

NREL's RFP entitled "Historically Black Colleges and Universities Photovoltaic Research Associates Program" was issued to about 50 Historically Black Colleges and

Universities with responses due June 30, 1998. Seven proposals were received. A final review committee meeting was held in September to complete the ranking of the proposals according to the stated Best Value Selection process in the RFP. During this meeting final reviewer scores were compiled, along with the weighting factors, to generate the rank order of the 7 proposals. Awards are scheduled for early FY 1999.

Finally, NREL's RFP entitled "University R&D for Future Generation PV Technologies" yielded 71 proposals for long-term research projects from many highly capable university researchers. After an extensive evaluation of these proposals, almost 20 awards are planned in FY 1999 to help support the DOE PV Program's long-standing strategy to support fundamental research at universities as a means for continued U.S. technical leadership in photovoltaics.

Liaison with Basic Energy Sciences in DOE's Office of Science

The High Efficiency PV Project is one project within the DOE/OS-supported Center of Excellence for Synthesis and Processing of Advanced Materials. The project has two teams: the Next Generation PV Team and the Thin Silicon-Based Team. These multilaboratory teams held four workshops during FY 1998. The two teams held a joint workshop early in FY 1998 followed by a Next Generation PV Team workshop in April. The attendees at the April workshop decided that, to be true to the project title (High Efficiency) and to the team title (Next Generation PV), work on the GaInNAs material leading to a 45% efficient solar cell would be the team's long-term focus. The Thin Silicon-Based Team held a meeting in conjunction with the 8th Workshop on Crystalline Silicon Solar Cells Materials and Processes in August. Finally, the Next Generation PV Team held a second workshop in September during the 15th NCPV (National Center for Photovoltaics) Program Review Meeting. All of these workshops have fostered interactions among researchers working in these areas regardless of their source of funding and therefore have provided an effective leveraging of PV program funds.

Research Task Reports

The following section contains highlights of the research activities in the seven task areas of the PV Fundamental and Exploratory Research Project. Five of these reports describe the results of NREL's in-house tasks. The remaining reports present research results from universities associated with the other two subcontract tasks. These researchers have been funded under earlier DOE/NREL subcontract programs for universities and almost all of them completed their subcontract programs in 1998.

Crystalline Silicon In-House Research

Title: **Crystalline Silicon Materials Research**

Organization: National Renewable Energy Laboratory, Golden, CO
Basic Sciences Center, Crystal Growth and Devices Team

Contributors: T. F. Ciszek (Principal Investigator), Y. S. Tsuo, T. H. Wang, and M. Landry

Introduction

Research on crystalline silicon (c-Si) materials was carried out in two task areas:

Task 1. Innovative methods for next-generation crystalline silicon materials growth

Task 2. Improvement of the fundamental understanding of silicon impurities and defects

The first task emphasizes research on innovative approaches to Si crystal growth methods, which complements work in industry by examining next-generation technologies [1]. The milestone for this task was to develop at least two innovative Si crystal growth methods. Task 2 seeks to develop a fundamental understanding of the role of defects and impurities in c-Si materials and device processing. A major activity in this task is the generation and characterization of samples with controlled concentrations of dopants, impurities, and defects [2]. The task milestone was to improve the fundamental understanding of impurity/defect behavior in photovoltaic silicon.

Task 1: Innovative methods for next-generation crystalline silicon materials growth

Fast and direct deposition of large-grain polycrystalline Si on glass substrates

Thin-layer crystalline Si solar cells are believed worldwide to be of vital importance to the next generation photovoltaic technology that promises low cost, high efficiency, low material consumption, and environmental friendliness. The most difficult challenge in the development of such PV technology is to produce an active silicon layer of sufficient electronic quality with a thickness on the order of 10 μm at a fast deposition rate of about 1 μm/min on a low cost substrate such as glass. Efforts over the world so far have only resulted in partial solutions (fast epitaxy of high quality layers on Si substrates, fast deposition of sub-micron grain size layers on high temperature glass, or slow solid-state crystallization from slowly deposited a-Si layers yielding highly stressed films). We were able to meet such a challenge with a new gas phase growth technique. It produces continuous Si layers of 5-20 μm thickness on high temperature glass at a growth rate of 1-3 μm/min. These Si layers exhibit large grains of 5-10 μm size. An effective minority carrier lifetime of about 5 μs was measured, implying a diffusion length far exceeding the layer thickness and low impurity content. A record of invention was submitted on the process [3], and additional details will be presented when intellectual property is secured. In related activities, a patent was issued on a new substrate material for thin-layer Si solar cells [4].

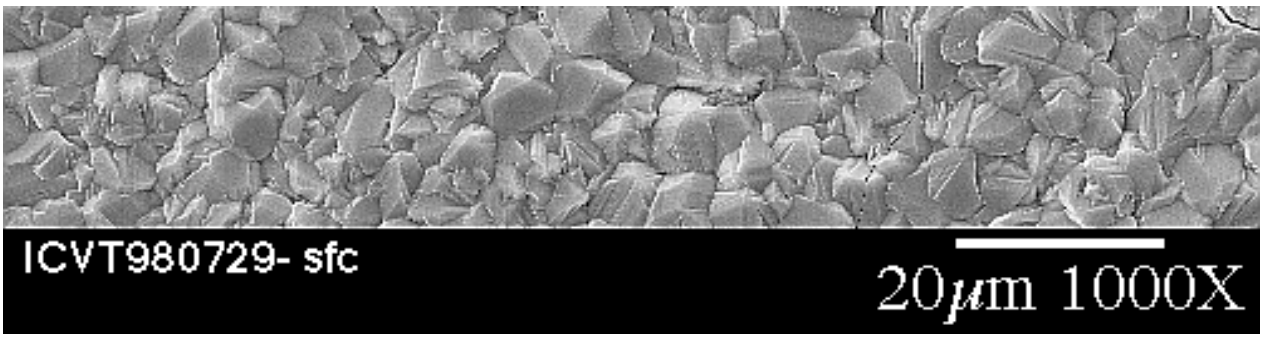

Fig. 1. The top view of a 10-μm-thick silicon film grown directly on glass at >1 μm/min.

Research on shaped crystalline silicon substrates

We grew Si tubes in collaboration with an industrial company interested in tubular silicon substrates for new applications, but unable to find a commercial supplier for them. The company manufactured hot zone parts to our specifications, as a part of an SBIR project, and sent them to NREL, where we conducted growth experiments using the capillary action shaping technique that we first published [5] in 1975, and recently explored for small diameter growth [6]. Our experiments produced prototype Si tubes 20 mm in diameter and 210 mm long. The growth hot-zone and a resultant tube are depicted in Fig. 2.

Fig. 2. The growth hot zone (left) and a resultant Si tube grown by capillary action shaping

Float-zone pedestal growth of thin silicon filaments

We continued our earlier work [6] on thin, high-purity, dislocation-free, single-crystal silicon filaments (SiFi's) grown from the melt by an RF-heated float-zone pedestal (FZP) method, particularly for the purpose of further characterizing the crystal structure and resistivity of the 0.3 – 2.0 mm dia., high-lifetime filaments. Some filaments were doped p-type with gallium. Good axial resistivity uniformity was observed in both undoped and deliberately doped filaments by spreading resistance measurements [7]. MoKα_1 X-ray topography verified that the filaments could be grown dislocation-free. The minority-carrier lifetimes resulting from the filament growth method (>100 ms) are more than adequate for consideration as active elements in linear photovoltaic concentrator devices and other semiconductor applications. We also grew Si dendrite filaments at 2-15 cm/min.

Other innovative Si crystal growth activities

In related Cooperative Research and Development Agreement (CRADA) activities with EBARA Solar Inc., the success rate of web crystal start-ups was more than doubled. Undesirable motion of the shallow silicon melt from which the ribbons are grown was reduced. A technique for starting wide webs without extraneous dendrites was demonstrated. A modified crucible/hot-zone arrangement that allows melt replenishment without excessive thermal perturbations was introduced. And defect analysis and thermal stress modeling to investigate reasons for premature web growth terminations was initiated.

A publication issued this fiscal year on another of our other innovative Si growth techniques [8].

We participated in the 1st International School on Crystal Growth Technology with an invited lecture [9].

Our R&D on an alternative MG purification method using porous Si etching was presented at the 15th European PV conference [10]. In our Initiative for Proliferation Prevention (IPP) project, our subcontractor, Intersolarcenter in Moscow, has developed a new chlorine-free method of producing solar-grade silicon feedstock. The process uses metallurgical-grade (MG) Si and ethyl alcohol as starting materials and produces solar-grade poly Si by using a fluidized bed reactor for the pyrolysis of silane.

Task 2: Improvement of the fundamental understanding of silicon impurities and defects

Iron-gallium pair defects

Work continued on understanding the role of Fe-Ga pair defects in degrading the electrical properties of silicon. Building on earlier work [11], we published our findings on lifetime degradation effects, trap levels, capture cross-sections, and defect concentrations [12]. We've extended the collaboration to the Lawrence Berkley Laboratory, where results are beginning to emerge on measurement of Fe concentration using high-resolution neutron activation analysis, which we will compare to those obtained from DLTS measurements and from dopant calculations. Sample growth has been hampered by major equipment repairs. We are currently focusing on diagnostic solar cell analysis of existing samples.

Minority carrier lifetime

In a Work-For-Others program with Siemens Solar Industries, we designed and built an apparatus for production-floor testing of bulk lifetime in Czochralski ingots. The novel probe method [13] coupled with new solid-state laser light source technology and a user-friendly computer control interface allows routine testing of all grown ingots to determine suitability for solar cell processing. We performed a 3-dimensional finite-element analysis to understand how much of an effect the non-passivated surface has on lifetime measurements in this two-probe, direct current photoconductivity decay (PCD) instrument.

A fixed voltage applied across the two probes in ohmic contact with one end of a cropped silicon crystal ingot results in an electric potential distribution and current distribution as shown below.

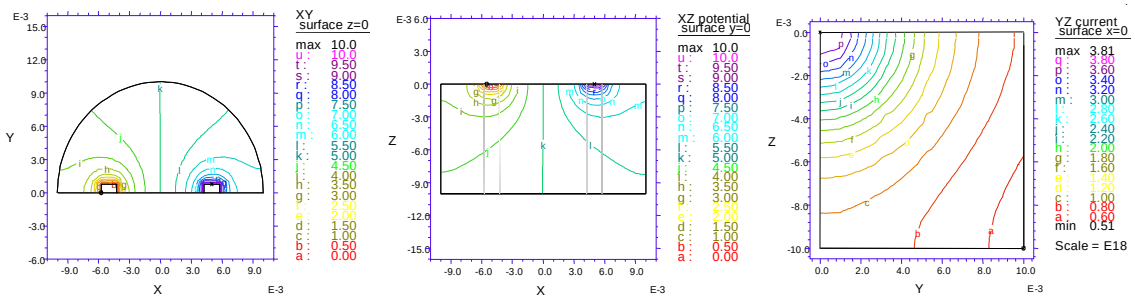

Fig. 3. *left* - potential on top surface, *middle* - potential in longitudinal section, *right* - current in center plane between the probes.

We found that a large voltage drop occurs around each probe tip and that only about one tenth of the total voltage is actually applied in the center excitation region of about 3-mm width. This makes PCD signal less susceptible to excess carrier sweep-out effects, but sensitive to mechanic-stability of the contacts. The current distribution in the center plane between the two probes indicates that the current is somewhat concentrated near the centerline (represented by the upper left corner) between the probes, and yet, it also spreads out as deep as 5 mm before the current density drops to half of the high values. This fact, coupled with the relatively low bulk lifetime that we normally encounter for commercial PV-grade CZ-Si, implies that the surface effect is minimal. In addition, the influence is confined to the top surface, which is much less than that of a double-sided wafer of similar thickness. The surface effect only lowers the effective lifetime to 18.8 μs from an actual bulk lifetime of 20 μs, for example. Therefore, as long as the measured lifetime is relatively low (~50 μs), the effective lifetime may be safely assumed to be the bulk lifetime, within measurement error.

Our work last year on analysis and modeling of lifetime measurement approaches has now been published [14], and we have extended it to examine the effects of sample inhomogeneity and geometry on photoconductivity decay [15].

Other Activities

We have begun to consider environmentally-friendlier ways of processing silicon, and a plenary lecture on this subject was presented at the 2nd World Conference on Solar Energy Conversion this year [16].

References

1. T.F. Ciszek and J.M. Gee, “Crystalline Silicon R&D at the U.S. National Center for Photovoltaics,” in: Proc. 14th European Photovoltaic Solar Energy Conference, Barcelona, Spain (1997) pp. 53-56.
2. T.F. Ciszek and T.H. Wang, “Silicon Defect and Impurity Studies Using Controlled Samples,” in: Proc. 14th European Photovoltaic Solar Energy Conference, Barcelona, Spain (1997) pp. 396-399.
3. Tihu Wang and Theodore F. Ciszek, "A Vapor Transport System for Silicon Crystal Growth,” NREL Record of Invention 98-47 (1998).
4. Theodore F. Ciszek, "Substrate for Thin Silicon Solar Cells," U.S. Patent 5,785,769 (1998).
5. T.F. Ciszek, "Melt Growth of Crystalline Silicon Tubes by a Capillary Action Shaping Technique," phys. stat. sol. (a) **32**, (l975) 521.
6. T.F. Ciszek and T.H. Wang, “Growth and Properties of Silicon Filaments for Photovoltaic Applications,” in: 26th IEEE Photovoltaic Specialist Conf. Record (IEEE, N.J., 1997) pp. 103-106.
7. T.F. Ciszek and T.H. Wang, “Float-zone Pedestal Growth of Thin Silicon Filaments,” in: High Purity Silicon V, Eds. C.L. Claeys, P. Rai-Choudhury, M. Watanabe, P. Stallhofer, and H.J. Dawson (The Electrochemical Soc., Proceedings Volume 98-13, New Jersey, 1998) pp. 85-89.
8. J. Moore, T.H. Wang, M.J. Heben, K. Douglas, and T.F. Ciszek, “Fused-Salt Electrodeposition of Thin-Layer Silicon,” in: 26th IEEE Photovoltaic Specialist Conf. Record (IEEE, New Jersey, 1997) pp. 775-778.
9. T. F. Ciszek, “Silicon Crystal Growth for Photovoltaic Applications,” invited lecture at the First International School on Crystal Growth Technology, ISCGT-1, Beatenberg, Switzerland, Sept. 5-16 (1998).
10. P. Menna, Y.S. Tsuo, M.M. Al-Jassim, S.E. Asher, R. Matson, and T.F. Ciszek, “Purification of Metallurgical-Grade Silicon by Porous-Silicon Etching,” in: Proc. 2nd World Conf. and Exhibition on Photovoltaic Solar Energy Conversion, Vienna, Austria, 6-10 July,1998 (to be published).
11. Y.S. Tsuo, Y. Petrovich, G.V. Grigorievich, et. al., "Method of High Purity Silane Preparation,” NREL Record of Invention 99-05, (1998)
12. T.F. Ciszek, T.H. Wang, W.A. Doolittle, and A. Rohatgi, “Minority-Carrier Lifetime Degradation in Silicon Co-Doped with Iron and Gallium,” in: 26th IEEE Photovoltaic Specialist Conf. Record (IEEE, N. J., 1997) pp. 59-62.
13. T.F. Ciszek, T.H. Wang, W.A. Doolittle, and A. Rohatgi, “Iron-Gallium Pair Defects in Float-Zoned Silicon,” in: High Purity Silicon V, Eds. C.L. Claeys, P. Rai-Choudhury, M. Watanabe, P. Stallhofer, and H.J. Dawson (The Electrochemical Soc., Proceedings Volume 98-13, New Jersey, 1998) pp. 230-240.
14. Theodore F. Ciszek, Tihu Wang, and Marc Landry, "Preparation-Free Contacting Method for Measuring Minority Carrier Lifetime in Large Silicon Ingots," NREL Record of Invention 98-06 (1998)
15. T.H. Wang and T.F. Ciszek, “Numerical Simulations of Transient Photoconductance Decay,” in: 26th IEEE Photovoltaic Specialist Conf. Record, Anaheim, CA, Sept. 29-Oct. 3, 1997 (IEEE, New Jersey, 1997) pp. 55-58.
16. Tihu Wang and Ted F. Ciszek, “Effects of Sample Inhomogeneity and Geometry on Photoconductivity Decay,” in *Silicon Recombination Lifetime Characterization Methods, ASTM STP 1340*, D.C. Gupta, F. Bacher, and W.H. Hughes, Eds., American Society for Testing Materials, (to be published, 1998)

Title: **Device Process Development**

Organization: National Renewable Energy Laboratory, Golden, CO
PV & EM Center, Device Process Development Team

Contributors: Bhushan Sopori, Wei Chen, Jamal Madjdpour, Yi Zhang, Mike Benallo, and Karen Nemire

Introduction

The objectives of our group are:

1. use defect engineering concepts to develop new processes that produce higher efficiency solar cells, at a lower cost,
2. generate new cell designs and fabrication processes based on rigorous modeling, and
3. assist PV industry by developing suitable methods for process control, cell design, and other analytical means.

Accordingly, the work is divided into 3 tasks – Device development and modeling, process development and modeling, testing and measurement for process control and monitoring.

Task 1: Device Development and Modeling

PV Optics and Emissivity Modeling

The following modifications were made on *PV Optics*: (i) reduction of calculation time, generally from days to a few hours, which is particularly important for multi-junction (MJ) cell analysis, (ii) bi-directional incidence of light, allowing analysis of both the substrate and the superstrate configurations, and (iii) ability to change the angle of incident illumination. Besides, PV Optics has been extended to make calculation of emissivity - an important parameter in RTP modeling and pyrometric measurements. Our emissivity model calculates the emissivity of Si wafers with the different surface morphologies, dopant concentrations, and temperatures. Our modeling package is the only software that handles non-ideal surfaces and multi-layer structures. Figure 1 shows an example comparing the calculated emissivities of a single-side polished Si wafer from the polished and the rough sides. Because the emissivity requires temperature dependence of the optical parameters, our model incorporates a new approach for modeling the refractive index (n) and absorption coefficient (k) as a function of temperature. The results of our calculations are in an excellent agreement with the experimental results (see Figure 2 for a comparison). Emissivity modeling is becoming increasingly important for PV because many PV manufacturers are using RTP.

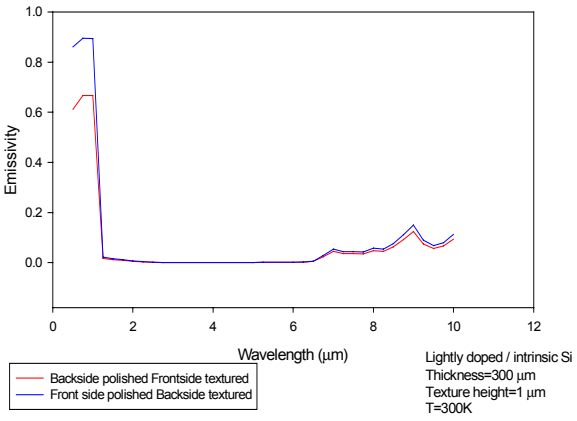

Figure 1

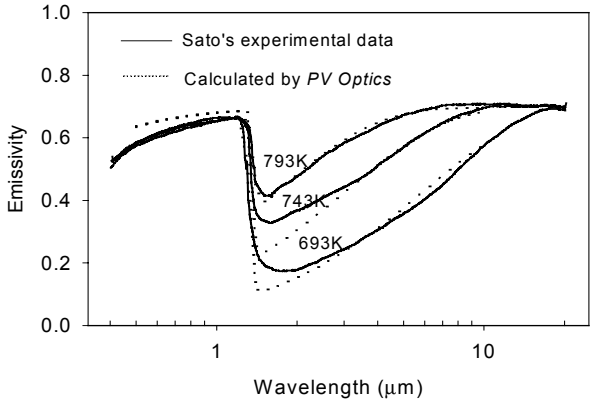

Figure 2

Thin Film Si Solar Cell

We are continuing to verify the features of our thin film Si-on-glass cell design. Si films were deposited at IEC using hot-wire process at 500º and 600º C and at North Carolina State University using low-temperature sputtering process. Several important results are:

a. During the Si deposition, our metallic interface layer enhances the nucleation of crystallites, which is later enlarged further by our optical processing. Figure 3 compares the morphologies of Si films deposited on glass substrate, with (a) and without (b) metallic layer, at temperatures lower than 80º C. The presence of the metal results in grain sizes in the range of 0.1-0.5 μm.
b. At low process temperatures, Al remains confined to Si-Glass interface during the deposition. Later optical processing does not seem to diffuse Al; furthermore, extended thermal processing at temperatures exceeding 500º C leads to the formation of alloyed films of large grains.
c. In our cell design, the metallic layer provides a stress relief buffer between the Si film and the glass substrate. We observed the Si films were cracked and peeled off without this layer, while staying normal with it.

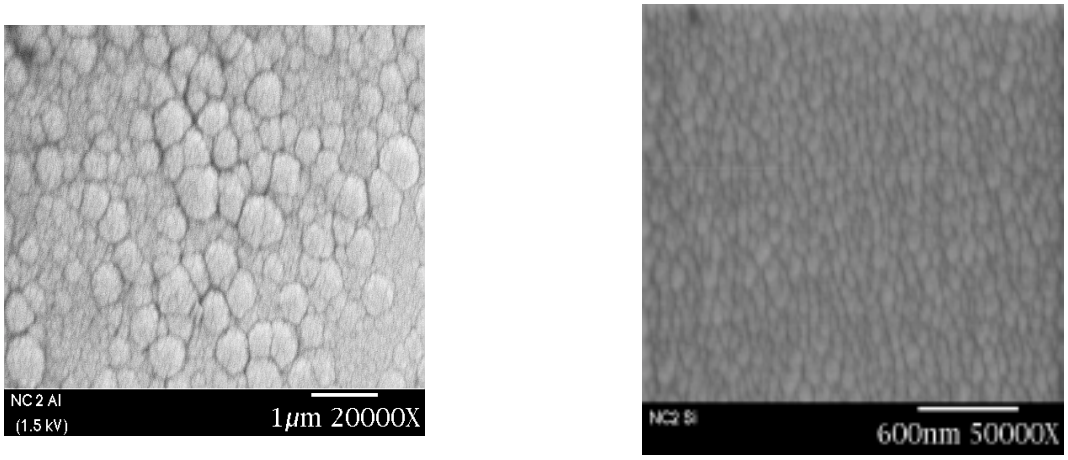

(a) (b)

Figure 3

Task 2: Process Development and Modeling

Gettering Process

We continued to investigate the validity of impurity gettering model we proposed earlier for low-cost PV-Si material. Originated by Sopori, Tan, and Jastrzebski, the model explains the properties of PV-Si and its gettering behavior, and asserts impurity precipitation occurs in the heavily defected regions during the crystal growth. We now have, for the first time, verified this phenomena, and shown that precipitation occurs predominantly at the defect clusters (see TEM picture in Figure 4). Our network analysis showed such regions limit the solar cell performance by shunting the device. Other studies show that the defect cluster regions have low photoluminescence and short lifetime. These results are expected to help understand mechanisms that cause shunting of solar cells.

Fig
clu
pre

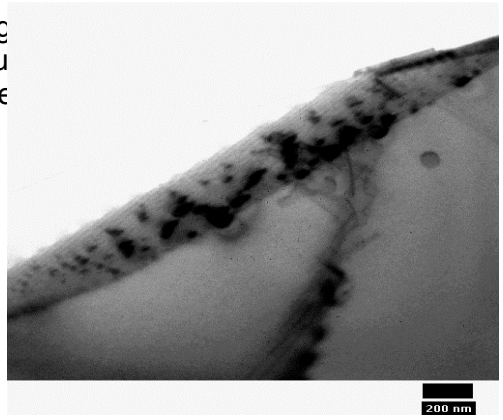

Further studies with other groups are in progresses: U.C., Berkeley is identifying the chemical nature of the precipitates using synchrotron X-ray florescence; we are investigating the possibilities of dissolving the precipitates with Optical Processing; and, Duke University is conducting the theoretical analysis.

PVSCAN

The assembly of new PVSCAN fell behind schedule due to the unexpected delay in the chassis fabrication. Recently, we also encountered several electronics-related problems in the system. PVSCAN has an electronics board specifically made by Labsphere Co. Since they do not support this instrument anymore, it was necessary for us to identify all the electronics operations. We spent an extensive amount of time to complete mechanical, electrical and optical drawings, as well as a parts/vendor list. A new system (with modifications covering new features) is expected to be operational early next year.

Fiber Optic Solar Simulator (FOSS)

The FOSS was moved to Lab C125 for two reasons – to allow III-V group an easy access to the system, and to relieve space congestion in C212. The objectives of FOSS are not only to serve as an accurate solar simulator, but also to get the capabilities for the testing that allow isolating the characteristics of cells in the MJ-stack. The current FOSS does not provide these capabilities because of its limited power out put. This system was primarily designed to verify proof-of – concept of producing a 2-in beam for 1-sun AM1.5 spectrum. During its use over last few years, the system's optical components have degraded, yielding merely 0.8 suns in a beam. We are currently redesigning a new FOSS that will include four additional, narrow-band sources to facilitate individual cell analysis. This work will be done in collaboration with the III-V Team.

Task 3: Testing and measurement for process control and monitoring

Lifetime Modeling

We continued theoretical modeling of the minority carrier lifetime in mc-Si, and addressed the questions of suitable techniques for lifetime measurement for monitoring purpose. This work is becoming particularly important, because PV industry is looking for an accurate means for substrate quality control. Previous work focussed on the steady-state measurement techniques of SPV and Quasi-steady State Photoconductive Decay (PCD) methods for mc-Si. We have now extended this modeling from steady state analysis to the finite element method to time-dependent transient PCD calculations. We have written the code and applied it to analyze the behavior of mc-Si wafers under various conditions. Some conclusions are: (i) In a material with more than one lifetime, there is a net flow of carriers from "good" grains to "bad" ones. This resulted carrier exchange among grains can strongly influence the measurement. (ii) A steady-state measurement technique can be more

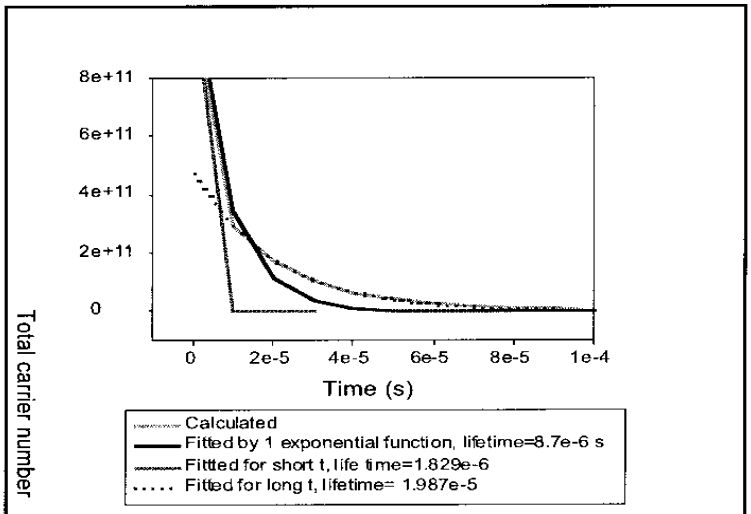

Figure 5. Calculated minority carrier concentration as a function of time, in a sample whose 95 % area has τ=1 μs, and 5% area has τ = 100 μs.

meaningful for the solar cell than a transient decay method. (iii) All techniques require low surface recombination velocities to yield meaningful results, and (iii) Even with the low surface recombination velocities or ideal conditions, the measured values depend on the technique. For example, the PCD results are dependent on the time-window used for data analysis. In order to demonstrate these effects, Figure 5 shows the PCD results on a wafer that has two regions – 95 % has 1-μs lifetime and 5% has 100-μs lifetime. Our calculation shows that the initial part can be fitted into a 1.83-μs-lifetime decay, while the "tail" into a 20-μs-lifetime decay. It is clear that the transient decay technique (even under ideal conditions) will not yield the correct lifetime(s). This is an important result that illustrates the reliability issues of using transient decay techniques for quality control in PV industry. This method favors "good" parts of the lifetime and overestimates the material quality.

The lifetime modeling is being extended to develop an electronic model of a poly-crystalline thin film Si solar cell.

Round Robin Lifetime (τ) Measurement

The lifetime round robin testing consists of seven groups. Each group has three different types: bare, oxidized, and P-diffused, corresponding to the different surface recombination velocities. The objective is to evaluate the influence of these material and measurement conditions in different techniques. Many participants have completed the measurements, and we are compiling the results. These results will be discussed at the 3rd Work Group Meeting that is now being planned for Feb. '99.

Papers published

1. Bhushan L. Sopori, Wei Chen, S. and S. Abedrabbo, and N. M. Ravindra, "Modeling Emissivity of Rough and Textured Si Wafers," J. Elec. Mat., accepted for publication
2. S. Abedrabbo, J. C. Hensel, O. H. Gokce, F. M. Tong, B. L. sopori, A. T. Fiory, and N. M. Ravindra, " Issues in Emissivity of Silicon, " J. Elec. Mat., accepted for publication.
3. B. L. Sopori, J. Madjdpour, W. Chen, and Y. Zhang, "Light-Trapping in a-Si Solar Cells: A Summary of the Results from PV Optics" presented at the NCPV Review, paper to be published in IAP
4. Bhushan Sopori, Wei Chen, Teh Tan, and Pavel Plekhanov, "Overcoming the Efficiency-Limiting Mechanisms in Commercial Si Solar Cells" presented at the NCPV Review, paper to be published in IAP
5. Bhushan Sopori, Wei Chen and Yi Zhang, " Development of A Thin Film Crystalline Silicon Solar Cell," presented at the NCPV Review, paper to be published in IAP.
6. Bhushan L. Sopori, Michael Cudzinovic, and Wei Chen, "Optical and Electronic Properties of Si-Al Interfaces Produced by Optical Processing", Symposium on the Transient Thermal Processing of Materials, TMS Meeting, San Antonio, TX, Feb. 15-19, 1998.
7. B. L. Sopori and W. Chen, S. Abedrabbo and N. M. Ravindra, (Invited Paper) "Modeling Emissivity and Time-Dependent Temperature Profiles of Rough and Textured Wafers", Symposium on the Transient Thermal Processing of Materials, TMS Meeting, San Antonio, TX, Feb. 15-19, 1998.
8. Bhushan L. Sopori, Wei Chen, Jamal Madjdpour and Marta Symko, "A Thin-Film Silicon Solar Cell: Design and Processing Approach", MRS Symposium on Thin Film Structures for Photovoltaics, Fall 1997.
9. B. L. Sopori, W. Chen, J. Alleman, R. Matson, N. M. Ravindra, and T. Y. Tan, "Grain Enhancement of Polycrystalline Silicon Films Aided by Optical Excitation", MRS Symposium on Thin Film Structures for Photovoltaics, Fall 1997.
10. Bhushan Sopori, Wei Chen, and Karen Nemire,"Influence of defect clusters on the performance of silicon solar cells"
11. Wei Chen, Bhushan Sopori, and N. M. Ravindra, "Theoretical Analysis of the minority carrier lifetime in a multi-crystalline wafer with spatially varying defect distribution"
12. M. I. Symko, B. L. Sopori, R. Reedy, S. Estreicher, and A. Rohatgi, "Hydrogen diffusion and defect passivation in silicon by forming gas anneal"
13. S. A. McHugo, A. C. Thompson, G. Lamble, A. MacDowell, R. Celestre, H. Padmore, J. Imaizumi, M. A. Yamaguchi, I. Perichaud, S. Martinuzzi, M. Werner, M. Rinio, H. J. Moller, B. Sopori, H. Hieslmair, C. Fink, A. Istratov, and E. I. Weber, "Direct correlation of solar cell performance with metal impurity distribution in polycrystalline silicon using synchrotron-based X-ray analysis"

Crystalline Silicon Subcontracts

Title: **Low Cost Glass and Glass-Ceramics Substrates for Thin Film Silicon Solar Cells**

Organization: * Cornell University, Ithaca, NY,
† Corning Incorporated, Corning, NY

Contributors: Dieter G. Ast*, Nikolay I. Nemchuk*, J. Gregory Couillard†, Chad B. Moore†, Linda R. Pinckney† and Sergey M. Krasulya*

Objective:

Develop novel, low cost, transparent glass ceramic substrates, capable of withstanding process temperatures up to 960 ºC and matched to the Coefficient of Thermal Expansion of silicon for the fabrication of thin film polycrystalline silicon solar cells.

Approach:

This is a joint development between Corning Inc. and Cornell University. Corning Inc. is developing the substrates, and Cornell University is investigating barrier layers and testing the substrate/ barrier layer combinations via the fabrication and electrical characterization of majority and minority carrier devices.

Results:

Multiple silicon nitride layers were found to be effective barriers against the outdiffusion of glass ceramic components (Fig. 1.) Device results to date indicate that barrier layer coated glass ceramic substrates appear suitable for the fabrication of both minority carrier devices (solar cells) and majority carrier devices (thin film transistors) at process temperatures up to 900 ºC. Performance of the thin film transistors on glass ceramics is comparable to those on oxidized silicon on fused silica wafers (see Fig 2 and 3, Table 1).

According to dark current-voltage (I-V) measurements, the performance of the minority carrier devices – thin film solar cells on glass-ceramic substrates - is as high as on silicon wafers and better then on fused silica substrates (Fig. 4). The forward I-V characteristics follow an exponential law with ideality factor of ~ 2 (Fig. 5). This behavior is expected for polycrystalline silicon, containing near midgap states.

Potential future research:

1) Simplify the barrier layer (currently triple LPCVD silicon nitride, separated by layers of LPCVD silicon dioxide).
2) Investigate via Deep Level Transient Spectroscopy the impurity transport from the substrate into deposited polycrystalline silicon film (‘substrate contamination’) and from the polysilicon film into the substrate (‘gettering’).
3) Begin joint work with M. Green (Pacific Solar) on testing these substrates for multilayer polycrystalline silicon solar cells fabrication.

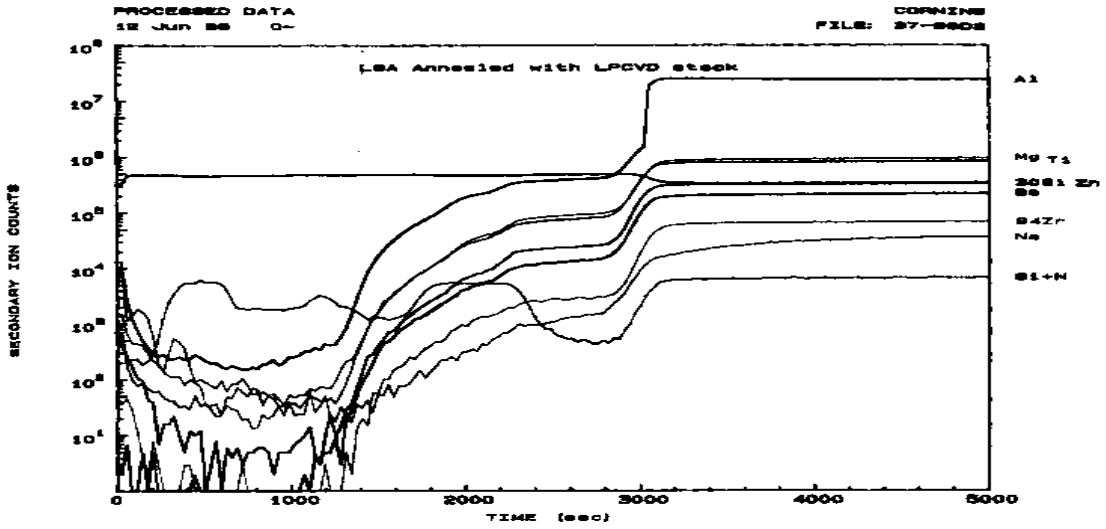

Figure 1. SIMS profile of a barrier layer/glass-ceramic combination, subjected to a 8 hour anneal at 900 ºC. The multiple barrier layer consisted of three 1000 Å thick LPCVD silicon nitride layers separated by 1000 Å thick LPCVD silicon dioxide layers. The location of the three SiNx layers is clearly indicated by the nitrogen + silicon peaks. The first oxide layer (the one in the contact with substrate) is saturated with glass components. However, the concentration of all glass components, except for Al, decreases within the first nitride layer to values below the detection limit of SIMS. The second nitride layer suppresses the Al signal to values below the detection level.

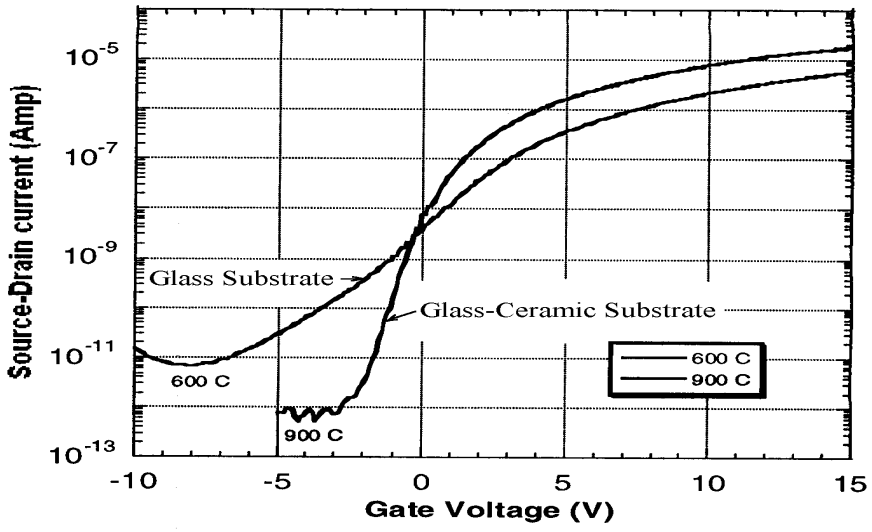

Figure 2. Current-Voltage characteristics of TFTs fabricated on 1737 glass at 600 ºC and LGA-139 glass-ceramic at 900 ºC. The lower leakage current and steeper sub-threshold slope both indicate that the polycrystalline silicon fabricated at high (900 ºC) temperature has improved electrical properties.

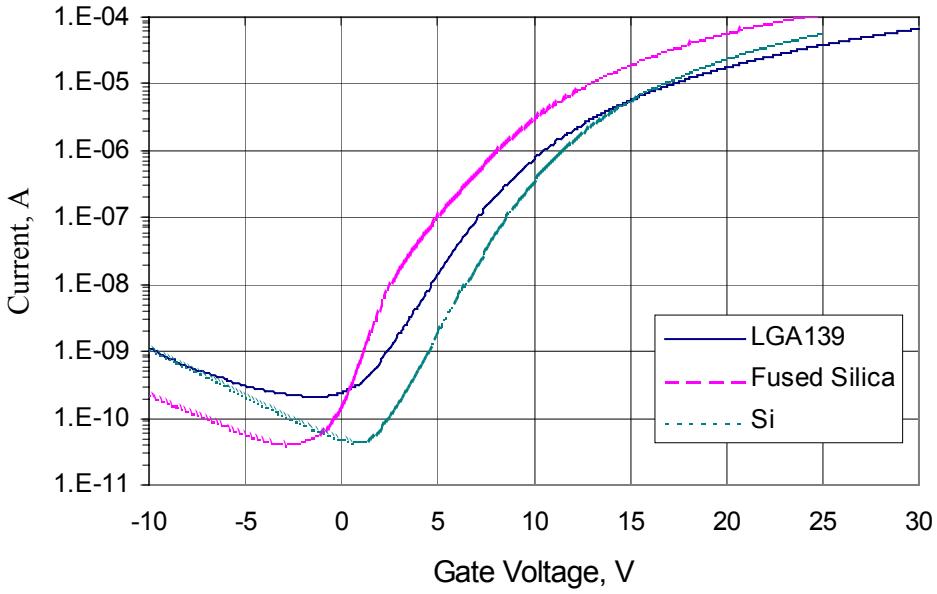

Figure 3. Current voltage characteristics of TFTs fabricated at 900 ºC on the LGA-139 glass-ceramic substrate and, for reference, on fused silica and oxidized silicon substrates. The lower saturation current of TFTs on glass-ceramic substrate is most likely caused by the high surface roughness (500 Å) of the particular wafers used. This roughness is replicated into the channel, resulting in additional carrier scattering.

	Vfb	Imin	I0	I15	μ	Qtrap	S	Vth	N
LGA-139	-1.2	231	260	5750814	34.31	5.05	2.19	7.8	118
	0.3	23	39	1515035	3.53	0.14	0.15	0.6	
Fused silica	-2.9	49	208	19006100	118.25	5.40	1.34	6.6	120
	1.1	9	220	8011165	43.17	0.25	0.12	0.7	
Silicon	0.6	45	435	5972658	76.61	5.18	1.90	9.4	120
	0.3	2	3127	3590079	5.90	0.09	0.10	0.2	

Table 1. TFT parameters for transistors made on LGA-139 glass-ceramic, fused silica and oxidized silicon wafers. The columns list, left to right, the flat band voltage, $\mathbf{V_{fb}}$; the source – drain current at the flat band voltage, Imin in units of pA; the source –drain current at zero gate voltage, $\mathbf{I_0}$ in units of pA; the source –drain current at a gate voltage of 15 V, $\mathbf{I_{15}}$ in units of pA; the intrinsic electron mobility **μ** in cm^2/Vs; the trap density $\mathbf{Q_{trap}}$ in multiples of 1E12 $/cm^2$; the subthreshold swing **S** in units of V/decade; the threshold voltage V_{th}; and the number of devices measured **N**. The line below lists the standard deviations of these parameters.

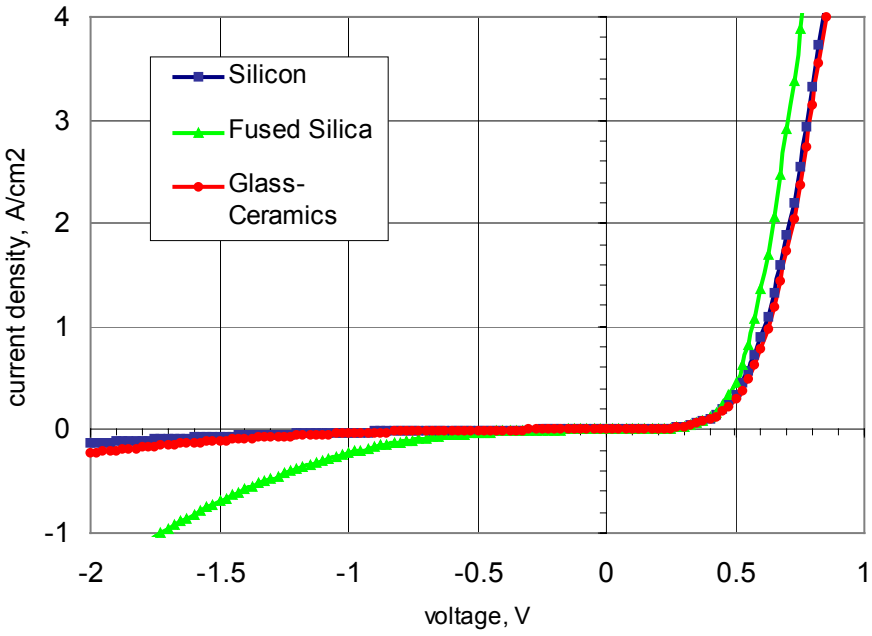

Figure 4. Dark Current-Voltage characteristics of thin film polycrystalline silicon solar cells fabricated on LGA-139 glass-ceramic, and for reference, on fused silica and oxidized silicon substrates. The performances of the cells made on glass-ceramics and on oxidized silicon are very close and far exceed those on fused silica, a high purity substrate that does not match the thermal expansion coefficient of polycrystalline silicon.

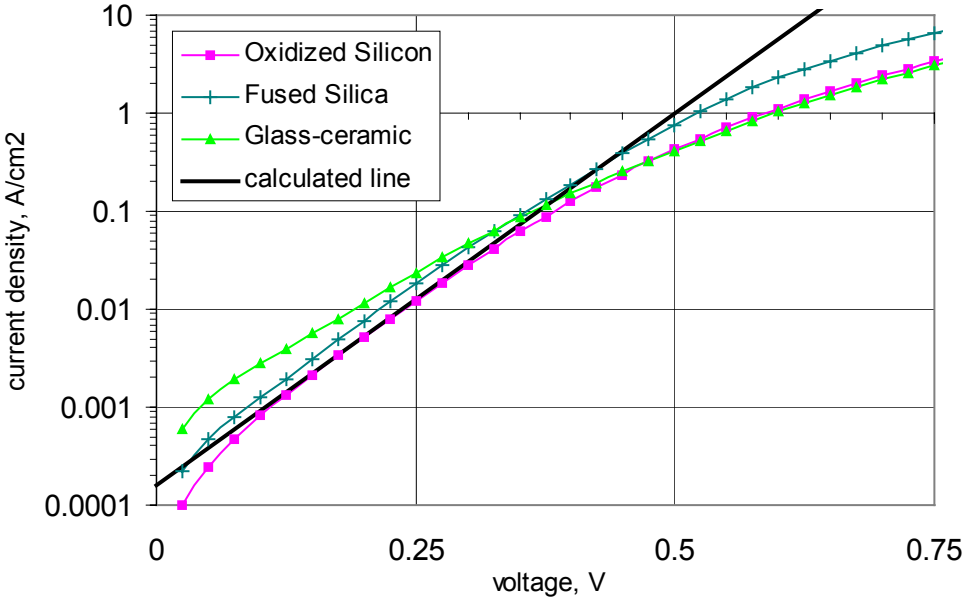

Figure 5. Forward Current-Voltage characteristics of thin film solar cells fabricated on different substrates. Black line is calculated for ideality factor N = 2.2. The curves follow an exponential law up to current density value of 0.1 A/cm^2. At higher currents, series resistant becomes significant.

Title: **Investigation of Gettering Mechanisms in Crystalline Silicon**

Organization: Department of Mechanical Engineering and Materials Science,
Duke University, Durham, NC 27708

Contributors: T. Y. Tan and U. M. Gösele, Principal Investigators;
S. M. Joshi and P. S. Plekhanov.

Objective

The goals of this program are to develop accurate physical models for gettering and apply the models to design efficient gettering processes for crystalline silicon materials. In this work, experimental evidence is presented to show that extended high temperature aluminum gettering can improve diffusion lengths in multicrystalline silicon wafers in regions of high or low starting diffusion length. Previously, the low diffusion length regions have been generally found to be unresponsive to gettering treatments. Modeling of the aluminum gettering process shows that gradually stepping or ramping down the temperature from a high starting value during gettering may give better results than a single step high temperature and long time anneal. The multi-step process is also likely to be more economical as the overall cycle time is reduced and the time at high temperature is also reduced, while giving comparable results.

Extended high temperature aluminum gettering of multicrystalline silicon wafers

While aluminum gettering has been shown to be successful in improving minority carrier diffusion lengths in single crystalline silicon [e.g., 1], results have been ambiguous in case of multicrystalline silicon [2], which often has localized regions of high dislocation and precipitate concentration. These localized regions do not show any improvement after typical aluminum gettering treatments at 800-850°C for a couple of hours as applied in industry, or at higher temperatures of up to 1000°C for short times as reported in literature. Most of the impurity atoms are in the precipitate form, while aluminum gettering can only remove impurity atoms dissolved in the silicon. Thus the gettering is limited by dissolution of precipitates, which proceeds quite slowly at low temperatures. Previous modeling results have shown that long times and high temperatures are required to allow substantial dissolution of precipitates and gettering of the dissolved impurity atoms.

Matched 4" square multicrystalline wafers of thickness 400-450 μm were used for these experiments, which used the ELYMAT technique for mapping of diffusion lengths across the wafers. After initial diffusion length maps were prepared of the experimental wafers, aluminum layers of 1 μm thickness were deposited on both sides of half of each wafer, while the other halves were left uncovered. The gettering anneal was done at 1100°C for 4 h in nitrogen in a quartz enclosure placed within a box furnace. After annealing, the Al-Si alloy layer was removed from the surface of the wafers and the diffusion length mapped across the wafers.

Figure 1 shows the initial and final diffusion length maps for a sample wafer. The half of the wafer that had the aluminum gettering layer shows an improvement in the diffusion lengths . In particular, the areas that initially had very low diffusion lengths also show substantial improvement in diffusion lengths which has not been observed before. The half of the wafer without a gettering layer shows degradation of diffusion length resulting from furnace contamination and from dissolution of precipitates without removal of the dissolved impurity atoms.

Figure 2 shows histograms of the diffusion length distributions before and after gettering in the half of the wafer that was Al gettered, which further illustrate the improvement. Before gettering, the distribution of diffusion lengths is wide, with a lot of data points at the lower end of the range. The diffusion lengths at the lower end of the range may, in fact, be even lower as the ELYMAT technique cannot resolve diffusion lengths below about one-fifth of the wafer thickness. After gettering, the distribution is much narrower and the data points are clustered at the higher end of the scale.

Modeling and optimization of high temperature aluminum gettering of iron precipitates in silicon

Previous modeling has indicated that, for successful aluminum gettering of impurities at high concentrations existing in precipitated state, extended times at high temperatures are required [3]. Besides, the high temperature gettering has a limited efficiency as the residual concentration of impurities after gettering is higher. As such high temperature anneals for extended times may prove uneconomical for industrial application, it is desirable to explore if shorter and more economical gettering procedures can be developed.

In order to evaluate the efficiency of the modeled gettering process in the case when impurities are present in the Si crystal in both dissolved and precipitated state, a new approach was developed [4]. It is based on the calculation of minority carrier diffusion length (or its reciprocal value, carrier recombination lifetime) integrated throughout the wafer, so as to simulate the recombination of carriers migrating from one side of the wafer to the other, as occurs in many experimental lifetime measurement setups. Proper accounting of precipitate contribution to the recombination rate is essential. Our theoretical derivations show that, due to the carrier diffusion effects, the capture cross-section of a precipitate is proportional to the cubic root of number of atoms in it. This approach allows us to easily compare the efficiency of different gettering processes.

In order to obtain low residual concentration of impurities and large lifetime improvement characteristic of low temperature gettering, but at the same time to maintain short process duration that can normally be achieved only in high temperature processes, we propose a variable temperature process. At the earlier, high te□□mperature stage(s), impurity precipitates are dissolved and substantial outdiffusion of impurity occurs. At the later, low temperature stage(s), the concentration of dissolved impurity is brought down to the desired level. The temperature can be either stepped down or ramped down. Our modeling has confirmed that as a result, low residual concentration of impurity can be achieved in comparatively short times. For instance, if Fe saturates Si at 900°C and precipitates at 700°C with precipitate concentration 10^{11} cm^{-3}, it will take about 55 hours to getter it from a 400 μm thick wafer at 700°C to the point where thermal equilibrium is achieved. In a variable temperature process, same results can be obtained in just about 1 hour (Figure 3).

Conclusions

Experiments on multicrystalline silicon show that localized regions of low diffusion length may be improved by extended high temperature aluminum gettering. Modeling results indicate that using multi-step gettering procedures which start at high temperature and progressively go to lower temperatures can give equal or better results than extended high temperature gettering, and thus provide a more economical alternative.

References

1. Joshi, S. M.; Gösele, U. M.; and Tan, T. Y. (May 1995). "Improvement of minority carrier diffusion length in Si by Al gettering." *Journal of Applied Physics* (11:1);p. 111-111.
2. McHugo, S. A.; Hieslmair, H.; and Weber, E. R. (1997). "Gettering of metallic impurities in photovoltaic silicon." *Applied Physics A* (64);p.127-137.
3. Tan, T.Y.; Gafiteanu, R.; Gösele, U.M. (1997). "Physical and Numerical Modeling of Impurity Gettering in Silicon." *NREL/SNL Photovoltaics Program Review, Proceedings of the 14th Conference*, C.E. Witt, M. Al-Jassim, J.M. Gee, eds. Woodbury, NY: American Institute of Physics; p. 215.
4. Plekhanov, P. S.; Gösele, U. M.; and Tan, T. Y. (1998). "Physical and Numerical Modeling of Gettering of Precipitated Metallic Impurities in Si." presented at *15th NREL/SNL Photovoltaics Program Review Meeting.*

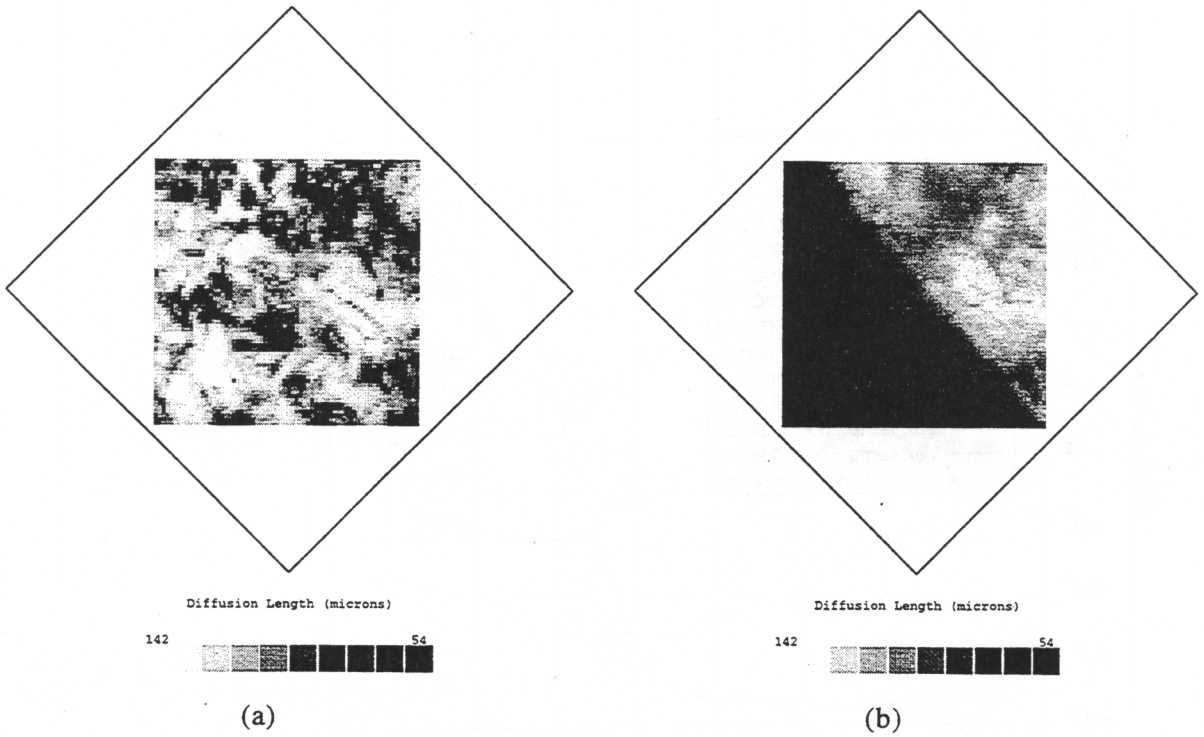

(a) (b)

Fig.1 Diffusion length maps of the same multicrystalline wafer : (a) Initial; (b) After annealing at 1100°C for 4 h with an Al gettering layer on both sides of half of the wafer. The initial diffusion length map has local regions of very low diffusion length. After gettering, the Al gettered half has much higher diffusion lengths than the ungettered half.

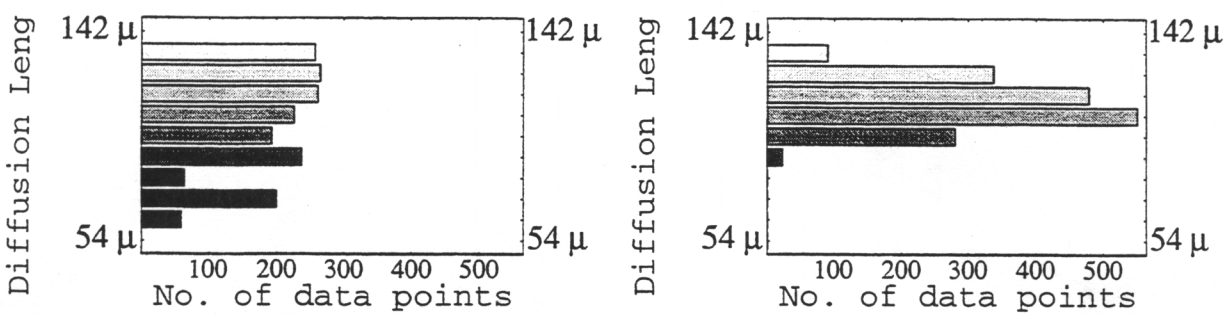

(a) (b)

Fig.2 Histograms of diffusion length values in the aluminum gettered half only as obtained from the diffusion length maps of Figure 1 : (a) Before gettering as seen in Fig. 1(a); (b) After gettering, as seen in Fig. 1(b). After gettering, the diffusion length distribution is clearly narrower and pushed to the higher end of the scale.

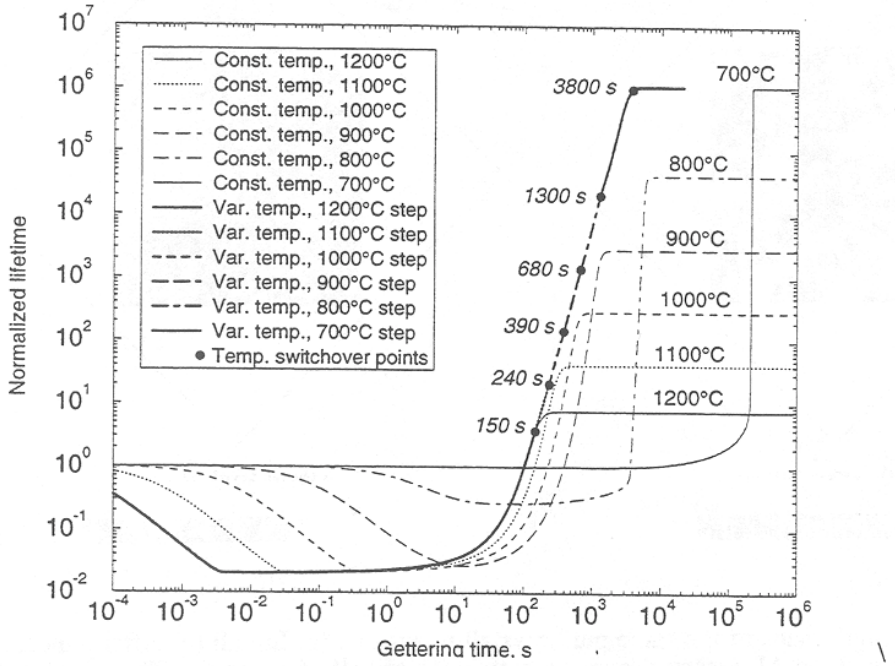

Fig.3 Normalized carrier lifetime as function of gettering time. The light lines correspond to constant temperature processes. The heavy line corresponds to variable temperature process with temperature switchover points shown. Normalization is done with respect to the lifetime at the beginning of the process.

Title: **University Research and Development in Crystalline Silicon**

Organization: School of Electrical and Computer Engineering
Georgia Institute of Technology, Atlanta, GA 30332-0250

Contributors: A. Rohatgi, Director; A. Ebong, Research Engineer; Vijay Yelundur and Ji-Weon Jeong, Graduate Research Assistants and S. Kamra, Research Scientist.

Objective

The objectives of this program are to investigate lifetime limiting defects and mechanisms in PV grade silicon materials, optimize and promote synergistic effects of promising gettering and passivation techniques; apply RTA to dissociate defect clusters; and design and fabricate high efficiency cells by integrating the most effective defect gettering and passivation techniques.

As grown lifetime of various silicon materials being investigated at UCEP

Figure 1 shows the as-grown lifetime of various silicon materials being investigated at UCEP. Lifetimes were measured by photo-conductance decay technique. Quasi steady state mode was used for the very low lifetime substrates while transient mode was used for the high lifetime materials. The bulk lifetime (τ) of these materials were measured in 0.001M solution of iodine to passivate the Si surface ($s < 25$ cm/s) so that the effective τ is essentially equal to the bulk τ. It should be recognized that the lifetime of the as-grown material can change dramatically during the course of cell processing. The degree of lifetime enhancement during the cell processing is found to be highly material specific. Thus the as grown τ is not always a good indicator of the final cell efficiency.

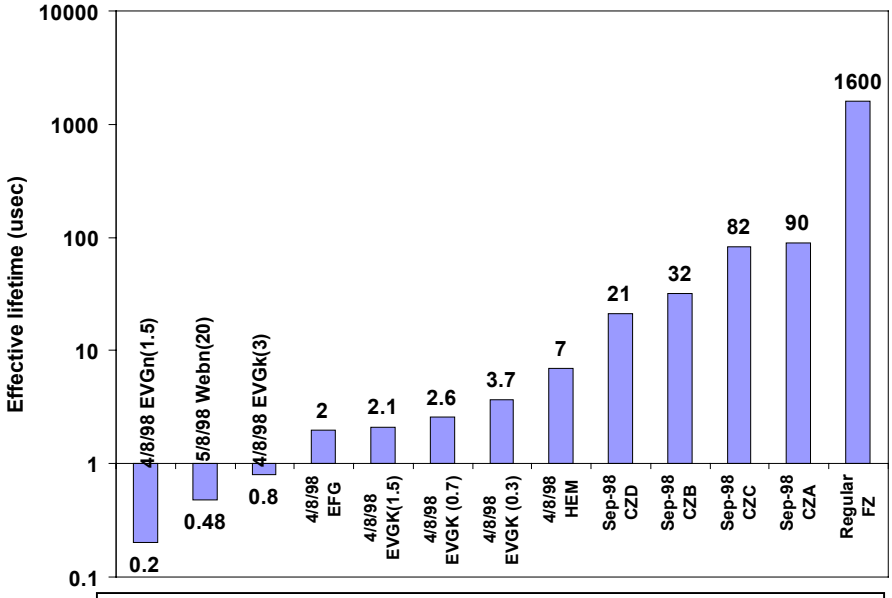

Figure 1: The as-grown lifetime of Si materials being investigated at UCEP.

Hydrogen passivation of multi-crystalline silicon without prior gettering

Solar cell can be fabricated by various technologies in a lab, including conventional furnace processing (CFP), rapid thermal processing (RTP) and belt line processing (BLP). Each technology involves phosphorus and Al diffusions to form the emitter and BSF, which are also known to getter metallic contaminants. In this section we report on the investigation of PECVD SiN induced hydrogenation prior to any gettering. BLP is the most manufacturable process,

which involves two high temperature treatments: 850°C for Al BSF formation and 730°C for front contact firing after the PECVD SiN AR coating deposition. The effect of these two high temperature steps on the SiN induced hydrogenation of multi-crystalline materials was investigated without the phosphorus diffusion. Several multi-crystalline materials were used in this experiment including HEM, Euro-Solar and Solarex - cast ingot, as well as EFG, Evergreen, and dendritic web ribbons. Figures 2a and 2b show the bulk lifetime of the cast multi-crystalline and ribbon silicon, respectively, before and after each high temperature treatment, including the effect of forming gas anneal at 400°C for 20 minutes. It was found that the bulk τ in some multi-crystalline materials, such as HEM, Euro-Solare, improved significantly due to hydrogenation from SiN and/or forming gas anneal even without any prior gettering. Whereas other materials like the string ribbon (Evergreen), Web, EFG and Solarex, did not show any improvement due to hydrogenation, prior to some kind of gettering. This could be due to the fact that lifetime limiting defects need to be gettered first in certain materials before hydrogenation induced lifetime enhancement can be observed.

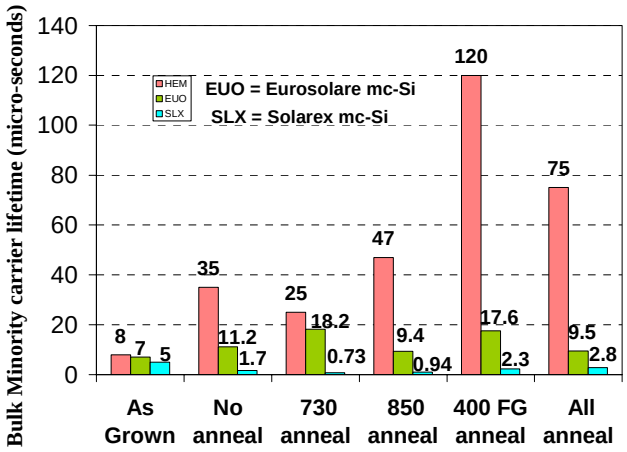

Figure 2a: Bulk lifetime enhancement of various cast mc-Si materials due to hydrogenation by annealing of RTO/SiN stack.

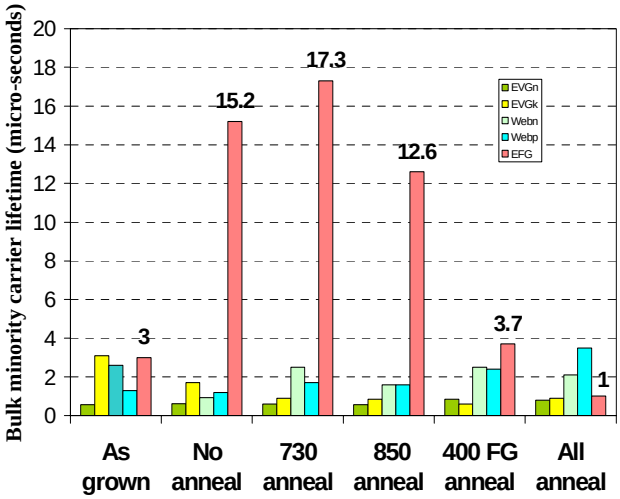

Figure 2b: Bulk lifetime enhancement in various ribbon Si materials due to hydrogenation by annealing RTO/SiN stack.

Synergistic effect of phosphorus and aluminum gettering, and PECVD SiN on Evergreen string ribbon silicon

After studying the effect of hydrogenation without any gettering, the synergistic effects of phosphorus and aluminum gettering with hydrogenation were investigated in belt line processing. Spin-on phosphorus, screen-printed aluminum and PECVD SiN films were used in this study. Figure 3 reveals the improvement in the bulk carrier lifetime of Evergreen string ribbon silicon after each processing step. A very significant improvement in the minority carrier lifetime was seen after phosphorus gettering and

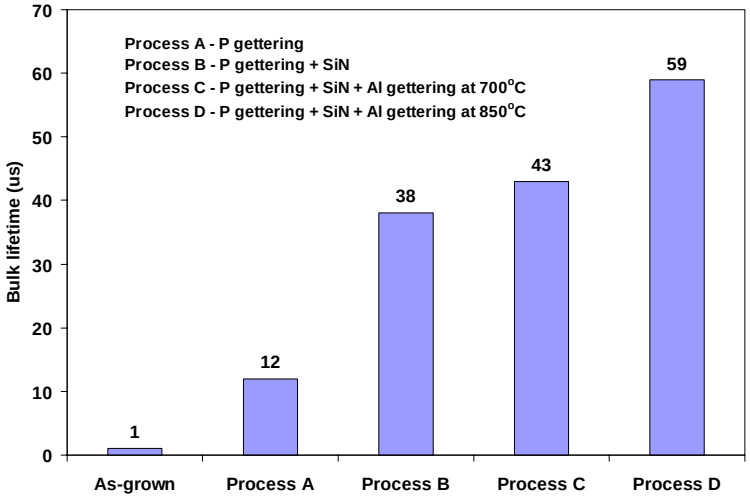

Figure 3: Bulk lifetime of Evergreen string ribbon silicon after gettering treatments

hydrogenation from the SiN film. The increase after phosphorus gettering and hydrogenation is very significant compared to the small change in lifetime observed after hydrogenation without the phosphorous gettering. These results indicate that effect of hydrogenation on τ in Evergreen string ribbon is much greater after the phosphorus gettering and it increases from about 1μs to 38 μs. Furthermore, addition of aluminum gettering increases the bulk lifetime to 59 μs. The beneficial effect of defect passivation by hydrogenation is not seen on the as-grown material (Figures 2b) because the lifetime is dominated by the impurities. Only after these impurities are gettered is the effect of defect passivation is observed on the minority carrier lifetime.

The effects of gettering and passivation were also studied on the EFG sheet silicon using the belt line processing. Figure 4a shows that the bulk lifetime in the as-grown wafers was found to be in the range of 0.6 and 8.2 μs. After the P-diffusion in the belt furnace, the bulk lifetime increased up to 30 μs (Figure 4a). Improvement in the bulk lifetime was found to be very different and dependent on the as-grown lifetime. The very low as-grown lifetime (<0.1 μs) did not show much improvement. However, moderate lifetimes (> 2 μs) showed significant improvement in the range of 100 to 340%.

Synergistic effect of screen-printed Al gettering and PECVD SiN hydrogenation on the bulk lifetime of EFG silicon was investigated. Al BSF was formed in the temperature range of 800 - 900°C after the phosphorous diffusion and PECVD SiN deposition. In the BSF firing temperature range of 810 and 890°C, no significant difference in the bulk lifetime was observed. After the SP Al BSF formation, the bulk lifetimes were in the range of 5 to 11 μs for the grown lifetimes in the range of 1 to 4 μs. Additional samples were prepared to decouple the effect of hydrogenation and Al gettering. These wafers were fired at 850°C in the belt furnace with and without the screen-printed Al on the back. Figure 4b shows the improvement in the bulk lifetime. Hydrogenation effect of PECVD SiN in the absence of Al was found to be quite small. More work is in progress to determine if the degree of hydrogenation is enhanced by the presence of Al or Al gettering by itself is responsible for higher lifetime in the sample with SP Al.

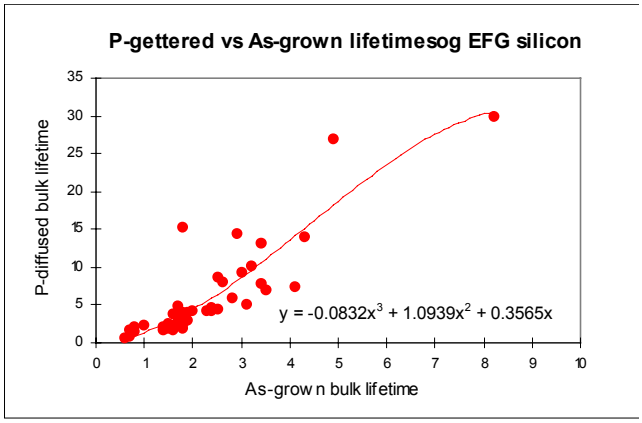

Figure 4a: P gettered versus as-grown lifetimes of EFG silicon.

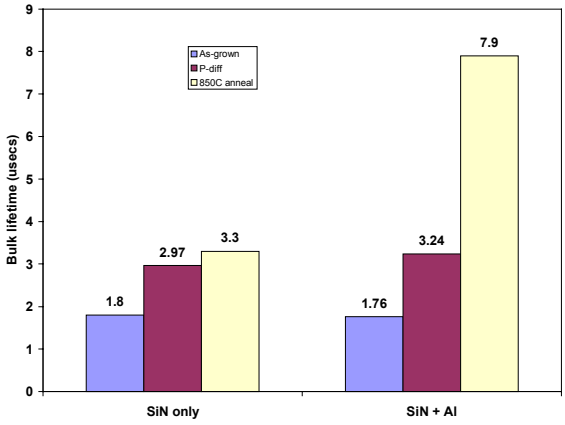

Figure 4b: Hydrogenation effect on bulk lifetime with and without Al.

FTIR measurement of Hydrogen content in SiN and oxide/SiN stacks before and after anneals

The FTIR measurements were performed to determine the total hydrogen content in the SiN and RTO/SiN stack. Figures 5a and 5b show the FTIR spectra of the RTO/SiN stack deposited on FZ Si and cast multi-crystalline silicon. The hydrogen content of the film is not influenced by the substrate type, however, the high temperature anneal has significant impact on the N-H and Si-H bond concentrations. It is interesting to note a similar trend in the FTIR spectra and the hydrogen content of the film on FZ and multi-crystalline silicon before and after the anneal, suggest that the substrate defect concentration does not influence the incorporation or the release of hydrogen from the SiN film.

Title: **Hydrogen-Defect Interactions Relevant to Si Solar-Cell Fabrication Studied by Vibrational Spectroscopy**

Organization: Department of Physics, Lehigh University, Bethlehem, Pennsylvania 18015

Contributors: Michael Stavola, Principal Investigator; Marcie Weinstein and J. Anna Zhou

Introduction

Even though hydrogen is commonly introduced into solar-grade Si to reduce the deleterious effects of deep-level defects, the mechanism for hydrogen introduction during low temperature processing steps and the hydrogen's subsequent interactions with defects and impurities are not well understood. In our work, vibrational spectroscopy is used to probe the introduction and subsequent defect reactions of hydrogen in crystalline Si. The properties of various hydrogen-containing defects are studied.

H_2 molecules

Isolated hydrogen in Si is mobile at low temperature (i.e., near 200K) so that at room temperature, H in semiconductors is bonded to other defects or present in the form of H_n aggregates. One of the simplest of these defects is the hydrogen molecule which has been proposed to play an important role during hydrogen indiffusion and in a variety of hydrogen reactions.[1-3] In spite of its proposed importance, the H_2 molecule was not observed directly until recently.

In two independent studies, a weak vibrational line associated with the H_2 molecule was discovered by infrared absorption spectroscopy and Raman spectroscopy.[4,5] Thus, it has become possible to probe the structure and properties of the H_2 molecule and to study its interactions with other defects and impurities.

In our experiments, we use uniaxial stress in conjunction with infrared absorption to obtain information about the symmetry of the H_2 defect so that its configuration in the lattice might be determined. Spectra measured for different orientations of the applied stress are shown in Fig. 1. The observed stress-splitting pattern is consistent with triclinic (C_1) symmetry for the H_2 molecule. A recent suggestion from theory is that the H_2 molecule is oriented along a [110] direction, giving a center with orthorhombic (C_{2v}) symmetry.[6] Our experimental results are inconsistent with this proposal.

Our understanding of the structure and properties of H_2 and its interactions with other defects is at an early stage. Nonetheless, the recent identification of the vibrational spectrum of H_2 promises rapid progress.

Hydrogenation of transition-metal impurities

An important role played by hydrogen in solar-grade Si is the reduction of the deleterious effects caused by deep-level defects. For example, the transition metals are common contaminants in Si that reduce minority carrier lifetime.[7] In pioneering studies of the hydrogen passivation of deep-level defects, it was discovered that exposure of Si samples to a hydrogen-containing plasma can eliminate many of the levels associated with the transition metals.[8] Until recently little was known about the microscopic properties of the hydrogenated defects or the mechanism of passivation. Several recent studies provide new insight, but also show that the hydrogenation of the transition metals is more complicated than the early studies suggested.[9-14]

In our group at Lehigh University, hydrogen is introduced at high temperature (1250°C) into Si doped with a transition metal impurity. In this way, hydrogen can be introduced throughout bulk samples that can be studied with structure-sensitive methods like EPR and vibrational spectroscopy.[9-11] A few hydrogenated transition metals (PtH, PtH_2, AuH, and AuH_2) have been identified and their structures determined.

Independently, a few groups have introduced hydrogen by wet chemical etching (at room temperature) into thin surface layers of Si doped with metal impurities.[12-14] Deep level transient spectroscopy (DLTS) was used to study the hydrogenated transition metals. Surprisingly, these DLTS results show that many of the hydrogenated transition metals remain electrically active. (The EPR and IR results mentioned above also showed that the hydrogenated metals remained active.)

In the absence of additional information, it is not clear that the different techniques even observe the same defects. In the following recent experiments, performed in collaboration with a group at the Max Planck Institute in Stuttgart, we are working toward bringing together the structure sensitive studies performed by our group and the DLTS studies of electrical properties.

1. To determine the electrical level positions of the hydrogenated metals observed by vibrational spectroscopy, we have prepared samples with their Fermi levels located in several well-defined positions, either by counter doping or electron irradiation. The charge state of the transition-metal-hydrogen complex being studied is then determined to provide information about its level position relative to the known Fermi level position of the Si sample. This experiment is repeated for several different Fermi level positions for each transition-metal-H defect. Such experiments have been carried out for Pt-H_n and Au-H_n centers. The levels of these defects have been determined approximately in these experiments so that they can then be associated with levels determined more accurately in previous DLTS experiments.

2. We are using a multiple-internal-reflection method in which the probing light is reflected from the internal surfaces of a sample tens of times to enhance the sensitivity of vibrational spectroscopy for the study of surface layers. In these experiments, we are attempting to observe by vibrational spectroscopy the same transition-metal-hydrogen complexes introduced into micron-thick layers by wet chemical etching that were studied previously by DLTS.

References

[1] J.W. Corbett, S.N. Sahu, T.S. Shi, and L.C. Snyder, Phys. Lett. **93A**, 303 (1983).
[2] A. Mainwood and A.M. Stoneham, Physica B **116**, 101 (1983).
[3] S.J. Pearton, J.W. Corbett, and M. Stavola, *Hydrogen in Crystalline Semiconductors* (Springer-Verlag, Berlin, 1992).
[4] A.W.R. Leitch, V. Alex and J. Weber, Phys. Rev. Lett. **81**, 421 (1998).
[5] R.E. Pritchard, M.J. Ashwin, J.H. Tucker, and R.C. Newman, Phys. Rev. B **57**, 15048 (1998); R.E. Pritchard, M.J. Ashwin, R.C. Newman, and J.H. Tucker, Mat. Sci. Eng. B, to be published.
[6] B Hourahine, R. Jones, S. Öberg, R.C. Newman, P.R. Briddon and E. Roduner, Phys. Rev. B **57**, 12666 (1998).
[7] For a review see chapt. 3 in S.J. Pearton, J.W. Corbett, and M. Stavola, *Hydrogen in Crystalline Semiconductors* (Springer-Verlag, Berlin, 1992).
[8] W. Schröter, M. Seibt, and D. Gilles, *Materials Science and Technology, Vol. 4*, edited by W. Schröter (VCH, Weinheim, 1991), p. 539.
[9] P.M. Williams, G.D. Watkins, S. Uftring, and M. Stavola, Phys. Rev. Lett. **70**, 3816 (1993).
[10] S.J. Uftring, M. Stavola, P.M. Williams, and G.D. Watkins, Phys. Rev. B **51**, 9612 (1995).
[11] M.J. Evans and M. Stavola, Mat. Sci. Eng. B, to be published.
[12] E.Ö. Sveinbjörnsson and O. Engström, Phys. Rev. B **52**, 4884 (1995).
[13] J.-U. Sachse, E.Ö. Sveinbjörnsson, W. Jost, J. Weber, and H. Lemke, Phys. Rev. B **55**, 16176 (1997).
[14] J.-U. Sachse, E.Ö. Sveinbjörnsson, N. Yarykin, and J. Weber, Mat. Sci. Eng. B, to be published.

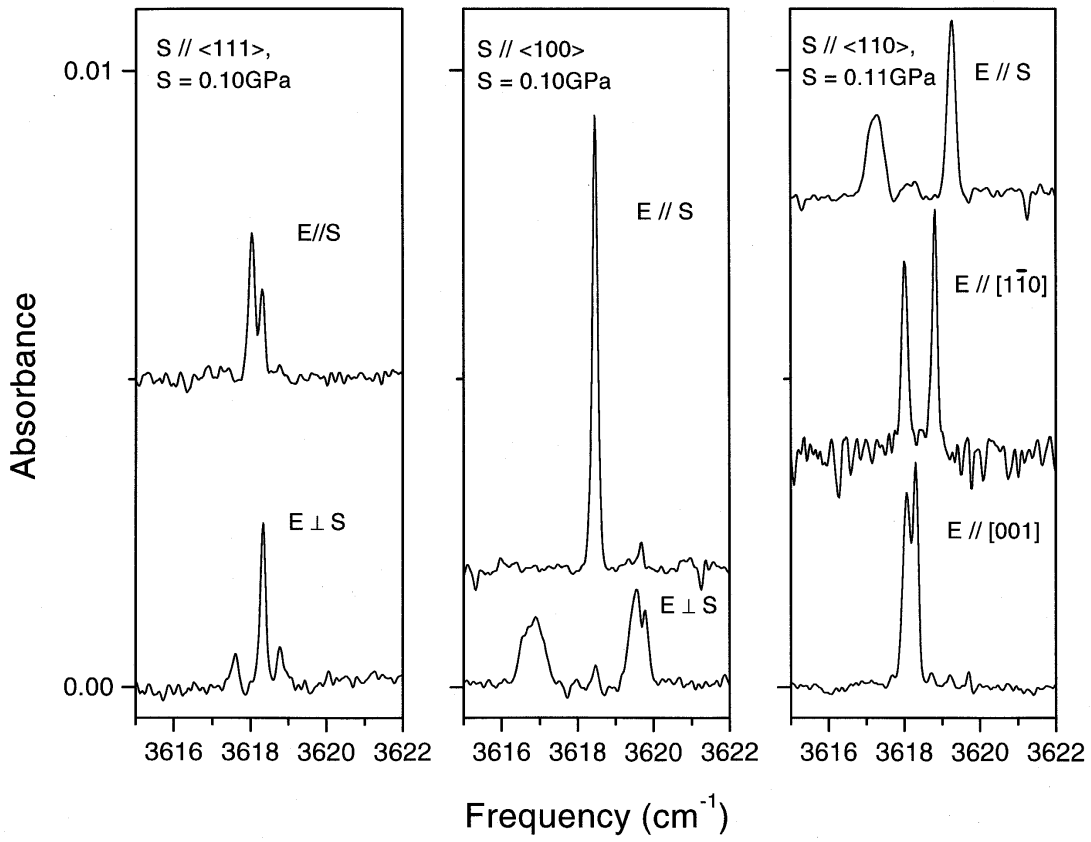

Fig. 1. The dependence of the H_2 vibrational spectrum (with a zero-stress absorption line at 3618 cm^{-1}) on uniaxial stresses applied along the different high symmetry crystal directions. Measurements were made for light polarizations both parallel and perpendicular to the applied stress direction.

Title: **Gettering Simulator and Aluminum Back Contact Optimization in a Manufacturing Environment**

Organization: Department of Materials Science & Engineering
Massachusetts Institute of Technology, Cambridge, MA 02139

Contributors: L. C. Kimerling, Principle Investigator; A. L. Smith in collaboration with
J. Coleman, G. Xaviar, and R. Balanga of Siemens Solar Industries

Introduction

Our research effort continues to focus on the structure, stability, and kinetics of lifetime degrading defects in Si for the optimization of solar cells [1,2]. We are continuing to develop an understanding of gettering processes to create a process simulator that is both quantitative and predictive. The goal is optimization of materials and processes for the solar cell production environment. The gettering simulator will yield a direct relationship between materials specifications and process design to achieve a desired minority carrier diffusion length. We have calculated the thermodynamic segregation coefficient of iron between a silicon wafer and a molten aluminum layer and have implemented simulations for back contact process design. In collaboration with the Siemens Solar Industries Camarillo facility, we have applied classic *design and analysis of experiments* to maximize the knowledge gained from a study of aluminum back contact formation. Cells with Al back surface contacts were fabricated and tested along side control cells to reveal a statistically significant improvement in performance.

Gettering Simulator

Last year we constructed a gettering simulator that quantifies the design and effectiveness of gettering treatments [3,4] based on the framework developed by Tan *et al* [5]. The simulator includes the competing gettering mechanisms of internal gettering (IG), segregation to molten Al and Al-dopant enhanced solubility. The initial contamination level, processing time-temperature, the materials specifications, and the device structure are simulator inputs. The resulting contamination profile of the wafer is the output that determines the minority carrier diffusion length. During this past year, we have used the simulator to examine the effects and interactions of the various gettering mechanisms of both local and extended length scales. In addition, we calculate the Fe segregation coefficient between a molten aluminum layer and a silicon substrate to be ~10^9 at 800C. This large value provides a substantial driving force for Fe removal from bulk silicon.

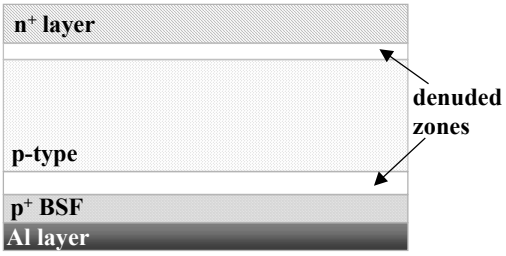

Figure 1. Wafer design includes several materials and device parameters. Included among these are the various doping levels in the emitter, wafer and p+ region, IG site size and density, and the widths of the denuded zones, emitter, p^+ layer and the molten aluminum during back contact formation.

Simulation Results

Design for gettering requires consideration of materials parameters, process conditions and the dynamic interaction of these. A simulator is useful for quantifying a particular process sequence with a particular set of material constraints. In addition, the simulator is useful in generating understanding of the tradeoffs and interactions of the various gettering mechnanisms. A solar cell wafer structure (Figure 1), such as that used at Siemens Solar Industries, might consist of a single crystal p-type wafer with an n^+ layer at the front surface. Oxygen precipitates are likely to be present with denuded zones at either face of the wafer caused by oxygen outdiffusion during high temperature steps such as in emitter diffusion. A p^+ back surface field region may be created by diffusion or liquid phase recrystalization. An Al molten layer will exist when aluminum back surface contacts are generated. Materials design for the solar cell structure includes substrate doping level, oxygen

content and distribution, denuded zone width, n^+ layer doping level and thickness, p^+ layer doping and thickness, and Al layer thickness. All of these materials properties are both determined by and dynamically vary with high temperature processing, to determine the gettering efficiency of a particular process stream.

The simulator serves to demonstrate important physical insights. In Figure 2 we show results for redistribution of Fe at a small length scale during a constant cooling rate step. The two curves contrast the impact of

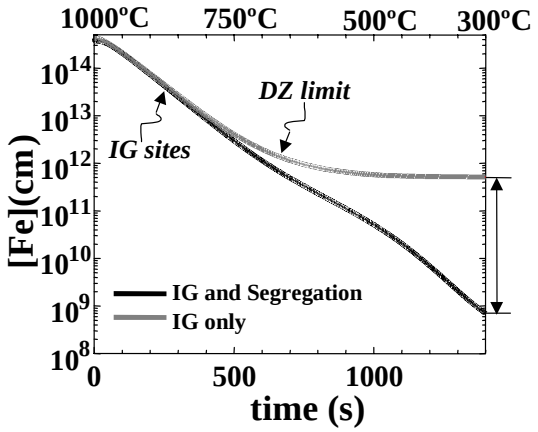

Figure 2. Cool for short range Fe redistribution for the case of gettering due to internal gettering only and that of internal gettering with segregation.

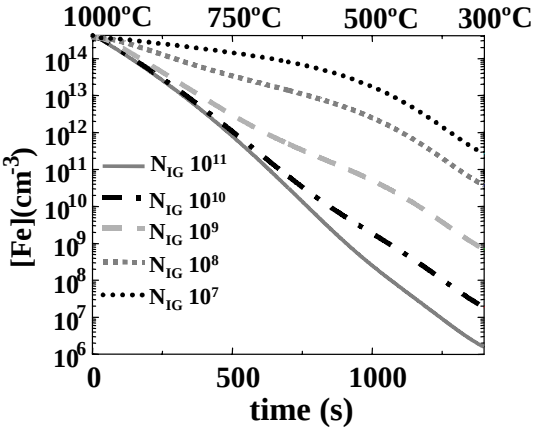

Figure 3. Cools comparing the impact of IG site density holding IG volume fixed.

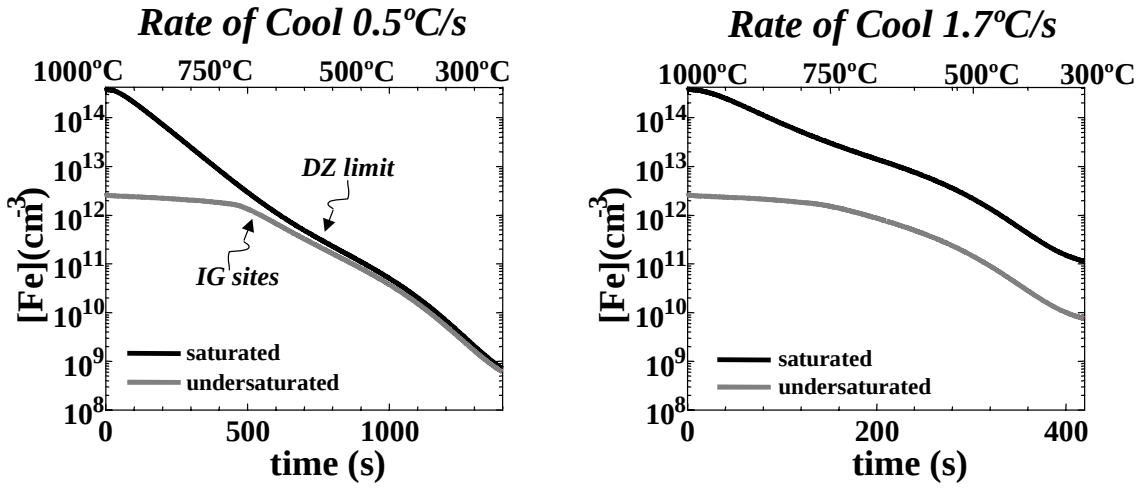

Figure 4. Cool for short range Fe redistribution comparing low and high initial levels of Fe contamination. Slower cooling, 0.5 C/s, shows no difference in final contamination level, where the faster cool shows more than an order of magnitude difference in residual Fe contamination.

gettering driven only by supersaturation against a case with both the supersaturation mechanism and a segregation redistribution mechanism. For the first case, Fe diffusion across the denuded zone limits the ability of the system to equilibrate; no precipitation at IG sites occurs below 700C, and the Fe concentration remains constant. For the case where a segregation mechanism is also active, one must consider the strong temperature dependence of the segregation coefficient. Whether it is segregation due to solubility enhancement or due to the molten aluminum phase, the segregation coefficient increases by several orders of magnitude throughout the cooling process. The increase in the gradient term in the diffusion

equation due to a stronger and stronger segregation effect more than compensates for the reduction in Fe diffusivity as during cooling.

Figure 3 shows how a greater number of smaller precipitates allows for faster equilibration than fewer large precipitates. An ideal process is robust to spurious introduction of contaminants. Figure 4 compares gettering capability for cooling over short length scales for varying initial contamination levels.
It remains to be experimentally determined whether internally gettered contaminants have less impact on minority carrier diffusion length than contaminants in solid solution in the bulk.

For the solar cell structure, where the entire bulk serves as the active device region, an understanding of the kinetics over large length scales is required to ensure optimal gettering. Figure 5 shows simulation results of constant temperature anneals for the case of an Al layer on one side of a silicon wafer. Internal gettering sites are included in typical density and number for Cz silicon. The appropriate thermodynamic values for the segregation coefficient for Fe between the Si and the molten Al layer are used. Each process was simulated with an initial contamination level of the Fe solubility in Si at 1000C. The wafers were then treated with an anneal of 700C, 800C or 900C for 10^4 seconds. There are three regimes of contamination removal. First, there is a drop due to supersaturation with a rate dependent on the Fe diffusivity at the respective temperatures and IG site density. This stage is followed by a plateau representing outdiffusion of Fe to the molten Al layer driving dissolution of Fe precipitates formed in the initial stage. Once the precipitates are dissolved, the Fe concentration decreases by segregation to the Al layer according to typical outdiffusion kinetics. For the case of 800C and 700C, the Fe diffusivity is small and this third regime is not reached within the time of the simulation. Just as Tan's results suggested, if "gettering" means internally gettered, then this can be accomplished quite quickly; if "gettering" means completely removing Fe contaminants form the wafer, a high temperatures or long times will be required [5,6]. Our key finding is that *high temperatures, where the segregation coefficient of Fe with respect to the molten Al-Si interface is still extremely large, can be used for reasonable lengths of time to achieve the outdiffusion gettering of regime 3.*

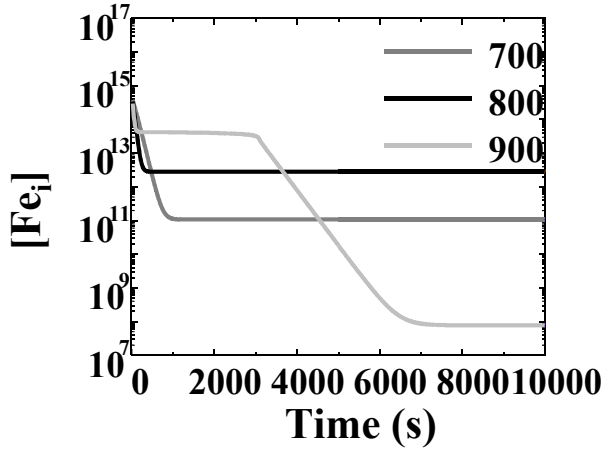

Figure 5. Time evolution of Fe contamination level initially at the solubility limit for Fe in Si at 1000C through various constant temperature anneals demonstrating that high temperature is required to substantially reduce the [Fe_i].

Al Back Surface Contact Study
At Siemens Solar Industries, a study of Al back surface contact formation was undertaken. Methods such as balanced experimental design, error control, and analysis of variance were used demonstrating a statistically significant improvement in short circuit current and open circuit voltage over control cells. The Al back contacted cells were subjected to environmental tests and passed. Preliminary results indicate that transition metal gettering is taking place and work is ongoing to quantify and maximize this effect. By using appropriate

statistical methods, this work shows that we can study the effect of Al contact formation in the most relevant context: the manufacturing facility.

Conclusion

This program addresses the factors limiting cell performance with low cost manufacturing. The understanding and development of robust process technologies are critical to the development of the global PV industry. This gettering simulator shows how fundamental knowledge generated by research has been incorporated into a predictive design tool. A partnership with a manufacturing facility has enabled the transfer of our fundamental understanding of gettering and Al contact morphology into product efficiency improvement.

References

1 L.L. Chalfoun, A.L. Smith, S. Zhao, and L.C. Kimerling, "Process Optimization of Alloyed Aluminum Backside Contacts for Silicon Solar Cells," poster at the 6th National Renewable Energy Laboratory (NREL) Workshop of the Role of Impurities and Defects in Semiconductors, August 12-14, 1996, Snowmass Village, Colorado

2 L.C. Kimerling, "The Role of Dislocations and Associated Defects in Determining Minority Carrier Lifetime", 7th National Renewable Energy Laboratory (NREL) Workshop of the Role of Impurities and Defects in Semiconductors, August 1996, Vail, Colorado

3 A.L. Smith, S.H. Ahn, and L.C. Kimerling, "A Gettering Simulator: Polished Wafers and p/p+ Epilayers," ECS Proceedings Volume 98-1, Eds. H.R. Huff, H. Tsuya, and U. Gösele, (Electrochemical Society, Inc., Pennington, NJ 1998) pp. 1138-1149.

4 A.L. Smith, S. Zhao, S. H. Ahn, G. Norga, L.L. Chalfoun, and L.C. Kimerling, "The Reaction Kinetics of Fe at Si Surfaces and Interfaces in Si Solar Cells," poster at the 7th National Renewable Energy Laboratory (NREL) Workshop of the Role of Impurities and Defects in Semiconductors, August 1996, Vail, Colorado

5 T.Y. Tan, R. Gafiteanu, and U. Gösele, Proc. 6th NREL Workshop on the Role of Impurities and Defects in Si Dev. Proc., 110 (1996).

6 T.Y. Tan, R. Gafiteanu, S.M. Joshi, and U. Gösele, "Science and Modeling of Impurity Gettering in Silicon," ECS Proceedings Volume 98-1, Eds. H.R. Huff, H. Tsuya, and U. Gösele, (Electrochemical Society, Inc., Pennington, NJ 1998) pp. 1050-1060.

Title: Characterization and Ti Gettering of PV Substrates

Organization: Department of Materials Science and Engineering, North Carolina State University, Raleigh, NC 27695-7916

Contributors: B. Sopori Program Manager; G. Rozgonyi, Principal Investigator;
A. Romanowski, A. Karoui, E. Covalla

Introduction

Four tasks are discussed in this work: (i) measurement of thermal-donors in n-type silicon using a contactless frequency resolved photoconductance (FR-PC) technique, (ii) transient metal identification using FR-PC, (iii) external gettering using Ti thin films, and (iv) variable wavelength microwave photoconductance (μ-PCD) system.

I. Emission and Capture Trapping Lifetimes of n-Type Silicon Wafers Evaluated Using Frequency Resolved Microwave Photoconductance

The FR-PC method is used for investigation of oxygen-related defects in non-thermal donor annealed wafers. A set of n-type silicon wafers doped with phosphorous at concentration of 10^{15} cm^{-3} were cut from the same CZ ingot and measured using the FR-PC. One group of these wafers was annealed in order to annihilate the thermal donors (TD) present in the material, while the second group was not annealed. The carrier kinetics is described using a two level recombination/trapping model [1] and characterized by surface recombination velocity v_s, and the bulk, emission, and capture lifetimes, denoted as τ, τ_e and τ_c, respectively. These four parameters have been evaluated by fitting the measured phase shift function to the calculated phase function. Since trapping does not play a role in annealed wafers, the four-dimensional fitting vector is reduced to two-dimensions, and two parameters v_s, τ describe the recombination phenomena of TD annealed wafers. A linear dependence between $\ln\{(\tau_e T^2)^{-1}\}$ and 1/T has been found, as shown in Fig. 1, indicating that $p_0 << p_1$. Therefore, both activation energy and hole capture cross section can be determined from τ_e, while trap populations $N_T(1-f_T)$ are found from τ_c. Several conclusions can be drown from the analysis of the Arhenius plots and trap population evaluated for different ingot positions: (i) a low capture cross section of 10^{-20} cm^2, indicating positive trap charge (it is assumed that holes are responsible for trapping and recombination processes), (ii) variation of trap activation energies from 0.26 eV to 0.4 eV, (iii) a high trapping population (concentrations) of 10^{16} cm^{-3} which decreases from the ingot shoulder to its tail, indicating

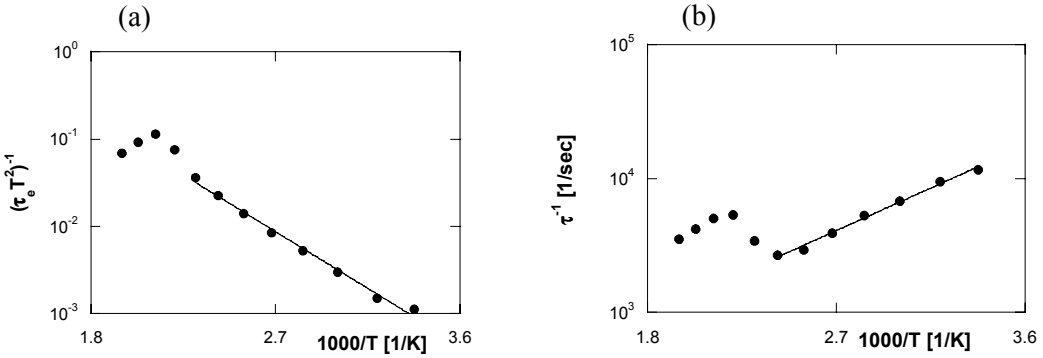

FIG. 1. Recombination parameters of n-type Si wafer placed near the ingot tail;
(a) emission lifetime, and (b) bulk lifetime.

oxygen clusters are most likely responsible for the trapping phenomena, (iv) domination of the carrier recombination near the ingot shoulder at low and high temperatures, (v) operative trapping processes at moderate temperature, (vi) an increase in trap populations with temperatures.

II. Metal impurity identification in silicon materials using contactless FR-PC methods

Previously, we have shown [2] that the recombination parameters, such as activation energy, impurity concentration, and minority carrier capture cross section can be evaluated from FR-PC spectra measured at different temperatures. However, it is known that the temperature variation changes the character of the recombination centers, e.g. dissociation can make impurity evaluation of pairs questionable for high temperature. Therefore, in this work a constant sample temperature is maintained, while the DC excitation level is varied, and the ac probing signal is kept constant. The DC variation of the injection level results in a shift of the quasi-Fermi levels, thereby changing the carrier recombination kinetics. The recombination parameters (activation energy, capture cross section, and concentration) are then determined from Nyquist plots of the microwave reflection coefficient. Carrier kinetics are described by a single level SRH model [2]. The fundamental ac microwave reflection coefficients have been obtained with the following assumptions: (i) low injection level, (ii) no recombination center saturation, (iii) homogenous quasi Fermi level distribution in the bulk, (iv) recombination parameters such as activation energy E_R, concentration N_R, and electron capture cross section σ_n do not depend on DC excitation level, and (v) only one recombination level is operative. The material parameters E_A, N_R, and σ_n are evaluated using a nonlinear simplex method by minimizing the error function χ. The main difficulty in minimizing χ is that it possesses several local minima. In order to overcome this, the initial error function is expanded by varying the injection level. Randomly localized individual minima can compensate, thereby enhancing "true" minima.

A set of n-, and p-type CZ, and p-type FZ wafers were contaminated with Ni, Fe, and Cu in an aqueous solution by a spin-on procedure, using $FeCl_3$, $Ni(NO_3)$, or $[Cu(NO_3)_2$ + 2% $HNO_3]$ solutions in DI water. Prior to the spin-on coating, the wafers were RCA cleaned, and then RTA annealed at 1000^{o}C for 5 min. The Nyquist plots for p-type CZ and FZ wafers contaminated with Cu reveal the occurrence of traps. No traps are revealed for either p-type FZ or CZ Ni contaminated wafers. Deep levels introduced by the diffusion of nickel were studied using many methods, including DLTS, admittance spectroscopy, PCD and Hall measurements. Four levels which are located symmetrically to the midgap have been reported [3, 4]: E_C -(0.15, to 0.21) eV, E_C - (0.36 to 0.47) eV and E_V + (0.31 to 0.35) eV, E_V + (0.15 to 0.21) eV. Using FR-PC the activation energies for Ni contaminated wafers are: E_V + 0.11 eV, E_C - 0.23 eV for FZ, and, E_V + 0.11 eV E_C - 0.17eV for CZ, which match the literature data well. The capture cross sections are moderate, i.e. 10^{-15} cm^2; therefore, we expect that these levels are acceptor-like, in agreement with the DLTS data [3]. For the Cu contaminated wafers two levels are also found for both CZ and FZ wafers at: E_V + 0.1eV, E_C - 0.1 eV and E_V + 0.17 eV, E_C - 0.22 eV. The Cu creates four donor levels in silicon [4]: E_V + (0.09 to 0.1) eV, E_V + (0.2 to 0.23) eV, E_V + (0.41 to 0.46) eV and E_C - (0.15 to 0.2) eV, and the evaluated levels reasonably match levels localized near both bands. The capture cross section of 10^{-14} cm^2 indicates their donor behavior. It is reported in the literature [4], that interstitial Cu forms the donor level at E_C - 0.16 eV, but with a small capture cross section of 10^{-17} cm^2. Therefore, these levels have to be excluded as effective recombination levels. Thus, the levels E_V + 0.1eV (CZ), E_V + 0.17 eV (FZ) are believed to be operative for Cu contaminated wafers. These levels are Cu-pair related defects [5,6]. Two levels are present for the FZ wafer containing Fe impurities. The first one, assigned to FeB pairs, has a capture cross section of 3 E-15 cm^2, in agreement with data obtained by SPV and μ-PCD [5], i.e. 3.5 E -15 cm^2. A second level has a large capture cross section of 10^{-14} cm^2 revealing its donor nature. Because this level is localized near the conductance band, should be acceptor-like [3, 4], contrary to our results, indicating that this level is not operative.

III. Ti Thin Film External Gettering

To obtain a better understanding of the thin film Al and Ti gettering process, a set of silicon samples were intentionally contaminated with Ni and Fe impurities (spin-on aqueous solution containing metallic impurities ($FeCl_3$ or $Ni(NO_3)_2$) [7, 8]. Three types of silicon wafers have been used in our investigation: #1: CZ, n-type, <100>, 10-20 Ωcm; #2: CZ, p-type, <100>, 14-25 Ωcm; #3: FZ, p-type, <100>, 13-22 Ωcm. After the contamination of the wafers from the back side by spin-on coating, the wafers were annealed at 1000 ^{0}C in RTA for 10 min. Three types of Ti thin films deposited by the magnetron sputtering system have been made: **G1** - Ti film of 600 A with Ar plasma; **G2** - Ti film of 600 A with Ar + N_2 plasma; **G3** - Al and Ti stack of 100A and 600A with Ar plasma; **G4** - Ti - Al alloy film of 600A with Ar plasma; **G5** - Al thin film of 600A with Ar plasma. N_2 gas was added for near surface nitridation in order to change the surface condition during the

deposition processes. Half of the wafers were covered by thin Al films of 600A thickness on the back, in order to investigate the double and single side external gettering methods. Two temperatures were used for wafer annealing in N_2 atmosphere: a low temperature of 500 ^{0}C for 300 min and a moderately high temperature of 700 ^{0}C for 150 min. After annealing, the residual metal layers and Ti-Si silicide were removed by dipping the samples into the CP-4 solution. Before gettering annealing, the lifetime was measured using μ-PCD.

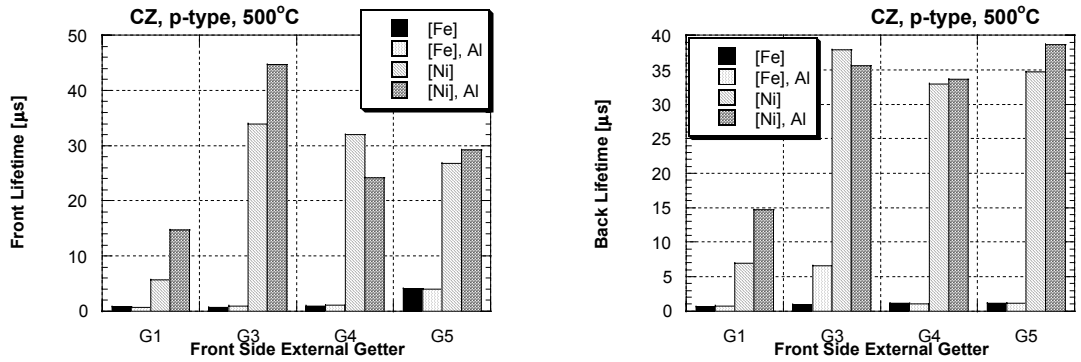

FIG. 2. Front (a) and back (b) side measured lifetimes of, p-type CZ wafers contaminated with Fe or Ni and front getters G1, G3, G4 and G5, (a) 500^{0}C, 300 min, (b) 700^{0}C, 150 min.

The following notation is used in the Figs. 2 and 3: [Fe]/[Ni] means single (front) side gettering of the iron/nickel contaminated wafers, while [Fe]/[Ni], Al means double side gettering of the iron/nickel contaminated wafers with the front side getters: G1, G2, …, or G5 and rear Al getter. Figure 2 shows

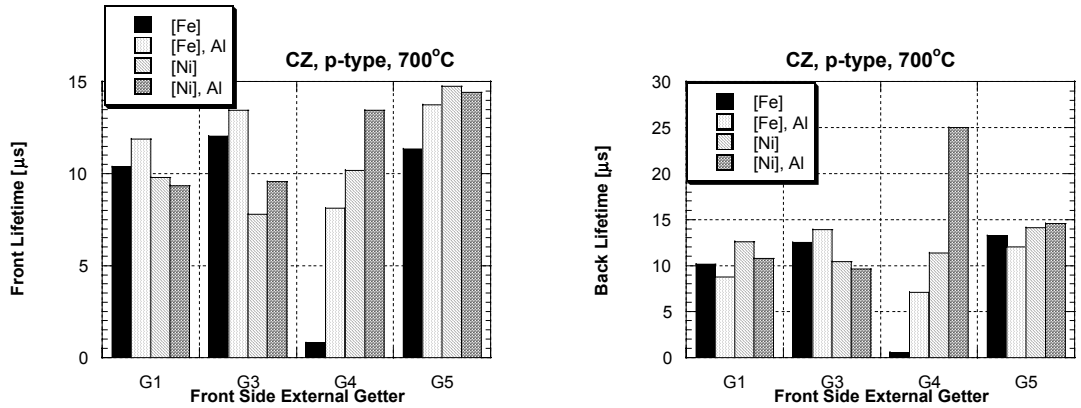

FIG. 3. Front (a) and back (b) side measured lifetimes of p-type CZ wafers contaminated with Fe or Ni and front getters G1, G3, G4 and G5, (a) 500^{0}C, 300 min, (b) 700^{0}C, 150 min.

the lifetime data of the p-type CZ wafers. The lifetime enhancement occurs only for the Ni contaminated wafers, and the best results (lifetime shrinks from 6 μm to ~35 μm) are obtained for G3 getter (Al-Ti stack), which are comparable with G4 (Ti-Al alloy) and G5 (Al film) getters. Generally dabble getter does not change the lifetime. The data set in Fig. 3 represent the lifetime measurements for the p-type CZ wafers gettered at 700 ^{0}C for 150 min. The lifetime improvement is seen for G1 (Ti film) and G3 (Al-Ti stack) getters and for both Ni (from 6 μm to ~15 μm) and Fe (from 1 μm to ~13 μm) contaminants. The lifetime results are comparable with the G5 getter (Al film). We can not explain the low lifetime of the Fe contaminated wafer with the single side G4 getter. Microscopic analysis reveals large microcrystalline structures on the film surfaces. It is worthy to note that adding N_2 gas into the plasma results in a color change of the Ti film that can have an impact on the reflection coefficient of the film layer.

IV. Variable Wavelength Pulsed Laser Excitation Source for μ-PCD and enhanced optical focusing system

We designed a laser-focusing system assuming a symmetrical waveform with TEM_{00} mode of the beam [9]. In order to reduce the beam divergence, a galilean beam expander has been used with synthetic fused silica (SFS) lenses (UV wavelength): the symmetric-concave SFS with a short focal lens and Plano-Convex SFS with a long focal length. The third lens, the objective one, is also Plano-Convex SFS with a long focal length. Theoretically, an output beam size of about 20 μm is expected for a 1 mm input beam size. A projected focusing optical system has been designed using the Integrated Optical Component Mounting System from Edmund Scientific. The input beam size can be set using an iris diaphragm. A new pulsed laser source LN300C has been added to our existing μ-PCD machine LIFETECH 88. The laser is triggered from a pulse generator, which is controlled by a PC. A Dye laser is used as the generation source with tuned wavelengths from 337 nm to 960 nm. The focusing system described above reduces the beam diameter from 1.5 mm to ~100 μm. Currently we are using the original data acquisition system of LIFETECH 88, which allows either 1/e or $1/e^2$ lifetimes to be mapped, or storage of the transient signal measured at five different points. In order to analyze multilayer structures or thin layer solar cells, the data acquisition system will be modified. An inconvenience with the new excitation source is its low repetition rate of 30 Hz. Such a low repetition time increases the time needed for mapping large areas; therefore, the new laser source can only be used for mapping small areas with high resolution, or for lifetime measurements at 5 or 9 points.

REFERENCES

1. Romanowski A., Buczkowski A., Karoui A., and Rozgonyi G., J. Appl. Phys. **83**, 7730(1998).
2. Romanowski A., Buczkowski A., Karoui A., and Rozgonyi G., Recombination Lifetime Measurement in Silicon, edited by D. Gupta, F. Bacher, and M. Hughes, ASTM 1998, STP 1340, pp. 68.
3. Graff K., *Metal Impurities in Silicon-Device Fabrication*, Springer-Verlag, Berlin, 1995.
4. Istratov A.A., Weber E.R, Appl.Phys. **A66**, 123(1998).
5. Istratov A.A., Flink C., Hieslmair H., Heiser T., and Weber E.R., Appl. Phys. Lett. **71**, 2121 (1997).
6. Rotondaro A.L., Hurd T.Q., Kaniava A., Vanhellemont J., Simoen E., Heyns M.M., and Claeys C., J. Electrochem. Soc. **143**, 3014 (1996).
7. Hourai M., Naridomi T., Oka Y., Murakami K., Sumita S., Fujino N., and Shiraiwa, Jap. J. Appl. Phys. **27**, L2361 (1988).
8. NREL Annual Report, May 1996, NREL XD-2-1104-6.
9. MELLES GRIOT, 1995/96 Catalog.

Title: **Theoretical analysis of hydrogen passivation of impurities and defects**

Organization: Physics Department, Texas Tech University
Lubbock, TX 79409-1051

Contributors: Stefan K. Estreicher, principal investigator
Jeffrey L. Hastings, MS student
Maen Gharaibeh, PhD student

Objectives

Rapidly-diffusing impurities in Si and poly-Si interact with the host crystal and can profoundly change the lifetimes of charge carriers. Poly-Si solar cells often benefit substantially from hydrogenation, as H often passivates[1,2] dangling bonds at vacancies, dislocations, grain boundaries, and other defects. On the other hand, common transition metal contaminants such as Cu. As an isolated interstitial, Cu is electrically inactive, but Cu precipitates reduce carrier lifetimes.[3,4] A microscopic understanding of the processes taking place is lacking and fundamental questions remain regarding the interactions between crystalline defects and rapidly-diffusing impurities.

The objective of this research is to investigate these issues theoretically at or near the ab-initio level, and provide new insights into (a) the properties of aggregates of intrinsic defects, (b) the interactions between such aggregates and H, (c) the configurations, binding energies, and electronic structures of Cu and its precipitates.

Theoretical approach

Static properties such as the equilibrium geometries, electronic configurations, diffusion paths, and potential energy surfaces are calculated at various levels of ab-initio Hartree-Fock (HF) theory in molecular clusters. These calculations provide total energy differences, electronic structures, and a wealth of chemical information.

The dynamics of complex formation and dissociation, vibrational frequencies, and diffusion properties are obtained with the ab-initio tight-binding molecular dynamics (MD) method developed by Sankey *et al*.[5,6] In the MD approach, the host crystal is represented by periodic supercells of 64 and 216 atoms.

For details about the theoretical techniques and the cluster and supercells approximations, see Refs. [1] and [7].

Hydrogen interactions with intrinsic defects

MD simulations have shown that the interstitial H_2 molecule, oftencalled "invisible hydrogen" is unstable in the vicinity of stretched, distorted, or imperfectly reconstructed Si–Si bonds. In particular, H_2 readily dissociates[8] in the vicinity of vacancies (V's) or self-interstitials (I's). Such defects are injected into the bulk by processes such as electron irradiation, ion implantation, etching, the deposition of n^+ layers or Al back-contacts, etc. Therefore, if a sample containing H_2 is processed, H will appear where none was seen before. This H can then participate in passivation reactions for example.

Recent calculations further connect this result to experiment. We have now observed[9] the reactions $H_{2+}+I \rightarrow \{I,H,H\}$ and $\{I,H,H\} + V \rightarrow H_2^*$, which convert H_2 into H_2^*. This conversion has been reported[10] in electron-irradiated material but was not understood. A movie of the last step in this reaction can be seen on the web.[11]

Studies dealing with the interactions between interstitial H and various V aggregates is continuing. The lowest-energy configuration for H in each of the aggregates containing 2 to 6 vacancies has been found and the

metastable states identified. The final energetics and the changes in positions of localized gap states are being investigated.

We have also initiated studies involving I's at the ab-initio MD level. They are generated by a number of processes such as implantation but also the precipitation of oxygen or the deposition of P-rich layers. It is remarkable how little is known about the interaction involving I's. We have calculated the lowest-energy configuration of I in Si, and are in the process of studying the consequences of I–I interactions and the formation of aggregates of self-interstitials.

Transition metals: Copper

All the Cu calculations are done at the HF level in clusters ranging in size from 38 to 100 host atoms. The calculated complexes include interstitial and substitutional Cu, copper-acceptor (B, Al, and Ga) pairs, and Cu precipitates at a ring hexavacancy (V_6).[12] Although some of the calculations are still being performed, preliminary results are already in print.[13] The key results can be summarized as follows.

1 It costs 1.6 eV to insert free Cu^+ into the T site in Si where it forms Cu_i^+. As an interstitial, it is electrically inactive, and diffuses with an activation energy of 0.24 eV. This calculated energy is very close to the experimental[14] value, 0.18 eV.

2. In the presence of a vacancy, Cu_i^+ becomes substitutional with a gain of energy of 2.7 eV. This value is rather small when compared to the energy one gains when other interstitials become substitutional: the V–I recombination leads to a gain of 8.2 eV, and a single H traps at a vacancy with over 3 eV energy gain.

3. Several Cu_i^+'s can precipitate inside V_6 at a gain in energy. The Cu impurities bind to the host atoms on the inner surface of the defect. The energy gained when V_6^0 traps Cu_i^+ and forms is $\{Cu,V_6\}^+$ is 3.4 eV. The tendency to precipitate shows up when one adds more Cu's into the same void. For example, the energy gained when $\{Cu_2, V_6\}^0$ traps Cu_i^+ and forms $\{Cu_3, V_6\}^+$ is 4.9 eV. Geometry optimizations dealing with $\{Cu_5, V_6\}^+$ are under way.

4. The reason why Cu precipitates are electrically active appears to be the formation of several weak Cu–Si bonds. Even in the simplest case – substitutional Cu – the energy spectrum clearly shows that localized states exist in the gap. The number of localized states in the gap increases for Cu precipitates in V_6.

5. Copper passivates the shallow B, Al, and Ga acceptors by forming a weak covalent bond with the acceptor at the antibonding site.[16] The calculated binding energies are comparable to the experimental ones and follow the trend observed. However, the pairs do not break up immediately into oppositely charged impurities such as $Cu_i^+ A^-$ where A is the acceptor. Instead, both impurities partially compensate each other up to rather substantial distances (over 10 Å in the largest cluster we are able to compute).

New electrically active C–C pair

We have studied a new EPR center associated with an unknown C-C pair.[17] The defect of a pair of C impurities at adjacent substitutional sites. This $\{C_s, C_s\}$ pair is unusual: although it is thermally stable up to rather high temperatures (about 500C), it is a high-lying metastable state which almost certainly requires a precursor.

Two C atoms do not like to be at adjacent substitutional sites: the C–C bond length should be much shorter than it is forced to be in this configuration. Substitutional C draws its Si nearest-neighbors toward itself in order to shorten the C–Si bonds. Having two C impurities at *adjacent* sites makes it that much harder to accomplish optimal bond lengths.

This defect probably occurs as follows. A self-interstitial kicks out C_s which becomes C_i. Then, C_i diffuses toward a substitutional C, forming the well-known $\{C_s, C_i\}$ pair. If a vacancy comes by, the complex is forced into a $\{C_s, C_s\}$ configuration which, although metastable, requires a high activation energy to dissociate. The details (configurations, electronic structures, spin densities, etc.) will be published as soon as the experimental group finishes collecting data.

Recent publications which acknowledge NREL support

S.K. Estreicher and P.A. Fedders: *Molecular-dynamics simulations of microscopic defects in silicon,* Mater. Sci. Forum **258-263**, 171 (1997).

J.L. Hastings, S.K. Estreicher, and P.A. Fedders: *Vacancy aggregates in silicon*, Mater. Sci. Forum **258-263**, 509 (1997).

S.K. Estreicher and J. Weber: *Photoluminescence centers associated with noble-gas impurities in silicon*, Mater. Sci. Forum **258-263**, 605 (1997).

S.K. Estreicher, J.L. Hastings, and P.A. Fedders: *Defect-induced dissociation of H_2 in silicon*, Phys. Rev. B **57**, R12663 (1998).

M. Stavola and S.K. Estreicher: *Recent experimental and theoretical results for H_2 in Si*, NREL Workshop on the Role of Defects in Si PV Processing (August 1998).

J. Weber and S.K. Estreicher: *Noble-gas-induced defects in Si*, MRS Proc. **510**, 531 (1998).

S.K. Estreicher and J.L. Hastings: *Cu-related complexes in silicon*, Mater. Sci. Engr. B (1998), in print.

S.K. Estreicher, J.L. Hastings, and P.A. Fedders: *Hydrogen-defect interactions in Si*, Mater. Sci. Engr. B (1998), in print.

S.K. Estreicher, J.L. Hastings, and P.A. Fedders: *Radiation-induced formation of H_2^* in silicon*, submitted.

References

1. S.K. Estreicher, Mat. Sci. Engr. R **14**, 319-412 (1995).

2. B.L. Sopori, X.J. Deng, J.P. Benner, A. Rohatgi, P. Sana, S.K. Estreicher, Y.K. Park, and M.A. Roberson, Sol. En. Mat. \& Sol. Cells **41/42**, 159 (1996).

3. A.A. Istratov and E.R. Weber, Appl. Phys. A **66**, 123 (1998).

4. T. Heiser, A.A. Istratov, C. Flink, and E.R. Weber, Mater. Sci. Engr. B, in print.

5. O.F. Sankey and D.J. Niklewski, Phys. Rev. B **40,** 3979 (1989).

6. O.F. Sankey, D.J. Niklewski, D.A. Drabold, J.D. Dow, Phys. Rev. B **41**, 12750 (1990).

7. S.K. Estreicher and P.A. Fedders in {\it `Computational Studies of New Materials', ed. D.A. Jelski and T.F. George (World Scientific, Singapore, in print).

8. S.K. Estreicher, J.L. Hastings, and P.A. Fedders, Phys. Rev. B **57**, R12663 (1998).

9. S.K. Estreicher, J.L. Hastings, and P.A. Fedders, submitted.

10. R.E. Pritchard, J.H. Tucker, R.C. Newman, and E.C. Lightowlers, Semic. Sci. Technol. (in print); S.K. Estreicher, J.L. Hastings, and P.A. Fedders, Mater. Sci. Engr. B (in print); T.S. Shi, G.R. Bai, M.W. Qi, and J.K. Zhou, Mater. Sci. Forum **10-12**, 597 (1986).

11. See http://jupiter.phys.ttu.edu/~guest/

12. S.K. Estreicher, J.L. Hastings, and P.A. Fedders, Appl. Phys. Lett. **70**, 432 (1997); J.L. Hastings, S.K. Estreicher, and P.A. Fedders, Phys. Rev. B **56**, 10215 (1997).

13. S.K. Estreicher and J.L. Hastings, Mater. Sci. Engr. B, in print.

14. A.A. Istratov, C. Flink, H. Hieslmair, and E.R. Weber, Phys. Rev. Lett. **81**, 1243 (1998).

15. D.E. Woon, D.S. Marynick, and S.K. Estreicher, Phys. Rev. B **45**, 13383 (1992).

16. S.K. Estreicher, Phys. Rev. B **41**, 5447 (1990).

17. B. Bech Nielsen and J. Byberg, private communication.

Title: Impurity Precipitation, Dissolution, Gettering and Passivation in PV Silicon

Organization: University of California at Berkeley, Department of Materials Science and Mineral Engineering, Berkeley CA.

Contributors: E.R.Weber, Principal Investigator; C.Flink, H.Hieslmair, and A.A.Istratov

Introduction

It is well established that the lifetime in PV silicon is limited by intragranular structural defects. These microdefects are effective precipitation sites for transition metals. High density of these precipitation sites, particularly in grains with low minority carrier diffusion length, and strong binding of metals to the precipitates result in low effectiveness of standard gettering techniques. This subcontract is focused on gaining quantitative physical understanding of processes involved in gettering of precipitated metals, i.e., in (1) dissolution of metal precipitates in the bulk of the wafer; (2) diffusion of metals towards gettering layer, and (3) their capture by gettering sites and competitive trapping of metals by intragranular defects in device-active region. To obtain a deeper insight into the physical mechanisms involved in precipitation/dissolution processes, and in agreement with the schedule of research approved by NREL, these studies were partly made on IC grade silicon.

Determination of intrinsic and effective diffusion coefficients of copper in silicon

Copper is one of the most prevalent and detrimental impurities in silicon device production [i]. The electrical and structural properties of copper in silicon are still poorly understood despite intensive research during the last 30 years (see, e.g., Istratov and Weber [ii] for a review). Even such a fundamental property as the diffusion coefficient of *Cu* in *Si* remains uncertain. In p-type silicon, copper diffuses as a positively charged ion [iii] in the presence of immobile acceptors. Reiss *et al.* [iv] showed that, due to the processes of trapping and releasing of donors by acceptors, the effective (apparent) diffusivity D_{eff} of donors in *p*-type material is lower than their diffusivity in intrinsic material D_{int} and in the case of $N_D << N_a$ is given by $D_{eff}=D_{int}/[1+\Omega N_a]$, where N_a is the acceptor concentration, N_D is the concentration of mobile donors and Ω is the pairing constant. The latter can be calculated theoretically, but requires knowledge of the interaction potential between copper and shallow acceptors. Numerous studies on copper diffusion[i,vx] obtained diffusion barriers between 0.39 eV and 0.43eV. Most of the studies were made on *p*-doped silicon and consequently only an effective diffusion coefficient of copper was measured. In this work, measurements were done using Transient Ion Drift (TID). To make sure that the diffusivity obtained from transient ion drift measurements are correct, we developed an exact model of transient ion drift obtained by solving the system of coupled differential equations. The model is described in the May & November NREL Quarterly Reports 1998 [xi]. From this model, an equation (Eq. 1) for the TID time constant was obtained. The first term on the right-hand side of Eq.1 describes the average drift time of unpaired copper ions through the depletion region. The second term describes the dissociation of copper-acceptor pairs. If $\tau_{TID} >> \alpha \times \beta \times \tau_{diss}$, the pairing is weak and the TID time constant is determined primarily by the intrinsic drift of copper ions through the depletion region. The intrinsic diffusivity D_{int} can in this case be determined directly from the experimental data. Eq.1 can be used to determine the time constant of *CuB* dissociation at temperatures where the pairing is strong (Eq. 2). The intrinsic diffusivity of copper calculated using Eqs.1 and 2 for experimental samples is presented in Fig.1 as an Arrhenius plot. Eq. 3 was obtained for the intrinsic diffusion coefficient for copper, and is valid in the temperature range between 265 K to 1173 K. It can be considered as the most accurate expression for the intrinsic copper diffusivity in silicon reported up to now.

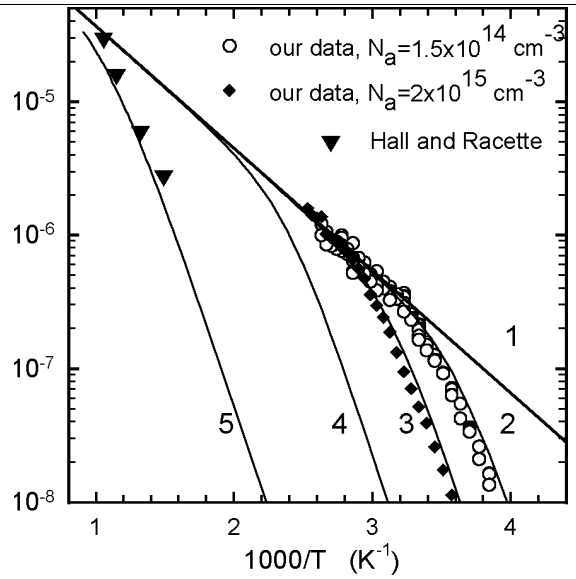

Fig.1. Effective diffusion coefficient of copper in silicon calculated for different boron doping levels (lines) and experimental data obtained in this study (circles, $N_a=1.5\times10^{14}$ cm^{-3} and diamonds, $N_a=2\times10^{15}$ cm^{-3}) and by Hall and Racette (triangles, $N_a=5\times10^{20}$ cm^{-3}). Curve 1 - intrinsic silicon, curve 2 - $N_a=1.5\times10^{14}$ cm^{-3}, curve 3 - $N_a=2\times10^{15}$ cm^{-3}, curve 4 - $N_a=1\times10^{17}$ cm^{-3}, curve 5 - $N_a=5\times10^{20}$ cm^{-3}.

$$\tau_{TID} = \alpha \times \frac{\varepsilon\varepsilon_0 k_B T}{q^2 N_a D_{\text{int}}} + \alpha \times \beta \times \tau_{diss} \qquad (1)$$

$$\tau_{diss}^{-1}(T) = (2.05 \pm 0.80) \times 10^{13} \times \exp\left(-\frac{0.61 \pm 0.01\ \text{eV}}{k_B T}\right) \qquad (2)$$

$$D_{\text{int}} = (3.0 \pm 0.3) \times 10^{-4} \times \exp\left(-\frac{0.18 \quad 0.01\ \text{eV}}{\text{k}_\text{B} T}\right) \quad (\text{cm}^2/s) \qquad (3)$$

$$D_{eff} = \frac{3 \times 10^{-4} \times \exp(-2090/T)}{1 + 2.584 \times 10^{-20} \times \exp(4990/T) \times (N_a/T)} \qquad (4)$$

We would like to emphasize that Eq.3 describes the copper diffusivity in the absence of copper-acceptor pairing and is valid only in intrinsic or *n*-type silicon, provided that no other trapping process exists. In *p*-type material, however, the effective diffusivity D_{eff} which describes copper diffusion and which is relevant for all practical applications is then given as Eq. 4.

Method of evaluation of precipitation sites density from the analysis of iron precipitation kinetics. So far, there was no reliable experimental technique to determine the density of heterogeneous precipitation sites in the bulk of silicon wafers. We developed an experimental technique which enables us to determine the precipitation site density from the analysis of precipitation kinetics. The technique is based on theoretical analysis of Ham [xii]. Taking into account the growth of the precipitates and the increase of their radii during growth, Ham solved the three dimensional diffusion equation and obtained an analytical equation to describe the kinetics of precipitation. This non-exponential equation can fit given experimental data by varying the precipitate site density, *n*, as long as the precipitation took place at a constant temperature. The implicit nature of this formulation makes it difficult to use, especially in computer simulations of gettering. To simplify the problem, Ham derived a solution assuming a fixed precipitate radius r_o. (Eqs. 5 & 6) The disadvantages of fitting this exponential approximation to experimental data are that it yields only the product nr_o. Furthermore, it is a poor metric to compare precipitation processes since the nr_o product is itself a function of the initial impurity concentration and the impurity density in the precipitate, and early in the precipitation process, when most experimental techniques are most accurate, the precipitate radius is growing, giving rise to a non-exponential curvature. Additionally, the product nr_o does not indicate whether the early precipitation was non-exponential (small r_o and large *n*) or exponential (large r_o and small *n*) However, an iterative technique based on the fixed radius solution provides a number of advantages. First, this method can simulate the growing radius solution by appropriately increasing the radius after each small time interval, Δt, it can be used in conjunction with other finite-difference simulations that require an explicit expression of the change in dissolved concentration as a function of time, and the precipitation can still be modeled *when the temperature is not fixed*, as during a slow cool. For the iterative solution of the Ham's equation, we have slightly modified Eqs 5 & 6 to obtain

$$\bar{c}(t) - c_s \cong (c_o - c_s) \cdot e^{-t/\tau_o} \qquad (5)$$

with

$$\tau_o = 1/4\pi n r_o D \qquad (6)$$

$$\Delta\bar{c}(\Delta t) = \bar{c}_{t+\Delta t} - \bar{c}_t = [c_s - \bar{c}_t]\left(1 - e^{-\Delta t/\tau}\right) \qquad \text{with} \quad \tau = 1/4\pi n r D$$

In this equation Δc is the change of the solute concentration from the starting concentration of the time interval Δt. We have verified that both the analytic growing radius solution and the iterative solution yield the same results. Thus, the developed iterative algorithm can be used to fit experimentally measured precipitation kinetics and enables us to predict the precipitation behavior even during a slow cool.

Application of the iterative technique to precipitation of iron at well-defined oxygen precipitates

The iterative technique described above was applied to perform the first quantitative study of precipitation of iron at oxygen precipitates was performed using these techniques. Previous studies succeeded only in establishing an unambiguous correlation between density and size of oxygen precipitates and kinetics of internal gettering of iron. Czochralski silicon samples used in our experiment were intentionally contaminated with iron at a high temperature and then annealed at a lower temperature to allow the iron to precipitate. Ham's equation, as discussed in the first section of the report, was fitted to the experimental data points. The decay of interstitial iron from experiment was exponential, indicating that the radius was large and not growing. Such an exponential decay could be explained if iron were precipitating on or decorating a larger defect such as the oxygen precipitate itself. One can see in Fig 2, that for low temperatures, $n_{Fe} \approx n_{Oxy}$, proving the model that iron precipitates on or decorates the surface of the oxygen precipitates. The data in Fig 2 can be used in a gettering simulator. The details of this study are presented in the August NREL Quarterly Report.

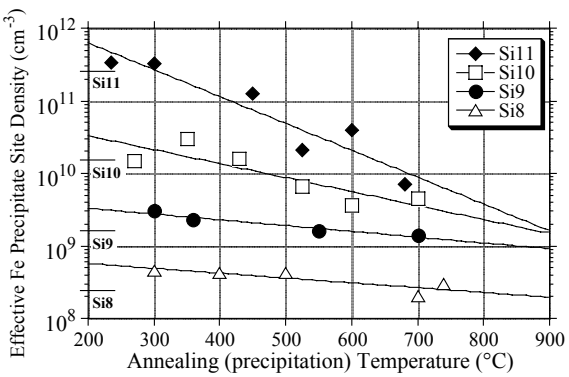

Figure 2: Effective iron precipitate density plotted for various temperatures using the radius of the oxygen precipitates for r_o. The horizontal bars on the y-axis indicate the oxygen precipitate density for the materials specified.

Iron precipitation and minority carrier difusion length

Previous studies indicated that the minority carrier diffusion length of iron contaminated samples does not improve and even degraded as the iron was precipitated. Results and studies by Henley et al.[xiii] made the quenching process, used in these studies, suspect. We performed a new study where the samples were fast cooled by removing the samples from the furnace and placing them in a crucible at room temperature. Subsequently, the samples are annealed at 425°C for various times. A significant improvement of minority carrier lifetime was observed as iron precipitates in samples which were not quenched. One sample which improved from 30µm to 137µm was annealed for approximately 10 hours. Thus, fast quenching introduces lifetime limiting defects.

Dissolution of Iron Precipitates

The next experiment was to observe dissolution from iron precipitated at oxygen precipitation sites. This process can be simulated using an iterative approach of Ham's law. The silicon sample contained $2x10^8$ oxygen precipitates/cm^3 and was contaminated with iron to approximately $3x10^{13}$ Fe/cm^3. The iron was allowed to precipitate during a slow furnace cool. The sample was then cleaned and annealed at 845°C. The dissolved iron concentration was monitored by DLTS as a function of time. A computer simulation was also performed using the above parameters. The simulation fitted the experimental results satisfactorily. The minority carrier diffusion length was already limited by the oxygen precipitates and did not correlate with the amount of dissolved iron. The studies of dissolution kinetics of iron precipitated at oxygen precipitates are now in progress.

Annealing Experiments

The results presented in the previous section suggest that anneals at 845^{0}C can dissociate iron precipitated at oxygen precipitates. In this section, we applied the same heat treatment to EFG material and FZ silicon with dislocations. The materials used for this study included high purity FZ polycrystalline silicon samples doped with iron, high purity FZ crystalline silicon samples with dislocations, and EFG silicon. The heat treatments did not improve the minority carrier diffusion length of any of the FZ samples, which indicates that iron is stronger bound at dislocations and intragranular microdefects than at oxygen precipitates. For the EFG samples, the heat treatments degraded the minority carrier diffusion length for all the samples. Additionally, iron was not detected in the EFG samples by DLTS or SPV techniques.

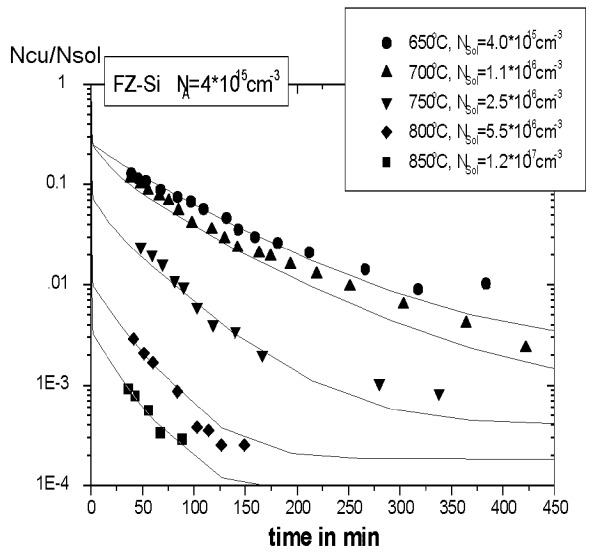

Figure 3: Decay of interstitial copper for various initial copper concentrations as determined by the in-diffusion temperature.

Copper Precipitation in Silicon

We reported the first systematic study of precipitation behavior of copper in silicon using Transient ion Drift and other experimental techniques. The major goal of this study was to prove the hypothesis that the precipitation behavior of copper is different in n-Si and p-Si. This is important for solar cells since they contain p-n junctions. To study the precipitation kinetics of interstitial copper the diffusion treatment was terminated by a quench of the samples to room temperature in ethylene glycol, resulting in a cooling rate of ~1000^{o}C per second. The interstitial copper concentration in the near-surface region in p-type silicon was then monitored with Transient Ion Drift (TID) in p-type silicon, and resistance measurements in n-type. The amount of precipitated copper in the bulk of n- and p-type silicon was profiled using X-Ray Fluorescence (XRF)

and quantitatively analyzed with Transmission Electron Microscopy (TEM).

In n-type silicon and for all copper contamination levels studied in this work, no significant changes in the resistance have been observed even five minutes after quench. This indicates the absence of the positively charged interstitial copper already several minutes after the quench and implies that copper precipitates in the bulk immediately after the quench. Correspondingly, copper precipitates throughout the wafer for all n-type samples as observed by TEM. In p-type silicon with copper concentrations below the doping concentrations no precipitates are formed. Thus the only available sink for the highly supersaturated copper is the surface and out-diffusion occurs. Furthermore, TID measurements have shown a decrease of the decay rate with increasing thickness of the samples. Analysis of the experimental data suggests that the copper kinetics in n-type FZ silicon is dominated by bulk precipitation and in p-type silicon by out-diffusion.

Summary

This report summarizes the following major achievements of FY 1998. Using Transient Ion Drift, developed at UC Berkeley with NREL support, we have obtained a diffusion barrier of 0.18 eV for the diffusion of interstitial copper. Previously reported values of Cu diffusivity at room temperature underestimated the diffusivity by more than two orders of magnitude. We have also reported the first studies on the precipitation kinetics of copper in silicon along with simulations of copper precipitation. We show that copper, in n-type FZ silicon, is dominated by bulk precipitation and, in p-type silicon, by out-diffusion. Since copper precipitates are known to be highly active recombination sites, this understanding of the behavior of copper in silicon will be of great value in designing better gettering processes for copper in silicon.

We have developed a technique of quantitative analysis of iron precipitation kinetics in silicon and demonstrated it on the example of gettering of iron by oxygen precipitates in silicon. For the first time, we reported a quantitative analysis of kinetics of the process of gettering of iron by oxygen precipitates. This technique enables us to determine the density of precipitation sites in the bulk of silicon and will be used in the next stages of the project to characterize other defects in PV silicon. We have observed the improvement of minority carrier diffusion lengths in iron contaminated silicon as the dissolved iron precipitated. Furthermore, we have reported the dissolution of iron which had already been precipitated on oxygen precipitates. Thus we are beginning to understand the kinetics and effects on diffusion length as iron interacts with oxygen defects in silicon. This methodology will then be applied to other defects common in PV silicon in order to better getter iron or minimize the effects of iron on the minority carrier diffusion length.

References

1. K. Graff, Metal Impurities in Silicon-Device Fabrication (Springer-Verlag, Berlin, 1995).
2. A.A. Istratov and E.R. Weber, Appl.Phys.A: Mater.Sci.&Process. 66, 123 (1998).
3. E.R. Weber, Appl.Phys.A: Solids&Surf. 30, 1 (1983).
4. H. Reiss, C.S. Fuller and F.J. Morin, The Bell System Technical J. 35, 535 (1956).
5. J.D. Struthers, J.Appl.Phys. 27, 1560 (1956).
6. R.H. Hall and J.H. Racette, J.Appl.Phys. 35, 379 (1964).
7. R. Keller, M. Deicher, W. Pfeiffer, H. Skudlik, M. Steiner and Th. Wichert, Phys.Rev.Lett. 65, 2023 (1990).
8. A. Mesli and T. Heiser, Phys.Rev.B 45, 11632 (1992).
9. T. Heiser and A. Mesli, Appl.Phys.A: Solids Surf. 57, 325 (1993).
10. A. Mesli, T. Heiser and E. Mulheim, Mater.Sci.Engin. B25, 141 (1994).
11. NREL Quarterly Report May 1998
12. F. S. Ham, J. Phys. Chem. Solids 6, 335 (1958)
13. W.B.Henley and D.A.Ramappa, J.Appl.Phys. 82, 589 (1997).

Title: **Optimization of Gettering Processes for Photovoltaic Silicon**

Organization: Center of Microelectronics Research,
University of South Florida, Tampa, Florida 33620

Contributors: B. Sopori, program manager
S. Ostapenko, principal investigator,
Y. Koshka, and I. Tarasov

Objectives

The effort was focused on a characterization of the "bad" regions in bulk polycrystalline silicon (poly-Si) wafers and solar cells using scanning room-temperature photoluminescence (RTPL). Luminescence mapping is recognized as a sensitive non-contact and non-destructive technique used to monitor crystalline Si quality. As previously reported [1], RTPL mapping applied to PV poly-Si is comparable to surface photovoltage with additional advantages. Specifically, we have found that spatial distribution of the defect luminescence band allows diagnostics of the "bad" regions with high recombination activity and reduced minority carrier lifetime.

Apparatus and samples

The basic components of the RTPL mapping set-up were described elsewhere [1]. An Ar^+- laser 514nm line with the power ranged from 30 to 80 mW was used as the excitation source. Alternatively, the 800nm AlGaAs laser diode (10nm bandwidth) operating in a pulse mode with peak power up to 130mW was used. The absorption coefficients of both laser lines in silicon are 1 □m^{-1} (514nm) and 12 □m^{-1} (800nm) which allowed us to compare PL mapping using near surface versus bulk excitation. For the RTPL study, polycrystalline silicon 10cmx10cm wafers were grown by the EFG technique and subjected to a standard solar cell processing including P-diffusion, hydrogenation, and Al backside alloying.

Experimental results

The PL spectrum of the as-grown and processed EFG wafers at 4.2 K consists of intense excitonic lines at a near-band-edge region dominated by the TO-phonon replica of the boron bound exciton at 1.093eV (Fig.1). It also exhibits the dislocation lines D_2 (0.87eV), D_3 (0.94eV) and D_4 (1.0eV) reported for plastically deformed Si. The D_1 dislocation line at 0.81eV, additionally found in dislocated silicon, is not clearly distinguished in our samples due to the superposition of an intense broad 0.8 eV PL band at this energy (Fig.1). The 0.8eV band has a half-width of about 0.05 eV at 4.2K (Fig.1). We denote this 0.8eV band the "defect" band here, and it is the focus of our RTPL mapping.

When temperature is increased above 120K, the PL spectrum consists of the band-to-band emission with $h\nu_{max}$=1.09eV and the 0.8eV band persisting up to room temperature. The following RTPL mapping was performed for both luminescence bands. First, we measured in a scanning mode the band-to-band PL intensity (I_{bb}), and compared it with the minority carrier diffusion length (L) over the entire sample. In Figure 2, we present typical line-scans of I_{bb} and L measured with an identical resolution of 3 mm. It is clear that regions of low L in the wafer correspond to reduced I_{bb} intensity. This observation was confirmed by mapping an entire 10cmx10cm EFG wafer, to verify our previous results [1]. Since L is a measure of bulk recombination, it is concluded that I_{bb} values represent a distribution of bulk non-radiative centers, which dominate the recombination rate of minority carriers in silicon at room temperature. The following relation is valid in this case:

$$I_{bb} \sim P_r / (P_r + P_{nr}) \sim \tau_n \sim L^2 , \quad (1)$$

where P_r and P_{nr} are the rates of radiative and non-radiative recombination, and τ_n is the minority carrier lifetime.

In regions along certain grain boundaries with low L values we found the intense 0.8eV PL band at room temperature (Fig. 1). The RTPL scan showed that this band is strongly localized in a form of narrow (of the order of mm wide) stripes around these grain boundaries. This is illustrated by the map in Figure 3a, covering an area of 38 mm x 51 mm. The white contrast corresponds to the highest PL intensity. As shown in Figs 3b and 3c, the regions with the most intense defect PL intensity, I_{def}, exhibit a substantially reduced I_{bb}. Here, two high-density PL maps of I_{def} and I_{bb} are obtained from scans over a 10 mm x 20 mm area with 0.25mm resolution. We have observed a strong signal from the defect band in this mapping study, with the peak amplitude a factor of about 20 above the background signal, accompanied by a ten-fold reduction of the I_{bb}. The inverse behavior of the intensities of these two bands around grain boundaries is shown in Fig. 4 in a point-by-point graph of I_{bb} versus I_{def}.

The 0.8eV defect band has the following features:

1. The defect band intensity I_{def} is observed both in as-grown material and after EFG processing including final solar cells. It is obvious that the defect PL band is localized in areas, which barely affected by conventional gettering/passivation techniques.
2. The I_{def} mapping contrast is temperature dependent. The defect band is observable over most of the sample below 200K. However, the stripe-like features shown in Figure 3 emerge only close to room temperature. This indicates that recombination properties of the 0.8eV PL band are modified at grain boundaries.
3. I_{def} can be suppressed by as much as a factor of 3 with a second hydrogenation of EFG beyond that normally provided in solar cell processing. This was done with a forming gas anneal (5% H_2 in N_2) at 450^o for 30 min on EFG wafers which already had undergone the regular hydrogen passivation.

Discussion

A key property of the 0.8eV PL defect band is the inverse correlation of the I_{bb} and I_{def} intensities shown in Figure 4. A competition of two radiative channels, I_{bb} and I_{def}, for minority carrier capture is unusual in Si at room-T due to the strong dominance of non-radiative centers. However, such a competition is possible if both the excitation and recombination occur in confined areas with high concentrations of the 0.8eV defects, e.g. such as at the grain boundary itself or at associated dislocations. These extended defects can provide potential wells to accumulate minority carriers (electrons) before the PL recombination. An alternative explanation of the data in Fig.4 is that a strong non-radiative center is affiliated with the 0.8eV band, and this serves as the luminescence probe. The simplest case is when the same deep defect features both a radiative and non-radiative recombination channel. This is very typical when the temperature is high enough to quench the radiative transition in favor of non-radiative one.

The observations that the 0.8eV PL band is accompanied at low temperatures by a weak D_2 line, as well as stronger D_3 and D_4 dislocation lines (Fig. 1), gives some suggestions as to possible origins for the defect center. Though the PL maximum of the defect band is close to the D_1 dislocation line at 0.812eV, it is much broader, ~ 50meV versus 5meV at 4.2K, and in contrast to the D_1 line, it persists up to room temperature. One possibility, therefore, is that the defects producing the D_1 line in EFG poly-Si are substantially modified due to grain boundary strains, and these produce the 0.8eV PL band broadening. Specifically, oxygen is very likely associated with the center responsible for the 0.8eV defect band. It was observed that oxygen precipitates in Cz-Si influence the spectral position, half-width and intensity of the D_1 line, presumably due to relaxation of the dislocation strain field [3]. An

absorption line at 1175 cm^{-1} in the FTIR spectrum is characteristically associated with oxygen precipitates in single crystal Si. This line is clearly observed in our EFG wafers. Grain boundaries in poly-Si wafers are known to be sinks for oxygen. Specifically, it was observed that the oxygen-enriched grain boundaries differ from oxygen deficient ones in terms of H-passivation [4]. In general, hydrogenation does not eliminate the detrimental effect of all defects at these boundaries during solar cell processing in poly-Si. Oxygen precipitates and complexes of transitions metals appear to remain in the low L regions, which for the most part limit solar cell efficiency.

In conclusion, scanning RTPL was applied to the study of high recombination regions in poly-Si EFG material used in solar cell fabrication, and has provided new insight into defects found in regions of low bulk minority carrier diffusion length L which limit solar cell efficiency. Defects exhibiting room-temperature PL maximum at about 0.8eV are localized around grain boundaries both in as-grown and processed wafers. These are regions not adequately passivated by hydrogen or having transition metals not gettered during cell processing. A new advance in the RTPL method described here is a mapping of a "defect" 0.8eV PL band, which is strongest in wafer regions with the lowest L values. We link this defect band to grain boundaries with accumulated impurities, such as oxygen. Low L regions are most detrimental to achieving high solar cell efficiencies, and their recombination is never completely eliminated during solar cell processing. Thus, the new defect PL signal can be used to assess the electronic quality of these low L regions in poly-Si, and to optimize various steps of solar cell fabrication in order to obtain better cell performance.

References

1. *Annual Report, Photovoltaic Program, FY 1997*
2. Koshka, Y.; Ostapenko, S.; Cao, J., and Kalejs, J. P. (1997). "Relationships Between Room Temperature Photoluminescence and Electronic Quality in Multicrystalline Silicon, Proc. 26th IEEE PVSC (Anaheim, CA), pp. 115-118
3. Bugajski, M.; Goorsky, M.; and Lagowski, J. (1991). "Oxide Precipitate-Related Photoluminescence in Silicon", Electron Technology, **24**, pp.85-92.
4. Kazmerski, L. L (1987). "Investigation of Impurity Neutralization and Defect Passivation in Poly-Si solar Cells", MRS Proceedings Vol. 106, pp. 199-210.

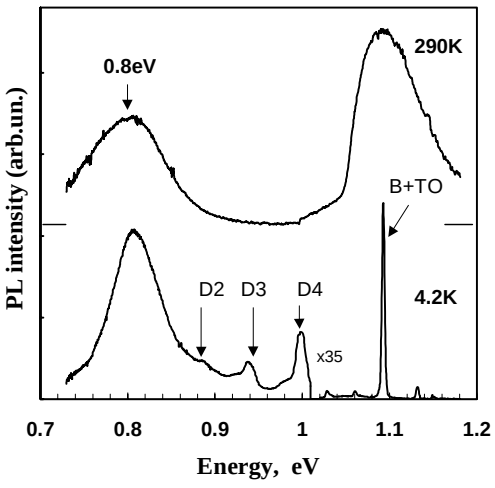

Figure 1: PL spectra in EFG wafer at the spot with strong "defect" band (see Fig.3)

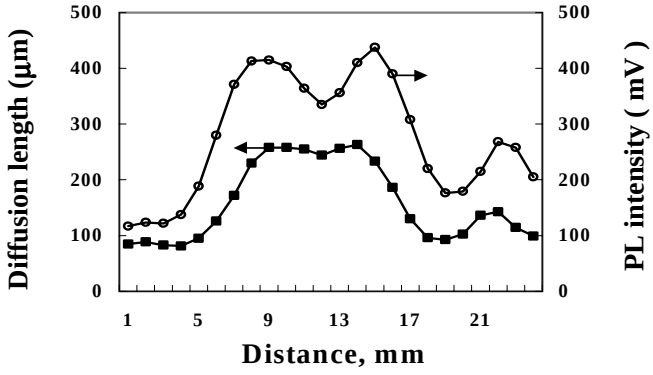

Figure 2: two line-scans of SPV diffusion length and band-to-band RTPL intensity. 'Bad" regions with L<100□m are observed.

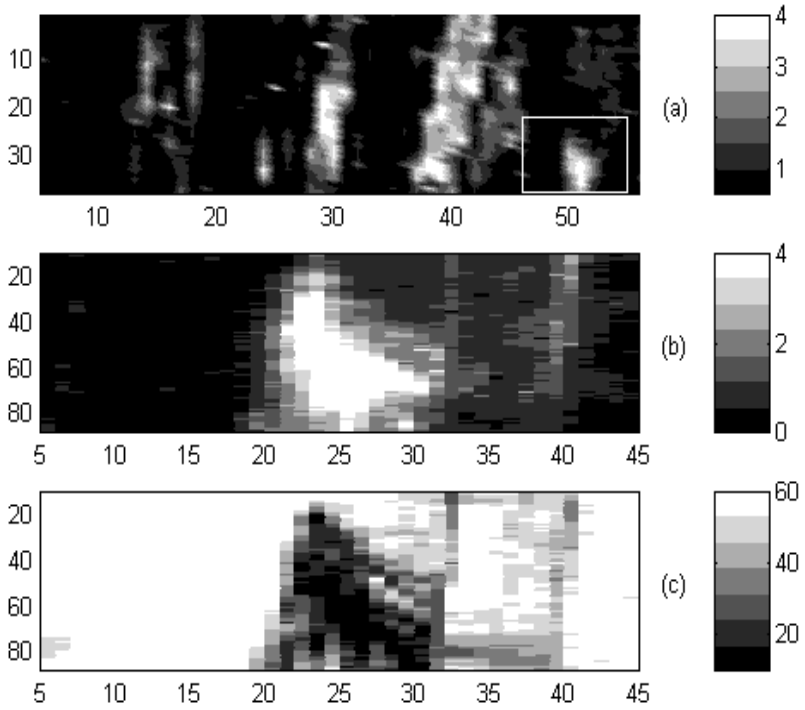

Figure 3: (a) RTPL mapping of the 0.8eV band shows a "stripe-like" localization at selected grain boundaries (38mmx51mm). The PL map fragment of (a) shown with white rectangular indicates a reverse correlation of the 0.8eV band (b) and band-to-band PL intensity (c).

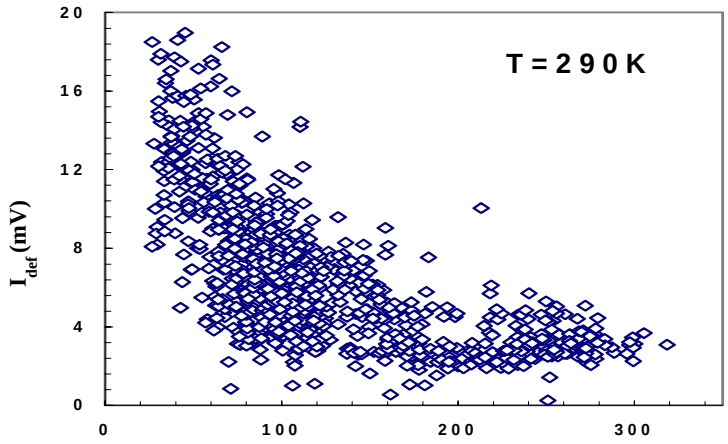

Figure 4: Reverse correlation of the band-to-band and 0.8eV luminescence measured by RTPL mapping in the region of the defect stripe indicated by rectangular in Figure 3a.

Fundamental and Exploratory Research— In-House

Title: **EE/ER Collaborative Research: Photochemical Solar Cell Development and Optimization**

Organization: National Renewable Energy Laboratory, Golden, CO
Center for Basic Sciences, Chemical Sciences Team

Contributors: A.J. Frank (Senior Scientist); B.A. Gregg (Senior Scientist); N.-G. Park (Postdoctoral Associate); J. van de Lagemaat (Postdoctoral Associate); A. Zaban (Collaborator); M. Grätzel (EPFL Collaborator); A.J. Nozik (Team Leader)

Results

(1) The AM 1.5-conversion efficiency of an NREL-produced dye-sensitized (anatase) TiO_2 solar cell (with no antireflection coating) was increased over the past year from 8.6% to 9.3%. This value approaches the best achieved by others to date (10-11%) and is substantially higher than efficiencies reported by other US laboratories. The 9.3% cell displayed a short-circuit photocurrent J_{sc} of 17.90 mA/cm^2, an open-circuit photovoltage V_{oc} of 756 mV, and a fill factor of 68%. In part, the improved advances in the cell performance were the result of our coordinated research activities under the ER/Chemical Sciences program.

(2) In collaboration with Dr. M. Grätzel, a dye cell was fabricated and measured at NREL's standard lab to be 10.4% efficient.

(3) The charge-collection efficiency of photoinjected electrons from dye sensitization was estimated from the respective time constants for charge recombination at open circuit τ_{oc} and the combined processes of charge collection and charge recombination at short circuit τ_{sc} obtained by intensity-modulated photovoltage spectroscopy IMVS and intensity-modulated photocurrent spectroscopy IMPS. A new method was developed to determine τ_{oc} and τ_{sc} from the steady-state electron-concentration profiles in the TiO_2 film calculated for constant light intensity. The continuity equation was modified to account for charge trapping and detrapping and the nonlinearity of the recombination rate on the electron-concentration profile. A simple expression was derived for calculating the charge-collection efficiency from the measured values of τ_{oc} /τ_{sc} and the light intensity dependence of τ_{oc}.

(4) The structure and photovoltaic properties of TiO_2 films deposited onto SnO_2 conducting glass from the hydrolysis of $TiCl_4$ and sintered at temperatures ranging from 100 – 500 °C were studied by Raman spectroscopy, X-ray diffraction, transmission electron microscopy, IMVS, IMPS, and other measurements. These studies show that $TiCl_4$-produced TiO_2 films have the rutile structure, regardless of sintering temperature. Both the AM-1.5 short-circuit photocurrent and open-circuit photovoltage of dye-sensitized rutile films increase significantly with sintering temperature. The increased of J_{sc} correlates with an increased concentration of adsorbed dye and improved light-scattering properties of the film associated with the growth of rutile particles. The sintering temperature is found to have only a minor effect on the charge-collection efficiency of the cell. IMVS and IMPS measurements indicate that the increase of V_{oc} with sintering temperature is due to a longer time constant for surface recombination associated with a decrease in the number of surface states. Treating nanocrystalline anatase TiO_2 electrodes with $TiCl_4$ produces an over layer of rutile, which increases the thickness of the overall TiO_2 film and improves its visible-to-near infrared light-scattering properties. Both of these factors are expected to play an important role in the observed high J_{sc}.

(5) Preliminary studies of a number of newly synthesized alkyl-substituted imidazolium iodide compounds indicate that the stability of the cell performance improves as the alkyl chain length of the imidazolium cation increases. However, the alkyl chain length of the salts was found to have no effect on the cell photocurrent and photovoltage. These results indicate that, at least for the alkyl-substituted imidazolium iodide salts, cation size does not influence the PV characteristics.

(6) Preliminary results indicate that extending the heating time for sintering or incorporating additional interparticle connecting structures within the TiO_2 particle film increases the fill factor.

(7) The energetics at the TiO_2/dye/solution interface, and the effect and extent of electric fields in the cells, are crucial and poorly understood parameters that govern the operation of the photochemical solar cells. Our studies have shown that the high concentration of electrolyte ions permeating the nanoporous films eliminates all but nanoscopic electric fields in the solution and in the TiO_2. The only substantial electric field is expected to occur at the TiO_2/solution interface, and it is primarily across this interface that the photopotential drops in operating cells. In the dark, the low conductivity of the TiO_2 and the high conductivity of the solution ensure that applied potentials drop over only a small fraction of the nanoporous TiO_2 film near the substrate electrode. Therefore, in contrast to the case with conventional solar cells, measurements of the dark currents cannot be directly compared to measurements of the photocurrents because the latter access most or all of the TiO_2 film. The sensitizing dye is located partially inside the electrochemical double layer at the TiO_2/solution interface and so its redox potential is not fixed relative to either the TiO_2 or the solution. If the dye is mostly inside the double layer, its potential will tend to follow that of the TiO_2; if it is mostly outside, it will be almost independent of the TiO_2. The fact that the potential of the sensitizing dye is not fixed relative to either the semiconductor or the electrolyte solution has important implications to the understanding and optimization of dye sensitized cells. Different photovoltage-limiting kinetic steps are expected to result in the two extreme cases, raising the possibility that the photovoltage can be optimized by controlling the position of the dye in the double layer. Experiments to test this proposition are in progress.

(8) The narrow absorption spectra of many dyes, as well as the ease with which optically thin cells can be made without electrical short circuits, provides the dye cells with a natural advantage over conventional solar cells in applications such as photoelectrochromic windows and power windows. A number of companies have expressed an interest in commercializing the photoelectrochromic window technology invented at NREL.

(9) The sensitization of nanocrystalline TiO_2 by [Fe^{II}(2,2'-bipyridine-4,4'-dicarboxylic acid)$_2$(CN)$_2$] was discovered. The electron injection apparently occurs from ultra short lived (<< 25 ps), initially populated metal to ligand charge transfer (MLCT) states before they are depopulated by internal conversion to ligand field (LF) states. This is the first report of photoreactivity from upper excited states and lends credence to recently reported femtosecond rates of electron injection from sensitizing dyes into TiO_2. Furthermore, the complex exhibits a unique "band selective" photosensitization, effectively sensitizing TiO_2 from only one of its two absorbance bands. Thus, "hot" electron injection is occurring before the upper excited state can relax to the lower one, a process that usually occurs in < 1 ps. This is the first efficient use of an iron bipyridyl complex for light-to-electricity conversion and greatly extends the realm of compounds in which sensitizing dyes may be sought.

(10) Further extending the realm of possible sensitizers, we have shown that sensitization of TiO_2 is possible using indium phosphide quantum dots. The quantum dots have a broader range of

absorption than most dyes and may also prove useful in all solid state devices. So far, however, the efficiency of these devices is less than that achieved with more conventional sensitizers such as the ruthenium dyes.

(11) One focus of current work is on finding ways to make an efficient solid state cell. The devices made to date are inefficient. We believe two factors are required for success: 1) the cells must be made thinner, that is, we need dyes with higher extinction coefficients, and 2) it is necessary to substantially decrease the recombination rate between electrons in the TiO_2 and the oxidized redox species in order to make a viable device using any other redox couple besides iodide/triiodide (that has intrinsically slow kinetics). We are pursuing several new approaches to these two problems.

Technology Transfer

Superconductive Components, in joint venture with Sustainable Technologies Australia, contacted us (A. J. Frank) regarding the possibility of an NREL CRADA to help them develop commercially viable photochemical solar cells as part of an ATP proposal to NIST (for $2 million). The proposed project was not funded.

Chemat Technology and Superconductive Components contacted us (A. J. Frank) independently regarding the possibility of an NREL CRADA to help in the characterization of their respective solar cells as part of a Phase I SBIR proposal. The proposed project was not funded.

Monsanto contacted us (A. J. Frank) for technical assistance to learn how we fabricate our solar cells and to request that NREL provide them with one of our solar cell for comparison with their own. A cell was sent to them.

Publications

R. J. Ellingson, J. B. Asbury, S. Ferrere, H. N. Ghosh, J. Sprague, T. Lian, and A. J. Nozik, "Dynamics of Electron Injection in Nanocrystalline Titanium Dioxide Films Sensitized with [Ru(4,4'-Dicarboxy-2,2'-Bipyridine)$_2$(NCS)$_2$] by Infrared Transient Absorption," *J. Phys. Chem. B* **102**, 6455 (1998).

A. Zaban, O. I. Micic, B. A. Gregg, and A. J. Nozik, "Photosensitization of Nanoporous TiO_2 Electrodes with InP Quantum Dots," *Langmuir* **14**(12), 3153 (1998).

R. J. Ellingson, J. B. Asbury, S. Ferrere, H. N. Ghosh, J. R. Sprague, T. Lian, and A. J. Nozik, "Sub-picosecond Injection of Electrons from Excited [Ru(2,2'-bipy-4,4'-dicarboxy)$_2$(SCN)$_2$] into TiO_2 Using Transient mid-Infrared Spectroscopy," to be published in the Proceedings of IPS-12, Berlin, 8/98.

A. Zaban, S. Ferrere, and B. A. Gregg, "Relative Energetics at the Semiconductor/ Sensitizing Dye/Electrolyte Interface," *J. Phys. Chem. B* **102**, 452 (1998).

S. Ferrere and B. A. Gregg, "Photosensitization of Semiconductors by [Fe^{II}(2,2'-bipyridine-4,4'dicarboxylic acid)$_2$ (CN)$_2$]: Band Selective Electron Injection from Ultra Short Lived Excited States," *J. Am. Chem. Soc.* **120**, 843 (1998).

A. Zaban, A. Meier, and B. A. Gregg, "Electric Potential Distribution and Short Range Screening in Nanoporous TiO_2 Electrodes," *J. Phys. Chem. B* **101**, 7985 (1997).

S. K. Deb, S. Ferrere, A. J. Frank, B. A. Gregg, S. Y. Huang, A. J. Nozik, G. Schlichthörl, and A. Zaban, "Photochemical Solar Cells Based on Dye-Sensitization of Nanocrystalline TiO_2," *Proc. 26th IEEE Photovoltaic Specialists Conference,* 1997, p. 507.

J. B. Asbury, R. J. Ellingson, H. N. Ghosh, S. Ferrere, T. Lian, and A. J. Nozik, "Femtosecond IR Study of Excited State Relaxation and Electron Injection Dynamics of Ru(dcbpy)$_2$(NCS)$_2$ in Solution and on Nanocrystalline TiO_2 and Al_2O_3 Thin Films," *J. Phys. Chem. B.*, submitted.

G. Schlichthörl, N.-G. Park, and A. J. Frank, "Estimation of the Charge-Collection Efficiency of Dye-Sensitized Nanocrystalline TiO_2 Solar Cells," In *Proc. Twelfth International Conference on Photochemical Conversion and Storage of Solar Energy*, Berlin, 8/98, in press.

G. Schlichthörl, N.-G. Park, and A. J. Frank, "Evaluation of the Charge-Collection Efficiency of Dye-Sensitized Nanocrystalline TiO_2 Solar Cells," submitted.

N.-G. Park, G. Schlichthörl, J. van de Lagemaat, H. M. Cheong, A. Mascarenhas, and A. J. Frank, "Dye-Sensitized TiO_2 Solar Cells: Structural and Photoelectrochemical Characterization of Nanocrystalline Electrodes Formed from the Hydrolysis of $TiCl_4$," submitted.

C. Bechinger and B. A. Gregg, "Development of a New Self-Powered Electrochromic Device for Light Modulation without External Power Supply," *Sol. Energy Mater. Sol. Cells*, in press.

B. A. Gregg, A. Zaban, and S. Ferrere, "Dye Sensitized Solar Cells: Energetic Considerations and Applications," *Z. Phys. Chem*, in press.

Presentations:

A. J. Frank (with co-author G. Schlichthörl) presented a poster entitled "A Study of Dye-Sensitized Nanocrystalline TiO_2 Solar Cells by IMVS and IMPS" at the 22nd DOE Solar Photochemistry Research Conference in Chantilly, Virginia, June 7-10, 1998.

G. Schlichthörl (coauthors: N.-G. Park and A. J. Frank) gave an invited talk entitled "Estimation of the Charge-Collection Efficiency of Dye-Sensitized Nanocrystalline TiO_2 Solar Cells" at the Twelfth International Conference on Photochemical Conversion and Storage of Solar Energy in Berlin, Germany, August 9-14, 1998.

A. J. Frank (coauthors: G. Schlichthörl and N.-G. Park) gave a keynote lecture entitled "Dye-Sensitized Nanocrystalline TIO_2 Solar Cells" at the 49th Annual Meeting of the International Society of Electrochemistry in Kitakyushu, Japan, September 13-18, 1998.

S. K. Deb, S. Ferrere, A. J. Frank, B. A. Gregg, S. Y. Huang, A. J. Nozik, G. Schlichthörl, and A. Zaban, "Photochemical Solar Cells Based on Dye-Sensitization of Nanocrystalline TiO_2," Proc. Twenty Sixth IEEE Photovoltaic Specialists Conference, Anaheim, CA, 1997.

B. A. Gregg, "Photoconversion Processes in Organic Semiconductors," Chemistry Department Seminar, University of Texas at Austin, January 22, 1998. (invited seminar)

B. A. Gregg, A. Zaban, and S. Ferrere, "Dye Sensitized Solar Cells: Energetic Considerations and Applications," Twelfth International Conference on Photochemical Conversion and Storage of Solar Energy (IPS-12), Berlin, August 1998. (invited seminar)

B. A. Gregg, et al. "Dye Sensitized Photochemical Solar Cells," NCPV meeting, Denver, September 1998.

A. J. Nozik presented invited seminars at the University of Georgia, Auburn University and Emory University, April 1998.

A. J. Nozik presented an invited colloquium at the University of Oregon in May 1998.

A. J. Nozik visited the University of Dublin in August 1998 to discuss the progress of the dye-sensitized photochemical solar cell project in Europe that is funded by the European community.

A. J. Nozik presented an invited talk at the Workshop on Photoelectrochemistry and Ultrafast Electron Transfer Processes at the 12th International Conference on Photochemical Conversion and Storage of Solar Energy (IPS-12) August 9-15, 1998. He also attended the IPS-12 Conference as a member of the International Organizing Committee to co-chair the workshop session on dye-sensitized photochemical solar cells.

Project Title : **Fundamental and Exploratory Research**

Task Title: Solid State Spectroscopy

Contributors: A. Mascarenhas, H. Cheong, B. Fluegel, J. Perkins (Solid State Spectroscopy)
Steve Smith, L. Kazmerski (Measurements and Characterization Center)
R. Dhere, P. Sheldon, Tim Gessert (CdTe Team)

Task Description and Results:

1) Recombination studies with submicron resolution in polycrystalline materials.

The performance of a polycrystalline thin film solar cell is strongly influenced by extrinsic material properties such as the effects of grain boundaries on photo-carrier transport and recombination.. In polycrystalline materials the grain size, chemical composition and doping can all vary between individual grains and across grain boundaries. So far, optical studies of such photovoltaic materials have relied on macroscopic techniques with probe sizes that are much larger than the average grain size. In these techniques, only *average* properties are measured. As a result, the current understanding is very limited regarding the microscopic fluctuations of the optoelectronic properties due to the grain structure, the role of the grain boundaries as recombination centers, and passivation of the defect states near grain boundaries. During the past year, in a collaboration with the CdTe team, we demonstrated that the microscopic variations in the material quality and the inter-diffusion of anions at the CdS/CdTe interface could be directly studied using the low-temperature scanning micro-photoluminescence (μPL) technique with a ~0.65 μm resolution (see Fig. 1). To perform these studies we completed the installation of a low-temperature near-field scanning optical microscope. The setup was tested at 4.2K and was shown to be capable of Atomic Force Microscope resolution capability. The software for integrating this setup with the spectrograph and signal acquisition electronics was developed. A systematic study of CdTe films that have been lifted off was undertaken as a function of film growth parameters and grain boundary passivation techniques.

2) Effects of Exciton Formation and Transport in Solar Cells

In a conventional device model, exciton effects are not considered, which is because of the fact that the exciton population is believed to be very low at room temperature. However, it has been pointed out recently by D. E. Kane et al and M. A. Green et al that even at room temperature, there may still be a significant amount of excitons in semiconductors like Si which have an exciton binding energy comparable to the thermal energy. Thus, the transport or diffusion of excitons may play an important role in determining the performance of a solar cell. We have now established a device model for the solar cell with the exciton effects included. Because of the difference in the diffusion coefficient and life time between the minority carrier and exciton, the existence of excitons affects the dark saturation current, short circuit current and spectral response. The conclusion drawn from this study was that the major effect of excitons on the performance of Si solar cells relies on whether the effective diffusion length of the coupled

exciton-electron system is significantly greater than that for the electron itself. These results have been published in J. Appl. Phys. **84**, 3966(1998).

3. Raman studies of alloying at the Cds/$CuInSe_2$ interface

We performed Raman scattering measurements on $CuInSe_2$ thin-film solar cell structures in an attempt to understand the possibility of Cd diffusion from the CdS top layer to the $CuInSe_2$ layer. Kannan Ramanathan prepared three samples for this study. We first measured a $CuInSe_2$ thin-film sample for comparison. A relatively strong phonon peak at 164 cm^{-1} and two weak peaks at 205 and 250 cm^{-1} was observed. Two $CuInSe_2$/CdS structures, one as deposited and another after being annealed at 200 ºC in air, were then measured. A strong phonon peak at 293 cm^{-1} and its two-phonon replica at 603 cm^{-1} are due to the CdS layer. The $CuInSe_2$-related features were also seen. In addition, a weak peak at 137 cm^{-1} was observed. This peak does not exist in the Raman spectrum of the $CuInSe_2$ sample nor does it correspond to any known phonon mode for CdS. This feature could be related to the heterojunction between $CuInSe_2$ and CdS. We plan to measure a thick CdS thin-film layer in order to establish the origin of the feature at 137 cm^{-1}.

4. Direct observation of Nitrogen resonant level in $GaAs_{1-x}N_x$

The alloy $GaAs_{1-x}N_x$ is of interest for potential use as an active absorbing layer in a triple junction monolithic tandem solar cell comprising of GaInP, GaAs, GaAs:N and Ge. For dilute concentrations of N where the lattice mismatch between $GaAs_{1-x}N_x$ is small its bandgap falls close to 1.2 eV. The giant bowing that occurs in dilute N doped GaAs is an intriguing scientific phenomenon. Measurements by John Perkins on $GaAs_{1-x}N_x$ samples grown by John Geisz at NREL directly revealed the reason for the giant bowing phenomenon. As shown in the electromodulated reflectance spectra in Fig.2, a new critical point transition denoted E_+ is observed above the conduction band edge. Most surprisingly, Fig. 2 shows that as opposed to the E_0 and $E_0+\Delta_0$ transitions which decrease in energy as the Nitrogen concentration is increased the E+ transition increases in energy. The opposite movements of the Impurity band and conduction band could be a result of level repulsion between the two and the reason for the giant bowing of the conduction band in dilute $GaAs_{1-x}N_x$ alloys. The NREL research provides the first direct observation of the Nitrogen resonant level in GaAs alloys. It showed that electromodulated reflectivity provides a simple means of characterizing the near band edge optical properties of $GaAs_{1-x}N_x$ alloys. These results have been submitted for publication.

Figure 1

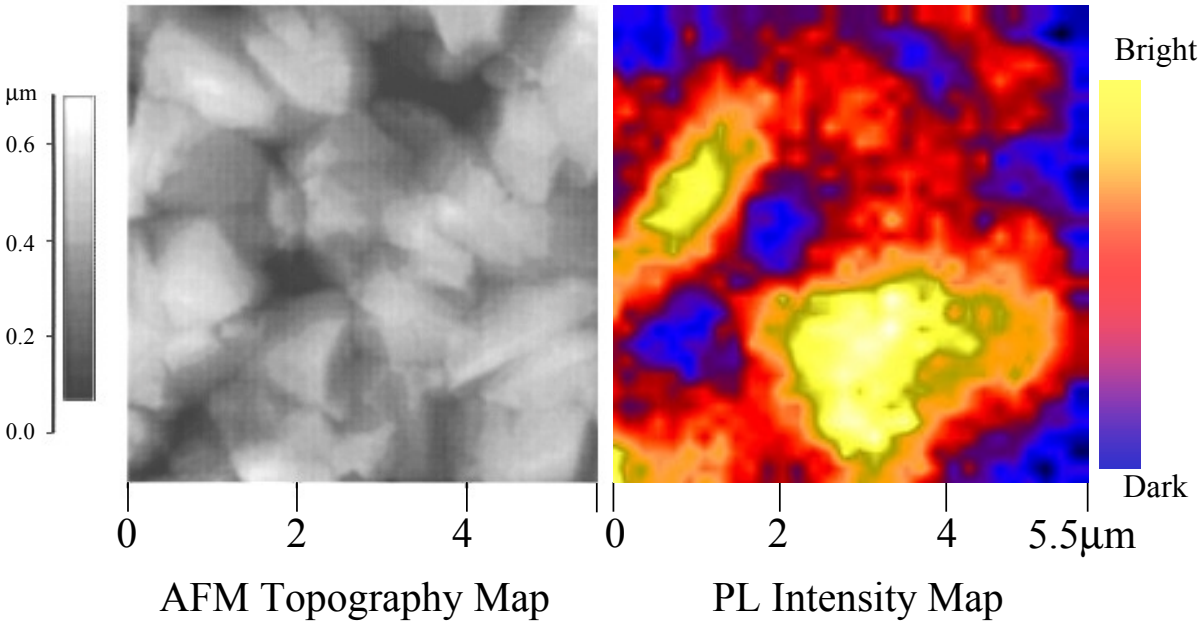
µm
0.6
0.4
0.2
0.0
Bright
Dark
0
2
4
0
2
4
5.5µm
AFM Topography Map
PL Intensity Map

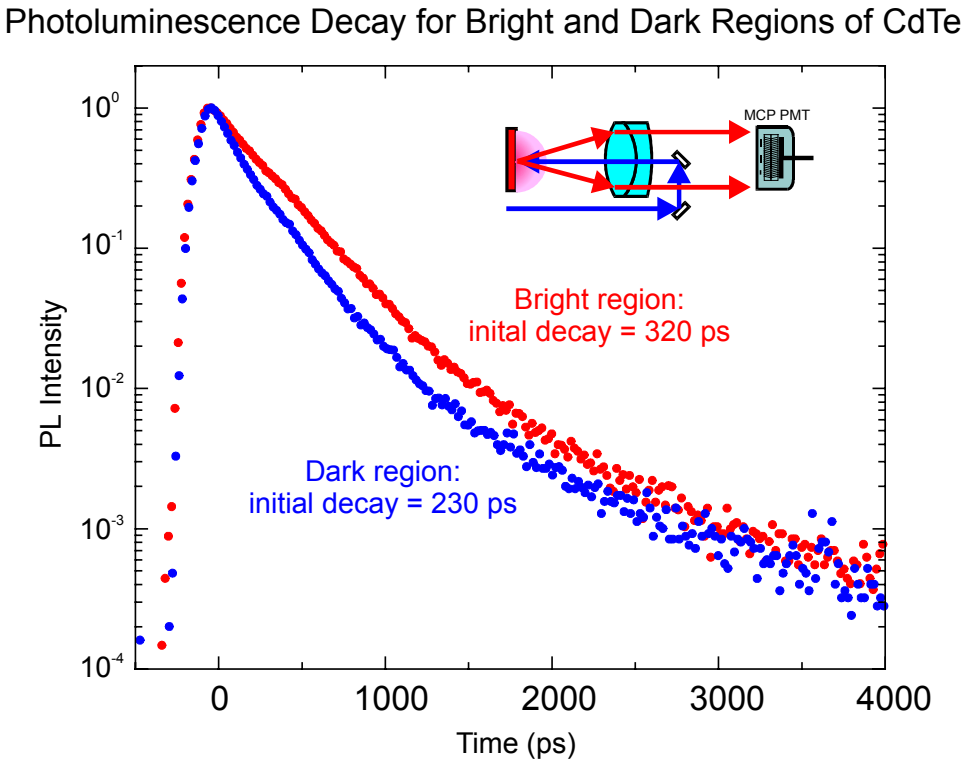
Photoluminescence Decay for Bright and Dark Regions of CdTe
MCP PMT
Bright region:
inital decay = 320 ps
Dark region:
initial decay = 230 ps
PL Intensity
Time (ps)
10^0
10^-1
10^-2
10^-3
10^-4
0
1000
2000
3000
4000

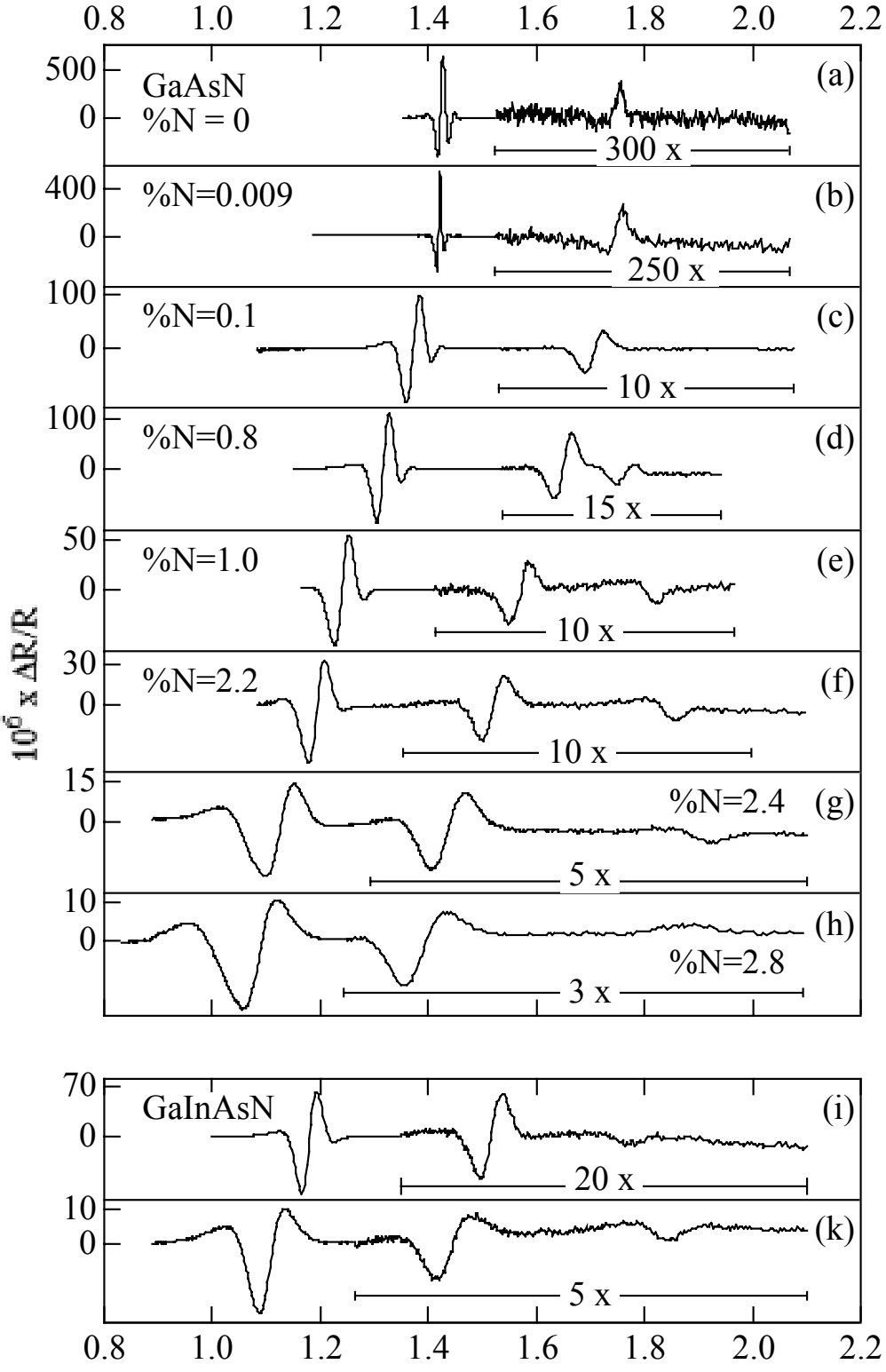

Fig. 2 (Perkins *et al.*)

Title: **Solid State Theory of Photovoltaic Materials**

Organization: NREL, Basic Science Center

Contributors: Alex Zunger (Research Fellow)
S: H. Wei (Career Scientist)
S.B. Zhang (Senior Scientist)
L:W. Wang (Senior Scientist)

This report provides a summary of the FY1998 research activities of the solid state theory group on

1. **Predicting the band offsets between II-VI and between III-V compounds**
2. **Crystal structure of $CuInSe_2$ ordered defect compounds**
3. **Dependence of band gaps of chalcopyrites on pressure**
4. **Theory of transparent conducting oxides**

5. The effects of Na on CIS Further details are available from the references at the end of this section and the solid state theory home page: http://www.sst.nrel.gov.

1. Predicting the band offsets between II-VI and between III-V compounds (1)

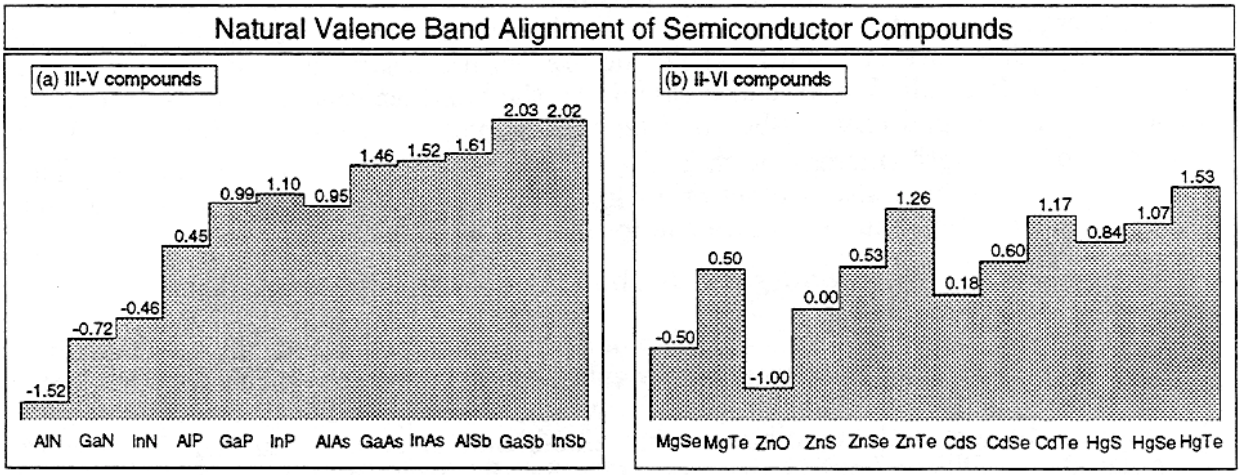

Figure 1. Calculated natural valence band alignment (in eV, relative to ZnS) of (a) III-V semiconductor compounds and (b) II-VI semiconductor compounds.

The offset ΔE_v,(*AX/BY*) between the valence (v) band maxima of two semiconductor compounds *AX* and *BY* forming a heterostructure is one of the the most important parameters in interfacial structures deciding both transport and device characteristics. Most of the experimental studies concerned only a particular pair and their results are somewhat scattered. Furthermore, many of the previous theoretical calculations involved approximations (e.g., model solid, no *p-d* coupling, etc.) whose validity has not been verified. Thus, overall regularities and trends were not apparent. We have systematically calculated the natural (unstrained) band offsets ΔE_v, via *ab initio*, all electron band structure method between all II-VI and between all III-V semiconductor compounds (Fig. 1). Clear chemical trends are apparent, for the first time. We find that for common-cation systems ΔE_v, decreases when the cation atomic number increases, while for common-anion systems ΔE_v, decreases

when the anion atomic number increases. The enclosed figure provides the *unstrained* offsets of most semiconductors. To add coherent strain effects, see S: H. Wei and A. Zunger, Phys. Rev. B, **49**, 14337 (1994).

2. Crystal structures of "ordered defect compounds"

It has been found recently that ordered defect compounds (ODCs) such as $CuIn_5Se_8$ and $CuIn_3Se_5$ may play an important role in the fabrication of device quality $CuInSe_2$ solar cells. However, despite extensive studies during the last few years, the stable crystal structures of the ODCs are still unknown. Using first-principles total energy method, we have studied systematically the crystal structures of the ODCs. For $CuInSe_2$ in chalcopyrite structure, each Se has four cation neighbors. We find that to minimize the total energy, the local deviation from the octet rule should be minimal. For example, the $CuIn_5Se_8$ ODC is stable only if it contains equal number of Se-centered clusters V+Cu+2In (denoted as k = 7) and V+3In (denoted as k = 9), where "V" denotes Cu vacancy. The $CuIn_3Se_5$ ODC is stable if we have 40% k=7 clusters, 40% k=9 clusters, and 20% k=8 (2Cu+2In) clusters. Our total energy calculation show that for $CuIn_5Se_8$ ODC, the crystal structure in which the atoms on the Cu sublattice form a -Cu-V_{Cu}-In_{Cu}-V_{cu}- (110) plane (the atoms on the In and Se sublattice are not changed) has the lowest total energy. However, the total energy differences between all the structures with the same number of clusters (k=7 and k=9) are fairly small (1-8 meV/atom), indicating that, at finite temperature the actual crystal structure may depend sensitively on the growth and annealing conditions. We also find that CuIn5Se8 in the spinal structure has even lower energy than the ODCs. For $CuIn_3Se_5$, we find that the lowest energy crystal structure is consistent with that observed by Hanada et al.. Again, the total energy difference between all the structures with the same number of clusters (k=7, 8 and 9) are fairly small. We have also calculated the bond lengths and the Se core level shift in the ODCs. We find that Cu-Se bond lengths are nearly constant in different ODCs, but the In-Se bond lengths increase with k: $R_{In\text{-}se}(k = 9) - R_{In\text{-}se}(k = 7) \sim 0.06$Å . The core level of the Se atom is also a function of k: The Se 1s core energy level in k=9 cluster is about 0.8 eV deeper than Se is core energy level in k=7 cluster.

3. Dependence of the band gaps of chalcopyrites on pressure [2]

The pressure (p) coefficient $a_i^{(p)} = dEi/dp$ of an interband transition i in a semiconductor is related to the volume (V) deformation potential $dEZ/dlnV$ via the bulk modulus B through the relation $dEZ/dp = -(1/B)(dEi/dlnV)$, where, i = $\Gamma_{15v} \rightarrow \Gamma_{1c}$ or i = $\Gamma_{15v} \rightarrow X_{1c}$, etc. For semiconductors with the diamond and zinc-blende structures, an "empirical rule" was formulated by William Paul in the late 1960s for the pressure coefficients of various band gap transitions. According to this rule, for a given transition i, $a_i^{(P)}$ is nearly the same for all semiconductors. While the foundation of the rule has never been examined rigorously, the rule has been used extensively in the past to identify the symmetry of optical transitions and to determine the band offset at zinc-blende semiconductor interfaces. The applicability of the rule to other tetrahedrally coordinated semiconductors has also never been investigated. We have examined the applicability of such a rule to chalcopyrite compounds ABC_2 using the latest experimental values of a_g (last column of Table I). We see from the data that (i) a_g in chalcopyrite is fairly constant when the group I transition metal A is varied, but (ii) when the group III cation B is changed from Ga to In, a_g can decrease by as much as 40%. (iii) a_g for chalcopyrites are much smaller than in the corresponding III-V compounds. (iv) In III-V compounds, a_g increases significantly as the anion atomic number increases. Using first-principles band structure method, we have investigated a_g theoretically in these materials and found good agreement between theoretical and experimental values (except for $CuInTe_2$ which we expect to have the value of ~ 5.9 meV/kbar,

rather than the much smaller known experimental value of 2.2 meV/kbar, see Table I). We explained why a_g is smaller and more cation dependent in chalcopyrites than in III-V's, and why a_g increases with anion atomic number. Based on our theoretical calculation we show that the "empirical rule" has to be modified.

Table I. Calculated pressure coefficients of the direct band gap of six chalcopyrite semiconductors. The results are given for the transition from the *highest* of the three crystal field split valence band states. For $\frac{dE_g}{dp}|_{calc.}$ we also give in parenthesis the value representing an average over the three crystal field split states.

Compound	$-\frac{dE_g}{dlnV}$ (eV)	$\frac{1}{B}$ ($Mbar^{-1}$)	$\frac{dE_g}{dp}|_{calc.}$ (meV/kbar)	$\frac{dE_g}{dp}|_{exp}$ (meV/kbar)
$CuGaSe_2$	4.13	1.24	5.1 (4.9)	5.0
$CuInSe_2$	2.32	1.41	3.3 (3.1)	3.0
$CuGaTe_2$	4.72	1.63	7.7 (7.5)	
$CuInTe_2$	3.25	1.76	5.7 (5.9)	2.2
$AgGaSe_2$	2.78	1.56	4.3 (5.0)	5.1
$AgInSe_2$	1.03	1.71	1.8 (2.4)	2.7

4. Defect Physics in ZnO — A Prototype Transparent Conducting Oxide

Transparent conducting oxides (TCO) are oxides that can sustain high concentrations of free charge carriers while, at the same time, maintaining a large bank gap. There are only a handful of them despite the vast number of oxides existing in ature. In many cases, one does not have to dope the TCOs, as free charge carriers are generated by native defects. Despite the technological importance of the TCOs, however, the origin of the native defect that controls the doping in TCO is poorly understood. Noticeably, we do not know why there is an asymmetry in doping (almost all TCOs are n-type, rarely p-type). We have carried out first-principles total energy calculations for the native defects in ZnO. We find a strong asymmetry in the formation energies ΔH_f of cation vs anion vacancy. For example, $\Delta H_f(V^0_O)$ for a charge neutral oxygen vacancy is only 2.1 eV (at the Zn-rich limit), whereas $\Delta H_f(V^0_{Zn})$ for a charge neutral Zn vacancy is as high as 6.2 eV (at the O-rich limit). The Zn- (or O-) rich limit here refers to the growth conditions at which the Zn (or 0) atomic chemical potential is that of bulk Zn (or molecular *OZ).* In other semiconductors, the formation energies of anion and cation vacancies are more similar. For example, the formation energies of charge neutral Ga and As vacancies in GaAs are both around 4 eV at the respective As- and Ga-rich limits. The significance of the asymmetry in the formation energy in ZnO is that we predict that Zn vacancies, regardless of their charge states and the growth conditions, will never form. Since the charged cation vacancies are the primary source of the "free electron killers", the high formation energy of V^{2-}_{Zn} means low concentration of electron traps. This enables high n-type doping densities in ZnO. On the contrary, we find a negative $\Delta H_f^{max} V^{2+}_O$ = *-0.8* eV in p- type *(E_F* = VBM*)* ZnO. Thus, V^{2+}_O will spontaneously form in p-type ZnO. Since V^{2+}_O is an effective hole trap, its formation compensates p-doping. The oxygen vacancy is interesting not only because of the low formation energy but also because when doubly ionized it has an empty energy level in the conduction. Persistent photo conductivity is thus expected since optical excitation will ionize V^0_O (deep) into V^{2+}_O (shallow)

which, after relaxation, cannot recapture the electrons in the conduction band by emitting photons. We also find that Zn interstitial has a negligible concentration in ZnO since the formation energy of Zn^{o}_{i} is about 5 eV higher than that of V^{0}_{O}.

5. Effects of Na in $CuInSe_2$ [3]

It has been observed that $CuIn_{1-x}Ga_xSe_2$ (CIGS) solar cells containing small amount of Na achieve higher efficiencies compared to those without Na. Reported effects include improved film morphology and grain sizes, better film orientation, increased film conductivity, increased uniformity of photocurrents and short-circuit current, increased hole density, higher open circuit voltage, higher fill factors and suppression of the formation of the "ordered defect compound" (ODC). Substantial efforts have been invested to model the role of Na in GIGS. Three models have been proposed to account for the increase in the hole density:
(a) *The oxygen model:* Ruckh et. al. suggested that the increase in the hole density is due to the neutralization of donor-like Se vacancies through an- enhanced chemisorption of oxygen in the presence of sodium. Thus, the Na-induced effects on CIGS are a consequence of oxidation effects. This assumption was further promoted by Kronik et al. who suggest that surface (including grain boundary) formation in CIGS is accompanied by the formation of surface Se vacancies. In their model, V_{Se} are electrically active donors which become shallow acceptors by oxygen substitution (they suggest that O_{Se} creates shallow acceptor levels at about ~ 130 meV). Na merely catalyzes O_2 dissociation, thus supplying the needed atomic oxygen.
(b) *The In_{Cu} model:* Contreras et al. suggest that the increase of the effective acceptor concentration is due to the elimination of the compensating antisite donor defect In_{Cu} in the film.
(c) The Na_{In} model: Niles et al. suggest that the increases in acceptor concentration in the presence of Na are due to direct creation of acceptors such as antisite defect NA_{In}.

Using first-principles total energy and band structure method, we have studied theoretically the Na-induced effects in $CuInSe_2$. Calculating the formation energies and the transition energy levels for a number of point defects: Nacu, Nal., Vs., and Os,, in $CuInSe_2$. We find that (1) If available in large quantities, Na will replace Cu, forming a stabler NaInSe2 compound having a large band gap (higher open-circuit voltage) and a (112)tt.d morphology. The ensuing alloy Na,,Cul-.,$InSe_2$ has a positive mixing enthalpy, so $NaInSe_2$ will phase separate, forming precipitates. (2) When available in small quantities, Na will form defect on Cu site and In site. Na on Cu site does not create electric levels in the band gap, while Na on In site creates acceptor levels that are shallower the CuI~.: The formation energy of Nal,,c,u is very exothermic, therefore as suggested by Contreras et al [(b) above], *the major effect of Na is the elimination of the Ins,, defects, thus increase the efective hole densities.* The quenching of Inc,, and Vcu by Na reduces the stability of the (2V- u + In~u), thus suppress the formation of the ordered defect compounds. (3) As suggested by Ruckh et al and Kronik et al [(a) above], Na catalyzes the dissociation of OZ into atomic oxygen that neutralizes Se vacancy (shallow donors), converts them into Os, However, we find, in contrast to (a) above that 0se is a deep (not shallow) acceptor. Having removed thereby the donors, 0 atoms in CuInSe2 form CU20 and In203 compounds, and phase separate, forming precipitates at the surface and grain boundaries.

References

[1] S: H. Wei and A. Zunger, "Calculated natural band offsets of all II VI and III-V semiconductors: Chemical trends and the role.of cation d orbitals ", Appl. Phys. Lett. 72 2011 (1998).
[2] S: H. Wei, A. Zunger, I: H. Choi, and P. Y. Yu, "Trends in band gap pressure coefficients in chalcopyrite semiconductors", Phys. Rev. B 58, 81710 (1998).
[3] S: H. Wei, S. B. Zhang and A. Zunger, "The effect of Na on the electrical and structural properties of CuInSe2", unpublished.

Fundamental and Exploratory Research—Subcontracts

Title: **Absorption Enhancement in Ultra-Thin Textured AlGaAs films**

Organization: University of California, Los Angeles
Electrical Engineering Department
420 Westwood Plaza
Los Angleles, CA 90095-1594

Contributors: E. Yablonovitch, Principal Inverstigator, M. Boroditsky, R. Ragan

Introduction:

We have studied light randomization and absorption in AlGaAs films textured by means of natural lithography. A reproducible thin film fabrication process was developed that provides 90% of ideally predicted band-edge absorption relative to our theoretical model. Since the 1μm diameter spheres are visible in the optical microscope, natural lithography with this sphere size is easy to monitor and optimize. Our technique is applicable for fabrication of thin film solar cells and LED's based on III-V compounds. Epitaxial lift-off technology allows us to fabricate very thin AlGaAs solar cells[1], making them lighter and cheaper and providing higher operating point voltages.

Enhanced absorption by light trapping:

It was proposed in late 1970s and early 1980's that light trapping by total internal reflection could be used to increase light absorption in semiconductor wafers. Several techniques were developed, such as natural lithography[2], metal islands[3] and anodical etch of the porous silicon[4] to texturize thin silicon sheets for light trapping. Yablonovitch[5] showed, that in the low absorption limit, total randomization of the light leads to the enhancement of absorption by the factor of $2n_f^2$**,** where n_f is film's refractive index. This results were confirmed experimentally by Deckman *et al*[6] by applying the natural lithography technique to amorphous silicon films. However, at the moment there is no theory for angular dependence of light scattering from surfaces produced by this process because perturbation methods require that the ratio of roughness height to the wavelength be small[7] while the quasi-classical small slope approximation[8] require a relatively smooth surface.

In this paper we report results of our study of light randomization and absorption enhancement in ultra-thin GaAs/AlGaAs films with a thickness of only a few optical wavelength. The ultra-thin films were textured using the natural lithography while varying the density of cylindrical surface structures. A modified photon gas model, which successfully describes the absorption at the band edge will be presented.

Sample Fabricaton:

The sample preparation method is by Natural Lithography: A GaAs/AlGaAs double hetero-structure wafer (see Table 1) is patterned with commercially available carboxylate modified 0.95μm polystyrene spheres. The sphere solution is first diluted with methanol to 1% concentration by weight and then surface deposited by dropping a small quantity of a solution on the wafer and spinning the wafer at 1500-2000 rpm. The wafer is spun to distribute the spheres across the surface, and to allow the methanol to evaporate. The sphere solution concentration and the revolution speed were varied until the conditions

Table 1. Structure of the GaAs/AlGaAs quantum well wafer

GaAlAs	0.32 μm	window layer
GaAs	0.20 μm	active layer
GaAlAs	0.44 μm	window layer
AlAs	0.05 μm	sacrificial layer
GaAs	>100 μm	substrate

were found such that approximately 50% of the wafer area is covered by spheres. The resultant sphere density distribution does not vary significantly across the surface of a given sample. The key point is to avoid building up multiple layers of spheres, which totally coat the surface and provide no patterning.

When the desired sphere distribution is obtained, the sample is etched using the chemically assisted ion beam etching process to transfer a pattern, using the spheres as a lithographic mask. In our work the transferred pattern consists of 0.25μm high mesas, which is approximately 3/4 of the thickness of the top AlGaAs layer. Following etching, the top three epitaxial layers (~1μm) of the wafer, containing the active layer of the device, are removed from the substrate using the epitaxial lift-off procedure (ELO)[9]. The sample is bonded to a glass slide with the untextured side against the glass by using a UV curable polyurethane adhesive.

Absorbance measurements:

The spectral reflectance, R(λ), of the textured and untextured film was measured over a white surface using a standard integrating sphere setup. Then, absorbance A(λ)of the sample simply becomes:

$$A(\lambda)=1-R(\lambda), \quad (1)$$

since there is no transmission outside of the sphere. Samples were held horizontally by gravity so that no optically absorbing adhesive materials were necessary inside the sphere. In all our measurements, the probe beam was incident on the glass side with the semiconductor film on the rear, as shown in Fig. 1. In this configuration specular reflections from the glass-air and the semiconductor/glass interfaces were identical for the textured and untextured samples. Thus, changes in reflectivity at the front surface ware not a concern, since the texturing was at the rear surface.

In all the textured samples, an increase in absorption was measured in comparison with the untextured films (see Figure 2). The maximum theoretical absorption, which can be attained is ≈80% due to incident beam reflectivity from the glass/air (4%) and semiconductor/glass (16%) interfaces. The best results were attained for samples, which were coated by approximately 50% area coverage of polystyrene spheres and the corresponding 0.25μm high mesas. An absorbance increase from 45% up to ≈75% of a maximally achievable result occurs for the sample in Figure 2 near the band edge. In our best samples, the experimental value nearly reaches the maximum absorbance predicted by theory, as can be seen in Figure 3. The absorbance oscillations, which occur for photon energies above the bandgap, are due to

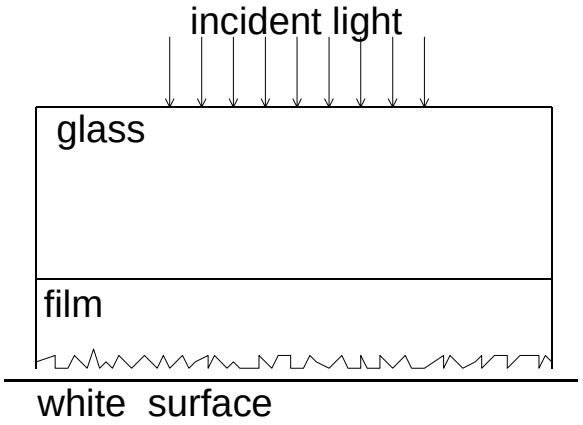

Figure 1. Experiment configuration.

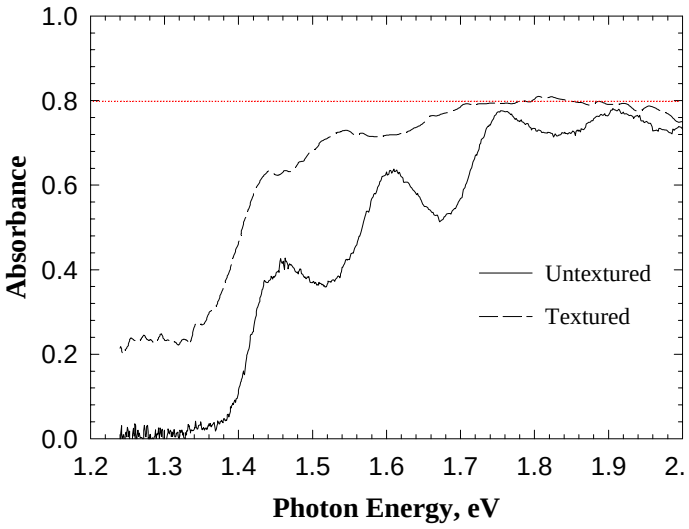

Figure 2. Sample with 50% of the surface area covered with spheres. A large absorption enhancement is obtained near the band edge.

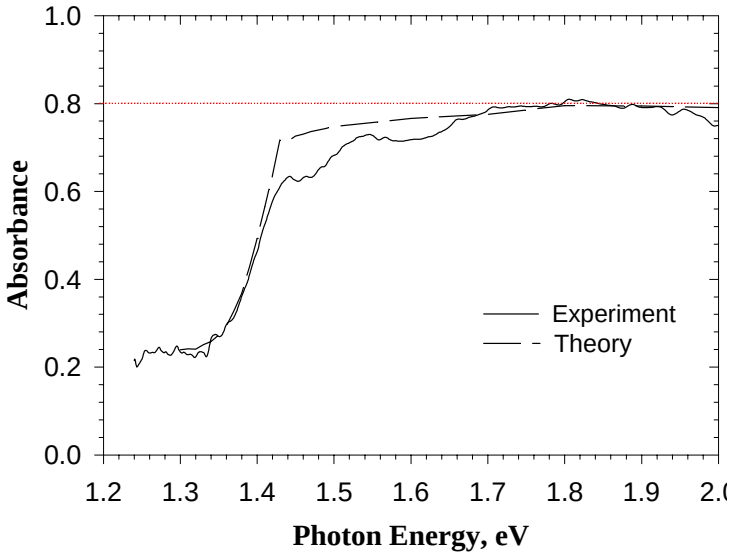

Figure 3. Comparison between the maximum theoretical absorption for a textured film and the values obtained experimentally.

Fabry-Perot fringes. The damping of these Fabry-Perot oscillations in the textured film is an additional evidence of light randomization produced through surface texturization. At energies below the bandgap, free carrier absorption is enhanced from <1% up to the level of ≈20%. Unfortunately, this produces heat rather then electron-hole pairs.

A modified photon gas model[10] was used to calculate the maximum achievable absorbance in the thin film. In the photon gas model in the work of Deckman *et al*[6], an average Lambertian length for absorption is used. This is not valid for the strongly nonlinear dependence of absorption on the propagation angle. Our theory, being more general, explicitly takes into account absorption of photons scattered at different angles. Instead of assumption of totally randomized photons, the model can deal with any angular dependence of scattering, such as Lambertian in this paper. It can also accommodate a dependence on incoming beam incidence angle. Instead of treating the freestanding film, the sample is treated as bonded on the glass or sapphire slide, thus taking into account a practical problem of the light trapping in the supporting slide.

Given this photon gas model, the amounts of reflected and absorbed light can be calculated. Knowing the absorption spectrum of the film and its dispersion, one can obtain the full spectral dependence of absorbance of the textured semiconductor film bonded to a glass slide. Since the samples we studied contained various $Al_xGa_{1-x}As$ alloy layers, the absorption coefficient α and the refractive index n_f in the above formulas are average values weighted by the thickness of the corresponding layers. The calculated absorbance dependence for perfect Lambertian texturing is presented in Figure 3 along with the experimental curve. Two curves show good agreement leading us to believe that in the samples which have approximately 50% of the surface area covered by 0.25μm high mesas at least 90% perfect light randomization has been achieved.

We have studied light randomization and the absorption enhancement in textured ultra-thin $Al_xGa_{1-x}As$ films, with a thickness corresponding to a few optical wavelengths. A correlation between the degree of light randomization and trapping, with the scale length of the texturization geometry was found. The observed absorption enhancement corresponds to 90% of the best possible theoretical value, or 90% light randomization. A modified photon gas model is proposed to calculate the light trapping and absorption at the band edge in the textured thin films.

---

[1] X.Y.Lee, A.K.Verma, C.Q.Wu, M.Goertemiller, E.Yablonovitch, "Thin film GaAs solar cells on glass substrates by epitaxial lift-off", Procedings of 25th PVSC, May 13-17 1996, Washington D.C., pp.53-55.

[2] Deckman, J.N. Dunsmuir, "Natural lithography," Appl. Phys. Lett **41**, 377-379 (1982)

[3] H.Stewart, D. Hall, "Absorption enhancement in silicon-on-insulator waveguides using metal island films," Appl. Phys. Lett **69,** 2327-29 (1996)

[4] A. Krotcus. V. Pacebutas, J. Kavaliauskas, I. Subacius, K. Grigoras, I. Simkiene, "Light trapping effect in silicon wafers with anodically etched surfaces", Applied physics A, **64**, pp.357-60, Springer-Vesrlag, April 1997.

[5] Eli Yablonovitch "Statistical Ray Optics," J.Opt.Soc.Am. **72** ,899-907(1982).

[6] H.W.Deckman, C.R.Wronsky, H.Witzke, E.Yablonovitch, "Optically enhanced amourphous silicon solar cells," Appl. Phys. Lett. **42**, 968-970(1982),

[7] P.M. van den Berg, T.J.Fokkema, "The Rayleigh hypothesis in the theory of reflection by a grating," J.Opt.Soc.Am. **69**,27-31(1979).

[8] A.G.Voronovitch, Sov. "Small slope approximation in wave scattering by rough surfaces", Sov. Phys. JETP 62, 65-70(1985).

[9] E. Yablonovitch, R. Gmitter, J.P.Haribson, R.Bhat "Extreme selectivity in the epitaxial lift-off GaAs films", Appl. Phys. Lett. **51**, 2222-24(1987).

[10] M. Boroditsky, R. Ragan, E. Yablonovitch, "Absorption Enhancement in Ultra-Thin Textured AlGaAs films," to be published in Solar Energy Materias and Solar Cells, Elsevier Sciences.

Historically Black Colleges and Universities

Title: **Photovoltaic Applications in Developing Countries--Small Energy Requirements**

Organization: Office of Sponsored Research, Central State University, Wilberforce, OH

Contributors: C.W. Fuller, Principal Investigator
H.K. Evans, Student Research Associate

Background

The National Renewable Energy Laboratory's Historically Black Colleges and Universities (HBCU) Photovoltaic Associates Program provides undergraduate support for photovoltaic energy research and education at HBCU's. The aim is to attract qualified science, engineering, and business students toward pursuing a career in these areas with emphasis in photovoltaic technology. Central State University currently has three students participating in a three year program entitled, "Photovoltaic Applications in Developing Countries". The following data includes the results of research conducted by the student research associates during Year Three.

Objectives

The primary goal for FY 1998 was to involve Central State University students in renewable energy research activities to inspire them to pursue careers in the renewable energy industry. By using practical, hands-on research methods, student research associates were expected to gain a basic understanding of renewable energy systems.

Approach

Since 1991, the CSU Office of Sponsored Research has been involved in the installation of water pumping windmills in West Africa. In recent years, student research associates have examined the practicality of marketing hybrid (sun/wind) powered water systems in developing countries. To help diversify CSU's renewable energy device marketing efforts, student research associates have completed the installation of a hybrid powered FIASA water pumping windmill at CSU's renewable energy research site. CSU student researchers also worked closely with student research associates from Wilberforce University.

Through a NASA sponsored project called the "Consortium for Advancing Renewable Energy Technology (CARET)", four students from CSU participated in an Applied Renewable Energy Technology (ENG 450) course at Wilberforce University. Major course objectives included: assisting in the design and installation of two PV based energy systems, (one on Wilberforce University's campus, the other at Antioch University's Glen Helen Ecological Institute), the creation of a website that included highlights of work completed on the PV installations, and the completion of individual background reports regarding specific aspects of renewable energy technology.

Research Results

Test Site Construction and Installation , Central State University

As a carry over from the previous fiscal year, CSU student researchers continued to focus on marketing renewable energy devices. To strengthen marketing efforts, CSU students helped expand a renewable energy test site into a replica of facilities found in a West African village. A 100' by 100' area encompasses a 32' FIASA windmill, an animal trough, a battery bank, a garden area and a Windseeker II turbine. A gravity feed water storage tank and a custom fabricated PV panel support will be added later.

The FIASA windmill has a hybrid power capability as its submersible pump can be operated using wind power or DC power supplied by the PV array.

Determining Solar Resource, Glen Helen Ecological Institute (GHEI)

Solar resource refers to the approximate amount of sun hours received per day at specific geographic sites. This data was retrieved from a CD ROM produced by the Weather Bureau Army/Navy (WBAN).

Shading of a PV array must be avoided so that power output at the site can be maximized. Using a device called the Solar Pathfinder, it was possible to determine the percentage of sunlight lost due to shading, the causes of the shading, and the approximate path of the sun.

The Solar Pathfinder is a portable device that consists of: a tripod stand, a template holder with compass, sun path evaluation sheets, and a convex dome. When oriented towards true south and viewed from 12-18 inches directly above, the dome yields a reflection of the horizon that will show any shade causing obstructions. Using a sun path evaluation sheet, a tracing of the horizon with chalk reveals the approximate horizon. Areas below the chalk line indicate periods of prevailing sunshine. Areas above the chalk line represent areas of no sunshine. Once the sun path is determined, solar resource at the site can be evaluated.

On each sun path evaluation sheet, there are twelve contoured lines representing the horizon for the indicated month. On each contour line is a series of numbers that run from left to right and total 100. Numbers outside of the chalk line are added together per the month and reflect the percentage decrease in solar resource. Table 1 displays approximate power output data per month for the given amount of sun hours.

Month and proper panel inclination	JAN (LAT+15)	FEB (LAT+15)	MARCH (LAT-15)	APRIL (LAT-15)	MAY (LAT-15)	JUNE (LAT-15)
sun hrs/day	3.1	3.8	5.7	5.1	5.7	6.1
% sun received	60%	84%	87%	91%	91%	87%
kW hrs/day	4.46	7.66	11.90	11.14	12.45	12.74
	JULY (LAT-15)	AUG (LAT-15)	SEP (LAT-15)	OCT (LAT+15)	NOV (LAT+15)	DEC (LAT+15)
sun hrs/day	6.0	5.7	5.1	4.4	3.0	2.5
% sun received	90%	91%	91%	80%	59%	61%
kW hrs/day	12.96	12.45	11.14	8.45	4.25	3.66
avg kW hrs/day						9.44
avg kW generated						0.40

Table 1: Solar Resource Analysis and Estimated Power Production for Glen Helen Ecological Institute

The expected output for the solar array is determined to be 1200 W. This figure was derived using the following formula: ***Expected Output = rated PV panel output # of panels per module # of modules*** Plugging in the appropriate numbers, we have 75 W 8 panels 4 modules = 1200 W. If there is a day with one hour of 100% sunshine, the panel will theoretically produce 1200 w in that one hour. Power output will vary depending on the percent of sun received and the length of time the sun shines onto the panel. Because the panel won't receive 100% sunshine, power output will be modified. The actual power

output formula follows: *Actual Power Output (kWh per day) = Expected Output # of sun hours % of sunshine received*

Determining Loads

The PV installation at the GHEI site was primarily put in place to supply power to GHEI's Trailside Museum. For this reason, power demand at the site had to be assessed (Table 2). To find the average kW required per item (Table 2, column 6), it is necessary to use the following formula:
Avg kW = Total Watts per item # of hours item used per day/# of hours in one day

Item	# of items	Watts/item	Total Watts	hrs/day	avg kW	% of load
Main Lights	40	40	1600	6	0.40	35%
Outdoor Lights	4	90	360	12	0.18	16%
Hot Water Heater	1	1500	1500	2	0.13	11%
Refrigerator	1	800	800	3	0.10	09%
Secondary Lights	10	60	600	5	0.13	11%
Snake Rocks	5	15	75	24	0.08	07%
Aquarium Pumps	6	10	60	24	0.06	05%
Furnace	1	500	500	4	0.08	07%
Total			5495		1.15	100%

Table 2: Load Analysis for Trailside Museum at GHEI

Power Production vs. Demand

In order to determine how effective the PV installation is, it is necessary to compare electricity use per the utility with expected electricity production at the GHEI site. Because the initial power output data from Table 1 was in units of kW hours per day, they must be changed to kW hours per month. A 30 day month was used when converting from kW hours per day to kW hours per month. Table 3 graphically presents this information.

Month	Average Electricity Use, GHEI (kWh) (Historical Demand)	Average Electricity Production, GHEI array (kWh) (Projected Power Production)	% of Electricity Supplied by PV Array
January	944	133.8	14%
February	956	229.8	24%
March	800	357.0	45%
April	930	334.2	36%
May	931	373.5	40%
June	750	382.2	51%

Month	Average Electricity Use, GHEI (kWh) (Historical Demand)	Average Electricity Production, GHEI array (kWh) (Projected Power Production)	% of Electricity Supplied by PV Array
July	692	388.8	56%
August	877	373.5	43%
September	595	334.2	56%
October	696	253.5	36%
November	879	127.5	15%
December	740	109.8	15%
Average			36%
TOTAL	9790		

Table 3: Projected Power Production vs. Historical Demand

On average, the PV array will be able to provide almost 40% of Trailside's energy requirements.

Cost Savings

GHEI seeks to reduce their energy costs using a clean source of power while educating the public about the viability of PV technology. Cost savings at GHEI were calculated by taking the price of power at .06/kWh. Converting the number of kW hours used into dollar figures gives the initial energy cost . Multiplying the initial energy cost by the percentage of power supplied by the array per the month , the savings are calculated:
Cost Savings = (# of kW hours used per month electricity cost % of electricity supplied by PV array)

Total savings for the year are estimated to be a little more than $204. At this rate, a PV system like GHEI's, costing $7500, would pay for itself in approximately 37 years.

Summary

A nature preserve like GHEI is ideal to educate the public about PV technology. In order to maintain green areas like nature preserves, sustainable technology must be used. Most of the town's residents were initially against the PV installation for aesthetic reasons. After a series of town meetings highlighting PV technology's positive attributes, the people were swayed. Student research associates experienced the difficulty involved with convincing traditionalists to adopt PV technology. Most importantly, student research associates assembled a windmill, learned how to determine loads, and estimated PV array output per geographic location. The additions to the CSU/CARET renewable energy test sites will allow future visitors to experience a village type environment while emphasizing the crucial role of renewable energy.

Title: **A Progress Report on Photovoltaic Application Research at MVSU**

Organization: Natural Sciences Dept. Mississippi Valley State University
Itta Bena, MS

Contributors: B.S. Balam and W.C. Mahone, Principal Investigator, S. Green, T. Pierre, and A. Robinson

This report constitutes a summary of the current state of Photovoltaic undergraduate research at Mississippi Valley State University. Our program objectives at Valley are centered on three areas. That is generation, storage and utilization of generated electrical energy.

Our vision of a Photovoltaic array would consist of multiple rotating platforms. We are researching the energy advantages of maintaining optimal alignment between the panels and solar incidence. Measurements we have made with standard panels at various angles of solar incidence has shown that for off normal angles of 45 degrees and greater one may be losing more than 50 percent of the available solar energy. Additionally Islands can be dispersed over an area without the environmental impact of very large arrays. An example application of this idea is shown in the very large phased array radio telescope. Instead of using a single large telescope, a number of smaller telescopes were mounted on movable platforms and dispersed over a wide area (several miles). The radio profile of the array is essentially equivalent to that of a radio telescope with a several mile wide receiving dish. A solar panel is simply a receiver for solar radiation. The next question is can we experience significant savings after allowing for the energy requirements of the rotation system.

In addition to developing rotating platforms for optimal power generation, we want to develop ways of storing electrical energy for long periods of time and efficiently retrieving it when desired. We will look at ways of storing electrical energy as chemical energy through an electrolytic reaction. In our effort we plan to generate chemical precursors of hydrogen from the electrical energy. Then we will use a chemical process to generate the hydrogen when we need it. We believe that hydrogen can be generated at any desired rate from its precursors using the proper design.

We are also investigating fuel cell technology. Fuel cells are in extensive use in new technology and their applications are increasing. The hydrogen for most fuel cells in operation today comes either from hydrogen storage systems or from hydrocarbon fuel via reformer technology. In our research we generate hydrogen from active metals and use pH as a control mechanism. The data in figure 1 show that the time required for our reaction to generate a particular volume of hydrogen is a strong function of the pH. The lower curve is for 8.0-M acid addition. The higher curve is for the 1.2-M acid addition. Table1 shows that while it takes the 1.2-M addition 242 seconds to generate .2 L of hydrogen, the 8-M treatment can do it one-fourth the time. Our experiments have also shown that the pH of the reaction mixture can be changed easily and quickly. Experiments are underway which will allow us to investigate other dynamic factors associated with hydrogen output.

Also fuel cell operation depends intrinsically on the ability of ions to cross porous media. To understand this we are investigating ion mobility using secondary voltaic cells incorporating salt bridges. We made a simple copper zinc cell using a potassium nitrate salt bridge. We fabricated three identical salt bridges from glass tubing. Using identical salt bridges we can increase the conductivity between the two half cells in a reproducible manner. The Voltage and current behavior of the cell was investigated as a function of loading and as a function of the number of salt bridges. (See figure 2). The initial part of the plot shows the cell voltage near the standard potential of 1.1 volts. A 5k-ohm resistor was then placed across the cell. The cell is unable to maintain its standard voltage with this power drain and it drops to

about a third of its standard value. When the second salt bridge is added the voltage increases by nearly 1.5 volts. The third salt bridge only increases the by .5 volts. Then the resistance is increased from 5k-ohm to 10k-ohm, then to 15 k-ohm, to 100k-ohm and then to 1meg-ohm. We see that as the resistance is increased that with diminished current requirements the cell voltage returns to the standard value. Voltaic cells whose half cell are separated by a salt bridge are compatible with an application of Hittorfs method which will allow us to determine the ion mobility for different kinds of ions in different media. Our future goal is to modify the cell by using a proton exchange mechanism as the salt bridge. We will also construct our fuel cell for research purposes.

Students involved in this research have learned about solar power generation and solar power measurement from direct experimentation. Additionally they have learned many auxiliary skills like making power measurements on active devices, the fundamentals of applied electricity, interfacing data acquisition devices with computers and programming them to acquire data, some optics and some celestial mechanics. These students are in the upper range of students at valley in terms of grades, career motivation, and maturity. This work has certainly helped to excite them about careers in science.

Table 1. Hydrogen Generation Data

Volume H2(mL)	Time(s) Run I	Time(s) Run II	RUN	mg Mg (s)	M HCl
	0	0			
50	60	7	**I**	**240**	**1.2**
100	101	20			
125	126	27	**II**	**310**	**8.0**
150	**152**	36			
175	190	42			
195	230				
200	**242**	59			
225		75			
230		88			
250		98			
270		136			

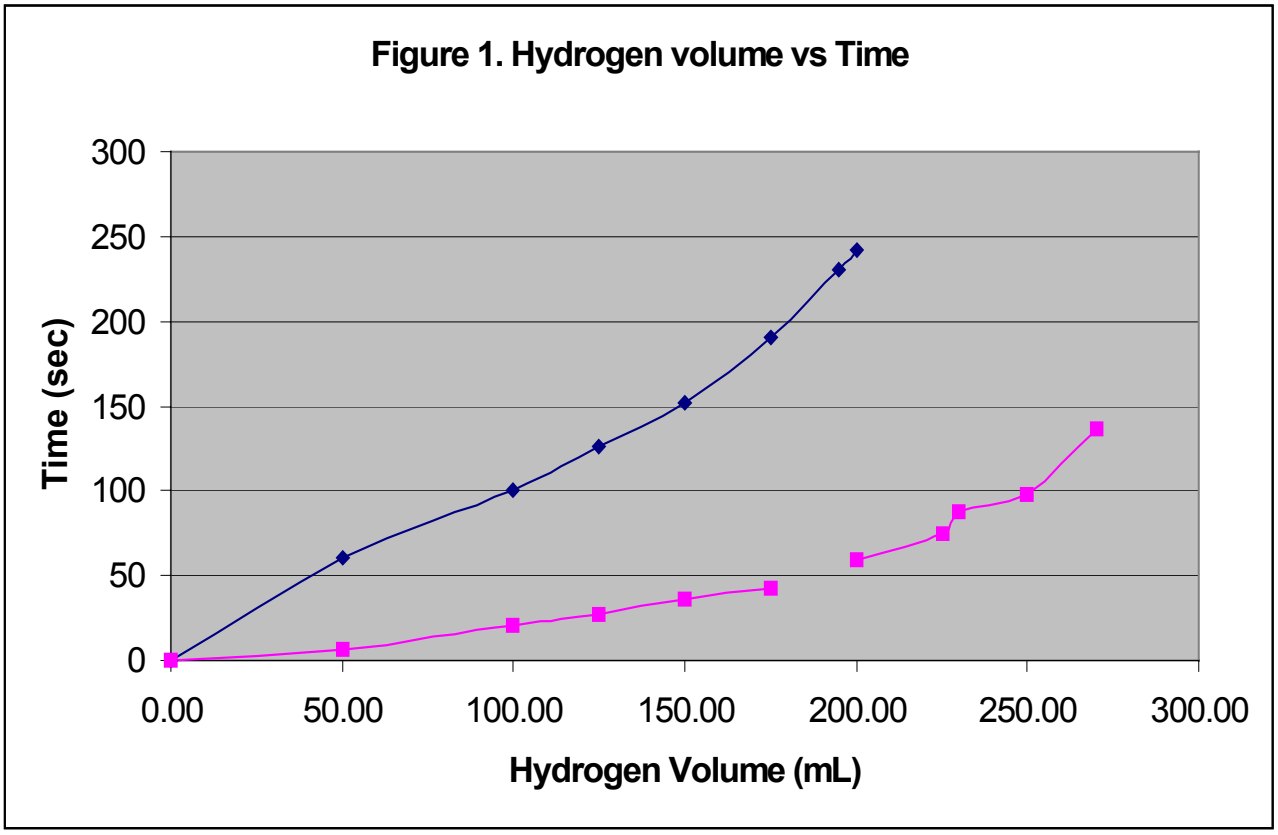
Figure 1. Hydrogen volume vs Time
300
250
200
150
100
50
0
Time (sec)
0.00
50.00
100.00
150.00
200.00
250.00
300.00
Hydrogen Volume (mL)

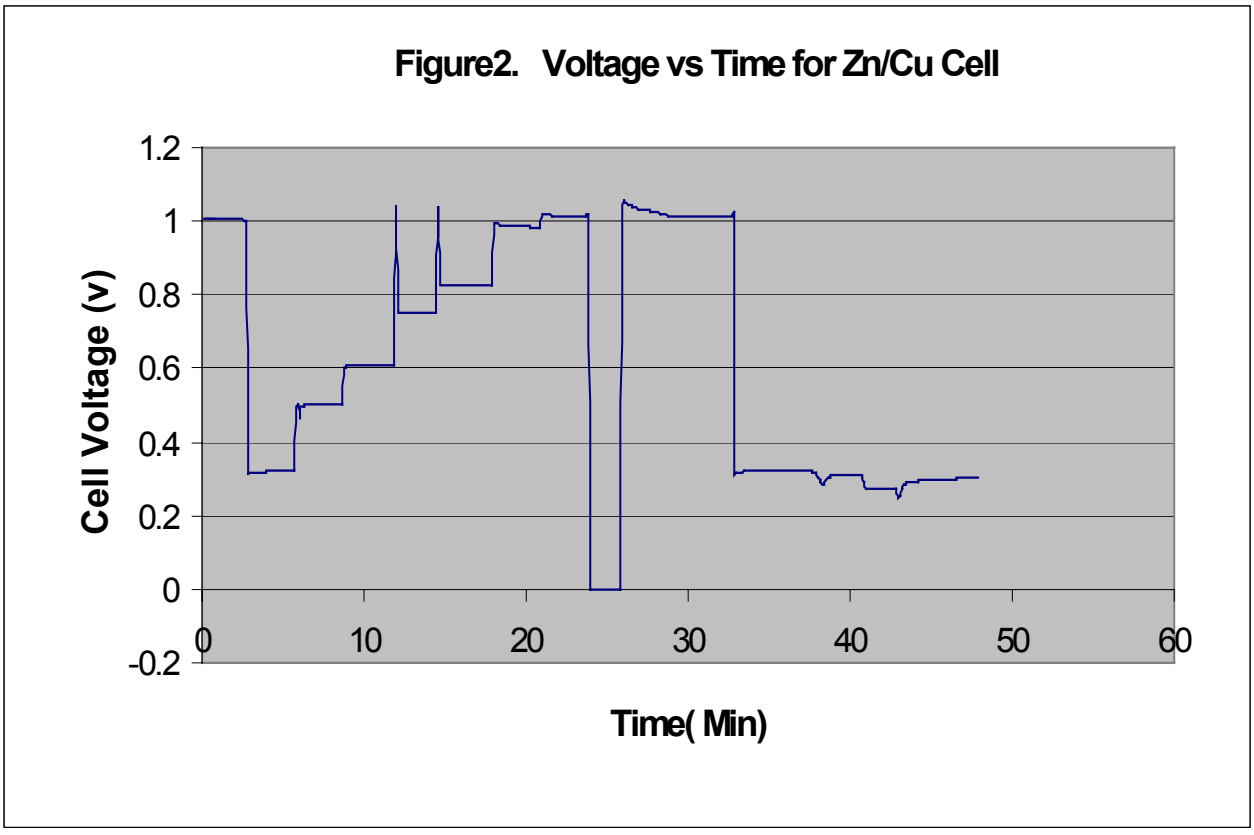
Figure2. Voltage vs Time for Zn/Cu Cell
1.2
1
0.8
0.6
0.4
0.2
0
-0.2
Cell Voltage (v)
0
10
20
30
40
50
60
Time(Min)

3.0 PV Electronic Materials and Devices Project

3.0 PV ELECTRONIC MATERIALS AND DEVICES PROJECT— Introduction

John P. Benner

The goal of the PV Electronic Materials and Devices Project is to establish competitive terrestrial PV technologies by developing electronic materials technologies and improved photovoltaic devices; advancing related science, engineering and research facilities to support continuing development; coordinating the allied efforts with our partners; and, facilitating commercialization.

The project includes tasks on High Efficiency Concepts and Concentrators, Amorphous Silicon, Copper Indium Diselenide, Cadmium Telluride, and New Ideas and User Functions. Within the project the tasks operate largely independently except for the last listed task that supports and coordinates activity in the clean room and other user facilities as well as draws upon the other tasks to guide future research. The thin film tasks all interact extensively (~20%) with investigations coordinated by the National Research Teams. Throughout the project we seek to balance our efforts in collaboration with industrial partners, applied research, and longer term investigations.

The degree of freedom presented by alloys and compound semiconductors yields the opportunity to develop solar cells and processing technologies that bypass constraints imposed by use of crystalline silicon – single bandgap with indirect transition, high growth and processing temperatures (>1000 C), exacting purity requirements, surface control, electronic activity of grain boundaries and dislocations, limited operation at higher intensities (< x200 suns), brittleness, and module design considerations such as operating voltage and hot-spot management. However, this degree of freedom comes at a substantial cost. These materials are more complex and lack the technology base and manufacturing infrastructure that has served silicon PV so well. The primary aim of the Electronic Materials and Devices Project is to build the foundation of knowledge in these materials systems and seek opportunities to expand the infrastructure through work with the PV industry, other electronics manufacturers, and equipment manufacturers. In order to accelerate the commercialization of these PV technologies, the NREL program must contribute in three areas. First, we must lead the development of the knowledge base and tools needed to understand and control these materials. Second, we apply our capabilities to assist industry and the National Research Teams in addressing current problems. Finally, we explore specific techniques and processes that anticipate improvements the industry will soon need.

FY1998 was an exciting year for the project with our teams demonstrating excellence in science, technology and technology transfer. American Physical Society News selected our work on vibrational properties of hot-wire Chemical Vapor Deposition (HWCVD) a-Si:H as a Physics Highlight. The model proposed in 1997 that provided an explanation for the metastability of amorphous silicon has passed peer review in the journals. Experiments in 1998 have provided evidence supporting the model. Our original work

in analyzing junction formation in CdS/CIGS and the CdS/CdTe interface is attracting attention from important groups pursuing similar approaches. Our investigations of 1 eV nitrogen bearing III-V alloys and solar cells appears to have stimulated a national adjustment of BES funded PV research to place greater emphasis on development of the bottom cell of a high efficiency stack. We set new PV efficiency records for advanced processes such as high-deposition-rate HWCVD a-Si:H, electrochemically deposited CIS, CIS on flexible stainless steel, and CdTe devices on conventional and novel conducting oxides. At the same time, our interactions with industry are becoming closer with more obvious benefit. In fact, NREL is now recognized as a leader in some aspect of each of these technologies.

The New Ideas and User Functions Tasks combine several of the activities that help to draw the Electronic Materials and Devices tasks together as a more cohesive and efficient project. For example, the Clean Room Task supports a core team that maintains the facility and coordinates the function of the large group of clean room users. In this way, the project gains efficiency in avoiding redundant purchases and operations as well as the technical improvement and cross-fertilization occurring during the Clean Room Users Group's meetings. In1998 investigation of nanostructured precursors for semiconductor deposition examined use of nanostructured Cu:HgTe for application in the graphite based contact to CdTe devices. These studies will continue in 1999.

PV Electronic Materials and Devices Project In-House Research

Title: **Development of Polycrystalline Cu(In,Ga)Se_2 Thin Films and Devices**

Organization: National Center for Photovoltaics (NCPV)
National Renewable Energy Laboratory, Golden, CO

Contributors:

Full Time	
R. Noufi, Principal Scientist and Team Leader	R. Bhattacharya, Senior Scientist
K. Ramanathan, Senior Scientist	J. Alleman, Master Technician
M. Contreras, Senior Scientist	W. Batchelor, student
F. Hasoon, Senior Scientist	B. Egaas, student
J. Dolan, Master Technician	H. Wiesner, Graduate Student
J. Keane, Master Technician	

Objective:

We seek to advance the development of CIS-based PV toward commercialization, and broaden the knowledge base of the material science and device physics.

Technical Approach:

We addressed the following technical problems:

(1) Demonstrate progress in developing CIGS absorber processing for potential manufacturing. The processes we addressed with varying degrees of emphasis were electrodeposition and sputtering
(2) Understanding of Junction formation and the development of an alternative junction; i.e., a direct ZnO/CIGS junction with no CdS buffer layer.
(3) The interaction of the glass/Mo substrate with the CIGS absorber and the affect on device performance.
(4) Partnership with industry to transfer knowledge and know-how relative to the CIS technology.

Results:

Process Development

CIGS From Sputtered Precursor: The CIS team has a long history of investigating various approaches towards CI(G)S absorber formation. One promising route being pursued has been via two-stage processes employing various precursor structures and subsequent recrystallization steps. Recently a new two-stage approach has been proposed and realized using the mulitchamber cluster tool. This particular pathway includes a novel sputtered Cu-In-(Ga)-Se precursor subsequently subjected to a recrystallization step. To date, the best CIS-only device of 0.43 cm^2 nominal area - without an AR-coating - yielded the following parameters: V_{oc} = 407 mV, J_{sc} = 34.77 mA/cm^2, FF = 66.95%, and

η = 9.48%. The best CIGS device was confirmed **13%** efficient, V_{oc} = 0.536V, J_{sc} = 34.65 ma/cm^2, FF = 70.1%. The particular emphasize of this work is on development of an industrially viable process, i.e., large-area, low-cost, high-throughput, and high-quality CI(G)S deposition. Current efforts focus on optimizing the process conditions for both materials (i.e., CIS and CIGS) and characterization of the obtained materials and devices. Details of the process will be discussed at a later date after it clears the patent disclosure process.

CIGS from Electrodeposited Precursors: We have fabricated **14.1%** efficient $CuIn_{1-x}Ga_xSe_2$ (CIGS) based devices from electrodeposited precursors. As-deposited precursors are Cu-rich films and are polycrystalline in nature. Additional In, Ga, and Se were added to the precursor films by physical evaporation to adjust the final composition to $CuIn_{1-x}Ga_xSe_2$. Addition of In and Ga and also selenization at high temperature are very crucial for obtaining high-efficiency devices. The X-ray analysis of the as-deposited precursor film indicates the presence of CIGS and Cu_2Se phases. The X-ray analysis of the film after adjusting the composition of the final film shows only the CIGS phase. The films/devices have been characterized by inductively coupled plasma spectrometry, Auger electron spectroscopy, X-ray diffraction, electron-probe microanalysis, current-voltage characteristics, capacitance-voltage, and spectral response. The parameters of the device are V_{oc} = 0.656, J_{sc} = 29 ma/cm^2, and FF = 74.1%.

CIGS from Electroless Deposited Precursors: The device fabricated using electroless Cu-In-Ga-Se (CIGS) precursors resulted in an efficiency of **10.5%** (V_{oc} = 0.6262 V; J_{sc} = 24.19 mAcm^{-2}; Fill Factor = 69.37%). The quality of CIGS-based films and devices prepared from electroless precursors is very promising. This may lead to novel and low-cost methods for absorber fabrication. Process details will be given after the patent disclosure procedure is concluded

ALTERNATIVE JUNCTION FORMATIONS

The nature of the interface between $CuInSe_2$ (CIS) and the chemical bath deposited CdS layer has been investigated. We show that heat-treating the absorbers in Cd- or Zn- containing solutions in the presence of ammonium hydroxide sets up a chemical reaction which facilitates an extraction of Cu from the lattice and an in-diffusion of Cd. The characteristics of devices made in this manner suggest that the reaction generates a thin, n-doped region in the absorber, creating a CdS/$CuInSe_2$ device with a buried, shallow junction with a CdS window layer, rather than a heterojunction.

Figs. 1 and 2 show a profile of the Cd incorporation in the CIGS thin film and single crystal. Zn incorporation also shows similar profile (not shown). These results were also confirmed by X-ray photoelectron spectroscopy (XPS) and photoluminescence (PL). The creation of a thin, heavily doped n-region can explain much of the observed phenomena. In a CdS device, the electric field will be supported entirely, or mostly, by this n-region, depending on the doping level. It is also quite possible that the Cu-deficient nature of the surfaces present natural sites for the occupation by Cd. In any case, we find that an enhanced n-doped region is more likely the heart of the device, rather than the CdS layer

itself. The latter undoubtedly offers the benefits of passivation and excellent lattice-matching, and it shields the absorber from ZnO and sputter damage. The foregoing discussion applies equally well to Zn as we have demonstrated with the Zn treated device. Fig. 3 shows the spectral response of devices treated with a Zn or Cd-solution. The gain in the blue region is obvious and substantial as compared to a CdS-containing device..

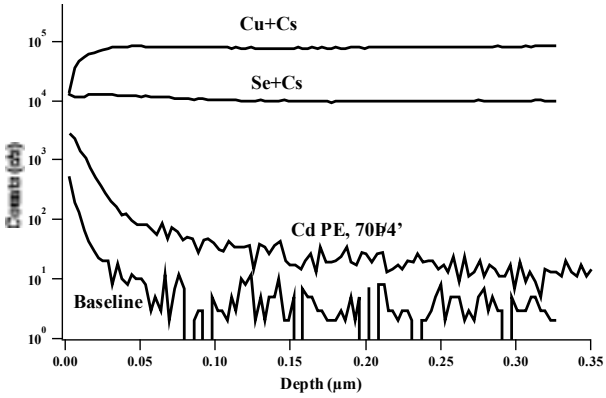

Fig. 1: SIMS profile of Cd, Cu, and Se in $CuInSe_2$ thin films. Baseline refers to the as-grown film. The Cd PE treatment was done at 70˚C for 4 min.

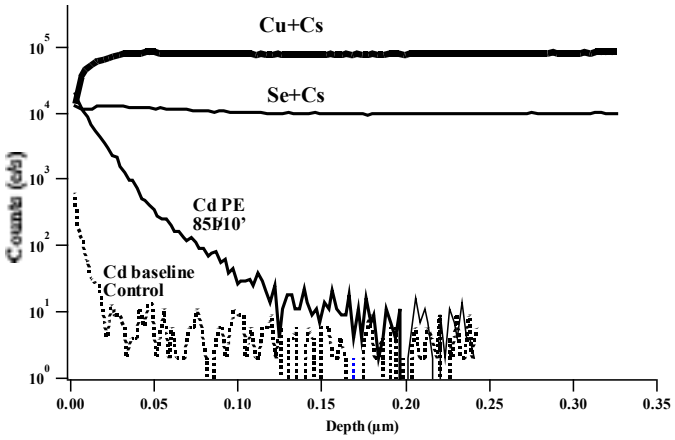

Fig. 2: SIMS profiles of Cd, Cu, and Se in as-grown and CdPE treated $CuInSe_2$ single crystals.

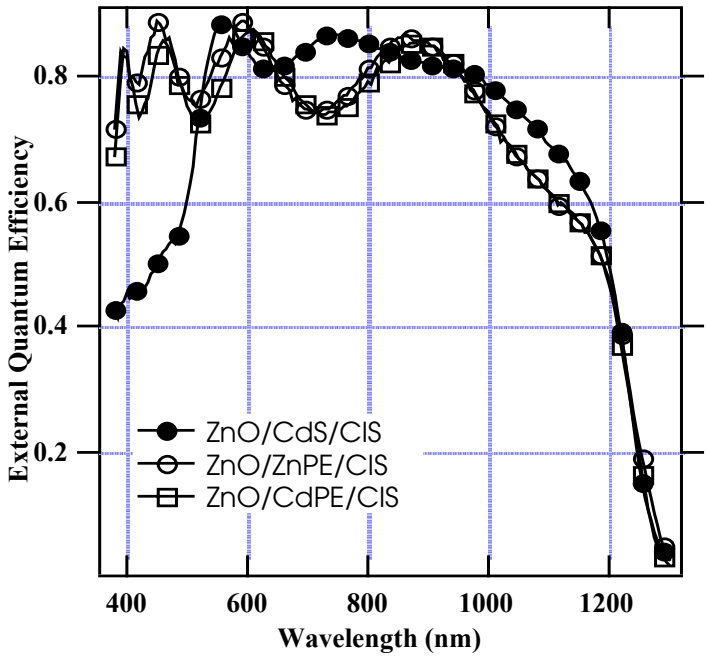

Fig. 3: Spectral response of the $CuInSe_2$ devices shown in Fig. 1. Measured before AR coating.

Alternative Junction Strategy: From a practical viewpoint, it would be most desirable to replace the wet chemistry step of fabricating CdSwith a vacuum process step. A second objective is the replacement of Cd to make the devices environmentally friendly. The ultimate goal is to make this the final step of the absorber preparation such that the entire processing can proceed in a seamless manner.

Our approach is to develop methods for forming an n- type, emitter region by extrinsic doping. The most obvious candidates appear to be the II_B elements substituting for Cu; IV elements for the In or Ga; and the halogens for the Se atoms. The efficiency of the Cd "doping" suggests that Zn is the logical choice. We have experimented with a variety of Zn sources, including elemental Zn. $ZnCl_2$ was chosen as the best candidate because of its low melting point and high vapor pressure at 200˚C. The method of delivering the $ZnCl_2$ to the absorber surface has been varied. The best result obtained by contact annealing $ZnCl_2$, described in the experimental section, is a 13.5% efficiency device, and it did not require a light soak or heat treatment to realize the efficiency. The parameters of this device are: V_{oc}= 0.527 V, J_{sc}= 36.01 mA.cm^{-2}, and FF = 0.71**. At the time of writing this paper, we have also fabricated a 14.2% device by optimizing the aqueous Zn PE treatment described above**. The above methods are viewed as temporary solutions that help establish our understanding of the junction formation, and they will be instrumental in the development of completely "dry" methods such as close-spaced annealing to make the processing more suitable for manufacturing. The current focus is to increase V_{oc} to obtain larger than 16% efficiency

The Impact of Na on the Performance of CIGS-based Devices

We, and others have shown that Na originating at the soda lime glass substrate migrates through the Mo back contact and incorporates in the CIGS absorber during growth. We

have deliberately incorporated Na during growth and studied the effects. Below we summarize our results.

Positive trends are observed in V_{oc} and FF. These results are manifested through increase in hole density. An optimum concentration of Na is centered around 0.1 at % which depends on the CIGS processing conditions. Most of the Na resides in grain boundaries.

The role of Na is proposed using two possible models:

1. Based on X-ray photoelectron spectroscopy (XPS) measurements, the most plausible interpretation of the data points to Na occupying In and/or Ga sites; i.e., Na_{In} and/or Na_{Ga}. These point defects act as double acceptors or compensate donors. This mechanism is mostly active at grain boundaries and internal surfaces. As a result, the Fermi level should move closer to the CIGS valence band maximum.
2. The incorporation of Na "annihilates" donor states stemming from the In_{Cu} anti-site. During growth, Na and In (and/or Ga) compete for a Cu site. Na is more likely to reside on the Cu site, therefore altering the number of defect pairs ($2V_{cu}$- In_{cu}). This model is based on XRD and photoluminescence measurements. If too much Na is incorporated, then $NaInSe_2$ secondary phase will form.

Both models are consistent with the experimental observations and both may impact the point defect pairs that are considered most likely to affect the carrier concentration in CIGS, i.e., the [$2V_{Cu}$-In_{Cu}] pair and the (Cu_{In}-In_{Cu}) pair.

Activities with the CIS National Team

We demonstrated progress in several areas as a result of focused teaming:

1. We explained the role of CBD CdS in the CIGS device based on experimental observations.
2. The interaction between the absorber and the glass/Mo substrate, especially as influenced by the Mo deposition conditions.
3. New understanding toward engineering a direct CIGS/ZnO junction

For more details, the reader is referred to a summary by the team dated April, 1998.

Technology Transfer/Industry Interaction

1. Optical Coating Laboratory (OCLI). Under an 8-month contract, we have transferred know-how of CIGS processing. NREL has confirmed a 15.1% cell efficiency, and a 8.3% AM 1.5 submodule. NASA confirmed this submodule (on 8 mil. Glass) at 7.8% AMO.
2. DayStar Technologies: The objective is to transfer the CIS technology to novel cell geometry/structure, which operates under moderate concentration. DayStar has demonstrated submodule approaching 9% efficiency.
3. We had substantial interaction with Global Solar Energy and ISET related to their planned effort of commercialization.

Title: **High-Efficiency Concepts and Concentrators**

Organization: National Renewable Energy Laboratory, Golden, CO

Contributors: Dan Friedman, John Geisz, Alan Kibbler, Charlene Kramer, Sarah Kurtz, Bill McMahon, Jerry Olson, Brian Keyes, Pat Dippo, Robert Reedy, Keith Emery, Halden Field

Objectives

- To establish III-Vs as a competitive terrestrial photovoltaic (PV) technology by developing III-V photovoltaic technologies, advancing related science and engineering, coordinating the allied efforts with our partners, and facilitating commercialization.
- To develop III-V concentrator cells and support the transition of III-V concentrator-cell technology to industry for future U.S. utility market needs.
- To reduce the cost of III-V cells in order to address lower concentration systems and, ultimately, to be able to achieve flat-plate costs.

Results

High-efficiency concept

The success of the $Ga_{0.5}In_{0.5}P$/GaAs tandem cell was further recognized this year by the 1998 IEEE Electrotechnology Transfer Award. The production volume of these cells continued to grow. Spectrolab reported on production of more than 250 kW of GaInP/GaAs/Ge dual-junction cells (1). NREL signed an agreement with TECSTAR licensing them to manufacture and sell the $Ga_{0.5}In_{0.5}P$/GaAs cells (2).

Perhaps the most exciting thing about this technology is the possibility of adding more junctions and achieving higher efficiencies (3). Fig. 1 shows some of the designs that are under study and their theoretical and estimated "practical" efficiencies. The more complex of these structures highlight the utility of the GaInAsN alloy that can be grown with a band gap of 1 eV and a lattice constant essentially equal to that of GaAs.

Optimization of GaInAsN material

Growth of the GaInAsN alloy began in September of 1997. Using dimethylhydrazine as the nitrogen source, this alloy is relatively easy to grow with an appropriate band gap and lattice constant (see Fig. 2) (4,5). Theoretical studies have predicted that nitrogen is not very soluble in single-crystal GaAs. Reports in the literature imply that the 1%-3% levels of nitrogen that are needed to achieve the desired band gap and lattice constant are not thermodynamically stable. The desired composition can be reached if low growth temperatures and relatively high growth rates are used to essentially "trap" the nitrogen into the material.

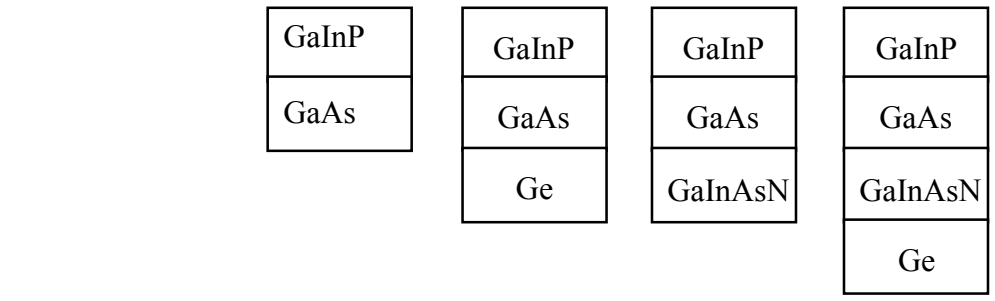

Theoretical efficiency	36%	42%	47%	52%
Practical efficiency	29-32%	34-38%	33-38%	36-42%

Figure 1. Theoretical and practical efficiencies of 2-, 3-, and 4-junction concepts assuming 500 suns irradiance and an AM1.5Direct spectrum. The practical efficiencies are taken to be 80%-90% of the theoretical efficiencies for the two simpler structures and 70%-80% of theoretical for the more challenging structures. A 30% efficiency has been achieved for the two-junction structure.

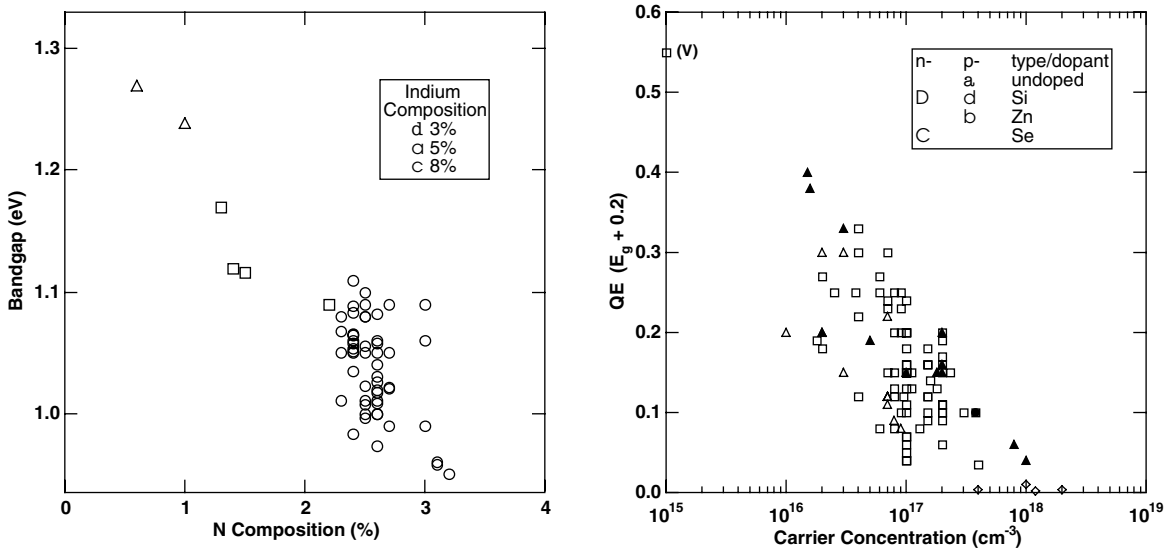

Figure 2. Bandgap of $Ga_{1-y}In_yAs_{1-x}N_x$ as a function of nitrogen composition, x, determined from x-ray data for indium compositions y = 3% (d), 5% (a), and 8% (c). Only data from nearly lattice-matched layers are shown.

Figure 3. The quantum efficiency of $Ga_{1-y}In_yAs_{1-x}N_x$ taken 200 meV above the bandgap as a function of carrier concentration. A variety of dopants and carrier type are plotted with different markers. All data shown are from layers with $E_g < 1.15$ eV. The point marked (V) was annealed under an As_2 flux in UHV.

GaInAsN samples were grown under a wide range of conditions. The hole concentration for nominally undoped material was typically measured to be about 1 X 10^{17} cm^{-3} (see squares in Fig. 3). This relatively high background hole concentration may be related to carbon contamination. The same growth conditions that "trap" excess nitrogen in the layers also cause trapping of other contaminants including carbon (which is present in large quantity in the growth system because precursors contain carbon) and oxygen (which is mostly excluded from the growth system).

Although the GaInAsN can be grown with excellent crystallographic quality, the electronic quality is poor. In order to quickly evaluate a large number of samples, a Polaron profiler was used to measure the photocurrent as a function of the photon energy. An example of this data is shown in Fig. 4. The line shows the photocurrent expected if carriers are collected from the 0.1-μm-thick depletion region. Fig. 5 compares the depletion width measured from capacitance-voltage (CV) measurements with the photocarrier-collection width measured from the quantum efficiency measurement, showing that carriers are collected only from the field region and not significantly from the flat-band region of the sample. Thus, we conclude that, for the wide range of conditions that we explored, the minority-carrier diffusion length is less than the depletion width.

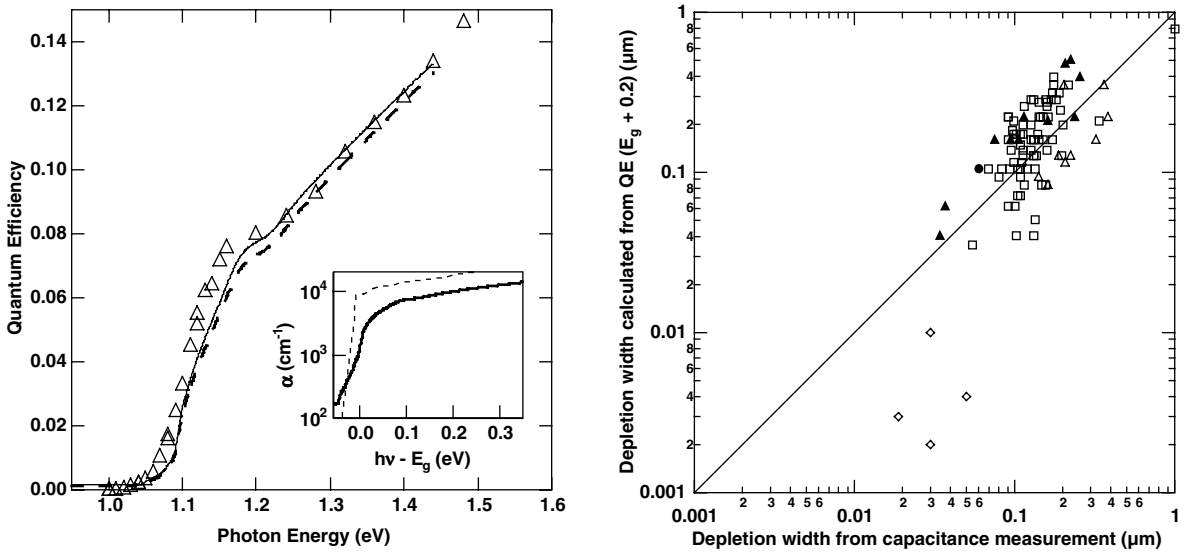

Figure 4. Quantum efficiency spectrum of a $Ga_{0.92}In_{0.08}N_{0.03}As_{0.97}$ layer. Points are data ; the lines are calculated. The inset graph is the absorption coefficient of $Ga_{0.92}In_{0.08}N_{0.03}As_{0.97}$ (solid line) and GaAs (dashed line).

Figure 5. The collection width calculated from quantum-efficiency data as in Fig. 3 as a function of the depletion width calculated from the measured capacitance of the junction. The dopants and carrier types are plotted with markers shown in the legend of Fig. 3.

The majority-carrier transport was investigated by measuring the Hall effect as a function of temperature as shown in Fig. 6. The Hall mobility is strongly dependent on the sample preparation. The carrier mobilities and carrier concentrations both changed after annealing. All of the mobilities are significantly less than typical room-temperature mobilities observed for GaAs (400 cm^2/Vs for holes and 8500 cm^2/Vs for electrons.) The one sample with the best hole mobility had a smaller nitrogen concentration and, therefore, a larger band gap. The very short minority-carrier diffusion lengths are partly a result of the reduced mobility, but appear to be more strongly degraded by a short minority-carrier lifetime.

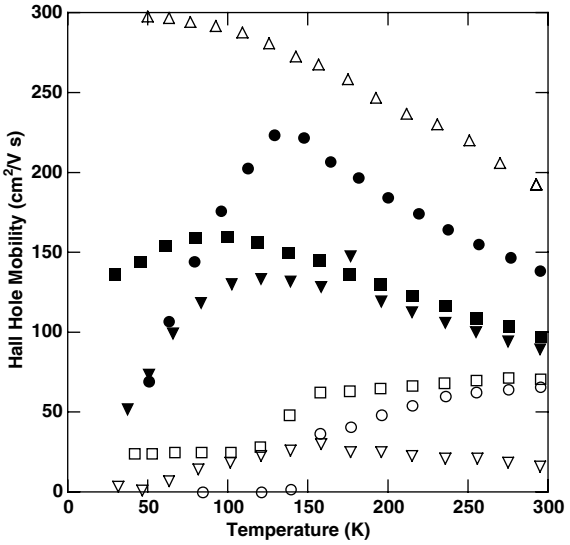

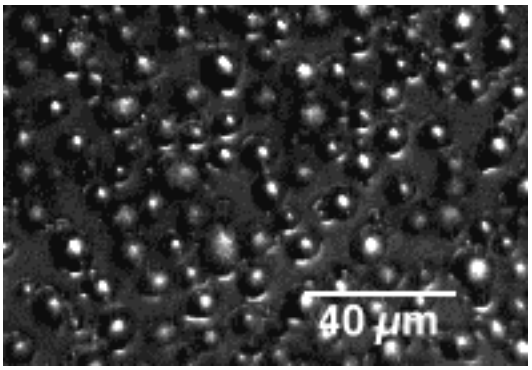

Figure 6. Temperature dependent Hall hole mobility data of $Ga_{0.92}In_{0.08}N_{0.03}As_{0.97}$.
Tg = 580°C, atm. pressure (○) as grown (●) annealed 650°C under N_2
Tg = 580°C, atm. pressure (□) as grown (■) annealed 700°C under UHV As_2
Tg = 560°C, low pressure (▽) as grown (▼) annealed 800°C under AsH_3/H_2
Tg = 650°C, atm. pressure (△) as grown $Ga_{0.95}In_{0.05}N_{0.01}As_{0.99}$.

Figure 7. Nomarski micrograph of GaInTlP surface for a layer grown at 350°C. Note the metal droplets.

Studies of other materials

In the literature have appeared reports that thallium can be used to grow an alloy that is lattice matched and has a band gap of 1 eV. Our attempts to duplicate the reported results were unsuccessful (6). Fig. 7 shows an example of the material obtained when thallium is added to the growth. At relatively low growth temperatures, thallium droplets were observed; at higher temperatures the droplets disappeared, but no evidence of thallium incorporation in the crystalline layer could be found.

Optimization of GaInAsN devices

Even with the poor quality of the GaInAsN alloy, a respectable device may be achievable if the design is optimized for the material quality (7,8). Fig. 8 compares the performance of a device grown with the conventional design (normally used for a high quality GaAs cell) with a design that improves the photocurrent collection. For the modified structure, the base doping is reduced in order to provide an electric field across a significant fraction of the device. The increase in field-aided collection results in a larger short-circuit current, but a reduced open-circuit voltage and fill factor, as expected. Although further optimization of the device performance is likely to result in slight improvements in the device, it is unlikely that the theoretical performance can be approached unless the material quality can also be improved.

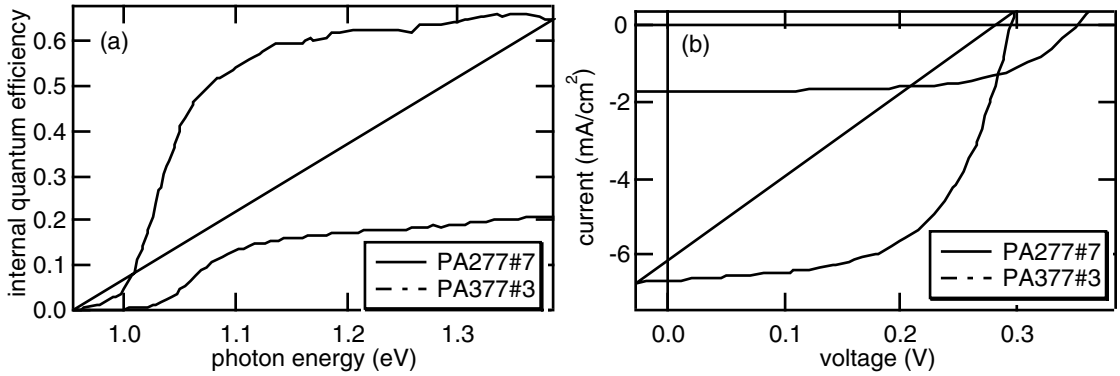

Figure 8. (a) Comparison of the internal quantum efficiency for device PA277#7, which has an n=10^{17}/cm^3 conventionally doped base, and device PA377#3, which has an n=5×10^{15}/cm^3 lightly doped base. **(b)** Comparison of the IV curves for PA277#7 and PA377#3.

Study of Ge surfaces

In addition to developing the new GaInAsN material, a key to fabricating the device structures shown in Fig. 1 is an understanding of the growth of GaAs on Ge. Although reports of growth of GaAs on Ge have appeared in the literature for years, the procedures used for growth in one chamber are not well understood and are often not transferable to other growth chambers. This study of germanium surfaces, undertaken as a collaborative project with Basic Energy Sciences, has led to significant understanding of the effects of arsenic exposure on germanium surfaces (7). Two sources of arsenic have been considered: As_4 and AsH_3. The choice of arsenic source affects both surface cleanliness and surface morphology. If a germanium surface is annealed under an As_4 flux, oxygen will be removed, but carbon contamination will not. Annealing under AsH_3 removes both oxygen and carbon contamination. Therefore, some AsH_3 exposure is desirable. Unfortunately, excessive AsH_3 exposure can have a negative effect on the surface morphology. As can be seen in Fig. 8, by annealing under an As_4 flux it is possible to obtain a single-domain surface with regularly spaced steps. Annealing the same surface under a high AsH_3 flux creates a less-desirable two-domain surface with bunched steps,

as seen in Fig. 9. This difference in surface morphology can be explained by the fact that AsH_3 etches germanium, while As_4 does not.

These results suggest that the AsH_3 exposure can be reduced and optimized to create carbon-free germanium surfaces with minimal step-bunching. In fact, the best GaAs/Ge interfaces are formed when the AsH_3 flux is very small prior to and during nucleation of GaAs. This result is somewhat unexpected, since one uses high fluxes of arsine or phosphine to grow III-V layers with specular morphology. For this reason, the reduced AsH_3 flux is only beneficial prior to and during GaAs nucleation. Once the germanium surface is fully covered with GaAs, it cannot be etched by AsH_3, and the remainder of the GaAs film should be grown at a higher AsH_3 flux.

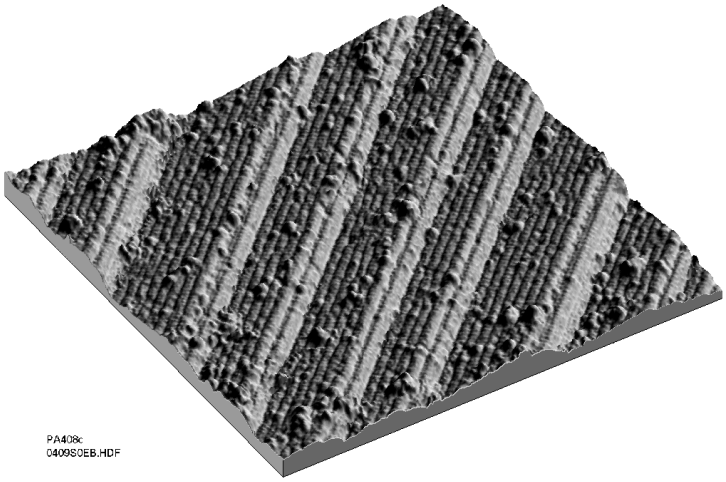

Figure 9. STM image of a Ge(100) surface miscut 6˚ towards (111) and annealed under arsenic and hydrogen. Dimer rows run parallel to step edges.

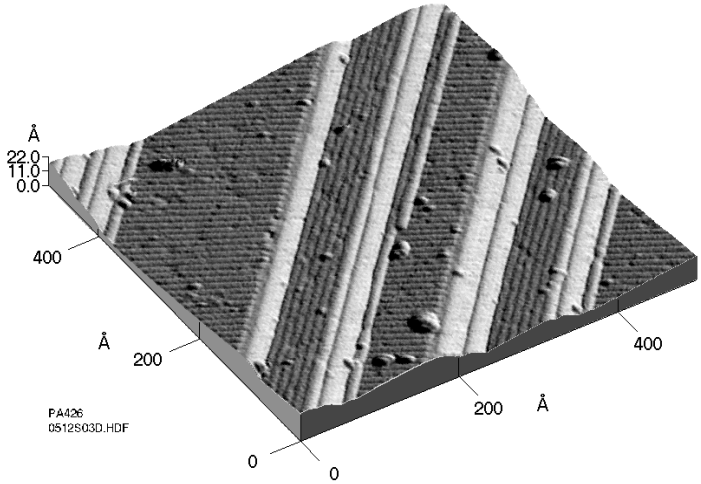

Figure 10. STM image of a Ge(100) surface miscut 6˚ towards (111) and annealed in AsH_3 at 640˚C for 15 min. The surface is two-domain with dimer rows both parallel and perpendicular to the step edges. The steps are bunching to form facets. The step bunching process is facilitated by a slow AsH_3 etching of the Ge.

References

1. Cavicchi, B. T., J. H. Ermer, D. D. Krut, D. E. Joslin, M. S. Gillanders and D. K. Zemmrich, "250,000 Watts of $GaInP_2$/GaAs/Ge Dual Junction Production," in *Proceedings of the 2nd World Conference on PV Energy Conversion*, 1998.
2. Kurtz, S. R. and D. J. Friedman, "Concentrator and Space Applications of High-Efficiency Solar Cells – Recent Developments," in *Proceedings of the NREL/SNL Review Meeting*, 1998.
3. Kurtz, S. R., D. Myers and J. M. Olson, "Projected Performance of Three- and Four-Junction Devices using GaAs and GaInP," in *Proceedings of the 26th IEEE Photovoltaic Specialists Conference*, 1997.
4. Geisz, J. F., D. J. Friedman, J. M. Olson, S. R. Kurtz and B. M. Keyes, *J. Cryst. Growth* (1998).
5. Geisz, J. F., D. J. Friedman, J. M. Olson, C. Kramer, A. Kibbler and S. R. Kurtz, "New Materials for Future Generations of III-V Solar Cells," in *Proceedings of the NCPV Review meeting*, 1998.
6. Friedman, D. J., S. R. Kurtz and A. E. Kibbler, "Exploration of GaInTlP and Related Tl-containing III-V Alloys for Photovoltaics," in *Proceedings of the NREL/SNL PV Program Review Meeting*, 1998.
7. Friedman, D. J., J. F. Geisz, S. R. Kurtz and J. M. Olson, *J. Cryst. Growth* (1998).
8. Friedman, D. J., J. F. Geisz, S. R. Kurtz and J. M. Olson, "1-eV GaInNAs Solar Cells for Ultrahigh-Efficiency Multijunction Devices," in *Proceedings of the 2nd World Conf. on Photovoltaic Energy Conversion*, 1998.
9. Olson, J. M. and W. E. McMahon, "Structure of Ge(100) Surfaces for High-Efficiency Photovoltaic Applications," in *Proceedings of the 2nd World Conf. on Photovoltaic Energy Conversion*, 1998.

Title: **Hydrogenated Amorphous Silicon Device Research**

Organization: NREL In-House Amorphous Silicon Research Team
National Renewable Energy Laboratory, Golden, CO

Contributors: H. M. Branz (Team Leader), R. S. Crandall, S. Heck, E. Iwaniczko, H. Mahan, B. P. Nelson, J. Thiesen, Q. Wang, Y. Xu

Objectives

The NREL Amorphous Silicon Team pursues breakthrough advances in materials and devices in order to improve the stabilized efficiency of amorphous-silicon-based PV cells and meet DOE PV cost goals. During FY '98, our objectives were to understand and overcome the light-induced degradation of hydrogenated amorphous silicon (a-Si:H), and to develop hot-wire (HW) CVD amorphous silicon for use as the midgap and lowgap cells of a triple junction amorphous-silicon-based solar cell. We collaborate closely with PV industry and academic collaborators through participation in and direction of the National Amorphous Silicon Teams.

Hot-wire n-i-p device fabrication

Having shown that they can produce 7-8% efficient stable amorphous silicon PV in medium-sized (5-10 MW/yr) plants, the amorphous silicon industry has focussed its attention recently on higher a-Si:H deposition rates. In the production environment, rapid deposition increases PV module production rates and reduces the capital cost per delivered watt. The longest deposition times have been needed to deposit the active semiconductor i-layer, so this is the most important layer to grow at a high rate.

The NREL Amorphous Silicon Team, in collaboration with United Solar Systems Corp., has set a new standard for high deposition rate amorphous silicon PV cells.[1] We used the hot-wire deposition technique to deposit the a-Si:H active layer. In this technique, silane is thermally decomposed onto a substrate by a 2000°C tungsten filament. For the cell, we deposited a thin n-layer by the standard PEVCD technique and a 2100Å i-layer by hot-wire onto a stainless steel substrate roughened and coated for high reflectivity by USSC. USSC finished the cell with a p-type microcrystalline layer and a transparent conductive top contact - and made the efficiency measurements. NREL deposited the cell's active layer at 16 Å/s and the initial solar conversion efficiency is 9.8%. After 1000 hours AM1 light-soaking, the efficiency of the cell falls to 7.7%.

Previously, no group had exceeded 9% efficiency in cells deposited more rapidly than 6 Å/s from low-cost precursor gas, and the industry typically deposits a-Si:H using PECVD at about 1 Å/s in production. Deposition of a 2000-Å i-layer by the standard industrial technique would take about 35 min. We deposited the active semiconductor layer of our cell in only about 2 minutes.

We have also dramatically improved the reproducibility of NREL's hot-wire deposition process. This has resulted in corresponding improvements in reproducibility of the HW devices we fabricate in-house. Previously, there was a problem with hot-wire tungsten filament degradation over time; this necessitated frequent filament changes that hurt run-to-run consistency. We believe that the degradation results from growth of a tungsten-silicide layer at the outer surface of the filament, especially at the cold filament ends. This would change the temperature of the filament and create other problems. We recently developed a new treatment in which we

introduce hydrogen gas into the system and break it into atomic H with the hot wire. This etches Si from the filament and the chamber and improves reproducibility. Poor reproducibility of results always slows device development; this improvement will allow us to more clearly determine the efficacy of process changes we implement.

We have successfully deposited 33 solar cells without changing the filament or cleaning the chamber. This was achieved by making 3 filament etch treatments. The low-light fill factor (FF) of nearly every baseline cell we make remains between 0.65 and 0.70. Without the treatment, baseline fill factors often fell below 0.60 and remained acceptable for only 8 depositions or fewer from one filament. After that, we needed to change filaments in order to maintain baseline efficiency.

As a result, we have made our best HW solar cell deposited entirely in-house, with an initial efficiency of 8%. The cell i-layer was grown at 16-18 Å/s. The best cell we have made in collaboration with Uni-Solar was deposited at the same high rate and showed an initial efficiency of 9.8%. We would need further improvements in our in-house p-layer and transparent conductor layer to equal the collaborative cell efficiency.

Staebler-Wronski metastability model

For twenty-three years, the Staebler-Wronski effect [2] has been a stumbling block to amorphous silicon PV reaching it's full potential. Our new microscopic model of light-induced metastable defect formation gives new vitality to the effort to understand the effect - and hopefully to eradicate it. The "H collision model" of a-Si:H metastability accounts quantitatively for the kinetics of defect creation and annealing by treating the light-induced emission and retrapping processes for mobile atomic H. For the first time, nearly all experimental results concerning the Staebler-Wronski effect can be understood within a single model.

A comprehensive 15-page paper entitled "Hydrogen collision model: Quantitative description of metastability in amorphous silicon," by H. M. Branz will appear in the 15 Feb. 1999 issue of the Physical Review B. [3] The work will appear back-to-back with a second paper that describes results of a light-induced H diffusion experiment to measures emission rates of H. [4]

During FY '98, we also obtained experimental confirmation of an important prediction of the "H collision" model. Extensions of the present experiment will enable us to measure key parameters of the model. With our confidence in the H collision model increasing, we will direct more work toward testing new ideas (based upon the model) for improving a-Si:H stability.

We degraded hydrogenated amorphous silicon (a-Si:H) using light pulses of 40 microsec to 2 millisec. Metastable photoconductivity degradations from pulsed light were compared to degradation with continuous light of the same intensity and same accumulated exposure time. Pulses were obtained by mechanically chopping a red light beam of 150 mW/cm2 intensity. Remarkably, for a given integrated exposure time, we observe higher photoconductivities (by up to 50%), as we shorten the pulses. For example, to obtain the same amount of degradation with 100 microsec pulses as with continuous illumination, the integrated sample exposure time to the pulses must be doubled. We conducted experiments to exclude thermal effects and other possible artifacts.

Our experiments show that light induced degradation of a-Si:H involves a second timescale of order 100 microsec, never before measured. Our result cannot be explained with a simple

carrier-driven degradation mechanism (as dominated previous metastability theories) because electron and hole populations rise and fall to steady-state values in less than 1 microsecond. In the hydrogen collision model, the newly observed timescale would be the time to reach a steady-state population of mobile hydrogen, precursors to defect creation. During illumination with pulses shorter than the mobile hydrogen rise time, the average mobile hydrogen population is lower than during continuous illumination, so defect creation is suppressed by breaking the illumination into pulses. In short, our theory predicted the existence of an unsuspected timescale associated with the mobile H and we did the experiment, and detected and measured this timescale. Of course, alternative models of metastability could still be formulated - but they must be consistent with our new experiment and timescale.

The importance of the theoretical and experimental work has been recognized by the organizers of two important international conferences. H. M. Branz was invited for extended talks at the 18th International Conference on Amorphous and Microcrystalline Semiconductors (ICAMS - 18, Aug. 1999) in Utah and at the 11th International Photovoltaic Science and Engineering Conference (PVSEC -11, Sept. 1999) in Sapporo Japan. These invitations were specifically for presentation about the H collision model.

References

1. A. H. Mahan, R. C. Reedy, E. Iwaniczko, Q. Wang, B. P. Nelson, A. C. Gallagher, H. M. Branz, and R. S. Crandall, in *Amorphous and Microcrystalline Silicon Technology-1998*, 507, edited by S. Wagner, M. Hack, H. M. Branz, R. Schropp, and I. Shimizu (Materials Research Society, Pittsburgh, 1998), in press.
2. D. L. Staebler and C. R. Wronski, Appl. Phys. Lett. 31, 292 (1977).
3. H. M. Branz, Phys. Rev. B 59, in press (1999).
4. H. M. Branz, S. Asher, H. Gleskova, and S. Wagner, Phys. Rev. B 59, in press (1999).

Selected 1998 PV publications from the NREL Amorphous Silicon Team

Refereed journals:

H.M. Branz, "The hydrogen collision model: Quantitative description of metastability in amorphous silicon," *Phys. Rev. B* , vol. 59, 1999, in press

H.M. Branz, S. Asher, H. Gleskova, and S. Wagner, "Light-induced deuterium diffusion measurements and metastability in hydrogenated amorphous silicon," *Phys. Rev. B*, vol. 59, 1999, in press

M. P. Petkov, A. T.Marek, , P.Asoka-Kumar K. G.Lynn, R. S.,Crandall, and A. H.Mahan, "An investigation of hydrogenated amorphous Si structures with Doppler broadening positron annihilation techniques," *Applied Physics Letters*, vol. 73, 1998, pp. 99-101

Z. Remes, Z., M. Vanecek, M., P. Torres, P., U. Kroll, U., A.H. Mahan, and R.S. Crandall, "Optical determination of the mass density of amorphous and microcrystalline silicon layers with different hydrogen contents, "*J. Non-Cryst. Solids,* vol. 227-230, 1998, pp. 876-879

R.S. Crandall, L. Xiao, and E. Iwaniczko,. "Recent developments in hot wire amorphous silicon" *J. Non-Cryst. Solids,* vol. 227-230, 1998, pp. 23-28

***Proc. Materials Research Society 1998 Spring Meeting Symposium A*, eds. R. Schropp, H.M. Branz, M. Hack, I. Shimizu, S. Wagner (MRS, San Francisco, CA, 1998) in press**

A.H. Mahan, R.C. Reedy, E. Iwaniczko, Q. Wang, B.P. Nelson, A.C. Gallagher, H.M. Branz, and R.S. Crandall, "H out-diffusion and device performance in n-i-p solar cells utilizing high-temperature hot wire a-Si:H i-layers"

H. Mahan, M. Vanecek, A. Poruba, V. Vorlicek, R. S. Crandall, and D. L. Williamson, "Low defect density microcrystalline Si deposited by the hot wire technique"

R. S. Crandall, E. Iwaniczko, A. H. Mahan, X. Liu, and R. O. Pohl, "Low temperature vibrational properties of amorphous silicon"

Q. Wang, E. Iwaniczko, A. H. Mahan, and D. L. Williamson, "Microcrystalline silicon n-i-p solar cells deposited entirely by the hot wire chemical vapor deposition technique"

B. P. Nelson, Y. Xu, D. L. Williamson, B. von Roedern, A. Mason, S. Heck, A. H. Mahan, S. E. Schmitt, A. C. Gallagher, J. Webb, and R. C. Reedy Jr. "Hydrogenated amorphous silicon germanium alloys grown by the hot wire chemical vapor deposition technique"

B. P. Nelson, Q. Wang, E. Iwaniczko, A. H. Mahan, and R. S. Crandall, "The influence of electrons from the filament on the material properties of hydrogenated amorphous silicon grown by the hot wire chemical vapor deposition technique"

X. Liu, E. Iwaniczko, R.S. Crandalland R.O. Pohl, "Molecular hydrogen in hot wire amorphous silicon"

L. Jiang, Q. Wang, E.A Schiff," Polarized electroabsorption spectra and light-soaking of solar cells based on hydrogenated amorphous silicon"

X. Geng, L. Wu, K. Price X. Deng, Q. Wang, and D. Han, "Internal electric field profile of a-Si:H and a-SiGe:H solar cells"

G. Yue, L. Chen, Q. Wang, E. Iwaniczko, G. Kong, J. Baugh, Y. Wu, D. Han, " Light-Induced change of Si-H bond absorption in hydrogenated amorphous silicon"

H.M. Branz, "Hydrogen collision model of the Staebler-Wronski effect: microscopics and kinetics"

Title: **Nanoparticles and New Ideas for Photovoltaics**

Organization: New Ideas Team, Center of Photovoltaics and Electronic Materials

Contributors: D.L. Schulz (Staff Scientist), C.J. Curtis (Senior Scientist), J.D. Perkins (Staff Scientist), P.A. Parilla (Senior Scientist), Renaud Stauber (Grad. Student), Joel Bertelson (NTEP High School Teacher/Summer Student), D.S. Ginley (Team Leader).

Objectives

The objectives of the team are two fold: 1) the continued exploration of nanoparticle precursors leading to low cost non-vacuum deposition technologies; and, 2) an exploration of new technological breakthroughs that could potentially impact photovoltaics (PV). Particular areas of interest include nanoparticle-derived contacts for both silicon and cadmium telluride solar cell technologies in the former, and the development of p-type $CuAlO_2$-based transparent conducting oxide films in the latter.

Technical Approach

Nanoparticle-Based Inks for PV: This project represents an integrated effort between the PV program and the Basic Energy Science's Chemical Sciences and Materials Sciences programs to evaluate the potential of nanoparticle-based inks as precursors for PV device elements and to develop an understanding of the mechanisms of nanoparticle interactions during the formation of electronic materials. The use of nano-sized particles could lead to narrower line-widths and patterns not easily attainable by conventional approaches. There are some challenges to this particle-based approach. First, small-grained materials have very large surface areas which leads to a large number of grain boundaries (GBs) in sprayed layers. As many device properties are limited by GBs, surface passivation and/or other treatments may be required to produce useful devices. Second, a tradeoff is made between ink stability and film contamination. Coordinating Lewis base species (e.g., diglyme, ethylene glycol, trioctylphosphine oxide) are often added to the solvent/particle mixture as a way of stabilizing the ink. Incorporation of these additives, sometime referred to as surfactants, as well as solvent into the deposited films should be avoided as this often leads to non-optimal device performance. This year we have focused on the formulation of 1) metal systems
(e.g., Al and Ag) as contacts to silicon; and 2) semiconductor contacts to CdTe.

p-Type TCO: Although there is very little budget for other work, we have been leveraging existing NREL projects (i.e. Superconductivity, Basic Energy Sciences Defective Oxides, and United States Industry Consortium) to initiate small projects with potentially large impacts on the PV program. These include an investigation of p-type oxides as contacts and junction partners.

Results

Nanoparticle Al and Ag Contacts to p- and n-Type Silicon

Aluminum-to-silicon contact metallizations via Al evaporation or Al-glass screen-printed pastes are well established techniques for large area contacts. In certain configurations, these metallizations lead to shading losses that degrade efficiency. Toward this end, a reduction in the present lithographic limitations of screen-printed conductors (i.e., linewidth > 100 μm) could serve to enhance overall solar-cell performance. The use of metallic inks that comprise nanosized particles could lead to smaller linewidths and maskless writing could also improve performance and reduce costs. Given suitable physical (i.e., particles < 0.5 μm in diameter) and chemical (i.e., reactivity) characteristics of the nanoparticles, this approach may be amenable to ink-jet printing.

Samples of Al and Ag powder prepared by Russian scientists via the electroexplosion process were characterized by TEM and found to be 50-300 nm and 100-300 nm in diameter, respectively. TEM-EDS indicated the Al sample particles contain a major O contaminant. The Al and Ag were applied onto p- and n-type Si, respectively, and subjected to typical contact anneals [1]. Figure 1 shows I-V characterization of these films after annealing. The Al to p-Si sample (Fig. 1a) shows a slight deviation from linearity in its I-V, whereas the Ag to n-Si sample (Fig. 1b) exhibits a linear I-V indicative of an ohmic contact [1, 2].

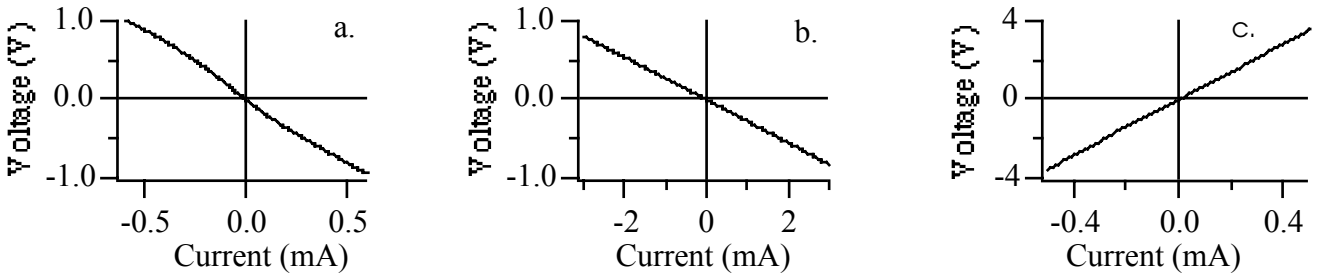

Figure 1. I-V characterization of (a) Al to p-type Si; (b) Ag to n-type Si; and (c) chemically-treated Al to p-type Si contacts.

In an effort to produce an ohmic contact to p-type Si using Al, we performed experiments to remove the surface oxide. After an NREL-developed wet-chemical treatment [3], the Al was observed to contain a much lower amount of O impurity by TEM-EDS. This treated Al was next applied as a contact to p-type Si and annealed as above. I-V characterization of this sample shows a marked improvement in the ohmic character of the treated Al (Fig. 1c) versus untreated Al (Fig. 1a).

Nanoparticle Semiconductor Contacts to CdTe

Cu-doped HgTe (Hg-Cu-Te) and Sb-Te particles have been applied as contacts to CdTe/CdS/SnO_2 heterostructures. The use of particulate systems is attractive for a number of reasons. First, given the existence of proper synthetic routes, particles with variable compositions (e.g., $Hg_{1-x}Cu_xTe$) can be synthesized with precise control over stoichiometry. This ability allows easy screening and optimizing as compared to, for instance, sputtering where changes in film stoichiometry often require the purchase of a new target.

Hg-Cu-Te

The standard NREL back-contact is a graphite-based Cu-doped HgTe material similar to that described by Britt and Ferekides [4]. The use of solution-synthesized Hg-Cu-Te particles in graphite-paste contacts was evaluated to determine the feasibility of nano-sized particles versus the micron-sized particles that are normally used. Hg-Cu-Te particles were characterized, mixed with graphite electrodag, and employed as contacts to CdTe [5]. Solar cells were produced by contact annealing at 220-270 ˚C with the current-voltage properties summarized in Table I. *While a contact anneal temperature of 220˚C is ~50˚ lower than that used for standard ball-milled Hg-Cu-Te/dag contacts, similar transport properties are observed.*

Metathesis preparation of Cu(I) and Cu(II) tellurides (i.e., Cu_2Te and CuTe, respectively) were attempted as a means of characterizing the valence state of Cu in the Hg-Cu-Te ink. Instead of Cu_2Te and CuTe, powder x-ray diffraction (PXRD) of product particles showed the formation of Cu_7Te_4 (PDF 18-456) and $Cu_{2.72}Te_2$ (PDF 43-1401), respectively. X-ray photoelectron spectroscopy of sputtered samples of these two product materials showed both are approximately 85% Cu^{1+} and 15% Cu^{2+} [5].

Table I. I-V Data for CdTe Solar Cells Contacted with Hg-Cu-Te Dag.

IV Characteristic	220˚C / 18 wt.%	20 min 37 wt.%	220˚C / 18 wt.%	40 min 37 wt.%	270˚C / 18 wt.%	20 min 37 wt.%	NREL baseline[6] 270˚C / 30min
V_{oc} (mV)	793	811	813	820	812	799	804
J_{sc} (mA/cm^2)	20.7	22.5	19.9	23.0	21.7	22.5	23.0
FF (%)	57.5	63.8	60.8	66.9	67.4	64.2	69.7
R_{series} (Ω)	5.8	5.0	6.1	4.4	4.5	5.0	N/a
R_{shunt} (Ω)	283	655	354	1063	433	452	Na/
Efficiency (%)	9.4	11.7	9.8	12.6	11.9	11.5	12.9

Sb-Te

Sb-Te particles were employed in preliminary studies as a contacting material based on the recent report of a Cu-free contact by the Parma group [7]. The metathesis reaction of 2 molar equivalents of SbI_3 with 3 molar equivalents of Na_2Te in methanol at –78˚C did not produce Sb_2Te_3. The PXRD pattern for the product powder consists of a mixture of Sb (PDF 35-732) and Te (PDF 36-1452) [5].

A preliminary study of Sb-Te contacts on CdTe was performed by spraying Sb-Te in methanol inks onto $CdCl_2$-treated CdTe films received as a gift from Doug Rose at Solar Cells Inc. (Toledo, OH). Bromine-methanol or NP acid surface treatments were performed on the CdTe films and the Sb-Te in methanol ink was immediately spray deposited at 150 ˚C. The contact anneal was varied from 200 to 300˚C under N_2. IV characterization of these solar cells showed V_{oc} increasing from less than 600 mV in the as-sprayed sample, up to ~750 mV for samples annealed at 200-250 ˚C, and >800 mV for a contact anneal of 300 ˚C. Efficiencies also increased with contact anneal temperature from 2.4% in the control cell up to 9.1% in one sample annealed at 300 ˚C for 60 min. This set of solar cells all exhibited $R_{se} > 20\ \Omega$; a seeming limit to device performance [5].

In an attempt to reduce R_{se}, a conducting material, acetylene black, was added to the Sb-Te/methanol mixture. For this round of solar cell preparation, CdTe films from Solar Cells Inc. were subjected to surface treatments in NP and Br_2/MeOH etches for 10 or 60 seconds prior to spray deposition of the Sb-Te-C mixture. A contact anneal was performed at 300 or 350 ˚C for 40 min under nitrogen gas. The performance of CdTe solar cells contacted with C-containing Sb-Te is not dramatically improved over the C-free Sb-Te contacted films. Except in one case, R_{se} remains greater than 20 Ω and R_{sh} is less than 400 Ω. Furthermore, V_{oc} never exceeds 800 mV, J_{sc} always remain less than 20 mA/cm^2, fill factors are less than 53% and efficiencies are limited to 7.2% in these devices [5].

$CuAlO_2$: A p-Type Transparent Conducting Oxide

In conjunction with their pre-existing n-type counterparts, transparent, p-type conducting oxide films would enable the fabrication of a variety of new PV structures and other new electronic devices with transparent p/n junctions. Almost a year ago Kawazoe, et.al. published an Applied Physics Letter on $CuAlO_2$ as a p-type TCO. Our initial attempts to duplicate this work using the same pulsed laser deposition (PLD) approach were not successful. While the correct phase was obtained in some cases, production was variable and inconsistent.

We have developed a robust method of forming c-oriented $CuAlO_2$ thin films. Preliminary measurements of the Seebeck and Hall coefficients confirm that these films are true p-type conductors, though the carrier density of 10^{17}/cm^3 is quite low. The transmittance spectra are similar to previously published results, with the fundamental absorption starting from about 350 nm (Figure 2). Unfortunately, the lowest achieved room temperature resistivity so far is 70 Ohm-cm, which is much larger than n-type ITO. Work is also underway to understand the mechanism of conductivity in these materials.

Industrial Interest

UNISUN is a small photovoltaic company based in Newbury Park, CA who are interested in the development of low cost routes to $CuInSe_2$ solar cells. CRADA research is underway.

Argonide is a small Sanford, FL-based company interested in the development of nano-sized metal particles produced by the exploding wire process. Thrust II proposal to USIC has been approved.

Recently, the Basic Energy Sciences Materials Sciences Division has provided a new source of funding for this research while the Chemical Sciences Division continues support.

A new interaction with Evergreen Solar has been initiated and preliminary experiments are underway.

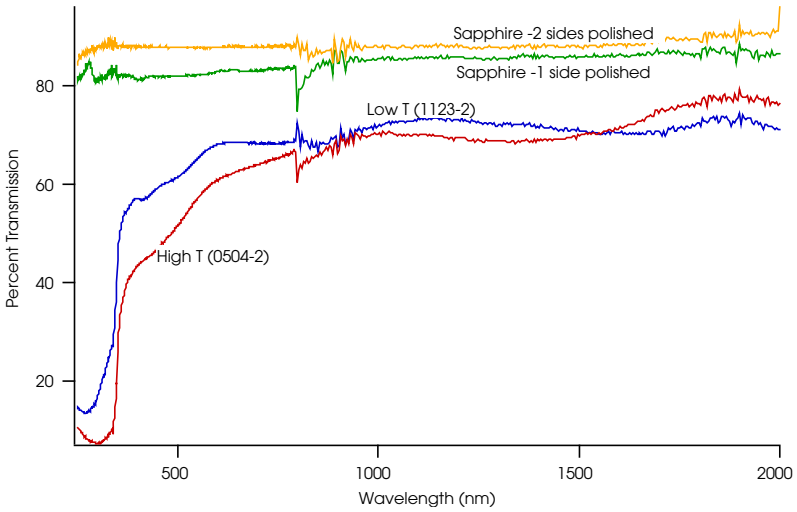

Figure 2. Transmittance spectra of $CuAlO_2$ thin films approximately 400 nm in thickness.

References (see above) and Relevant 1998 Publications[8] **and Patents**[9-11]

[1] D. L. Schulz, R. Ribelin, C. J. Curtis, and D. S. Ginley, "Particulate Contacts to Si and CdTe: Al, Ag, Hg-Cu-Te, and Sb-Te" *1998 National Center for Photovoltaics Annual Review AIP Conference Proceedings*, (in press).

[2] D. L. Schulz, C. J. Curtis, D. S. Ginley, and F. Tepper, "Nanosized Al and Ag Particulate Contacts to Silicon: Materials Characterization and Preliminary Electrical Results," *Extended Abstracts of the 8th World Conference on Silicon, Copper Mountain, CO*, 1998.

[3] D. L. Schulz, C. J. Curtis, and D. S. Ginley, "Passivating Etchants for Metallic Particles," U.S. Provisional Patent Application on File.

[4] J. S. Britt and C. S. Ferekides, "Ohmic contact using binder paste with semiconductor material dispersed therein," U.S. Patent No. 5,557,146, 1996.

[5] D. L. Schulz, R. Ribelin, C. J. Curtis, D. E. King, and D. S. Ginley, "Nanoparticle-Based Contacts to CdTe," *Materials Research Society Symposia Proceedings*, (in press).

[6] From a 38 cell baseline test. June 1998 CdTe BiMonthly PV Program Report.

[7] N. Romeo, A. Bosio, R. Tedeschi, and V. Canevari, "High Efficiency and Stable CdTe/CdS Thin Film Solar Cells on Soda Lime Glass," presented at 2nd World Conference and Exhibition on Photovoltaic Solar Energy Conversion, Vienna, Austria, 1998.

[8] D. S. Ginley, C. J. Curtis, R. Ribelin, J. L. Alleman, A. Mason, K. M. Jones, R. J. Matson, O. Khaselev, and D. L. Schulz, "Nanoparticle Precursors for Electronic Materials," *Materials Research Society Symposia Proceedings*, (in press).

[9] M. Pehnt, D. L. Schulz, C. J. Curtis, and D. S. Ginley, "Preparation of a Semiconductor Thin Film," U.S. Patent No. 5,711,803, 1998.

[10] D. L. Schulz, D. J. Curtis, and D. S. Ginley, "Solution Synthesis of Mixed-Metal Chalcogenide Nanoparticles and Spray Deposition of Precursor Films," U.S. Patent Application Filed January 27, 1998.

[11] D. L. Schulz, D. J. Curtis, and D. S. Ginley, "Method for Forming Thin-Film Conductors Through the Decomposition of Metal-Chelates in Association with Metal Particles," U.S. Provisional Patent on File, 1999.

Title: **NREL Clean Room / Device Fabrication Team Activities**

Organization: NREL Center for Photovoltaics and Electronic Materials

Contributors: **Team Members:** Scott Ward (team leader), Tim Gessert, J. Alleman, C. Allman (Admin. Assistant), M. Contreras, A. Duda, D. Friedman, D. Ginley, J. Keane, C. Kramer, S. Kurtz, M. Landry, X. Li, W. McMahon, K. Melerberg, J. Olson, M. Page, P. Parilla, R. Ribelin, L. Roybal, S. Smith, 7. Thiesen, S. Tsuo, X. Wu, D. Young.

Objectives

The Clean Room / Device Fabrication Team provides the tools and procedures necessary to produce state-of-the-art test structures and devices from semiconductor materials synthesized by NREL or its subcontractors: The Team also provides a "crossroads" at which researchers working on various technologies can mutually benefit from shared information and experience. The Team maintains an integrated, multi-disciplinary facility comprising ~3500 square feet of Class 1000 clean room space and housing ~$2M of equipment. Major equipment includes photolithographic processing, vacuum metallization, electrolytic metallization, and thermal processing. The Team also maintains characterization equipment and techniques appropriate for process monitoring and development. ~25 researchers were Team members during FY98. These individuals were from various "home" teams in the PV&EM, Basic Sciences, and Measurements and Characterization Centers. Most Team members use the Team facilities on a daily-to-weekly basis.

Technical Approach

The Clean Room/Devices Fabrication Team utilizes the SERF Clean Room facility and related characterization equipment to fabricate devices from semiconductor materials produced by their home teams or subcontractors. Processes activities can also by performed for non-Team members either by mutually beneficial collaborations between Team and non-Team members or by providing project-specific funds. Although the individual Team members work with a wide variety of material systems and related technologies, the procedure used to develop processes for device fabrication is similar. This will often involve review of related literature/documentation, design and production of required photomasks, preliminary process experimentation to optimize individual processing steps, process feasibility studies to determine how steps interact, and use of an entire process sequence to produce desired device or structure. The time required for process development sequence can range from hours to months, depending on the complexity of the process and availability of related information. Because of this extensive effort to develop individual processes, Team members are encouraged to maintain awareness of other activities, and share information and/or experiences when appropriate. Team organizational functions are aimed at facilitating this transfer of process information. Within guidelines established by the Team, a Team member is free to use the Clean Room facilities on an as-needed basis. Team members that charge to Clean Room/Device Fabrication task, (presently 0.3 F17E plus one unfilled FIE position) perform functions related to developing Team organization, maintaining facility equipment, providing training in the use of process equipment and procedures, acquiring and providing process and ES&H documentation, performing Business Development activities, and providing long-term planning for the Team and facilities. They are also available to trouble-

shoot and engineer specific processes as well as providing process support for small internal activities such as FIRST projects.

Studies and Accomplishments

Following is a partial summary of studies and accomplishments resulting from work by Clean Room Team members and related collaborations. The list is organized by citing the home team of the researcher that performed the work, or the home team of the collaborating partner.

III-V Materials and Devices Team (Center for PV&EM)

- Use of vacuum deposition equipment for applications of antireflection coatings.
- Routine processing of III-V devices including use of plated Au for front and back contacts, and vacuum evaporation for processing of Ti/Pd/Ag/Pd top contacts. Processing and chemical etching for device isolation and to enable profilometry of epi-layer thickness.
- Studies to investigate the use of very-thick photoresist layers for the production of thick depositions of plated Au as well as chemically amplified negative resists.
- Continued process development of an improved metallization for high-concentration devices. This multi-layer metallization involved high-profile grid lines (3 gm wide x 9 gm high).

CdTe Team (Center for PV&EM)

- Routine deposition of MgF_2 antireflective coatings (~1000 Å) onto the glass side of finished CdS/CdTe devices prior to efficiency measurements.
- Use of the Clean Room's cleaning apparatus and procedures became routine for preparation of all 3" x 3" Corning 7059 glass used for CSS device fabrication by the CdTe Team.
- Use of Clean Room automatic ellipsometer to assist in development of CVD Si02 and Sn02 layers. This instrument can produce numerous measurements of optical index and layer thickness very quickly and is invaluable for analyzing CVD deposit uniformity.
- Developed photolithographic / chemical etch process to isolate CdTe devices fabricated with sputtered ZnTe back contacts.
- Developed a technique using the infra-red alignment capabilities of one of the mask aligners to deposit a metal aperture to more accurately define the area of in-house processed diagnostic devices

CIS Team (Center for PV&EM)

- More work was performed to produce a CIS mini-module using wet-chemical etching.
- Utilized clean environment for routine production of Mo-coated substrates for CIS growth. By cleaning the substrates in the clean room (Class 10 hood), and locating the Mo sputtering system in an adjacent area (Class 1000), pinhole formation is reduced.

TPV Team (Center for PV&EM)

- This externally funded activity performed routine processes to fabricate photovoltaic devices with band gaps required to convert the thermal radiation directly into electricity. The activity developed and utilized several novel processes that are now part of the Clean Room Team's experience base and available for the PV Program. Many of these have already been utilized by other Teams (e.g., See fabrication of "free-floating films" for the Spectroscopy Team).

- Expanded processes and tooling of monolithic interconnected module (MIM process) to enable fabrication of a 5.2 cm2 device (18 interconnected 0.74 eV devices on a single substrate with two contacts
- Developed processes required to fabricated a 0.6 eV mismatched MIM device. Efforts are presently underway to increase device area from 0.25 cm~ to 1.0 cm 2.

- Vacuum (electron-beam) deposition of high-quality Au for backside-reflector layers (BSR's) onto TPV devices, and Cr/Pd/Ag/Pd front contacts.

- Vacuum deposition of MgF2 films (1300 A) for use as a dielectric-spacer layer/diffusion barrier layer/optical element between a Au back surface reflector (BSR) and the active TPV device.

- Routine use of vacuum deposition of ZnT/MgF_2 antireflection coatings on TPV devices.

Crystal Growth and Devices Team (Center for Basic Sciences)

- Routine fabrication of diagnostic crystalline silicon solar cells using electron-beam A1 for the back contact, and Ti/Pd/Ag metallization (through shadow masks) for the front contact. Photolithography is used for mesa etching to isolate the small diagnostic devices.
- A computer control system for the eight-tube quartz furnace of the Thermal Processing Clean Room was installed, tested, and is now in routine use. A dedicated wet processing bench for silicon solar cells was also installed in this laboratory.
- A 12-inch by 12-inch format screen printer became operational in the Thermal Processing Clean Room in FY98.
- Study effect of various heat treatments, including optical processing, on high-quality Al metallizations on crystalline Si. This work involved use of dedicated Al E-Beam evaporator to deposit numerous high quality Al films, and thermal processing of these samples.

Sunerconductivity Team Center for Basic Sciences)
- Electron-beam deposition of 300A Ag onto LaAl substrates for use as electric contacts. Deposition rate optimized to enhance thickness uniformity.

Spectroscopy Team (Center for Basic Sciences
- Clean Room Team members fabricated "free-floating films" of GaInP for PL analysis. The ability to remove these -2-gm-thick epitaxial films from the GaAs substrate enabled improved PL analysis that was helpful in understanding "ordering" in IH-V materials.

- Performed "groove etching" on GaAs to expose (111) surface to enable investigation of ordered growth. This activity is now a collaborative effort with the e-beam lithography team at NIST.

Analytical Microscopy Team (Center for Measurement and Characterization)
- Production of metallized fiber optic probes used to obtain a sub-wavelength point source of light has continued. In this process, the tapered portion of a specially prepared optical fiber is coated with evaporated Al during rotation to produce a sub-wavelength aperture at the apex of the taper. These probes are used for near-field scanning optical microscopy (NSOM) by members of the Center for Measurements and Characterization.

Chemical Sciences Team (Center for Basic Sciences

- Clean Room Team members produced Pt metallizations on soda-lime glass substrates for use in dye-synthesized solar cell research. To produce the required film adhesion, alkaline cleaning procedures were used to prepare the substrate prior to multi-level E-beam metallization of a Ti adhesion layer (400 A) and Pt (600 A). The cost of processing and precious metal consumption were shared between the Clean Room and Chemical Sciences Teams.

Electro-Optical Characterization Team (Center for Measurement and Characterization)

- The automatic ellipsometer in the clean room was used routinely to calibrate the wavelength scanning ellipsometer. The automatic ellipsometer is well suited for this application because the Clean Room Team maintains ellipsometric calibration standards.

- Electron-Beam evaporation of metals (Cr, Sn, Pt, Al, Au, Ag, and Pd) onto thin-film CdTe for use in PL analysis of contacted vs. non-contacted CdS/CdTe devices (collaborative effort between Electro-Optical Characterization, and CdTe, and Clean Room Teams).

Enhanced Capabilities

During FY 98, the K&S wirebonder was received and set up. Digital image capturing capabilities were added to the optical microscopes. A probe station was acquired and set up.

Conclusions and Future Directions

The Clean Room / Device Fabrication Team was created in 1996. Because of the Team's brief history, efforts continue to focus on providing the process capability critical to enhance the PV program, while developing longer-term objectives within the framework of available personnel, equipment, and program support. This involves identifying and the prioritizing needs of the Team members, developing a method to assign critical maintenance and administrative responsibilities, fostering beneficial collaborations, and learning how to share and transfer the Team's information base effectively. As indicated by the preceding list of the Team's studies and accomplishments, these efforts have led to some significant accomplishments and synergistic collaborations during the past year. However, several important Team objectives remain undeveloped, and it is here where a portion of next year's efforts will be placed.

Future New Capabilities

Acquisition of a Personal Scanning Electron Microscope (SEM).

Development of Reactive Ion Etching (RIE) capabilities.

Title: **Thin-Film CdS/CdTe Solar Cell Development**

Organization: National Renewable Energy Laboratory

Contributors: T.A. Gessert (Team Leader), D.S. Albin, M. Al-Jassim, S.A. Asher, R. Bhattacharya, T.J. Coutts, R.G. Dhere, F. Hasoon, B. Keys, D. Levi, X. Li, Y. Mahathongdy, A. Mason, C. Narayanswamy, D. Niles, R. Ribelin, D. Rose, D. Schulz, A. Swartzlander-Guest, P. Sheldon, D. Waters, L. Woods, X. Wu.

Objectives/Technical Approach:
The three primary objectives of the CdTe Team are: 1) To develop reproducible processes for high efficiency CdS/CdTe devices and to improve our fundamental understanding of the physics and chemistry of the device; 2) To explore alternative processes and device structures which lend themselves to improved device performance, improved fundamental understanding, improved reproducibility, and/or improved ease of manufacture; and 3) To provide strong industrial partner support.

The CdTe Team has developed a 3-year roadmap outlining long-term research goals and activities. This roadmap is divided into four sections addressing critical portions of the device structure. These include the transparent conducting oxide (TCO) layer, the CdS/window layer, the CdTe absorber/junction, and the back contact. In support of these activities, we have dedicated significant resources towards developing new characterization tools and techniques allowing us to probe critical interfaces.

Results:
NREL-Record Efficiency CdS/CdTe Device Produced - In December of 1997, the NREL CdTe team fabricated a CdS/CdTe device demonstrating an NREL-confirmed efficiency of 15.4% (Global). This new in-house record device represented influences from several on-going research activities within the NREL CdTe team.

Solar Cells, Inc./NREL Collaboration - A collaborative effort between Solar Cells, Inc. (SCI) resulted in a thin-film CdTe solar cell with an NREL-verified efficiency of 14.1%; the first time SCI has reached this level. NREL's contribution to this device was the deposition of a high-quality bilayer SnO_2 front contact on a low-Fe "water-white" glass product supplied by AFG Industries. With the addition of NREL's CVD SnO_2 deposition capability, SCI had access to customized TCO-coated glass substrates. Reduced absorption in the water-white glass and a thinner CdS layer, facilitated by the resistive SnO_2 layer, resulted an improved short wavelength response and improved device J_{sc}.

Cadmium Stannate (CTO) Related Device Development - A CTO-based CdS/CdTe solar cell device was fabricated demonstrating an NREL-confirmed efficiency of 15.0% (V_{oc} = 828 mV, J_{sc} = 24.5 mA/cm^2, FF = 73.8%). The device integrates a CTO film demonstrating improved transparency, reduced sheet resistance, and an NREL-developed zinc stannate (Zn_2SnO_4, ZTO) buffer layer. The integration of the ZTO buffer layer into both SnO_2-based and CTO-based CdS/CdTe devices significantly improves the ease of device manufacture (improved layer adhesion following $CdCl_2$ treatment), performance, and reproducibility. This is clearly seen in Figure 1, which shows the efficiency of 30 identically processed devices, all of which include the ZTO buffer layer. This device set has an average efficiency of 13.78% with a standard deviation of 0.37%.

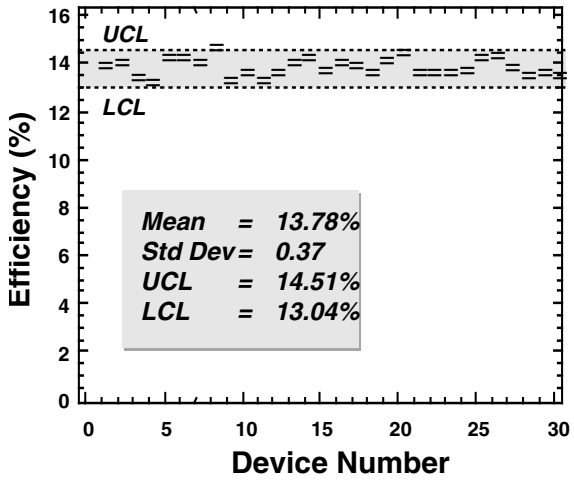

Figure 1. Reproducibility of thirty CdS/CdTe devices with a ZTO buffer layer.

In related work, CTO-based CdTe cells incorporating sputtered CdS layers have been initiated to investigate processes that are more manufacturable than chemical bath deposition (CBD. Literature review indicates that incorporation of sputtered CdS typically results in reduced V_{oc}'s, unless the thickness of the sputtered CdS is more than 2000 Å. However, results from our work indicates that the sputtered CdS thickness can be significantly reduced (to improve J_{sc}) without impacting V_{oc} if a ZTO buffer layer is used. We have fabricated a CTO-based CdTe cell incorporating a sputtered CdS layer that demonstrated an NREL-confirmed efficiency of 14.4%. To our knowledge, this is the highest efficiency for CdTe cell with a sputtered CdS window layer.

In another related study, a more manufacturable process for the fabrication of CTO-based CdS/CdTe solar cells has been demonstrated (e.g., reduced thermal budget, capital investment, process time, and manufacturing costs). Preliminary device results have demonstrated CdTe cells with an efficiency of 12.5% and good reproducibility. A patent related this new process is presently being filed.

SnO_2 Bilayer Development – We have observed that placing a high-resistivity SnO_2 (i-SnO_2) between the conductive SnO_2:F and the CdS can assist in maintaining high shunt resistances and high V_{oc}'s while using thinner CdS layers. Nevertheless, these results were inconsistent, partly because i-SnO_2 sputtered at room temperature was not thermally stable in the hydrogen ambients used just prior to CSS CdTe deposition. We now have the capability to deposit SnO_2 from low-pressure CVD reaction of TMT and oxygen, and have further determined that the CVD i-SnO_2 is much more resistive to reduction in high-temperature hydrogen ambients (e.g., stable at 500°C in H_2).

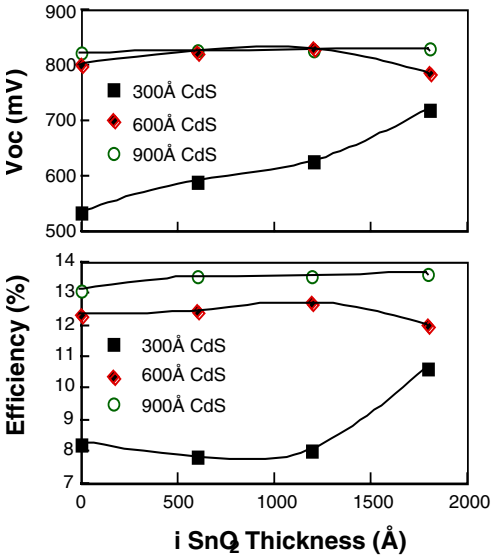

Fig. 1. Effect of CVD-Grown i-SnO_2 and CdS thicknesses on device performance.

A study to determine if the CVD i-SnO_2 would produce a more controllable effect on device performance indicated that, varying the i-SnO_2 thickness from 500-2000 Å and the CdS thickness from 300-1000 Å, the CdS thickness impacts device performance strongest. Only when CdS film thickness is reduced to 300Å, do we observe an affect with varying the i-SnO_2 layer the device performance (mainly V_{oc}). Considering this data, we have chosen a bilayer SnO_2 for our baseline process that uses a 2000 Å thick i-layer.

CdS Window Layer Development/Interface Alloying – The goal of this project is to understand the role that interdiffusion between CdS and CdTe plays in device formation and performance. To date, we have studied the compositional differences between $CdTe_{1-x}S_x$ layers formed by interdiffusion of CBD CdS/CdTe layers and CSS CdS/CdTe layers in two ways: 1) The "lift-off" approach in which finished CdS/CdTe devices are separated directly at the interface; and 2) The "thin-film couple" approach where only a thin (2000-3000 Å) CdTe film is grown on the respective CdS layer.

Preliminary analysis indicates that the "thin-film couple" approach can yield information which may not be representative of actual devices. For example, if we compare the degree of $CdTe_{1-x}S_x$ interfacial alloying measured by both techniques for CdS/CdTe interfaces grown at 600°C, we observe a strong difference. The lift-off approach shows that the amount of S in CdTe, at the interface, approaches ~12-14 at.% S for CBD CdS/CdTe interfaces but only ~2-3 at.% S for CSS CdS/CdTe interfaces (see Fig. 2a). In contrast, the amount of alloying revealed by the "thin-film couple" approach is much less for both types of CdS (on the order of 1 at.% or less, see Fig. 2b). The reduced CdTe deposition time in the thin-film couple approach may explain the reduced alloying shown in Fig. 2b.

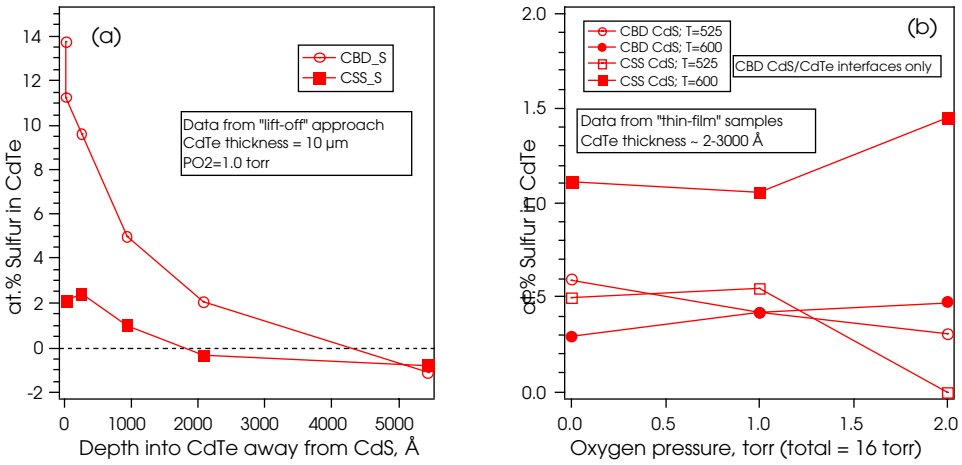

Fig. 2 Alloying measured in lift-off (a) and thin-film couple (b) samples using XRD.

We have also studied how alloying affects optical bandgap. Optical R-T measurements were performed on $CdTe_{1-x}S_x$ alloy thin films that were produced by laser ablation (films supplied by A. Compaan of the University of Toledo as part of a National CdTe Team study). From the R-T data, the variation in optical band gap as a function of the alloy parameter x was determined. The results are shown in **Fig. 3**, along with the parabolic fit reported by Ohata et al. (Jap. J. of Appl. Phys, 12(10) 1973). It should be noted that the parabolic equation reported by Ohata was a poor fit to both the NREL and Ohata's data. Rather, as indicated in the caption of **Fig. 3**, a better estimate of the S-alloying in Te-rich alloys is arrived at using a 4th degree polynomial.

$CdCl_2$ Process Development - The baseline $CdCl_2$ treatment used by the NREL CdTe Team is a wet process that produces significant enhancement of device performance while requiring inexpensive equipment. Nevertheless, this process is inconsistent with dry, in-line processing envisioned for large-area CdTe PV manufacturing. Further, even laboratory conditions do not produce the level of control required for systematic device research. For these reasons, we are developing equipment and studying procedures to enable a dry $CdCl_2$ process that will be manufacturable and also result in the level of control required for device research. Efforts toward this goal include construction and development of apparatus that allows dry processing of individual small samples (0.75" x 0.75"), and the recent purchase and installation of apparatus allowing for larger batches and higher throughput.

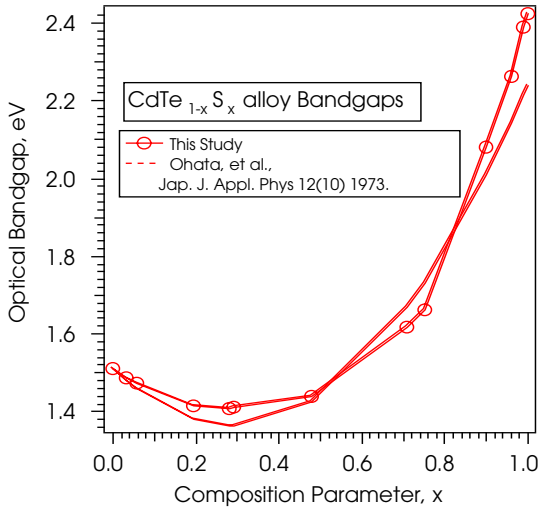

Fig. 3. Optical Bandgap as a function of Sulfur content, x, in $CdTe_{1-x}S_x$ alloys. Various analytical fits to the data:

3rd degree: Eg = 1.4963 - 0.22296(x) - 0.88536(x)^2 + 2.038(x)^3; R2=0.999

4th degree: Eg = 1.5063 - 0.62662(x) + 1.2355(x)^2 - 1.3812(x)^3 + 1.700(x)^4; R2=0.999 (this is better at low S)

Because the relative importance of variables in this dry process are uncertain, our investigation included a statistical experimental design and related screening experiments. A second order, rotatable, Central Composite Design (CCD) was chosen because it provided efficient second-order modeling for quantitative factors, and provides flexibility in the resolution selection. From the screening experiments, statistically significant factors were identified for further study. The design also indicated that the optimum vapor $CdCl_2$ process conditions should include a higher source temperature, higher substrate temperature, oxygen containing ambient, longer treatment times, programmed cool down profile, porous source plates, sources without moisture, no pre-anneal, higher pressures, and faster ramp up rates.

In collaboration with members of the NREL Characterization Division, a systematic study involving PL, AES, and XPS was initiated. This study has produced results that significantly advance our understanding of the surface and bulk chemistry that occurs during the vapor $CdCl_2$ process. For example, initially the benefits of a vapor $CdCl_2$ process were viewed purely in manufacturing terms (i.e., it was quicker, cleaner, and inherently, more reproducible). However, results indicate that chlorine-containing residues remaining on the CdTe surface after solution $CdCl_2$ are more adherent to the CdTe surface than similar residues remaining after the "dry" modification. This difference between the two processes, shown in Fig. 4, could have a serious impact on manufacturing.

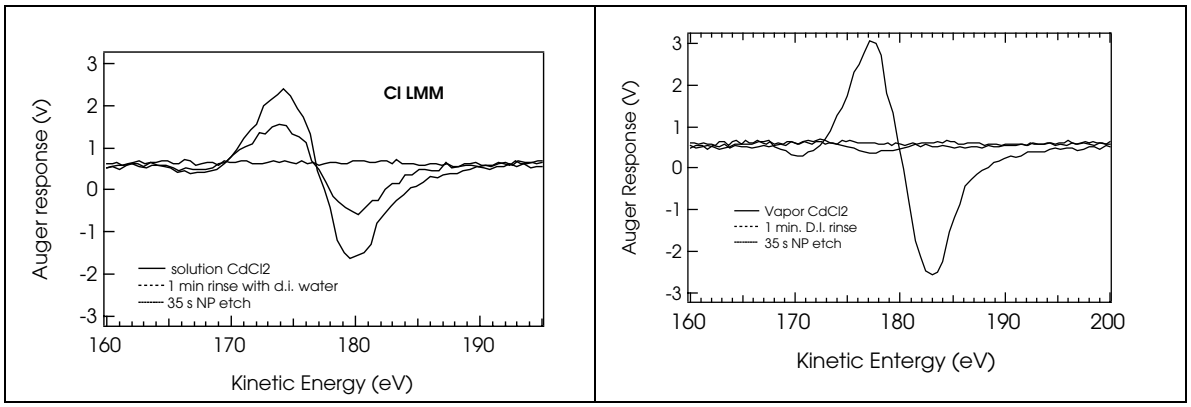

Fig. 4. AES data for Cl residues on wet (left) and vapor (right) $CdCl_2$ treated films.

Because it was found that the NP etch is not necessary when vapor $CdCl_2$ is used, studies to evaluate various means of preparing the CdTe surface prior to back contacting were initiated. We found that thermal anneals of the CdTe surface in vacuum were adequate when vapor $CdCl_2$ was used. Such anneals (not requiring acid etches) are consistent with manufacturing. The performance of solution and vapor $CdCl_2$ treated devices is shown in Fig. 5.

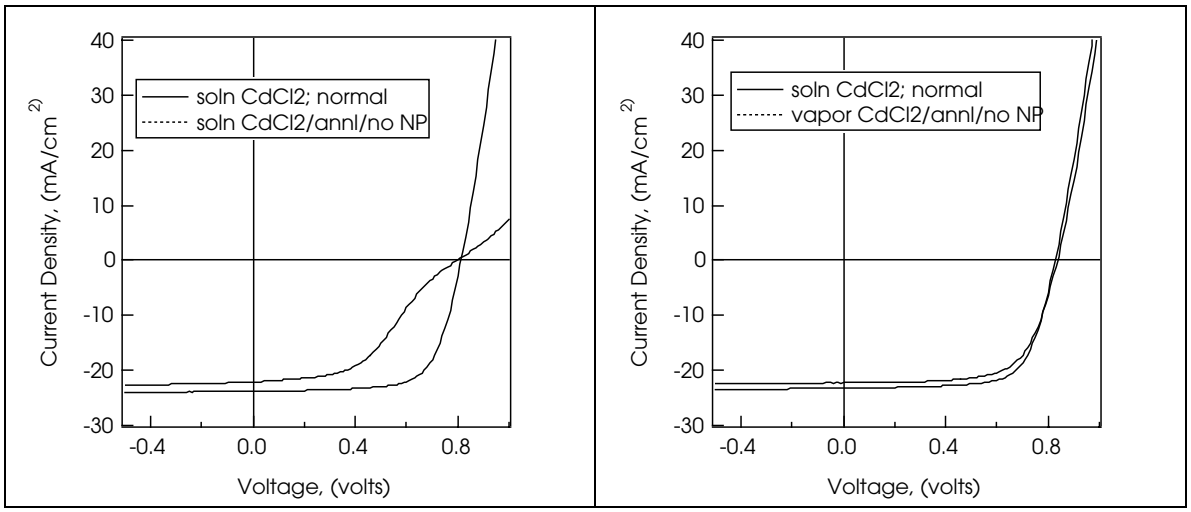

Fig. 5. I-V data showing the effectiveness of vacuum anneals as a post $CdCl_2$-precontact treatment for both solution (left) and vapor (right) $CdCl_2$ treated cells.

Baseline Contact Studies – Our baseline back contact has consisted of a mixture of carbon electrodag (dag) and Cu-doped HgTe, the latter crystal supplied by the U. South Florida (USF). During FY98, our supply of the latter HgTe crystal was depleted and an effort was undertaken to find a replacement. As a precursor to this project, ICP analysis was performed on two USF-supplied Cu:HgTe crystals: an "old" sample and a more recent supplied "new" sample. ICP results showed that the "old" USF material (used in the baseline process) contained about half as much Cu and Hg as the "new" material, and that the Cu/Hg ratio of the "old" was lower by about half. X-ray diffraction measurements of the USF crystals were performed in parallel with two types of Cu_xTe phases and a pure HgTe "standard" sample.

Rather than find only HgTe and possibly elemental Cu as a precipitate, XRD indicated that both USF samples contained HgTe in equilibrium with predominantly $Cu_{1.44}Te$ and a little Cu_2Te. No elemental Cu, at least within the sensitivity of the XRD technique, was identified. Having established that our existing back contact pastes were in essence a mixture of HgTe and Cu_xTe, we investigated whether pre-weighed mixtures of HgTe and Cu_xTe could replace our USF supplied Cu:HgTe crystal powders. In addition to offering us the ability to realize our own back contact compositions, this new approach allowed us to evaluate the effect of Cu on device performance and reliability. We also considered pastes where only pure HgTe was used (i.e., no Cu), and where only C-dag was used (no Cu or HgTe). Device results indicated that the $Cu_{1.44}Te$ +HgTe paste is an excellent substitute for our baseline (control) paste. A subset of devices produced using these pastes was delivered to Colorado State University (CSU) to study the effect of Cu on device stability. Their report of an inverse correlation between Cu content and performance during stress testing (reported at the Fall 98 PVARD meeting) was a direct result of our developing this new back contacting procedure.

SIMS Analysis of Diffusion in ZnTe Back Contact - SIMS analysis was performed on SCI-produced CdS/CdTe device material that was processed using the NREL ZnTe contact sequence (i.e., undoped ZnTe + ZnTe:Cu + Ni). The study compared devices that were pre-etched in the NP etch with similar devices that were prepared with the ion-beam (IB) pretreatment used in the "all-dry" ZnTe contacting process developed at NREL.

SIMS indicated that Cu diffuses from the outer ZnTe:Cu layer into the adjacent undoped ZnTe layer and builds up at the ZnTe/CdTe interface. Standard-resolution SIMS indicated Cu in the CdTe for all of these devices, including those contacted without using Cu. The Cu in the CdTe could be due to the residual Cu impurities in the starting CdTe source material. However, it was also possible that an interference between $^{63}Cu^{+}$ and $^{126}Te^{2+}$ could conceal a small Cu signal within a much larger signal due to the ^{126}Te isotope. High-resolution SIMS was performed to investigate these possibilities. This data confirmed that some Cu in the CdTe diffuses from the ZnTe:Cu layer into the CdTe layer and collects near the junction.

Future Directions:
In FY99, we will study the potential of Cd as a dopant to produce higher resistivity i-SnO_2 as well as continue to develop the CTO-based TCO. We will continue to study the use of ZTO as a barrier layer as well as begin to explore the low-resistance potential of this material. We will continue to develop a dry $CdCl_2$ process to replace the wet treatment, and integrate the process into our baseline. We will continue our efforts to characterize CdS/CdTe interface alloying and identify how it impacts device parameters. We will focus on fundamental aspects of the back contact, including current transport at critical interfaces, contact stability and degradation mechanisms. We will also continue to work on collaborative projects initiated with our industrial and team partners through the Thin Film Partnership program. A detailed description of tasks is outlined in the CdTe FY99 Annual Operating Plan.

References:

Papers:

1. T.J. Coutts, X. Wu, P. Sheldon, and D.H. Rose, "Development of High-Performance Transparent Conduction Oxides and their Impact on the Performance of CdS/CdTe Solar Cells", 2nd World Conference on PV Energy Conversion (2WCPVEC).
2. D.M. Waters, D. Niles, T. Gessert, D. Albin, D. Rose, and P. Sheldon, "Surface Analysis of CdTe After Various Pre-Contact Treatments", 2WCPVEC.
3. D.H. Levi, L.M. Woods, D.S. Albin, T.A. Gessert, R.C. Reedy, and R.K. Ahrenkiel, "Influence of Grain Boundary Diffusion on the Electro-Optical Properties of CdTe/CdS Solar Cells," 2WCPVEC.
4. R. Dhere, H.R. Moutinho, S. Asher, D. Young, X. Li, R. Ribelin, and T.A. Gessert, "Characterization of SnO_2 Films Prepared Using Tin Tetrachloride and Tetramethyl Tin", 2nd NCPV Program Review Meeting (2NCPVRM).
5. C. Narayanswamy, T.A. Gessert, S.E. Asher, Analysis of Cu Diffusion in ZnTe Based Contact for Thin-Film CdS/CdTe Solar Cells, 2NCPVRM.
6. X. Wu, P. Sheldon, Y. Mahathongdy, R. Ribelin, A. Mason, H.R. Moutinho, and T.J. Coutts, "CdS/CdTe Thin Film Solar Cell with a ZTO Buffer Layer," 2NCPVRM.
7. X. Li, R. Ribelin, Y. Mahathongdy, D. Albin, R. Dhere, D. Rose, S. Asher, H. Moutinho, and P. Sheldon, "The Effect of High-Resistance SnO_2 on CdS/CdTe Device Performance," 2NCPVRM.
8. Y. Mahathongdy, D.S. Albin, C.A. Wolden, R.M. Balwin, "Vapor $CdCl_2$ – Optimization and Screening Experiments for an All Dry Chloride Treatment of CdS/CdTe Solar Cells", 2NCPVRM.
9. D.H. Levi, L.M. Woods, D.S. Albin and T.A. Gessert, and Dave Albin, "Back Contact Effects on the Electro-Optical Properties of CdTe/CdS Solar Cells," 2NCPVRM
10. D. Albin, R. Dhere, A. Swartzlander-Guest, D. Rose, X. Li, D. Levi, D. Niles, H. Moutinho, R. Matson, and P. Sheldon, "Interface Reactions in CdTe Solar Cell Processing, Mat. Res. Soc. Symp. Proc. Vol. 485, p. 215 (1998)
11. D.H. Rose, F.S. Hasoon, R.G. Dhere, D.S. Albin, R.M. Ribelin, X.S. Li, Y. Mahathongdy, T.A. Gessert, and P.Sheldon "Fabrication Procedures and Process Sensitivities for CdS/CdTe Solar Cells, Accep. For Pub. Prog. In Photovoltaics.

Allowed Patents:

1. X. Wu, P. Sheldon, T.J. Coutts, "PV Devices Comprising Cadmium Stannate Transparent Conduction Films and Method for Making", NREL IR#95-35.
2. X. Wu and T.J. Coutts, "Thin Transparent Conducting Films of Cadmium Stannate", NREL IR#95-45.
3. T. A. Gessert, "Use of Separate ZnTe Interface Layers to Form Ohmic Contacts to p-CdTe Films", NREL IR#96-49.

Filed Patents:

1. T.A. Gessert, "Ion-Beam Treatment to Prepare Surfaces of p-CdTe Films", NREL IR#96-48
2. T.A. Gessert, "Plasma & Reactive Ion Etching to Prepare Ohmic Contacts," NREL IR#96-52
3. X. Wu, P. Sheldon, T.J. Coutts, "PV Devices Comprising Zinc Stannate Buffer Layer and Method Making," NREL IR#98-39.

4.0 PV Measurements and Characterization Project

4.0 PV MEASUREMENTS AND CHARACTERIZATION PROJECT— Introduction

Project Leader: Lawrence L. Kazmerski

The NCPV Photovoltaic-Program laboratories within this project perform thousands of measurements each year, partnering with industry, universities, research laboratories, and internal research efforts. The Measurements and Characterization Team within the NCPV includes more than 40 experts, providing analytical support covering the test and measurement range from atoms through arrays. With state-of-the-art equipment and facilities, these laboratories embody cell and module performance, electro-optical characterization, analytical microscopy, and surface and interface characterization capabilities. The laboratories contribute analytical service support and collaborations, as well as measurement technique research to enhance and assist the PV R&D and industry communities. Scientists and engineers in these laboratories work closely with the major PV programs, leading and assisting efforts within the Thin-Film Partnership, PVMaT, and the Concentrator Alliance. Staff also work with international efforts for technology transfer, standards development, and standard reporting assurance.

These laboratories offer more than 40 techniques to determine the electrical and optical properties of materials and devices, as well as the chemistry, composition, topography, structure, and physical nature of materials, surfaces, and interfaces. Through its website (www.nrel.gov/measurements), this NCPV operation offers its collaborators and clients a secured data transfer facility to enhance customer interactions and improve measurement turn-around time. This facility currently links some 40 laboratories using the NREL measurement and characterization facilities, providing real-time and archival methods of data transfer, retrieval, and observation. In this period, more than 20 DOE teams have collaborated in the evolution of this new method of electronic interaction. The majority of the NREL sample evaluations require independent analysis for *quality assurance*—especially for contract deliverables and for validation of milestones and record results. NREL maintains standards (physical standards and techniques), knowledge of standard conditions, and leads in the world PV standards community to ensure *quality* and *validity* of results. These programs are the models for quality assurance for the NCPV, the PV Program and the National Renewable Energy Laboratory.

The organization maintains technical leadership in the standard testing of solar cells and modules—and assists R&D and industry efforts by providing cost-effective measurement and characterization service, research, and technique development. In FY 1998, the technique-development efforts of this project were recognized through the Harold Hubbard Research Award to Richard Ahrenkiel for his pioneering work and instrument development in the minority-carrier lifetime spectroscopy area. In FY1998, the measurements and characterization laboratories performed more than 45,000 measurements on some 16,000 samples representing every photovoltaic technology. The majority of these tests and measurements are tied to contract deliverables, program milestones, and standard verifications—prioritized in the annual operating plan of the Photovoltaics Program. Cost analysis of these efforts continue to support that these

centralized facilities provide cost savings for the PV program in terms of turn-around time, expert-based analysis, responsiveness, and cross-technology information exchange and documentation. The leadership roles in the characterization area has provided the PV Program with a central position in assuring worldwide uniformity in reporting and measurement/test procedures. The Measurements and Characterization Division will continue to focus its efforts to assist the validation and deployment strategies for this important program element, including the Million Solar Roofs Program and PVMaT. The technique development efforts address measurements specific to photovoltaic industry needs and the evolvement of manufacturing-environment methods. Several examples are summarized in each of the more detailed summaries that follow this introduction. The contributory nature of these laboratories work is partially indicated by the 80 journal, conference proceedings, and book publications during this past year, with some 70% of these with research collaborators from the internal and subcontractor communities.

About 15% of the activities are directed toward the research and development of measurement techniques, many of which are specific to PV technologies. New or improved analytical offerings during this past year include:

- temperature-controlled, large-area, continuous solar simulator for the evaluation of cells and modules under standard conditions for flat-plate and concentrator technologies,
- novel, minority-carrier lifetime spectrometer for contactless, non-intrusive, industry-based and in-line evaluation of solar cell materials,
- development and implementation of a defect evaluation procedure and instrumentation, leading to a planned user facility during FY1999 for evaluation of intragrain regions in polycrystalline photovoltaic semiconductors.

With this ensemble of analytical capabilities, the Laboratories for Measurements and Characterization offer customers and collaborators a complete, one-stop site for diagnostic evaluation and correlation of events from single-atom to the macroscale dimensions. The following summaries provide some examples and highlights of service, collaborations, research, and technique development activities in the four, defined interactive groups (Cell and Module Performance, Electro-Optical Characterization, Analytical Microscopy, and Surface and Interface Characterization) supporting the NCPV and Photovoltaics Program with both extraordinary analytical capabilities and expertise.

PV Measurements and Characterization In-House Research

Title: **Analytical Microscopy Characterization of PV Materials**

Organization: NREL

Contributors: Mowafak Al-Jassim, Kim Jones, Rick Matson, Helio Moutinho, Andrew Norman and Amy Swartzlander.

Introduction

The *Analytical Microscopy* task has provided extensive support for both our in-house and subcontract groups. A wide variety of techniques was used to characterize PV materials and devices. Quantitative compositional measurements are performed by fully computerized electron probe microanalysis (EPMA) using either energy dispersive or wavelength dispersive X-ray analysis. Structural and defect analyses are carried out by transmission electron microscopy (TEM). Additionally, scanning electron microscopy (SEM) in its various modes, such as secondary electron imaging, backscattered electron imaging, cathodoluminescence (CL) and EBIC imaging, is providing a wide support for measuring the topographical, compositional, luminescent and microelectrical properties of PV materials and devices. In the nano-scale area atomic force microscopy (AFM) is providing indispensable, high resolution examination of the morphology of thin films. Furthermore, we have maintained the X-ray diffractometer as a multiuser facility for the PV program.

The majority (~60%) of analyses carried out by this task is of short-term nature. The emphasis in this category is on high-quality data with short turn-around time. However, due to the routine and/or the proprietary nature of this work, it probably suffices to state here that we analyze over 150 of this type of samples a month. In addition to routine analysis, approximately 40% of our resources are committed to research support. Most of the research activities carried out by this task are planned through other in-house and subcontractors activities. The following is a brief account of some examples of our research support during 1998. These are divided according to material technology.

CIS

In response to the needs of a CRADA for spatially identifying the location and cause of shunting problems in thin film modules, the NREL-developed large scale laser scanner (LSLS) with its automated shunt screening program has been applied to both thin film CIGS and a number of a-Si modules. In particular, laser scanning of CIGS mini-modules was used to identify inter- and intra-cell non-uniformities, create maps of the shunt resistance of the devices, identify the specific locations of shunting problems (such as pinholes and laser scribe areas), and also provide a measurement of the shunt resistance of the corresponding individual cells.

High resolution EBIC has been deployed in the field-emission SEM. One recent interesting application was the determination of the junction positions in both ZnO/CIS and ZnO/CdS/CIS devices. The result was that a homojunction was formed in the CIS in both cases at essentially the same position in the absorber material, thereby suggesting the possibility of deleting CdS from the device structure altogether.

In order to study the effect of Na concentrations on device properties and to correlate that with structural and microelectronic properties, CIS films with varying Na concentrations were grown on four different substrates (alumina, 7059 glass, soda lime glass (SLG), and $Si0_2$/SLG). The five levels of Na incorporation were introduced by co-evaporating 0, 2, 8, 35, and 230 mg of Na_2Se with Cu, In, and Se. In general, we observed the following: the device parameters all improved with the first addition of Na (2mg) and then remained relatively constant over the next steps of 8 and 35 mgs. At 230 mg, where the material apparently became the equivalent of supersaturated, the microstrucure disintegrated into small grain material and the device parameters plummeted, except the hole density—which increased. The electron-beam-induced current (EBIC) characterization of the devices indicated that the first bit of Na served to create a narrower, much more uniform, space charge region nearer the hetero-face (hence the higher V_{OC}, J_{SC}, FF, N_A). Reflecting the device data reasonably well, the charge collection efficiency profile revealed by EBIC, varied in average junction position, space charge region, diffusion current contributions which reflected, in turn, the complex defect chemistry of the material.

A novel approach in the formation of CI(G)S was studied using the high resolution SEM. The formation pathway follow a two-step process via various precursor structures using a matrix consisting of several process parameters, the influence on precursor growth and subsequent compound formation is under study. The SEM was used to identify the structural growth of the precursor structures and their dependence on the various process parameters under investigation. Furthermore, examining the final CI(G)S films allowed the correlation between structure and morphology to the respective precursor and, finally, to the device performance of the finished photovoltaic devices.

CdTe

Induced recrystallization of CdTe thin Films deposited by Close-Spaced Sublimation (CSS) was investigated by AFM and X-rays diffraction (XRD). This work complemented the study we did last year on CdTe films deposited by Physical Vapor Deposition (PVD) and CSS. In the previous study we attributed the changes observed in PVD samples treated with $CdCl_2$ to a recrystallization and grain growth process. The fact that CSS samples did not show any changes with the treatment was attributed to their initial good quality, when compared to PVD samples. If our interpretation of the results were correct, and the changes observed in CdTe films after $CdCl_2$ heat treatment are due to recrystallization, we should be able to induce this process in CSS films if we increase their initial stress. With that objective, we deposited CSS films at lower temperatures, which had smaller grains than films deposited at higher temperatures, and consequently more stress. AFM images (Fig. 1) and XRD patterns from these samples after treatment at 350°C showed new grains over the original matrix, and two lattice parameters, respectively, confirming ongoing recrystallization. This is the first time recrystallization in CSS CdTe films has been observed.

Furthermore, a major advantage of preparing CSS CdTe films at lower temperatures is the economy of energy during growth, and the simplification of the process, since the problem of diffusion of impurities and softening of the sodalime glass used as substrate is eliminated. We prepared solar cells using CSS CdTe films grown at low (420° to 474°C) and high (620 °C) temperatures. Although the $CdCl_2$ parameters have not been optimized, we obtained cells

deposited at low temperatures with efficiencies close to ones deposited at high temperatures. We believe that after the optimization of growth and chemical treatment parameters we can achieve high efficiencies in solar cells using CSS CdTe films deposited at lower temperatures.

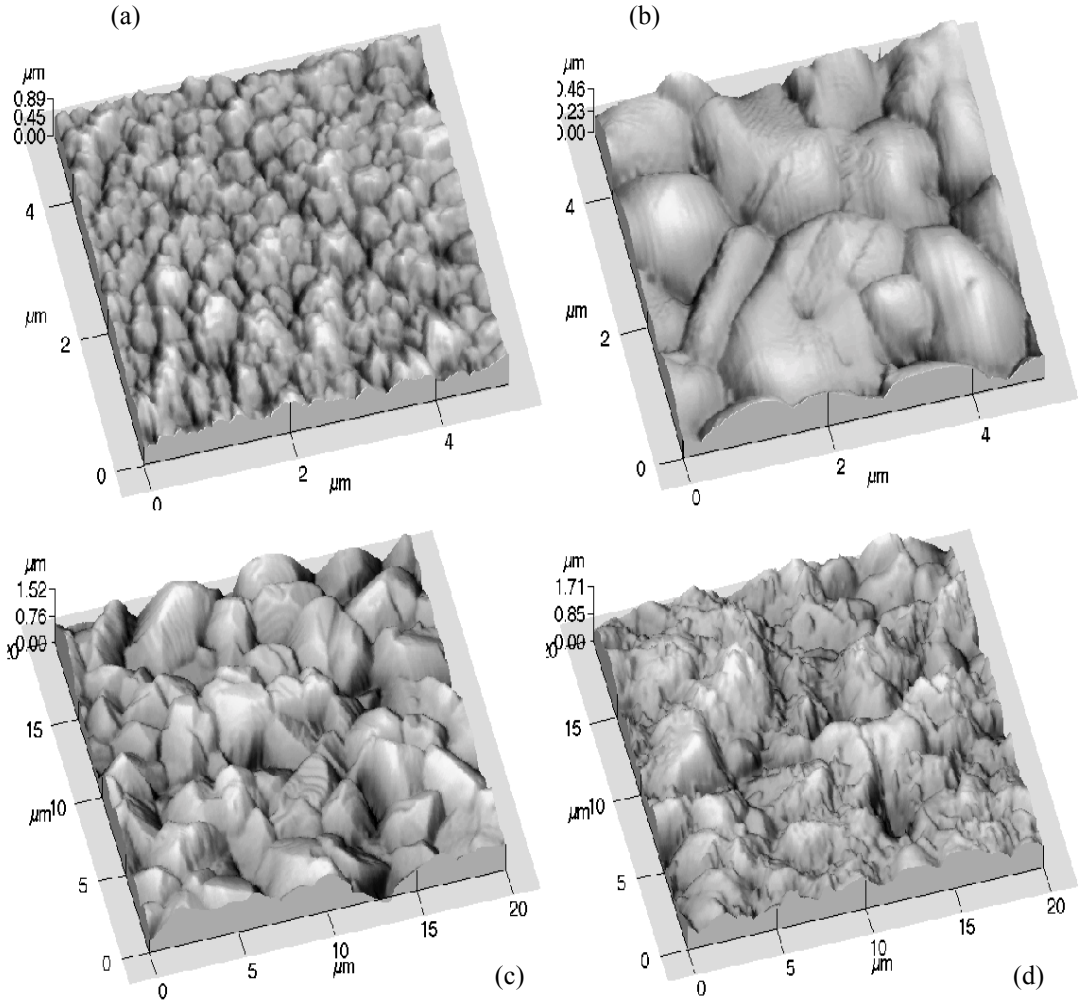

Figure 1: AFM images of CSS CdTe films. (a) Low-temperature deposition, untreated. (b) Low-temperature deposition, $CdCl_2$-treated at 400ºC, 30min. (c) High-temperature deposition, untreated. (d) High-temperature deposition, $CdCl_2$-treated at 400ºC, 30min.

Si

An inter-comparison of the OBIC maps of the polycrystalline Si cells of several companies (Solarex, Astropower, Evergreen, Shell, and ASE in collaboration with Daystar Technologies) demonstrated an overall acceptable spatial uniformity of response amongst the cells, the extreme being no worse than about 5% variation from the device peak response across the entire device. This is at issue because non-uniformity in thin film module and sub-module device properties can be dramatic. This information was shared with all concerned parties.

Over this past year, we have worked closely with the a-Si group on the development and optimization of a low-temperature homoepitaxial Si growth process, using hot wire chemical vapor deposition (HWCVD). TEM analysis has played a crucial role in providing microstructrual information which has lead to the optimization of several important parameters critical to the growth of good quality epitaxial layers. The first and most obvious is substrate cleaning. While this may seem trivial, the development of an effective cleaning process that works at low temperatures without the introduction of H platelets into the substrate has proved problematic. Figure 2 shows a 120 nm HWCVD epitaxial Si layer grown on a (001) Si wafer. This TEM cross-sectional view reveals a high density of hydrogen platelets at the interface, in the layer, and deep in the Si substrate. Through experimentation, we have found a series of ex-situ cleaning techniques that provide us with a relatively stable H terminated surface. We also have determined several parameters in the growth process itself which have helped us to optimize the layers grown. Chief among these is the fact that an increase in the amount of atomic H in the ambient gas must be offset by an increase in substrate temperature to inhibit the formation of substrate damaging platelets. Since this process produces atomic hydrogen as a direct by-product of the decomposition of SiH_4 on the hot filament, it is imperative to find appropriate substrate temperatures which depend on gas flow rate, filament temperature, and ambient pressure. Shown in figure 3, is an epitaxial Si layer that was deposited at a low temperature incorporating a refined cleaning process and by optimizing a variety of growth conditions. This TEM cross-section illustrates a significant reduction in interfacial contamination and almost complete elimination of hydrogen platelet formation.

III-Vs

The main activity in this area has been supporting NREL's III-V Materials and Devices Team in developing 1.0eV bandgap materials for multijunction cells. Metastable $(GaAs)_{1-x}(Ge_2)_x$ alloys were investigated by TEM and AFM in support of NREL's High Efficiency Devices Team. These alloys, with direct band gaps varying from 0.67 to 1.42 eV, can be grown lattice-matched to GaAs making them a candidate material for use in high efficiency multijunction cells. Bulk $(GaAs)_{1-x}(Ge2)_x$ alloys are unstable to phase separation into GaAs-rich zincblende and Ge-rich diamond structure phases. However, there have been reports that single phase metastable alloy layers may be grown by non-equilibrium techniques such as molecular beam epitaxy, metal organic vapor phase epitaxy (MOVPE) and sputtering. The results we obtained so far are on $(GaAs)_{1-x}(Ge2)_x$ layers, $0 < x < 0.22$, grown by low pressure (≈50 Torr) MOVPE at temperatures between 640-690°C on vicinal (001) and (115) GaAs substrates. Cross-sectional TEM dark-field images taken with the chemically sensitive (002) reflection revealed pronounced segregation of Ge in all the layers examined. In $x \approx 0.1$ layers, grown on vicinal (001) substrates at 640°C, Ge segregation occurred on {115}B planes inclined at 15.6° to the (001) plane forming an interconnecting network of Ge-rich plates ≈ 5 nm thick (see Fig. 4). AFM of the growth surface revealed {115} surface facets associated with this segregation. Increasing the growth temperature to 690°C resulted in a change in the segregation microstructure towards irregular, (001) oriented, plates of diamond structure Ge-rich material with antiphase boundaries quite often being formed in the zincblende GaAs-rich material overgrowing these plates. Growth on a (115)B substrate resulted in a spontaneously formed superlattice-like structure of alternating layers of Ge-rich and GaAs-rich material along the (115) growth direction.

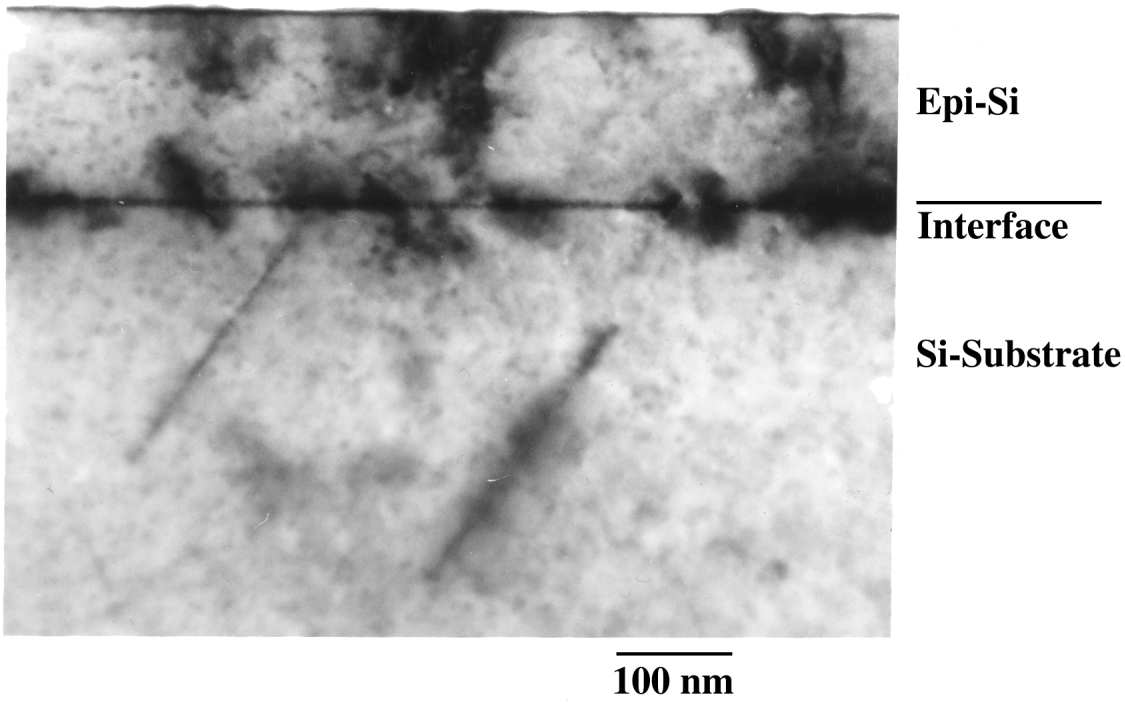

Figure 2: HWCVD epitaxial Si containing a high density of platelets

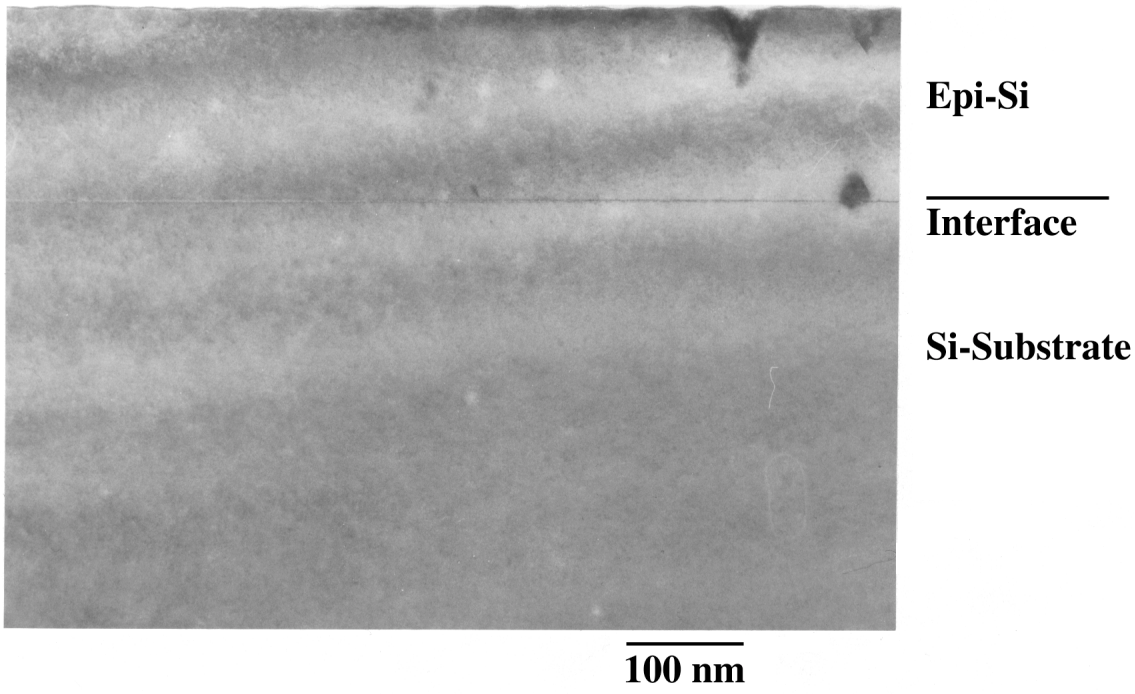

Figure 3: HWCVD epitaxial Si with low defect density

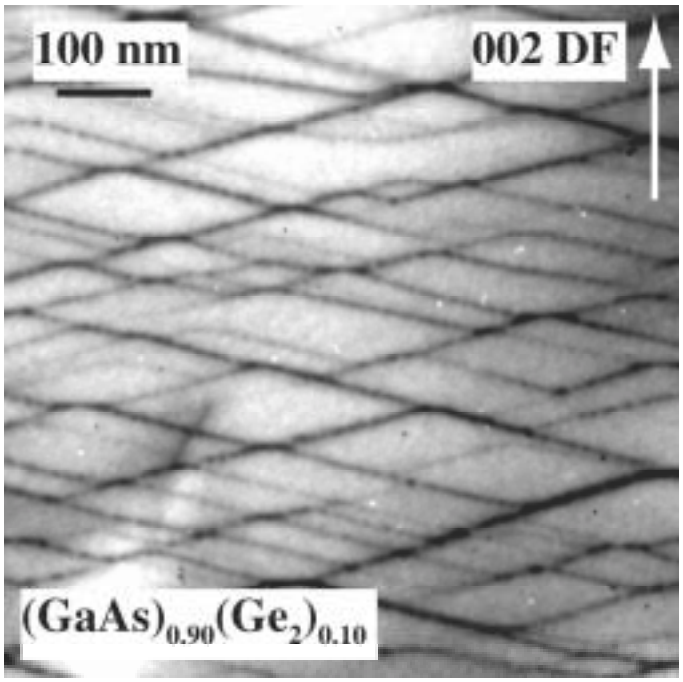

Figure 4: **[002]DF micrograph of x ≈ 0.1 layer grown at 640°C on vicinal (001) GaAs substrate showing Ge segregation on {115}B planes.**

For x ≈ 0.22 layers, grown at 640°C on vicinal (001) substrates, Ge segregation again occurred but without the formation of the regular faceted structure observed in the x ≈ 0.1 layers. The Ge-rich regions in these layers formed an almost cellular structure when viewed along [110] but appeared as thin bands inclined at ≈ 2° to the $(GaAs)_{1-x}(Ge2)_x$ layer/buffer layer interface when viewed along [-110]. AFM revealed surface hillocks elongated along [110] that correlated with the observed pattern of Ge segregation. It is believed that surface segregation of Ge coupled with the development of anisotropic surface roughness during growth leads to the characteristic patterns of Ge segregation observed in the layers. The effect of growth temperature, growth rate, alloy composition, and substrate orientation on the compositional uniformity and electrical and optical properties of these layers is being further investigated.

Title: **Electrooptical Characterization**

Organization: Laboratory for Measurements and Characterization,
National Renewable Energy Laboratory, Golden, Colorado 80401

Contributors: R. K. Ahrenkiel, Principal Investigator, F. Abulfotuh,
P. Dippo, B. M. Keyes, D. Levi, J. Webb, L. Gedvilas.

Objectives

The overall objective of the electrooptical characterization task is to develop and provide electrical and optical measurement support for both in-house and subcontract photovoltaic (PV) device research, so as to accelerate commercialization of the respective technologies.

Results

The following describe contributions of the above measurement technologies to the principal device technologies of the national PV program.

CdS/CdTe thin film Solar cells.

During this period, extensive studies of CdS and CdTe were performed for both in-house and external researchers. The studies included energy resolved photoluminescence measurements taken at different powers and at different temperatures for the specified sets of samples from different researchers. The temperatures spanned the range from room temperature to 4.25°K. Work is on-going to examine the results and determine what information can be extrapolated from the data.

L. Woods has measured light and dark grain boundary diffusion potentials on CdTe "lift-off" films using three different electrical techniques. All films received a $CdCl_2$ treatment and some received the NP etch. The dark diffusion potential values from the different techniques are in good agreement and show that the NP etch reduces the grain boundary potential by half. This is in agreement with the model proposed by D. Niles for Te on CdTe surfaces. When this model is applied using SimWindows, a device emulation program, there is a reduction in the bimolecular recombination in the sulfur alloyed region near the grain boundary of a grain with a thick (50 Angs.) layer of Te. This result is consistent with the photoluminescence of these films.

NREL CdTe Team: Golden, CO:

Dean Levi is participating in the National CdTe team stability study by providing measurements of junction PL on samples under bias and at 10 suns.

CdTe Contact Studies:

We are continuing our studies of the effects of back contact processing on the electro-optical properties of the near-junction region of the CdTe absorber. In a recently initiated experiment, we deposited 10 different metals on the back surface of a CdTe/CdS device structure. Almost all of these metals produced a significant perturbation in the junction PL spectrum. We will study the systematics of these effects in an attempt to further clarify the effect of NP etch on the junction PL spectrum. This work was reported at the WCPEC conference in Vienna.

CdS studies

The FTIR lab staff began FTIR micro-spectroscopic analyses of impurity precipitates on CdS/SnO_2 samples cleaved from CdTe overlayers provided by the in-house CdTe Team. The chemical-bath deposited (CBD) CdS films exhibited much higher impurity coverages than the close-spaced sublimated (CSS) CdS films. Impurity precipitates identified at the cleaved CBD CdS surfaces included sulfates and stannates, but few organics, which are apparently vaporized or oxidized prior to CdTe deposition. The inorganic interfacial impurities may contribute to the reduced adhesion of CBD CdS to CdTe relative to

that of the CSS CdS. We also performed FTIR analyses which indicated that the polymeric components of the CBD reactor do not contribute contaminants to the as-deposited CBD CdS films.

CIGS thin film solar cells

Our Team to examined a number of CIS, CdS, ZnO, and CdS/CIS films on various substrates using far-infrared (15 □m to 100 □m FTIR spectroscopy. The objectives of this work were to correlate the far-IR reflectance of the films with their conductivity, and to measure the lattice vibrational spectra of the films (especially of the CIS films). We were able to measure the lattice vibrational spectra of CIS films on Mo substrates at room temperature by obtaining the unpolarized reflection-absorbance spectra of the CIS/MO film relative to an uncoated Mo substrate.

DLTS studies was carried out on 12 CIGS devices, which required 50 DLTS measurements of the transient spectrum and C-V characteristics.

Crystalline and multi-crystalline Silicon solar cells

Measurements for AstroPower

A project with AstroPower, to measure the minority-carrier lifetime in a large number of wafers prior to device fabrication, was described in an earlier report. The project will be completed when the wafers are fabricated into devices by AstroPower and the short circuit current compared with the minority-carrier lifetime and relative minority-carrier mobility measured by RFPCD. We measured 55 wafers by RFPCD using a laser wavelength of 850 nm and a spot size of about 2 inche diameter. The data showed a range of low injection lifetimes ranging from 150 ns to 300 ns. The range of electron mobilities in the p-type materials varied by about a factor of 3. The relative diffusion length was calculated for all samples and varied by about a factor of 3 among the sample lot. The ratio of high-injection lifetime to low-injection lifetime was very close to 2.0 for all samples measured. These data are indicative of recombination at Fe-B complexes for which the electron and hole capture cross-sections are equal producing the result that (high)/(low)=2.0. From the measured lifetime values, one can calculate a density of active Fe-B recombination centers of about $1x10^{14}$ cm^{-3}. We are attempting to find alternative techniques for identifying these complexes including DLTS and FTIR.

These wafers were returned to Astropower for a proprietary heating processing treatment that has been found to increase the device performance. The 55 wafers were remeasured and the heating processing does not change the electron mobility. However, the low-injection lifetimes increase by about a factor of 10 resulting in an increase in the diffusion length of about a factor of 3. The range of low-injection lifetimes now varies from about 1.5 s to 4.0 s. Again the ratio of (high)/(low)~2.0 indicating Fe-B complexes but with a concentration reduction of about 10. The wafers were returned to AstroPower for device fabrication. The finished devices were measured and the open-circuit voltage and short-circuit current were recorded. The open-circuit voltage changed very little. The short circuit current correlated well with our measured minority-carrier parameters.

The FTIR group worked AstroPower to provide FTIR analyses of carbon and oxygen, and carbide and oxide precipitates in the polysilicon silicon samples. Correlations observed between impurity concentrations and carrier diffusion lengths in the AstroPower samples were investigated and presented at the NCPV national meeting in October.

Evergreen Solar

FTIR micro-spectroscopic analyses of carbon-containing impurity precipitates in string-ribbon silicon samples provided by Evergreen Solar.

We peformed a number of minority-carrier lifetime measurements on string-ribbon samples using the RFPCD technique.

High Efficiency Devices

Support has been provided for the NREL III-V team, in their search for the optimal growth conditions for high quality epitaxial GaAs on the new MBE system, using the time-resolved photoluminescence technique. The two projects pursued were 1) the investigation of ordering properties of epitaxial GaAs films and 2) the production of device quality MBE material through the growth and characterization of GaAs/GaInP double heterostructures.

Research has been in an attempt to use Photoluminescence (PL) and Time-Resolved Photoluminescence (TRPL) to improve the low-temperature GaAs-related compounds. These 1 eV compounds are excellent candidates for a third junction in the already successful GaInP/GaAs tandem cells, allowing for an increase in the device efficiency from 30% to 37%. Current material issues include the presence and effect of dislocations, interfaces, and the presence of carbon on the lifetime of photogenerated carriers. Measurements on low-temperature GaAs have shown that a spectral response of about 0.7 can be achieved with measured lifetimes of about 0.5 ns. The correlation between these parameters can further be seen by measurements on 1.2 to 1.3 eV compounds which exhibit a spectral response of 0.3 to 0.4 and a lifetime of about 0.2 ns. Current 1eV material is limited to a quantum efficiency of about 40 %. The cause for this is being investigated.

We performed far-infrared FTIR measurements of the substitutional nitrogen lattice mode in GaInNAs, to complement the mid-infrared measurements performed earlier this year. The intensity of the substitutional nitrogen band does not correlate with XRD and SIMS measurements of nitrogen content, despite using the far-infrared measurements in an attempt to identify additional nitrogen modes. We plan to perform far-IR analyses of lifted-off GaInNAs films to eliminate interference from the GaAs substrate modes

Photoluminescence (PL) measurements were very useful in characterizing the 1eV GaInNAs latticed matched to GaAs. As a result of the short diffusion length, the standard spectral response measurements have proven to be sensitive only to changes in carrier concentration. In contrast, PL has been successful in monitoring changes in material quality as a result of post growth annealing processes. This is a very important finding and forms the basis for future work in this area.

DLTS measurements were made on the GaInNAs samples and a number of deep level defects were discovered in the material.

Amorphous Silicon Solar Cells

Performed innovative room-temperature FT-PL and FT-Raman analyses of microcrystalline silicon films to identify defects and to measure the crystalline/amorphous ratio, respectively. Our clients were the Hans-Meitner Institute and the IEC.

We developed software for rapid quantitative analysis of hydrogen in a-SiH and a-SiGeH in support of H. Mahan's and B. Nelson's teams, respectively.

.

Technique Development

A RFPCD lifetime measurement system was developed that measures lifetime as a function of sample temperature. Measurements were made on a number of PV materials including thin film CdS, CIGS, and CdTe, GaAs, InGaAs and single and polycrystalline silicon wafers over the temperature range 80 K to 300 K. These data provided additional information about the principal recombination mechanisms in these materials.

Work was completed on the active quenching circuit for the new IR-TRPL system under the FIRST program. Data were obtained on a 1.0 ev sample fabricated by the in-house III-V Team.

An inexpensive CdS thickness measurement system has been designed and built for the CdTe team. This nondestructive optical technique constitutes a major improvement over the current destructive and time consuming profilometer based system. Furthermore, by varying the beam diameter and/or the location of the beam on the sample, information on sample uniformity can easily be obtained. This system is fully operational.

Work for Others

The new analytical services agreement (ASA) system was put in operation. ASA contracts were put in place with Spire Corporation, Hewlett-Packard Corporation, and Penn State University.

Patents: A patent application was allowed by the U. S. Patent Office. The patent was entitled "Apparatus for measuring Minority Carrier Lifetime in Semiconductor Materials" and the inventor is Richard K. Ahrenkiel

Publications:

Journal Articles

R. K. Ahrenkiel, R. Ellingson, S. Johnston, and M. Wanlass, Appl. Phys. Lett. **72**, 3470 (1998).

R. K. Ahrenkiel and S. Johnston, Solar Energy Materials and Solar Cells **55**, 59-73, (1998).

F. Alsina, H. M. Cheong, J. D. Webb, A. Mascarenhas, J. F. Geisz, and J. M. Olson, Phys. Rev.**B, 56**, 20, 13126 (1997),

H.R. Moutinho, M.M. Al-Jassim, D.H. Levi, P.C. Dippo, L.L. Kazmerski. Journal of Vacuum Science and Technology. A, Vol. **16(3)**, May/June 1998.

J. F. Geisz, D. J. Firedman, J. M. Olson, S. R. Curtz, and B. M. Keyes, J. Cryst. Growth **175** (1998).

Conference Papers

R. K. Ahrenkiel and S. Johnston, Mat. Res. Soc. Symp. Proc. Vol. **510**, pp. 575-581 (1998).

S. Johnston and R. K. Ahrenkiel, Mat. Res. Soc. Symp. Proc. Vol. **510**, pp. 607-612 (1998).

D. Albin, R. Dhere, A. Swartzlander-Guest, D. Rose, X. Li, D. Levi, D. Niles, H. Moutinho, R. Matson, P. Sheldon, Mat. Res. Soc. Symp. Proc , Vol**. 485**.

D.H. Levi, L.M. Woods, D.S. Albin, T.A. Gessert. D.W. Niles, A. Swartzlander, D.H. Rose, R.K. Ahrenkiel, P. Sheldon, Mat. Res. Soc. Symp. Proc , Vol. **485**. (1998), pp. 209-214.

M. Contreras, H. Wiesner, and J. Webb, AIP Conference Proceedings **Vol. 401**, 40 (1998), 403

K. Ramanathan, R. N. Bhattacharya, J. Granata, J. Webb, D. Niles, M. A. Contreras, H. Wiesner, F. S. Hasoon, and R. Noufi, *Twenty-Sixth IEEE Photovoltaic Specialists Conference-1997*. p. 319-322, (1998).

J. D. Webb, D. H. Rose, D. W. Niles, A. Swartzlander, and M. M. Al-Jassim, Proc *Twenty-Sixth IEEE Photovoltaic Specialists Conference-1997*. (1998), pp. 399-402 ,(1998).

M. A. Contreras, B. Egaas, P. Dippo, J. Webb, J. Granata, K. Ramanathan, S. Asher, A Swartzlander, and R. Noufi, *Twenty-Sixth IEEE Photovoltaic Specialists Conference-1997*, 359-362 (1998).

T. L. Wangensteen, M. W. Wanlass, J. J. Carapella, H. R. Moutinho, A. R. Mason, J. D. Webb, and F. A. Abulfotuh, *Twenty-Sixth IEEE Photovoltaic Specialists Conference-1997*, (1998, pp. 967-969.

R. K. Ahrenkiel, S. P. Ahrenkiel, and M. M. Al-Jassim and R. Venkatasubramanian, *Twenty-Sixth IEEE Photovoltaic Specialists Conference-1997*, (1998), pp. 527-529.

R. K. Ahrenkiel and S. Johnston *Twenty-Sixth IEEE Photovoltaic Specialists Conference-1997*, (1998), pp. 119-122.

R. K. Ahrenkiel, D. H. Levi, S. Johnston, W. Song, D. Mao, and A. Fischer, *Twenty-Sixth IEEE Photovoltaic Specialists Conference-1997*, (1998), pp. 535-538.

B. Jagannathan, R. L. Wallace, W. A. Anderson, and R. K. Ahrenkiel, *Twenty-Sixth IEEE Photovoltaic Specialists Conference-1997*, (1998), pp.675-678.

R. Venkatasubramanian, B. C. O'Quinn, E. Siivola, B. Keyes, and R. K. Ahrenkiel, *Twenty-Sixth IEEE Photovoltaic Specialists Conference-1997*, (1998), pp. 811-814.

D. H. Levi, L. M. Woods, D. S. Albin, T. A. Gessert, D. W. Niles, A. Swartzlander, D. H. Rose, R. K. Ahrenkiel, and P. Sheldon *Twenty-Sixth IEEE Photovoltaic Specialists Conference-1997*, (1998), pp. 351-354.

F. A. Abulfotuh, A. Balcioglu, T. Wangensteen, H. R. Moutinho. F. Hasoon, A. Al-Douri, A. alnajjar, and L. L. Kazmerski, *Twenty-Sixth IEEE Photovoltaic Specialists Conference-1997*, (1998), pp. 451-454.

B. M. Keyes, F. Hassoon, P. Dippo, A. Balcioglu, and F. Abulfotuh, *Twenty-Sixth IEEE Photovoltaic Specialists Conference-1997*, (1998), pp. 479-482.

Title: **PV Efficiency Measurements - Standard Reporting Conditions**

Organization: Center for Measurement and Characterization

Contributors: K.A. Emery task leader; S. Rummel, H. Field, D. Dunlavy
A. Anderberg
Tom Moriarty (leveraged as part of TPV work for others)

Objectives

The performance of photovoltaic devices of all sizes and technologies are evaluated within this activity. This team supports the entire photovoltaic community by providing: secondary calibrations of photovoltaic modules and cells, efficiency measurements with respect to a given set of standard reporting conditions, efficiency verification of contract deliverables, current versus voltage (I-V) measurements under varying temperature, spectral irradiance and total irradiance. Support is provided for in-house programs in device fabrication, module stability, module reliability, PV systems, and alternative rating methods by performing baseline testing, specialized measurements and other assistance when required. This activity also supports the entire PV community by providing information on: PV measurement equipment and systems that are appropriate for the end user, I-V measurement procedures, and uncertainty analysis. Included in the uncertainty analysis are the determination of potential artifacts in the I-V results because of equipment or procedures, and realistic estimates of the elemental error sources. This activity is committed to obtaining the lowest possible uncertainty in the measurement of the standardized PV performance of single- and multi-junction cells and modules.

Technical Approach

The photovoltaic current versus voltage characteristics are measured with respect to standard terrestrial reporting conditions (25°C temperature, 1000 Wm^{-2} total irradiance and ASTM E892 global reference spectrum). The intensity of the Spectrolab X-25 solar simulator (30 cm square beam) is adjusted until the measured short-circuit current of a reference cell is equal to it's calibration value corrected for spectral mismatch. The current versus voltage characteristics are then measured using 4-terminal Kelvin connections to the PV device with a custom data acquisition system designed to give a random error of less than ±0.1% and a non random error of less than ±1% . The uncertainty in efficiency measurements with respect to standard reference conditions is ±2-5% depending on the sample size, geometry and number of junctions. The I-V system has a voltage range of ±50 V (0.1 μV resolution) and ±16 A to ±1 pA. These procedures have been shown to be valid for any given tabular reference spectrum including AM0 and the ASTM direct normal reference spectrum. Because of the wide current and voltage range the system is also used for concentrator and dark I-V measurements. For two-terminal multi-junction devices the spectrum of the Spectrolab model X25 solar simulator is adjusted, using a special filter plate developed at NREL, until each junction is producing the correct photo-current. The I-V system is also used for examining the effects of pre-measurement conditions, bias rate, maximum power versus illumination time, V_{oc} *vs*. time, and I_{sc} *vs*. time on the PV performance.

The filter spectral response system uses periodic monochromatic light directed through one of 68 10 nm bandwidth interference filters covering the spectral range from 280 to 1900 nm. The system is capable of providing steady-state light bias levels up to 200 mA and voltage bias levels

from ±1 mV to ±40V. Higher current bias levels are possible with an external shunt resistor. The intensity of the bias light is normally adjusted to give the short-circuit current under standard reporting conditions. The custom operational amplifier current-to-voltage-converter allows for a wide range of gains (1 to 10^6). The intense light from the 1000 W lamp illuminating the 5 cm diameter filters allows for small cells to large modules to be illuminated with adequate signal to noise. The uncertainty in the relative spectral response as a function of wavelength is less than ±5%. The data can be made absolute by forcing the integrated quantum efficiency to agree with the measured spectral response. The absolute spectral response can also be measured directly with this system giving an uncertainty of ±10%. The limiting factor in the uncertainty is the ±5-10% spatial nonuniformity of the monochromatic beam. The second grating monochrometer based system has a wavelength range from 300-5,000 nm with a 1 nm wavelength resolution and a 1-5 nm selectable bandwidth. The grating system was designed for accurate absolute spectral response measurements by illuminating a small 1 mm by 3 mm rectangular area and measuring the power of the entire beam. The system uses all reflective optics so chromatic aberrations and beam wander with wavelength are not present. The grating system uses an operational amplifier for the current-to-voltage conversion allowing a ±15 V voltage bias range with 0±1 mV being the normal configuration. A lock-in amplifier is used to detect the ac signal. The system is capable of broadband or filtered light bias for multi-junction or nonlinear devices. Both systems rely on accurate pyroelectric detectors or NIST calibrated semiconductor detectors for the measurement of the light power.

The efficiency versus concentration measurements are measured with a Spectrolab High Intensity Pulsed Solar Simulator (HIPSS). This system has been used to measure the performance as a function of concentration for several GaInP/GaAs concentrator cells fabricated at NREL to 1500 suns. The concentrator lamp housing allows measurement from 1 to 2000 suns. The cell performance as a function of concentration can also be measured using an unfiltered 1000W Xe-arc continuous light source that is focused to a small area. Using the cell's I_{sc} measured at one sun (ASTM E891-87 direct normal reference spectrum at a total 1-sun irradiance of 1000 Wm^{-2}) and assuming linearity in the current with total irradiance, the I-V characteristics are measured. The linearity can be determined by using calibrated wire mesh filters over a range of irradiances. Using a technique developed at NREL the temperature of the space charge region temperature can be accurately set to a given value under continuous illumination even though large temperature gradients (>10°C) may exist between the plate temperature and junction temperature. The procedure involves setting the sample temperature to the reference temperature e.g. 25°C without illumination (no heat load). Using a high speed shutter and voltmeter the open-circuit voltage is sampled (1000 readings/sec). The highest measured V_{oc} is then taken to be the V_{oc} under concentration. The thermoelectrically controlled vacuum plate is then cooled until this V_{oc} is reached. This same procedure is used in the Spectrolab X25 system for samples on thermally insulating substrates where temperature gradients of 5-10°C are typical.

The primary reference cell calibration procedure involves measuring the short-circuit current (I_{sc}), total irradiance (E_{tot}), and spectral irradiance ($E_S(\lambda)$) at the same time outdoors with the same 5° field of view. E_{tot} is measured with an Eppley HF primary absolute cavity radiometer, and $E_S(\lambda)$ is measured with a LICOR LI-1800 spectroradiometer. The uncorrected average

calibration value $<CV_u>$ is calculated for the 30 I_{sc} and E_{tot} readings taken during the 30 seconds required to measure $E_S(\lambda)$. Once a valid $<CV_u>$ is obtained the short-circuit current is corrected for temperature and the spectrally corrected calibration value CV is computed. Since the measurement of $E_S(\lambda)$ does not encompass the limits of the reference spectrum, the measured spectrum is extended using a computer model developed by the group to encompass the range of the reference spectrum (300-4000 nm). The calibration value CV is computed at least 20 times for at least 3 separate days giving a single primary calibration value. This procedure has been shown to have a total uncertainty of less than ±1% by rigorous uncertainty analysis, intercomparison with the World Photovoltaic Scale, primary AM0 standards and other intercomparisons.

The I-V characteristics of modules are routinely evaluated using the Spire 240A Solar Simulator. This system has a 0-100V and 0-20 A range for a 61 by 122 cm area. During FY 1998 the Spectrolab model X200 Large-Area Continuous Solar Simulator (LACSS) was used to evaluate the I-V characteristics of modules under continuous illumination. The custom LACSS I-V measurement system is capable of handling devices with an area less than 150 by 120 cm and a maximum voltage of ±300 V and current of ±60 A with a ±0.01 mV and ±1μA minimum. The system is routinely used to perform dark I-V measurements on modules without changing anything. Light soaking and pre-measurement procedures that have been developed for cells are routinely performed on the LACSS for thing-film CIS and CdTe modules. The Spectrolab Large Area Pulsed Solar Simulator (LAPSS) produces a one-sun beam of light (2m by 2m area and could illuminate a 4m by 4m area). The Spectrolab data acquisition system has a 0-100 V, 0-40 A measurement range. The system has been used to evaluate the I-V characteristics of modules.

During FY98 standardized Outdoor module I-V measurements were performed on a variety of one-sun modules using our variable tilt and azimuth test bed. For flat-plate modules the total irradiance was measured with an Eppley pyranometer and a crystal-Si reference cell in a module package mounted in the plane-of-array. A normal incidence pyrheliometer calibrated against NREL's cavity radiometers is used to measure the direct normal irradiance for concentrator modules. The module temperature is measured with a temperature sensor attached to the back surface of the module. The spectral irradiance is measured during the I-V measurement using a LICOR LI-1800 spectroradiometer with a Teflon dome and temperature controlled detector. Meteorological parameters at the time of measurement including direct to diffuse ratio, wind speed, wind direction, barometric pressure, air temperature and relative humidity are stored with the data. The outdoor I-V measurement system is capable of handling devices with a voltage and current range of ±300 V and ±60 A maximum to ±0.01 mV and ±1μA minimum.

Results

During FY96 the team performed 3814 I-V and QE measurements on 1383 cells and modules (I-V under standard reporting conditions). These figures do not include measurements on thermophotovoltaic cells. The cell and module calibrations were performed for the following groups:

U.S. Industry - AP Corp. (Si ribbon), ASE Americas (Si ribbon, extensive optical characterization of an encapsulated cell with a proprietary means of optical enhancement at the module level), ASM (a-Si), AstroPower (Si film, mono-Si), BP Solar (CdTe,

mono-Si, US plant), DayStar (low concentration prototype submodule of mono-Si, CIGS and triple-junction a-Si), ECD PVMat a-Si/a-Si/a-Si:Ge), ECD/Sovlux CRADA (a-Si/a-Si/a-Si:Ge), Evergreen Solar (multi-Si), Global Solar (mono-Si), Iowa Thin films (a-Si/a-Si), ISET (CIGS), Lockheed Martin Associates (CIGS), OCLI (CIGS CRADA), Photowatt - CEPFL (multi-Si), Sharp (multi-Si for SPIRE Corp.), Siemens (mono-Si, CIGS), Solarex (multi-Si, a-Si:Ge, a-Si/a-Si:Ge, filtered Si reference cells), Solar Cells Inc. (CdTe), Solec Int. (mono-Si), Solar Fabrik modules from Spire (mono-Si), Solar Solutions Inc./Koncar (a-Si), Solar World (Siemens mono-Si cell), SunPower (bifacial mono-Si), Sunwize (mono-Si), Tecstar (GaAs on Ge), Tideland (mono-Si cells imbedded in glass module), Unisun (CIGS), United Innovations (GaInP/GaAs cusp concentrator modules), Uni-Solar (a-Si/a-Si), and USSC (a-Si/a-Si:Ge, a-Si/a-Si:Ge/a-Si:Ge, a-Si:Ge, filtered Si reference cells)

Universities and other Groups in US -ASU Photovoltaic Testing Laboratory (reference devices), Burdick Technologies Unlimited (Si and filtered Si solar radiometers), Colorado School of Mines (CdTe), Colorado State University (mono-Si), Florida State Univ. (Si detector), Georgia Institute of technology (mono-Si), Oregon State Univ. (mono-Si reference cell), Penn State (a-Si, filtered Si reference cell), Sinton Consulting (mono-Si), Univ. of Utah (a-Si), and Univ. S. Florida (CdTe)

NREL internal groups - (a-Si, μC-Si/mono-Si, CIGS, CdTe, dye sensitized nano crystal dye, mono-Si, mono-Si, multi-Si, GaAs, GaInP, GaInNAs, GaInP/GaAs tandems, various reference cells for the user facility)
Modules for exposure studies and systems evaluation, including most of US industry in addition to Kanaka (a-Si/a-Si), APS (a-Si/a-Si),

Foreign Groups - Belgium (IMEC multi-Si, mono-Si), China (BSERI mono-Si, TIPS mono-Si), Czech Republic (Solartec mono-Si), Germany (Univ. Konstanz bifacial Si), Mongolia (Post Telecommunications Authority multi-Si to evaluate SPIRE 240A Solar Simulator), Russia (Inter Solar Center mono-Si), Switzerland (EPFL nano-crystalline dye sensitized cell), Taiwan (Sinonar filtered Si reference cell), Univ. Neuchatel Switzerland (a-Si/μc-Si), Univ. Sao Paulo Brazil (mono-Si)

Approximately 40 papers acknowledged the support of this group during FY98. This team has assisted nearly all module manufactures with their QA/QC programs by providing telephone consultations on measurement strategy and procedures, and a calibration tractability path for their cells and modules. The technology of PV I-V and spectral response measurements was transferred to a variety of university and manufacturing groups through phone conversations and visits. The group also supported work in spectral irradiance modeling and energy rating methods resulting in several co-authorship's. In support of international programs trips to China and India were made to transfer efficiency measurement technology. The team participated in the International intercomparison of calibration procedures for new technologies by performing extensive post-intercomparison analysis of the sample set.

A new system for measuring the quantum efficiency of solar photovoltaic devices has been developed. The spectral range is 250 to 1350 nm with a bandwidth of the monochromatic

beam of 2 nm. The light source is a xenon arc lamp with an ellipsoidal reflector. A three-section, custom fiber-optic bundle provides monochromatic and bias light to the sample and a reference signal to a monitor cell. Further development will involve the system's noise performance, increasing its bias light capability, reducing stray light effects, and improving its accuracy.

A new technique to more accurately measure the spectral response of a module has been developed. Previous module quantum efficiency measurements at NREL involved illuminating the entire module and setting the bias to the normal zero volts. The new technique is essentially a generalization of the procedures to measure the quantum efficiency of multi-junction cells. This procedure involves setting the light bias conditions so all cells are illuminated with broad-band light with the cell in the module that you wish to measure having less light so it is current limiting. The module is forward biased to the open-circuit voltage - the open-circuit voltage / number of cells in series. This procedure has been successfully used for CIS, mono-Si and CdTe modules.

Publications

M.A. Green and K. Emery, K. Bücher, D.L. King, and S. Igari "Solar Cell Efficiency Tables (version 11)," Progress in Photovoltaics Research and Applications, vol. 6, pp. 35-42, 1998.

M.A. Green and K. Emery, K. Bücher, D.L. King, and S. Igari "Solar Cell Efficiency Tables (version 12)," Progress in Photovoltaics Research and Applications, vol. 6, pp. 265-270, 1998.

Steve Rummel, Keith Emery, Halden Field, Tom Moriarty, Allan Anderberg, Don Dunlavy, and Larry Ottoson, "PV Cell and Module Performance Measurement Capabilities at NREL," Proc. 15th NCPV Program Review meeting, Denver, CO, September 8-11, 1998, AIP proceedings, 1998.

Halden Field, "UV-VIS-IR Spectral Responsivity Measurement System for Solar Cells," Proc. 15th NCPV Program Review meeting, Denver, CO, September 8-11, 1998, AIP proceedings, 1998.

M.A. Green and K. Emery, K. Bücher, D.L. King, and S. Igari "Solar Cell Efficiency Tables (version 11)," Progress in Photovoltaics Research and Applications, vol. 6, pp. 35-42, 1998.

K. Emery, D. Dunlavy, H. Field, and T. Moriarty "Photovoltaic Spectral Responsivity Measurements," proc. 2nd World Conference and Exhibition on Photovoltaic Solar Energy Conversion, Vienna Austria July 6-10, 1998.

Related publications funded by work for others TPV contract

T. Moriarty and K. Emery, "Thermophotovoltaic Cell Temperature Measurement Issues, Proc. 4th NREL TPV Conf., Denver, 1988.

M. Wanlass, J. Carapella, A. Duda, K. Emery, L. Gedvilas, T. Moriarty, S. Ward, and J. Webb, X. Wu, "High - Performance, 0.6 -eV, $Ga_{0.32}In_{0.68}As/InAs_{0.32}P_{0.68}$ Thermophotovoltaic Converters and Monolithically Interconnected Modules," proc. 4th NREL TPV Conf., Denver, 1998.

Title: **Surface and Interface Characterization**

Organization: National Renewable Energy Laboratory
National Center for Photovoltaics
Measurements and Characterization Division

Contributors: Sally Asher, David King, Alice Mason, David Niles, Robert Reedy, Amy Swartzlander, and Matthew Young

Introduction

The Surface and Interface Analysis Team uses a powerful array of sophisticated techniques for the analysis of the surface and near surface regions of materials. These include scanning Auger electron spectroscopy (AES), X-ray photoelectron spectroscopy (XPS), ultra-violet photoelectron spectroscopy (UPS), and dynamic and static secondary ion mass spectrometry (SIMS). XPS and AES spectroscopies are related techniques for determining the composition and chemistry of surfaces. Dynamic SIMS is used to perform trace element analysis for contaminants and dopants in materials. Static SIMS gives trace elemental and chemical information from surfaces.

Many of the research activities performed by this task are in support of work planned through other in-house and subcontractors activities. Team members have also been made significant improvements to equipment during this reporting period. The following is a brief description of some of the highlights of our work during 1998. The work in this report is divided according to the technique applied to the problem.

AES Study of Sulfur Distribution in ISET Grown $CuInSe_2$

ISET has begun to investigate the incorporation of S into their CIS based devices. The objective of this experiment was to study the S content of sulfidized CIS films as a function of the Cu/In stoichiometry. To this end, ISET prepared CIS absorber films with various Cu/In ratios. All samples were subsequently sulfidized in H_2S at 575°C for 20 minutes. Compositional information was obtained from AES depth profiles while microstructural information was obtained from SEM cross-sections. This information has helped ISET understand how their process control variables affect absorber layer composition.

AES depth profiles showed that there is a definite trend in the S diffusion as a function of Cu/In stoichiometry. Figure 1 shows that for a Cu-rich film the S is almost uniformly distributed. The profile in Figure 2 shows that as the Cu/In ratio nears 1, the S incorporation is restricted to the top surface near the junction area. The highly In rich

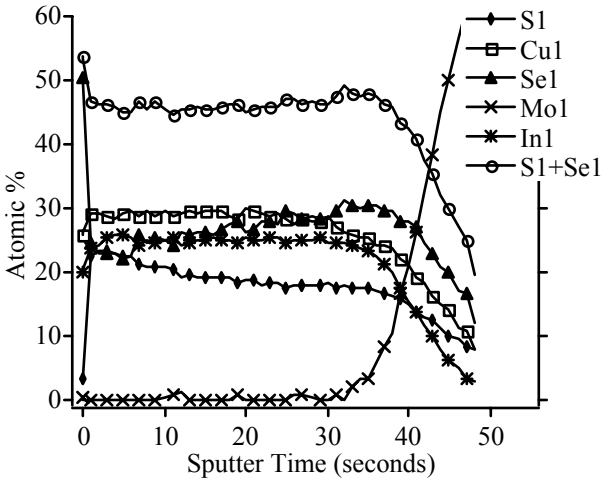

Figure 1. AES profile of sulfidized Cu rich CIGS (Cu/In > 1).

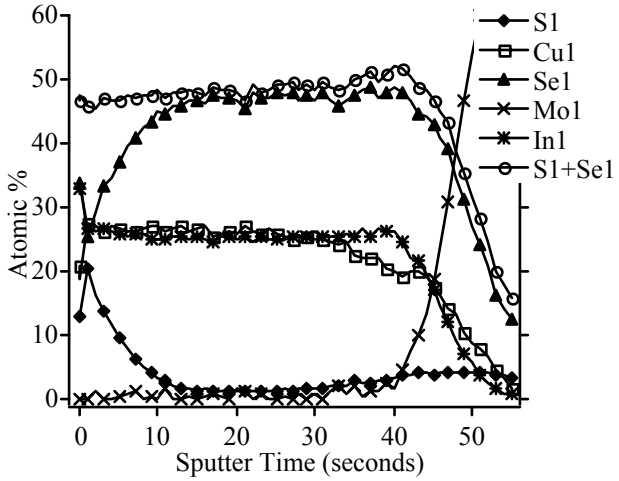

Figure 2. AES depth profile of sulfidized stoichiometric CIGS (Cu/In ≈ 1).

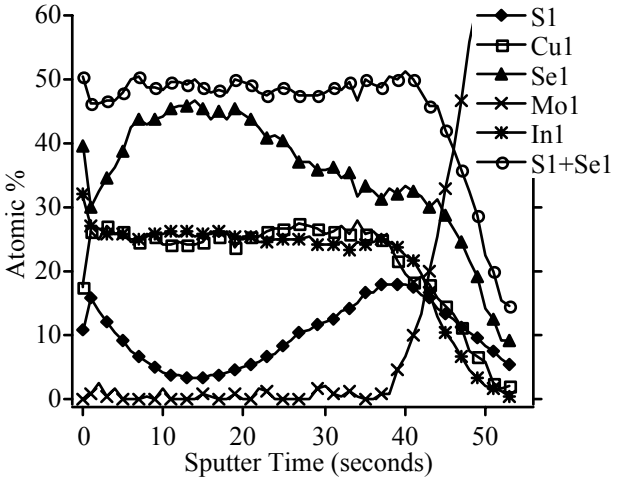

Figure 3. AES depth profile of sulfidized In rich CIGS film (Cu/In < 1).

sample, shown in Figure 3, has a peaks of S at the front and back of the absorber layer. For all conditions the total of (S+Se) is constant and near 50 atomic %.

An explanation for this behavior can be formulated by combining the AES results with SEM cross-sectional analysis. The SEM micrographs show that as the In content increases, the grain size near the back of the absorbers becomes smaller. If S diffuses rapidly along the grain boundaries and then continues into the grains, the small grains near the back can be completely converted into the sulfa-selenide. In the Cu-rich sample the AES results show that the liquid phase present during growth carries the S through the entire device. The compositional analysis also shows that the sum of the (S + Se) contents is near 50 atomic % for all samples, indicating substitution of the S for Se in the lattice.

AES Study of Defects in Global Solar Energy $CuInGaSe_2$ Films

Numerous samples were analyzed this year for GSE using Scanning Auger Microscopy. These samples were CIGS/Mo grown on a flexible substrate. Many parameters of the film

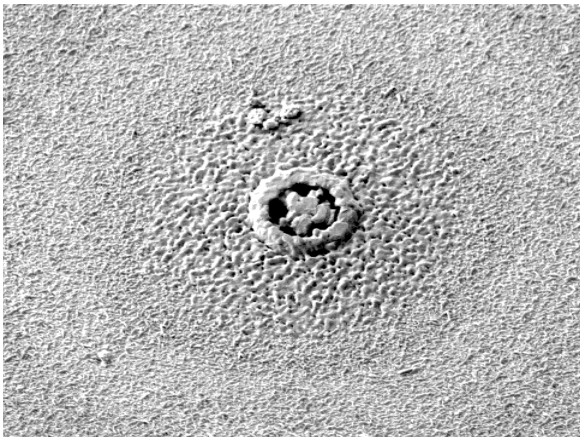

Figure 4. SEM micrograph of defect on CIGS film.

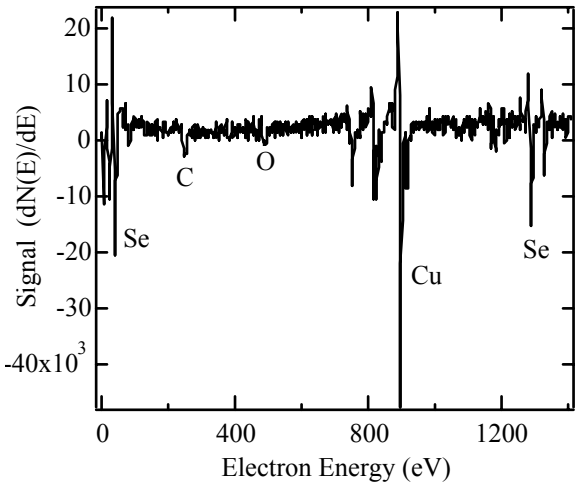

Figure 5. AES survey spectrum from the defect showing the presence of $CuSe_2$.

growth were monitored by using the chemical mapping and depth profiling capabilities of the AES. The data has allowed GSE to understand and explain variations in the electrical properties of their films as a function of growth conditions. Figures 4 and 5 illustrate one particular set of samples in which defects on the surface of the films were determined to be $CuSe_2$ growths.

XPS Studies of CdTe Back Surface Treatments

A sample matrix was created by the CdTe team to study the effect of different process treatments on the surface chemistry of the CdTe, and ultimately on the performance of the devices. The focus of this study was to determine the surface composition and chemistry of CdTe samples treated with wet and dry $CdCl_2$, nitric and nitric-phosphoric acid etches, and de-ionized water rinses, all combined with different anneals. XPS analyses suggest that the ultimate performance of the CdTe cell is greatly dependent upon the chemistry of the CdTe back-surface material. Treatment combinations that yield an oxidized back surface clearly result in poor devices. Cells that have a *metallic* back surface perform best, both in total efficiency and in terms of the measured IV curves. This is in contrast to pervious work, which had suggested that a p-type back-contact surface is needed for maximum cell performance. A manuscript describing these results is now in progress.

SIMS Analysis of GaInNAs and GaInNP Materials

The Surface Analysis team has provided extensive analytical support to the High-efficiency Concepts and Concentrators team in the past year to characterize both the contaminants and the N levels in the new low-bandgap semiconductors GaInNAs and GaInNP. These analyses have been important tools for understanding the problems faced in growing these materials both by MOCVD and MBE techniques. SIMS depth profile analysis was used to study the growth parameters affecting the incorporation of N and contaminants in MOCVD-grown single layers of GaInP:N and GaInAs:N deposited on GaAs. The SIMS results were important in showing that for GaInP:N films there were high levels of O and C incorporated with little addition of N. However, analysis of standard $GaInP_2$ without intentional N incorporation showed that the C and O levels were at or below the SIMS instrumental background limit. In the GaInAs:N films, C, O, and N were observed at levels which were lower than in the $GaInP_2$:N case. This work led to suspicions that the dimethyl-hydrazine N source was contaminated. In addition, super- lattice and other multi-layer structures have also been investigated.

In support of this work, the SIMS staff had ion-implant standards fabricated to facilitate quantitative analysis of dopants and contaminants in these materials. The new standards contain all of the element and matrix combinations encountered in this work, and will allow the team to achieve much higher accuracy and precision when

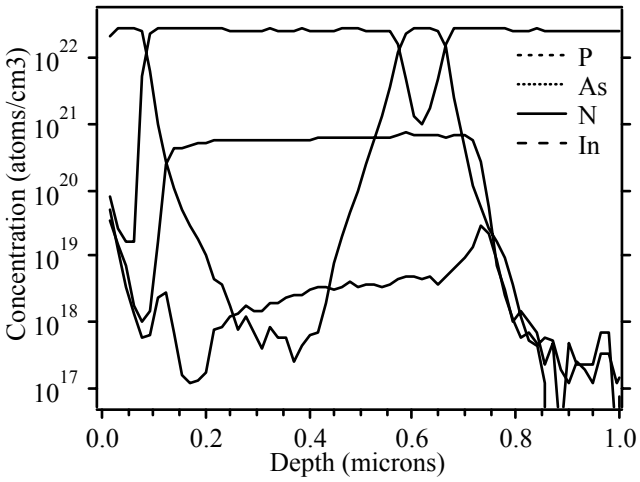

Figure 6. SIMS depth profile of N in GaInNAs/GaInNP multi-layer structure.

analyzing these materials. Figure 6 shows the result of quantifying the nitrogen though all the layers in a depth profile from one of the multi-layer samples.

SIMS Characterization of Amorphous Silicon Germanium Alloys

Silicon germanium alloys are commonly used in a-Si:H-based photovoltaic devices to reduce the optical bandgap. It is known that a-Si:H materials with excellent electronic and structural properties can be grown by the hot-wire chemical-vapor deposition (HWCVD) process. This process was recently used to investigate the possibility of growing a-SiGe:H at a high deposition rate with properties superior to that of plasma-enhanced chemical-vapor deposition (PECVD). SIMS is often the technique of choice to obtain information from hydrogenated amorphous materials due to its sensitivity and ability to detect H directly. A common difficulty with SIMS, however, is that ion yields can change for a given element in different matrices and for different elements in the same matrix. This causes problems when trying to quantify H and Ge contents through these amorphous multi-layer device structures where the matrix material is actually a Si-Ge alloy. The purpose of these experiments was to develop methods for characterizing the composition of the germanium-containing amorphous alloy material with a single analysis and analytical technique, SIMS.

SiGe alloy samples with compositions ranging from pure a-Si:H to pure a-Ge:H were grown from silane and germane gas mixtures using the HWCVD process. Electron probe X-ray microanalysis (EPMA) was used to provide the atomic concentrations of Si and Ge. The hydrogen concentrations were measured by nuclear reaction analysis (NRA). SIMS measurements were then performed. The concentrations of H and Ge were calibrated by measuring ion implant standards into pure Si to obtain relative sensitivity factors, or RSFs, that were then applied to the alloy samples. This standardization procedure references the signal for the element of interest to the Si matrix signal. However, in the SiGe alloy samples it becomes necessary to apply an alloy correction to the Si signal based on the amount of Ge in the matrix. Once the alloy correction has been applied, a linear regression analysis can be performed to find the best fit between the SIMS data and the EPMA results for Ge, and similarly between the SIMS data and NRA results for H. The results of this procedure are shown in Figures 7 and 8.

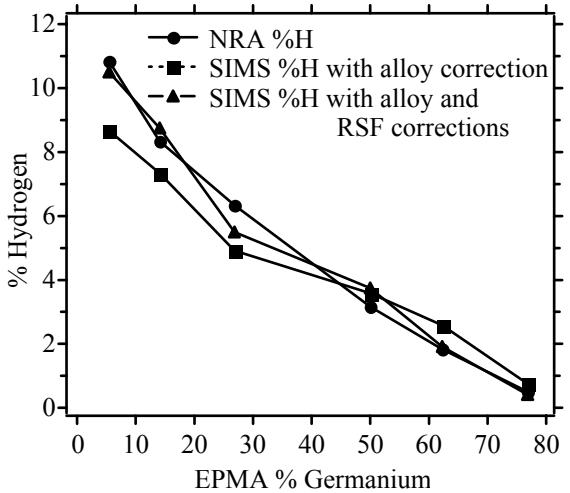

Figure 7. SIMS H after alloy correction and RSF correction compared to NRA results.

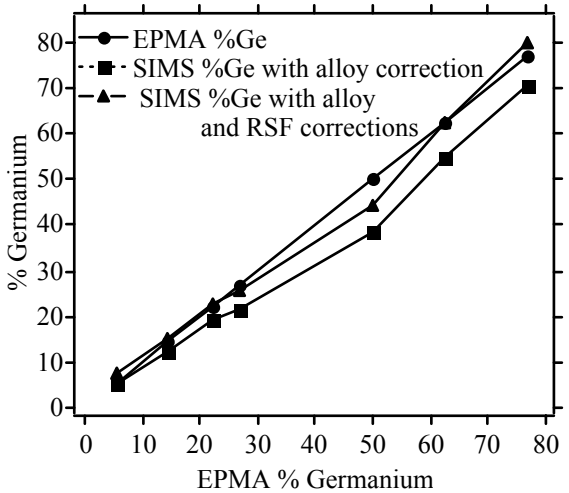

Figure 8. SIMS Ge after alloy correction and RSF correction compared to EPMA results.

This work shows that SIMS measurements of hydrogen can be performed in alloy materials within the generally stated accuracy of 50%, or in this case, 15%. In addition, compositional analysis of SiGe-alloys which generally is accomplished by AES or EPMA analysis, can now be performed by SIMS to an accuracy of at least 50% at the same time the H measurements are made. This will allow quantitative analysis of the thin layers in actual device structures. This method can be extended to dopant and contaminant elements as well.

SIMS and XPS Study of Cd-Partial Electrolyte Treated $CuInSe_2$

A major effort in the CIS team during the past year has been the understanding of the CdS/CIS junction interface. It has been shown that treatment with a Cd-containing solution, but without the actual growth of CdS, is enough create a junction in the CIS. The Surface Analysis team has participated in this study by providing SIMS and XPS analysis to study the chemical changes and distribution of elements at the CIS surface after treatment with the Cd partial electrolyte (PE) solution. Figure 9 shows the SIMS results for treating a CIS polycrystalline thin film and a CIS single crystal in the Cd-PE solution for 10 minutes at 85°C. The crystal contains a higher level of Cd at the surface and apparently shows slightly greater diffusion of Cd into the CIS. Additional study of these same samples showed that surface roughness affected the measurement and that care must be taken in interpreting the data. Subsequent SIMS analysis at lower primary ion impact energies showed that most of the Cd resides in the near surface region of the CIS with only shallow diffusion into the crystal and thin film. Figure 10 shows the comparison of the XPS Auger parameter (□) taken from the spectrum of a crystal treated in concentrated Cd-PE solution with □-values from several pure compounds. This analysis shows that the Cd at the surface of the crystal is likely bound as the chemical species CdSe. This work has helped further the understanding of junction formation between CdS and CIS polycrystalline devices leading to improved device performance.

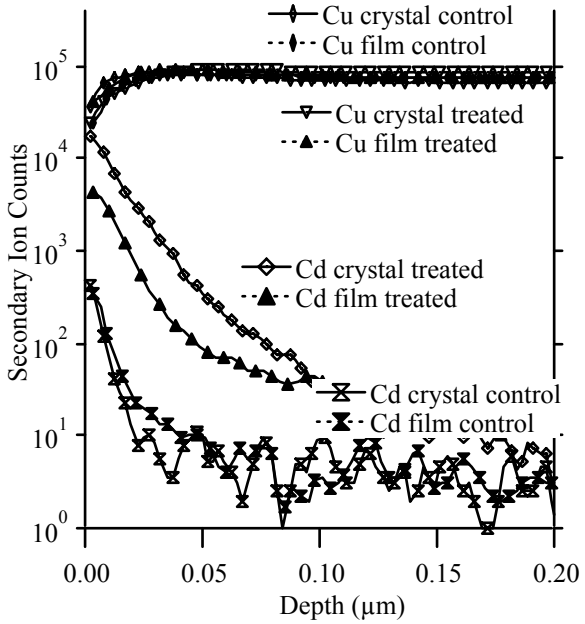

Figure 9. SIMS depth profiles of CIS polycrystalline thin film and CIS single crystal treated with Cd-PE solution.

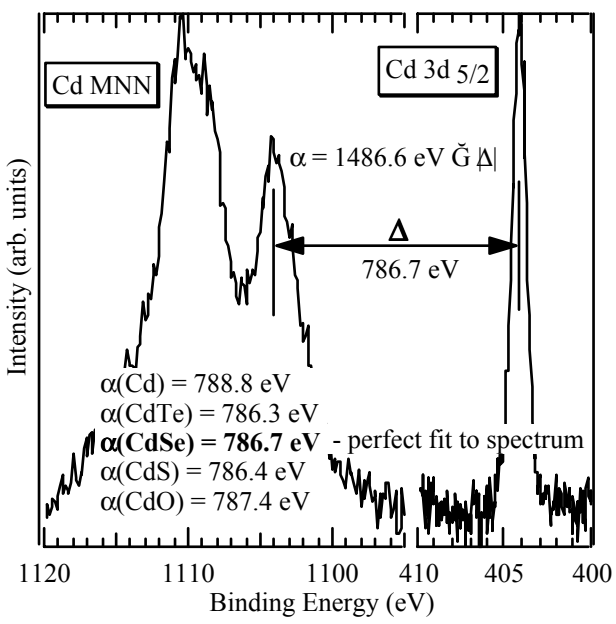

Figure 10. XPS Auger parameter analysis of CIS single crystal treated with Cd-PE solution.

Equipment Modifications and Technique Development Activities

During the past year, the Surface Analysis team has been able to complete several significant improvements to existing equipment. New computer systems were installed on the PHI-5600 XPS instrument and the PHI 670 AES instrument. The new Pentium PC controlled systems replaced outdated Apollo workstations which had become difficult to service and repair. The new hardware and software have already lead to improved efficiency in data acquisition, data processing, and dissemination of results to customers from these instruments. The Cameca IMS-3F SIMS instrument has undergone two significant modifications in FY98. First, laboratory personnel designed and fabricated electronic circuitry to improve primary ion beam control during analysis. This has led to a substantial improvement in the depth resolution of depth profiles from this instrument. A manuscript detailing this work was accepted for publication in the Journal of the American Vacuum Society. One of the reviewers for the article commented that "there are probably at least 100 sites with the Cameca IMS-3F that could benefit from this simple modification". The second modification to the 3F fitted video cameras on the sample-viewing microscope and at the output of the secondary-ion image detection system. The cameras improve the ability to position samples prior to analysis, as well as allowing the acquisition of digitized direct secondary-ion images.

5.0 Thin-Film Technologies Project

5.0 THIN FILM TECHNOLOGIES PROJECT—Introduction

Ken Zweibel

The Thin Film Technologies Project includes in-house R&D in CIS, CdTe, and amorphous silicon as well as subcontracted R&D within the Thin Film PV Partnership. Research is conducted by research teams within each organization and by cooperative National Research Teams in amorphous silicon, cadmium telluride, CIS, and Thin Film ES&H.

Some of the highlights for the fiscal year include:

In CIS:

NREL researchers added substantially to their world record cell efficiency (see Figure 1) by reaching 17.7% efficiency on a CIGS cell.

In CdTe:

Solar Cells Inc. fabricated a 9.1% efficient very large area CdTe module (see Table 1), meeting several of our Annual Operating Plan milestones for the CdTe technology. This is the most efficient thin film module of its size.
Solar Cells Inc. CdTe systems (1-10 MW) demonstrated 1-3 year outdoor stability at various locations (e.g., NREL, PVUSA, Ohio Edison).
Golden Photon fabricated the highest efficiency CdTe cells made on low-cost, soda lime glass (14.8% efficient). They also produced a near-30 W CdTe module of about 3400 cm^2 area.
Golden Photon identified stability as a critical issue for their approach to manufacturing CdTe modules.

In amorphous silicon:

United Solar made a significant advance in the world record efficiency for a-Si cells, reaching a NREL-measured stabilized efficiency (total area basis) of 11.8%. The previous best was about 10.9%. This is the first significant advance in a-Si cell efficiency in more than 5 years.

The thin film technologies made progress toward commercial readiness. In amorphous silicon, both Technology Partners (Solarex and United Solar) began construction of amorphous silicon production plants of sizes larger than had previously existed (USSC Troy, MI, 5 MW plant; Solarex, 10 MW Virginia plant). The two CdTe Technology Partners, GPI and SCI, delivered about 200 kW of product from pilot lines, including 25 kW each to a Navy-sponsored experiment at Edwards Air Force Base in California. Several of the CIS companies are experimenting with sub-MW pilot lines. Despite this progress, no thin film technology has yet reached substantial commercial presence in PV measured by annual worldwide production. Further technological and transitional scale-up to manufacturing issues must be addressed on an ongoing basis.

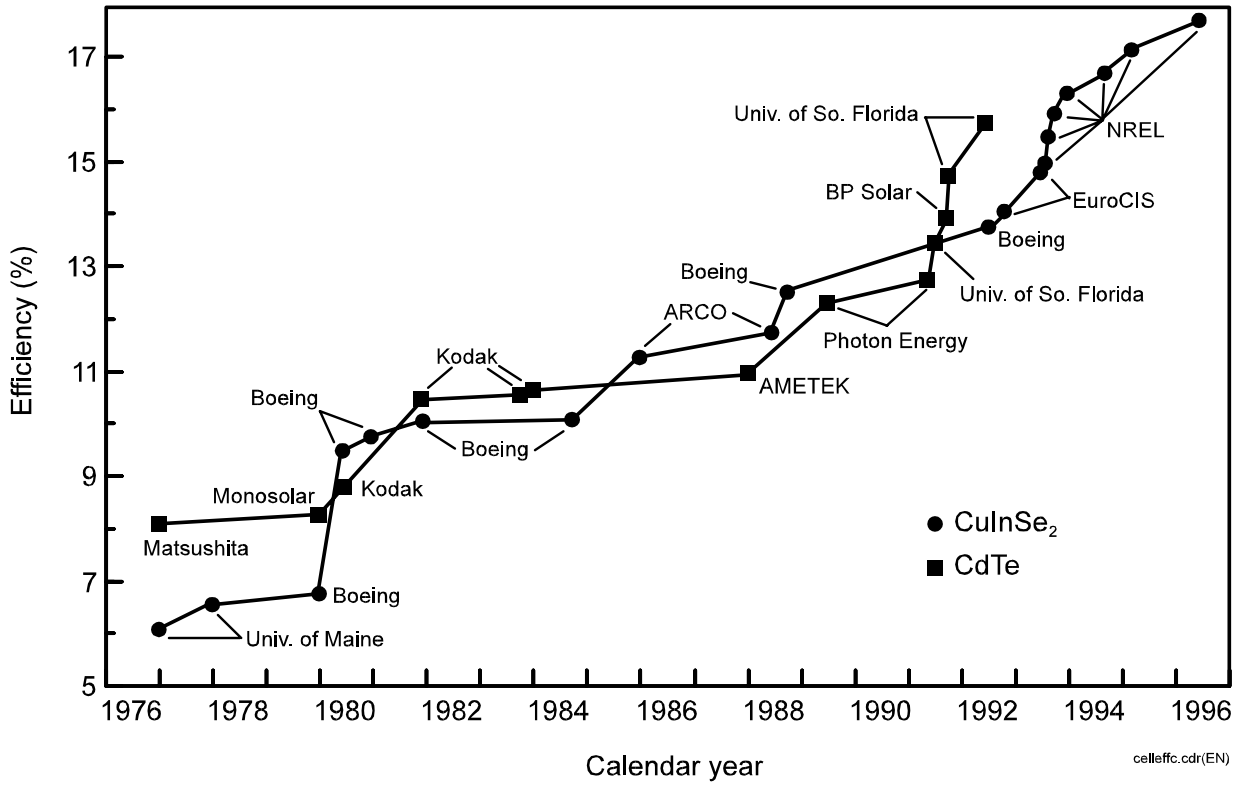

Table 1. The Best Thin Film Modules (1996)

Material	Size (cm^2)	Efficiency (%)	Power (Watts)	Company & comments
CdTe	6728	9.1%	61.3 W	Solar Cells Inc.
$CuInSe_2$ (CIS)	3859	10.2%	39.3 W	Siemens Solar Industries
Amorphous silicon	3906	7.8%	30.6 W	Energy Conversion Devices
CdTe	3350	8.7%	29.3 W	Golden Photon Inc.
Amorphous Silicon	3432	7.8%	26.9 W	United Solar Systems (USSC)
Amorphous Silicon	1200	8.9%	10.7 W	Fuji (Japan)
$CuInSe_2$ (CIS)	938	11.1%	10.4 W	ARCO Solar (now Siemens Solar Industries)
CdTe	1200	8.7% (reported)	10.0 W	Matsushita (Japan)
Amorphous Silicon	902	10.2	9.2 W	USSC

Note: Efficiencies verified independently at NREL unless noted as 'reported'; for a-Si they are after 600 hours light-soaking.

Thin-Film Technologies Subcontracts

Title: **Monolithically Interconnected Silicon – Film™ Module Technology**

Organization: AstroPower, Inc., Solar Park, Newark, DE, 19716-2000 USA

Contributors: D.H. Ford and J.A. Rand, Co-Principal Investigator; E.J. DelleDonne, R.B. Hall, A.E. Ingram, and A.M. Barnett

Abstract

AstroPower is developing an advanced thin-silicon-based, photovoltaic module product. A low-cost monolithic interconnected device is being integrated into a module that combines the design and process features of advanced light trapped, thin-silicon solar cells. This advanced product incorporates a low-cost substrate, a nominally 50-μm thick grown silicon layer with minority carrier diffusion lengths exceeding the active layer thickness, light trapping due to back-surface reflection, and back-surface passivation. The thin silicon layer enables high solar cell performance and can lead to a module conversion efficiency as high as 19%. These performance design features, combined with low-cost manufacturing using relatively low-cost capital equipment, continuous processing and a low-cost substrate, will lead to high-performance, low-cost photovoltaic panels.

Technical Approach

Thin film polycrystalline silicon grown on a low-cost substrate is one of the most sought after paths to low cost photovoltaic power [1]. Further cost reductions can be realized through the fabrication of large-area, series-interconnected submodules. This design incorporates a method of partitioning the thin-film photovoltaic layer into sub-elements and reconnecting them as a series array. A 36 segment 321.3 cm^2 monolithically interconnected device with an efficiency of 9.79% (verified by NREL) was fabricated as proof of concept for the interconnect process. Although this device exhibited many of the features required in a thin-film, monolithically-interconnected submodule, this device structure required a high number of process steps for device fabrication and did not incorporate light-trapping.

Figure 1 illustrates the schematic view of the monolithic interconnect device that AstroPower is presently pursuing.The sub-element device design consists of a thin (35-50 μm) polycrystalline silicon layer which is grown on a low-cost substrate. The thin silicon enables the use of imperfect materials and increased doping levels and lowers cost by minimizing the use of relatively expensive feedstock material. Diffusion lengths equivalent to twice the device thickness are required to assure high carrier collection through the bulk of the base layer. The addition of light-trapping and back surface passivation leads to improved solar cell voltage and fill factor.

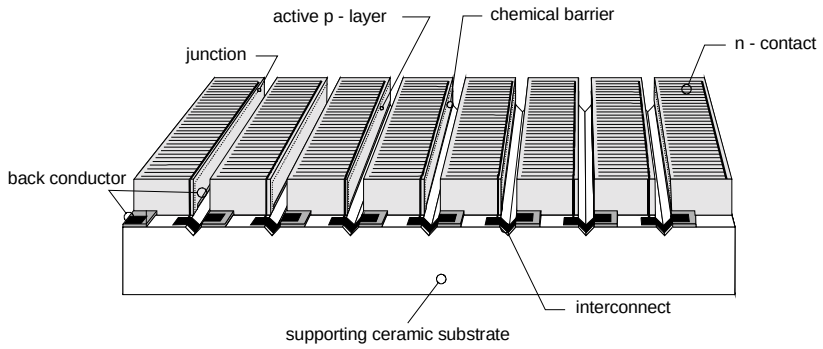

Figure 1. Schematic view of present monolithic device design.

Results

Substrate

When designing a substrate for thin-film silicon growth, the primary issues that must be addressed are:

- Mechanical stability at growth temperatures.
- Thermal expansion matched to silicon.
- Minimizing diffusion of impurities to the active silicon layer.

Structured ceramic substrates have been formulated to incorporate these properties and it has been demonstrated that the substrates can be manufactured in a cost-effective manner using a tape casting process.

The tape casting process pictured in Figure 2 is used to form large-area, thin, flat ceramics on a continuous basis. The advantage to tape casting, over other ceramic forming processes such as dry pressing or extruding, is that it forms flat pieces with thicknesses in the 25-1250 μm range. AstroPower presently has the capability to cast ceramics up to 12.5 inches wide.

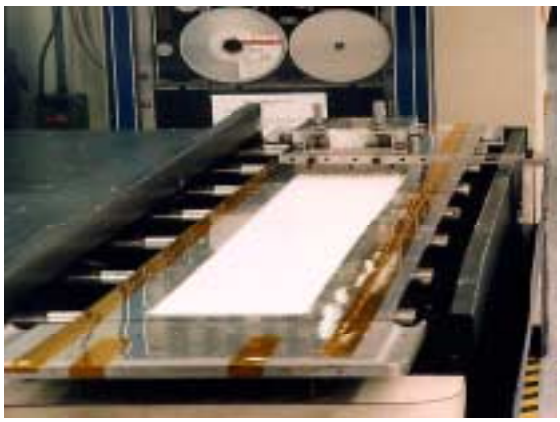

Figure 2. View of ceramic tape casting process

In order to obtain a flat crack free substrate with the tape cast process, a "slip" must be carefully formulated. The "slip" is a solution which contains all of the chemical ingredients required for the ceramic, and the proper chemicals for binding the particles together during the drying process. The slip is dried to form a "green-state" tape which is cut to size and then fired (sintered) to form a flat ceramic body. From this "green-state" a density is measured known as the "green density". The green density is a function of the particle distribution of the ceramic powder and the binder/solvent system. It is important to maximize the green density in order to reduce curling and cracking of the ceramic during the sintering process as well as to provide a higher sintered mass density for mechanical support of the silicon layer and prevent wet chemicals from leaching into the ceramic during subsequent solar cell fabrication processes.

Silicon Growth

Polycrystalline silicon films have been grown on ceramics utilizing AstroPower's Silicon-Film™ process. Uniform 50-75 μm thick films with columnar grains extending through the thickness of the film have

been grown on the ceramic substrate. Aspect ratios of 5:1 have been achieved. Figure 3 shows the typical cross sectional morphology of the film.

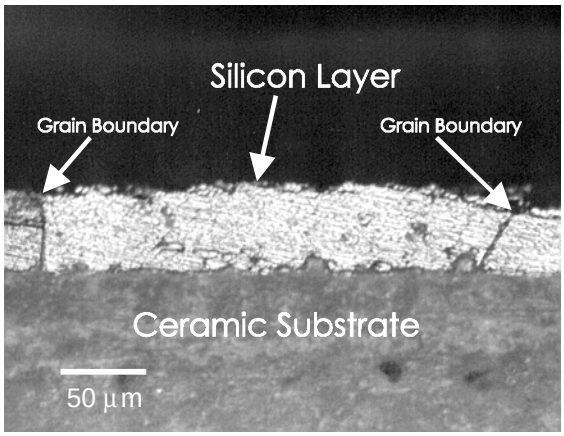

Figure 3. Cross-sectional view of silicon layer grown on ceramic.

Light Trapping

The optical path length of light in a thin-film crystalline silicon solar cell must exceed the thickness of the device to generate high light-generated currents. Extended path lengths can be achieved by making the interface surfaces of the silicon layer and ceramic reflective through pigmenting [2] and random texturing.

Since the front surface of the device requires an antireflective coating that provides little or no reflection to normally incident light, internal reflection requires some degree of texturing to redirect the trapped light.

Texturing of a thin silicon film can be done on either surface; the surface exposed to light, or the imbedded surface at the film-support interface. The present approach is to utilize the natural texture of the silicon-ceramic interface to texture the back surface of the thin film device. Optical measurements of silicon on ceramic structures can be analyzed to extract significant optical design parameters [3].

Figure 4 displays reflectance data for a 5µm silicon film deposited on a ceramic substrate. Included in Figure 4 as a control is the reflectance data for a conventional, 500-µm thick, polished silicon wafer. The near-bandgap region (900 to 1300-nm) indicates that some degree of light trapping is occurring in the thin film. The front surface reflection, (R_{front}), of both samples is approximately 30%, expected for silicon in this range. The escape reflection (light that enters the device and escapes after some number of internal reflections) varies considerably for the two structures. The control wafer reaches a total reflectance value of approximately 47% for non-absorbed light. This implies a back surface reflectivity of 27% [3], which agrees well with the R_{front} of 30%. The escape reflectance of the silicon on ceramic continues to increase with increasing wavelength. The optical properties of the ceramic, as well as redirection of the light through texturing are leading to this change.

Assuming the simple model of non-absorbed light, the effective reflectance of the silicon-ceramic interface is over 60%. This effect combined with the slow increase of escape reflectance with wavelength

for such a thin film imply a high degree of internal reflections and randomization of the light is occurring. Devices will be fabricated on these films to establish the effective level of light trapping.

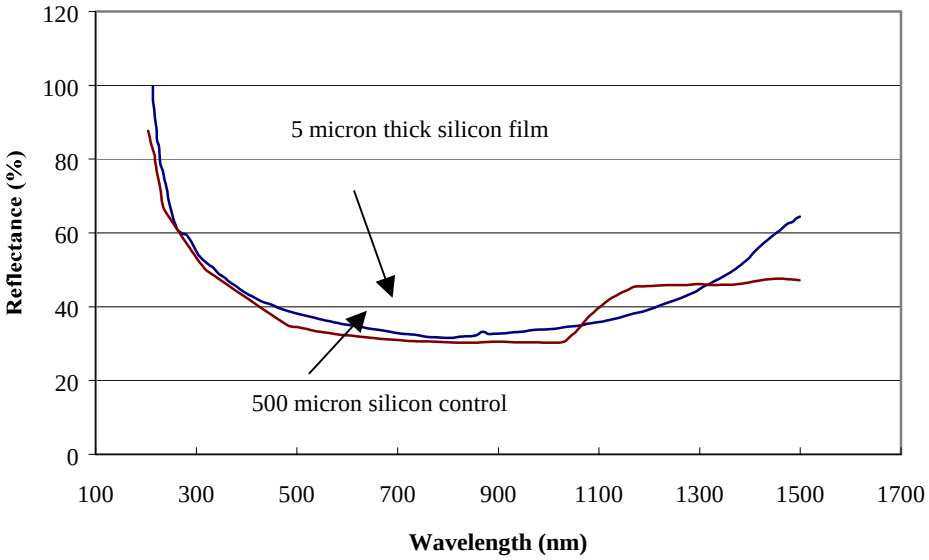

Figure 4. Reflectance of a 5 μm thick silicon film deposited on a ceramic substrate and a 500-μm thick conventional polished silicon wafer.

Conclusions

A 9.79% efficient, 321.3 cm^2 monolithically interconnected photovoltaic array has been achieved. Analysis of this result has led to an improved light-trapped device design which reduces the cost/watt by reductions in the number of process sequence steps and reductions in process complexity. A pigmented, high temperature, insulating ceramic has been developed as the supporting substrate for the monolithic interconnect. The ceramic provides the optical properties and random texturing required for light trapping. The improved design will lead to near-term efficiencies of 13% for large-area, monolithically interconnected devices and 19% in the long term.

Acknowledgements

This work is funded in part by the U.S. Department of Energy through the cost shared Thin-Film Partnership Program which is managed by the National Renewable Energy Laboratory. We would like to thank Roger Aparicio of the Institute of Energy Conversion at the University of Delaware, for providing thin film depositions and reflectance measurements.

References

1. 2nd World Conference on Photovoltaic Solar Energy Conversion, Proceedings (in press), Vienna, Austria, July 6-10, 1998.
2. J.E. Cotter, Ph.D. Thesis, University of Delaware (December, 1996).
3. J.A. Rand and P.A. Basore, “Light-Trapping Silicon Solar Cells Experimental Results and Analysis”, 22nd IEEE PVSC, (1991), pp. 192-197.

Title: **Apollo® Thin Film Process Development**

Organisation: BP Solar Inc.
Fairfield, California.

Contributors: D W Cunningham, J Healy, M Sadeghi, M Rubcich, K Davies,
T Trumbly, L Grammond, D Skinner.

Introduction

This paper documents progress at BP Solar for the first 5 months of a 3 year PV Partnership program started on May 1st 1998. The objective of this project (subcontract RAK-7-17619-27) is to use the PV Partnership program to help introduce the Apollo® process into a production environment, to establish a base line performance at volume and to increase device efficiency, output and reliability.
The areas defined below are seen to be key and need to tackled as major challenges in scale up. These are areas are:

The Semiconductor. Optimisation of the CdTe electroplating bath operation. This process must be fully characterised and engineered in order for stoichiometrically correct CdTe to be deposited at low temperatures on large areas. The BP Solar CdTe film is deposited onto a CdS window layer by electrodeposition. The CdS coated tin oxide glass cathode is immersed in an aqueous solution containing cadmium and tellurium salts. During the deposition, cadmium and tellurium components are co-deposited to form the semiconductor alloy on the CdS window layer. Extensive qualification has been performed at BP Solar on a laboratory scale. The laboratory process shall be scaled to a high volume capable of producing a per annum output in excess of 5MW per reactor. There are a large number of device and process issues that must be considered as part of this scale up. The following list highlights a number of the major issues that must be addressed as part of process development and device optimisation:

- Optimise electroplating for large scale deposition
- Increase device efficiency.
- Improve semiconductor deposition uniformity.
- Increase deposition rate for greater productivity.
- Investigate larger (>6sqft) cathode areas.

Device Performance. The role of impurities in the bulk and starting materials will prove to be a major issue on scaling. These impurities need to be identified and characterised. It is hoped that under the program BP can engage in collaborative work with experts in the field with respect to device degradation and stress testing. The impurity and device properties will be tracked using SPC methods.
Semiconductor processing. High volume production will require concentrated effort in more than one field. BP Solar believes that semiconductor processes including laser techniques are important areas which affect throughput and cost of product.
Bench marking and environmental testing. This is key as a new technology is brought into production. The tasks will include: Determination of the outdoor performance in a variety of applications, evaluation of performance in accelerated conditions and to identify what factors contribute to long term module reliability.
Health Safety and the Environment. BP Solar will work to minimise the total volume of production waste from its plant and move to a zero discharge scenario. In addition to this BP will utilise existing work on CdTe recycling and adapt this to its own plant process.

Process Development

Optimise CdTe Electroplating Bath Operation.

During the first quarter of Phase I considerable emphasis was placed in the electroplating operation with respect to equipment design. It was decided to build a dedicated single plate, large area tank to be used exclusively for the NREL funded program. This way specific experiments can be performed under the program without affecting production activities at Fairfield.

The equipment design was based on a single plate bath capable of accommodating 61" by 14", tin oxide coated glass substrates. For ease of operation in a manual mode, the plate was orientated with the 61" length parallel to the horizontal. Bath details are as follows:

Solution volume:	200 litres
Maximum cathode size:	115cm x 35.6cm.
Heating capacity:	8 kW (Electric)
Construction materials:	All stabilised polypropylene.
	Exposed metals are Teflon™ coated.
Solution components:	Cadmium sulphate
	Tellurium oxide
	18 MΩ DI water.

On installation of the bath, activities included solution purification by electrolysis and impurity analysis. Impurity concentration was determined using BP Solar's in-house ICP-AES. Work will continue into phase 2 (Q1) to optimise the plating conditions and impurity level.

Enhanced Laser Processing Techniques.

The aim of this task is to optimise laser scribing and, therefore, optimise any aspects that affect device performance. Various beam powers were utilised and cutting speeds up to 8 inches per second were investigated. Laser table travel speed is important to achieve high throughput and manufacturing economies. Laser scribing is critical in the BP Solar thin film process as it needs to be selective with respect to cutting the tin oxide in the first cut but, for the second and third cut, the tin oxide needs to be left untouched. Damaging the tin oxide during these scribes could lead to high series resistance, device instability and, in the worst case, breakdown in the device series interconnect.

BP Solar hope to incorporate a single high power laser split six times to improve throughput at the laser station. The plan for the next quarter is to continue with analysis and qualify the necessary beam power and parameters for a high throughput system.

Outdoor Testing Program for Apollo® Modules.

An important area for qualification of a new thin film process is outdoor testing. During the first quarter an interim test structure was erected on the roof of the Fairfield building. Some of the first modules to be produced at Fairfield were placed into this structure. A total of 18 25W modules were connected in 6 parallel strings of three modules. This configuration was chosen to fit the nominal 48V (Vmp) input requirement of the grid tied inverter. The inverter is a 4kW utility tied device.

As this is an interim system, no continuous data logging was installed. All measurements are performed by dismantling the modules and measuring on a Spire 240A. This is not a convenient method to measure modules. A plan has been drafted in co-operation with the BP Solar systems engineering group to build a 2kW ground-mounted system adjacent to the factory. Advantages of this approach are the incorporation of a data logger into the system design, easier access for installing/removing test modules, and more efficient operation of the inverter at 2kW.

To date the stability data is encouraging and commensurate with R&D results, with no performance degradation during the first 4 months under load. The average module power (Apollo® ref. module (1sqft) measured at NREL in 1997) over this period was 27.4W. See attached graph for performance trends.
The graph above shows a selection of modules and their performance over 4 months

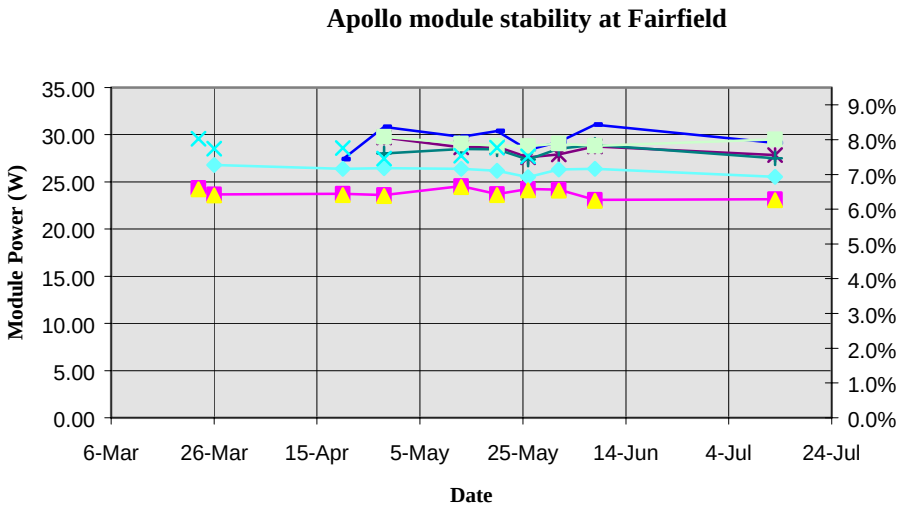

These modules will be transferred to the new outdoor system when it is ready in addition to new modules to make up the 2kW.

It is planned that the system will be in place in the last quarter of this year.

Health, Safety and Environment Program.
BP Solar used the first quarter of the Phase 1 to define work program details relating to task 4.1, Production Waste Abatement. The aim of this task is to attempt to close loop the aqueous waste stream and then extract the cadmium so that, ultimately, it can be converted into a reusable form. Close looping any aqueous waste stream is a challenging task as the make up of the stream can complex often a composite of many different sources. The study will be conducted with Radian International as a subcontractor. The areas of study are listed as follows:

1. Feasibility Study of Closed-Loop Treatment for Apollo® Process Wastewater
   - Identify candidate waste streams
   - Perform analysis of waste stream characteristics and quantities generated
   - Conduct economic analysis of closed-loop alternatives
   - Devise strategy for implementing multiple treatment steps for closed-loop operation

2. Review Wastewater Treatment Technologies for BOD/COD Reduction and Closed-Loop Operation
   - Review commercially available treatment technologies for organics reduction
   - Investigate novel, less commercial, new technologies
   - Conduct treatability studies on composite and/or segregated waste streams
   - Identify feasible purification technologies for closed-loop water reuse

3. Evaluate Process Improvements for Waste Reduction
   - Identify waste streams that are difficult to treat cost-effectively
   - Investigate options for segregating waste streams to optimise treatment efficiency
   - Implement improvements and recharacterize waste
   - Evaluate performance of product manufactured with improved process

4. Identify Opportunities for Waste Material Recycle/Reuse
   - Evaluate the purity of cadmium produced on electrowinning anodes made from various metals (stainless steel, titanium, other metals)
   - Identify steps required to process reclaimed cadmium into cadmium salts suitable for reuse in BP solar plating processes
   - Investigate potential off site recycling of cadmium waste for metal reclamation or smelting
   - Identify possible opportunities for recycling/reuse of other wastes besides cadmium.

BP Solar has also worked on determining Cd leachate levels from the module package using the EPA toxic characteristic leaching procedure (TCLP). BP Solar attended and presented a paper on EPA TCLP sample preparation protocol and its effect on extract metal concentrations. The paper was presented at Keystone, CO as part of the PV/Environment Workshop on July 24th 1998. The data presented showed Apollo® CdTe modules produce trace Cd levels well below the EPA limit for cadmium.

References

1) J.M. Woodcock, M.E. Özsan, A.K. Turner, D.W. Cunningham, D.R. Johnson, R. J. Marshall, N.B. Mason, S. Oktik, M.H.Patterson, S. J. Ransome, S. Roberts, M. Sadeghi, J.M. Sherborne, D.Sivapathasundaram and I.A.Walls, Proceedings 12th E.C. Photovoltaic Solar Energy Conference (1994) 948.

2) MH Patterson, AK Turner, M Sadeghi and RJ Marshall, Proceedings 12th E.C. Photovoltaic Solar Energy Conference (1994)

Title: **Nanostructure of a-Si:H and Related Alloys by Small-Angle Scattering of Neutrons and X-rays**

Organization: Colorado School of Mines, Golden, Colorado
Department of Physics and Department of Chemical Engineering

Contributors: D.L. Williamson and D.W.M. Marr, Principal Investigators

Objectives

The objective of this project is to improve the understanding of which nanostructural features are related to electronic materials properties that determine the performance of a-Si:H-based solar cells. The primary techniques utilized are small-angle x-ray scattering and x-ray diffraction. A major new focus of the project is to determine whether small-angle neutron scattering can be used to determine hydrogen nanostructure and any changes of it that might occur during light soaking. In addition, the anomalous small-angle x-ray scattering technique will be further applied to determine the degree of non-uniform Ge incorporation into a-SiGe:H materials.

Approach

A combination of several structural characterization methods including small-angle x-ray scattering (SAXS), small-angle neutron scattering (SANS), anomalous SAXS, and x-ray diffraction (XRD) is being used to study nanostructural features ranging in size from the atomic up to approximately 30 nm. Features such as nanovoids, hydrogen-rich clusters, columnar-like growth, microcrystallites, medium-range-order, surface roughness, and alloy composition fluctuations or segregation can all be detected with a high degree of sensitivity. For example, nanovoids of volume fraction 0.1 % are readily seen and their average size can be determined. Information on medium-range-order can be inferred from the XRD line width of the first diffraction peak of a-Si:H. Anisotropy in the SAXS, as detected by a sensitivity of the SAXS to sample orientation relative to the x-ray beam, is direct evidence of oriented nanostructural features such as columnar-like growth. Much better sensitivity to the hydrogen nanostructure is expected from SANS due to the large interaction cross-section between the neutrons and hydrogen or deuterium.

The approach involves collaboration with the NREL Low-gap, Mid-gap, and High-gap National Research Teams, particularly the film-making and device-making groups that supply relevant, systematic sets of samples to help address specific issues within the above objectives. We also collaborate with several groups around the world not supported directly by NREL but recognized as experts in the field.

Results

The discussion will be separated according to materials appropriate to the low-gap, mid-gap, and high-gap components of a multijunction solar cell. The latter is the structure being developed to meet the long-range goal of 15% stabilized efficiency modules with the amorphous silicon thin-film technology. Only brief summaries will be presented and the reader is referred to the appropriate publication for details.

Low-bandgap Material

A series of a-Si1-xGex:H alloys with 0 £ x £ 1 has been prepared by the hot-wire chemical-vapor deposition (HWCVD) method and characterized by SAXS. All samples are inhomogeneous on a nanometer scale with a significant increase in the amount of heterogeneity above x=0.1 and this correlates

with degraded opto-electronic properties. Oriented features detected in the nanostructure are associated with a directed flux of deposition species from the heated filament. We conclude that the new HWCVD alloys prepared to date have nanostructures and opto-electronic properties similar to those of device-quality PECVD alloys and this has been accomplished with deposition rates about an order of magnitude faster [see ref. 1 for more details].

The nanostructures of hydrogentated amorphous silicon germanium alloys, a-Si1-xGex:H (x~0.5 to 0.6), prepared by plasma enhanced chemical vapor deposition, were examined by anomalous small-angle x-ray scattering (ASAXS). Clear evidence of inhomogeneous distributions of Ge was found with correlation lengths of 1.0 - 1.4 nm. This non-uniformity was removed by enhanced ion bombardment during growth and resulted in improved photovoltaic performance. The anisotropic ASAXS from the Ge composition fluctuations is consistent with Ge enrichment along the boundaries of a columnar-like nanostructure [see ref. 2 for more details].

Mid-bandgap Materials

Four high-quality a-Si:H films were selected for another look at possible changes in the nanostructure induced by light soaking. An early study by our group found no evidence for light-induced changes [3] but our techniques have improved and a more careful procedure was developed. All four samples were relatively thick and showed void fractions below or near our detection limit. All four samples were first annealed at 180oC for 2 hours and then subjected to light soaking under 1 Sun for 1000 hours to place the samples in the degraded state B. SAXS measurements were then made in this state followed by in-situ annealing in the SAXS system to place each sample in state A. This allowed careful comparison of the SAXS in the two states by simply taking a difference in count rate at each q. The average deviations from zero (for the q-range from 0.4 to 6.2 nm-1) for the four sample are all below 0.1 count/s and three are negative and one is positive. Thus it is concluded that there is no significant difference in the nanostructure as determined by SAXS between states A and B of the Staebler-Wronski effect [see ref. 4 for more details].

A systematic study by SAXS and Raman spectroscopy was performed on hydrogen implanted a-Si and standard device-quality PECVD a-Si:H, both having a hydrogen concentration of 11 at.%. The modifications of short-range and medium-range structural order induced by annealing were investigated. Annealing causes the formation and growth of nanoscale H complexes in both materials. However, the volume content of the H nanoclusters is strongly influenced by the disorder of the original structure, remaining smaller by a factor of three in the a-Si:H compared to the H-implanted sample. Qualitative resemblances and quantitative differences of the structural evolution of H-implanted a-Si and a-Si:H in terms of H solubility and defect structure are discussed [see ref. 5 for more details].

A study has been made of the structural, defect, and device behavior of a-Si:H near and above the onset of microcrystallinity. High-hydrogen-diluted films of a-Si:H, 0.5 mm in thickness and optimized for solar cell efficiency and stability, are found to be partially microcrystalline (mc) if deposited directly on stainless steel (SS) substrates but are fully amorphous if a thin n-layer of a-Si:H or mc-Si:H is first deposited on the SS. In these latter cases partial microcrystallinity develops as the films are grown thicker (1.5 to 2.5 mm) and this is accompanied by sharp drops in solar cell open circuit voltage. For the fully amorphous films, x-ray diffraction (XRD) shows improved medium-range-order compared to undiluted films and this correlates with better light stability. Capacitance profiling shows a decrease in deep defect density as growth proceeds further from the substrate, consistent with the XRD evidence of improved order for thicker films. The tendency toward improved order and fewer defects as the film

becomes thicker is in agreement with a recently proposed "phase diagram" in which the a/mc boundary varies both with thickness and with the H-dilution ratio [6]. Operation near this boundary tends to enhance the sensitivity to the nature of the starting substrate, the bare SS somehow inducing partial microcrystallinity. Thus it is possible that the recent record device [7] benefited from the predeposition of the n-layer such that a fully amorphous i-layer could form under the high-H-dilution condition.

Of particular interest is the observed improvement in the medium-range-order induced by the high-H-dilution as evidenced by the narrowing of the first diffraction peak of a-Si:H. It is observed that the narrowest width in the fully amorphous state can be achieved by PECVD at a 300oC substrate temperature, or by HWCVD at higher temperatures (~360-425oC). Previously it had been suggested that the improved structural order and stability of the hot-wire a-Si:H was related to its significantly lower hydrogen content (1-3 at.%) when prepared at higher temperatures [8,9]. However, this study makes it clear that the same improvement in medium-range-order and enhanced stability is possible in material with a typical hydrogen content of ~10 at.%. Thus we suggest that the improved properties of a-Si:H are more likely related to the improved medium-range-order and the associated lower defect density [see ref. 10 for more details].

High-bandgap Materials

SAXS and deuterium secondary ion mass spectrometry (DSIMS) studies have been made of the nanostructure and hydrogen dynamics in rf-sputter-deposited a-Si1-xCx:H alloys (x £ 19 at.%). The SAXS showed that the films contained elongated features larger than 20 nm with preferred orientation, consistent with a residual columnar-like growth of the films. In addition, the SAXS also included a clear nanostructural component consistent with roughly spherical nanovoids ~1.1 nm in diameter, of total content 0.5 £ f £ 1.0 vol.%. f increased by ~100% after isochronal 1 hour annealing at 300, 350, and 375oC, followed by further annealing for 2 - 15 hours at 375oC. The growth of f was apparently due largely to a ~20% increase in the average void diameter. For x £ 3 at.%, the DSIMS yielded power-law time dependent H diffusion coefficients D(t) = Do(wt)-a, where the dispersion parameter a varied from 0 to ~0.5±0.1 among the samples, but was temperature independent at 350 £ T £ 475oC. The moderate values of a are consistent with the moderate nanovoid contents f £ 1.0 vol.% determined by SAXS. The weak dependence of a on T is consistent with the weaker growth of the SAXS with annealing as compared to a-Si:H. The activation energy Ea(100nm) for a diffusion length L=100 nm was ~1.4 eV, similar to that of a-Si:H [see ref. 11 for more details].

Summary

SANS experiments are expected to be performed in 1999 to determine the viability of this technique to characterize details of the H nanostructure. Special samples containing D in place of H will be prepared for these studies. We continue to accumulate evidence supporting the premise that a homogeneous nanostructure in a-Si:H-related materials yields the best devices. The use of a substrate bias to induce ion bombardment during high-rate deposition leads to a dramatic reduction in the heterogeneity and to better solar cell efficiencies. However, these cells are not as stable as those made by conventional PECVD. New a-Si1-xGex:H alloys made by the hotwire method show opto-electronic properties comparable to the best PECVD material; however, they also show significant heterogeneity similar to the best PECVD material. Clear evidence has been acquired by ASAXS for non-uniform Ge distributions in a-SiGe:H alloys by ASAXS. Such composition fluctuations are likely to be detrimental to carrier transport. New results on the medium-range-order of a-Si:H suggests that more ordered material is more stable under illumination.

References

1. D.L. Williamson, Y. Xu, and B.P. Nelson, AIP Conf. Proc. (NCPV Program Review Meeting, Sept. 8-11, 1998- in press).
2. G. Goerigk and D.L. Williamson, Solid State Commun. 108 (1998) 419.
3. D.L. Williamson, Y. Chen, S.J. Jones, and G.D. Mooney, Annual Report, Photovoltaic Subcontract Program FY 1991, NREL/TP-410-4724 (1992) p. 18.
4. D.L. Williamson, Final Subcontract Report, NREL/SR-520-25844 (1998).
5. S. Acco, D.L. Williamson, W.G.J.H.M. van Sark, W.C. Sinke, W.F. van der Weg, A. Polman, and S. Roorda, Phys. Rev. B58(1998) 12853.
6. J.H. Koh, Y. Lee, H. Fujiwara, C.R. Wronski, and R.W. Collins, Appl. Phys. Lett. 73 (1998) 1526.
7. J. Yang, A. Banerjee, and S. Guha, Appl. Phys. Lett. 70(1997) 2975.
8. A.H. Mahan, D.L. Williamson, and T.E. Furtak, Mat. Res. Soc. Symp. Proc. 467 (1997) 657.
9. A.H. Mahan and M. Vanecek, AIP Conf. Proc. 234 (1991) 195.
10. S. Guha, J. Yang, D.L. Williamson, Y. Lubianiker, and J.D. Cohen (submitted for publication).
11. J. Shinar, R. Shinar, D.L. Williamson, S. Mitra, H. Kavak, and V.L. Dalal (submitted for publication).

Titles: **Polycrystalline Thin Film Cadmium Telluride Solar Cells Fabricated by Electrodeposition (finished June 1998).**
Process Development and Basic Studies of Electrochemically Deposited CdTe-Based Solar Cells (started May 1998).

Organization: Department of Physics, Colorado School of Mines,
Golden, Colorado 80401-1887

Contributors: J.F. Trefny, V. Kaydanov, T.R. Ohno, Co-Principal Investigators;
R.T. Collins, T.E. Furtak, C. Wolden, W. Song, J. Tang, M.H. Aslan,
A.M. Al-Kaoud, A. Gilmore, T. Wen, L. Feng, J. Xi, U. Laor.

Objectives

Advance the processing for high-performance stable CdTe photovoltaic devices, by: (1) advancing the understanding how the basic electronic properties of CdTe thin film solar cells are related to composition, structure and processing procedure of the constituting layers; (2) studying microscopic processes in different parts of the cell responsible for degradation of electronic properties as a function of stress conditions; (3) optimizing the composition of the constituting layers, deposition procedures and postdeposition treatments to enhance cell performance; and (4) contributing to the development of accelerated lifetime prediction tests for the CdTe solar cells.

Technical Approach

In FY 1998 our research and development efforts were focused on: (1) development and adjustment of new methods for characterizing polycrystalline thin films constituting the cell: SnO_2, CdS, CdTe; (2) influence of postdeposition treatment and CdS/CdTe interdiffusion on CdS and CdTe optical and electrical properties and cell performance; (3) cell stability under stress conditions and mechanisms of degradation; (4) preparation by APCVD and studies of optical and transport properties of SnO_2 thin films. Systematic studies of the processing procedures, stress tests and resulting changes in electronic properties of materials and cell performance were aimed at a better understanding of basic issues related to device performance and stability of the CdTe-based solar cells.

Characterization Methods

Film resistance measurements in a wide frequency range

This method is aimed at separate measurement of individual contributions of intragrain material and grain boundaries, GB, to the total electrical resistance of a polycrystalline thin film. As the frequency of AC measurements increases the GB impedance becomes lower due to shunting by capacitance connected in parallel to the GB resistance, R_B. At a very high frequency range the total impedance of the film is defined completely by the resistance of intragrain material, R_I. Thus by comparing DC and high frequency AC measurements, one is able to determine separately R_I and R_B [1]. Measurement of the GB resistance over a range of temperatures can be used to determine the dominating transport mechanism, potential barrier height and doping level in the vicinity of the GB [2].

CSM has purchased the equipment for the impedance and admittance measurement in a frequency range from 75 KHz to 30 MHz (funded by NREL, Subcontract #XAK-8-17619), and started to use it for measurements at room temperature. Designing of a probe station for the variable temperature measurements is in progress.

Near-Field Scanning Optical Microscopy (NSOM).

While conventional far-field optical techniques are limited by diffraction to spatial resolution of ~1m, spatial resolution of 100 nm is routinely achieved for NSOM. As the optical fiber tip, with an aperture size much smaller than the wavelength of light, is scanned, maintaining a constant separation (~10 nm) from the sample, a microphotographic image is obtained simultaneously with a reflected light image. The NSOM technique developed at CSM was successfully used for topography studies of the polycrystalline GaAs, CIGS, as well as for the photocurrent mapping .

Scanning Tunneling Microscopy and Spectroscopy(STM and STS)

This method permits atomic scale characterization by using a metal tip held much closer to the sample surface than in the NSOM case. In this FY we used a scanning tunneling microscope to map the topography of ZnTe and SnO_2 thin films. For thin ZnTe layers prepared on various substrates there is little structural change upon annealing. The first steps were also made in STS: tunneling J-V measurements were performed at the center of the ZnTe grain and in the GB region revealing considerable differences. Further work will be understanding the origins of these changes.

Ellipsometry

Systematic studies of tin oxide thin films using variable angle spectroscopic ellipsometry verified applicability of this method for comprehensive characterization of TCO films [3]. The data on film thickness, surface roughness, optical properties, carrier concentration and mobility (the latter two from the plasma and collision frequencies) were in a good agreement with those obtained by more conventional methods. Now we try to clarify the options provided by the method with respect to characterization of CdS thin films and multilayer structures.

Thermopower measurements.

A simple equipment was designed and constructed for measurements of the Seebeck effect (thermopower) on thin film samples. For the tin oxide films it was shown that these measurements provide an opportunity to measure carrier concentration and its distribution over the area of a sample of arbitrary size and shape. Thermopower measurements can be also used for identification of the scattering mechanism.

Postdeposition treatment of CdS/CdTe films and interdiffusion

Interdiffusion

The band gap of the ternary phase $CdTe_{1-x}S_x$ decreases as S content increases for $x<0.2$. In this study [4], PL measurements were used to detect the ternary phase presence and its composition using the relationship between energy gap and S content. The CdTe/CdS films were coated with $CdCl_2$ and annealed at different temperatures. Profiles of the S concentration as a function of depth were obtained by sequentially removing the CdTe layer using a Br-methanol etch. The amount of S diffused into the CdTe and its depth profile changes substantially with the annealing temperature increase. For 350^0C the x value does not exceed 0.01 near the CdTe/CdS interface and drops to undetectable levels at 3m distance. At 410^0C (our standard processing procedure) x=0.04-0.05 near the interface (quite close to the S solubility limit at this temperature) and drops to $x<0.01$ at the 2m distance. Nearly pure CdTe and $CdTe_{1-x}S_x$ coexist, which could be attributed to preferential diffusion along grain boundaries. At 460^0C x is around 0.05 and does not change much in 3m distance.

Change in postdeposition treatment. "Sandwich" structures.

It was shown that S diffusion into the CdTe can be beneficial for the cell performance, mostly due to the increase of the Jsc. Unfortunately consumption of the CdS by the CdTe layer occurs non-uniformly and leads to the appearance of pinholes if the CdS is not thick enough initially. To preserve the positive effect of S diffusion, make the S depth profile more uniform, and to limit at the same time CdS

consumption, we have tried an alternative processing procedure [5]. A thin CdS layer was deposited on the top of the electrodeposited CdTe, then the CdS/CdTe/CdS film, "sandwich" structure, was coated with $CdCl_2$ and annealed at the standard temperature (410^0C) but for a shorter time than usually (25 min instead of 45 min). The residual CdS was etched out and the cell was completed with a Au back contact. As compared to the cells with a single CdS layer and the same initial thickness (125 nm which is two times lower than the standard one) the "sandwich" cells demonstrated a considerable increase in Voc (~17%), Jsc (~8%), FF (~6%) and efficiency (~30%). It should be mentioned that the CdS thickness, annealing time and back contact were not optimized. These studies will be continued with ZnTe:Cu/Au back contact, electrodeposited CdTe as well as with SCI material.

CdS thin film properties under different postdeposition treatments.

Studies of optical absorption and transmission spectra, PL, and photoconductivity decay were performed on as-prepared CBD CdS films, films annealed with and without $CdCl_2$ coating, and also after $CdCl_2$ treatment of CdTe/CdS structure with the subsequent removal of the CdTe [6]. $CdCl_2$ treatment of CdS before CdTe deposition provides the lowest concentration of shallow defects and recombination centers, and hence the highest transmittance in the wavelength range of 500-600 nm and the highest lifetime of the minority carriers. All this leads to the increase of Jsc and is beneficial for the cell performance.

Stability studies

Small area solar cells were fabricated at CSM by applying ZnTe:Cu/Au back contacts to the CdTe/CdS/TCO structures provided by Solar Cells, Inc. (SCI). The cells were stress tested for about 700 h. in dark, at enhanced temperatures in vacuum oven.

A new method for characterization of the degraded cells was developed based on the analysis of the dynamic resistance, R=dV/dJ, dependencies on current and voltage [7]. It was shown that the "series resistance" increase is due to decrease in saturation current of the back contact Schottky diode. The latter occurs mostly due to decrease in carrier concentration in the CdTe which is caused by a small change in a very high compensation degree in this material. Saturation current of the main diode as well as diode quality factor do not change considerably under open circuit conditions. Degradation of the main diode is much more pronounced when stress testing is performed under bias.

We analyzed the possible influence of electromigration of Cu dopants, which can exist in CdTe as both interstitial donor and substitutional for Cd acceptor [7]. It was shown that the built-in electric fields in the CdTe-based cell, as well as their changes under bias and light influence, should affect strongly migration of Cu and degradation processes in different parts of a cell. These conclusions were verified by experiments performed at CSM, University of Toledo and Colorado State University at Fort Collins.

Stress testing of the cells is continued at CSM under variety of stress conditions and their combinations.

Preparation and studies of Tin Oxide Thin Films.

SnO_2 thin films were deposited on soda lime and Corning 1737F glass substrates using APCVD method. $SnCl_4$ and H_2O were used as precursors, methanol as a catalyst, and difluoroethane as a doping source. Sheet resistance and optical transparency of the films were close to those (sometimes better) for the commercially available Nippon Glass, Asahi and LOF materials.

The Hall effect, resistivity, thermopower, plasma and collision frequencies were measured on a series of films with a thickness of around 500 nm and carrier concentration ranging from $1 \cdot 10^{20}$ cm^{-3} to $5 \cdot 10^{20}$ cm^{-3} [3]. Comparison of plasma frequency and Seebeck coefficient, S, with the Hall concentration, n_H, did not indicate any manifestation of non-parabolicity in this concentration range. Effective mass, m*, was found to be close to 0.275 m_0, in agreement with handbook data [8]. Mobility calculated based on the collision frequency data, "optical mobility", m_o, turned out to be very close to the Hall mobility, m_H.

Estimated mean free path length, l»5 nm, is much smaller than the grain size. Together with m_o»m_H, that means that grain boundaries do not contribute considerably to the carrier scattering and to the measured sample resistivity and sheet resistance. The scattering parameter value determined from S and n_H, and the temperature independence of the mobility leads to the conclusion that scattering by impurity ions screened by free carriers is the dominating scattering mechanism.

Preliminary calculations of mobility were made based on theory for this scattering mechanism, taking into account the spatial dispersion of dielectric constant. The results obtained are close to the experimental values. If it is correct, the mobility measured in SnO_2, produced by Nippon Glass and by APCVD in our facility, is close to the theoretical limit. It was shown that compensation of donor impurities by some acceptors can lead to a significant decrease in mobility.

References:

1. John J.Kester, Scot Albright, Victor Kaydanov, Rosine Ribellin, Lawrence M. Woods and Jeffrey A.Phillips, "CdTe Solar Cells: Electronic and Morphological Properties", *NREL/SNL PV Program Review; Proceedings of the 14th Conference, Lakewood, CO, 1996*; AIP Conference Proceedings, pp. 162-169.
2. L.M. Woods, D.H. Levi, V. Kaydanov, G.Y. Robinson, and R.K Ahrenkiel, "Electrical Characterization of CdTe Grain-Boundary Properties from As Processed CdTe/CdS Solar Cells", *Proceedings of the 2nd World Conf. on Photovoltaic Solar Energy Conversion*, July 6-10, 1998, Vienna, Austria, (in press).
3. Al. Al-Kaoud, T. Wen, A. Gilmore, V. Kaydanov, T.R. Ohno, C. Wolden, J.U. Trefny, J. Xi, L. Feng, "Atmospheric Pressure Chemical Vapor Deposition of SnO_2: Processing and Properties", *NPCV Photovoltaic Program Review: Proceedings of the 15th Conference, Denver, CO, 1998*; AIP Conference Proceedings (in press).
4. M.H. Aslan, W. Song, J. Tang, D. Mao, R.T Collins, D.H. Levi, R.K. Ahrenkiel, S.C. Lindstrom, M.B. Johnson, "Sulfur diffusion in Polycrystalline Thin-Film CdTe Solar Cells", *Proceedings of Material Research Soc. Symp.* 485, 1998, pp.203-208.
5. W. Song, D. Mao, V. Kaydanov, T.R. Ohno, J.U. Trefny, R.K. Ahrenkiel, D.H. Levi, S. Johnston, B.E. McCandless, "Effect and Optimization of CdS/CdTe Interdiffusion on CdTe Electrical Properties and CdS/CdTe Cell Performance", *NPCV Photovoltaic Program Review; Proceedings of the 15th Conference, Denver, CO, 1998*; AIP Conference Proceedings (in press).
6. W. Song, D. Mao, J.U. Trefny, R.K. Ahrenkiel, D.H. Levi, and S. Johnston, " Influence of $CdCl_2$ Treatment on the Electrical and Optical Properties of CdS Thin Films", *Ibid*.
7. D. Morgan, J. Tang, V. Kaydanov, T.R. Ohno, and J.U. Trefny "Degradation Mechanisms Studies in CdS/CdTe Solar Cells with ZnTe:Cu/Au Back Contact", *Ibid*.
8. O. Madelung, "Data in Science and Technology. Semiconductors Other than Group IV elements and III-V Compounds", *Springer Verlag, Berlin-Heidelberg, 1992*, p.45.

Title: **Device Physics of Thin-Film Polycrystalline Solar Cells**

Organization: Colorado State University, Fort Collins, Colorado
Department of Physics

Contributors: J.R. Sites, Principal Investigator; J.E. Granata, J.F. Hiltner, P.K. Johnson, Y. Shelton, and D.W. Warner, A.L. Fahrenbruch

Objectives

The objectives of this program are to (1) quantitatively separate individual performance losses in CI(G)S and CdTe solar cells using currently available techniques, (2) expand the tool set for measuring and separating the losses, and (3) suggest fabrication approaches or modifications to minimize the losses.

Loss Analysis

One loss analysis project was assistance to K. Ramanathan at NREL for a comparison of CIS and CIGS cells he made using only a Zn-solutions instead of the usual chemical-bath deposition needed to form a CdS layer. The efficiencies when sulfur was omitted from otherwise similarly processed cells were only modestly lower (~0.5%), but there were several specific differences noted: (1) short-circuit current in the Zn-treated cells as expected was higher due to better blue-light collection, (2) reflection from the Zn-solution cells was slightly higher and more specular, (3) open-circuit voltage was lower with the Zn-solution cells, presumably due to a somewhat poorer junction, (4) hole density, another junction indicator, was also less in this case by about a factor of two, (5) the Zn-solution cells were leakier by a factor of 3-10 implying a somewhat less robust structure than when a finite-thickness sulfide layer was used. The important conclusion is that although no other buffer layer has surpassed CdS for CIS or CIGS cell performance, the differences have substantially narrowed, and Cd-free CI(G)S cells have become considerably more credible.

A second loss-analysis collaboration, this one with ISET, identified differences in recombination between two sets of CIS cells made under nominally identical conditions, and a third collaboration with MRG tracked the optical differences in their ITO as conductivity was varied. A final study related to modules under uneven illumination documented the effect of forcing a reverse current up to 110% of typical photocurrent through CIS cells. As one might expect, cells with shunt resistance below 1000 Ω-cm^2 were generally unaffected, but one manufacturer's, which had higher shunt resistance, was damaged.

Sodium in CIS Cells

A number of CIS and CIGS films and solar cells were fabricated and analyzed to determine how much sodium is needed to optimize device performance and what is the likely mechanism for improvement due to sodium [1]. A broad range of sodium concentration from 0.001 to 0.15 at % was found to yield similar performance with modest fall-off below this range and significant degradation above it.

Fig. 1a shows the pattern for open-circuit voltage and 1b for the hole density deduced from capacitance. There is scatter in the data, but the open circuit voltage at 0.1 at %. Na is 50-100 mV above that at the lowest concentrations, and the hole density is a facctor of ten larger. The fill-factor, not shown, typically increases by 10%. Cells made on sodium-containing substrates show smaller changes in final sodium concentration and performance as sodium is added. The general interpretation is that one needs sufficient sodium for well-passivated grain boundaries, but not so much as to produce secondary phases.

Small-Spot Measurement

A new piece of apparatus has been built and tested to focus a solid-state laser beam to a very small spot and step a solar cell through it in the x-y plane under computer control. The purposes of this apparatus are (1) to reliably probe grain and intergrain regions before and after anneal cycles, and (2) by varying spot size to separate lateral and normal contributions to series resistance. The apparatus is now working, it records features on a distance scale of one micron, and it can reproduce its path with submicron precision.

Stress Tests

Both CIS and CdTe cells have been stressed at elevated temperatures under a variety of bias and illumination conditions. For CIS cells made at Siemens Solar Industries, there is a nearly reversible pattern where 80^{o}C in the dark leads to lower efficiency (~1%), primarily through an increased series resistance, while the same temperature in the light restores the efficiency [2]. Much of the change occurs in the first hour, but it continues for at least 20 hours. The effect does not seem to be dependent on bias during the light part of the cycle. At the same time that series resistance goes up under dark stress, the hole density decreases, but it also recovers, or nearly recovers, during the light half of the cycle. These particular transient patterns have not been seen in cells from other labs, thought the general theme of CIS improving slightly under illumination is common, and certainly in the preferable direction for solar cell operation.

An extensive set of measurements following stress at elevated temperatures has also been made on CdTe cells from Solar Cells, Inc., NREL, and ANTEC [3, 4]. At 100^{o}C under illumination, there are usually observable changes, thought the onset ranges from a few hours to over a month, and it is accelerated by roughly a factor of 1000 over what might be expected under field conditions. Initial changes are attributed to the back-contact barrier as deduced from reverse curvature of the J-V curve. Often the barrier is first reduced, due to annealing, then gradually increased, presumably because when copper is used in junction fabrication, it can be quite

mobile through a polycrystalline material. In some cases at still later times, there is clear degradation of the primary junction seen in both current-voltage and capacitance-voltage measurements. This change is attributed to significant copper diffusing to the front-junction region. The rate of change for the CdTe cells is often a strong function of bias. It is generally less pronounced at operating conditions than at open circuit, which is consistent with an electric field opposing a concentration gradient. The general observation to date is that CdTe cells with copper-free or minimal-copper back contacts tend to be the most stable.

Modeling

Computational modeling of CdTe cells uses the AMPS software supplied by Pennsylvania State University. Baseline calculations for current-voltage curves with parameters typical of CdTe cells have been contrasted with those where one parameter at a time, such as the back-contact barrier, is varied.

References

1. J.E. Granata and J.R. Sites, "Impact of Sodium in the Bulk and in Grain Boundaries of $CuInSe_2$". Proc. 2nd World Conf. on PV Solar Energy Conv. (Vienna, July 1998).

2. J.F. Hiltner and J.R. Sites, National CIS Team Meeting, April 16, 1998, Golden, CO.

3. J.F. Hiltner and J.R. Sites, National CdTe Team Meeting, September 8, 1998, Denver, CO.

4. J.F. Hiltner and J.R. Sites, "Stability of CdTe Solar Cells at Elevated Temperatures: Bias, Temperature and Cu Dependence," AIP Conf. Series. (in press)

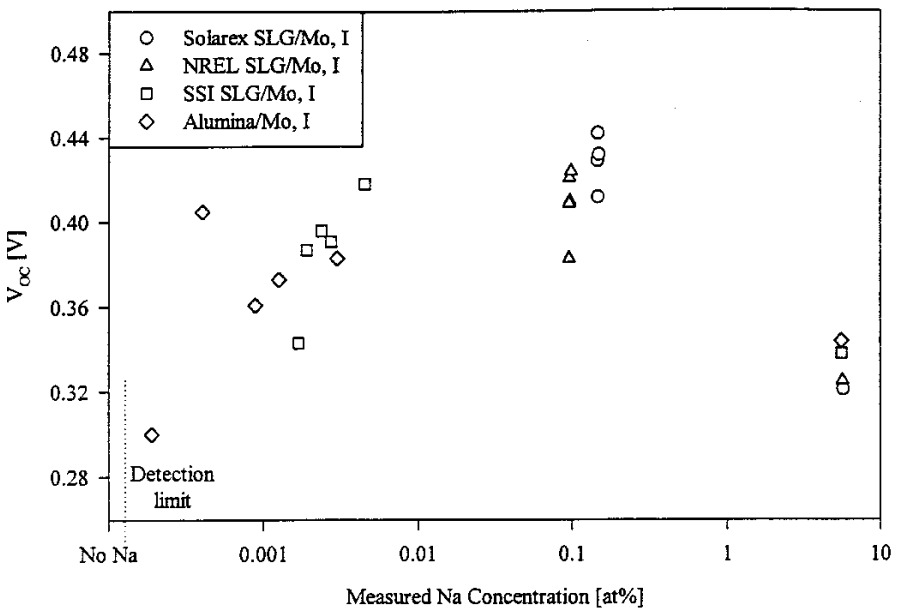

Fig. 1. CIS Open-circuit voltage as a function of Na concentration for cells on four types of substrate.

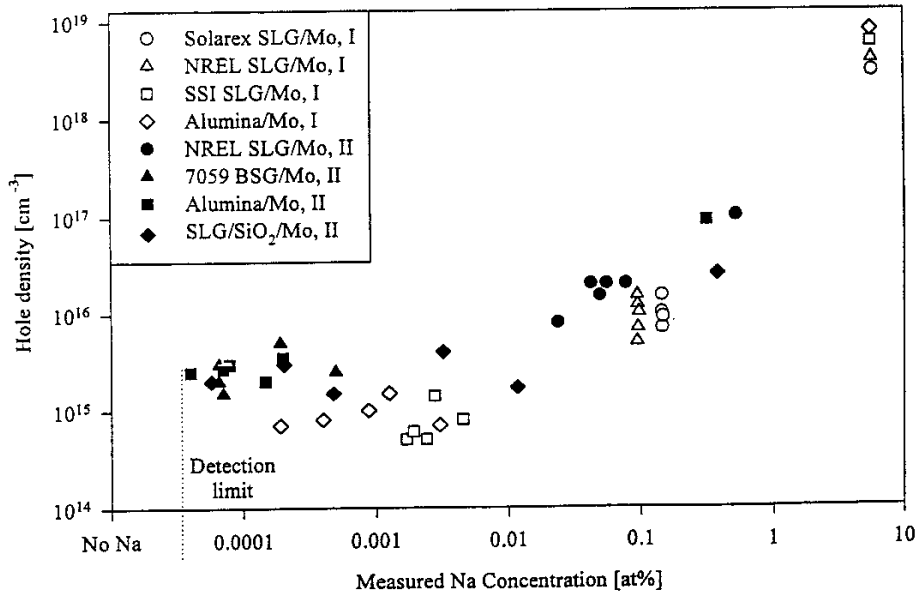

Fig. 2. CIS hole density for CIS cells on several substrates.

Title: **Development of a Thin-Film Based "Micro-Concentrator" Photovoltaic Technology**

Organization: DayStar Technologies, Inc., Denver CO

Contributors: J.R. Tuttle, E.D. Cole, T.A. Berens, A. Szalaj

Project Objective

DayStar Technologies, Inc. was founded in 1996 to commercialize a photovoltaic (PV) cell and module technology based upon a thin-film cylindrical filament cell and non-planar refractive optics. In order to accelerate development, the module was redesigned to accept thin-film industry cell components that could be integrated into a new planar plastic and glass optical package. With limited thin-film products reaching commercial availability, we expanded our efforts to include wafer Si (single- and poly-crystal) cell components. Concentration is not a new idea, but DayStar's product design leads to a module with an equivalent form-factor to that of a standard 1-sun flat-plate module. In the 4-8 sun design range, the full solar electric system will require single axis tracking to an accuracy of + 2.5˚. If we lower the concentration to 2.5 suns, a 15˚ acceptance angle allows for passive tracking, or none at all for certain applications. In this subcontract, we intend to work out design, prototype, and manufacturing issues pertaining to the integration of thin-film single-junction $Cu(In,Ga)Se_2$ and triple junction a-Si solar cell components into our concentrator module package. We report here on progress towards development and commercialization of this PV module technology.

Approach / Background

Design Considerations

Present module designs include either series- connected wafers of Si cell material, or monolithically integrated cells of thin-film heterojunctions. There are particular challenges in each of these approaches that compromise their cost effectiveness. Wafer Si cells are raw-material intensive and efforts to reduce manufacturing costs ($\$/m^2$) have invariably led to reductions in performance (W/m^2), the net effect being little change in their quotient, \$/Wp. The projected supply problems with Solar-grade Si further complicates the picture. When thin-film technologies were first introduced, they promised much lower manufacturing costs with only slightly lower performance. The former was a result of a module design that incorporated "monolithic" integration, or cell integration that occurred simultaneous with cell fabrication, and economies of scale - the bigger the cheaper. Both design criteria have led to low yields that effectively drive the manufacturing cost back up to that of crystalline Si (at lower performance levels). Although these issues will likely be resolved in the long run, it has created a continuing void in the industry for cheaper module product.

DTI has addressed these issues in a design that either requires only 1/4 of the more expensive Si cell material, or obviates the need for monolithic integration and insulating glass substrates for the manufacturing of a thin-film based module product. Although concentrator technologies are under development by several companies, their bulky form-factor leads to a moderately high cost of the optical package introduced to replace the semiconductor material.

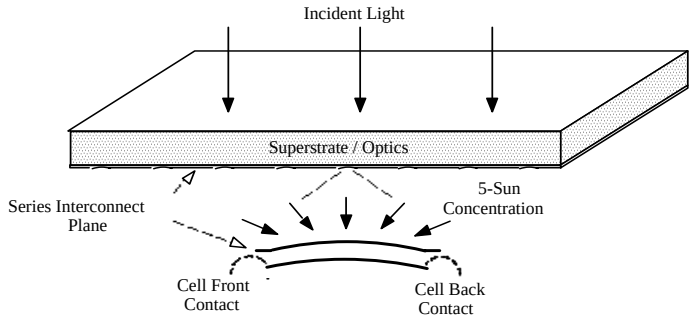

Figure 1. Schematic of DayStar module package.

DTI's module (Fig. 1) is designed with a similar form-factor of a conventional flat-plate module and can accept, with minor modifications, various types of thin-film and crystalline cell materials. The components include series-connected / encapsulated cell strings, thin plastic optics, coverglass, and encapsulant. With the exception of the custom cell integration process, all other packaging materials and processes do not differ from what is used in the 1-sun, flat-plate module incorporating the same cell technology. This makes for simple integration of DTI's technology into existing manufacturing lines.

Cell & Module Fabrication

Both thin-film and crystalline cell materials have been incorporated successfully into this module design. The thin-film CIGS was fabricated for these purposes at the National Renewable Energy Laboratory first under a Cooperative Research and Development Agreement (CRADA) (7/96-7/98) and then under this contract. The cell processing was modified to improve its series resistance at 4x short-circuit current (Jsc). The a-Si is a stabilized multi-junction stack purchased from United Solar Systems Corp. The wafer-Si technologies included single and polycrystalline from various manufacturers. In the latter two cases, cell materials were non-optimally designed for this application, but would only require simple process modifications to reach optimal performance at 4-suns intensity.

For the thin-film CIGS and a-Si cell materials, completed 7.5cm x 10cm cell stacks on metallic sheets are subsequently processed into 7.5cm x 0.4cm cell strips (Fig. 2). For the c-Si cells, strips were cut from wafers along individual grid lines, and then integrated. Modules are completed by mating the integrated cell strings to the optics, and then mating the optics to the coverglass.

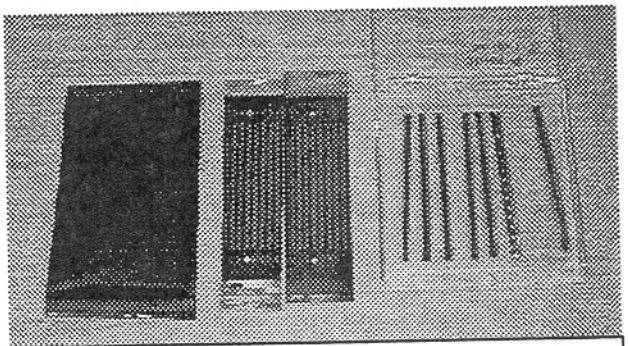

Figure 2: Processed CIGS sheet cell material as (a) a completed cell stack; (b) after bussbar deposition; and (c) after shearing into cell strips.

Research Results

Cell & Module Performance

We have previously reported on the operation of specially designed CIGS based solar cells under 2-20 suns of concentration [1]. Typical results included an improvement in performance (under Direct AM1.5 illumination) from 14.8% (total area) at 1-sun to 17.7% at 20-suns intensity. For cells used in the DTI module package, the only cell processing modification made was to the ZnO where the sheet resistivity was reduced from 20 ohm/sq. to 10 ohm/sq. To begin, several completed cells were characterized at 25˚C at 1&5 suns illumination. The cell performance, in all cases, improved. The average change was +.065V in Voc and +1.5% (abs.) in performance. The conclusion here is that the positive impact of concentration on voltage more than compensates for its negative (or neutral) impact via series resistance losses in the TCO.

A test jig was constructed for characterization of unencapsulated cell material under 5-suns, without cooling, to measure performance and operating temperature over a 50+ hour time period. One of the cells measured at 25˚C was subsequently mounted onto the test fixture with a thermocouple attached to the backside. The cell now will operate, after equilibration, at a temperature greater than 25˚C. After a 1-sun measurement was accomplished, a cylindrical focusing lens was placed over the cell and adjusted until the short-circuit current density (Jsc) was 5-times the one-sun photocurrent. The Jsc, for the purposes of these measurements, is exactly linear with concentration level. An initial I-V was performed before heating could occur. Thereafter, the cell was operated under constant 5-sun illumination at the cells maximum power point voltage (Vmp). At various time intervals, I-V curves were taken and the cell returned to this dynamic operating condition.

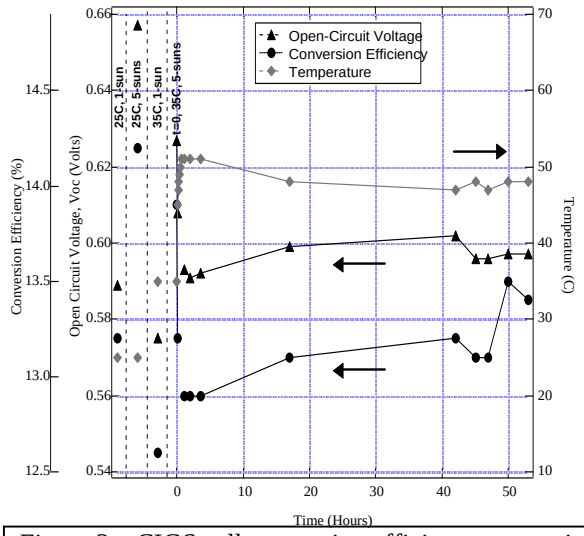

Figure 3. CIGS cell conversion efficiency, open-circuit voltage, and operating temperature over 53 hours of continuous operation.

In Fig. 3, results are presented over a 50 hour period. The maximum operating temperature was 52˚C. In short, the results are exemplary. There exists a nearly even correlation between 1-sun, 25˚C performance (standard industry benchmark) and 5-sun ambient performance for CIGS cell materials. Or, in other words, the gains observed due to concentration offset any losses due to thermal effects. This, in fact, is a superior characteristic of this cell and module configuration to that of a 1-sun, flat-plate technology where field operating performance is typically several percentage points below laboratory performance due to both thermal and interconnect effects. The conclusion here is that CIGS is well suited for operation under the conditions of DayStar's module package.

Stabilized multi-junction a-Si cells were also obtained for 5-sun reliability testing. It appears that this cell nearly levels off in performance after 40+ hours of operation at 5 suns. There are some yet understood behaviors that are present when the cell is removed from the light and cooled down. Discussions with experts in the a-Si field will proceed to better understand the data. The results do suggest that cell operation under the conditions produced in DayStar's module package would not degrade over time. It is, of course, worthwhile to note that the performance at 5-suns under operating conditions is superior to that of 1-sun operation at 35˚C.

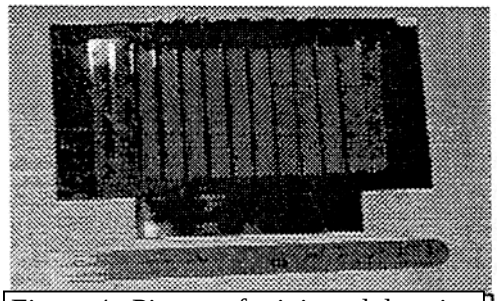

Figure 4. Picture of mini-module using thin-film cell components.

10-cell string integrated mini-modules have been fabricated with CIGS, c-Si, a-Si cell materials. A typical prototype is pictured in Fig. 4. Voltage output is on the order of 5.5V, 5.5V, and 20V, respectively. The CIGS module has been deployed and measured outdoors by NREL (Fig. 5). The aperture area performance was measured to by 5.5%. The "active-area" performance is calculated to 7.2%. The difference between "aperture" and "active" areas lie in the optics design and the module scale in use. The optics as presently designed and fabricated includes a fixed edge area where light is lost. The "active-area" is therefore defined here as the area over which all light reaches the solar cell for conversion and represents the

upper limit on aperture-area conversion potential for a larger module. In fact, however, the edge losses have been significantly reduced with emerging designs.

The overall low performance for the CIGS technology is a consequence of an interconnect scheme that is better suited to low-Jsc cell materials. 13% 10-cell strings of CIGS have been fabricated and should produce greater than 11% active-area module performance.

Conclusions

In this development effort, we have successfully demonstrated the following:

- Operation and stability of CIGS and a-Si thin-film cell technologies under 5-sun concentration.
- Performance enhancement of CIGS, a-Si, and c-Si under 5-sun concentration. In the latter two cases, appropriate cell design will further improve performance.
- Efficacy of cell interconnect resulting in no loss of performance (1-cell vs. 10-cell).
- Efficacy of mating of cells to optics and optics to coverglass.

With continued development work, the ability to put all of the above pieces together into a 10% or greater module product will improve.

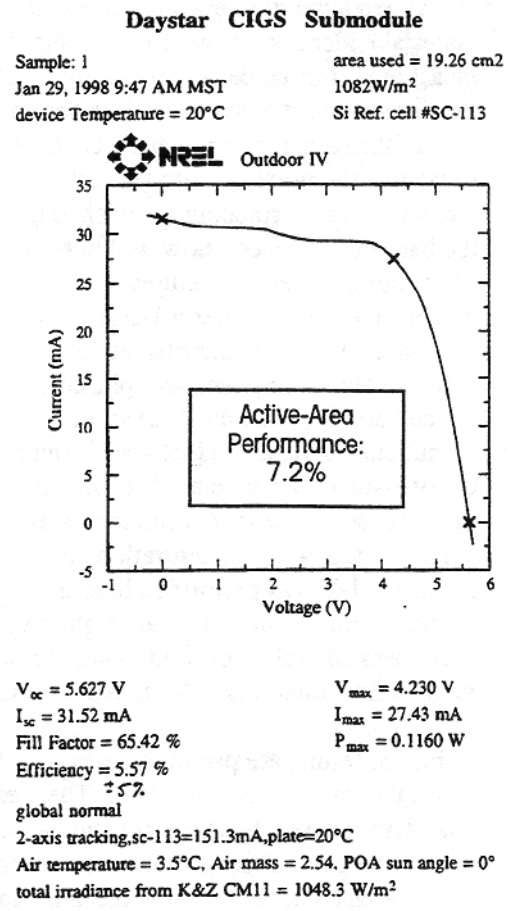

Figure 5. I-V measurement of CIGS-based mini-module.

Acknowledgements

We are grateful to NREL for their technical assistance and support through Subcontract ZAK-8-17619-25.

References / Publications

1. J.R. Tuttle, E.D. Cole, J. Alleman and J. Keane, Proceedings of the 1st Conference on Future Generation Photovoltaic Technologies, Denver, March 4-26, 1997, AIP Conference Proceedings 404, p243.

2. J.R. Tuttle, E.D. Cole, T.A. Berens, A. Szalaj, J. Keane, J. Alleman, "A Novel Flat-Plate PV Concentrator Package", *NCPV Photovoltaics Program Review; Proceedings of the 15th Conference, Denver, CO, 1998;* AIP Conference Proceedings (in press).

3. J.R. Tuttle, E.D. Cole, T.A Berens, J. Keane, and J.Alleman, "A Crystalline and Thin-Film Cell PV Concentrator Package", *Proceedings of the 2nd World Conference and Exhibition on Photovoltaic Solar Energy Conversion*, Vienna, Austria, 6-10 July 1998 (in press).

Title: **Use of Very High Frequency Plasmas to Prepare a-Si:H Based Triple-Junction Solar Cells at High Deposition Rates**

Organization: Energy Conversion Devices Inc.
1675 West Maple Road, Troy, MI 48084

Contributors: S. J. Jones, T. Liu, and M. Izu

Objectives

The overall objective of this program is to develop a very high frequency (70 MHz) plasma enhanced chemical vapor deposition process for the fabrication of intrinsic layers for high efficiency amorphous silicon-based triple-junction solar cells at high deposition rates. These intrinsic layers (i-layers) are either amorphous silicon (a-Si:H) or amorphous silicon germanium alloy (a-SiGe:H) materials. The goal is to prepare these materials at rates of 10 Å/s while maintaining the cell efficiencies at the high values presently obtained for devices made using the standard 13.56 MHz frequency and low deposition rates (near 1 Å/s). Upon completion of a successful program, application of this high rate process to ECD's roll-to-roll solar cell production design will lead to higher machine throughput and reduced solar module cost.

Technology

Over the past 20 years, ECD and it's joint venture company United Solar Systems Corp. (United Solar) have played key roles in the development of a-Si:H based PV technology for having designed and developed an a-Si:H/a-SiGe:H/a-SiGe:H triple junction, spectrum splitting cell structure and a continuous roll-to-roll solar module manufacturing process. The triple junction solar cell device structure is comprised of a blue-green light absorbing a-Si:H layer, two green-red light absorbing a-SiGe:H layers and supporting doped layers for each of the absorbing layers. Indium-Tin-Oxide contacts and metal grids are used for carrier collection and Silver/Zinc Oxide or Aluminum/Zinc Oxide back reflectors are used to allow for multiple light passes through the absorbing layers. The roll-to-roll manufacturing process uses a flexible stainless steel web as a substrate material on which the light absorbing layers are deposited. This process is an inexpensive method to prepare the solar modules and offers significant economy-of-scale advantages which result in significant cost savings as the volume of production increases. ECD has developed the process through generations of manufacturing machines, including the recently built 5MW plant for United Solar [1].

Approaches

In this program, we are further advancing ECD's existing PV technology by performing the following tasks:

Task 1: Optimization of a-Si:H single-junction cells with i-layer prepared at rates near 10 Å/s;
Task 2: Optimization of a-SiGe:H single-junction cells with i-layer prepared at rates near 10 Å/s;
Task 3: Optimization of a-Si:H/a-SiGe:H/a-SiGe:H triple-junction cells with all i-layers prepared at rates near 10 Å/s; and
Task 4: Development of conditions and/or hardware for the uniform deposition of i-layers at rates near 10 Å/s over a large area .

Generally, the deposition conditions used to prepare single-junction amorphous silicon (a-Si:H) and silicon germanium alloy (a-SiGe:H) cells by the very high frequency (VHF) technique are being optimized to obtain the highest cell efficiencies. These component cells are then combined to create high efficiency a-Si:H/a-SiGe:H/a-SiGe:H triple-junction cells. The deposition conditions for these multi-junction cells are also being optimized to further increase the device performance. For the future

incorporation of the technique into an ECD built roll-to-roll solar cell production line, deposition conditions will be optimized and/or cathode hardware designs will be tested which will allow for the uniform deposition of i-layers over a large area using the VHF technique and high deposition rates.

Accomplishments

1) Optimization of a-Si:H Cells

Much of the work completed involving a-Si:H cells prepared at high i-layer deposition rates by the VHF technique was discussed earlier[3] The general conclusion from these studies was that by using the VHF technique and careful selection of deposition conditions, the initial and stable cell efficiencies could be made to remain relatively constant with varying i-layer deposition rate up to 10 Å/s. Beyond 15 Å/s, the efficiencies are lower. Much of this work focused on cells made without current enhancing Ag/ZnO back reflectors. This was done because in the a-Si:H/a-SiGe:H/a-SiGe:H triple-junction structure, the top a-Si:H cell gets virtually no current enhancement from the back reflector. In order to again demonstrate the quality of the a-Si:H devices prepared by the VHF technique at rates near 10 Å/s, we have prepared some a-Si:H devices with Ag/ZnO back reflectors. These cells have initial efficiencies greater than 10 % as is demonstrated by the JV curve shown in Figure 1. The efficiencies degrade to stable 8% efficiencies with long term light exposure (1000 hrs. under AM1.5 conditions at 50ºC).

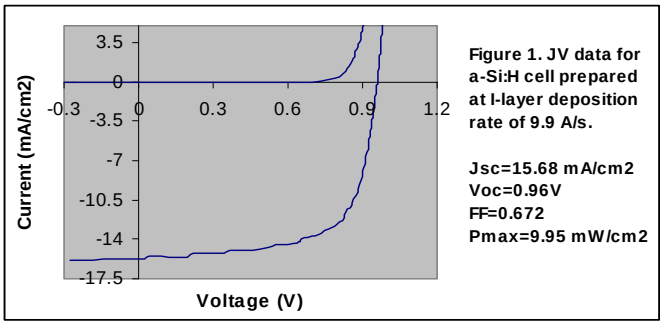

Figure 1. JV data for a-Si:H cell prepared at I-layer deposition rate of 9.9 A/s.

Jsc=15.68 mA/cm2
Voc=0.96V
FF=0.672
Pmax=9.95 mW/cm2

2) Optimization of a-SiGe:H Cells

During this year, we have made great strives towards optimizing the deposition conditions for the preparation of a-SiGe:H layers for their use in middle and bottom cells for the triple-junction structure[4]. The optimization process included varying the substrate temperature, the Si and Ge source gas flows, the hydrogen flow, the applied power and the chamber pressure. Table I lists JV data for some of our more recent cells whose i-layers were prepared using the different plasma frequencies and various deposition rates. Since our goal is to test the potential use of the VHF technique as a method to prepare middle and/or bottom a-SiGe:H cells for triple-junction structures, the J-V data listed in the table was obtained using 530 nm filtered AM1.5 light. The 530 nm filter is used to eliminate light typically absorbed by the a-Si:H top cell that would not reach the middle and bottom cells in the triple-junction cells. Since the middle cell in the triple-junction structure only receives roughly a 0.5 mA/cm^2 increase in current from the back reflector, we chose to compare data for cells without back reflectors in the table. Comparing data, both initial and light soaked, for cells made by the VHF technique at around 10 Å/s with the data for cells made using the standard 13.56 MHz frequency at around 1 Å/s, the cell properties are very similar. For the cells made using the 13.56 MHz frequency, poorer properties are still observed as the i-layer deposition rate is increased. Thus, these results are consistent with the results for the a-Si:H cells where at high i-layer deposition rates, the VHF technique was found to be a far superior deposition method. In terms of the exact efficiency values, they are not as high as we would like them even for the cells prepared at the low rates. Thus, in the next year we plan to improve these baseline efficiencies through changes in our deposition procedures and/or the system hardware.

Table I

JV results for a-SiGe:H cells whose i-layers were prepared at different plasma frequencies.

Frequency (MHz)	Light SoakTime (hrs.)	Dep. Rate (Å/s)	i-layer thickness (Å)	J_{sc} (mA/cm^2)	V_{oc} (V)	FF	R_s (Ωcm^2)	P_{max} (mW/cm^2)
13.56	0	0.92	2100	7.97	0.752	0.575	11.8	3.45
	622			6.92	0.704	0.510	24.3	2.48
13.56	0	6.1	2260	7.43	0.711	0.550	14.4	2.91
70	0	9.5	2000	8.07	0.760	0.579	10.7	3.55
	622			7.10	0.682	0.506	21.1	2.44
70	0	10.2	2150	8.15	0.750	0.571	12.1	3.49
	622			7.30	0.676	0.497	23.1	2.46

In terms of understanding the changes in the film growth process which allow for improved material properties with the use of the VHF plasma rather than the 13.56 MHz plasma, several studies of the plasma kinetics have shown that as the frequency of the plasma increases, the average energy of the ions which bombard the growing film surface decreases while their number increases. This increased bombardment could be a key factor in the ability to use higher deposition rates since a moderate amount of bombardment has previously been found to be beneficial in increasing the surface mobilities of adatoms during the growth of a variety of thin film materials.

In an effort to test the effect of different ion bombardment conditions on the i-layer quality, we have prepared a number of cells using different substrate dc biases. Table II summarizes data for a-SiGe:H cells. These cells were made without the benefit of the current enhancing back reflector and the JV measurements were again made using 530 nm filtered AM1.5 light to simulate absorption due to a top a-Si:H cell. With increasing positive electrical bias, the deposition rate of the a-SiGe:H i-layer was found to drop significantly from nearly 10 Å/s at a bias of 0V to less than 4.8 Å/s at 50V. Accompanying this drop in deposition rate was a significant decrease in V_{oc} from 0.75V to 0.64V. Increasing the positive bias further to 100V led to a much smaller change in deposition rate and no change in V_{oc}. With increasing negative bias, there is also a decrease in the deposition rate for the a-SiGe:H i-layers, however the decrease is not as great as in the case of positive bias. Between 0 and –100V bias, there is only a small (less than 7%) decrease in deposition rate and very little change in the cell properties. Beyond –100V, the deposition rate decreases more rapidly and a significant drop in V_{oc} is apparent.

Table II

Effect of substrate bias on the properties of single-junction VHF a-SiGe:H cells

Substrate Bias (V)	Deposition Rate (Å/s)	i-layer thickness (Å)	J_{sc} (mA/cm^2)	V_{oc} (V)	FF	R_s (Ωcm^2)	P_{max} (mW/cm^2)
0	9.5	2000	8.15	0.750	0.571	12.1	3.49
50	5.8	1220	7.62	0.638	0.561	15.9	2.73
100	4.4	920	6.74	0.641	0.632	11.9	2.73
-30	10.5	2210	8.15	0.742	0.562	10.3	3.40
-50	9.3	1950	8.18	0.749	0.559	11.1	3.43
-100	8.9	1860	7.74	0.745	0.580	11.1	3.46
-150	8.5	1780	7.33	0.736	0.531	14.5	2.87
-200	6.8	1430	7.40	0.730	0.555	15.4	3.00

For the a-Si:H cells, we observed many similar trends with varying bias. With increasing positive bias, there is a significant decrease in the i-layer deposition rate as was observed for the a-SiGe:H cells. Also, there is the same decrease in V_{oc} observed for the a- SiGe:H cells with increasing positive bias. Thus, the decrease in V_{oc} for the a-SiGe:H alloys is not, for at least the most part, due to a decrease in Ge content. The changes in V_{oc} for both types of cells are likely due to decreases in the hydrogen content and/or changes in the film microstructure. With increasing positive bias, no change in the V_{oc} is observed however a decrease in deposition rate is seen. Thus this method of altering the ion bombardment, in particular the ion energy, of the film surface does not lead to higher efficiencies. However, other alternative methods that more effectively alter the ion flux may.

3) Optimization of Triple-Junction Cells

During this time period, we have made our first a-Si:H/a-SiGe:H/a-SiGe:H triple-junction cells using the VHF technique and high deposition rates. For these cells, all of the i-layer deposition rates were near 10 Å/s (±1 Å/s). Table III compares cell data for one of the best triple-junction cells made using the VHF technique and a deposition rate near 10 Å/s with those for the best cell made in the same deposition system using the VHF technique but a lower deposition rate (3 Å/s). The data demonstrates that we have achieved a 10% active area efficient cell at the high deposition rate and the efficiency is close to that for the cell made using the lower deposition rate. The differences in J_{sc}, V_{oc} and FF may be related to differences in the current matching and the Ge contents in the different i-layers. We are presently exploring this possibility. We also plan on improving the baseline efficiencies through changes in our deposition procedures and/or the system hardware. We have completed limited light soaking experiments on the triple-junction cells. On cells with efficiencies between 9.5 and 10%, the efficiencies for both the high rate and low rate cells degraded by 10-15% after 600 hrs. of light soaking.

Table III
Data for triple-junction cells.

Frequency (MHz)	i-layer Deposition Rates (Å/s)	J_{sc} (mA/cm^2)	V_{oc} (V)	FF	R_s (Ωcm^2)	P_{max} (mW/cm^2)
70	3	6.70	2.23	0.683	38	10.22
70	10	6.90	2.28	0.645	41.5	10.13

Acknowledgment

We would like to thank H. Fritzsche, S. R. Ovshinsky, A. Banerjee, J. Yang, S. Guha and other members of the ECD photovoltaic project team and the Thin Film Partnership team who have contributed to this research program through either collaborations and/or helpful discussions. This work was supported by NREL (subcontract: ZAK-8-17619-18) under the Thin Film Partnership Program.

References

1. S. Guha, J. Yang, A. Banerjee, K. Hoffman, S. Sugiyama, J. Call, S.J. Jones, X. Deng, J. Doehler, M. Izu and H.C. Ovshinsky, 1997 IEEE PV Specialist Conf. Proc., 607 (1997).
2. X. Deng, M. Izu, S. J. Jones, T. Liu, S. R. Ovshinsky, and B. Vier, "Development of High, Stable-efficiency Triple-junction a-Si Alloy Solar Cells", Final Subcontract Report under NREL subcontract ZAN-4-13318-11, February 1998 (available through NTIS).
3. X. Deng, S. J. Jones, T. Liu, M. Izu and S. R. Ovshinsky, , in Proceedings of 26th IEEE Photovoltaic Specialist Conference, 591 (1997).
4. S.J.Jones, X. Deng, T. Liu and M Izu, Spring 1998 Mat. Res. Soc. Symp. Proc. (to be published).

Title: **Thin Film CIGS Photovoltaic Technology**

Organization: Energy Photovoltaics, Inc. (EPV)
Princeton, NJ

Contributors: Alan Delahoy, Principal Investigator; Jeff Britt, Co-Principal Investigator; Zoltan Kiss, Program Manager; G. Butler, D. Chorobski, G. Jachura, B. Price, P. Ripish, A. Varvar, F. Ziobro.

Objectives

The principal objective of this program is to successfully transfer an R&D scale, high efficiency CIGS process to manufacturing scale equipment in a manner that allows efficient production. A major milestone is the demonstration of a well-controlled supply of Cu to the growing film by linear source evaporation. A further objective is the incorporation of a junction-forming process into the vacuum chamber used for CIGS growth. Using these techniques, the fabrication of encapsulated CIGS modules 4300 cm^2 in area and with a power exceeding 30W is a high priority.

Approach

As previously described, EPV operates a complete pilot line for production of 4300 cm^2 CIGS modules, and a 4-source R&D scale CIGS deposition system for recipe development. EPV is seeking to consolidate large area CIGS growth and junction formation in a single machine. For CIGS growth this has been accomplished, thereby avoiding air exposure and time consumption in shuttling a substrate between separate high temperature evaporation and magnetron sputtering systems. The new CIGS formation process (EPV's third) is termed the FORNAX process, and the historical evolution of EPV's processing is described in [1]. The FORNAX process is a sequential, not a selenization, process, and requires co-deposition of Se with the other elements. The uniform supply of material in a hot, Se-containing atmosphere is non-trivial, and EPV has pioneered the use of linear evaporation sources to accomplish this [2,3]. While junction formation is routinely accomplished via chemical bath deposition of CdS, EPV has initiated a new program to explore direct deposition of ZnO on small samples of CIGS using a novel growth technique for the ZnO, viz. the reaction of fluxes of Zn and atomic oxygen [4].

Results

The best module produced using EPV's second process generated 25.0 watts in sunlight at an irradiance of 1052 W/cm^2, corresponding to an aperture area (3100 cm^2) efficiency of 7.65% and an active area efficiency of 8.7%. The PV parameters were V_{oc} = 31.0 V, I_{sc} = 1.46 A, and FF = 55.4%. The I-V curve is shown in Figure 1. This module required both evaporation and sputtering systems for its CIGS formation.

The performance of cells produced in an R&D scale system by the new FORNAX process is shown in Table 1. This table compares the average and best device characteristics obtained with the FORNAX process to the average characteristics obtained with the well-optimized second process over an area of about 14 cm x 22 cm. An average V_{oc} of 569 mV was obtained with the FORNAX process compared to 459 mV for the second process. The best FORNAX cell had a V_{oc} of 611 mV and FF of 74.5%, but a rather low current density of 27.5 mA/cm^2, despite the 2μm cell thickness. Nevertheless, because of the high cell voltages achieved, the FORNAX process appears to offer long term potential for exceptional cell efficiencies, and the higher band gap material is better suited to modules. Fornax cells are also better behaved in terms of exhibiting no measurable degradation during storage (this has been checked up to 50 days) and only a small enhancement upon light soaking.

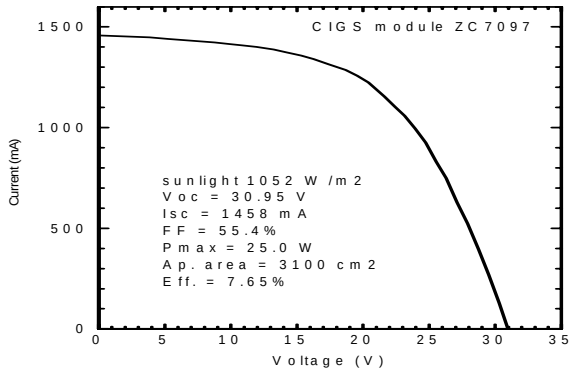

FIGURE 1. I-V curve as measured in sunlight for a 25 watt, 7.65% CIGS module.

TABLE 1. Device characteristics obtained using EPV's second and FORNAX CIGS processes, and under the direct junction initiative.

CIGS process	Source of CIGS	Junction formation	V_{oc} (mV)	J_{sc} (mA/cm^2)	FF (%)	Effic. (%)
second	EPV (R&D)	CdS/ZnO (EPV)	459	37.0	69.1	11.7 <22>
FORNAX	EPV (R&D)	CdS/ZnO (EPV)	569	27.3	73.3	11.4 <24>
FORNAX	EPV (R&D)	CdS/ZnO (EPV)	611	27.5	74.5	12.5
FORNAX	EPV (pilot)	CdS/ZnO (EPV)	537	25.5	70.3	9.6
3-stage	NREL	CdS/ZnO (EPV)	628	35.9	74.1	16.7
3-stage	NREL	ZnO (EPV)	565	35.7	61.1	12.3

A series of eight, 16-cell minimodules was fabricated using FORNAX CIGS [1]. Laser scribing was used for the Mo, while the 2nd and 3rd scribes were performed mechanically on a small x-y table. The I-V data for the highest efficiency minimodules are shown in Table 2. An average V_{oc} of 607 mV per cell was obtained for one of the minimodules. The difference in performance between the two runs is due to the different Ga/(In+Ga) ratio used in their preparation. The area lost at the interconnects is about 10%, so that the active area J_{sc} is about 27 mA/cm^2.

TABLE 2. Performance of unencapsulated minimodules prepared using FORNAX CIGS.

Module #	Area (cm^2)	V_{oc} (volts)	V_{oc}/cell (mV)	I_{sc} (mA)	J_{sc} (mA/cm^2)	FF (%)	P_{max} (mW)	Effic. (%)
1765b	36.4	8.97	561	53.5	23.5	67.0	312	8.84
1766a	34.0	9.58	599	52.0	24.5	69.8	332	10.24

Implementation of the FORNAX process on the pilot line has required development of a new version of linear source to allow better control of Cu deposition. Both rate and uniformity have been improved, and Figure 2 shows the thickness distribution achieved for a relatively thick deposition from the Cu linear source. Devices produced on CIGS material grown in the pilot line by the FORNAX process on 96.5 x 44.5 cm^2 soda lime glass substrates have exhibited good voltages and fill factors. The I-V parameters for such a device are shown in the 4th entry in Table 1. The open-circuit voltage was 537 mV and FF 70.3%.

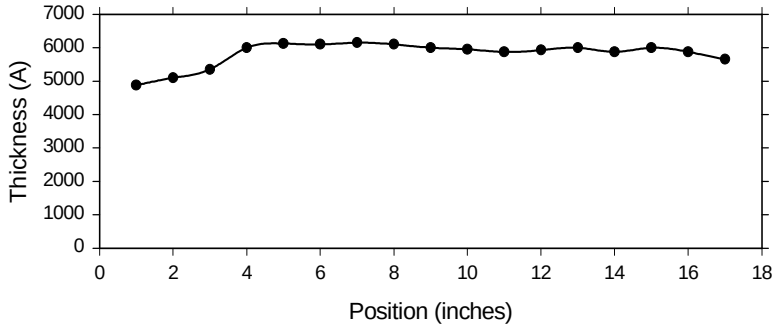

Figure 2. Thickness distribution across the narrow dimension of a glass substrate (perpendicular to the direction of substrate travel) after Cu deposition from a linear source.

At the National CIS R&D Team Meeting (Denver, Sept. 1998) EPV announced a new program to form direct junctions using reactive ZnO prepared under a DOE SBIR award, and invited the collaboration of NREL. Some of the goals of this program are: 1) to eliminate Cd, and develop a dry junction formation process, 2) to develop a CIGS/reactive ZnO/sputtered ZnO process for short term manufacturing purposes, and 3) to further understand metastable effects in direct junction devices. One of the best device results obtained so far is shown as the 6th entry in Table 1 above. Although cell voltages are often in the 300-400 mV range, it is encouraging that a V_{oc} of 565 mV has been observed. The cell efficiency was 12.3%. The cells exhibit a variety of light soaking effects, the most noticeable being an increase in V_{oc}. The effect relaxes in the dark, and can also be induced by voltage bias. Two examples are shown in Figure 3 below. A plot of V_{oc} versus illumination time at three different temperatures is shown in Figure 4. It is found that the V_{oc} versus log(t) curves can be described by a stretched exponential, and scale with t.exp(-E/kT) as a parameter, with E = 0.51 eV. The underlying mechanisms have yet to be elucidated. Most of these experiments were conducted with CIGS provided by M. Contreras, NREL.

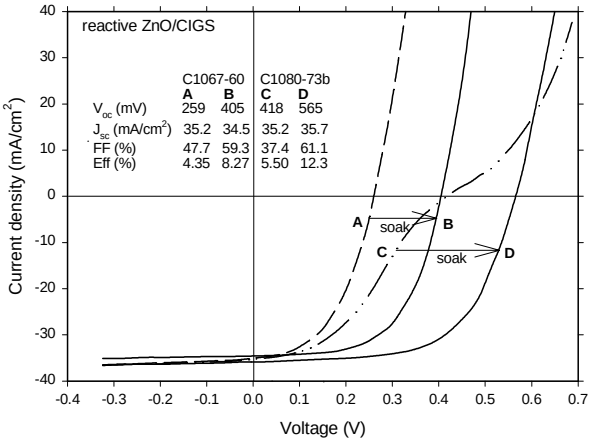

Figure 3. I-V curves before and after voltage soaking for two direct junction ZnO/CIGS devices.

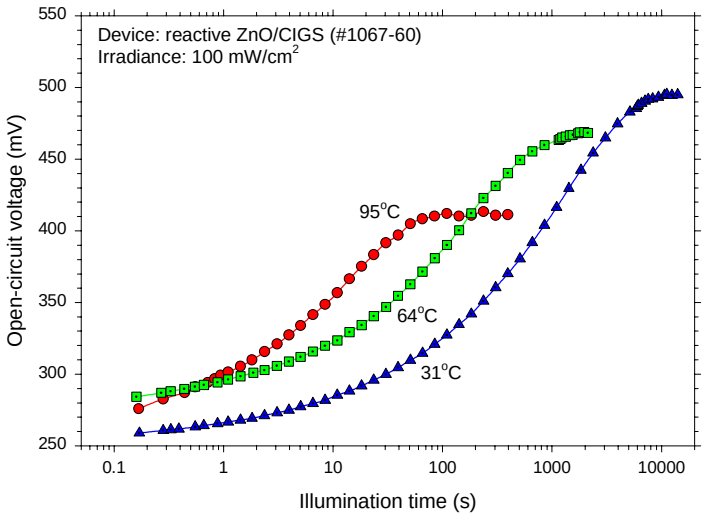

Figure 4. V_{oc} versus log time for a direct junction (ZnO/CIGS) device at three temperatures, showing earlier achievement of saturation at elevated temperatures.

Conclusions and Future Plans

Using a new CIGS formation process, termed the FORNAX process, 16-cell minimodules were prepared with efficiencies up to 10.2% and cell voltages averaging 607 mV. The successful operation of an improved type of linear source for Cu delivery has allowed implementation of the FORNAX process in the pilot line on 96.5 cm x 44.5 cm glass substrates. The significance of this accomplishment is that a pilot scale CIGS formation machine of extreme versatility has been constructed, one that is capable of emulating all known vacuum CIGS processes. We look forward to trials and engineering development of this new source, and renewed efforts on the module front using this machine. Encouraging results have been obtained in preparing direct ZnO/CIGS junctions by a new method, including cells in the 12-13% range, and experiments with in-situ junction formation are being contemplated.

References

1. Delahoy, A.E., Chorobski, D., Ziobro, F., and Kiss, Z.J. "Baseline Process Development for Pilot Line Production of CIGS Modules" NCPV Program Review Meeting, Denver, CO, Sept. 8-11, 1998.
2. Delahoy, A.E., Britt, J.S., Kiss, Z.J. (1998) "CIS Photovoltaic Technology," Final Technical Report, NREL/SR-520-25713, 29pp. Available from NTIS, Springfield, VA 22161.
3. Delahoy, A.E. and Meyers, P.V., "Thin-Film PV Modules: Manufacturing Technology and Issues," Tutorial III, 26th IEEE Photovoltaic Specialists Conference, September 29, 1997.
4. Delahoy, A.E. and Ruppert, A.F., "Zinc Oxide Film Formation using Atomic Oxygen and Metal Flux Sources," Presented at the 2nd World Conference and Exhibition on Photovoltaic Solar Energy Conversion, Vienna, July 6-10, 1998.

Title: $CuIn_{1-x}Ga_xSe_2$ Thin Film Solar Cells

Organization: Florida Solar Energy Center, Cocoa, FL

Contributors: Neelkanth G. Dhere, Principal Investigator; Shashank R. Kulkarni, Kevin W. Lynn,

Objective

The goals of this research is to improve the efficiency of $CuIn_{1-x}Ga_xSe_2$ (CIGS) thin-film solar cells by determining device limitations by carrying out detailed analysis of CIGS solar cell parameters; optimizing the bandgap of CIGS thin films by controlled gallium and sulfur incorporation; and improving the morphology by providing controlled amounts of sodium prior to selenization-sulfurization.

Technical Approach

Detailed analyses of $CuIn_{1-x}Ga_xSe_2$ thin film solar cell can elucidate their limitations and loss mechanisms. Addition of gallium and sulfur can raise the band gap of CIGS thin films closer to the optimum value. Initially attempts were made to raise the bandgap by incorporating more gallium. In earlier experiments, CIGS films were prepared by the two-selenization process using Se vapor of metallic precursor layers sputtered from CuGa(22%) and In targets. The process consisted of preparing a Cu-rich $CuIn_{1-x}Ga_xSe_2$ thin-film during the first stage, followed by the preparation of an overall Cu-poor, large-grain film during the second stage. Higher rates of temperature ramp-up to 550 – 560 °C and a controlled cool-down to 300 °C under continued selenium evaporation helped in enhancing gallium content. Overall gallium content, x, was limited to 0.21, while the best efficiency for a CIGS solar cell was 9.02%. Use of a higher gallium-content CuGa(66%) alloy target in conjunction with CuGa(22%) and In targets would enhance gallium content in the CIGS film. Controlled minute traces of sodium in the form of a sodium added to growing CIGS films can improve the morphology and enhance p-type doping. Sodium may be supplied to the growing film by evaporation of small quantities of Na_2S prior to selenization.

Results

Detailed analyses of the 9% $CuIn_{1-x}Ga_xSe_2$ thin film solar cell were carried out at IEC. The JxV characteristics in light and dark were compared to verify if the light characteristic was essentially a translated curve with light short circuit current J_{sc} or J_l (Figure 1). A cross–over would have meant photoconducting heterojunction partner layer. In the present case, there is not much of crossover. I-V characteristic under illumination provided values of $J_{sc,}$ V_{oc}, FF, and η, in addition to R_s, R_p. Ascending and descending curves were obtained to verify hysteresis.
The main (middle) part of log ($J+J_{sc}$) versus V_t curves showed diode behavior (Figure 2). The offset between dark and light curves is attributed to the higher J_o under illumination. At low values of voltage, the curve shows the value of the shunt resistance. In the present cell, shunting effects became predominant below 0.1 mA cm^{-2}. Slopes are modified due to series resistance at high currents. In the present cell, series resistance effect was observed over 50-60 mA cm^{-2}. The dJ/dV versus V curve measures ac conductance around J_{sc} (Figure 3). For the dark curve, it gave a reasonable value of 1 kΩ cm^2. The light curve showed slight change of collection with voltage. The unsmoothed light curve was noisy due to flicker in xenon arc lamp. The scatter was reduced by using values of dJ/dV calculated by the nine-point differential method. dV/dJ versus $1/[J_o+J_{sc}]$ curve was plotted to estimate ac resistance in forward bias. The straight lines show diode or exponential behavior (Figure 4). The intercept at ∞ current gave a reasonable value of series resistance of ~ 2 Ω cm^2. Non-coincidence between ascending

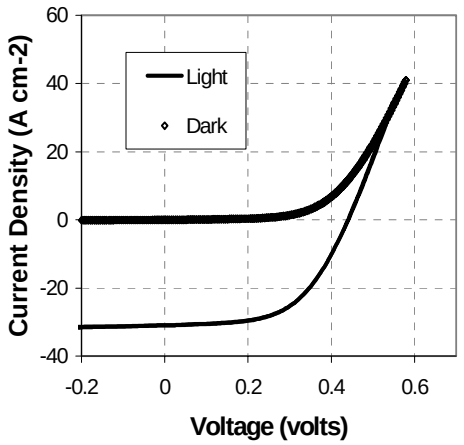

Figure 1: Variation of light and dark current density with voltage

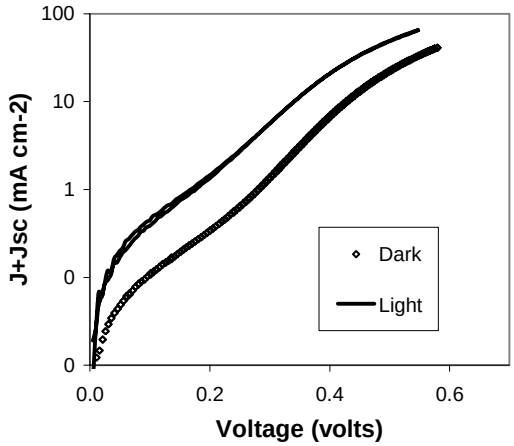

Figure 2: Log($J+J_{sc}$) versus total voltage V_t curves

and descending curves indicated hysteresis. This was not always the case.
The quantum efficiency (QE) curves were obtained in the dark, under AM1 light illumination bias, in reverse (-1 V) bias under AM1 light bias (illumination), and in forward (+0.3 V) bias under AM1 light bias (Figure 5). There was not much light sensitivity in the QE curves, with and without AM1 light bias. The observed better collection under reverse bias and reduced collection under forward bias were as expected.
Another set of curves was obtained for normalized QE versus photon energy in eV (Figure 6). Here the peak value of each curve was normalized to 1. The curves showed a slight difference in collection at low

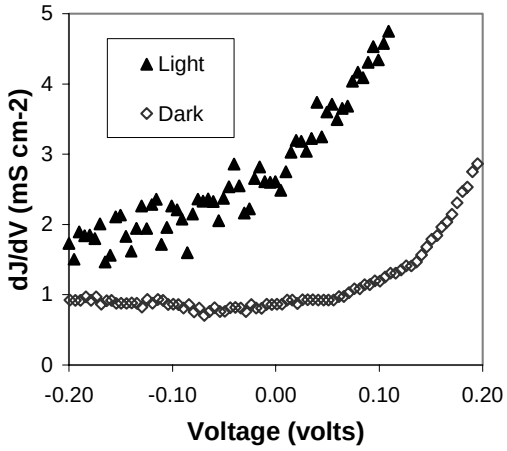

Figure 3: dJ/dV versus Voltage characteristics

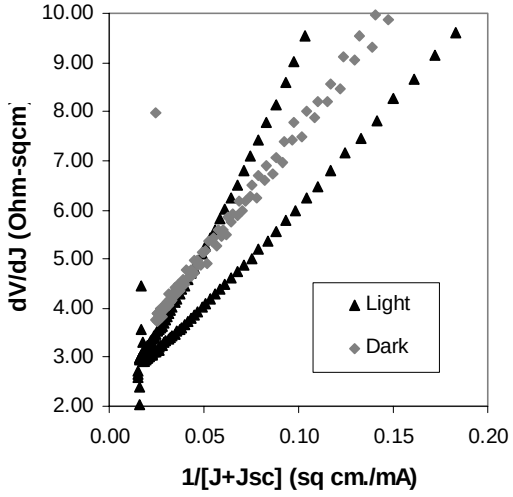

Figure 4: Variation of dJ/dV with $1/[J+J_{sc}]$

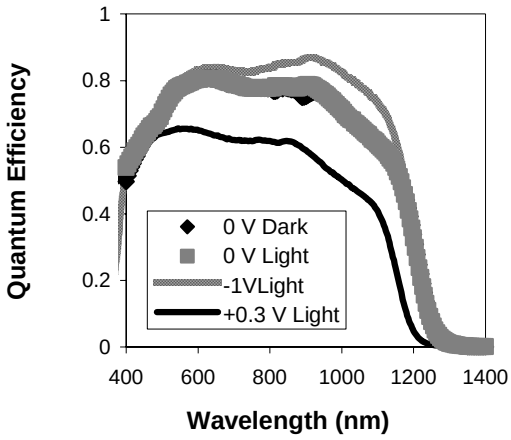

Figure 5: Variation of quantum J+Jsc Efficiency with wavelength

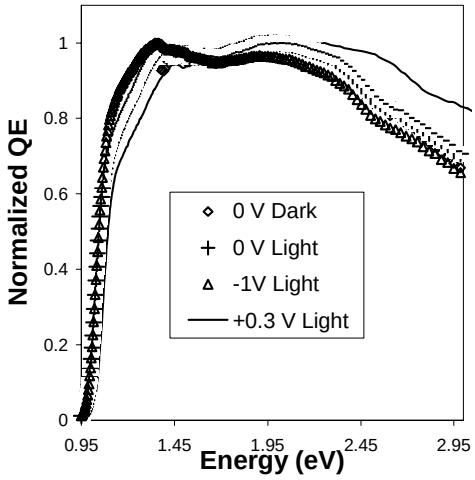

Figure 6: Normalized quantum efficiency with photon energy in eV

energy. The curve showed QE cut off at low (~0.94-0.95 eV) energy and CdS absorption at the high energy. The log of normalized quantum efficiency (QE) versus photon energy showed a linear behavior at low energy because of the exponential shape of collection (Figure 7). This is not unusual. Again there was a slight difference at low photon energy due to increase in collection as a result of a higher field in the reverse bias. These curves also showed QE cut-off at low energy, that was ~ 0.2 eV below that of cell

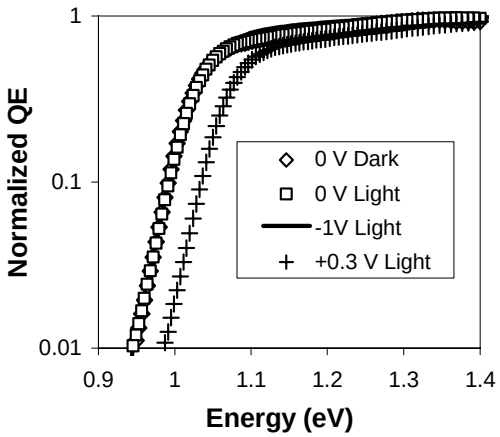

Figure 7: Log Normalized QE versus photon energy

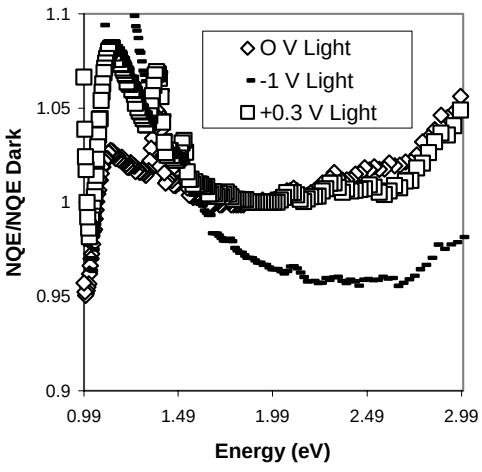

Figure 8: NQE/NQ E_{dark} x photon energy

fabricated at IEC having higher effective Ga incorporation. Normalized QE/(Normalized QE in the dark) i.e. NQE/NQ E_{dark} versus photon energy curves were plotted so as to amplify even small differences up to 5-10% (Figure 8). NQE/NQ E_{dark} was slightly above 1 because of slightly better collection under light bias. The NQE/NQ E_{dark} values were significantly higher under light bias and reverse bias due to better collection, and lower under light bias and forward bias due to poorer collection. A few extra peaks were observed due to glitches during filter changes, etc.

On the whole, the characteristics of the $CuIn_{1-x}Ga_xSe_2$ thin film solar cells were normal and the cells did not have serious limitations. It was decided to achieve higher efficiency by bandgap enhancement through incorporating higher proportions of gallium. Initially attempts were made to raise the bandgap by incorporating more gallium. CIGS films were continued to be prepared by the two-selenization process using Se vapor. A higher gallium-content CuGa(66%) alloy target was used in conjunction with CuGa(22%) and In targets so as to enhance gallium content in the CIGS film. In the first sequence, a 2.75 μm thick film with a composition of $Cu_{0.93}In_{0.72}Ga_{0.28}Se_2$ was attempted. In it a total of ~4060 Å of CuGa(22%), ~620 Å of CuGa(66%), and ~5340 Å of In were deposited. The majority (80%) of the CuGa(66%) was deposited on the back contact, followed by 80% of the CuGa(22%), 65% of In, and the remaining 20% of CuGa(22%). After the first selenization, the remaining 35% of In and 20% of CuGa(66%) were deposited, followed by a second selenization. Most of the high gallium material was placed toward the back contact in order to form the concentration gradient. Higher rates of temperature ramp-up to 550 – 560 °C and a controlled cool-down to 300 °C under continued selenium evaporation that had helped in enhancing gallium content in earlier experiments, were employed also in the new series of experiments. Since gallium content was similar to films made using only the CuGa target, a series of attempts were made using both the low (22% Ga) and high (66% Ga) targets to increase the gallium content. After considerable experimentation with the order of the deposition sequence, 3μm thin films with a composition of $Cu_{0.94}In_{0.57}Ga_{0.41}Se_2$, as verified by electron probe microanalysis, were prepared. X-ray diffraction of CIGS thin films having Ga content to >40% showed the presence of both $CuIn_{0.5}Ga_{0.5}Se_2$ and $CuIn_{0.7}Ga_{0.3}Se_2$. However, morphology and device properties deteriorated. High (~600 ^oC) temperature annealing or triple-selenization have been shown to be useful for effective gallium incorporation. However, the processes become more and more difficult to scale-up. In post-deposition selenized films, gallium has a tendency to diffuse towards the back contact. Ga incorporation near the back contact provides the back-surface field. The so-called double-profiling of gallium may result in a front surface field. It would oppose the electrons diffusing towards the junction. This may be detrimental to device performance. It was decided to replace the second selenization by sulfurization. Sulfur incorporation does not pose a similar problem. With sulfur incorporation near the junction, the bandgap increase takes place by a downward shift of the valence band rather than an upward shift of the conduction band as is the case with gallium incorporation. This approach seems to be more promising. Controlled minute traces of sodium added to growing CIGS films in the form of Na_2S prior to selenization so as to improve the morphology and enhance p-type doping improved film morphology. Large-grain films with faceting were observed by scanning electron microscopy and atomic force microscopy. These CIGS films, are, therefore, expected to result in higher efficiency devices.

Publication

1. N. G. Dhere and K. W. Lynn, Band Gap Optimization by Gallium and Sulfur Incorporation in $CuIn_{1-x}Ga_xSe_{2-y}S_y$ Thin Films Prepared by Selenization-Sulfurization Process, Proc. 2nd World Photovoltaic Solar Energy Conf. Vienna, Austria, July 6-10, 1998.

Title: **Process Development of Large Area, Thin Film CIGS**

Organization: Global Solar Energy, LLC, Tucson, AZ

Contributors: J. Britt, Principal Investigator, R. Wendt, S. Wiedeman, S. Albright, M. Misra, J. Fogleboch, R. Hensley, B. Howard, L. Kostroski, D. Mason, R. Nelson, F. Ratel, and D. Shah

Objective

The objective of this project is to develop the technology for producing flexible thin film PV modules sectioned from continuous rolls having 13% conversion efficiency over 1000 cm^2 area and 11% efficiency on larger modules with a 3500 cm^2 area.

Approach

Global Solar Energy (GSE) has developed the technology to deposit and monolithically integrate CIGS photovoltaics on a flexible substrate. In the GSE approach, long continuous rolls of polymer substrate are processed as opposed to individual small glass plates. Not until final module buss and power lead attachment is the continuous roll sectioned into individual panels. Roll-to-roll vacuum deposition has several advantages over glass coaters that translate directly to reduced capital costs, greater productivity, improved yield, greater reliability, lower maintenance, and a larger volume of PV. Specific advantages include: (1) elimination of expensive entry, exit and holding chambers in the deposition line; (2) smaller and less complicated chambers than glass coaters, (3) fast heat-up and cool-down times, and (4) elimination of thermal and mechanical breakage associated with glass.

In combination with roll-to-roll processing, GSE has developed sputtering and evaporation deposition operations that enable low cost and high efficiency CIGS modules. In-line multi-source evaporation has been demonstrated at GSE to deposit high quality CIGS in a continuous roll-to-roll operation. For the Mo, CdS, i-ZnO, and TCO layers, GSE has developed controllable and reproducible high-rate vacuum deposition techniques.

Three tasks are identified in this project, namely,

Task 1: CIGS Absorber Improvement

Task 2: Monolithic Integration of PV

Task 3: Encapsulation Development and Reliability Testing

The overall objectives of Task 1 are to optimize the electronic quality of the absorber material while maintaining compatibility with vacuum CdS junction formation and to improve and scale up the source design for multi-source co-evaporation over large area (33cm x 300 meter rolls of substrate) with adequate uniformity. Control and reproducibility are critical issues in this task. Materials utilization for the metals of greater than 50% and a deposition rate that allows 10 cm/minute roll coating speed must be maintained.

The objective of Task 2 is to fully develop and optimize scribe and interconnect processes for module formation. The approach includes layer-specific, all laser-scribing methods, coupled with the

development of ink-jet deposition over scribes. Key factors are excellent electrical isolation for front and back contact scribes, low series resistance for the interconnect scribe, minimal debris generation and minimal scribe area loss.

The objective of Task 3 is to begin development of viable encapsulation and finishing methods to produce flexible and rigid mounted PV products. Front and backsheet materials, methods for mounting and forming buss and power output connections must be developed.

Results

Individual evaporation sources for each element (Cu, In, Ga, and Se) have been fabricated and installed in a research reactor that accommodates 6-in. wide web and in a manufacturing-scale system for depositing CIGS on a 13-in wide web. The insulation and source component materials and designs have been improved through a number of iterations. The microscopic and macroscopic compositional uniformity of CIGS deposited from the sources has been demonstrated thus far to be adequate over deposition areas greater than 50 ft^2. Additionally, the sources have proved to be robust and reliable over the course of many depositions.

Optimization of the absorber deposition process involves adjustment of substrate temperature, evaporative source flux rates, source placement and sequence, selenium delivery rate, and substrate web speed. The individual evaporation sources for Cu, In and Ga can be configured in many different sequences. At present, the best small-area device had an efficiency of 9.8% (Figure 1). This device was made from a CIGS film deposited at a relatively low rate of 2.5 cm/min. in the research reactor. Perhaps a more significant result was an 8.8% device (V_{oc} = 0 .441 V, J_{sc} = 31.9 mA/cm^2, FF = 63.1%) made from CIGS deposited on a web moving at greater than 12 cm/min., suggesting that the practical limits of CIGS deposition rate have not yet been reached.

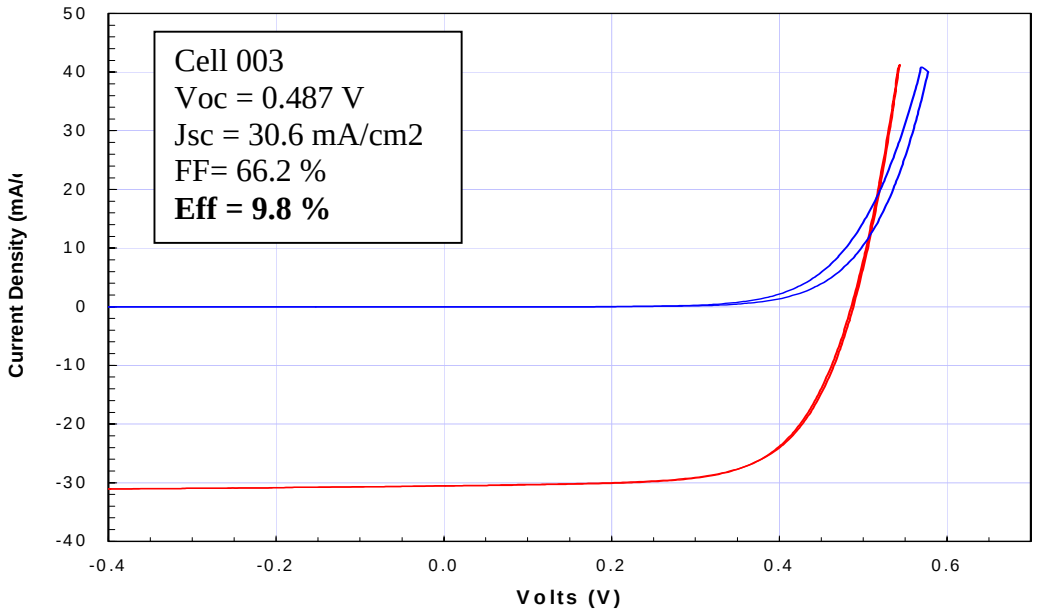

Figure 1. Light and dark J-V characteristic of a 9.8% efficient CIGS device deposited in a continuous process on Mo/polyimide. The J-V parameters for the 0.31 cm^2 device were measured at the IEC on a total area basis.

A series of round robin experiments were conducted between the Institute of Energy Conversion (IEC) and GSE during this phase. The goal of the experiments was to identify the major differences between the device finishing process predominately used in research laboratories (CBD CdS/i-ZnO/c-ZnO) and the process GSE intends to use in manufacturing (vacuum deposited CdS/i-ZnO/ITO). CIGS deposited on a continuous polyimide web at GSE was used for all the experiments. Only slight differences in device characteristics were observed between the two CdS deposition processes (Table 1). A greater difference was observed when comparing the two TCO films, ZnO and ITO (Table 2). The lower short-circuit current density and efficiency of the device with ITO is presumably due to poorer optical transmission through the ITO film. Further improvements in the ITO deposition process are expected to lessen the differences in quality (transmission/sheet resistance) between ZnO and ITO.

Table 1. Comparison of devices with CBD and sputtered CdS (common CIGS and ZnO TCO)

	V_{oc} (V)	J_{sc} (mA/cm^2)	FF (%)	Eff. (%)
CBD CdS (IEC)	0.465	25.8	64.0	7.68
vacuum CdS(GSE)	0.443	27.0	62.7	7.50

Table 2. Comparison of devices with ITO and ZnO (common CIGS and CBD CdS)

	V_{oc} (V)	J_{sc} (mA/cm^2)	FF (%)	Eff. (%)
i-ZnO/c-ZnO (IEC)	0.478	31.2	63.6	9.47
i-ZnO/ITO (GSE)	0.457	26.0	64.5	7.67

Interconnecting cells on a soft, semi-opaque polymer substrate presents several challenges not encountered when working on glass substrates. Several interconnect schemes have been investigated to address these and other challenges (Table 3). With the exception of the cascade configuration, all of the options require an ink-printing step [1].

Table 3. Interconnection options under investigation for CIGS on flexible substrates. (s1 = Mo scribe, s2= via scribe, s3 = TCO scribe, p = print, w = weld)

Configuration	Interconnect Sequence	
Cascade	Mo/S1/CIS/CdS/S2/TCO/S3	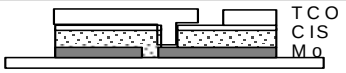
Post Absorber 1	Mo/CIS/CdS/S1/P1/TCO/P2/S2&W	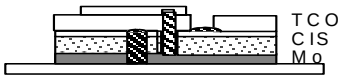
Post Absorber 2	Mo/CIS/CdS/S1/P1/TCO/S2	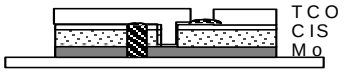
Post Absorber 3	Mo/CIS/CdS/S1/P1/TCO/S2	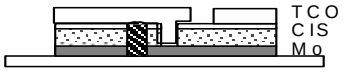
Post Device (TCO)	Mo/CIS/CdS/TCO/S1/P1/P2/S2& ‴	

A production laser scribing station has been installed in the GSE facility in Tucson. Equipment for high-speed, high accuracy ink-jet printing is an integral part of the scribing station. Either insulating or conductive ink can be applied with the equipment. A significant amount of effort has been devoted to narrowing the ink lines since scribe area loss will likely be governed strongly by the width, uniformity, and registration accuracy of the printed lines rather than by the laser scribes themselves. Continuous, accurate, uniform ink lines as narrow as 200 μm have been deposited and cured thus far.

Two prototype laminators each capable of simultaneously laminating two 1-ft. x 4-ft. modules have been designed, assembled, and installed in the GSE facility. The laminators are PC controlled and have a small thermal load for a shortened cycle time. A lamination process has been developed that reproducibly yields bubble-free flexible modules. The lay-up of the encapsulation materials is done manually and is presently the most time consuming part of the lamination process. Techniques for automating the lay-up process are being investigated.

Two types of module product types have been planned for, one flexible and the other semi-rigid. For the semi-rigid module, the polyimide film will be encapsulated against an unbreakable, inexpensive substrate. Prototype semi-rigid modules have been successfully fabricated with this approach. Buss bar and termination schemes have also been demonstrated but still require rigorous testing to verify their durability.

Conclusions and Future Directions

Substantial progress in CIGS deposition, patterning, and encapsulation was made during the first phase of this subcontract. For CIGS deposited on a continuous polyimide web, total area cell efficiencies near 10% were achieved, and the tools and understanding necessary to achieve this result were improved. A production patterning station capable of laser scribing and ink-jet printing was installed. Uniform and continuous ink-jet lines less than 200 μm wide were demonstrated with the station. In the encapsulation area, a laminator for flexible modules was designed, assembled, installed, and successfully demonstrated for both flexible and semi-rigid modules.

The next phase of this work will focus on the following areas: a) further improvement of CIGS material quality, with emphasis on the 13-in production system, b) demonstration of successful laser scribing in conjunction with ink-jet printing to produce efficient monolithically interconnected modules, and c) initial qualification of encapsulation, buss bar, and termination techniques on live modules.

References

1. Wiedeman, S.; Wendt, R.G.; and Britt, J.S. (1998). "Module Interconnects on Flexible Substrates" Presented at the National Center for Photovoltaics (NCPV) Program Review Meeting, September 8-11, 1998, Denver, CO, and to published in the American Institute of Physics (AIP) Proceedings Series.

Title: **Transparent Conductors and Barrier Layers for Thin Film Solar Cells**

Organization: Department of Chemistry,
Harvard University, Cambridge, MA.

Contributors: R. G. Gordon, Principal Investigator;
R. N. R. Broomhall-Dillard, X. Liu, D. Pang, D. Teff

Summary of Current Project Objectives

Transparent conducting materials are essential components of many kinds of solar cells, in which they serve as front-surface electrodes. Most designs for highly reflective back contacts also call for a transparent conducting layer. The compositions of these transparent conducting layers are usually based on oxides of tin, indium and/or zinc, and are referred to as transparent conducting oxides (TCO). In addition to having low electrical resistance and low optical absorption, the structure of a front-surface TCO must minimize reflection losses. The TCO must also resist degradation during cell fabrication and use. Finally, the method for making the TCO must be inexpensive and safe.

Our objectives are to improve the performance of TCO materials and the methods for their production. We aim to reduce their electrical resistance, optical absorption and reflection losses, and to lower the deposition temperature to avoid thermal degradation of other cell components. For the production method, the prime consideration is to deposit the TCO layers at a high rate with relatively simple apparatus. The method chosen is chemical vapor deposition (CVD) at atmospheric pressure, since it has been demonstrated in the glass-coating industry to be the most cost-effective method for making large areas of TCO coatings.

CVD of Zinc Stannate Films

Sputtered zinc stannate transparent conductors has been shown to be more stable, both thermally and chemically, than either zinc oxide or tin oxide.[i] In this task we are trying to discover a process for CVD of zinc stannate, which should be more cost-effective for large-area deposition.

The first challenge was to find zinc and tin precursors that react under similar CVD conditions. Tin oxide is usually deposited from an oxygen-containing CVD atmosphere, which is too reactive for the most commonly-used zinc sources, based on diethylzinc. Hence we looked for zinc sources that are less reactive with oxygen. Zinc acetylacetonate was identified as a promising less reactive zinc source. Its main problem as a CVD precursor is that it is a solid with relatively low volatility. Thus we searched for a suitable solvent so that its solution can be flash vaporized as a source of zinc acetylacetonate vapor.

The solubility of zinc acetylacetonate was tested in a wide variety of organic solvents. Only solvents with fairly high boiling points (over about 130ºC) should be used, so that premature evaporation of the solvent will not cause precipitation of solid zinc acetylacetonate, blocking the evaporator. Ethoxyethanol (b. p. 134ºC) was the best of the solvents tested. Initial use of these solutions successfully deposited zinc oxide from an oxygen-containing carrier gas at substrate temperatures around 500ºC.

Study of the safety data on this solvent showed, however, that it is a toxic teratogen, and may be banned from new industrial uses. Thus a search was made for safer alternative solvents. One likely candidate is di(ethylene glycol) methyl ether, a chemically similar high-boiling solvent (b. p. 194ºC) with no reported teratogenic effects. This solvent will be tested next.

Most CVD reactions for tin oxide are run at high temperatures, over 500ºC, whereas most zinc oxide depositions are run at temperatures below 500ºC. Thus we searched for a more reactive tin precursor that can be used below 500ºC. Dibutyltin diacetate was identified as an appropriate tin precursor for low-temperature depositions. It is a liquid at room temperature, so we will test it for miscibility with the solvents identified for zinc acetylacetonate.

CVD of Fluorine-doped Zinc Oxide Films

The highest priority is to find out why a-Si solar cells grown on ZnO:F superstrates have lower voltages and fill factors than those grown on standard SnO_2:F. Three sets of zinc oxide films were sent to Solarex, for use in preparing a-Si solar cells. One set was doped with fluorine, the second with aluminum, and the third with both fluorine and aluminum. The approximate free electron concentrations in these samples were as follows:

Sample	Electron Concentration
ZnO:F	2×10^{20} cm^{-3}
ZnO:Al	2×10^{20} cm^{-3}
ZnO:(F+Al)	4×10^{20} cm^{-3}

The reason for preparing the doubly-doped samples was to test zinc oxide films in which the carrier concentrations were as high as those typical of commercial fluorine-doped tin oxide.

The relevant cell parameters from the Solarex cells were as follows:

TCO	Voc, volts	FF	Jsc, ma/cm^2
ZnO:Al	1.43	0.647	14.94
ZnO:(F+Al)	1.45	0.642	16.29
SnO_2:F	1.56	0.681	15.25

The higher free electron concentration in the double-doped ZnO:(F+Al) failed to make a significant improvement in Voc or FF.

In contrast, our studies last year with Steven Hegedus at Delaware showed that increasing the boron doping level in the p-Si did improve these parameters.[ii] Thus the major barrier to carrier transport lies within the p-layer of the a-Si, not within the transparent conductor. One focus of future efforts should be on forming micro-crystalline p-layers, through which the holes can tunnel more freely because they have higher mobility than in a-Si, and in which the tunneling distance is reduced because the hole concentration is higher in micro-crystalline p-Si.

Some success in increasing the voltage and fill factor by deposition of micro-crystalline p-Si layers on zinc oxide has been reported.[iii] However, their short-circuit currents were reduced by about 10%, indicating that some absorption was being introduced by their p-layers.

Solarex cells made on one ZnO:F sample were shunted, presumably because of the sharp points of the crystallites on this textured sample (10% haze). Thus we will make some new ZnO:F samples in which the texture is developed by etching a smooth sample. This approach should produce a cratered textured

surface without any sharp projections that may lead to shunts. A similar approach to etch texturing zinc oxide films has been reported by a group at Juelich.[iv]

For a TCO to form a low-resistance contact to p-Si, the TCO should have a high work function (corresponding to a low Fermi energy). There are few reported measurements of work functions for TCO materials, and they were made by different methods in different laboratories, so comparisons are not meaningful. Recently, Minami and co-workers [v] reported work function measurements on a wide range of TCO materials using the same method in the same laboratory, so comparisons should be more meaningful. Of particular interest, they found the following values:

TCO	Work Function (eV)	Electron Conc.(cm^{-3})
ZnO:Al	4.55	probably $>10^{20}$
SnO_2:F	4.9	probably $>10^{20}$
SnO_2	4.8	2×10^{17}
$ZnSnO_3$	5.3	6×10^{19}
ZnO	5.3	7×10^{19}

The work function for fluorine-doped tin oxide is indeed higher than that of aluminum-doped zinc oxide (no measurements were made for ZnO:F), confirming our suspicion that highly-doped zinc oxide has too low a work function to make a low-resistance contact to p-Si.

The work functions for nominally undoped ZnO and $ZnSnO_3$ are even higher than that of SnO_2:F. Thus, if the work function argument is correct, even better contact to p-Si should be obtained by either lightly doped ZnO or $ZnSnO_3$ as a layer between the usual heavily-doped TCO layer and the p-Si.

CVD of Aluminum Oxide Films

Soda-lime glass contains a high concentration of sodium, which can out-diffuse into TCO layers during their deposition and increase their resistance. In the case of tin oxide, deposition normally takes place at temperatures of 550 ^{o}C or higher, and a sodium barrier of silica or alumina is normally employed between the soda-lime glass and the tin oxide. In the case of ZnO:F, we have in the past not used any barrier layers because the deposition temperature was only 450 ^{o}C, so the sodium mobility was much lower, and we did not see significant effects of using a diffusion barrier.

In more recent ZnO:F depositions, we increased the substrate temperature up to nearly 500 ^{o}C, so we decided to re-investigate the possible effects a sodium diffusion barrier. Amorphous aluminum oxide was chosen as the material for the sodium diffusion barrier, because previous studies in our laboratory [vi] had identified it as a more effective barrier than the more commonly used silica barriers.

A batch of triethyltriisopropyldialuminum was prepared by heating together commercially available triethylaluminum and triisopropylaluminum, and distilling the product.[vii] This liquid was used for CVD of amorphous aluminum oxide coatings on a number of soda-lime glass substrates.

Conditions were adjusted so that smooth, transparent, low-haze coating were obtained. The refractive indices of the alumina coatings were generally between 1.55 to 1.60. No X-ray diffraction lines could be

seen from a sample, showing that the alumina is amorphous as deposited. Generally, an amorphous structure is desirable for good performance as a diffusion barrier.

Nano-indentation tests of the alumina showed that its hardness is similar to that of quartz. Its adhesion is good, and it could not be scratched easily with a sharp glass point. Its chemical stability is excellent, and it could not be etched by common acids or bases. The alumina was etched by hydrofluoric acid. This observation also shows that it is not crystalline, because crystalline alumina is impervious to HF.

Alumina films were deposited on soda-lime glass, and then ZnO:F films. The samples with alumina barriers had resistances about 10% lower than those deposited directly on soda-lime glass under the same conditions.

CVD of High-Resistance Tin Oxide Films

Certain thin-film solar cell designs, such as cadmium telluride, benefit from a surface layer of high-resistance tin oxide on top of the usual low-resistance layer of fluorine-doped tin oxide. This task is directed to finding a process for CVD of high-resistance tin oxide.

In order to produce high resistance CVD tin oxide films, we will of course omit the normal fluorine dopant source. Chlorine can also act as an n-type dopant in tin oxide films, so a precursor must be chosen without any chlorine in it. Dibutyltin diacetate seems like one appropriate non-halogenated tin precursor for high-resistance tin oxide films.

Oxygen vacancies are another source of free electrons in tin oxide. In order to minimize oxygen vacancies, a high oxygen concentration needs to be used during deposition. In preliminary tests, it was found that use of oxygen as a carrier gas for dibutyltin diacetate produced powdery deposits that could be wiped off the glass substrates. Further runs with lower dibutyltin diacetate concentrations and lower substrate temperatures did moderate the reaction so that undoped tin oxide films could be deposited under high-oxygen conditions. These films are, however, still fairly conductive, with sheet resistances in the ten kilo-ohm range for thicknesses of 100 nm, corresponding to resistivities of 0.1 ohm-cm. Presumably this conductivity arises from oxygen vacancies in the lattice. In order to increase the resistance to the desired 10^4 level, it will be necessary to introduce acceptor doping to trap some of the free electrons. A trivalent metal, such as aluminum or gallium, substituting for the tin should provide the traps needed to reduce the free electron concentration.

---

i. Minami, T. et al. (1994). *Japanese J. Appl. Phys.*, Vol. 33, pp. L1693-L1696.
ii. Gordon, R. G. et al. (January 1998). *Annual Technical Report*, NREL Subcontract XAN-4-11318-05, B. von Roedern, technical monitor.
iii. Winz, K., et al. (1996). *Mat. Res. Soc. Symp. Proc.*, Vol. 420, pp. 819-824.
iv. Kluth et al. (1997). *Proc. IEEE 26th PVSC*, Anaheim, p. 715; Rech et al. (1997). *Proc. IEEE 26th PVSC*, Anaheim, p. 619; Loffl et al. (1997). *Proc. 14th EC-PVSEC*, Barcelona.
v. Minami, T. et al. (1998). *Surface Coatings Technology*, in press.
vi. Chapple-Sokol, J. D. (1988). *Ph.D. Thesis*, Harvard University.
vii. Liu, X.; Kramer, K.; and Gordon, R. G. (1997). *Mat. Res. Soc. Symp. Proc.*, Vol. 446, pp. 383-388.

Title: **Research on Improved Amorphous Silicon and Alloy Devices Prepared Using ECR Plasma Techniques**

Organization Iowa State University, Ames, Iowa 50011

Contributors Vikram L. Dalal(PI)
Tim Maxson, Robert Girvan, Kay Han, S. Haroon, K. Erickson, J. Herrold, B. Oliver, Xi Huang, Z, Zhou, H. Sathwane, A. Sanford

Report

Introduction

Amorphous Silicon and (Si,Ge) alloy materials are of significant interest for fabricating photovoltaic energy conversion devices. The qaulity of the material depends critically upon the deposition conditions. In previous reports [1], we have shown that the plasma conditions used to deposit the materials can fundamentally alter the chemistry of growth, and thereby alter material properties. In particular, we showed that high hydrogen dilution can be expected to homogenize growth and achieve materials with low microstructural defects, and therefore, with better stability. We also showed that one can make very good devices in a-Si:H by using the ECR growth technique as a fine chemical tool to control growth chemistry[2]. In this report, we extend this work to a-(Si,Ge) alloys. We show that the influence of plasma chemistry in this case is very profound, and that ion bombardment, in particular, seems to play a rather large role in making the better a-(Si,Ge) materials and devices.

Experimental Method

A series of a-(Si,Ge) materials and devices were made using the remote, low pressure ECR deposition technique [3]. The materials were grown from a mixture of silane, germane and hydrogen, with the dilution ratio of hydrogen/(silane+germane) being about 20:1. The hydrogen gas was introduced into the ECR resonance zone, where it decomposed, and the energetic beam of H radicals and ions was directed towards the sample. The precursor gases, silane and germane, were introduced near the sample. The plasma and the H beam decomposed the gases, resulting in a deposition of (Si,Ge) alloys. By changing the ratio of silane to germane, the bandgap of the films could be changed. The samples were grown at low pressures, from 5 to 15 mT, and temperatures in the range of 300-340 C. The films were deposited on 7059 glass, and the devices, on a rough stainless steel substrate.

The following optical and electronic properties of the films were measured:
Tauc gap, E04 gap, Dark conductivity, photo-conductivity, sub-gap absorption and activation energy.

Results on properties of films

1. Bandgap: To our surprise, we discovered that the Tauc bandgap of a-(Si,Ge) films itself was a function of pressure in the reactor. In Fig. 1, we show the Tauc gap vs.pressure for two sets of films made with differing silane/germane ratios. As the pressure decreases, the Tauc gap seems to increase.
2. Photo/dark conductivity ratio: We discovered that the photo/dark conductivity ratio of the materials depended on the pressure. In Fig. 2, we show the results for photo/dark conductivity ratio for films deposited at different pressures as a function of Tauc gap. Clearly, the films deposited at lower pressures have better photo/dark ratio, and indication of better quality in such films.
3. Urbach energy of valence band tails. We measured the Urbach energy of valence band tails from sub-gap absorption data. We show the results in Fig. 3, where we show Urbach energy vs. Tauc gap for films made at two different pressures. Once again, the material deposited at lower pressures has the lower Urbach energy, i.e. higher electronic quality.

From these results, then, we conclude that the properties of the films seem to deteriorate as the pressure in the reactor increases. This was an unexpected result, never observed previously.

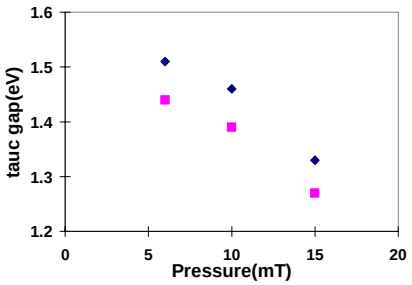

Fig. 1 Influence of pressure on Tauc gap

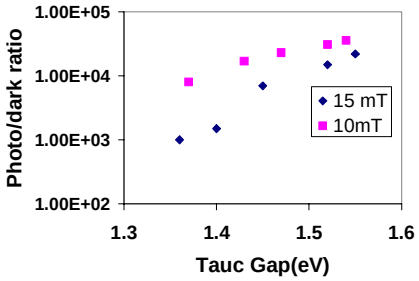

Fig. 2 Influence of pressure on photo/dark Conductivity ratio

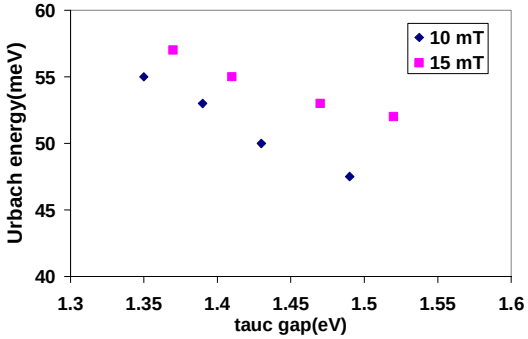

Fig. 3 Influence of pressure on Urbach energy of a-(Si,Ge)

Results on Devices

We next made substrate type p-i-n devices on stainless steel substrates. We discovered the following phenomena:

1. The open circuit voltage of the devices made at higher pressures were always much lower than the open circuit voltages of devices made at lower pressures.
2. The fill factors were poorer in devices made at higher pressures.
3. The plot of subgap QE vs. energy revealed that the devices made at higher pressures, while keeping all other conditions constant, had a lower Tauc gap than devices made at lower pressures.
4. We measured the hole mobility-lifetime product in devices by using a quantum efficiency vs. applied voltage technique [4]. The results for our materials are shown in Fig. 4 as mobility-lifetime vs. Tauc gap for devices made at different pressures.
   From Fig. 4, we observe that the mobility-lifetime product becomes worse as the pressure is increased.

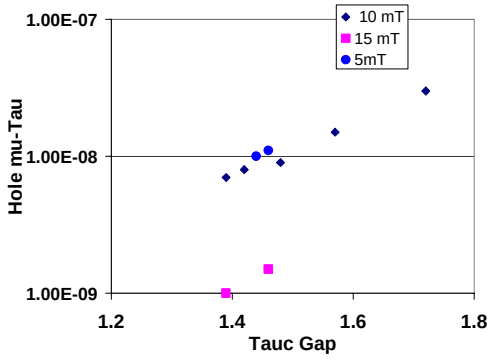

Fig. 4 Mobility-lifetime products for a-(Si,Ge) cells
Made at three different pressures

Thus, from both material and device results, we can conclude that the deposition pressure has some impact on the properties of a-(Si,Ge) films in our ECR reactor. We speculate that this result arises because in a remote ECR plasma, one changes the ion bombardment conditions significantly when one changes the pressure; a lower pressure leads to increase in both ion flux and ion energy. See Fig. 5. We speculate that the ion bobmardment changes the fundamental growth chemistry; a higher bombardment results in a greater mobility for the less mobile radical, namely the germyl radical. The higher mobility results in a more homogeneous film, with less Ge-Ge clustering. Such clustering can lead to a film which has an apparently lower bandgap [higher absorption] than a homogeneous film. The more homogeneous the film, the better the electronic propeprties. The reason why ion bombardment is so important for a-(Si,Ge) but not for a-Si is because the two radical mobilities are so different when growing (Si,Ge).

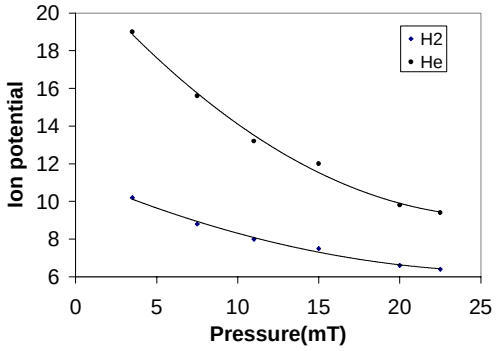

Fig. 5 Ion potential as a function of pressure
ECR reactor for H or He discharge

The implications of this discovery are potentially significant. If one can design a deposition process to improve radical mobilities further, the materials would improve. Such work is in progress.

References

1. V. L. Dalal et al, Proc. Of Amer. Inst. Of Physics, 394, 33(1998)
2. V. L. Dalal et al, Proc. Of 26th. IEEE Photovolt. Conf., p. 695(1997)
3. V. L. Dalal et al, J. Non-Cryst. Solids, 198, 1101(1996)
4. V. L. Dalal and F. Alvarez, J. de Physics, Vol. 42,C-4,491(1981)

Title: **Application of CIS to High Efficiency PV Module Fabrication**

Organization: International Solar Electric Technology (ISET)
8635 Aviation Blvd., Inglewood, CA 90301

Contributors: B.M. Basol, Principal Investigator; V.K. Kapur, Program Manager;
C.R. Leidholm, A. Halani, G. Norsworthy and R. Roe

Objectives

The objectives of this R&D partnership program are the development and demonstration of a novel, low-cost, non-vacuum deposition technique for the growth of CIS and related alloy absorbers and the use of these absorbers for the fabrication of high efficiency solar cells and modules.

Approach

In this program ISET's efforts were concentrated on the development of a non-vacuum deposition process for CIS absorber layers. The novel technique developed by ISET involves nano-size particle deposition. The basic idea is to fix the stoichiometry of the material in a starting powder which can later be deposited on the selected substrate in the form of a precursor film. This in effect is similar to screen printing which to date has not given any good results due to the fact that there is no good sintering agent for CIS type materials. In ISET's approach sintering and densification of the deposited films do not present a big problem. The key is to have a very small (sub-micron) particle size in the starting powder and to utilize a film deposition technique that can put down a thin (1-4 μm) layer of this powder for further processing. The stoichiometry is fixed within the deposited powder layer and therefore the uniformity of the deposited layer is not of concern. The thickness, however, needs to be controlled to a certain extent within the range indicated above.

The general steps of depositing CIS layers by the non-vacuum technique is given in Fig. 1. The advantages and unique features of this process are; (i) excellent compositional uniformity of the deposited CIS film which is easily achieved since the composition of the precursor is fixed at the molecular level, (ii) high materials utilization which may be over 85%, and (iii) low cost capital equipment.

.

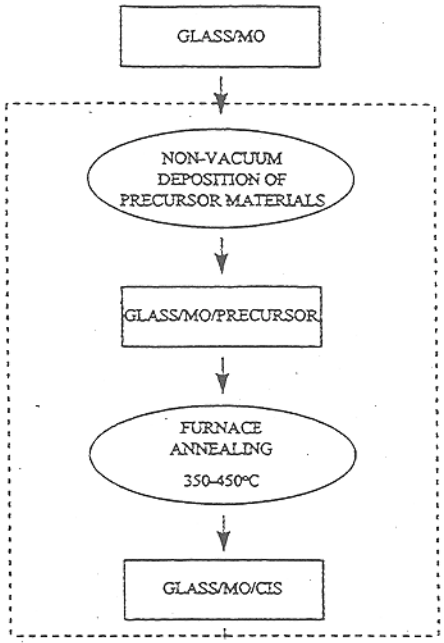

Fig.1 General processing steps for ISET's novel non-vacuum technique.

Results and Discussion

Fig. 2 shows the SEM of a precursor film deposited in the form of a layer of nano-particles on a Mo/glass substrate. The typical particle size in the precursor is about 0.2 Fm. When this film is further processed the resulting CIS compound layer has a grain size of 0.5-2.0 Fm with near-columnar structure.

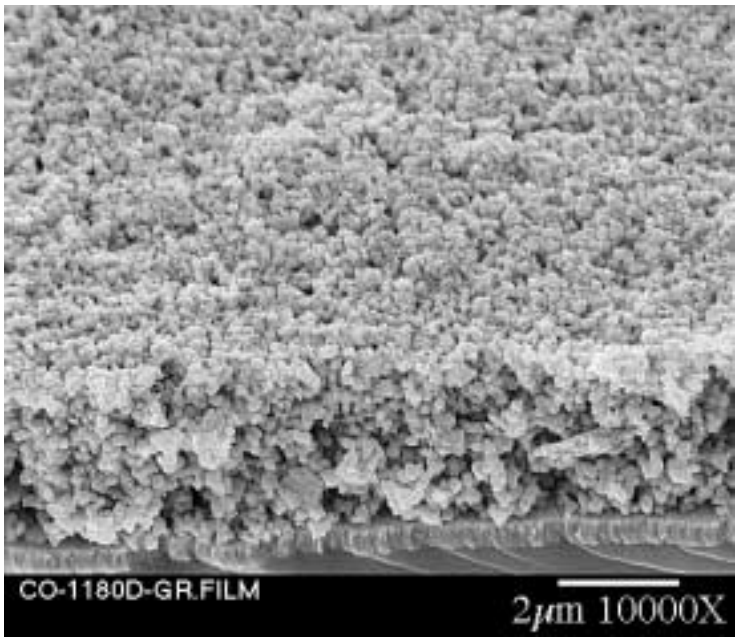

Fig. 2 SEM of a precursor layer consisting of nano-size particles. This film can be converted in a dense CIS layer through post-deposition annealing steps.

Soda-lime glass substrates were used in this work. Mo contact layers were deposited on the soda-lime glass substrates by D.C. magnetron sputtering. CIS films were grown on the Mo surface by the non-vacuum technique. Solar cell fabrication steps included deposition of a thin CdS layer by the commonly used chemical bath deposition approach. A ZnO layer was then deposited on the CdS surface using a MOCVD method. Solar cells of 0.09-1.00 cm^2 area were defined on the substrates using photolithographic techniques. Modules were also fabricated using films of typically 50 cm^2 area.

Single cell fabrication continued during this period, mostly for yield studies rather than efficiency improvement. CIS cells without S and Ga were fabricated with efficiencies ranging from 10%-13%. In this range of efficiencies the main difference between the high and low efficiency cells was the voltage which, through device analysis, could be directly correlated with the carrier densities in the absorbers. The statistical data so far indicates that the efficiencies of the devices fabricated on CIS absorbers will be at best in the 10-13% range. Higher efficiency and tighter yields will require the development of higher bandgap absorbers.

Module integration for devices fabricated by the non-vacuum technique offered unique challenges. In the general module integration approach the Mo layer is first scribed by laser forming isolated Mo pads, and then a CIS layer is grown over the whole substrate. In our non-vacuum approach, however, we determined that the film nucleation on the glass surface was very different from its nucleation on the Mo layer. The SEM of Fig. 3 shows the surface view of a CIS layer deposited near a scribed Mo region. The white line on the SEM indicates the glass/Mo boundary. To the left of this boundary is the glass/CIS structure and to the right is the glass/Mo/CIS region. Clearly, the CIS layer grown directly on the glass surface by the non-vacuum technique is discontinuous and the glass surface is visible through the large nodules of CIS. The adhesion between the CIS nodules and the glass substrate is not good and the portions of the CIS film within the scribed lines peel off, especially during the ZnO deposition. Exposed Mo edges then give rise to low shunt resistance between adjacent devices.

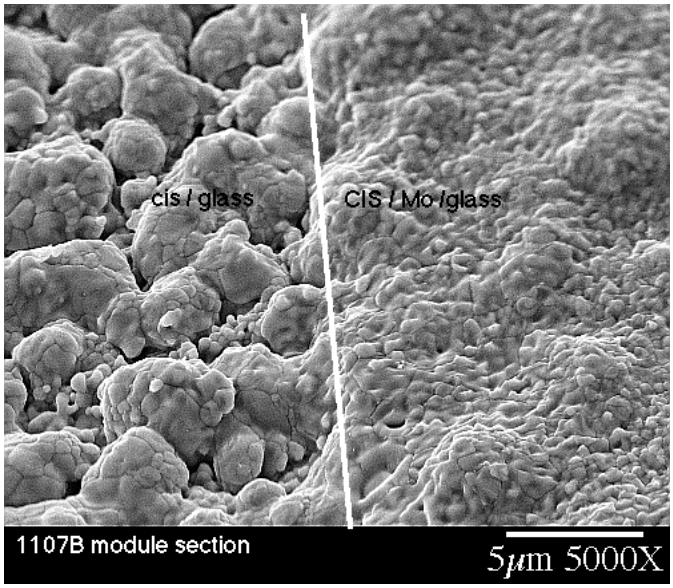

Fig.3 CIS layer grown near a scribed Mo line. Region on the left is the CIS grown on glass surface. Region on the right shows the CIS grown over the Mo layer.

Faced by this challenge ISET has adapted another approach to module integration. In this approach Mo/CIS structure was first formed on the glass substrate and then the scribing step was carried out. Two techniques were evaluated for the isolation of adjacent devices, laser scribing and chemical etching. It was observed that with laser scribing, there is clearly a melted region along both edges of the scribed line. The composition of this melted region was studied by micro probe and was found to be In and Se poor. Heat generated by the laser beam apparently causes preferential evaporation of In and Se species which are known to have low vapor pressure. What is left behind is a Cu-rich region that is relatively conductive. Such a conductive path would cause low shunt resistance in the finished modules once the top ZnO contact is deposited. Photolithography followed by chemical etching was another approach that was evaluated to form isolated devices for module integration. In this case a photoresist process and chemical etching was used to form the isolating grooves in CIS/Mo structures. The grooves were then filled with an insulating material and the devices were interconnected.

We have fabricated many mini-modules of 40-60 cm^2 area using this second approach. The illuminated I-V characteristics of a 74 cm^2 device consisting of 16 cells connected in series is shown in Fig. 4. The efficiency is 7.95%.

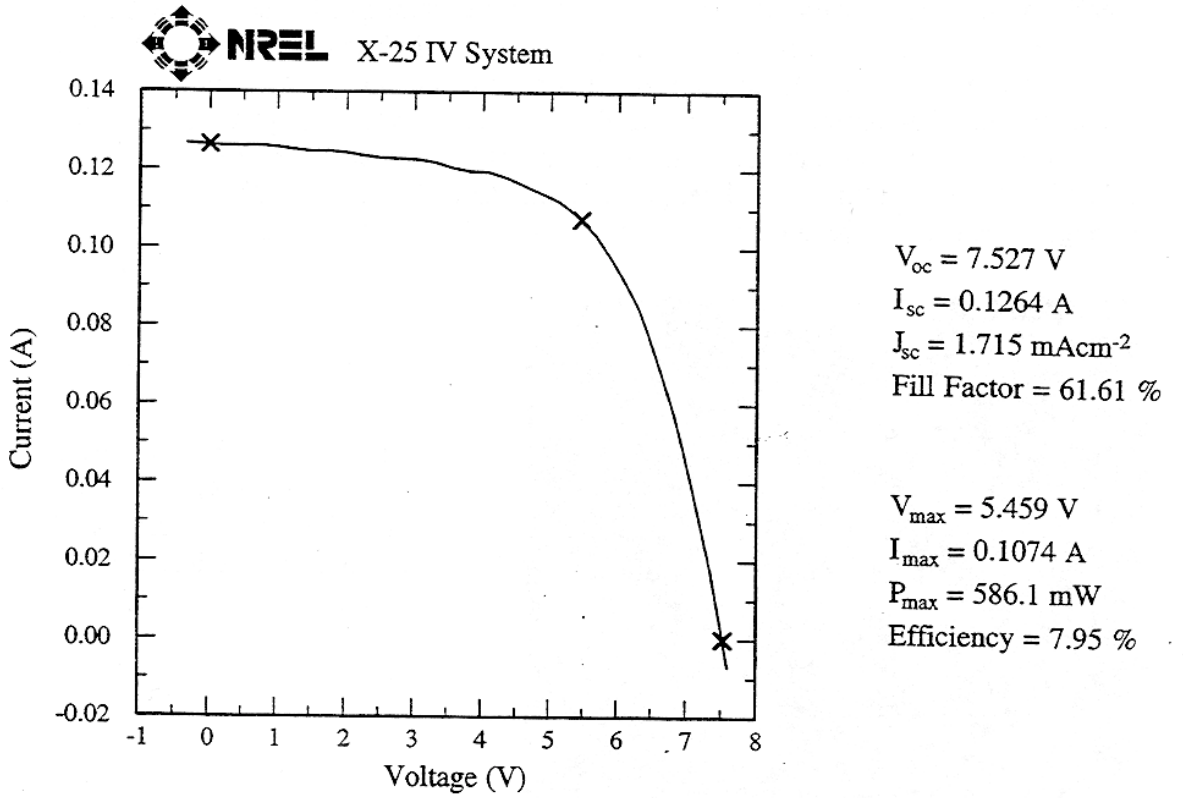

Fig. 4 Illuminated I-V characteristics of a module fabricated on a non-vacuum grown CIS layer.

Conclusions

During this research period ISET has concentrated its efforts on the further development of its novel non-vacuum technique which is based on nano-particle deposition. CIS layers without Ga or S were deposited by this technique to demonstrate up to 13% efficient solar cells. Modules with 40-75 cm~ area were fabricated with efficiencies close to 8%. Problem areas in. module integration were identified.

Acknowledgments

Part of this work has been carried out under National CIS Partnership Program.. The authors are grateful to the members of the working group which included J. Britt of EPV, T. Gillispie of Lockheed Martin, A. Rockett of University of Illinois, J. Sites of CSU; R Matson, A. Swartzlander-Franz, S. Asher and M. Al-Jassim of NREL. We are also thankful to K. Emery of NREL for characterization and measurements of films and devices, and to H. Ullal, R Noufi and K. Zweibel for technical discussions.

Title: **Atmospheric Pressure Chemical Vapor Deposition of CdTe for High Efficiency Thin Film PV Devices**

Organization: ITN Energy Systems, Wheat Ridge, CO

Contributors: Peter V. Meyers, principal investigator; R. Kee[†], C. Wolden[†], L. Raja[†], V. Kaydanov[†], T. Ohno[†], R. Collins[†], A. Fahrenbruch[‡]
† Colorado School of Mines, Golden, CO
‡ALF, Inc., Stanford, CA

Project Objective: Overall objective is improved thin film CdTe PV manufacturing technology with increased power conversion efficiency. Tasks required to accomplish the overall goal are grouped into 1) development of deposition apparatus and procedures which enable control of film growth over large area and 2) development of advanced measurement and analytical procedures which provide useful and effective device characterization.

Approach/Background: CdTe deposition by Atmospheric Pressure Chemical Vapor Deposition (APCVD) employs the same reaction chemistry as has been used to deposit 16% efficient CdTe PV films (Close Spaced Sublimation) but employs forced convection rather than diffusion as a mechanism of mass transport. APCVD enables discovery of fundamental mass transport parameters which, through application of established engineering principles, can be used to design high throughput, high yield manufacturing equipment. Device analysis goes beyond conventional one-dimensional device characterization and analysis toward two dimension measurements and modeling.

Although there are many demonstrated methods for producing high-efficiency CdTe solar cells, large-scale commercial production of thin-film CdTe PV modules has not yet been realized.[1] An important contributor to the commercial production of thin-film CdTe will be development of advanced deposition reactors. Close Spaced Sublimation (CSS) has produced the highest efficiency CdTe PV cells to date.[2,3] APCVD combines proven CSS reaction chemistry with state-of-the-art engineering principles to enable design of thin film deposition reactors for the manufacturing environment. APCVD's anticipated advantages include:

- Low equipment cost compared to vacuum processing because equipment will need neither the structural strength nor the pumping systems of a vacuum chamber.
- Large area uniformity is achieved through control of temperature and gas flow - both of which are subject to rigorous engineering design.
- Process control and source replenishment are simplified because the source gas generation is physically separated from the deposition chamber.
- Process compatibility is attained in that APCVD is presently used commercially to deposit transparent conducting oxide (TCO) films commonly used in CdTe solar cells. In fact, the processing sequence: deposit TCO, deposit CdS, deposit CdTe, dry $CdCl_2$ heat treatment and metalorganic CVD of electrodes could be performed in a single continuous process.
- Raw material costs are low as CdTe is used in its least expensive form - chunks.
- Continuous processing is simplified because gas curtains replace load locks.

Reaction Chemistry CdTe film deposition by CSS or APCVD is a three-step process that involves (i) generation of elemental vapors, (ii) vapor transport, and (iii) condensation and reaction to form CdTe. Congruent sublimation of CdTe occurs through the reaction

$$CdTe + heat \leftrightarrow Cd(g) + \frac{1}{2}Te_2(g). \quad (1)$$

Vapor pressure over solid CdTe in a chemically inert environment depends only on temperature and is described by the Antoine equation

$$log\ [P_{sat}] = 6.823 - 10{,}000/T\ . \quad (2)$$

where T is temperature Kelvin and saturation pressure, P_{sat}, is expressed in atmospheres. In both APCVD and CSS, Cd and Te_2 vapors are transported to a substrate that is maintained at a somewhat lower temperature than the source. At the substrate temperature, the source gas is supersaturated causing Cd and Te_2 vapors to react and form CdTe. The degree of supersaturation and the rate of material delivery to the surface determine deposition rate. Cd and Te_2 can also condense to form their elemental condensed phases, but at all temperatures the elemental vapor pressures of Cd and Te_2 over their respective condensed phases is much higher than either gas over CdTe, thus CdTe is the equilibrium solid phase. In practice, for substrates held above ~500°C and deposition rates ~ 5 μm/min the deposited films are single phase CdTe.

It is emphasized that these reactions depend only on temperature and on the concentrations of the source gases immediately above the superstrate. In particular, the reactions do not depend upon the pressure of inert gases such as N_2, Ar or He. Thus the heterogeneous reaction chemistry, i.e., the set of reactions that take place on the substrate, is the same for CSS, elemental vapor deposition, or APCVD. The primary difference between CSS and APCVD is the mechanism of mass transport.

Mass Transport

Diffusion - Mass transport of the gas source species occurs through a combination of diffusion and convection. Most previous work, including CSS and elemental vapor deposition, has been performed in closed systems where diffusion is the lone transport mechanism. Mass flux due to diffusion is proportional to the product of concentration gradient and diffusion coefficient. In CSS, the concentration gradient is determined by the difference between the equilibrium partial pressures at the source and superstrate and by the physical separation between them.[4] For typical CSS conditions (P = 10-50 torr, source-superstrate spacing of 3-10 mm, and temperature differences of 10-80°C) deposition rates are on the order of 4 μm/min. Use of CSS at atmospheric pressure has been demonstrated, but deposition rates were in the 0.2 μm/min range.[5]

Forced Convection - Mass transport rate can be increased and control improved over that achieved by diffusion alone by using forced convection. Convection processes are critical in APCVD for both generating elemental vapors and for transporting material to the substrate. Vaporization of source material occurs in a packed bed containing CdTe chunks as illustrated in Figure 1. Mass transport from a packed bed is an efficient and well-characterized method of producing source material-laden gases.[6] Flow in packed beds is turbulent, creating high mass transport coefficients. Partial pressure of CdTe vapors, P_{CdTe}, coming out of the source gas generator is given by

$$P_{CdTe}/P_{sat} = (1-\exp\{- h_m * A_{p,t} * \varepsilon /[v_o * A_{c,b}]\}) \quad (3)$$

where P_{sat} is the equilibrium partial pressure at the bed temperature (Eq. 2), $A_{p,t}$ is the total surface area of the particles in the packed bed, $A_{c,b}$ is the cross sectional area of the bed, h_m is the mass transfer coefficient, v_o is the "open velocity" of the gas (i.e., the velocity the gas would have if there were no particles in the bed), and ε is the void fraction of the bed. Calculations for the case of a 10 cm diameter bed packed with ~4 kg of 1 cm diameter particles, maintained at 1000 K (727 °C), and a gas flowrate of 7.6 l/s indicate that the outlet gas will be >99% saturated and the pressure drop will be ~4.5 psi. Source gas of this throughput and saturation level is sufficient to coat a 100 cm^2 superstrate with 10 μm of CdTe in one minute.

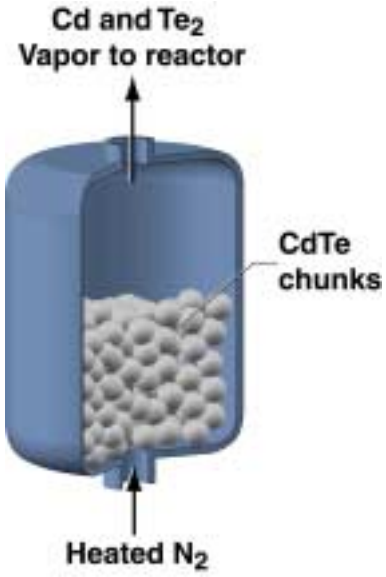

Figure 1 Schematic of the "packed bed" source gas generator

Source gas is convected to the deposition chamber via transport piping. Deposition onto piping walls is retarded by heating them to temperatures above the packed bed temperature.

Status/Accomplishments: During Phase I the APCVD reactor has been designed, all components have been constructed and assembly is nearly complete. Initial device modeling is being performed using AMPS 1-D. Equipment for two-dimensional characterization of films using AC impedance and Near Field Scanning Micro Photoconductivity is in place and initial studies have begun.

Conclusions: Atmospheric Pressure Chemical Vapor Deposition (APCVD) of polycrystalline thin-film CdTe appears to offer several practical advantages over state-of-the-art manufacturing techniques**.**

Planned FY 1999 Milestones:

- Demonstration of device quality CdTe films.
- Demonstration of 12% power conversion efficiency.
- Presentation of two-dimensional methods for characterization and analysis of device operation on a microscopic scale.

Major Articles Published in FY 1998:

P. Meyers, R. Kee, L. Raja, C. Wolden and M. Aire, "Atmospheric Pressure Chemical Vapor Deposition of CdTe – Reactor Design Considerations", NCPV Photovoltaics Program Review; Proceedings of the 15th Conference, Denver, CO, 1998; AIP Conference Proceedings (in press).

[1] P.V. Meyers and R.W. Birkmire, *Prog. in PV:Res. & Appl*., Vol 3 (1995) pp 393-402.

[2] C. Ferekides and J. Britt, *Solar Energy Mat. & Solar Cells* 35 (1994) pp 255-262.

[3] H. Ohyama, T. Aramoto, S. Kumazawa, H. Higuchi, T. Arita, S. Shibutani, T. Nishio, J. Nakajima, M. Tsuhi, A. Hanafusa, T. Hinino, K. Omura, and M. Murozono, "16.0% Efficient Thin-Film Solar Cells", *Proc. 26th PVSC* (1997) pp 343-346.

[4] T.C. Anthony, A.L. Fahrenbruch, and R.H. Bube**,** *J. Vac. Sci. Technol*. A 2 (3), (1984), pp 1296-1302.

[5]K. Mitchell, C. Eberspacher, F. Cohen, J. Avery, G. Duran and W. Bottenberg, "Progress towards high efficiency, thin film CdTe solar cells", *Proc 18th IEEE PVSC* (1985) pp 1359-1364.

[6] C. J. Geankopolis, *Transport Processes and Unit Operations*, 2nd Ed., (Allyn and Bacon, Inc., Boston, 1983) Chapter 7.

Title: **In-Situ Sensors for Process Control of $CuInGaSe_2$ Module Deposition**

Organization: Materials Research Group, Inc.
Wheat Ridge, Colorado

Contributors: I.L. Eisgruber, Principal Investigator; P.K. Bhat, B. Carpenter, J. Engel, R. Hollingsworth, C. Marshall, and T.L. Wangensteen

Introduction

Yield and reproducibility issues remain an important challenge in $CuInGaSe_2$ (CIGS) photovoltaic module fabrication. Although champion cells report impressive efficiencies, reproducing these efficiencies, particularly in large numbers, remains problematic. Materials Research Group, Inc. (MRG) is developing the use of in-situ sensors to improve yield, reproducibility, average efficiency, and prevention of "lost processes". In-situ x-ray fluorescence (XRF) will be used to monitor composition and thickness of deposited layers, and in-situ optical emission spectroscopy (OES) will be used to provide real-time feedback describing the deposition plasma. Characterization techniques will be examined ex-situ in the first two years of the contract, which started February 10, 1998. The characterization techniques will be applied to existing deposition systems in the final year of the contract.

The composition of the CIGS layer is the most critical and sensitive for device performance. Thus, a sensor for the CIGS layer is being investigated during the first year of the contract. XRF signal is being examined ex-situ on CIGS films and all precursor layers. By correlating thickness measurements and XRF signal from Se layers, Cu layers, In layers, and Ga layers of different thicknesses, the constants required to translate XRF peaks into thickness values will be determined.

Research Results

Progress in XRF interpretation on CIGS has advanced in three areas in FY1998. The first area is the development of software allowing interpretation and prediction of XRF signals. This software was written and verified. Second, numerous test samples were fabricated. Third, analysis of XRF measurements on test samples was begun.

To gain an understanding of how a given change in film properties should change XRF signals, MRG has written code that simulates x-ray fluorescence of multi-layer structures. Such an understanding is important to determine implications of various conditions – such as noise in the XRF signals, systematic XRF error (e.g. x-ray tube drift), nonuniformity of the samples as one moves to different spots on the substrate, uncertainty in the compositonal measurements, or differing through-film compositional profiles – for an effective sensor. The equations that predict magnitude of x-ray fluorescence signals from a sample are well-known, although complicated [1]. Therefore, predicting x-ray fluorescence signals from a known sample can be achieved from first principles by computer calculation. The simulation created at MRG can predict the magnitude of primary and secondary fluorescence emission lines from multi-layer samples, where each layer contains multiple elements. The simulation output has been tested against simplified expressions for very thick and very thin films, as well as against data in the literature, to verify its accuracy.

The simulation software has predicted a number of the complexities of interpreting XRF data from CIGS films. For example, Figure 1 shows the calculated effect of varying Ga content in a typical CIGS film on

XRF signal. Varying Ga/(In + Ga) ratio is plotted on the x-axis. On the y-axis, the fraction of emission for each peak, relative to that from a sample with Ga/(In + Ga) = 0.25, is plotted. As expected, Ga signal increases and In signal decreases nearly linearly with Ga addition. Figure 1b is a magnification of the data shown in figure 1a, emphasizing the effects of interaction between elements. Over the range of Ga concentrations shown, the Cu signal increases by 6% even though the number of Cu atoms in the sample is constant. This increase occurs for two reasons. First, the mass absorption coefficient of In (in m^2/mole) is about 6 times greater than that of Ga at the Cu emission wavelength. Thus, replacing In atoms with Ga atoms allows more Cu fluorescence to escape the sample. Second, Cu fluorescence is excited very efficiently by Ga-Kα emission, so as the amount of Ga increases, Cu emission from secondary fluorescence also increases. The Se signal, on the other hand, shows very little change with the addition of Ga, because the mass absorption coefficients of Ga and In are nearly equal at both the incident and the Se emission wavelength. Furthermore, the Se absorption edge is at a higher energy than the Ga emission, so no secondary fluorescence signal enhancement occurs. Variations in back contact thickness and through-film concentration gradients can complicate XRF interpretation in similar manners.

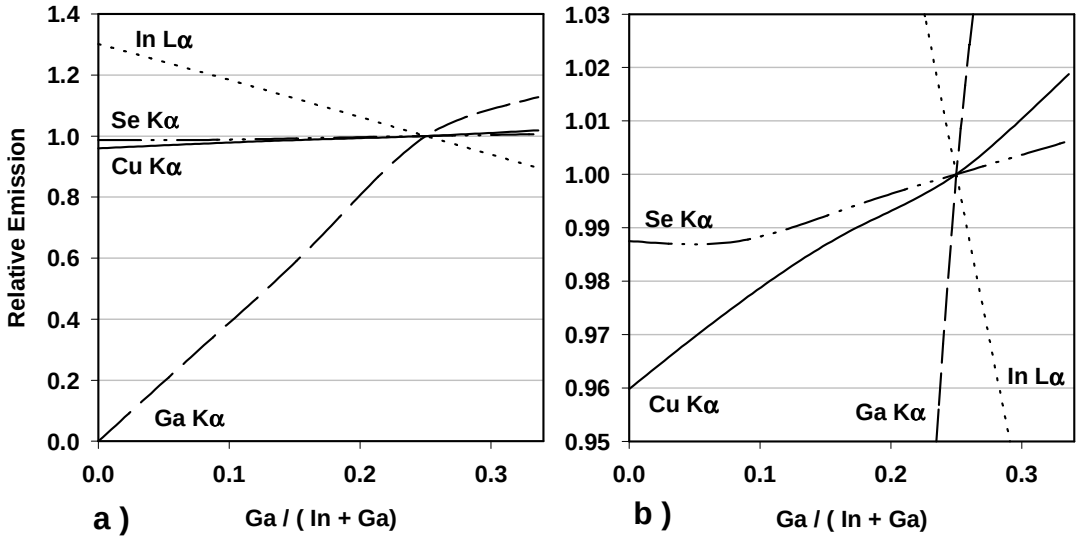

Figure 1: Calculated effect of varying Ga content on XRF Cu-Kα, In-Lα, Ga-Kα, and Se-Kα signals, for a uniform 2.5 μm CIGS film illuminated by 20 keV x-rays. The graph is shown a) over the entire data range, and b) with the y-axis magnified.

A number of XRF test samples were fabricated. These samples were fabricated by special services provider Lockheed Martin Astronautics (LMA) using equipment built by MRG. Required transport speeds as a function of time to allow controlled compositional grading over each 12”x12” LMA substrate were calculated at MRG. Calculations were verified by profilometer measurements on single-element layers. Samples already fabricated include CIGS samples of varying Cu and Ga content, and Cu and In stacks of various thicknesses. Electron probe microanalysis (EPMA) and inductively coupled plasma (ICP) measurements have been performed at the National Renewable Energy Laboratory on selected samples to begin evaluating which type of compositional measurements should be routinely performed on XRF samples.

Analysis of XRF measurements on test samples has begun using ex-situ XRF equipment at LMA. Some results of initial measurements are as predicted. Uncertainty in raw peak counts showed the expected statistical dependency on number of counts. Peaks for the elements of interest were well-resolved in energy and contained many more counts than the background, as shown in figure 2. Use of Nb backing material behind the sample eliminated signals from the sample carrier. Trends observed in XRF signals

versus known film thicknesses are qualitatively as expected. The typical relationships between detector dead time and shifts in apparent peak energies were observed, and x-ray tube current was set appropriately.

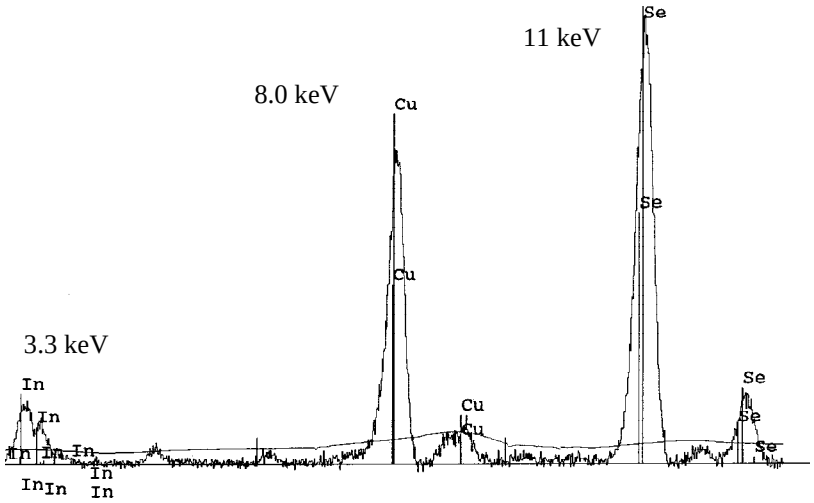

Figure 2: Typical XRF spectrum of CIS sample on Mo/glass substrate.

Other results of the initial measurements require further investigation. For example, a significant amount of Cu was measured in plain glass samples, and in glass\ Mo samples. These measurements were made with clean Nb backing material that shows no evidence of Cu contamination. Since Cu/In+Ga ratio in the CIS film is probably the most critical quantity to be measured with XRF, the presence of this excess Cu is very important. If it is not evenly distributed over all substrates, it could prevent even an accurate *relative* measurement. There are several possibilities for the origin of the Cu. It is possible that either (i) the Cu is very nonuniformly distributed in the glass (ii) the Cu diffuses into the Mo during Mo deposition, (iii) or the Mo target is contaminated with Cu. Experiments are underway to determine the nature of the excess Cu. Second, large variations in Mo signal across a single sample have been measured. The expected magnitude of Mo signal due to measured Mo roughness must be compared with the measured Mo signal variations. If the Mo signal variation is determined to be simply a consequence of Mo roughness, its effect on measured Cu, In, Ga and Se signals secondary fluoresence, must be predicted and included in the CIGS analysis. Third, Cu signals from Cu/Mo/glass samples of varying thickness have not followed the calculated quantitative relationship, although results are qualitatively reasonable. Figure 3 shows the measured and predicted Cu counts as a function of thickness. The open points are the simulated data points, and the filled points are measured. The predicted counts were normalized to match the measured counts for the thickest film on the graph, since a precise determination of the tube intensity and the detector solid angle is very difficult. Experiments are currently being performed to determine the source of the quantitative disagreement, possibly Cu in the substrate, back contact thickness variations, or a detector issue.

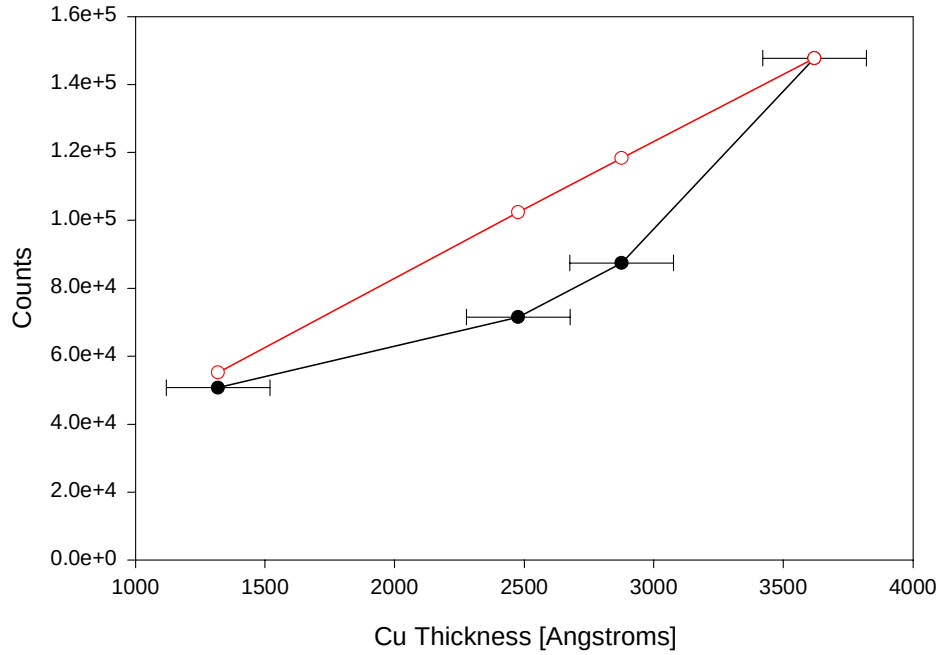

Figure 3: Calculated and measured number of counts for Nb/glass/Mo/Cu samples. Open points are calculated, and filled points are measured.

Conclusions

In summary, progress in ex-situ examination of XRF signal from CIGS films and precursor layers has been made in FY 1998. The goal of this examination is the development of in-situ sensors to improve yield, reproducibility, and average efficiency during the manufacture of CIGS modules. Software allowing interpretation and prediction of XRF signals was written and verified. The simulation software has predicted a number of the complexities of interpreting XRF data from CIGS films. Additionally, numerous test samples were fabricated, and analysis of XRF measurements on these samples has begun. Peak statistics and resolution, as well as qualitative relationships between film thicknesses and XRF signals, behaved as expected. Further investigation is needed regarding Cu detected in glass\ Mo samples, large variations in Mo signal across a single sample, and quantitative disagreement between measured and predicted XRF signals from Cu/Mo/glass samples of varying thickness.

References

1. R. Tertian, F. Claisse, *Principles of Quantitative X-Ray Analysis*, London: Heyden & Son Ltd, 1982, ch. 4, pp-56-64.

Title: **High Efficiency, Stable Hot Wire CVD Prepared Amorphous and Polycrystalline Silicon Film Solar Cells**

Organization: MVSystems, Inc., 17301 West Colfax Avenue, Unit 305, Golden, CO 80401

Contributors: Arun Madan, J. Xi, D. Arendall, A. Bakhtin, K. Coates, G. Jones, S. Morrison, and E. Valentich

Objectives

The overall objectives of this R&D contract is to develop a high quality amorphous(a-) and micro-crystalline (μc-) Si-based thin film alloy materials by the "Hot Wire" Chemical Vapor Deposition (HWCVD) technique, with the goal, at the end of the three year program, to demonstrate and deliver 12% stable a-Si-based devices and 10% μc-Si based devices. The interim goal for the first year (Phase I) is to build, test, and finalize a HWCVD and plasma enhanced chemical vapor deposition (PECVD) apparatus, and to establish a "baseline" for a-Si and μc-Si based alloy materials and PV devices.

Accomplishments

During FY1998 (contract commenced in April 1998), we have made a significant progress in building and upgrading existing equipment to support the material and device research; in parallel, we have made a significant inroad into fulfilling the research tasks concerned with material and device development.

The accomplishments can be summarized as,

1: We have successfully developed a new HWCVD deposition technique, which overcomes the problems encountered in the conventional technique, namely a very short lifetime of the the filaments, poor reproducibility of the deposited films due to the sagging of such filaments. To date, the new filament design has deposited in excess of 100um of a-Si material; we believe its logevity could be extended much beyond this level. Hence, this potentially provides an opportunity for large area commercialization of this promising approach.

2: We have established "device quality" intrinsic a-Si films by our new proprietary HWCVD technique, and have successfully incorporated this material into a Schottky barrier diode structure. Further, our preliminary results on intrinsic μc-Si films reveal the electronic transport properties to be reasonably good.

Following is a brief summary of the tasks accomplished in the breif time of our involvement with this program.

A. Equipment development:

1: Developed and tested an innovative new HWCVD technique.

2: Built a thermal evaporation system for supporting the material and device fabrication effort.

3: Rebuilt a RF and DC magnetron sputtering system for supporting the material and device fabrication effort.

4. Built a residual gas analyzer for leak detection and for in-situ analysis of gas species.

5. Built an integrated device and material characterization system enabling measurements of light and dark J-V in devices, their spectra response and temperature-dependent conductivity.

All of the above tasks have been completed, except item 5 which is almost complete.

B. Materials and device research:

1: Intrinsic a-Si films by the new HWCVD technique.

We have reproducibly fabricated "high quality "intrinsic a-Si films, at a deposition rate of about 5 Å/sec. Table 1, shows the comparison of these films with those of the PECVD produced samples.

Table 1. Typical properties of the intrinsic a-Si films prepared using the PECVD and HWCVD techniques.

Deposition Method	Dark Conductivity $(\Omega\cdot cm)^{-1}$	Photo Conductivity $(\Omega\cdot cm)^{-1}$	Gamma
PECVD	$5x10^{-10}$	$8x10^{-5}$	0.95
HWCVD	$1.2x10^{-10}$	$1.3x10^{-5}$	0.91

In the above, gamma is derived from, $\ln(\sigma_{ph}) \propto \gamma \cdot \ln(F)$, where F is the intensity of illumination and σ_{ph} is the photo-conductivity; it is known, that the recombination kinetics are dictated by the density of defect states (DOS) and that the value of γ is linked to it. Although a γ value above 0.9 indicates low DOS, it seems that the HWCVD sample may possess higher DOS as the photo-conductivity is lower and the gamma value shows a slight decrease in comparison with the PECVD samples.

2: Doped (p+ and n+) a-Si films.

The new technique is able to dope the samples well. p- and n-type a-Si films have been produced with the addition of B_2H_6 and PH_3 as the doping gas respectively. Table 2 lists the conductivity and the activation energy values; it should be noted that the p-type films exhibit properties which are similar to the "low band gap" p+ layers prepared by the PECVD technique.

Table 2. Typical properties of HWCVD prepared p+ and n+ type films.

Type	Dopant Gas	Dark Conductivity(1/Ohm*cm)	Ea (eV)
n	Phosphine	1.30E-03	0.32
p	Diborane	1.50E-05	0.46

3: Intrinsic μc-Si films.

We have made a brief effort to produce intrinsic micro-crystalline silicon films by using a hydrogen dilution ratio of about 10 in silane gas. Figure 1 shows the X-ray diffraction data and we note a 220 orientation and an average crystal size of about 390 Å. This film showed a dark conductivity of 2.7 X 10^{-6} $(Ohm*cm)^{-1}$. By applying the photo-mixing technique, University of California at Los Angles, have measured the carrier mobility as 3.22 cm^2/vs and lifetime as 783ns, (hence $\mu\tau = 2.5x10^{-6}$ cm^2/v), which is interestingly high.

4: Schottky barrier device with PECVD and HWCVD deposited intrinsic a-Si layer.

We have successfully produced Schottky barier (SB) devices which is used as a basic diagnostic device structure. Table 5 compares the performance of the SB with i-layer fabricated using the PECVD and the HWCVD technique.

Table 5: Comparison of a Schottky Barrier Device with i-layer fabricated using the PECVD and HWCVD technique.

Sample #	803	809
Composition	SnO2/n/i/Pd (all PECVD)	SnO2/n/i/Pd (HWCVD i-layer)
White Response		
Voc (mV)	415	375
Jsc (mA/cm^ 2)	12.7	10.7
FF	0.66	0.53
Red Response		
Voc (mV)	370	315
Jsc (uA/cm^ 2)	1250	1190
FF(Red)	0.67	0.64
Blue Response		
Voc (mV)	335	270
Jsc (uA/cm^ 2)	313	256
FF (Blue)	0.66	0.61
Diode Quality Factor	1.34	1.7
Barrier Height (eV)	1	0.94

These results suggest that the DOS may be higher in the HWCVD material and supported by the material results discussed earlier. Further improvement in material and device fabrication is required.

5. Solar cell p-i-n type device using HWCVD intrinsic a-Si layer.

It is recognized that the most viable device structure would be a p/i/n or an n/i/p device structure. To this end, we are in the process of laying the foundations such that these types of devices could be fabricated, in the near future, with all of the layers fabricated using the new HWCVD technique.

Acknowledgement

We thank Dr.'s A. Rohatgi (Georgia Tech University), C. Taylor, (University of Utah), D. Williamson (Colorado School of Mines), R. Braunstein (University of California at Los Angeles), D. Myers (NREL) for their assistance in evaluating the samples produced at MVSystems Inc..

This work was supported by NREL (subcontract:ZAK-8-17619-16) under The Thin Film Partnership Program.

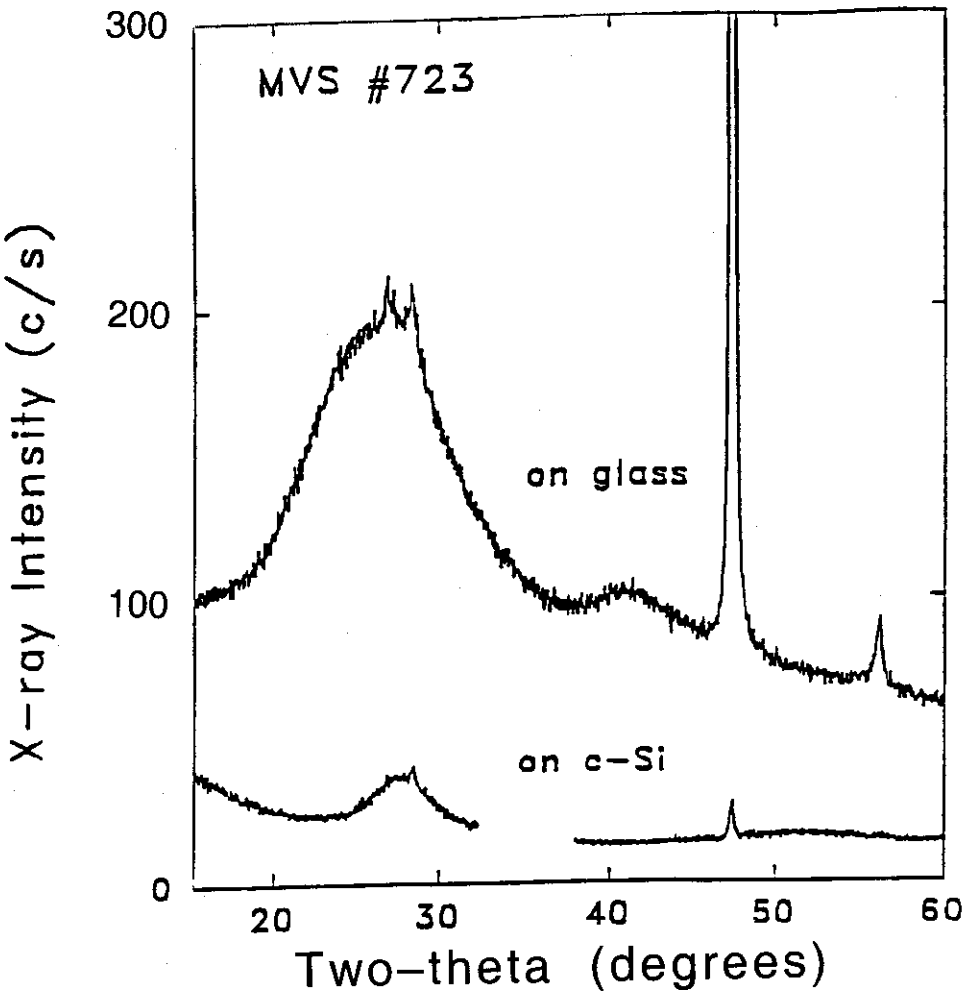

Fig. 1: XRD of HWCVD μc-Si on glass and crystalline silicon substrates

Title: **Atomic Scale Characterization of Hydrogenated Amorphous Silicon Films and Devices**

Organization: National Institute of Standards and Technology (KIST)
Boulder, Colorado

Contributors: A. Gallagher, principal investigator, M. Childs, K. Rozsa, and S. Barzen

Objective

The overall objective is to assist the development of a cost-effective hydrogenated amorphous silicon (a Si:H) photovoltaic (PV) technology. There are two trusts to this effort: (1) improving understanding of the film growth mechanisms that limit the efficiency of current PV devices, and devising ways to overcome these limitations, and (2) studying the internal electrical characteristics of thin-film PV cells.

Technical Approach and Results

Particulate incorporation into a-Si*H films

Obtaining high quality a-Si:H PV cells by deposition from a silane discharge requires relatively low deposition rates, and this is an important limitation to the throughput of a production line. We have shown that silicon particles grow and accumulate in the plasma, particularly at higher pressures and powers. We also observe that a significant number of the smaller particles escape the plasma and incorporate into the growing film [1]. It appears likely that these particles are causing the limitation in deposition rate, and that film quality at lower deposition rates is also effected by particle incorporation. To devise methods to mitigate this particle incorporation into films, we are studying particle growth and behavior in the plasma, as well as particle removal techniques.

Negative molecular ions SiH_n^- form in the plasma, and are suspended there by the discharge-sheath electric field. Due to collisions with radicals and positive ions, they grow into $Si_xH_n^-$ ions of increasing size, or silicon number (x). When x exceeds perhaps 50, the Si are believed to be cross linked, producing a "particle" of ~0.6 run radius (R_p) with approximately the same internal properties as the growing a-Si:H film. Similarly to the film, the particle surface is H passivated and it does not react with stable gases such as SiH_4. Again similarly to the film, it grows by the addition of Si atoms from radicals, primarily SiH_3, and ions, primarily SiH_3^+. During this growth in particle size, or x, particles usually remain negatively charged due to electron collisions. However, a fraction become neutralized for small time intervals, allowing a small fraction of the particles to escape to the electrodes and incorporate into the film. This produces a competition between growth and escape, such that the number and size of suspended particles is a very sensitive function of the discharge power and pressure, and the electrode gap. The data presented in our previous reports clearly demonstrates this sensitivity for the particles suspended in the

plasma. We expect the size and quantity of particles in the film to be an equivalently sensitive function of these discharge parameters, but we have not yet established this experimentally. However, we have developed a quantitative model that predicts the particle growth rate, the size and density of particles suspended in the plasma, and their rate of escape into the film. By comparing to our measurements of suspended particles, we largely verify the model, including its predictions for particle escape and incorporation into the film.

We will first review the measurements of particles suspended in the plasma; these have been completed this year for discharges in pure SiH_4. The most direct way to detect particle growth and behavior in the plasma is by light scattering, so we use this method to investigate particle behavior versus discharge and deposition parameters. Particles with 2nm $<R_p<$8 nm have been observed in films [1], so we would like to study this range of suspended particle sizes. However, light scattering by small particles is proportional to $n_p R_p^6$, where np is the particle density and R_p the radius, and due to the R_p^6 factor we can only observe $R_p > 4$ nm particles. Thus, we study 4nm $< R_P <$ 25 nm suspended particles. It is necessary to establish R_p by a separate technique, and we utilize a measurement of the time (τ) of particle diffusion to surfaces in the discharge afterglow, where $\tau \propto R_p^2$. The discharge is turned on for varying times to establish R_p versus discharge operating time (τ). The data shows that, for lower pressures and powers R_p grows linearly with t, except for a slightly accelerated initial growth up to 2 run. Our growth model quantitatively fits this measured growth rate, for a range of discharge conditions. It finds that this particle growth is almost entirely due to consecutive attachments of Si from SiH_3 collisions with the negatively charged particles. For higher pressures and powers, the measured particle growth rate somewhat exceeds that calculated as due to SiH_3 collisions, implying that heavier radicals begin to play a significant role. These radicals result from radical-radical collisions and buildup of Si_2H_6 in the gas. (This also implies that a significantly different radical mix produces the film for these plasma conditions.)

With increasing discharge time t, the increase in R_p is accompanied by a major decrease in n_p, implying that particles are disappearing from the plasma region. We have shown, theoretically, that this decrease in n_p is not due to the agglomeration of particles, so the only feasible explanation is particle loss from the plasma region between the electrodes. This is, of course, consistent with our STM observations of particle incorporation into the a-Si:H film. We have also studied the spatial distribution of particles in the afterglow, to see if this corresponds to particles sticking to both electrodes, or only the lower electrode. The unfortunate result is that these small particles stick to both electrodes with an equal and large probability. Gravity plays a very minor role in the motion of these particles, so this is not be surprising. However, we also find that thermophoresis plays a major role in the motion of these small particles, driving them towards the cooler electrode. While we have not yet made quantitative measurements or developed a quantitative model for how this operates during the active discharge, it is apparent that this is one of the most promising approaches to preventing particles from incorporating into films. Since the a-Si:H substrate is typically at ~220C during device production, it is relatively easy to cool the lower, rf electrode to a lower temperature. However, this is not done in most or all production facilities, and the effect of such particle mitigation on device properties remains to be seen.

Other aspects of the spatial distribution of particles within the operating rf plasma are also interesting. Particles reside in the neutral plasma region, which typically fills the central 1/3 of the gap between the electrodes. Also, without gas flow the observed (r_p=4-25nm) particles reside everywhere above the rf electrode, but the density is considerably higher near the edges of the electrodes. As particle size increases, this tendency becomes stronger, and when gas flow is added, this higher density occurs near the downstream edge of the rf electrode, particularly near the electrode corners. This tendency of larger (R_p > 20 rim.) particles to reside near the electrode edges probably explains the absence of such particles in the films studied by STM in Ref. 1. However, another possible explanation is suggested by our model, which shows that larger particles have a lower probability of being occasionally neutralized, and this decreases their escape to the film. It is important to recognize that small particles are continually being formed and are escaping to the electrodes. These are not visible in the experiment, because they scatter less light than the large particles, but they are the primary cause of particle incorporation into films. We therefore depend on the model to predict the behavior of these smaller particles, while checking the validity of the model with observations of the larger particles.

We will now briefly describe the model for particle growth and escape from the rf, a-Si:H deposition plasma. This has been developed this year, and tested against the measurements described above. The model initiates particles from the SiH_3 and SiH_3^- radicals that result from electron collisions with SiH_4. Due to radical and ion (mostly SiH_3^+) collisions these radicals grow into Si_xH_n and $Si_xH_n^-$ molecules, and as x increases these molecules take on the character of a-Si:H particles, with most of the Si atoms bonded to each other. It is convenient to label all of these molecules as "particles" containing x Si atoms. For each x value the ratio of charged to uncharged particles depends on the rate of electron versus +ion attachment, and these rates depend on the electron (n_c) and ion (n_+) densities. These densities, as well as the SiH3 density, are established self-consistently from the film growth rate and charged-specie conservation arguments. For each x value, a fraction (f_x) of particles are neutral, and these neutral particles diffuse toward the electrodes at an x-dependent rate (D_x). This loss rate competes with growth due to radical attachment (rate G_x), yielding $n_p(x)$ that is a gradually decreasing function of x. D_x is proportional to R_p^{-2} or $x^{-2/3}$, while G_x varies as R_p^2 or $x^{2/3}$ and f_x decreases slowly with increasing x. Thus, the fraction of particles lost per $x \rightarrow x+1$ growth step, f_xD_x/G_x, is a rapidly decreasing function of x. This means that small particles are lost much more frequently than large particles. In addition, the density of large-x particles is very sensitive to the plasma conditions, because the small loss that occurs for each growth step occurs repeatedly. (A R_p=3.6 nm particle, which is typical of those measured in the films [l], corresponds to $x=10^4$; the result of 10^4 growth steps.) For example, doubling the film growth rate (G_{film}) doubles G_x, and this typically produces ~10^4 higher density of R_p=5 nm particles. A similar change results from increasing the electrode gap by $\sqrt{2}$.

An example of the model prediction for the steady state distribution of particles without gas flow is shown in Fig. 1. Here the density of particles ($Si_xH_n^q$) is plotted versus x and the charge q on the particle, up to $x=10^4$ or R_p=3.6 nm. The solid line labeled q=0 refers to neutral radicals as well as neutral particles, but not stable silane gases. The line labeled "Total" is the sum over all particle charges, and $f_x=n_p(q=0)/n_p(\text{Total})$. Note that as x increases, particles of increasing

negative charge occur and f_x slowly decreases. This total density of size x particles is converted to the density per nm range of R_p in the top (dashed) curve; this is closely related to the measurements described above. The circles labeled "Escape" are the rate of particle escape to the electrodes, per unit volume of neutral plasma. region. To put this on the same graph as the densities, this rate is in units of 10^6 particles/cm^3s. The x=1 value represents the SiH_3 transport to the film, which is largely responsible for the 0.2 nm/s film growth rate. The distribution of particles escaping to the film falls rapidly with increasing x, but it must be integrated over x to obtain the entire number. As an example, ~10^9 particles/cm^2s with $R_p \geq^2$ nm escape to the substrate, and these deposit ~$4x10^{12}$/cm^2s Si atoms. This is ~0.4 % of the total deposition of 10^{15}/cm^2s. This is consistent with the particle density observed in the experiment described above, as well as with the particle densities deposited into the film, as reported in Ref. 1.

The structure of these particles should be similar to that of the film, but it is very likely that the interface between particles and film is not well structured. The radicals and ions which ordinarily produce the film structure within the top few monolayers can not easily reach below particles that have just stuck to the film, and Si atoms at this film-particle interface are not as free to coordinate their locations and bonds, as occurs at the film surface. The density of these particle-surface states far exceeds the defect density in a-Si:H films, so this is a very serious film quality issue.

Conclusions

We have completed analysis of our measurements of the growth of Si particles in a silane plasma, for a range of discharge conditions. This has provided sufficient understanding of particle growth and transport to allow us to develop a quantitative model that takes into account all of the reactions between radicals, ions and particles. This model provides a detailed understanding of the growth mechanisms and the transport of neutral particles to the film. In large part, the major particle transport to the film results from a relatively high ratio ("50) of +ion/electron densities in the plasma, as this causes a relatively large fraction of particles to be neutral and thereby capable of escaping the plasma.

1) D.N. Tanenbaum, A.L. Laracuente, and A.Gallagher, Appl. Phys. Lett. **68**,1705 (1996)

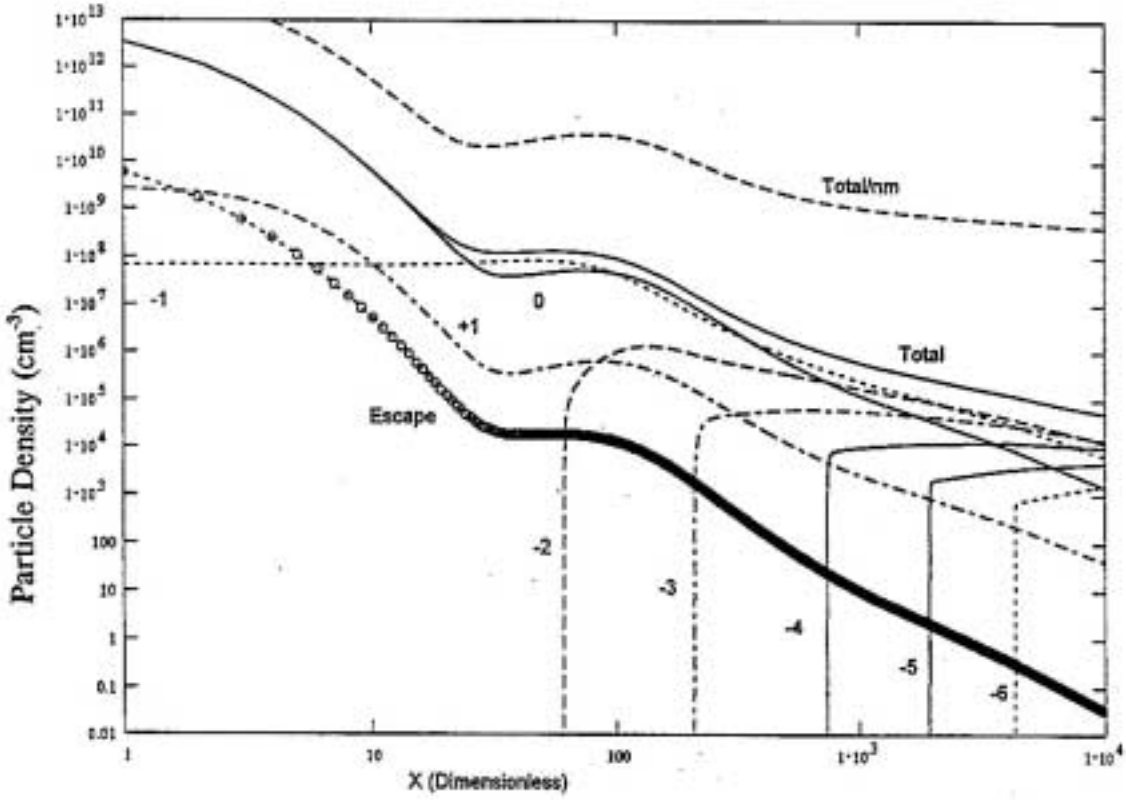

Fig. 1. Calculated particle densities versus number of Si atoms (x) in the particle, for an rf discharge in 0.3 Torr of SiH_4, with a film deposition rate of 0.2 nm/s and an electrode gap of 1.3 cm. The circles indicate the rate of particle escape from the discharge to the electrodes, in units of 10^6 $cm^{-3}s^{-1}$.

Titles: **Wide-Band-Gap Solar Cells with High Stabilized Performance;**

Stable a-Si:H Based Multijunction Solar Cells with Guidance from Real Time Optics

Organization: The Pennsylvania State University, University Park, PA;
Center for Thin Film Devices.

Contributors: C.R. Wronski and R.W. Collins, Principal Investigators;
Hiroyuki Fujiwara, Lihong Jiao, Joohyun Koh, Yeeheng Lee, Andre S. Ferlauto, Randy J. Koval, Zhou Lu, Xinwei Niu, Pablo I. Rovira

Introduction and Overview

In order to optimize amorphous silicon (a-Si:H) and microcrystalline silicon (μc-Si:H) component layers for use in a-Si:H-based single and multijunction solar cells, multistep processes are often required to control the evolutionary development of film properties with thickness. Thus, real time optical measurements are important because they provide the microstructural evolution and optical properties continuously as a function of film thickness. This allows one to design multistep processes based on an in-depth understanding of deposition, rather than on trial-and-error experimentation. In this report, we highlight the latest advances in the application of real time optics to the optimization of a-Si:H based solar cells.

Optimization of a-Si:H i-Layers for Solar Cells

Figure 1 depicts a phase diagram that identifies the amorphous–to-microcrystalline (a→μc) transition continuously as a function of H_2-dilution gas flow ratio R=[H_2]/[SiH_4] and bulk layer thickness d_b for Si film growth on a-Si:H substrate films, the latter prepared with R=0. This diagram was deduced from real time spectroscopic ellipsometry (RTSE) studies that identify the critical thickness at which the a→μc transition occurs for a given substrate and set of deposition conditions [1]. The phase diagram is relevant for the optimization of the i-layers of p-i-n and n-i-p solar cells since the substrate layer in all such cases is an amorphous film. In particular, the phase diagram shows that for a 4000 Å thick layer, typical of the bulk i-layer in a solar cell, R must be less than 15 in order to ensure the amorphous phase throughout growth. In contrast, for a 200 Å layer, typical of an interface buffer layer in a solar cell, R must be less than 50. In our research, we have demonstrated that the optimum solar cell fabrication process is one that is maintained on the amorphous side of the a→μc boundary, but as close as possible to this boundary *versus thickness* [1]. The bold vertical lines in Fig. 1 denote such an optimized two step i-layer process that leads to high performance, high stability p-i-n cells.

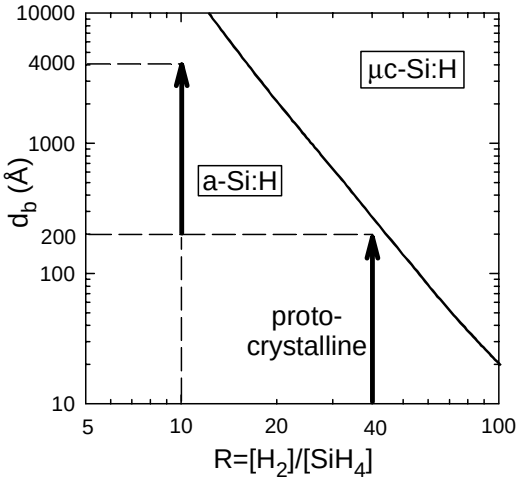

FIG. 1 Phase diagram for the preparation of Si films at 200°C on a-Si:H (R=0) substrates vs. H_2 dilution ratio R and bulk thickness d_b. The bold lines depict an optimized two step i-layer process.

In the so-called "protocrystalline" regime in Fig. 1, the Si film grows initially as a-Si:H, but after a critical bulk layer thickness, crystallites nucleate and then μc-Si:H develops. The fact that p-i-n solar cells are optimized with an initial i-layer step in the protocrystalline regime suggests that the a-Si:H films

prepared in this regime are of high electronic quality. The thinness of these films, however, precludes conventional ex situ characterization. We have fit the dielectric functions $\varepsilon=\varepsilon_1+i\varepsilon_2$ of the a-Si:H obtained in real time just prior to the a→μc transition using a Kramers-Kronig (K-K) consistent model in which ε_2 is expressed as a product of the Tauc Law and a Lorentz oscillator. Figure 2 shows the oscillator linewidth and Tauc optical gap at 200°C for films prepared vs. R. With increasing R, films of decreasing thickness are probed in order to remain within the protocrystalline regime. From the figure, it is clear that the linewidth decreases and the gap increases monotonically with R. Because the linewidth scales inversely with the excited state lifetime τ for electronic transitions well into the bands, then the increase in τ with R suggests increasing order in the protocrystalline films. The increasing order can give rise to improved solar cell performance and stability.

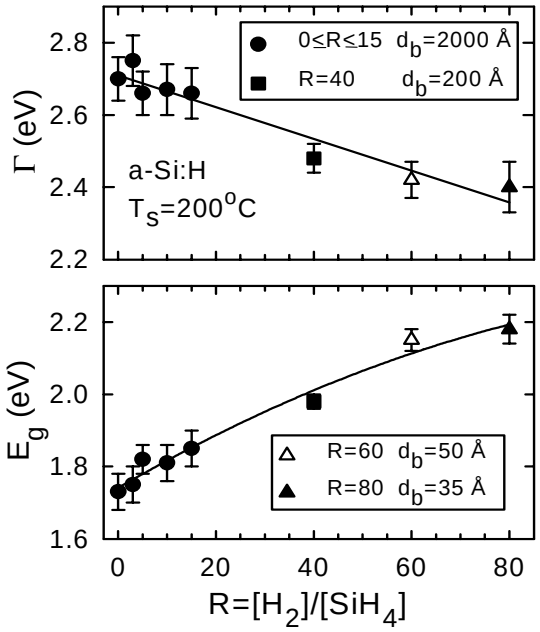

FIG. 2 Best fit Lorentzian linewidth and Tauc gap at 200°C that describe the optical properties of a-Si:H films as a function of the H_2-dilution ratio R. For increasing R greater than 15, decreasing thicknesses are characterized in order to remain within the amorphous growth regime.

Real Time Optics of Solar Cells on Textured SnO_2 Surfaces

RTSE studies performed before 1998 utilized rotating polarizer multichannel ellipsometry [2]. Such an approach is unsuitable for characterizing textured surfaces owing to the scattering and non-uniformity that lead to depolarization of the incident polarized beam upon reflection. A rotating polarizer instrument erroneously interprets a randomly polarized component superimposed on linear polarization, for example, as elliptical polarization. In contrast, recently developed rotating compensator multichannel ellipsometry allows one to analyze the polarized and unpolarized components of the beam separately [3]. Thus, it provides not only (ψ, Δ) versus photon energy and time, which characterize the polarization change induced by the sample, but also the degree of polarization p. The rotating compensator instrument has also been developed with the capability of determining the reflectance spectrum [4]. As a result, the spectra in (ψ, Δ) can be analyzed to determine the microscopic structure of the film stack at a given time during the growth process, whereas the deviation of the measured reflectance spectrum from that predicted theoretically from the analysis of (ψ, Δ) can be applied to characterize the integrated scattering and the macroscopic structure at any given time.

This approach can be demonstrated through an analysis of Asahi U-type textured SnO_2 on glass. Figure 3 shows spectra in (ψ, Δ) and the reflectance for the bare textured SnO_2. Analysis of the (ψ, Δ) spectra yields the SnO_2 film microstructure and optical properties at room temperature before heating as shown in Fig. 4. The best fit microscopic model of the textured SnO_2 consists of three layers. The first layer simulates a low density region at the interface to the glass, the second describes the bulk region, and the third top-most layer describes the microscopically rough surface. The best fit K-K consistent model for the dielectric function of Fig. 4 uses a sum of Tauc-Lorentz and Drude expressions for ε_2. In Fig. 4, the minimum value of ε_2 near 2.5 eV is 0.02, corresponding to an absorption coefficient α of ~1×10^3 cm^{-1}. This is near the sensitivity limit of RTSE. Higher accuracy in α for $\alpha<10^3$ cm^{-1} is expected using transmission measurements with index matching fluid at the surface to avoid scattering.

The microstructure and optical properties from Fig. 4 yield the fit to the (ψ, Δ) spectra in Fig. 3 given by the solid lines. An analysis of the reflectance in Fig. 3 starts with the microscopic optical model of Fig. 4; however, such a model leads to a reflectance spectrum that exceeds the experimental one by

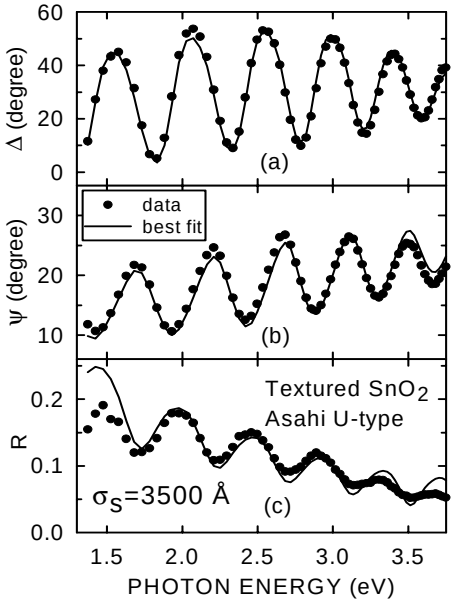

FIG. 3 (a) Δ, (b) ψ, and (c) the reflectance spectra for Asahi U-type textured SnO_2. The fits to (ψ, Δ) (solid lines) are obtained using the microscopic structural model of Fig. 4. The fit to the reflectance employs in addition a macroscopic roughness distribution with a width of 3500 Å.

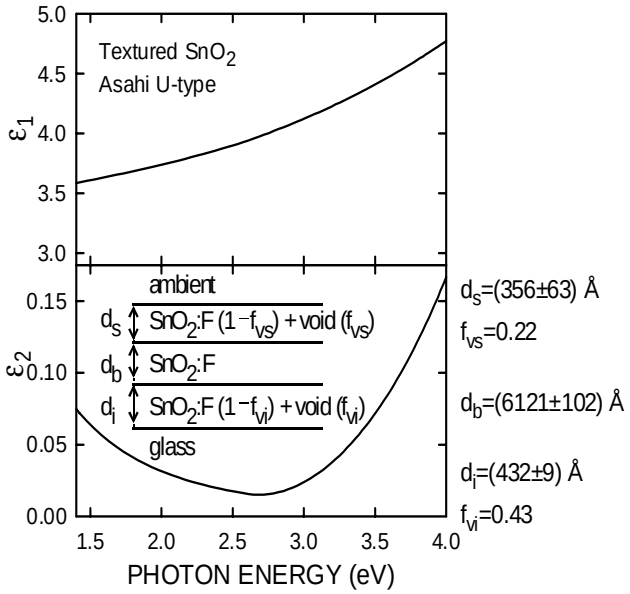

FIG. 4 The best fit dielectric function for the bulk layer of Asahi U-type textured SnO_2 at 25°C using Tauc-Lorentz bound electronic and Drude free electronic contributions. The inset shows the microscopic structural model for the SnO_2, along with the best fit structural parameters (right).

0.2-0.3, owing to the fact that losses by scattering are not included in the model of Fig. 4. By adding a macroscopic roughness distribution having a Lorentzian surface profile $w(z) = \sigma_S[\pi(z^2+\sigma_S^2)]^{-1}$, where z is the distance of the surface from the plane that describes the mean surface level and σ_S is the width of the distribution, then an excellent fit (solid line) to the measured reflectance can be obtained for σ_S = 3500 Å. Thus, an optical model for the Asahi U-type SnO_2 includes the microscopic structure of Fig. 4 with a macroscopic modulation of the top two interfaces having a width of 3500 Å.

Such surface structure makes it very difficult to analyze ellipsometric spectra collected during the growth of a p-i-n cell on the SnO_2. Figure 5 shows the evolution of the effective thickness d_{eff} for a p-layer growth process. d_{eff} is deduced using a two layer model consisting of (i) an interface roughness layer formed from the surface roughness on the SnO_2 and (ii) an overlying a-$Si_{1-x}C_x$:H roughness layer. No bulk-like a-$Si_{1-x}C_x$:H layer forms because the microscopic roughness on the SnO_2 substrate film is thicker than the final p-layer. The three parameters determined versus time include the volume fraction f_i of a-$Si_{1-x}C_x$:H that penetrates the d_i=360 Å thick microscopic modulations on the SnO_2 surface, and the roughness layer

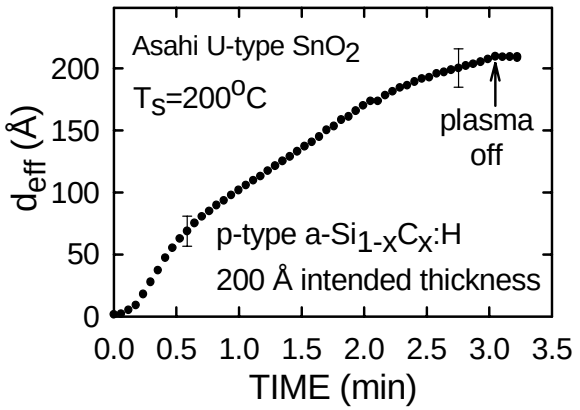

FIG. 5 RTSE analysis results for the evolution of the effective thickness during the growth of an intended 200 Å a-$Si_{1-x}C_x$:H:B at 200°C on the Asahi U-type textured SnO_2 film of Figs. 3 and 4.

thickness d_s and volume fraction of free space f_{vs} in the evolving roughness associated with the a-$Si_{1-x}C_x$:H film. Thus, the effective thickness of the growing a-$Si_{1-x}C_x$:H film at any given time is given by $d_{eff} = d_i f_i + (1-f_{vs})d_s$. The deposition time was chosen in Fig. 5 to yield a d_{eff} value of 200 Å, based on the bulk layer deposition rate obtained in an identical p-layer deposition on c-Si. The result for the final d_{eff} value of 209 Å from the analysis of p-layer growth on textured SnO_2 is in excellent agreement with the expected value.

Summary and Future Directions

We have described recent progress in real time optical analysis of the growth of a-Si:H and µc-Si:H films for optimized solar cells.
(1) A phase diagram for Si:H film growth has been developed that describes the regimes of H_2 dilution ratio and thickness leading to a-Si:H and µc-Si:H films. It has been proposed that the optimum i-layer materials for a-Si:H solar cells are prepared in such a way as to maintain the deposition as close as possible to the a→µc boundary *vs. thickness* while remaining on the amorphous side. In this regime, the growing a-Si:H appears to exhibit improved ordering as indicated by a longer lifetime for band-to-band electronic transitions. The concept of the phase diagram will be expanded in the future to direct optimum deposition of individual doped layers and tunnel junction layers of single and multijunction devices.
(2) Instrumentation and analysis procedures been developed to characterize the evolution of the microscopic and macroscopic surface structure during the growth of solar cells on textured substrates. The procedures have been applied to Asahi U-type SnO_2, and to a-$Si_{1-x}C_x$:H p-layer growth on the SnO_2. Remarkably, the evolution of the effective thickness during p-layer growth has been obtained with better than 5% accuracy in the presence of 360 Å of microscopic roughness and 3500 Å of macroscopic roughness. The latter capability will assist in the design of µc-Si:H p-layers on textured SnO_2.

References

1. J. Koh, et al., Appl. Phys. Lett. 73, 1526 (1998).
2. R.W. Collins, et al., Thin Solid Films 313-314, 18 (1998).
3. J.C. Lee, P.I. Rovira, I. An, and R.W. Collins, Rev. Sci. Instrum. 69, 1800 (1998).
4. P.I. Rovira and R.W. Collins, J. Appl. Phys. (in press, 15 February 1999).

Selected Bibliography of Recent Papers

J. Koh, et al., "Nucleation of p-Type µc-Si:H on a-Si:H for n-i-p Solar Cells Using $B(CH_3)_3$ and BF_3 Dopant Source Gases", Mater. Res. Soc. Symp. Proc. 507 (1998).

J. Koh, et al., "Real Time Spectroscopic Ellipsometry for Characterization and Optimization of a-Si:H-Based Solar Cell Structures", Thin Solid Films 313-314, 469 (1998).

J. Koh et al., "Microstructural Evolution of a-Si:H Prepared using Hydrogen Dilution of Silane Studied by Real Time Spectroellipsometry", J. Non-Cryst. Solids 227-230, 73 (1998).

H. Fujiwara, et al., "Optical Depth Profiling of Band Gap Engineered Interfaces in Amorphous Silicon Solar Cells at Monolayer Resolution", Appl. Phys. Lett. 72, 2993 (1998).

H. Fujiwara, et al., "Real Time Spectroscopic Ellipsometry Characterization of Structural and Thermal Equilibration of Amorphous Silicon-Carbon Alloy p-Layers in p-i-n Solar Cell Fabrication", J. Appl. Phys. 84, 2278 (1998).

J. C. Lee and R. W. Collins, "Real Time Characterization of Film Growth on Transparent Substrates by Rotating Compensator Multichannel Ellipsometry", Appl. Opt. 37, 4230 (1998).

Title: **CIS-Based Thin Film PV Technology**

Organization: Siemens Solar Industries
Camarillo, California
Contributors: Robert R. Gay, Jürgen Bauer, Melinda E. Dietrich, Christine Köble, Ulfert Rühle, Dale E. Tarrant, Robert D. Wieting, Dennis Willett

Objectives and Goals

The primary objective of this subcontract (#ZAF-5-14142-03) is to establish reliable high-throughput, high-yield thin film deposition processes in order to make CIS a viable option for the next generation of photovoltaics. The primary goals are to demonstrate performance as well as commercial viability via the milestones of a champion prototype 13% efficient large area module and sets of modules in 1-kW arrays of steadily increasing efficiency, culminating in delivery of a 1 kW array of 12% efficient large-area modules by the end of the subcontract. This paper reports on progress toward these goals through approximately the third year of this three year, three phase subcontract, October 1997 through December 1998.

Introduction

Multinary $Cu(In,Ga)(Se,S)_2$ absorbers (CIS-based absorbers) are promising candidates for reducing the cost of photovoltaics well below the cost of crystalline silicon. CIS champion solar cell efficiencies have reached 17+% efficiency for devices fabricated at NREL (i). Small area, fully integrated modules exceeding 13% in efficiency have been demonstrated by several groups (ii). Long-term outdoor stability has been demonstrated at NREL by 1x1 ft. and 1x4 ft. SSI modules which have been in field testing for as long as ten years (iii). Cost projections based on current processing indicate cost well below the cost of crystalline silicon (ii). However, challenges remain to scale process to larger substrates and higher capacity, and to pass accelerated environmental testing. The origin of thermal transient behavior needs to be identified and eliminated if possible. A package design needs to be developed to pass standard environmental qualification testing.

From an industrial perspective, the full process sequence anticipated for use in the final product must be mastered and rigorously demonstrated. Application of statistical process control (SPC) techniques is used to rigorously demonstrate yield and reproducibility. SSI abandoned development based on individual cells and defined a 10x10-cm twelve-cell monolithically interconnected "mini-module" baseline process which exercises all aspects of large area module production (iv). During Phase 1 of this subcontract, SSI repeatedly executed the baseline process, rigorously demonstrating process reproducibility and yield for over two thousand CIS-based mini-modules (v). During Phase 2 of this subcontract, SSI demonstrated that absorber layer property and cell performance differences between large-area circuits and baseline circuits were related to design differences between the baseline and large area absorber formation reactors (vi,vii). Differences in absorber layer properties remaining after adjusting the large area reactor process conditions to closely mimic process conditions in the baseline reactor were isolated to differences in the materials of construction and the physical design of the large reactor. Based on these studies, and the associated advances in understanding regarding the influence of reactor design on performance, SSI designed and built a new large area reactor which is a more direct scale-up of the baseline reactor. Success with this reactor was demonstrated by comparable performance for baseline circuit plates and 28x30-cm circuit plates fabricated in the large area reactor. Also during Phase 2 of this subcontract, SSI delivered a 1 kW array of $Cu(In,Ga)(S,Se)_2$ modules with significant improvements in efficiency and the temperature coefficient for power over the previously installed array which was based on an older absorber formation technology without sulfur incorporated in the absorber ($Cu(In,Ga)Se_2$). SSI introduced two new 5 (ST5) and 10 watt (ST10) CIS-based products designed for use in 12 V systems, and NREL confirmed a new world-record efficiency of 11.1 percent on an SSI large area (3665 cm^2) module.

Process Development

During this subcontract phase, substrate size was scaled from ~1x1 ft. to ~1x4 ft. in the new large area reactor. Success for ~1x4 ft. circuit plates was demonstrated by performance comparable to baseline performance. Large area circuit plates are now processed through absorber formation and all subsequent device formation processes. These 1x4 ft circuit plates are then laminated as 1x4 modules or cut to smaller sizes to form 30x18 cm ST5 or 30x36 cm ST10 products. Low capacity production of prototype 1x4 ft. circuit plates was conducted while applying SPC and Analysis of Variation methodologies to develop a low variation process through repeated “cycles of learning.”

Figure 1 presents performance data for all 1X4 circuit plate produced between January and November of this year including 18% of the circuits plates that were dedicated to experiments. Average efficiency, 10.8%, is indicated by the heavy solid horizontal line and the SPC upper and lower control limits by the horizontal dashed lines. This control chart shows that the process exhibited generally good control for extended periods although a troubling tendency toward shifts in the process average is evident (viii). This behavior is not yet understood but appears to result from batch-to-batch variability in precursor or base electrode preparation. An extended period when defective circuits resulted from shunting along the laser scribed pattern lines in the Mo base electrode is indicated in Figure 1. This behavior is also not yet well understood but appears to result from batch-to-batch variability in base electrode preparation. Mechanical yield, the fraction of all substrates introduced into production which pass intermediate inspections before IV testing, is 74%. Electrical yield depends upon the choice of lower specification limit; 85% yield at 10% minimum circuit efficiency and 96% yield at 9% minimum efficiency.

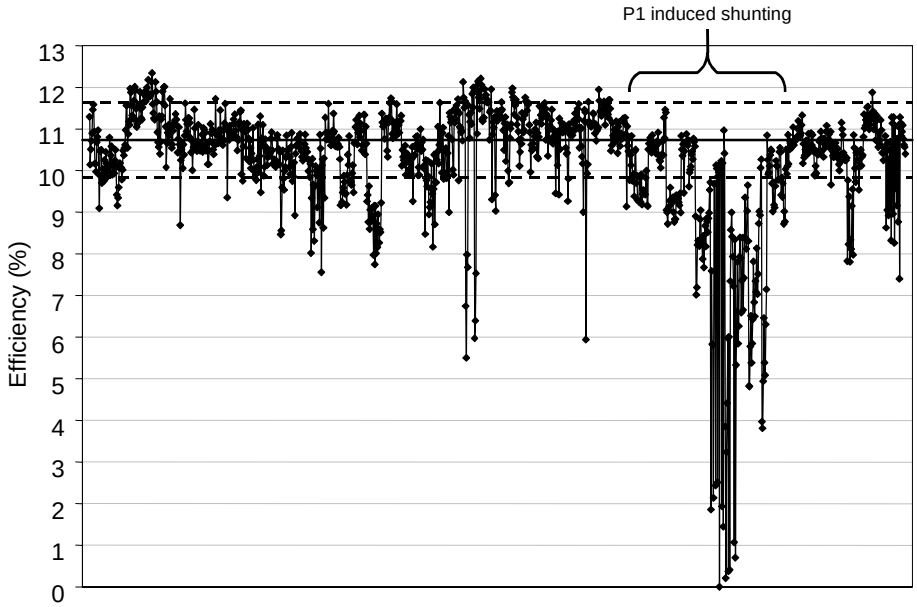

Figure 1. Performance of 1X4 circuit plates produced between January and November 1998.

Although long-term outdoor stability has been demonstrated at NREL and thermally induced losses from thermal cycling and humidity-freeze cycling tests recover with outdoor exposure, water vapor ingress resulting from extended damp heat testing (85°C, 85% R.H. for 1000 hours) permanently degrades performance for typical glass/EVA/circuit laminate structures. As depicted in Figure 2, long-term outdoor stability has been demonstrated at NREL where 1x1 ft. and 1x4 ft. modules have undergone testing for as long as ten years (iii). Measurements on both modules and 1kW arrays indicate good stability with no seasonal variation in performance and thereby demonstrate that thermally induced transients observed after exposure to accelerated environmental testing are not observed in the field despite daily and seasonal changes in module temperature.

Packaging designs have been demonstrated that protect against water vapor ingress during damp heat testing and allow modules to pass the damp heat test after thermally induced transient effects are reversed by outdoor exposure. For example, a 10x10 cm circuit plate laminated using EVA between an oversized cover sheet and an aluminum back sheet, and including an edge seal, was successful. A package design similar to a thermopane window was also successful. However, these package designs typically exhibit low yield through damp heat testing and are not desirable for commercialization. Additional lamination, edge sealing, and pseudo lamination experiments have been conducted including tests of package design options based on the replacement of EVA. The preliminary results indicate that transients introduced by long term exposure at 85°C or temperature cycling are reduced by soft encapsulating materials such as silicone grease, two part silicone, or partially cured EVA. Damp heat exposure resulted in an acceptable loss of only ~2% for one glass/silicone/circuit/TPAT structure with edge seals and desiccant incorporated in the package.

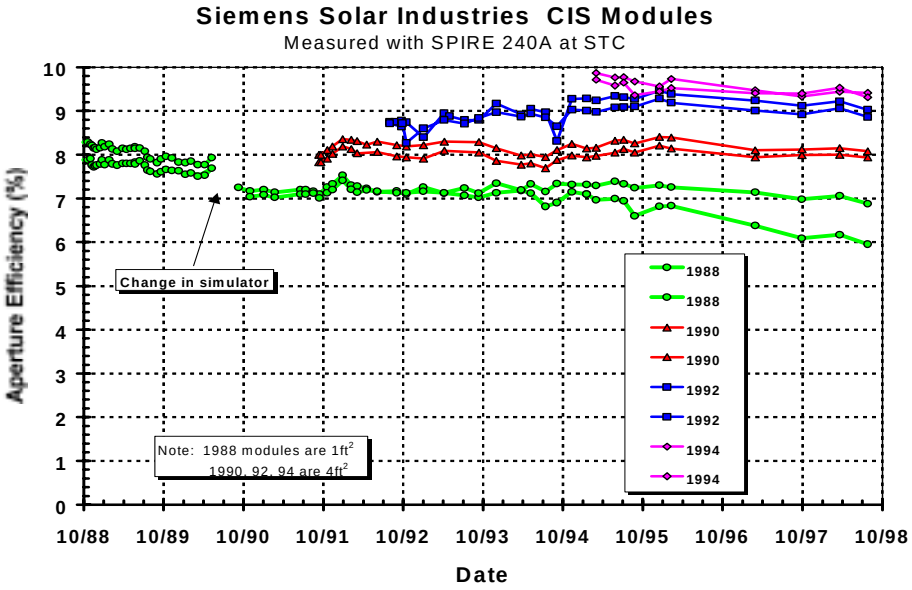

Figure 2. Results of outdoor testing at NREL showing excellent long-term stability.

1kW Array

SSI delivered 32 ~1x4 ft. modules, ~1.2 kW, to upgrade the test array at the NREL Outdoor Test Facility. The NREL measured average efficiency at standard test conditions of 11.4% is the highest array efficiency for any thin-film technology. NREL confirmed a world-record 11.8%, 3651 cm^2 aperture area efficiency for the champion module (Figure 3). The efficiency of all modules far exceeds the DOE year 2000 goal of 10% for commercial CIS modules.

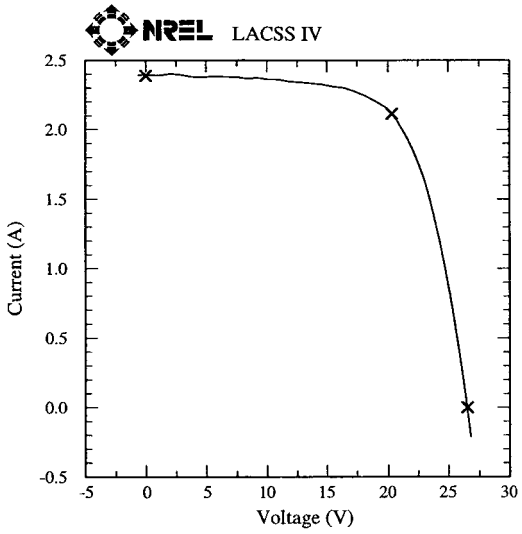

Area	3651.1	cm^2	(125.9 x 29.0 cm)	
Voc			26.50	V
			0.530	V/cell
Isc	2.389	A	32.72	mA/cm^2
Vmax	20.34	V	0.407	V/cell
Imax	2.113	A	28.94	mA/cm^2
FF	0.679			
Pmax	42.99	W		
Efficiency	11.8%			

Figure 3. NREL confirmed world-record large area thin film module.

Acknowledgments

The author gratefully acknowledges NREL for valuable measurement and analytical assistance. This work was supported by the National Renewable Energy Laboratory, Golden, CO, under subcontract No. ZAF-5-14142-03 of the Thin Film Photovoltaic Partnership Program through the U. S. Department of Energy.

1. Ken Zweibel, Harin S. Ullal, Bolko von Roedern, “Progress and Issues in Polycrystalline Thin-Film PV Technologies,” 25th IEEE Photovoltaic Specialist Conference, 1996, pp. 745-750.

2. R. Gay, “Status and Prospects for CIS-Based Photovoltaics”, 9th International Photovoltaic Science and Engineering Conference, Miyazaki, Japan, November 1996. Published in Solar Energy Materials and Solar Cells, 47 (1997) pp.19-26.

3. H.S. Ullal, K. Zweibel, B.G. von Roedern, “Current Status of Polycrystalline Thin-Film PV Technologies”, 26th IEEE Photovoltaic Specialists Conference, Sept. 29-Oct. 3, 1997, Anaheim, California, NREL/CP-520-22922, UC Category: 1250.

4. D. E. Tarrant and R. R. Gay, “Research on High-Efficiency, Large-Area CuInSe2-Based Thin-Film Modules, Final Subcontract Report,” NREL/TP-413-8121 (1995).

5. D. Tarrant, R. Gay, "Thin-Film Photovoltaic Partnership Program - CIS-based thin film PV technology. Phase 1 annual technical report, September 1995--September 1996", (Apr 1997) NREL report DE97000236.

6. R. Gay, J. Bauer, R. Dearmore, M. Dietrich, G. Fernandez, O. Frausto, C. Fredric, C. Jensen, A. Ramos, J. Schmitzberger, D. Tarrant, R. Wieting, D. Willett, “Thin-Film Photovoltaic Partnership Program CIS-Based Thin Film PV Technology”, NREL Photovoltaic Program, FY 1996 Annual Report, August 1997, NREL/BK-210-21966, pp. 243-246.

7. D. Tarrant, J. Bauer, R. Dearmore, M. Dietrich, G. Fernandez, O. Frausto, C. Fredric, C. Jensen, A. Ramos, J. Schmitzberger, R. Wieting, D. Willett, R. Gay, “Progress in CIS-Based Module Development”, 14th NREL/SNL Photovoltaics Program Review, Lakewood, Colorado, November 1996. Published in AIP Conference Proceedings 394, (1997) pp. 143-152.

8. R. D. Wieting, “CIS Product Introduction: Progress and Challenges”, National Center for Photovoltaics Program Review Meeting, Denver, Colorado, September 9, 1998, to be published in AIP Conference Proceedings.

Title: **Technology Support for Initiation of High Throughput Processing of Thin-Film CdTe PV Modules**

Organization: Solar Cells, Inc.
1702 N. Westwood Ave.
Toledo, OH 43607

Contributors: G.L. Dorer, R.C. Powell, J.J. Hanak, U. Jayamaha, J. Bohland, S. Cox, J. Christiansen, T. Kahle, N. Reiter, G. Rich, M. Steele

Objectives:

The research effort in FY1998 consisted of four major areas of activity:

1) Equipment, process and fabrication development, which addressed the issue of improved prototype module fabrication, processes with the goal of near-term manufacturing.
2) Efficiency improvement, that was geared towards increasing module performance.
3) Characterization and analysis, that focused on the issues of verification and improvement of product reliability as well as on providing support for all process development activities.
4) Cell interconnects, including further development of SCI's proprietary Dot Matrix process and alternative means of cell patterning.

Summary of Results

Solar Cells Inc. (SCI) has set out to create the technology to produce photovoltaic modules in volumes sufficient to compete with the economics of conventional electric technology [1, 2]. In FY1998 significant accomplishments have been realized. The following is a summary of the results.

Deposition of Semiconductor Films

Major achievements have been made in the development of the production prototype VTD system for continuous coating of glass plates with CdS/CdTe semiconductor layers. They included accurate means of metering of source powders, reliable transport of heated glass in vacuum and required uniformity of film thickness. The VTD process has achieved a status in which linear coating speeds in excess of 8 ft/min have been realized for the semiconductor, equal to about two modules per minute, or 144 kW per 24-hour day. The process has been implemented in a production line, which is capable of round-the-clock continuous production of coated substrates 120 cm x 60 cm in size at a rate of 1 module every four minutes, equal to 18 kW/day. Currently the system cycle time is limited by the rate of glass introduction into the system and glass heating, but not by the rate of the semiconductor deposition.

Pilot Production

A successful test of the VTD system has been conducted under an environment of PV module production, in a continuous run lasting 18 hours, during which 140 plates were coated. At present the difference between the coating speed and the coated module production is due to the substrate handling capability by the vacuum load locks and glass heating capacity. The thickness of the glass substrate for modules has been reduced from 5 mm to 3 mm, thereby achieving higher optical transmission, faster heating and lower cost. With the thinner glass coating speeds of 9 ft/min have been achieved. The 3-mm thick glass has now become the standard substrate for module production.

Vapor Distributor
A key component of the VTD process is the vapor distributor into which the semiconductor source materials are injected and where they are vaporized. The design allows source introduction and vapor supply on demand. Although several versions of the vapor distributor already exist, its development is still continuing, as SCI's plans call for increased production capacity.

Source Materials
One of the major activities in the VTD process was the development of the semiconductor source materials in forms appropriate for introduction into the vapor distributors. Proprietary processing methods have been developed that facilitate the delivery of the source materials on demand and with uniform distribution.

Chloride Treatment of CdS/CdTe Layers
Three variants of chloride treatment were studied with some success. One of them include the standard, wet $CdCl_2$ treatment, the second, a soak, dip and dry treatment, both followed by heat treatments at ca. 400 ^{o}C. For the standard treatment, cell efficiency was studied as a function of time and temperature of the heat treatment. The optimized values are available in form of contour plots. The third, newly developed method, still under study, is a dry, vapor-chloride treatment, in which the samples are heated rapidly to the process temperature, heat treated in a vapor of $CdCl_2$, and rapidly cooled. It is anticipated that this method might save considerable process time and equipment by circumventing rinsing and drying.

Interconnects
The effort in the SCI's Dot-Matrix process has resulted in achieving efficiency of 7.4% for full-size modules and 8.0% for 1/4 modules. A new version of the Dot-Matrix process has also been introduced that uses only laser scribing for the patterning process. More accurate laser tables are needed to continue this development. In the search of a new 'line-patterning' method, other than laser scribing, good quality patterning of TCO has been achieved.

Performance
A new SCI record efficiency of 14.1% has been achieved for small cells by the combination of the use of low-iron glass, intrinsic tin oxide over the TCO, thinning of the CdS layer, and various improvements in the film deposition, back contacts and device processing (tested by NREL). For the 60 cm x 120 cm modules produced by the new, rapid VTD process, the top aperture-area efficiency achieved thus far is 8.4 %, compared with the SCI record of 9.1 % for the established CSS process. The difference in performance was found to be caused by dust particles and pinholes in the CdS layers, variation in the substrate temperature and film thickness and variation in laser patterning.

Accelerated Life Testing
The ALT program has been established, with the participation of four laboratories. Extensive data on accelerated degradation effects under electrical bias and elevated temperature have been collected and presented. All SCI-made CdTe devices in the field, including modules and arrays, some in their fourth year of outdoor exposure, continue showing excellent stability (see Figure 1).

Instrumentation
Extensive development has taken place in instrumentation and means of automated or accelerated testing of device performance, data collection and data processing to keep up with the rapid throughput of the VTD process.

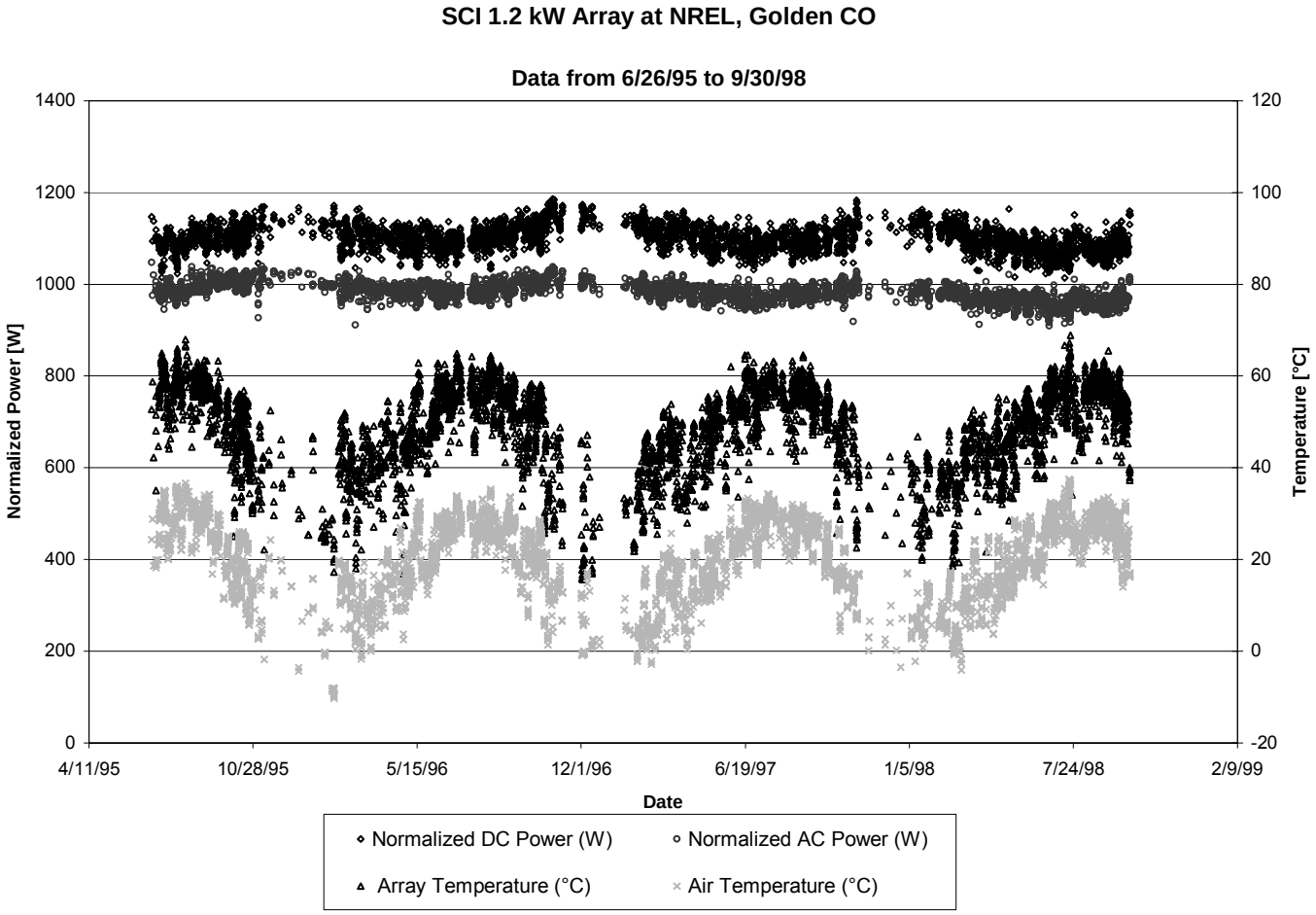

Figure 1. Performance of the 1kW array installed at NREL (Data courtesy of NREL)

Module Encapsulation

A significant item in the cost reduction of high-throughput manufacture of PV modules is final encapsulation that currently utilizes EVA. A liquid polyester resin is a candidate material that may meet the expectations of low cost of unit assembly and product longevity. Styrene-based polyester resin systems are already used worldwide in architectural glass laminating applications and aliphatic-based resins are used in challenging environmental conditions. Two resin systems were tested for encapsulation of mini-modules and modules. The initial tests have shown promising results, comparing well with EVA and exceeding stability with respect to high-intensity UV irradiation.

References

1. R.C. Powell, G.L. Dorer, Upali Jayamaha, J.J. Hanak, "Technology Support for Initiation of High Throughput Processing of thin-Film CdTe PV Modules," NREL Subcontract ZAF-5-14142-05, Solar Cells Inc., Subcontractor Phase III Technical Report, (1998).
2. R.C. Powell, G.L. Dorer, Upali Jayamaha, J.J. Hanak, "Technology Support for Initiation of High Throughput Processing of thin-Film CdTe PV Modules," NREL Subcontract ZAK 18-17619-17, Solar Cells Inc., Subcontractor, Quarterly Technical Report No. 1, (1998).

Title: **Research on Amorphous Silicon Cells and Modules**

Organization: Solarex, A Business Unit of Amoco/Enron Solar, Toano, Virginia

Contributors: R. Arya, Program Manager, T. Bao, M. Bennett, D. Carlson, L. Chen, G. Ganguly, G. Lin, F. Liu, R. Middya, F. Willing, J. Newton

Introduction

Solarex has been performing research in the area of amorphous silicon (a-Si) photovoltaics for about 15 years, and started manufacturing single junction a-Si solar cells for consumer applications at Newtown, Pennsylvania, in 1984. In 1997, Solarex started the commercial production of large area (8.6sq. ft.) multijunction a-Si PV modules at Toano, Virginia. Over the last year, the Solarex a-Si research program has focused on improving the performance the scribing processes, the back reflector, processes for small area single junction and tandem devices, and higher growth rate processes. There has also been a systematic study of the light induced degradation effects in a-Si versus a-SiGe devices, and of treatments that improve the stabilized performance of small area devices. The amorphous silicon process transfer from small area research machines to larger area production machines has also been investigated as efforts are made to introduce newly developed processes into the production line at the plant. -

Front Contact Research

We fabricated tandem device structures on some samples of ZnO coated glass from Harvard University; the ZnO was deposited by atmospheric pressure CVD and was textured for use as front contact. As shown in Table 1, the Harvard ZnO that was doped with both fluorine and aluminum (H-D) exhibited the highest transmission and the lowest sheet resistance, and gave rise to the devices with the largest photocurrents (J_{SC} = 16.29 mA/cm^2).

Table 1. Properties of small area Tandem Devices on Harvard ZnO and AFG CTO

CTO	*Dopant*	*Trans.*	**Haze**	*R (Ω)*	**Voc** *(V)*	*FF*	*Js1*	**Js2**	*Total Jsc*
AFG					1.565	0.681	7.69	7.56	15.25
H-A	F	0.814	0.099	108	0.392				
H-B	Al	0.748	0.027	54	1.43	0.647	7.37	7.57	14.94
H-C	Al	0.810	0.045	76	1.376	0.605	7.6	7.52	15.12
H-D	F+Al	0.848	0.034	44	1.45	.0.642	8.1	8.19	16.29
AFG					1.55	0.67	7.77	7.44	15.21

We have developed ZnO on 1mm thick soda lime glass for use as front contacts. In Table 2 below. we compare commercial SnO_2 with ZnO using our standard tandem process. We find that higher currents are obtained when using ZnO compared to commercial SnO_2

even though the haze is lower. However, the fill factor is lower using ZnO, which may be associated with a higher contact resistance. The degradation is also larger on cells made on ZnO.

Table 2. The performance and degradation of tandem cells on commercial SnO_2 and Solarex ZnO

CTO	*Voc* (V)	*FF*	*Jscl (mAlcm2)*	*Jsc2 (mAlem2)*	*Efj.* (O)	*Normalized Eff.*
$Sn0_2$						
Initial	1.56	0.69	8.17	7.91	8.65	1.00
Stable	1.47	0.61	8.17	7.73	7.14	0.83
ZnO						
Initial	1.57	0.67	8.37	8.39	8.75	1.00
L Stable-	1.47	0.58	8.21	7.58	6.68	0.76

Improved Amorphous Silicon Processes

New improved processes have been developed for single junction a-Si cells.[1] The stabilized performance of small area cells using these new processes is compared to standard cells in Table 3. We see a ~6% improvement in stabilized performance. Incorporating these new processes in the small area Tandem Cell Process allowed the stable performance to reach~9%.

Table 3. Performance after Light-Induced Degradation of small area Single junction Cells prepared using the Standard and New Processes on Asahi CTO and AFG CTO

	Asahi CTO				AFG CTO			
Process	*Voc (V)*	*FF –*	*Jsc (mAlcm2)*	*Efficiency* (%)	*Voc* (V)	*FF*	*JsC (mA/cm 2)*	*Efficiency (%)*
Standard	0.88	0.60	13.2	6.96	0.87	0:59	12.05	6.18
New	0.89	0.61	14.0	7.58	0.87	0.61	12.96	6.90
	0.89	0.61	14.0	7.59	0.88	0.62	12.66	6.82
	0.90	0.63	13.3	7.60	0.86	0.63	12.43	6.69
	0.88	0.63	14.0	7.69	0.86	0.62	12.72	6.83
	0.88	0.63	14.0	7.75	0.88	0.60	13.14	6.97

Table 4. Performance after Light Induced degradation of small area Tandem Cells prepared using the Standard and New Processes on Asahi CTO.

Process	*Voc (V)*	*FF*	*Jsc_1 (mAlem2)*	*Jsc_2 (mA/cm2)*	*Efficiency (%)*
Std.	1.48	0.64	8.83	9.02	8.50
New	1.50	0.66.	8.76	8.82	8.69
	1.49	0.63	9.19	8.91	8.48
	1.51	0.64	7.74	9.85	8.51
	1.52	0.65	8.30	9.35	8.74
	1 51	0.64	8.55	9.41	8.98

We have made a series of process changes to improve the performance of Tandem Cells. The performances of some of these cells are shown in Table 5. The highest efficiency is about 11.3%.

Table 5: Performance of small area Tandem Cells on Asahi CTO

#	*Voc (V)*	*FF*	*Jsc (mA/cm2)*	*Efficiency* (%)
1	1.618	0.699	9.99	11.30
2	1.627	0.701	9.47	10.80
3	1.628	0.705	9.3 5	10.73
4	1.614	0.701	9.89	11.12
5	1.624	0.709	9.82	11.31
6	1.620	0.717	9.28	10.78

Faster a-Si Deposition Processes

Our standard I-layer process uses a deposition rate of about lA/s, and the performance drops when we use a faster (~3A/s), deposition rate. We have developed several new processes that improve the stable performance of single junction a-Si cells.[1]

Table 6: The stabilized performance of a-Si single junction cells prepared under standard and new process conditions at ~3A/s on Asahi CTO.

Process	*Rd (A/s)*	*Voc (V)*	*FF*	*Jsc (mAlcm2)*	*Efficiency* (%)
Std.	3.08	0.88	0.56	11.10	5.48
New	3.16	0.89	0.54	11.41	5.43
New	3.00	0.89	0.55	11.69	5.65
New	3.10	0.91	0.57	12.14	6.29

Back Contact Research

We have developed a silver-based back contact. Table 7 below, shows the comparative performance of our standard devices with our standard Al based back contacts and the newly developed silver-based back contacts. There is a clear gain in the red response and in the overall Jsc, but the number of shunted segments is not observed to increase.

Table 7: The performance of standard, small area, tandem devices completed using standard and new, silver based back contacts

Back Contact	*Voc (V)*	*FF*	*Jsc1 (mA/cm^2*	*Jsc2 (mA/cm^2)*	*Shunted segments*	*Gain in Jsc*	*Gain in QE800*	*Eff. (%)*
Ag	1.62	0.63	8.99	8.91	1/36	4%	18%	9.15
Al	1.63	0.64	8.93	8.28	3/36			8.99

Degradation of a-Si vs. a-SiGe cells

In earlier work [2J, we had examined the effect of a reverse bias at elevated temperatures on the performance of a-Si:H single junction cells. In the current work, we extended the study to single junction a-SiGe:H cells and find that a reverse bias treatment at 120 °C causes the efficiency of both a-Si:H and a-SiGe:H cells to increase, but the effect is much slower and smaller in the a-SiGe:H cell. Fig. 1 below shows that a 170 nm thick a-SiGe:H single junction p-i-n cells degrades more slowly than a 300 nm thick a-Si:H p-i-n cells when exposed to 60 suns illumination at 60 °C under open-circuit conditions, and while the a-Si:H cells appear to saturate after a few hours of exposure, the a-SiGe:H cells still continue to degrade.

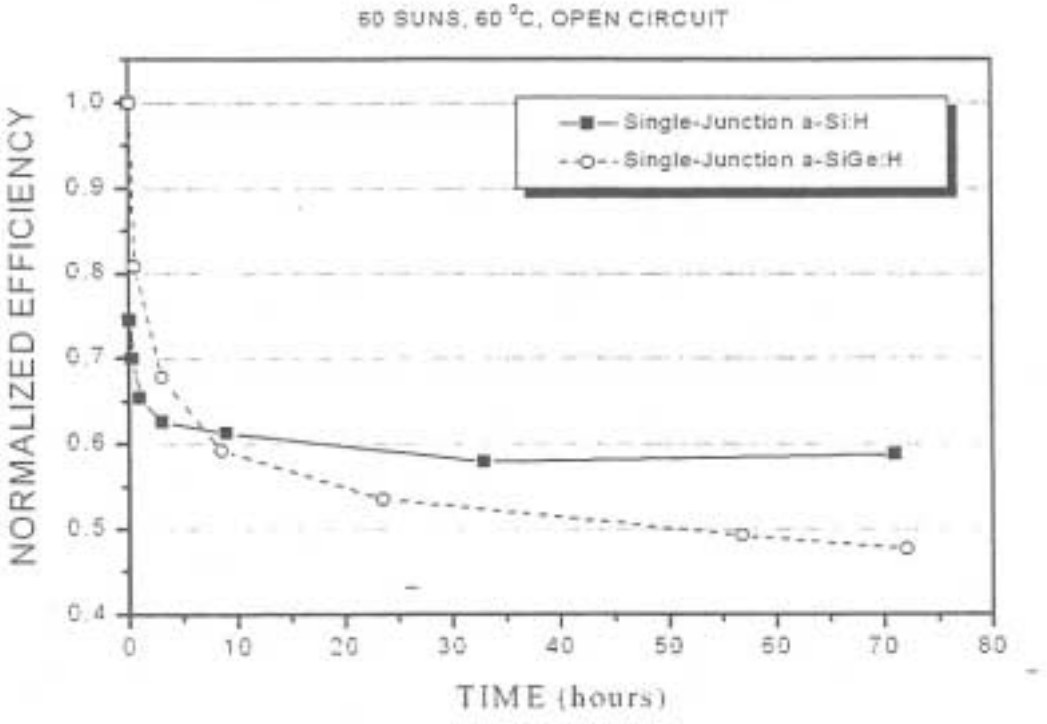

Fig. 1. Normalized conversion efficiency as a function of exposure time to 60 suns illumination at 60 °C for both a-Si:H and a-SiGe:H single junction cells.

We conducted some experiments to determine the diffusion coefficient of deuterium in both a-Si:H and a-SiGe:H films. The data indicate that more than half of the deuterium diffuses out quite rapidly leaving a component that appears to be diffusing quite slowly. The hydrogen that diffuses out rapidly may be associated with hydrogen on the internal surfaces of columnar voids. The more slowly diffusing hydrogen may be associated with the degradation and annealing kinetics that we observe in our a-SiGe:H films.

References

1. R. Arya et. al., NCPV Review Meeting. Denver. Colorado. September 1998.
2. D. Carlson and K. Rajan, Appl. Phys. Lett. 70 [16] 2166 (1997).

Title: **Electroabsorption and Transport Measurements and Modeling Research in Amorphous Silicon Based Solar Cells**

Organization: Syracuse University, Department of Physics, Syracuse, New York 13244.

Contributors: Eric A. Schiff, principal investigator; Jonghun Lyou, visiting scientist; Nikos Kopidakis, research associate; Lin Jiang, Prasanna Rao, Quan Yuan, research assistants. Lyou is Professor of Physics at Korea University in Seoul; Jiang is presently employed at Guidant Corporation in Minneapolis, Minnesota.

In 1998 our research has focused on the following topics:

- *Electroabsorption studies* of a-Si based solar cells. The studies have several purposes: (i) to probe the built-in potential V_{bi} of a-Si:H based solar cells, and (ii) to exploit the electroabsorption spectrum for insight into the optical properties of novel materials. In this year's report we summarize some recent measurements addressing V_{bi} in cells with a-SiGe:H absorber layers. We present some tantalizing data on doped microcrystalline Si, and show an unexpected electroabsorption spectral feature in the infrared which we associate with optical absorption at the *n/i* interface.

- *Electron and hole mobility measurements* in a-Si based materials. Our work has two thrusts. We are surveying the mobility properties of novel a-Si:H based materials (hot-wire, triode-deposited, etc.) to check for the achievement of *exceptional* mobility properties, and we are improving our quantitative techniques to help in assessing *incremental* improvements in a-Si:H based materials. In the last year we have worked on drift mobilities in hydrogen-diluted a-Si:H and on hot-wire a-Si:H.

- *Computer Modeling of a-Si Based Solar Cells*. We have commenced work with the AMPS program developed by Steve Fonash's research group at Pennsylvania State University. We are exploring parameter choices and comparing the output with analytical approximations; ultimately we seek a better understanding of the open-circuit voltages in a-Si based cells based on our group's experience with drift-mobility and built-in potential measurements.

Our research contract was acknowledged in the following publications in 1998:

"Polarized Electroabsorption Spectra and Light Soaking of Solar Cells Based on Hydrogenated Amorphous Silicon," L. Jiang, Q. Wang, E. A. Schiff, S. Guha, and J. Yang, *Appl. Phys. Lett.* **72**, 1060--1062 (1998).

"Direct Observation of Dangling Bond Motion in Disordered Silicon," N. Nickel and E. A. Schiff, *Phys. Rev. B* **58**, 1114--1117 (1998).

"Polarized Electroabsorption Spectra and Light-Soaking of Solar Cells BAsed on Hydrogenated Amorphous Silicon," Lin Jiang, Qi Wang, and E.A. Schiff, in *Amorphous and Microcrystalline Silicon Technology - 1998*, edited by S. Wagner, M. Hack, H.M. Branz, R. Schropp, I. Shimizu (Materials Research Society, Symposium Proceedings Vol. 507, 1998), *in press.*

Electroabsorption and Built-in Potentials

A crucial parameter of any solar cell is the "built-in" electrostatic potential across it. The associated internal electric field is responsible for transporting photocarriers across the absorber layer in amorphous silicon based cells. There is as yet no consensus regarding the best method for measuring the built-in potential, but for some time we have been working with the electroabsorption method originally used in a-Si:H based cells by the Osaka University group.

We received a series of *pin* solar cells with a-SiGe:H intrinsic layers from United Solar Systems Corp. spanning the optical bandgap range 1.45 - 1.75 eV. We have measured the

electroabsorption signal S vs. external bias V as a function of wavelength and for a significant range of sample thicknesses. The principal parameter extracted from this type of study is the voltage axis intercept V_0 obtained by least-squares fitting to the remarkably accurate experimental proportionality $S \propto (V\text{-}V_0)$. Ideally V_0 would estimate the built-in potential of the solar cell.

The resulting data are presented as Fig. 1. While not yet completely understood, they are the most promising we have yet obtained for extracting a built-in potential. This is because several comparable samples with varying thicknesses all have a common long-wavelength limit for V_0; in our past studies [1] of cells with a-Si:H intrinsic layers, V_0 had a much larger wavelength-dependence. We have attributed this wavelength-dependence to p^+-layer electroabsorption, which competes in a wavelength-dependent way with absorber layer electroabsorption. The present measurements do not appear to have this complication, presumably because the electroabsorption from the doped layers is negligible near the bandgap of the a-SiGe:H intrinsic layers. The long-wavelength limit then yields an estimate for $V_{bi} \approx 1.17$ V.

This value is a very interesting one; it is presumably primarily a joint property of the microcrystalline silicon p^+ and the amorphous silicon n^+ layers of the cells. It is sufficiently large that it is unlikely to present a noticeable limitation for solar cells with smaller bandgaps (such as the present cells with a-SiGe absorbers), but it would very likely limit achievements of open-circuit voltages much greater than the current record near 1.05 V.

We believe that the short-wavelength potential limit of about 2.0 V can probably be interpreted in terms of the *p/i* interface field being somewhat higher than the mean field in the cells. If we can make this argument quantitatively, it will yield useful insight into the profile of the internal electric field.

Electroabsorption Spectra of Microcrystalline Silicon

"Microcrystalline" silicon layers are very useful in solar cells with amorphous silicon based absorber layers; in particular doped microcrystalline p^+ layers are incorporated in cells with the best reported open-circuit voltages. Despite the importance of microcrystalline layers, they represent a daunting problem for characterization: a given "microcrystalline" thin film can incorporate small crystallites exhibiting quantum confinement effects on their optical properties, various degrees of disordered "tissue" between crystallites, as well as larger crystallites with properties similar to those of bulk crystalline silicon.

Electroabsorption spectroscopy should be a good approach for unraveling the optical properties of microcrystalline materials. The shape of an electroabsorption spectrum is typically a well-defined band near the bandedge, which makes for simpler interpretation than the broad, featureless spectra observed in direct absorption. This feature is illustrated in Fig. 2, where we show the electroabsorption spectra for two a-Si:H films with varying bandgaps (from United Solar Systems Corp.), as well as for four phosphorus-doped microcrystalline Si films prepared by plasma deposition at Forschungszentrum Jülich with varying volume concentrations of silane in hydrogen diluent [2]. Strong interference fringe effects have been manually removed from the spectra, accounting for their overly smooth appearance.

The microcrystalline spectra are certainly *not* what would be anticipated for materials with large grains of silicon, for which electroabsorption should be a weak line-spectrum near the bandgap of 1.1 eV. At first glance, the electroabsorption is remarkably similar to that for amorphous silicon, but with very strong blue shifts. However, the polarization properties of the spectra are inconsistent with this interpretation, although we shall not present these measurements here. It does appear that the material has a considerable volume of very fine diameter (1-10 nm) crystallites, thus accounting for the blue shift by quantum confinement. This interpretation bears a similarity to that proposed a few years ago to account for internal photoemission measurements in a-Si:H based solar cells incorporating microcrystalline Si doped layers. The strength of the electroabsorption is much stronger than expected for crystalline silicon, and we speculate that the strong blue-shift in the optical properties is accompanied by a corresponding increase in electroabsorption strength.

Infrared Electroabsorption Spectra

We have found an infrared electroabsorption band near 0.9 eV. At first thought this might seem to be simply a defect to conduction (or valence) band transition from the absorber layer. However, the dependence upon bias field is quite different than for interband transitions, and the strength is much larger than expected from the relative strengths of interband and defect absorption. These effects are illustrated in Fig. 3, where we show the spectrum measured in a *pin* solar cell from United Solar Systems Corp.. Comparable effects have been observed in several samples including a series of TCO/*i*/*n* Schottky barrier samples prepared at the Institute of Energy Conversion at University of Delaware.

We believe that the infrared spectrum is due to a completely different mechanism than the interband electroabsorption. Interband electroabsorption is quadratic in electric field, and is associated with a very small modification of the matrix element for the optical transition by an electric field. We attribute the infrared spectrum to depletion of carriers from the n^+ layer. In this model, depletion reduces the density of electrons near the Fermi energy, and thus enhances the rate for defect to bandtail transitions; note that the proposed transition is a localized-localized one, and is thus strongly sensitive to the extension of electron wavefunctions in the bandtail of the n^+ layer.

We are still assessing the utility of this effect for solar cell characterization; it offers an interesting approach to characterizing the i/n^+ interface of a solar cell.

References

1. "Electroabsorption Measurements and Built-in Potentials in Amorphous Silicon *pin* Solar Cells," L. Jiang, Q. Wang, E. A. Schiff, S. Guha, J. Yang, and X. Deng, *Appl. Phys. Lett.* **69**, 3063--3065 (1996).
2. "Structure and Growth of Hydrogenated Microcrystalline Silicon: Investigation by Transmission Electron Microscopy and Raman Spectroscopy of Films Grown at Different Plasma Excitation Frequencies," *Phil. Mag. A* **75**, 31--47 (1997).

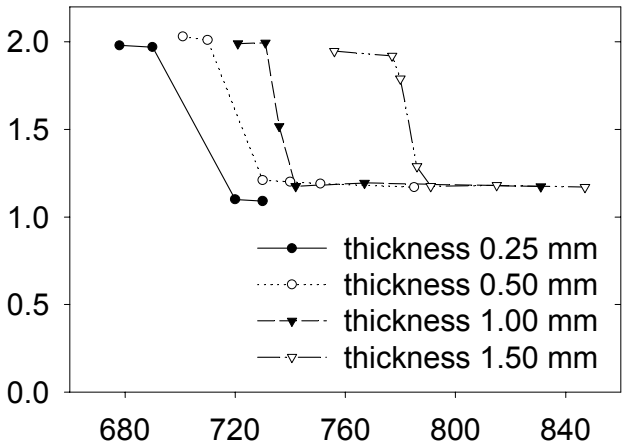

Fig. 1: Wavelength dependence of the electroabsorption offset potential V_0 for four *pin* solar cells (prepared at USSC) with a-SiGe:H absorber layers of differing thicknesses; the typical optical gap was 1.5 eV. The long wavelength limit of about 1.17 V is an estimate of the built-in potential; open-circuit voltages ranged from 0.65 - 0.79 V under AM1 conditions.

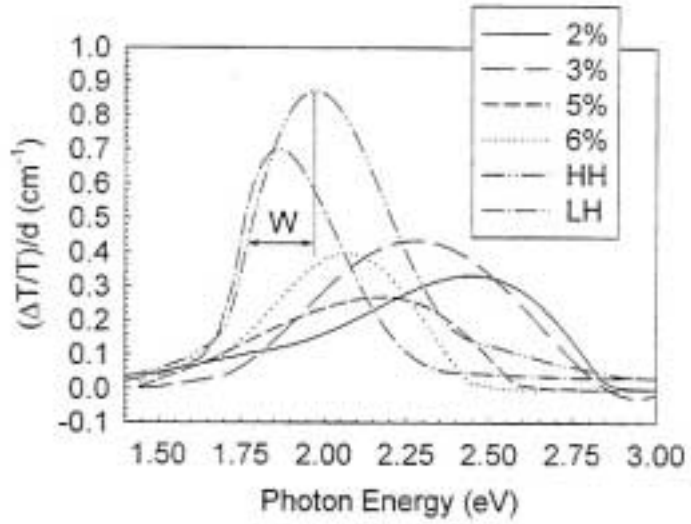

Fig.2: The electroabsorption spectra of amorphous silicon and microcrystalline silicon prepared using plasma deposition from silane/hydrogen mixtures. Samples denoted LH and HH and completely amorphous; samples denoted 6% to 2% are increasingly crystalline.

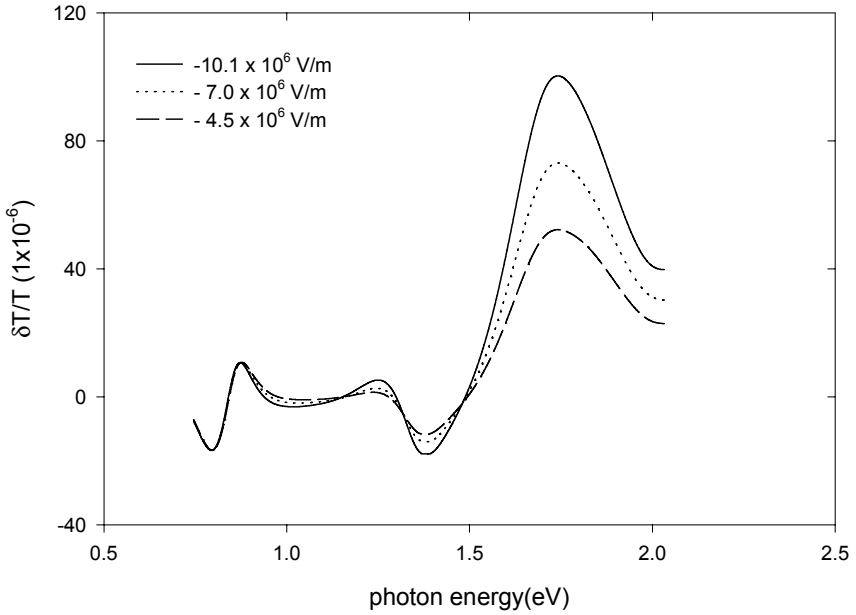

Fig. 3: Electromodulation spectrum measured using a fixed modulation voltage, and variable DC bias voltages (indicated). Negative signals are attributed to interference effects in the thin film. Note that the infrared feature near 0.9 eV is independent of bias voltage, whereas the interband feature rising above 1.5 eV depends linearly on bias. This distinction leads to the model proposed in the text.

Title: **High-Efficiency Triple-Junction Amorphous Silicon Alloy Photovoltaic Technology**

Organization: United Solar Systems Corp.
Troy, Michigan 48084

Contributors: S. Guha, principal investigator; A. Banerjee, E. Chen, J. Edens, T. Glatfelter, G. Hammond, M. Hopson, N. Jackett, K. Lord, A. Mohsin, J. Noch, T. Palmer, I. Rosenstein, D. Wolf, B. Yan, J. Yang, and K. Younan.

Objective

The principal objective of this R&D program is to expand, enhance and accelerate knowledge and capabilities for the development of high-performance, two-terminal multijunction hydrogenated amorphous silicon (a-Si) alloy cells and modules with low manufacturing cost and high reliability. The program goal is to obtain 12% stable modules that will qualify IEEE-Std 1262-1995 reliability testing.

Approach

In order to improve efficiency, United Solar uses a spectral-splitting, triple-junction cell structure. In this configuration, the top cell uses an amorphous silicon alloy of ~1.8 eV bandgap to absorb the blue photons. The middle cell uses an amorphous silicon germanium alloy (~10% germanium) of ~1.6 eV bandgap to capture the green photons. The bottom cell has ~ 40% germanium to reduce the bandgap to ~1.4 eV to capture the red photons. The cells are deposited on stainless steel with a predeposited silver/zinc oxide back reflector to facilitate light trapping. A thin layer of antireflection coating is applied to the top of the cell to reduce reflection loss.

During this year, research activities were carried out in the following four areas: 1) fundamental studies to improve our understanding of materials and devices, 2) small-area cell research to obtain the highest cell efficiency, 3) large-area cell research to obtain the highest module efficiency, and 4) deposition of small-area cells using a modified very high frequency (MVHF) technique to obtain higher deposition rates.

Status/Accomplishments

1. Fundamental Studies

We have shown previously that hydrogen dilution plays a very important role in improving material and cell performance. The highest efficiency cells are obtained when the intrinsic material is deposited at a level of hydrogen dilution that is at the threshold between amorphous and microcrystalline transition. Collaborating with the Colorado School of Mines, we have now demonstrated that the structural order in this material is determined by the substrate on which the film is grown and also the film thickness. The order improves as the thickness increases. This results in the improvement of material quality in the direction of film growth and has been confirmed by the measurement of defect density at the University of Oregon.

2. Small-area Cell Research

We have worked on improving the component cells of the multijunction structure by changing the deposition conditions. The highest efficiencies obtained in the multijunction structure are given below.

- Achieved 14.4% initial and 12.4% stable active-area (~0.25 cm^2) cell efficiency in a dual-bandgap, double-junction structure.
- Achieved 15.2% initial active-area (~0.25 cm^2) cell efficiency in a triple-junction structure.

3. Large-area Module Research

Uniformity in deposition over a large area is key to the achievement of high module efficiency. We use a large-area reactor where the component cells are deposited over one-square-foot area and the uniformity is investigated by evaluating the performance of small-area cells deposited over the entire area. Using this method, we have made high efficiency component cells and have fabricated large-area, triple-junction modules. The highlights of this activity are given below:

- Deposited array of single-junction top cells (~0.268 cm^2) on stainless steel substrates without back reflector using a-Si alloy over areas greater than 900 cm^2 and achieved an average total-area stabilized cell efficiency measured under global AM1.5 of 5.4% after 1031 hours of one-sun light soaking at 50 ^oC.
- Deposited array of single-junction middle cells (~0.268 cm^2) on stainless steel substrates without back reflector using a-SiGe alloy over areas greater than 900 cm^2 and achieved an average total-area stabilized power density measured under global AM1.5 with λ>530 nm filter of 3.5 mW/cm^2 after 211 hours of one-sun light soaking with an appropriate filter at 50 ^oC.
- Achieved 14.48% initial and 12.86% stable active-area (~0.25 cm^2) efficiency in a triple-junction structure using a large-area (1 ft x 1 ft) reactor.
- Achieved 12.3% initial aperture-area (~919 cm^2) efficiency in an encapsulated module using a triple-junction structure.
- Achieved 10.5% stable aperture-area (~905 cm^2) efficiency in an encapsulated triple-junction module after 1000 hours of one-sun light soaking at 50 ^oC carried out and measured by NREL.
- Fabricated and delivered two large-area prototype modules with a total area of 216" x 29.6" and 216" x 15.5" to NREL; the initial power outputs for the two modules are 317.8 W and 155.5 W, respectively.

4. Cells Deposited at High Rates

We have previously shown that deposition at high rates results in poorer cell performance and stability. This was attributed to a poor microstructure of the film grown at high rates. Since the characteristic of the plasma can influence the film property significantly, we have carried out experiments to determine the energy distribution of the ionized species in the plasma excited by both radio frequency and very high frequency power sources. The energy of the positive ions is found to increase as the pressure is lowered. Using the MVHF technique, the following results have been obtained:

- . Achieved 11.1% initial active-area (~0.25 cm^2) cell efficiency in an a-Si alloy *p i n* device using MVHF at ~6 Å/s.
- . Achieved 10.8% initial active-area (~0.25 cm^2) cell efficiency in a triple structure using MVHF at ~6 Å/s.

Publications

1. Guha, S., Yang, J., Banerjee, A., and Sugiyama, S. (1998). "Material issues in the commercialization of amorphous silicon alloy thin-film photovoltaic technology." *MRS 1998 Spring Meeting Proceedings; April 13-17, 1998, San Francisco, CA.*

2. Yang, J., Sugiyama, S., and Guha, S. (1998). "Effect of excitation frequency on the performance of amorphous silicon alloy solar cells." *MRS 1998 Spring Meeting Proceedings; April 13-17, 1998, San Francisco, CA.*

3. Chen, C.C., Lubianiker, Y., Cohen, J.D., Yang, J., Guha, S., Wickboldt, P., and Paul, W. (1998). "The electronic structure, metastability and transport properties of optimized amorphous silicon-germanium alloys." *MRS 1998 Spring Meeting Proceedings; April 13-17, 1998, San Francisco, CA.*

4. Mahan, A.H., Reedy, Jr., R.C., Iwaniczko, E., Wang, Q., Nelson, B.P., Xu, Y., Gallagher, A.C., Branz, H.M., Crandall, R.S., Yang, J., and Guha, S. (1998). "H out-diffusion and device performance in *n-i-p* solar cells utilizing high temperature hot wire a-Si:H i-layers." *MRS 1998 Spring Meeting Proceedings; April 13-17, 1998, San Francisco, CA.*

5. Yang, J., Banerjee, A., Lord, K., and Guha, S. (1998). "Correlation of component cells with high efficiency amorphous silicon alloy triple-junction solar cells and modules." *2nd World Conference and Exhibition on Photovoltaic Solar Energy Conversion Proceedings; July 6-10, 1998, Vienna, Austria.*

6. Guha, S., Yang, J., Banerjee, A., Hoffman, K., and Call, J. (1998). "Manufacturing issues for large volume production of amorphous silicon alloy photovoltaic modules." *NCPV Photovoltaics Program Review Proceedings; September 8-11, 1998, Denver, CO.*

Title: **Photocharge Transport and Recombination Measurements in Amorphous Silicon Films and Solar Cells by Photoconductive Frequency Mixing**

Organization: Physics Department, University of California at Los Angeles
Los Angeles, CA 90024-1547

Contributors: R. Braunstein, Principle Investigator;
S. Dong, J. Liebe, G.S.Sun, A. Kattwinkel

Program Outline

This program is concerned with the characterization of the photoconductive properties of a-Si:H, a-SiC:H and a-SiGe:H films and solar cells from "round robin" sources by the photoconductive mixing technique so as to separately determine drift mobilities and photomixing lifetimes. By measurements of the temperature and electric field dependence of the drift mobility in the annealed and the light-soaked states, the effects of the sample deposition conditions on the transport properties are investigated.

The materials studied during this period were:

1. Hot-wire assisted PECVD a-Si:H from NREL
2. GD diluted and undiluted a-Si:H from the Wronski group
3. ECR-a-Si:H from the Dalal group
4. Hot-Wire a- SiGe:H from the Nelson group
5. $CuInSe_2$ from NREL

Results

The mobilities and lifetimes were determined for the above samples in the annealed and the light-soaked states by the photoconductive frequency mixing technique. It was found that for all substances the mobilities and lifetimes decayed at different stretched-exponential rates.The mobility increased as a function of electric field indicating that the charged carrier transport takes place in the presence of long-range potential fluctuations (LRPF); to account for this observation, a model was developed which considered that the charge carriers overcome these barriers by thermal activation instead of going around the barrier due to scattering or even tunneling through the barrier.

Hot-Wire Results (NREL)

The range and the depth of the long range potential fluctuations were determined for the hot-wire samples. It should be noted that the range decreases as the substrate temperature increases in the annealed state. In addition, the depth of the potential increases. In the light-soaked state, the depth of the potential increases as the substrate temperature increases.

Diluted and Undiluted

Figure (1) shows the results obtained for the diluted and the undiluted samples of a-S:H from the Wronski group. It should be noted that for the undiluted sample the lifetime and the mobility decay at approximately the same rate; while for the diluted sample the drift mobility decays more rapidly than the lifetime.

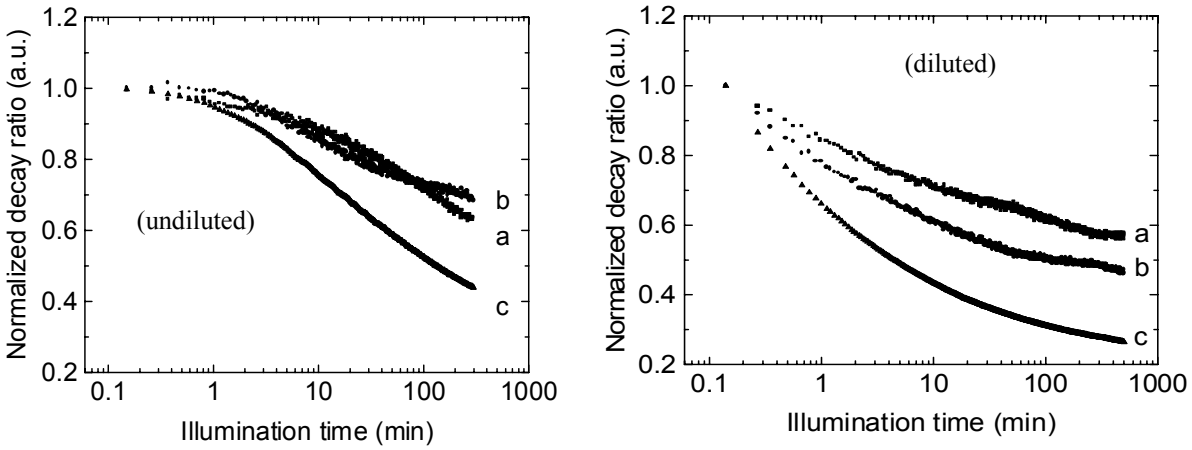

Figure 1. The decay of photoconductivity (c), lifetime (a), and drift mobility (b) as a funtion of illumination time with 4 suns intensity of a He-Ne laser line.
(Diluted a-Si:H: dilution ratio 10:1 H_2 SiH_4)

The light-soaked state was obtained by *in situ* employing the He-Ne laser with an intensity of 4 suns over a period of 5 hours illumination.

ECR Results

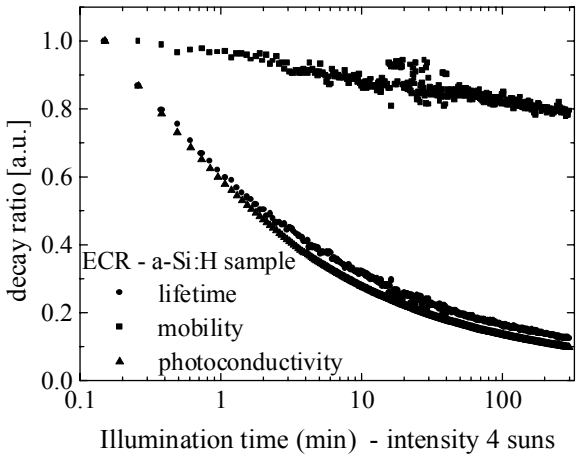

Figure 2. The decay of mobility (μ), lifetime (τ), and photoconductivity (σ).

The measurement of ECR produced samples of a-Si:H from the Dalal group are shown in figure 2.
It should be noted that for this case the mobility decays at a slower rate than the life. This is different from the case for the diluted a:-Si:H shown in Figure 2 where the mobility decays more rapidly than the lifetime.The drift mobility and lifetime decay at different rates depending upon the sample preparation. Since the lifetime is generally determined by the number of neutrals while the mobility is determined by the number of charges, it is indicated that during light soaking, the rates of production of neutral and charges differ for different samples.

Hot-Wire a-Si:Ge:H Alloys (Nelson)

Brent Nelson supplied us with a series of samples of a-SiGe:H alloys prepared by the hot- wire technique using varying growth parameters to explore the parameter space between pure a-Si:H: and pure a-Ge:H to produce a-SiGe:H alloys to optimize the transport parameters within the two bandgap regimes: 1.40-1.45 eV and 1.60.eV and 1.60-1.65 eV. The photoconductivity, mobility and lifetime were determined and in addition the electric field dependence of the mobility was measured enabling a determination of the range and the depth of the long range potential fluctuations. Figure 3 shows plots of the photoconductivity, drift mobility, lifetime, and mobility as a function of the Tauc gap. It should be noted, that the photoconductivity decreases as the Ge content increases is due to the decrease in the mobility the lifetimes remain relatively constant. The range of the LRPF increases slightly with the decrease in the Tauc gap while the depth increases.

Atomic Force Microscopy Study of the Morphology of Hot-Wire a-Si:H and its Correlation With the Electrical Properties.

There is evidence that the surface morphology of a-Si:H may play a role in the transport properties. To this end, we initiated a study with Dr. David Braunstein formerly of Parks Scientific, presently at IBM, San Jose, to employ Atomic Force Microscopy to systematically study the surface morphology of a series of hot-wire samples . Figure 4 shows the RMS roughness of the surface and the photoconductivity of hot-wire samples as a function of substrate temperature. The decrease in the photoconductivity, mobility and range of the long-range potential fluctuations as the deposition substrate temperature is increased seems to be correlated with a decrease in surface roughness! Further analysis of the images by fractal analysis are to be performed to arrive at the grain sizes to understand these observations.

Determination of the Built-in Electric Field near Contacts to $CuInSe_2$

The built-in electric field in polycrystalline $CuInSe_2$ (CIS) near gold co-planar contact was quantitatively revealed for the first time by the photomixing technique. A He-Ne Laser beam was focused locally on the CIS sample near one of its contacts .While both dc dark and photocurrents showed ohmic behavior, the high frequency (252 MHz) photomixing current showed significant non-ohmic behaviour, as it was non-zero under applied dc bias, which reveals a built-in electric field ~ 1000V/cm. The capability of the photomixing technique to probe local charge transport properties is expected to be very useful for, e.g., the quantitative evaluation of the quality of ohmic contacts and the investigation of electric field induced p-n junction formation in CIS and related materials. This work was published:

"Determination of the built-in field near contacts to polycrystalline $CoInSe_2$ – Probing Local Charge Transport Properties by Photomixing" – Yi Tang, Shirung Dong, G. S. Sun, R. Braunstein, B. von Roedern
NCPV Photovoltaics Program Review; Proceedings of the 15th Conference, Denver, CO, 1998; AIP Conference Proceedings (in press)

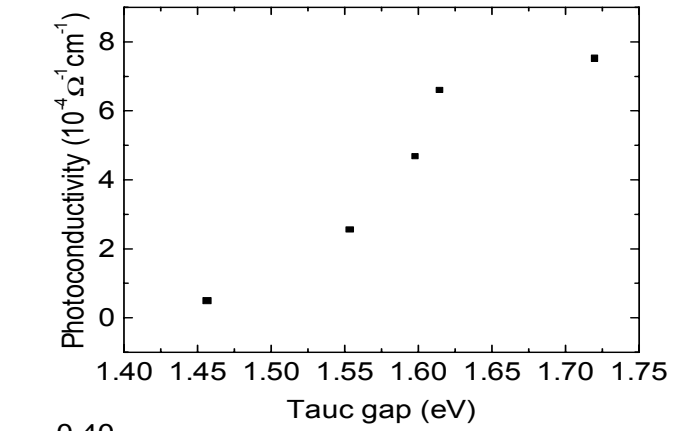

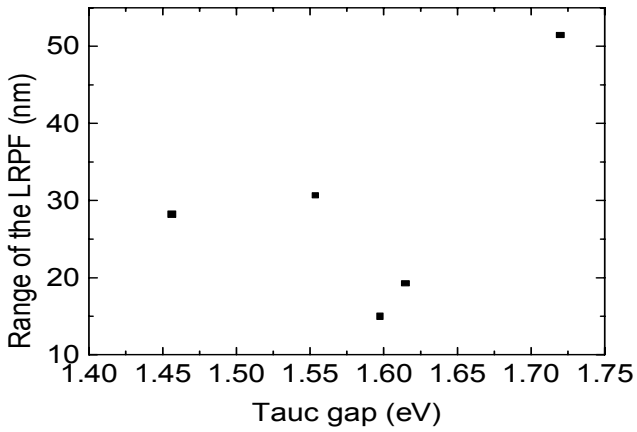

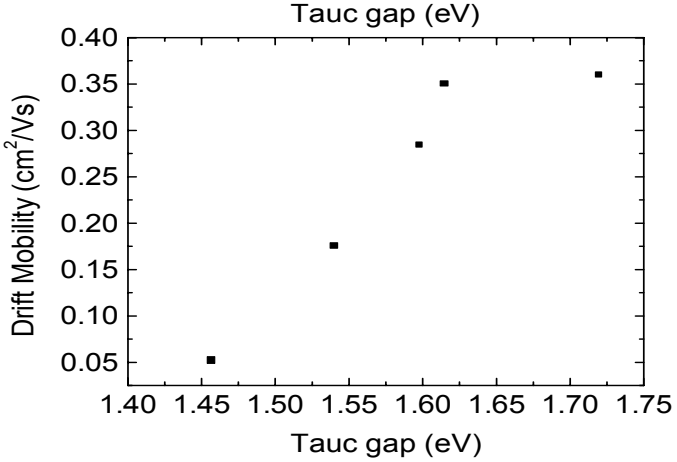

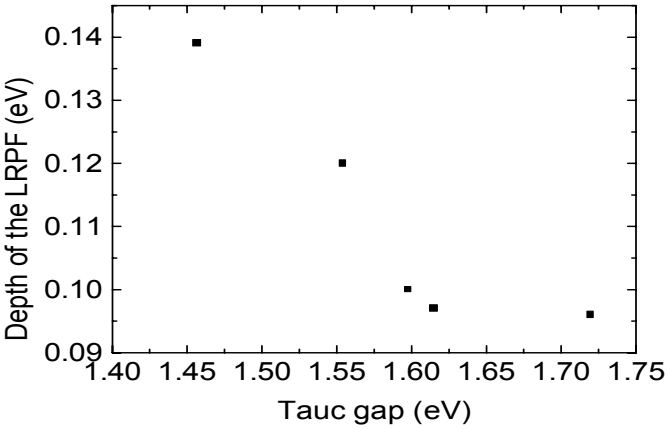

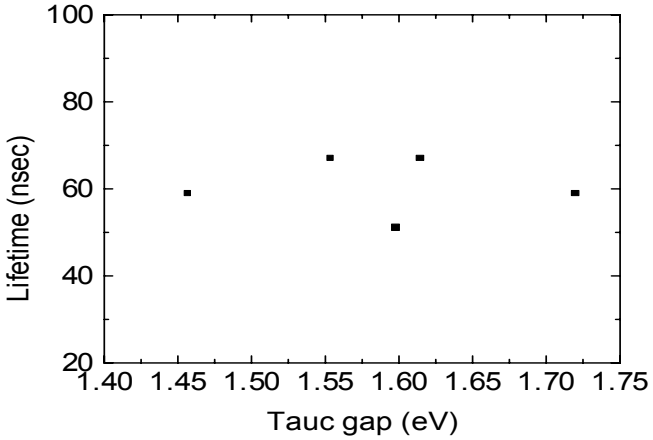

Figure 3. The photoconductivity, drift mobility, lifetime, range and depth dependence on the Tauc gap.

Figure 4, below: (a) The RMS rough as a function of the substrate temperatures. (b) Theannealed state photoconductivity as a function of the substrate temperatures.

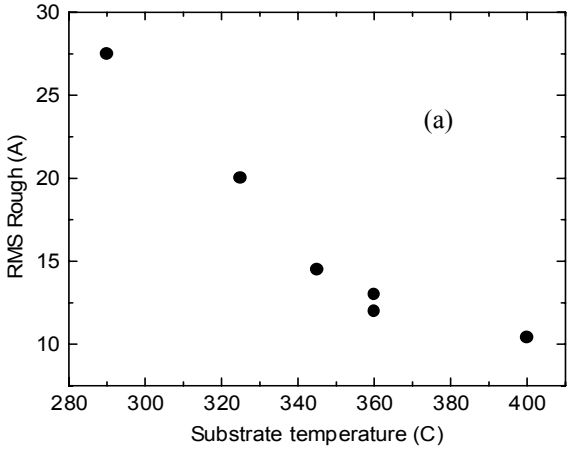

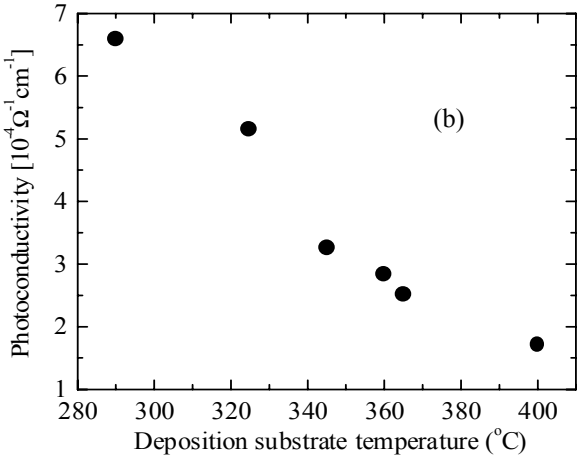

Title: **Optimization of Processing and Modeling Issues for Thin-Film Solar Cell Devices Including Concepts for the Development of Polycrystalline Multijunctions**

Organization: Institute of Energy Conversion, University of Delaware, Newark, DE 19716

Contributors: R. Birkmire, W. Buchanan, E. Eser, S. Hegedus , B. McCandless, T.W.F. Russell, J. Phillips, W. Shafarman

Objectives

The objectives of this research program are to develop the science and engineering base required to advance the development of PV module technology by: 1) developing quantitative relationships between process parameters, film growth, material properties and device performance; 2) developing next generation materials and device structures; and 3) participating in the national PV team activities.

Technical Highlights

$CuInSe_2$ based solar cells: A process to grow $CuIn(SeS)_2$ films using metal precursors reacted in a S-Se atmosphere was developed and quantitatively modeled. $CuIn(SeS)_2$ films were grown with uniform and graded S/Se2 ratios through the film thickness. $Cu(InGa)Se_2$ solar cells with increasing Ga content were analyzed using bi-facial spectral response measurements and the results indicate that the minority carrier diffusion length decreases with increasing bandgap. Solar cells with greater than 13% efficiency were made with evaporated $Cu(InGa)Se_2$ films deposited at 400˚C substrate temperature using a Cu-rich growth process.

CdTe based solar cells: XRD spectra obtained from $CdTe_{1-x}S_x$/CdS thin-film structures were analyzed using a model which incorporated grain size distributions and treatment times to estimate diffusion coefficients and activation energies for bulk and grain boundary diffusion of CdS into CdTe. Techniques for reducing CdS diffusion into the CdTe layer during post-deposition treatment have been developed. Degradation in CdS/CdTe devices only occurs when they are stressed after the application of Cu and/or C contact layers. Irreversible loss in V_{oc} occurs with all contact variations examined to date. The increase in blocking contact behavior at forward bias is related to Cu and can be reversed. Several TCO bi-layer configurations were found that allow the use of thin CdS, less than 100 nm while maintaining V_{oc} greater than 0.8.

Si based solar cells: Attempts to deposit μc-SiC p-layers were unsuccessful. No evidence of Si-C bonding was identified in the Raman spectra of the samples deposited over a wide range of CH_4 and H_2 partial pressures and power densities. However, high conductivity p-layers, >1 S/cm, having a c-Si volume fraction of ~85% were deposited at a power density of 84 mW/cm^2 which is compatible with superstrate p-i-n cell structure. Thin polycrystalline silicon films, ~10 microns, were grown in a hot wire CVD system equipped with a high resolution mass spectrometer. The films had grain size of 30 nm based on XRD with crystalline fractions of as high as 85% based on Raman.

Results

$CuInSe_2$ based solar cells: High bandgap alloys of $CuInSe_2$ are being investigated for their potential to improve manufacturability and performance of modules [1]. $CuInS_2$ films, with Eg = 1.5 eV, were formed by the reaction of sputtered Cu-In layers in a CVD reactor with a flowing gas mixture containing H_2S, O_2 and Ar. After a KCN etch to selectively remove Cu_xS_y from the films, devices were fabricated with efficiency = 8.9%. $CuIn(SeS)_2$ films were formed by reaction in a H_2Se-H_2S-O_2-Ar gas mixture and a quantitative model of the reaction and resulting film composition was developed and verified. Uniform $CuIn(SeS)_2$ films were formed after reaction at 450˚C for 120 min. The composition of the $CuIn(SeS)_2$ film was controlled by the concentration of H_2Se + H_2S in the gas phase and was modeled in terms of a steady state equilibrium based on:

$$2H_2Se + CuInS_2 \Leftrightarrow 2H_2S + CuInSe_2$$

A thermodynamic analysis of this reaction was carried out to predict the solid-vapor phase equilibrium which included the effect of O_2. The results are shown in Figure 1 along with

experimental data used to verify the model. Based on the analysis, graded films were also formed by annealing either $CuInSe_2$ or $CuInS_2$ films in a controlled Se and/or S containing atmosphere.

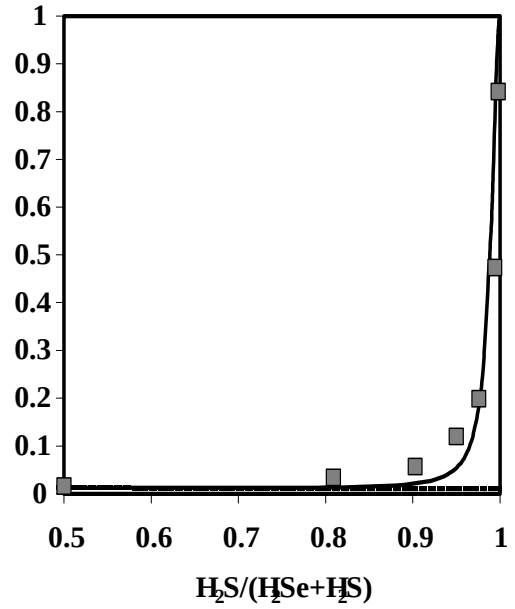

Figure 1. Steady state model for $CuIn(SeS)_2$ formation in $H_2Se + H_2S$. Symbols = data; solid line = model.

We have previously shown that solar cells fabricated from $Cu(InGa)Se_2$ films with $Ga/[In+Ga] \leq 0.3$ corresponding to $Eg \leq 1.3$ can be made with efficiency, ~15%. However, with higher bandgap, the device efficiency decreases due primarily to a decrease in fill factor and open circuit voltage. Current-voltage and quantum efficiency measurements have shown that the main cause of this decrease is a voltage dependent light generated current, $J_L(V)$. The cause for this $J_L(V)$ was analyzed by bi-facial spectral response measurements as a function of applied voltage to determine the changes in collection efficiency [2]. Devices were made from $Cu(InGa)Se_2$ films with uniform composition deposited by elemental evaporation at two different Ga compositions, $Ga/[In+Ga] = 0.30$ and 0.65. The films were deposited on soda lime glass coated with a semi-transparent Mo having a transmission of ~10% to allow the spectral response measurements through the back contact. There was no significant difference in the current-voltage behavior due to the thin Mo other than an increase in series resistance. Spectral response measurements through the CdS window layer and Mo back contact were made and expressions for minority carrier collection were then used to analyze the data to determine the minority carrier diffusion length, the space charge width, and the absorption coefficient. The analysis showed that the decrease in the light generated current with increasing voltage was primarily due to a reduction in minority carrier diffusion length from about 0.8 to 0.1 μm.

The effect of reducing the substrate temperature for $Cu(InGa)Se_2$ deposited by elemental evaporation from 550 to 400˚C is being evaluated because lower deposition temperature has significant potential manufacturing advantages. Using a 'standard' process, evaporation rates are varied to give a Cu-rich initial stage of growth with $Cu/(In + Ga) > 1$ followed by an In-Ga-Se layer to achieve a final composition with $Cu/(In + Ga) \approx 0.9$. The grain size in the $Cu(InGa)Se_2$ films decreased as the temperature decreased with no change in performance of solar cells as discussed below.

An alternative process, in which the Cu, In, Ga and Se fluxes are kept constant throughout the deposition, results in $Cu(InGa)Se_2$ films with smaller grains than those formed using the Cu-rich growth phase and the grain size decreases with decreasing temperature. There are no other apparent differences between the $Cu(InGa)Se_2$ films grown by both processes. All films have uniform composition through the films based on Auger measurements and the same crystallographic texture. Solar cells were fabricated on $Cu(InGa)Se_2$ samples deposited by both processes at different temperature and the results for the best cells are summarized in Table 1. The films all have $Ga/(In+Ga) \approx 0.3$ and the devices have the structure of glass/Mo/$Cu(InGa)Se_2$/CdS/ZnO/Ni/Al grids. The deposition using constant flux gives better cell performance at $T_{ss} = 550$˚C, despite the smaller grain size. Conversely, at $T_{ss} = 400$˚C, the process with a Cu-rich phase gives much better device performance. The results indicate that there is not a simple relationship between grain size and device performance.

Table 1. Summary of the J-V results for the best cells obtained in recent experiments using $Cu(InGa)Se_2$ films deposited with graded and uniform processes and T_{ss} = 550 and 400˚C.

T_{ss} (˚C) process	550 Graded	400 Graded	550 Uniform	400 Uniform
V_{oc} (V)	0.582	0.594	0.633	0.536
J_{sc} (mA/cm^2)	32.6	32.9	31.5	28.1
FF (%)	71.7	68.1	75.7	63.4
η (%)	13.6	13.3	15.1	9.5

CdTe based solar cells

CdTe-based solar cells are made using physical vapor deposited CdS and CdTe films and vapor processing techniques to quantify and control the physical and chemical interaction between CdS, CdTe, $CdCl_2$, and O_2 [3,4,5,6]. Cells are also fabricated on materials provided by other organizations at different processing stages.

Analysis of the microstructure and microcomposition of $CdTe_{1-x}S_x$/CdS thin-film structures using symmetric and glancing x-ray diffraction, EDS, and TEM has led to a chemical basis for the CdTe-CdS-$CdCl_2$-O_2 system. XRD spectra have been evaluated to estimate the bulk and grain boundary diffusion coefficients and activation energies using a model that incorporates measured grain size distributions and treatment time. The diffusion coefficients for CdS into CdTe at fixed $CdCl_2$ and O_2 partial pressures were estimated to be 10^{-13} cm^2/sec for bulk and 10^{-8} cm^2/sec for grain boundary and the corresponding activation energies estimated from data over the 380˚C to 480˚C temperature range are 2 eV and 3 eV, respectively.

Techniques for reducing CdS diffusion into the absorber layer during post-deposition treatment have been developed: 1) using a $CdTe_{1-x}S_x$ alloy absorber layer, with x less than or equal to the solubility limit of CdS in CdTe to reduce the concentration driving force for diffusion; 2) incorporating a brief, less than 5 minute, anneal at T ~ 600˚C prior to the $CdCl_2$ treatment to reduce the CdTe grain boundary density; and 3) using vapor $CdCl_2$ treatments to control the vapor species responsible for enhancing diffusion. Alternative TCO structures have been evaluated in conjunction with the National CdTe Team. Several bi-layer configurations have been found that maintain high V_{oc} when the final CdS film thickness is less than 100 nm. For example, Libbey-Owens-Ford conductive tin oxide over-coated with more resistive tin oxide made at Golden Photon yielded CdTe/CdS devices with V_{oc} = 800 mV and 730 mV for final CdS film thickness of 80 nm and < 10 nm, respectively. Similar results were obtained from structures with a conductive indium-tin oxide layer coated with a resistive inter-layer of indium-tin oxide.

Many CdTe devices exhibit degradation in V_{oc} of 0.1-0.2 V and in FF of 10 to 20% when exposed to elevated temperatures of 80-100°C in air under forward or reverse electrical bias. Typically, a “roll-over” in forward bias associated with a blocking contact is observed. Key results have been obtained this year providing insight into degradation of CdS/CdTe solar cells by stressing at various stages of the post deposition processing. Devices were made on CdTe/CdS material supplied by Solar Cells, Inc. Post deposition contact treatments were performed at IEC and the cells were stressed at open circuit at 1.5 suns and 100°C for 6 days. CdS/CdTe layers stressed after $CdCl_2$ heat treatment but before receiving Cu layer exhibited no degraded behavior after contacts were applied. Devices stressed after receiving the 150Å Cu layer but before the C contact showed only the loss in V_{oc}; “blocking contact” behavior was completely absent. Re-stressing the same devices with the C contact results in a blocking contact and further loss of FF but no further loss in V_{oc}. However, devices receiving an additional Cu layer after being stressed with the first Cu showed no blocking contact after being re-stressed with C contacts, also with no change in V_{oc}. Physically removing the initial C contact of a degraded device and re-contacting with C eliminated the blocking contact behavior but did not restore V_{oc}. Finally, devices stressed without Cu but with the C contact had

poorer initial performance, as expected from the lack of Cu doping, but still showed comparable degradation in both V_{oc} and FF.

Si based solar cells

During 1998 efforts were concentrated on the development of a process leading to SiC p-layers compatible with a superstrate p-i-n cell structure, deposited in a RF PECVD system. Experimental variables were dopant gas, CH_4 and H_2 gas flows normalized to the sum of SiH_4 and CH_4 flows, and power. For convenience the normalized gas flow parameters are labeled as "c" and "h" respectively.

No evidence of Si-C bonding was identified in the Raman spectra of the samples deposited with $c<0.5$, $0<h<227$ and power densities from 80 mW/cm^2 to 400 mW/cm^2. The only crystalline phase identified was Si [7]. Compared to B_2H_6, doping with $B(CH_3)_3$ lowered the conductivity by a factor of 40 and reduced the fraction of crystallinity from 87% to 53% [7]. Also, crystalline Si fraction decreased strongly with increasing c. Finally, it was demonstrated that high conductivity p-layers (>1 S/cm) having high c-Si volume fraction (~85%) can be deposited on glass at a power density of 84 mW/cm^2 which is compatible with deposition on TCO substrates for device fabrication.

In the films deposited with $c \geq 0.5$, we observed again no crystalline SiC phase. For $c = 0.83$ and 0.94, films had no c-Si or a-SiC:H phases. However, films deposited with $c = 0.5$ at a power density of 160 mW/cm^2 showed the presence of both crystalline Si and a-Si:C:H phases. The actual structure of the films depended on hydrogen dilution h and on the nature of the substrate. Films deposited on SnO_2 have no identifiable structure for $h = 5$ but as h is increased change gradually from a-Si:C:H to c-Si. On glass, however, the films were a-Si:C:H at h=5 but become almost entirely c-Si at all higher hydrogen dilution levels.

A new effort was initiated to develop a process to deposit thin polycrystalline Si films at low temperature, < 700˚C ,and collaborations with AstroPower and NREL researchers were established to support the research. Thin polycrystalline Si films, ~10 microns, were grown in a new hot wire CVD system equipped with a high resolution mass spectrometer. The primary efforts have focused on: 1) establishing the system control and reproducibility; 2) eliminating contamination in the Si films; 3) calibrating the mass spectrometer to determine radical concentrations during film growth; 4) developing diagnostic tools to characterize the crystallinity of the films; and 5) determining growth condition to form polycrystalline Si films.

Thin polycrystalline films were deposited using both pure SiH_4 and a mixture of H_2 and SiH_4 on 7059 glass substrates over a range of total flow rates, pressure and wire temperatures. The impurity concentration in the films was evaluated by SIMS. The levels of O and C were comparable to that seen in typical a-Si films grown by plasma CVD. The structure of the films correlates primarily with residence time of the gas in the deposition zone and wire temperature. The structure of the films varied from amorphous to microcrystalline with grain size of 30 nm based on XRD with crystalline fractions of as high as 85% based on Raman. Concentration of Si, SiH, SiH_2 and SiH_3 resulting from the decomposition of SiH_4 during film growth have been measured for residence times from 4 to 12 sec. to determine how the radical concentrations affect film structure.

References:

1. R.W. Birkmire and M. Engelmann, presented at the 15th NCPV Prog. Rev. Mtg., Denver, CO, Sept 9, 1998.
2. J.E. Phillips and W.N. Shafarman, presented at the 15th NCPV Prog. Rev. Mtg., Denver, CO, Sept 9, 1998.
3. B.E. McCandless, L.V. Moulton, and R.W.Birkmire, *Prog. in PV*, Vol. 5 (1997), 249.
4. B.E. McCandless, I.Youm, and R.W.Birkmire, *Prog. in PV*, Vol. 6 (1998).
5. B.E. McCandless, J.E. Phillips, and J. Titus, *Proc. 2nd WCPVEC*, Vienna, 1998.
6. B.E. McCandless and R.W. Birkmire, presented at the 15th NCPV Prog. Rev. Mtg., Denver, CO, Sept 9, 1998.
7. E. Eser, S. Hegedus, W. Buchanan, presented at the 15th NCPV Prog. Rev. Mtg., Denver, CO, Sept 9, 1998.

Title: **Future CIS Manufacturing Technology Development Current)/ Processing of $CuInSe_2$ - Based Solar Cells: Characterization of Deposition Processes in Terms of Chemical Reaction Analysis**

Organization: Chemical Engineering, Electrical Engineering, and Materials Science and Engineering Departments, University of Florida, Gainesville, FL 32611

Contributors: T. Anderson, Principal Investigator; O. Crisalle, P. Holloway, and S. Li, Co-Investigators; C.H. Chang, C. Huang, M. Ider, S. Kim, S. Kincal, L. Reith, and B. Stanbery, Graduate Research Assistants.

Objective

The primary objective of this continuation project is to develop improved processing schemes for the fabrication of $CuInSe_2$-based solar cells. The previous project initiated research on the development of a high-rate process to produce device quality thin films of CIS-based materials. Important components of this program included the use of plasma sources, novel precursor film structures, dry buffer-layer processing, and rapid thermal processing. The current project continues the effort with added research in process control and the addition of Ga to the absorber material.

Approach

A team of researchers from 3 disciplines is working to demonstrate a process for rapid fabrication of CIS absorber layers which is suitable for the manufacture of high efficiency thin film modules. This process first deposits a thin 'seed' layer of large grain size CIS at low rate by a migration enhanced process, followed by high rate deposition of a mixed phase precursor material using a plasma assisted process. An analysis of the phase equilibria in the Cu-In-Se system has suggested the use of stacked binary compounds of CuSe, Cu_3Se_2 or $CuSe_2$ and InSe, In_6Se_7 or In_4Se_3 will produce a low temperature liquid phase to assist in the formation of large grain size CIS films. This work will verify the approach in CIS, extend it to CIGS, explore the use of Rapid Thermal Processing (RTP) and implement advanced process control strategies.

The program is also comparing the performance of cells incorporating the buffer layer materials $In_x(OH, S)_y$ and Mg (S, Se), which are potential alternatives to conventional CBD CdS. Initial deposition of these materials will be attempted using CBD, and if found promising, work will be directed at dry processing (e.g., MOCVD). The motivation for this approach includes the elimination of a wet processing step and incorporation of a Cd-free material.

It is believed that the carrier mobility in the ZnO TCE layer can be increased by improving the film microstructure. Increasing the carrier mobility would allow the carrier concentration to be reduced and thus improve the transparency of the film. This hypothesis is being investigated, and the critical microstructural features and the relation of their formation to processing parameters are being identified.

A significant effort is being made to accurately describe the phase equilibria and thermochemistry of the Cu-In-Ga-Se system. This knowledge will assist in understanding such issues as conductivity type conversion in the near surface region of CIGS, interactions of CIGS with buffer layer materials, and absorber film formation processes. The approach is to first collect literature data and perform a full assessment on subsystems. The initial assessment then suggests inconsistencies and critical missing thermodynamic properties. An experimental effort that involves synthesis and equilibration, DTA, XRD, XFAS, and e.m.f. is then pursued to measure key properties.

Precursor Film Deposition

CIS and binary precursor film deposition is being conducted in our laboratory in a custom- designed, rotating-disc reactor that accommodates multiple substrates. A rotating platen to translate substrates through four reactor zones: chalcogen deposition, heating, metal deposition, and a relaxation zone. This modulation of reactant fluxes allows longer adatom diffusion time and thus achieves good crystallinity at lower processing temperature. As an example, this process was used to deposit CIS in a single stage, three-layer process using periodic heating to peak temperature on the order of 550° C [1]. In this process layer 1 was deposited with a Se/In molar ratio 5, layer 2 with a Se/As molar ratio 5, and layer 3 with a Se/Cu molar ratio 9 and In flux 60% of that used in layer 1. Compositional and structural characterization showed that single-phase α-$CuInSe_2$ films were formed by this process, but In segregates to the surface (Figure 1).

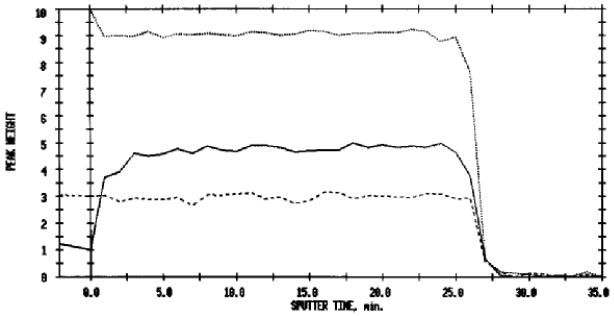

Figure 1. AES sputter profile of CIS absorber.

The Na background concentration was determined by SIMS analysis, and the doping levels were estimated to be an order of magnitude lower than those reported for growth on soda-lime glass by conventional processes with larger thermal budgets. The lower background Na level has permitted us to control the location and extent of Na doping by incorporating a NaF source in the deposition chamber.

Considerable interest exists on the role of Na in improving the absorber microstructure and the cell performance. A model was developed [2] for the incorporation of Na based on the reported existence of the ternary compound $NaInSe_2$ and the published phase diagram for the analogous Li-Cu-In-Te quaternary system. The proposed role of Na is that of a surfactant, enhancing cation sublattice defect aggregation and surface segregation of excess indium as either a quaternary compound or solid solution of $NaInSe_2$ and $CuInSe_2$.

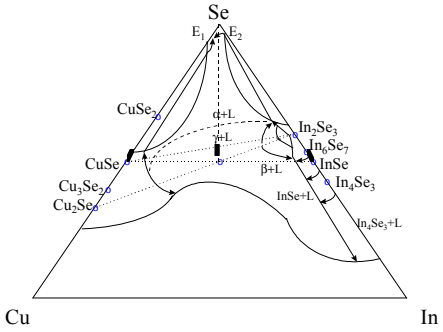

Figure 2. Liquidus projection for Cu-In-Se ternary system.

The work on the role of Na was extended to CIGS with the use of high resolution XPS to study the near surface region of the absorber film [3]. The analysis of measurements performed on device quality films indicates the computed ratio [Cu + Na]/[In + Ga] is constant to within the accuracy of measurement, although the Cu is depleted in the near surface region. This result is consistent with the substitution of Na and Cu lattice vacancy sites, leading to the formation of a thin Na-containing phase at the surface.

Rapid Thermal Processing

Rapid Thermal Processing is an attractive technique with the advantages of high throughput, low thermal budget, and better control of process kinetics. In this program, stacked binary compounds rather than elemental layers were used as the precursor structure for RTP synthesis of $CuInSe_2$ thin films [4,5]. To assist in identifying suitable compositions for the binary layers, the Cu-In-Se phase diagram was estimated and a liquidus projection is shown in Figure 2. It is noted that the eutectic valley between the binary eutectic composition E_1 and E_2 is nearly degenerate and thus exists at slightly below 220° C. The dash line in Figure 2 connecting the pure Se corner to the $CuInSe_2$ $_{compound}$ indicates it should be possible to form CIS in the presence of an intermediate low temperature liquid phase to produce the α-phase and Se, which should volatilize. To test this prediction a series of bi-layer, binary precursor films were deposited using our deposition system and processed using RTP. XRD and Raman scattering measurements confirmed the precursor structure In_4Se_3 / $CuInSe_2$ / Cu_2Se resulted from the deposition of the first and third layers at the deposition temperature 200 °C and their limited reaction at their interface. Three values of the set point temperature (220, 290, 500 °C) were used to RTP the precursor film. Characterization of the processed films showed that no reaction occurred at 220 °C, but that most of the In_4Se_3 phase disappeared and formed CIS at 290 and 500 °C. Work is now underway to fully explore this reaction pathway.

Buffer Layer Deposition

Prior studies of CBD CdS have reported that films contain a mixture of crystal structures. Although the hexagonal wurtzite phase of CdS is slightly more stable than the cubic phase, both crystal structures have been reported in the literature. Both XRD and Raman were used to characterize CBD CdS films, but the similarity of the cubic and hexagonal structures in combination with the low signal level from thin film samples render these techniques ineffective for differentiating the crystal structure. Selective Area Diffraction, however, was successfully used to identify the hexagonal phase in our films. Plan view TEM micrographs indicated the grain size was on the order of 10 to 30 nm.

To better understand why a CBD CdS is a critical component of high efficiency cells, the effect of various CdS buffer layer processes (i.e., CBD, MOCVD and sputtering) on the excess carrier lifetimes and material properties of CIGS cells was studied. A contactless, non-destructive reflection or transmission mode Dual Beam Modulation (DBOM) technique [6] was developed by this group and applied to the films produced by the different buffer layer processes. The results show that the excess carrier lifetime increases in all CIGS films received from 3 different laboratories when CdS was deposited, regardless of the method [7,8]. Furthermore, the increase in the lifetime after CdS deposition was less for water and Cd-partial electrolyte treated samples than for as-deposited samples. It was also observed that Ar plasma cleaning prior to deposition of CdS had a negative effect when sputtering, perhaps as a result of ion damage. Intermediate surface treatments such as DI water rinse, Cd-partial electrolyte dip, or Ar plasma cleaning do not offer a significant advantage. These results suggest that the CdS influence goes beyond the CIGS surface layer.

Thermochemistry and Phase Equilibria

A comprehensive assessment of the Cu-In-Ga-Se system is being performed with full assessments of the Se unary, and the Cu-In, Cu-Se, and In-Se binaries having been performed. In addition, estimates of the Cu_2Se-In_2Se_3 pseudobinary and the Cu-In-Se ternary phase diagrams have been made. To supply critical property values, selected experiments have been performed using e.m.f., DTA, and XRD determinations. Specifically the Gibbs energy of formation of the compounds Cu_2Se, Ga_2Se_3, $CuInSe_2$ (α and δ), $Cu_2In_4Se_7$, $CuIn_3Se_5$, and $CuIn_5Se_8$ has been measured. Additionally, component activities were measured in the Cu-Se and In-Se, along with the range of solid solution in $Cu_{2-x}Se$ by coulometric titration. DTA was also performed on selected compositions

around the compound $CuInSe_2$. These results will be incorporated in future assessment activities and used to estimate more complicated phase diagrams.

Collaborations

The team at the University of Florida has been an active collaborator in the Thin Film Partnership through its participation in the various teams. Specific collaborations have been established with Global Solar Energy and International Solar Electric Technology, Inc.

References

1. Stanbery, B.J.; Huang, C.H.; Chang, C.H.; Anderson, T.J. (1998). "Characterization and Processing of $CuInSe_2$ Solar Cells." *Proc. 2nd World Conference on Photovoltaic Solar Engineering.* Vienna, Austria (to be published).

2. Stanbery, B.J.; Chang, C.H.; Anderson, T.J. (1998). "Engineered Phase Inhomogeneity for CIS Device Optimization." *Institute of Physics Conference* Ser. No.152; pp. 915-922.

3. Stanbery, B.J.; Lambers, E.S.; Anderson, T.J. (1997). "XPS Studies of Sodium Compound Formation and Surface Segregation in CIGS Thin Films." *Proc. 26th IEEE Photovoltaic Specialists Conference*, Anaheim, CA; pp. 499-502.

4. Chang, C.H.; Stanbery, B.J.; Morone, A.; Davydov, A.; Anderson, T.J. (1998). "Novel Multilayer Process for $CuInSe_2$." *Materials Research Society Symposium Proceedings* (485); pp.163-168.

5. Stanbery, B.J.; Davydov, A.; Chang, C.H.; Anderson, T.J. (1997). "Reaction Engineering and Precursor Film Deposition for CIS Synthesis." *NCPV Photovoltaics Program Review; Proceedings of the 14th Conference; Lakewood, CO; American Institute of Physics Conference Proceedings (394); pp. 579-588.*

6. Li, S.S.; Stanbery, B.J.; Huang, C.H.; Chang, C.H.; Chiang, Y.S.; and Anderson, T.J. (1996). "Effects of Buffer Layer Processing on CIGS Excess Carrier Lifetime: Application of Dual-Beam Optical Modulation to Process Analysis." *Proceedings 25th IEEE Photovoltaic Specialists Conference*, Washington, DC; pp. 821-824.

7. Chang, C.H.; Morone, A.A.; Stanbery, B.J.; McCreary, C.; Huang, M.; Huang, C.H.; Li, S.S.; Anderson, T.J. (1998). "Growth and Characterization of CdS Buffer Layers by CBD and MOCVD." *NCPV Photovoltaics Program Review; Proceedings of the 15th Conference; Denver, CO.*

8. Huang, C.H.; Li, S.S.; Stanbery, B.J.; Chang, C.H.; Anderson, T.J. (1997). "Investigation of Buffer Layer Processing on CIGS Excess Carrier Lifetime: Application of Dual-Beam Optical Modulation to Process Analysis." *Proc. 26th IEEE Photovoltaic Conference*, Anaheim, CA; pp. 407-410.

Title: **Properties of Wide-gap Chalcopyrite Semiconductors for Photovoltaic Applications**

Organization: Department of Materials Science and Engineering
University of Illinois, Urbana, IL

Contributors: A. Rockett, Principal Investigator; G. Berry, Shawn O'Conner, Dongxiang Liao, graduate research assistants; Benjamin French, Jessica Nelson, and Jens Niemax, undergraduate research assistants.

Objectives

The objectives of this project are to develop a fundamental understanding of wide-gap chalcopyrite semiconductors and photovoltaic devices. Information to be obtained includes significant new fundamental materials data necessary for accurate modeling of single and tandem-junction devices, new information on the basic materials science of wider-gap chalcopyrite semiconductors to be used in next-generation devices, and practical information on the operation of devices incorporating these materials.

Approach

Thin film epitaxial and polycrystalline layers of $Cu(In,Ga)(S,Se)_2$ are to be produced and characterized. Deposition uses a hybrid sputtering and evaporation method shown previously to produce high-quality epitaxial layers of $Cu(In,Ga)Se_2$. Initial depositions of sulfide alloys will produce polycrystalline materials for purposes of rough stoichiometry and deposition temperature determination. Upon satisfactory results on glass, we will switch to GaAs substrates and increase the deposition temperature consistent with our experience for deposition of selenides. We will characterize the layers using a wide array of state-of-the-art optical, electrical, microchemical and microstructural analysis available at the University of Illinois. The deposition of sulfides is just beginning with the design and installation of a sulfur effusion cell in the hybrid deposition system. This will be completed shortly. Initial sulfide depositions have not yet begun.

We are continuing our previous experiments characterizing the effect of impurities in single crystals where Hall effect measurements are more effective than in common device materials. The results described below were recorded for CIGS deposited in a single step from magnetron sputtered Cu and In fluxes and evaporated molecular Se. The single crystal $CuIn_{1-x}Ga_xSe_2$ layers were deposited directly on "epi-ready" GaAs (001) or $(111)_{As}$ wafers. Deposition temperatures were ~650°C. Samples were ion implanted with elements which may occur as contaminants by diffusion across CIGS heterojunctions. In the current work, Zn and Cd were used. In addition, Ar, an inert species, and O, a common impurity in deposition chambers, were tested. The results to date are preliminary but suggestive.

We have begun a new effort this fall in simulation of devices using the AMPS model developed by S. Fonash and coworkers at the Pennsylvania State University. The purpose of this project is to evaluate the data obtained previously by this project in device performance. No results have been obtained yet.

Microstructural studies for this project were carried out by X-ray diffraction and by scanning electron microscopy. Composition analyses used secondary ion mass spectrometry (SIMS), and energy-dispersive spectroscopy. Hall-effect measurements were obtained as a function of temperature using gold contacts in a van der Pauw pattern. Characterization of Na transport in CIGS and Mo deposited at several industrial laboratories has been continued out using SIMS as part of the NREL CIS team effort. Finally, we have established an active collaboration with Professor Larry Olson from Washington State University and Siemens Solar Industries to investigate interaction across ZnO/CIGS heterojunctions.

Results (10/1/97 - 9/30/98)

Point Defects in CIGS

This year we have spent some time considering the implications of our previous results in the context of device performances. We plan to make the following more quantitative with modeling work now underway. The following is a summary of Reference 1 where complete details and arguments are given.

Typical CIGS photovoltaic devices consist of heterojunctions between group III-rich p-type CIGS and an n-type window layer. The material contains large numbers of In_{Cu} (divalent, double donor) antisite defects and Cu vacancies (monovalent acceptors) clustered via $In_{Cu}^{+2} + 2\ V_{Cu}$ □ $[V_{Cu}In_{Cu}V_{Cu}]^{0}$. We suggest that these ordered defects then form a lattice of defect superclusters such that each In_{Cu} antisite defect is surrounded by V_{Cu} and each vacancy by antisite defects. The result, platelets of defects surrounded by nearly perfect lattice is supported this structure has been found by TEM characterization of the "135" ordered defect phase $CuIn_3Se_5$. If defect clusters did not themselves cluster, defects would occupy such a large portion of the lattice that it would be impossible to find relatively undisturbed areas of CIS. This would radically change the band structure. Around the perimeter of these superclusters, unpaired defects would occur which we propose act as acceptors. The number of acceptors would then change little with changes in composition because the perimeter area of superclusters varies slowly with fraction of clusters, as observed. The number and type of defects observed by us previously are consistent with this interpretation.

We have proposed a model involving decomposition of such superclusters near the front contact of a CIGS solar cell. This pins the Fermi level the Cu_{In}^{+2} ionization energy energy until sufficient charge has accumulated to convert all of the defects in the affected region to the double charge state. In device-quality material, this pinning is probably insignificant because of a low density of these defects. Much more important is the double ionization level for the In_{Cu} defect. Raising the Fermi energy above the ionization level of the In_{Cu}^{+2} defect destabilizes the defect clusters. It is unlikely that at equilibrium, the Fermi energy could rise above this defect state energy. It is proposed that pinning of the Fermi energy by changes in the charge state of the antisite defects may limit the collection field. It is proposed that this limits the open circuit voltage of CIGS solar cells and may result in the light soaking improvement in these devices.

Ga is an important alloying element, significantly improving the performance of CIGS devices ~25% Ga. Larger amounts of Ga decrease performance. Our data suggest that Ga reduces the enthalpy of formation or clustering of defects. This results in a dramatic rise in electrically active states in CIGS grown at high temperatures. In CIGS devices, this would result in reduced depletion lengths and greater recombination rates in high Ga content devices. The results are consistent with analysis of high Ga content devices. Ga also affects the ratio of donors to acceptors as a function of composition, increasing acceptor formation far beyond formation of donors. This is consistent with general observations of polycrystalline CIGS as well.

Finally we proposed that Na forms stable clusters with In_{Cu} donor defects at supercluster perimeters. In heavily-compensated material such as is typical in devices this may have the effect of raising the carrier concentration and could have the effect of increasing clustering of existing defects. Device performances degrade with excessive Na addition. We conclude that the amount of Na needed is only that necessary to eliminate compensating states and to modify microstructure. Additional Na causes disorder and damages the resulting crystals.

Other Research Efforts

Many new efforts have begun this year and are at a preliminary stage. Consequently many of the results reported below are preliminary. We anticipate establishing the results more conclusively in the coming year.

The Effect of Impurities on CIGS

We have performed preliminary characterization of the effect of Cd and Zn ion implantated into CIGS single crystals. The results indicate that while significant ion damage is done by these elements as previously found for Cr and Se implantation, the damage can be almost completely removed by annealing at 650°C. Preliminary results suggest that Zn has almost no effect on the properties of the CIGS after annealing. However, some changes at lower temperatures were observed with Cd implanation. A full analysis of the data is currently underway. Until this analysis is complete it is difficult to say what the detailed effect of Cd is, although it is probably not a deep trap state.

Even more preliminary results are available for implantation of oxygen and argon. Data obtained to date indicate that ion damage is non-recoverable upon annealing or that these atoms significantly degrade the conduction properties of CIGS thin films. Implantation of species at other ion doses will beconducted during the coming year to determine the effect quantitatively.

This result is signficant in that Cd is occasionally found distributed throughout a wide region of the CIGS in polycrystalline device layers (data from SIMS analysis performed at both NREL and in this group). While this Cd is presumably located in grain boundaries, it may have some effect on the conduction properties of the material. ZnO is a common heterojunction material, consequently the effects of Zn and O on the device are important for understanding heterojunction behaviors in the absence of a CdS layer. The Zn data indicates that Zn diffusion across the interface may not be critical but oxygen could have a detrimental influence on device performances. Both Zn and O diffusion have been observed (see below) in work conducted in collaboration with Siemens Solar Industries and Washington State University.

Na and Ga Redistribution During Selenization Reactions

Several studies of the behavior of Na have been in progress this year as part of our participation in the CIS Mo Team. Results of characterization of thin films of Mo deposited by dc magnetron sputtering on soda lime glass (Mo/SLG) and $CuInSe_2$ (CIS) on Mo/SLG had as the primary objective to clarify the factors determining the concentration of Na in commercial-grade CIS. Mo films were deposited by three laboratories manufacturing CIS thin film solar cells. Analysis was by secondary ion mass spectrometry (SIMS), scanning electron microscopy (SEM) and X-ray diffraction (XRD). Changes in Mo deposition parameters in general_affected the_Na level but there was no obvious link to any single Mo deposition parameter. Oxygen content directly affected Na level. The Na behavior was not obviously connected to film preferred orientation. Na distributions in CIS deposited on the Mo were not limited by diffusivity of the Na. The Na concentration in the CIS was increased by annealing the Mo films both with and without intentionally added Na. The Na level in the CIS appears to be set more by the CIS deposition process than by the Na concentration in the Mo so long as the Mo contains sufficient Na to saturate the available sites in the CIS.

Na behavior has further been examined in commercial CIGS formed by selenization using H_2Se and elemental Se vapor. Several preliminary conclusions can be drawn from this work. First, under optimal conditions, added Na has a larger effect on the films than does the choice of substrate glass. The Na is found primarily in the areas of the CIGS where Ga is also found. This is probably due to the decrease in grain size in those regions rather than to the presence of higher amounts of Ga or O there. S, deposited with the Na does not end up in the same area as does the Na. Rather, it tends to move toward the surface and accumulate in a buried layer. This is probably due to the reaction process rather than to the microstructure. Device performances improved with modest amounts of added Na on borosilicate glass. Device performances on soda-lime glass were not improved by adding Na. The supply of Na appears to have been adequate from the glass itself. A study is currently underway of dynamic process of redistribution of Na and Ga during selenization using H_2Se.

Selenization of Mo layers was also examined. Elemental Se vapor was found to produce significantly less selenization than H_2Se. The amount of selenization was also strongly

dependent upon Mo deposition conditions, although a specific source of the change in reaction rate was not found.

ZnO Work

Preliminary results have been obtained on the distribution of Zn and O across ZnO/CIGS interfaces as part of a study of the performance of solar cells lacking a CdS buffer layer. This study has compared the depth distribution of Zn and O across ZnO/CIGS heterojunctions with both single crystal epitaxial CIGS and in standard device layers. Device layers were deposited at Siemens Solar Industries, single crystal epitaxial layers were deposited by us, and all ZnO layers were formed at Washington State University. SIMS analyses were conducted by us. Results are highly preliminary but suggest that ZnO diffuses into the grain boundaries of the CIGS polycrystals even at relatively low temperatures. This work will be continued during 1999.

Conclusions

All of our work in the past year has continued to demonstrate the importance of point defects and their migration on the performance of CIGS for solar cells. We conclude that it is the careful control of point defect densities and clustering that determines the success or failure of a standard CIGS solar cell. Work in progress will establish the validity of this conclusion. In addition, we are collecting data on several specific issues of interest to the solar cell community.

Title: **Search for Factors Determining the Photodegradation in High-Efficiency a-Si:H-based Solar Cells**

Organization: Department of Physics & Astronomy, University of North Carolina at Chapel Hill, Chapel Hill, North Carolina

Contributors: Daxing Han, principal investigator; investigators; Jonathan Baugh, Lei Wu, Guozhen Yue, and Jing Lin.

Introduction

The central unsolved problem in the study of hydrogenated amorphous silicon (a-Si:H) is the metastability. The microscopic origin of such metastability is still unclear. Recently, Branz at NREL suggested a H-collision model that explains most of the photo-induced-degradation dynamics including low temperature defects creation.[1] On the other hand, Carlson et al [2,3] at Solarex suggested that the local motion of protons near silicon dangling bonds results in the acceleration recovery. Both the models suggested that H motion is crucial for the photo-degradation and recovering. Can we observe this microscopic local motion? Can we link the H microstructure to SWE? These are the major issues of our research program and studied by NMR, DIR and stress. The other issue is to improve understanding of carrier collection andopen-circuit voltage limitations of a-Si:H-based solar cells. The offer will carry out internal field profile determinations using the null-currenttransient measurements and the recombination losses via midgap and tail-state defects using the luminescence measurements.

Light-induced Changes of Si-H Bond Absorption in a-Si:H Films Studied by DIR[4]

Device-quality a-Si:H films with more or less SWE prepared by GD and hot-wire CVD were studied. The total H content varies between 2-15 at.%. There were no measurable light-induced changes of the IR absorption by the IR spectrometer. However, by using the differential infrared (DIR) technique, we have observed 0.5-1% photoinduced changes upon AM1 light-soaking: (a) for the less stable sample prepared by pure SiH_4, there is a simultaneous decrease near 2040 cm^{-1} and an increase near 1880 cm^{-1}. Light-induced H-bond redistribution [1,5] could be the origin for such changes. At this point, we are not sure whether the Si-H trapped in microvoids or the SiH_2 species are responsible for the 2040 cm^{-1} peak. (b) for the more stable samples prepared by GD with H-diluted SiH_4 and hot-wire CVD, the DIR absorption near 2000 cm^{-1} increases upon light soaking. One possibility is the change of the oscillator strength caused by the change of local environments (e.g., local charge distribution) of the Si-H bonds.

Correlation between Photoinduced Volume Expansion and SWE in Hot-wire a-Si:H[6,7]

We observed that the less Si-H bonds, the lower compression in the hot-wire films.[6] A photoinduced increase of the compression in the order of 10^{-4} of the initial value was found in all the a-Si:H films that have been studied. [6,7] Rana's recent calculations [8] showed a change in the oscillator strengths of Si-H vibrations due to the flipping of H to Si back-bond induced a 10^{-4} increase in the 2000 cm^{-1} absorption. Meanwhile, the distortions of the structure could increase the strain of the network about 10^{-4}. The question is: does the photoinduced volume expansion relate to the SWE? By measuring the optoelectronic properties before and after light-soaking for

the same group of hot-wire films, we show that these changes are not directly related. In the films deposited at 280< T_S <360 °C, a factor of 4-6 photodegradation of the photoconductivity was obtained, but there was no obvious degradation of the photoconductivity for the films deposited at 360 < T_S < 440 °C. Whereas, photo-induced increase of the compression in the order of 10^{-4} was found in all the a-Si:H films.

^{1}H Motion Studied by Dipolar Order Relaxation and High Temperature NMR

Dipolar order relaxation studies in GD a-Si:H [9,10] have provided some evidence for the existence of a significant amount of relatively mobile H (~ 15% of the H content); H_2 molecules trapped in nanovoids have been suggested as the origin. We present in Fig. 1 indication that significant differences of the relaxation time exist between GD and hot wire a-Si:H. From early dipolar relaxation time (< 20 ms), we deduced the T_{1D} by fitting the data to f(t) exp(-t/T_{1D}). The T_{ID} of the clustered H is slightly shorter but the T_{ID} of the isolated H is 4 times longer in HW film than that in GD films. The results indicate that the local motion of the isolated H is much slower in HW compared to that in GD film.

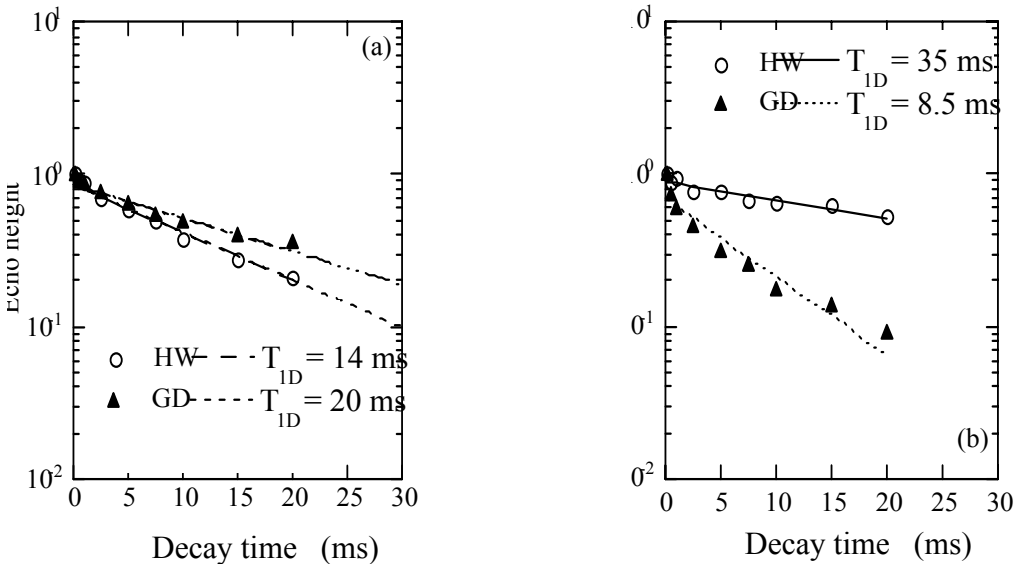

Fig. 1 Early decay of (a) clustered and (b) isolated ^{1}H in HW and GD a-Si:H.

Furthermore, high temperature NMR is applied to investigate the hydrogen dynamics and microstructure of a-Si:H. A home-made high temperature NMR probe was used in the temperature range from room temperature to 200 C. Preliminary results show an indication of hydrogen motion within the film from room temperature to 150 ˚C (above 150 ˚C, the ^{1}H effusion occurs). In addition to the generic broad and narrow lines observed in all a-Si:H, a second narrow line (less than 1 kHz wide) is identified as the temperature is raised. This very narrow line is particularly visible and sensitive to temperature in hot-wire a-Si:H.

Internal Electric Field Profile of a-SiGe:H Solar Cells with Varied Ge Content[11]

We show the electric field profile of 0.15-μm-thin a-SiGe:H cells with varied Ge contents. Figure 2(a) plots the measured V_a vs. λ. We fit the data by using the functions in Fig. 2(b). The fits to the data are shown in Fig. 2(a) as the dashed lines. The cell performance, the fitting

parameters of $E_i(x)$ and the deduced defect density N_d are listed in Table I. We can see that the electric field is stronger for the cell with less Ge content. This is because of a larger optical gap and less defects in the a-SiGe:H i-layer with less Ge content. In Fig. 1(a), the V_a decreases quickly when $\lambda > 500$ nm in the thin cells, perhaps, due to the hole effect near n/i interface.

Table I. ss/n-i-p/TCO solar cell performance and the fitting parameters of $E_i(x)$

Sample ID	Ge:Si	V_{oc} (V)	J_{sc} (mA/cm^2)	FF	P_{max}	E_o (V/cm)	□ (μm)$^{-1}$	L_o (μm)	N_d (cm^{3}eV)$^{-1}$
L1	55:45	0.574	14.83	0.540	4.60	9.31×10^4	9.886	0.10	9.7×10^{16}
L2	50:50	0.673	13.60	0.556	5.09	1.06×10^5	12.02	0.083	1.4×10^{17}
L3	40:60	0.700	12.01	0.630	5.33	1.20×10^5	14.01	0.071	2.0×10^{17}

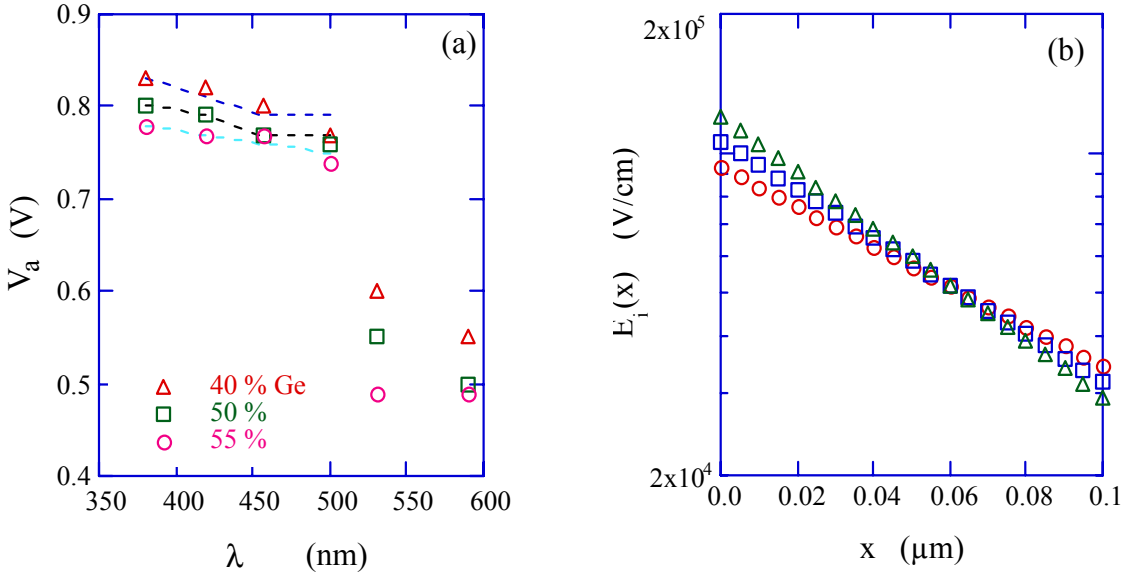

Fig. 2 (a) V_a vs. □ for a-SiGe cells. The dotted lines are the fits by using the $E_i(x)$ functions in (b)

Electroluminescence Spectrum in Amorphous Silicon p-i-n Diodes[12]

Last year, we reported a complete model to explain the EL features as dispersive-transport-controlled non-geminate recombination processes.[12] However, most of the EL spectra were taken by the home-made filter wheels. There were only 12-14 data points of a spectrum in the energy range of 0.6 eV to 1.6 eV as shown in Fig. 3a. Therefore, we were looking forward to using a grating spectrometer to study the spectral lineshape in more detail. We have successfully upgraded our EL systems by installing a grating spectrometer (SPEX TRIAX-180) and the LabVIEW software. We now obtain EL spectra not only more precisely but also more efficiently as shown in Fig. 3b. We have measured EL spectra from a group of a-SiGe:H cells from Univ. Toledo. Meanwhile, we use the same system for PL studies.

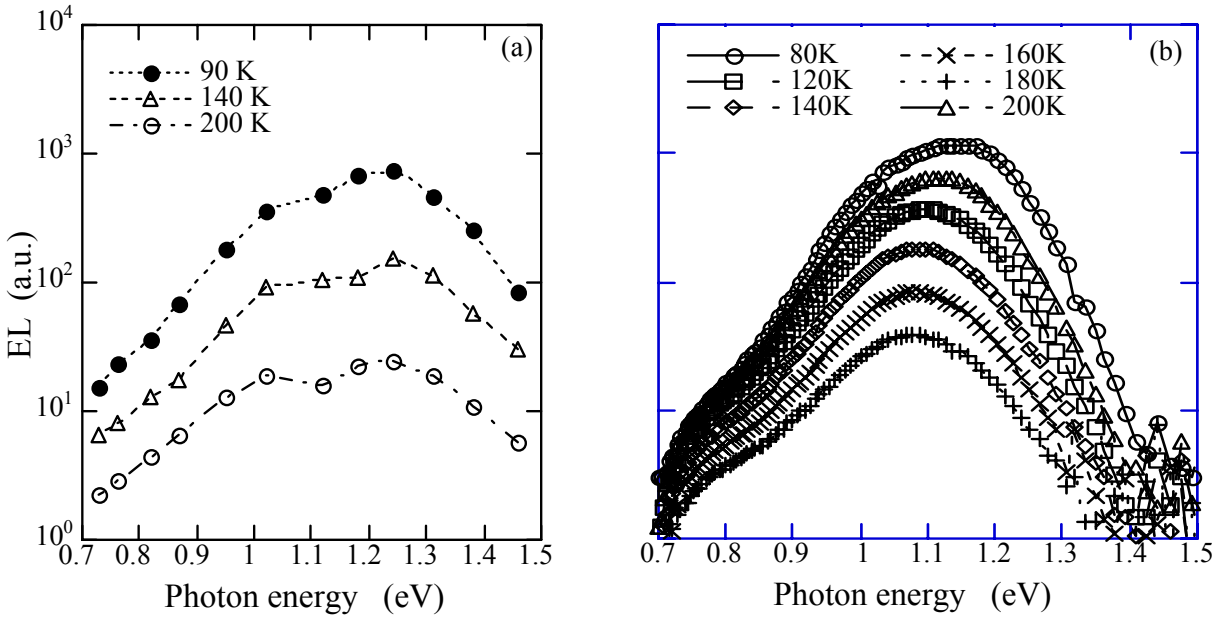

Fig. 3 The EL spectra taken by (a) the filter and (b) the grating spectrometer from a-Si:H p-i-n cell made at Solarex.

References:

1. H. M. Branz, "Hydrogen collision model of light-induced metastability in hydrogenated amorphous silicon", *Solid State Communications*, **105/6**, 387 (1988).; MRS Spring Meeting Proc. Symp. A, 1998, in press.
2. R. Arya, Final Technical Report (13 Sept. 94-28 Feb. 98), NREL/SR-520-24854, June 1998.
3. D.E. Carlson, R.W. Smith, P.J. Zanzucchi, and W.R. Frenchu, in *Pro. IEEE Photovoltaics Specialists Conf.*, 16th, (SanDiego, CA, pp. 1372-1375. IEEE, New York, 1982).
4. Light-induced change of Si-H bond absorption in Hydrogenated Amorphous Silicon, Guozhen Yue, Jonathan Baugh, Liangfan Chen, Qi Wang, Eugene Iwaniczko, Guanglin Kong, Yue Wu, Daxing Han, to be published in MRS-98 proc.
5. R. Darwich et al., *Philosophical Magazine* B, **72**, 363-372 (1995).
6. Correlation of stress with hydrogen micro-structure in Thin Film Hydrogenated Amorphous Silicon, Daxing Han, T. Gotoh, Motoi Nishio, S. Nonomura, S. Nitta, Qi, Wang, E. Iwaniczko. MRS Symp. Proc. Vol **505** (Material Research Society, 1998), p.445.
7. Photo-induced Structure Metastability and the SWE in a-Si:H, Daxing Han, Tamihiro Gotoh, Motoi Nishio, Tomonari Sakamoto, Shuichi Nonomura, Shoji Nitta, Qi Wang, Eugene Iwaniczko, Harv Mahan, to be published in NCPV Program Revive Meeting (Sept., 1998).
8. 10th NREL/EPRI a-Si Team meeting, Aug. 1998
9. "Effect of light soaking on the local motion of hydrogen in hydrogenated amorphous silicon", P. Hari, P. C. Taylor, and R. A. Street, Mater. Res. Soc. Proc. **336**, 329 (1994).
10. "Nuclear magnetic resonance studies of hydrogen in amorphous silicon", R. E. Norberg, P. A. Fedders, and D. J. Leopold Mater. Res. Soc. Symp. Proc. **420**, 475 (1996).
11. Internal Electric Field Profile of a-SiGe p-i-n Solar Cells, Xinhua Geng, Xunming Deng, Qi Wang, and Daxing Han, to be published in MRS-98 proc.
12. Daxing Han, Final Subcontract Report (July 7, 94-Jan.15, 98), NREL/SR-520-24741, May. 1998.

Title: **Microscopic Origins of Metastable Effects in a-Si:H and Deep Defect Characterization in a-Si,Ge:H Alloys**

Organization: University of Oregon, Eugene, Oregon

Contributors: J. David Cohen, principal investigator; Yoram Lubianiker, Chih-Chiang Chen, and Kimon Palinginis

The primary research goals of this program are to elucidate the basic mechanisms by which a-Si:H degrades with light exposure, and to study the defect structure in low bandgap a-Si,Ge:H alloys. During the past year we carried out the following studies: (1) Developing a model to account for the light-induced degradation kinetics in amorphous silicon produced by DC reactive magnetron sputtering containing a small microcrystalline component; and (2) Examining the spatial distribution of defects in a-Si:H films deposited under high hydrogen dilution to look for improved properties close to the onset of microcrystallinity.

Approach and Results

Last year we reported results obtained on several amorphous silicon samples deposited by dc reactive magnetron sputtering in the presence of either hydrogen or deuterium from John Abelson's group at the University of Illinois. We established that, by using TEM and Raman spectra studies, these samples included a considerable density of microcrystallites, but consisted predominantly of an amorphous component.[1] The deep defect density was determined by drive-level capacitance profiling (DLCP).[2]

The degradation kinetics of these samples is quite unusual as is displayed for one such sample in Fig. 1. This shows the variation in defect density with light exposure at an intensity of 4.5 W/cm^2. One observes that the defect density increases very slowly until roughly 10 minutes of exposure (hereafter called "stage 1"). Following this, the defect density increases quite rapidly in the next time interval (stage 2), and then at a more moderate pace similar to standard a-Si:H (stage 3). Finally, we reach saturation (stage 4). All these results, including the abrupt increase in stage 2, were found to be completely reproducible and were independent of the specific Pd barrier junction used.

Figure 2 presents a comparison of the increase in deep defect density obtained through the DLCP technique for three different intensities. It can be seen that most of the features found for the high light intensity are present also at the lower intensities. The main differences are that the increase in defect density during stage 1 becomes even slower as the light intensity decreases, while the rapid increase regime (stage 2) becomes less evident. The other apparent differences, i.e. the lower overall defect density and the longer times required to achieve saturation under lower light intensity, are already well known and generally occur for all a-Si:H samples.

While the results displayed in Fig. 2 were reported by us at the end of last year, we did not yet know how to account for this fairly complex degradation behavior. During the past year we have begun to obtain some insight into the processes involved. The most common way to account for the degradation kinetics in a-Si:H is by the rate equation [3]:

(1)

where N is the density of the dangling bond defects and G is the light intensity. The coefficients C and λ determine the rates of the light induced defect creation and annealing processes, respectively. We assume that light induced annealing process is initiated via the capture of one type of carrier into the metastable defects, and thus we take f(G,N) = G/N. This equation neglects any thermal processes, but this is a good approximation since the light soaking was carried out at temperatures which did not greatly exceed room temperature. When the light induced annealing term is negligible, the solution of the rate

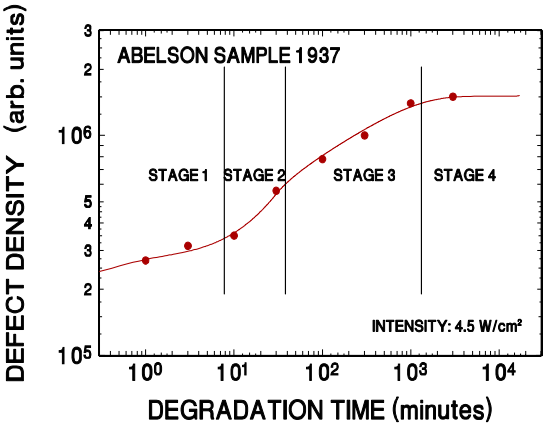

FIG. 1. Deep defect density *vs.* degradation time for a mixed microcrystalline/amorphous si-licon sample using red filtered ELH light at an intensity of 4.5W/cm^2. The solid line is a guide to the eye. The increase in defect density with time falls into 4 distinct behavioral regimes which have been labeled as "stages". For standard amorphous silicon only the last 2 stages of degradation are found to occur.

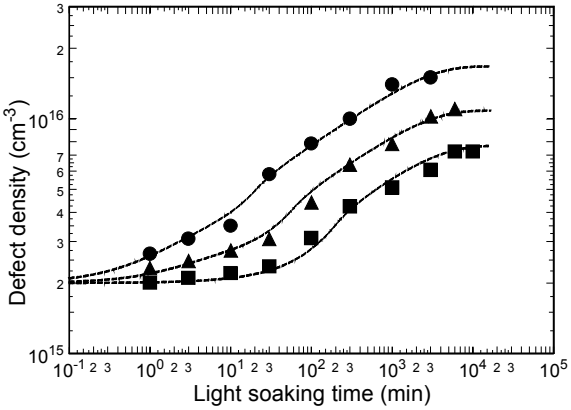

FIG. 2. Defect density vs. light soaking time for three different light intensities: 4.5W/cm^2 (circles), 2.9W/cm^2 (triangles), 1.7W/cm^2 (squares). The solid lines in this figure represent the fits obtained from the mixed phase model described above.

equation produces the well known $t^{1/3}$ rule. However, this solution does *not* agree with the complex degradation behavior displayed in Figs. 1 and 2.

We have found that the simplest model that can account for the entire degradation kinetics is of a material which contains three phases. The first phase is high quality amorphous silicon. The second phase is a more disordered type of a-Si:H, believed to lie adjacent to the microcrystallites. The higher degree of disorder of this second phase might be due either to extra stress caused by the presence of the microcrystallites, or to a deficit of diffusing hydrogen which is able to passivate a larger fraction of the bulk defect states. The third phase is that of the microcrystallites, whose contribution to the defect density can be neglected. The total defect density will thus be given by $f_1N_1+f_2N_2$ where N_i and f_i are the defect density and the effective volume fraction of the i^{th} phase, respectively. Since the second phase is assumed to be much more defective we start with $N_2 >> N_1$, but we also know that $f_2 << f_1$ from the TEM micrographs that indicate the vast majority of the film is amorphous silicon.

Turning to the degradation kinetics, we assume that N_2 degrades like equation (1). However, due to the high initial defect density of this phase, the light induced annealing term in this equation will be significant even for short light soaking times. Furthermore, because this phase is highly defective, the corresponding coefficients C and λ have relatively high values. For Phase 1 we assume that initially the recombination is governed not by the dangling bonds within this phase, but by states associated with the other two phases into which the carrier can diffuse and recombine. We denote these states by Z.

As the dangling bond density begins to increase, it will shift the quasi Fermi level towards midgap, but will not initially alter the free carrier lifetime since the collapse of the quasi Fermi level will simply deactivate an equal number of the Z states. However, once the density of the dangling bonds in Phase I is high enough the recombination will be dominated by those defects and the kinetics will become "normal" again. In Fig.2 the fit lines indicate how this model indeed accounts for all the features of our data.

Our second area of study has been a joint collaboration with researchers at Uni-Solar and at Colorado School of Mines to examine the properties of a-Si:H films grown under hydrogen

dilution close to the onset of microcrystallinity. Uni-Solar provided hydrogen diluted samples of several thicknesses (0.5, 1.5, and 2.5 μm on n^+ a-Si:H coated stainless steel) to Don Williamson for X-ray analysis. They also provided him with 0.5 μm thick films on 3 types of substrates (bare stainless, n^+ a-Si:H coated stainless steel, and n^+ □c-Si coated stainless steel). They provided my group with two hydrogen diluted a-Si:H films of thicknesses 1.05 and 1.3 μm on n^+ a-Si:H coated stainless steel, plus one undiluted (standard glow discharge) a-Si:H on n^+ a-Si:H coated stainless steel. For all samples we evaporated a semi-transparent Pd contact onto the top surface to produce a Schottky barrier for our junction measurements. For the samples deposited on n^+ a-Si:H coated stainless steel, Don Williamson's X-ray analysis indicated that the films were purely amorphous at 0.5 μm thick, were mixed microcrystalline/amorphous for the 1.5□m thick film, and were largely microcrystalline at 2.5 μm. The implication of his results was that the hydrogen diluted a-Si:H was approaching the onset of crystallinity as the film got thicker, and that the onset of distinct crystallinity occurred somewhere in excess of 1μm.

The role of my laboratory was to assess whether the electronic properties of these films were also varying as these hydrogen diluted films increased in thickness. Last year scientists at Uni-Solar and ECD had reported that a-Si:H films grown under hydrogen dilution close to the onset of microcrystallinity exhibited a higher degree of stability [4]. Therefore, it seemed possible that the density of deep defects in the light-degraded state of these films would become lower as these films became thicker, at least until the onset of microcrystalline was reached.

The three films (one standard, two deposited with hydrogen dilution with different total thicknesses) were characterized in a light-degraded state produced by exposure to red-filtered light from a tungsten-halogen source at an intensity of $2 W/cm^2$ for 100 hours. We used the DLCP method to obtain defect profiles for each of these samples using a measurement frequency of 33Hz and a series of measurement temperatures. Based upon cross correlation studies between ESR and DLCP on previous samples [5], we believe that a good estimate of the total defect density will be obtained by doubling the profile values obtained at 370K. Figure 3 shows such DLCP profiles at different measurement temperatures obtained for the two a-Si:H grown with hydrogen dilution (in the light degraded state). Note that the profiles for the two samples of different thicknesses are nearly identical except for the lowest temperatures where the profile distances approach the edge of the thinner sample. These profiles indicate defect densities for these films lying between 1.2 to 1.5×10^{16} cm^{-3}.

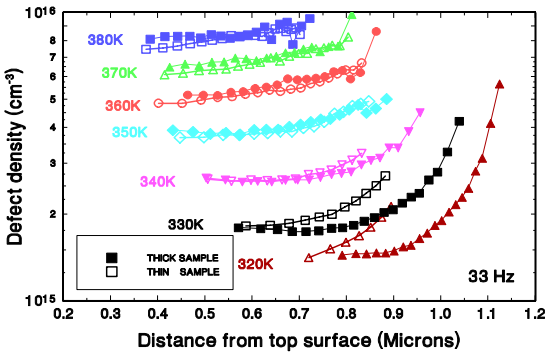

FIG. 3. Drive-level capacitance profiles for the two hydrogen diluted Uni-Solar standard glow discharge samples in their light degraded state at 33 Hz and several measurement temperatures. Note the good agreement between the profiles obtained on the two samples. Also note that the profiles show a considerable spatial variation than those of the standard sample.

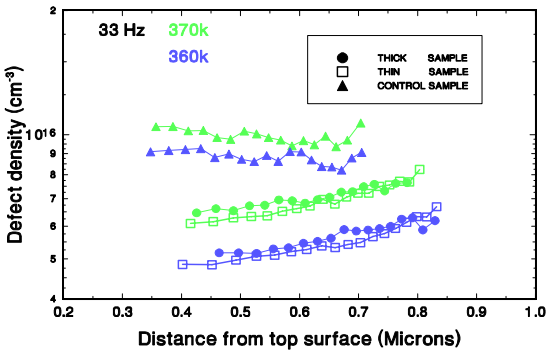

FIG. 4. Comparison of drive-level profiles for all three samples at the highest profiling temperatures. The total defect density in each film is estimated to be twice the value shown for the 370K curves in each case. Note that the profiles for the hydrogen diluted samples are significantly lower than for the standard sample and also indicate a much greater spatial variation.

In Fig. 4 we display a direct comparison between the profiles for all three samples. These are shown for the two highest measurement temperatures where the profiles should be encompassing a larger part of the deep defect band. We see that the hydrogen diluted samples exhibit defect densities roughly a factor of 1.5 lower than the standard sample, and we also note the much stronger spatial variation of the profiles for the hydrogen diluted samples. This variation indicates a decrease in deep defect density toward the top surface of those films. That is, the density of light-induced deep defects becomes smaller as we move toward the onset of microcrystallinity as deduced from the X-ray studies carried out by Don Williamson on Uni-Solar samples deposited under the identical conditions. This tends to support the conclusion that it is this approach to microcrystallinity which leads to a more stable a-Si:H material evidenced, in this case, by a lower defect density.

Finally, in Fig. 5, we display photocapacitance spectra taken for the two hydrogen diluted samples. The spectrum for the thinner sample is nearly identical to those of very high quality glow discharge samples reported previously [5,6]. The thicker sample spectrum matches that of the thinner sample in both the bandtail regime and also at optical energies below 1.0eV where the signal is believed to originate solely from dangling bond defects in a-Si:H. However, the thicker sample has an additional feature at intermediate optical energies which we identify with the presence of silicon microcrystallites. Our results are thus consistent with Don Williamson's X-ray results that indicate a small degree of microcrystallinity for the 1.5 μm thick samples grown in this fashion.

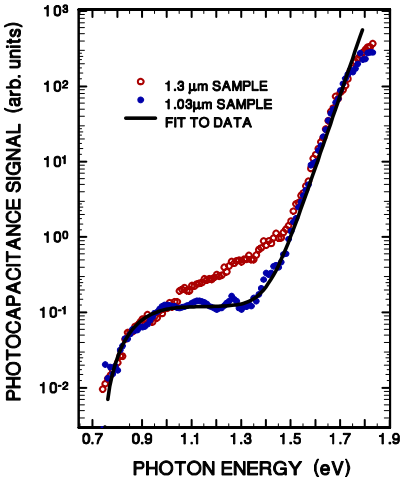

FIG. 5. Photocapacitance spectra for the two Uni-Solar hydrogen diluted a-Si:H samples of different thickness. The thinner sample spectrum is quite similar to many published results for sub-band-gap spectra of a-Si:H in the literature. The thicker sample shows an additional feature at intermediate energies that we associate with the presence of a very small fraction of microcrystallites. The solid line is a fit to the thinner sample data which indicates an Urbach energy of 46meV and an estimated deep defect density of 1.5×10^{16} cm^{-3}. This latter value agrees quite closely with the defect density obtained from the DLCP measurements for this sample.

1. D. Kwon, H. Lee, J.D. Cohen, H.-C. Jin, and J.R. Abelson, J. Non-Cryst. Solids **227-230**, 1040 (1998).
2. C.E. Michelson, A.V. Gelatos, and J.D. Cohen, Appl. Phys. Lett. **47**, 412 (1985).
3. Z.Y. Wu, J.M. Siefert and B. Equer, J. Non-Cryst. Solids **137-138**, 227 (1991).
4. D.V. Tsu, B.S. Cho, S.R. Ovshinsky, S. Guha and J. Yang, Appl. Phys. Lett. **71**, 1317 (1997).
5. Thomas Unold, John Hautala, and J. David Cohen, Phys. Rev. B**50**, 16985 (1994).
6. A.V. Gelatos, K.K. Mahavadi, J.D. Cohen, and J.P. Harbison, Appl. Phys. Lett. **53**, 403 (1988).

Title: **Advanced Processing Technology for CdTe and High Band Gap $CuIn_xGa_{1-x}Se_2$ Solar Cells**

Organization: Department of Electrical Engineering
Center for Clean Energy and Vehicles
University of South Florida
Tampa, FL

Contributors: D. L. Morel and C. S. Ferekides, principal investigators
S. Jaganathan, A. Jayapalan, V. Komin, D. Marinsky, V. Palekis, P. Panse, H. Sankaranarayan, P. Salvaraj, M. Shankaradas, B. Tetali, V. Viswanathan, Y. Ying and Z. Zhao, graduate assistants

$CuIn_xGa_{1-x}Se_2$

Objectives

The objectives of this project are to develop improved processing techniques for $CuIn_xGa_{1-x}Se_2$ (CIGS) solar cells and to correlate performance and processing mechanisms.

Approach

A key aspect of the approach which we take to improving performance while maintaining manufacturing constraints is to separate the formation of bulk and surface properties so that each can be optimized independently of the other. In our last report we reported the achievement of this objective. We then went on to optimize the bulk properties and presented data that indicated the consistent achievement of high J_{sc}'s. The task that we now face is the optimization of surface and interface properties that largely determine V_{oc} and FF. To assist this process we have under development a new photocapacitance technique that provides useful information about the interface region. The discussion which follows will highlight the results we have attained thus far with this technique.

Results

The primary parameter of interest for these studies is V_{oc}. It is generally believed that V_{oc} is dominated by recombination in the space charge layer in these devices. It is thus of interest to determine information about the states responsible for recombination and to further understand the effect of processing parameters on these states. The photocapacitance technique that we are developing uses both frequency and wavelength to probe the space charge region both spatially and energetically. First, however, we establish a correlation between our probe signal and V_{oc} as shown in figure 1. This data is taken from a cross section of representative devices. The photocapacitance factor is the ratio of capacitance at one sun intensity to that in the dark. As can be seen, there is a clear correlation between this parameter and V_{oc}. A correlation between photocapacitance and performance has been reported previously for a small sample of devices(1). Our results are generally in agreement in that device

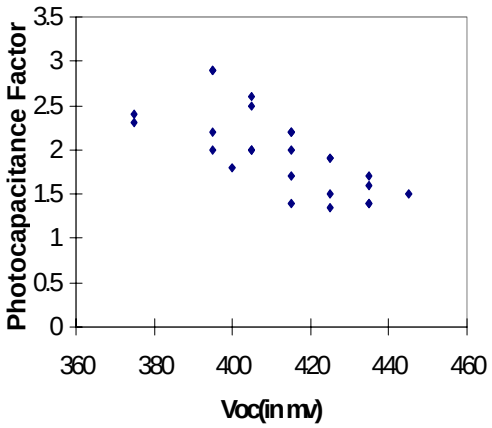

Figure 1. Photocapacitance vs. Voc.

efficiency for the devices in figure 1 scales directly with V_{oc}.

Our interpretation of these results is that the states responsible for recombination also trap light induced charge carriers. The trapped charge can be either positive or negative which can either expand or contract the space charge layer resulting in a change in capacitance. In white light at one sun intensity we always see an increase in capacitance corresponding to a decrease in space charge width of a couple of thousand angstroms. In low intensity monochromatic light the behavior is much more complex. In this case we also monitor the time dependence of the photocapacitance signal and often see a reversal of sign with time as positive and negative charge settle into traps. The time constants for these phenomena are as long as minutes indicating that deep levels are responsible for much of the activity.

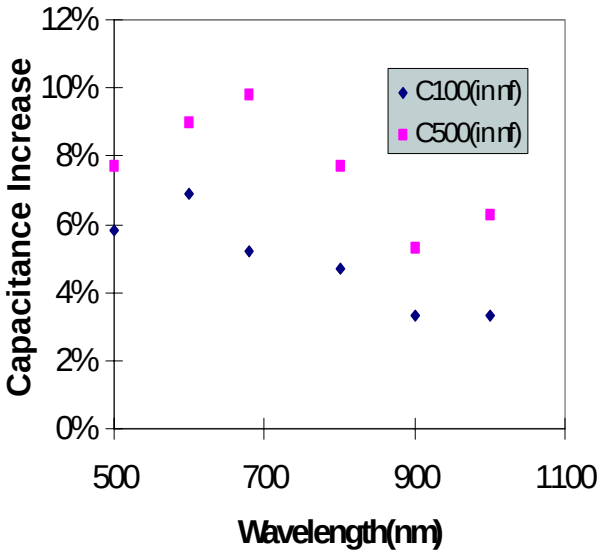

Figure 2. Wavelength dependence of photocapacitance.

In figure 2 we show the wavelength dependence of photocapacitance at two frequencies. Notwithstanding the effect of photon energy on generation and trapping, variation of the wavelength allows spatial control of the generation. Looking first at the 500 kHz data the peak at 700 nm indicates that the trapping centers are located near the metallurgical junction with CdS. At the lower frequency of 100 kHz the peak is seen to shift to shorter wavelengths which indicates that the centers associated with this signal are closer to the CdS interface. Deeper states are observed at lower frequencies, so these results collectively indicate that the levels that are dominating the trapping kinetics are deep and are peaked in the vicinity of the CdS interface. Since these are correlated with the recombination centers that control V_{oc}, we conclude that these centers are also in the vicinity of the CdS interface.

These results indicate where we must focus our efforts to improve overall performance. Additional details about these effects can be found in reference (2). A key issue that must be resolved is whether the states controlling performance are determined by formation of the CIGS surface during growth, or whether they are at least partially linked to junction formation procedures. To address this and other important issues we are extending these studies to include time dependent phenomena and correlation with compositional profiles. We will report our findings in future reports.

CdTe

The primary objectives of this project are to develop improved solar cell processing schemes for CdTe solar cells which are capable of further enhancing the performance and long-term stability and to reduce the manufacturing costs of thin-film photovoltaic modules. The process being developed for the deposition of the semiconductors (CdTe and CdS) is the close spaced sublimation (CSS); CSS has demonstrated high throughput and efficient material utilization. Alternative window materials and TCO's, back contact schemes, and long term stability studies are issues also being addressed.

CSS Process

The effects of the main CSS process parameters, such as source/substrate temperatures and ambient, on film and solar cell properties are being investigated. The process is being optimized for temperatures below 550°C, a restriction imposed to alleviate problems associated with soda lime glass substrates. Oxygen was found to be a critical process parameter for the CSS

deposition of both CdTe and CdS films. Its use leads to improved solar cell performance. These deposition processes are often optimized on borosilicate glass and subsequently transferred to soda lime glass. The most significant solar cell results obtained to date are listed in table I. Both devices shown have been fabricated at substrate temperatures below 550°C and the performance was verified at the National Renewable Energy Laboratory.

Table I.

Glass Substrate	V_{OC}, (mV)	J_{SC}, (mA/cm^2)	ff	Efficiency, (%)
Corning 7059	848	24.16	73.1	15.0
Soda lime (LOF)	839	23.11	73.5	14.3

$CdCl_2$ Heat Treatment - Processing Temperatures <500°C

The $CdCl_2$ heat treatment is an important processing step utilized by most CdTe solar cell researchers. However, this is often the time limiting step in the entire cell fabrication process and also leads to the generation of cadmium containing liquid waste. A vapor $CdCl_2$ heat treatment process is being developed as an alternative to the typical wet $CdCl_2$ process. The effects of the substrate temperature and ambient are being investigated and being optimized for high efficiencies and short processing times. The solar cells used for these studies are fabricated at temperatures below 500°C (CSS-CdTe). The most significant results obtained to date are listed here:

CSS-CdTe T_{SUB}=480°C Wet $CdCl_2$ V_{OC}= 835 mV J_{SC}=20.22 mA/cm^2 ff=66.0%
CSS-CdTe T_{SUB}=480°C Vapor $CdCl_2$ V_{OC}=790 mV J_{SC}=20.20 mA/cm^2 ff=62.2%

More recent experiments have yielded V_{OC}'s over 800 mV for cells processed using the vapor $CdCl_2$ treatment; further optimization of this process is expected to lead to state-of-the-art cell efficiencies.

Alternative Window Layers - Transparent Conductive Oxides

In addition to further advancing solar cell efficiencies, one of the objectives associated with this task is to improve our understanding of the junction formation process and device operation. Most of the to-date activities have focused on SnO_2, ZnO, CdO, and ZnSe. Zinc oxide has been routinely used as the TCO for the fabrication of solar cells. The use of oxygen at various cell fabrication steps, in particular during the deposition of the CSS CdS films, leads to an increase in the sheet resistance of ZnO which eventually leads to high series resistance and low ff's. However, ZnO maintains its as-deposited electrical characteristics if no oxygen is used during the deposition of the CdS layer, therefore making it a good candidate for "oxygen free" cell processing schemes.

ZnSe has been used for the fabrication of CdTe/ZnSe junctions; an advantage of using ZnSe instead of CdS is the possibility of enhancing J_{SC} due to the larger bandgap of ZnSe. This task has to date proven to be the most challenging due to extensive and difficult to control interdiffusion between the two semiconductors. It has been determined that the interdiffusion can be significantly limited by lowering the processing temperatures. CdTe/ZnSe solar cells have exhibited efficiencies over 11.0%.

Back Contact Schemes - Stability Studies

Baseline solar cells are being fabricated using HgTe:Cu doped graphite paste as the contact material. This type of contact has been successfully utilized in the past for high efficiency devices. In addition to the graphite paste two more contacting schemes have been developed. A new method based on sputtered Cu_xTe films has produced devices with efficiencies over 15.0%. An important characteristic of this process is its ease of manufacturing. A ZnTe (copper doped) based contact, an approach often used by other CdTe groups, has also been developed. Although not completely optimized, this method has already yielded devices with state-of-the-art V_{OC}'s (>830 mV) and ff's (>70%). The ultimate performance factor for the back contact will be its

long-term stability. To date, it is believed that in most cases where cell performance degradation has been observed, it was due to degradation of the back contact. To this end, preliminary stability studies are underway to evaluate the above contact approaches. Solar cells are being stressed at temperatures in the range of 70-90°C, under dark and light (AM1.5) conditions, in a controlled ambient (to date only devices fabricated with doped graphite back contacts have been studied). The cells are characterized using light and dark measurements (I-V, C-V). Devices stressed at the highest temperature (90°C) have exhibited the highest degree of degradation due to losses primarily in the ff; changes in V_{OC} are within 10 mV while J_{SC} remains essentially unchanged. In the future a larger number of devices will be tested in order to perform statistical analysis on the data, and devices fabricated with the other two contacting schemes will also be included. The stress temperature range will be expanded to 50-100°C. The figures below show the ff and V_{OC} for three devices stressed in the dark at the three temperatures mentioned above.

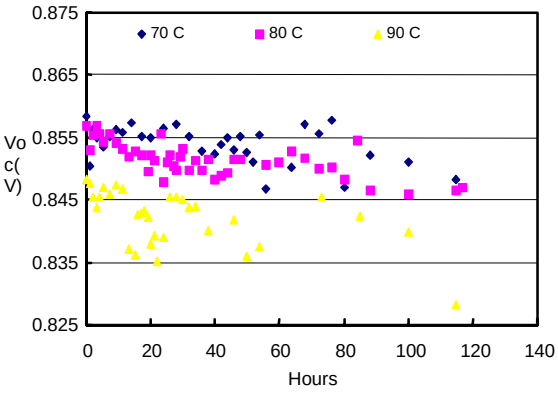

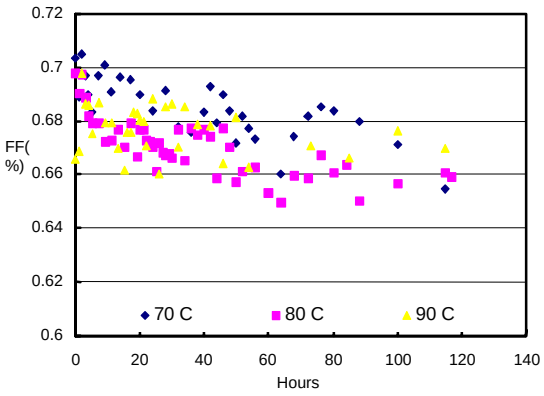

References

1. R. Ahrenkiel, *J. Appl. Phys*., **59**(1), (1986), 181.
2. A.Jayapalan, H. Sankaranarayanan, H. Lin, R. Narayanaswamy, C. S. Ferekides and D. L. Morel, "Determination of Fundamental Parameters and Mechanisms in CIGS Solar Cells Using Photocapacitance Techniques", *Proceedings of the Second World PV Conference*, Vienna, July, 1998.

Title: **High Efficiency Thin-Film Cadmium Telluride and Amorphous Silicon Based Photovoltaic Cells**

Organization: Department of Physics and Astronomy
The University of Toledo
Toledo, OH 43606

Contributors: Alvin D. Compaan and Xunming Deng, principal investigators; Randy G. Bohn co-investigator; Xianbo Liao (visiting scholar); Kent Price (postdoc); Ronghua Wang, Greg Miller, James Walker, Dan Grecu, Ilvydas Matulionis, Xianda Ma, Diana Shvydka, Konstantin Makhratchev, Chitra Narayanswamy (graduate assistants)

Objectives

The objectives of this work are to develop improved processing schemes for CdTe and a-Si:H-based solar cells which are capable of further enhancing their performance and long-term stability, and reducing the manufacturing costs of commercial thin-film photovoltaic modules. An important part of this work involves collaborative efforts with the CdTe and a-Si:H national teams. The discussion below is divided into the CdTe-related work and the a-Si:H-related work.

CdTe

Technical Approach

The University of Toledo effort emphasizes rf sputtering of both CdS and CdTe from compound semiconductor targets. In addition, we have begun to use sputtering for deposition of back-contact structures. During the past year we have optimized the vapor $CdCl_2$ treatment process for three-inch substrates and continued work on laser scribing of PV thin films [1a] generally in collaboration with other team members. The deposition effort is supported by studies of photoluminescence [1b], optical absorption, Hall/conductivity measurements, and, through collaboration, ellipsometry [2] and grazing incidence x-ray fluorescence. [3]

Absorption measurements on CdSTe alloy films

In the final technical report of previous subcontract [4] we summarized measurements on CdS_xTe_{1-x} alloy films prepared by pulsed laser deposition (PLD) covering the full alloy range. These measurements included x-ray diffraction, Raman scattering [5,6], electrical conductivity, persistent photoconductivity, and optical absorption. Recently we have performed optical absorption at 10K on PLD films and rf sputtered films for x near 0 and 1 before and after $CdCl_2$ treatment. One goal was to examine the detailed wavelength dependence of the fundamental absorption edge including the broadening due to phonons, alloy fluctuations, and strains.

Figure 1 shows the absorption coefficient for two lightly alloyed films of CdS_xTe_{1-x} as-deposited and after vapor $CdCl_2$ treatment for 30 minutes at 387^o C. In the CdTe-rich film (x=0.04) annealing sharpens the edge significantly so that the exciton peak can clearly be observed. For the sulfur-rich film (x=0.95), there is very little sharpening of the absorption edge after annealing although there is a small blue shift upon annealing of about ~30 meV. For the sulfur-rich alloy there is a substantial density of tail states extending to at least 1 eV below the absorption edge. This may point to the importance of deep-level Te-related defect states at low densities in CdS and may help explain the lack of observed photoresponse from electron-hole pairs created in the CdS layer of CdS/CdTe solar cells. We expect to examine further this absorption edge behavior in even more lightly CdTe alloyed CdS films.

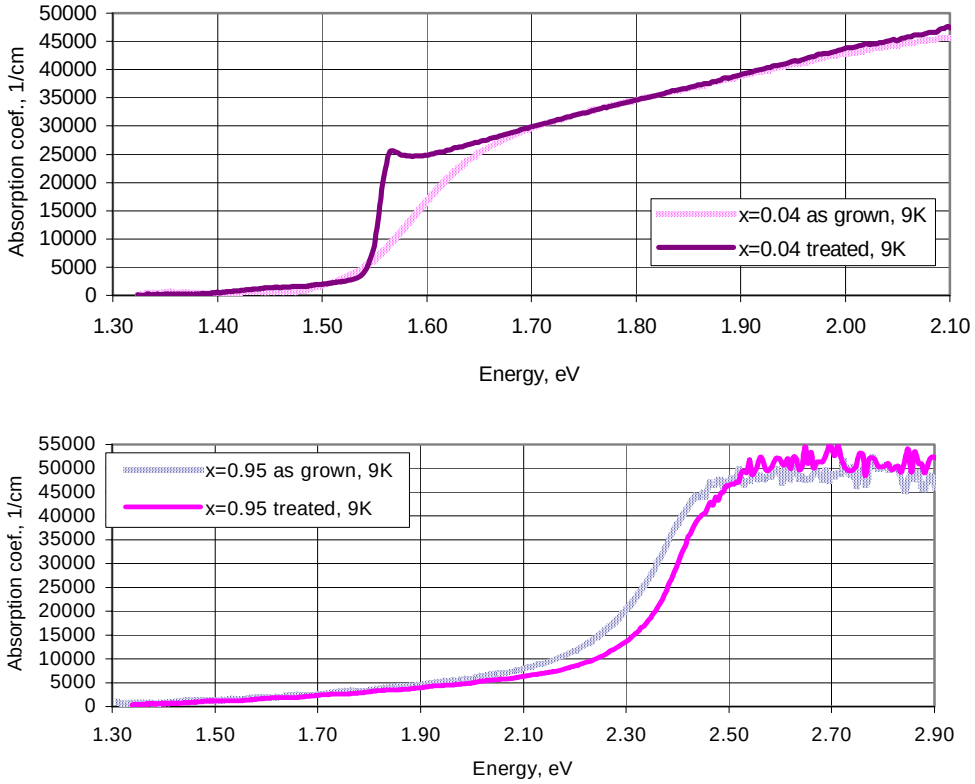

Fig. 1. Absorption coefficients for ~2 μm thick CdS_xTe_{1-x} films rf sputtered on Corning 7059 glass before and after vapor $CdCl_2$ treatment. upper: x=0.04; lower: x =0.95

Cell performance vs. CdTe thickness

Various groups have fabricated high efficiency CdTe solar cells with CdTe thicknesses from ~1.5 μm to ~15 μm. The best cells typically have CdTe thicknesses above 3 μm. As a start toward understanding the CdTe thickness dependence, we prepared a series of rf sputtered cells with CdS layer thickness held constant at 0.13 μm and CdTe layer thickness from 2.4 μm to 0.5 μm.

At the minimum CdTe thickness of 0.5 μm, V_{OC} dropped to about 85% of the value for 2.4 μm CdTe. J_{SC} dropped the most, to about 70%; and the fill factor dropped to about 75% of the best value. Since the overall efficiency is the product of all three of these factors, it dropped to about 40% of the best efficiency. In these cell structures, in which we made no attempt to use light trapping or back surface fields to enhance carrier collection, one expects a loss of current due to deep penetration of red light. However, the drop in fill factor and open circuit voltage ought to be avoidable. Furthermore, the spectral quantum efficiency curves on these devices do not indicate a serious loss of collection in the red end of the spectrum. (Nor would one expect this from the absorption data. [4]) We expect to continue to work on aspects of reducing the absorber layer thickness. Thinner CdTe layers would reduce deposition time, and also would reduce the quantity of materials with potentially negative impacts on the environment.

a-Si:H

Technical Approach

We have divided our research into several sub-task areas: wide bandgap research, mid bandgap research, narrow bandgap research, non-semiconductor research [7] and multi-junction solar cell fabrication. [1c]

Triple Junction Cell Results

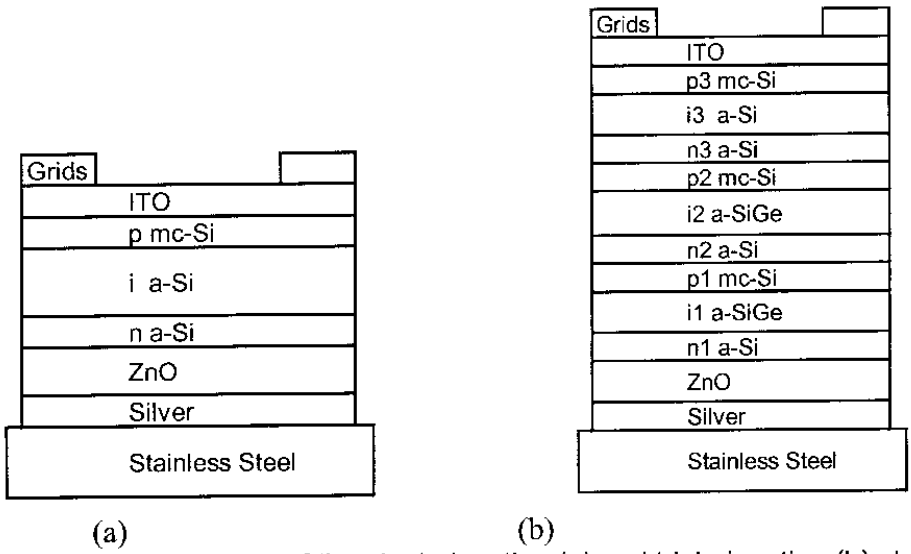

Figure 2. Schematics of the single-junction (a) and triple-junction (b) structures of a-Si solar cell devices fabricated in this program.

The device structures for single and triple cells are shown in Figure 2 (a) and (b).

We deposit wide bandgap a-Si alloy solar cells with the structure SS/Ag/ZnO/a-Si n^+/a-Si-intrinsic/μc-Si-p^+/ITO. Various deposition conditions for the i-layer and p-layer were explored. A high hydrogen dilution and relatively low temperature were used for the i-layer deposition. With this, we have obtained a-Si single-junction solar cells with 1.02 V open circuit voltage, although the fill factor is still low and needs to be further improved. In the mid bandgap research area, we have explored various deposition conditions to improve the solar cell FF while maintaining relatively high V_{oc}. A typical optimized a-Si solar cell, deposited on bare stainless steel without the use of a back-reflector, shows a 0.732 fill factor. and short circuit current of 6.9 mA/cm^2, which is approximately the current that we need from the top cell of a triple-junction device.

A high-quality narrow-bandgap material is critical to the achievement of high efficiency triple-junction solar cells. We explored the deposition of a-SiGe alloys and solar cells with different Ge content in the alloy and under different hydrogen dilution conditions. Table 1 summarizes the results for a series of a-SiGe samples deposited on Ag/ZnO back-reflectors. The i-layers in all of these devices have graded bandgaps to enhance hole collection. Sample GD109 was deposited under standard condition with a hydrogen dilution ratio of 10. The data in the J_{ph} column was obtained by integrating the QE curve with AM1.5 global spectrum. The FFs are relatively low in this set of devices due to the lack of metal grids. Figure 3 shows the QE curves for this set of a-SiGe devices. The red response at 800 nm is around 50% for both GD109 and GD110. An improved a-SiGe solar cells were deposited on back-reflector and aluminum grids were evaporated on top. Such improved a-SiGe devices show an initial efficiency of 8.3%.

Table 1. Device data for a series of a-SiGe solar cells having i-layers deposited under different deposition conditions.

Samples	V_{oc} (V)	J_{ph} from QE (mA/cm^2)	FF	P_{max} (mW/cm^2)
GD109 (Standard)	0.681	19.3	0.530	6.97
GD110 (+15% Ge)	0.634	21.3	0.473	6.39
GD111 (-15% Ge)	0.714	20.0	0.527	7.53
GD112 (2.5x H dilution	0.813	18.2	0.486	7.19

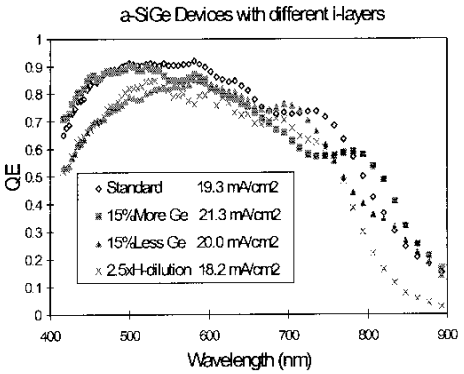

Figure 3. Quantum efficiency curves for the four a-SiGe solar cells described in Table 1.

Using the preliminary optimized component cells and sputter deposited ITO, we fabricated a series of triple-junction solar cell devices, having a structure shown in Figure 2(b). These triple cells achieved 8.8% initial efficiency (V_{oc}=2.289 V, J_{sc}=6.39 mA/cm^2, and FF=0.604). Since our sputter deposition of ITO films is not fully optimized yet, we asked scientists at United Solar to deposit their ITO films on UT's triple-junction solar cells. This device showed a 9.7% initial efficiency.

References/Publications

1. Three papers to appear in the *Proc. of the NCPV Program Review*: (a) A.D. Compaan, I Matulionis, and S. Nakade, "Lasers and Beam Delivery Options for Polycrystalline Thin-Film Scribing"; (b) D. Grecu and A.D. Compaan, "Photoluminescence Study of Cu Diffusion in CdTe"; (c) X. Deng , "Study of Triple-Junction Amorphous Silicon Alloy Solar Cells".
2. K. Wei, F.H. Pollak, J.L. Freeouf, D. Shvydka, and A.D. Compaan, "Optical Properties of $CdTe_{1-x}S_x$ Experiment and Modeling," submitted to J. Appl. Phys.
3. Y.L. Soo, S. Huang, Y.H. Kao, and A.D. Compaan, "Investigation of interface morphology and composition mixing in CdTe/CdS heterojunction photovoltaic materials using synchrotron radiation," J. Appl. Phys. **83**, 4173 (1998).
4. A.D. Compaan and R. G. Bohn, *Annual Subcontract Report: High Efficiency Thin Film Cadmium Telluride Photovoltaic Cells*, August 1997 NREL/SR-520-23404.
5. A. Fischer, Z. Feng, E. Bykov, G. Contreras-Puente, A. Compaan, F.Castillo-Alvarado, J. Avendano, and A. Mason, "Optical phonons in laser-deposited CdS_xTe_{1-x} films," Appl. Phys. Lett. **70**, 3239-41 (1997).
6. A. Fischer, L. Anthony and A.D. Compaan, "Raman Analysis of Short-Range Clustering in Laser-Deposited CdS_xTe_{1-x} Films," Appl. Phys. Lett., **72**, 2559 (1998).
7. X. Deng, G. Miller, R. Wang, L. Xu, and A.D. Compaan, "Study of Sputter Deposition of ITO Film for a-Si:H n-i-p- Solar Cells, *2nd World Conference and Exhibition on Photovoltaic Solar Energy Conversion—Proceedings* (to be published).

Title: **Characterization of Amorphous Silicon Thin Films and PV Devices**

Organization: Department of Physics, University of Utah, Salt Lake City, Utah 84112

Contributors: P.C. Taylor, principal investigator; G. A. Williams, W. D. Ohlsen, J. M. Viner, S. L. Chen, N. Schultz, T. Su, W. Xu

Objectives

The major objectives of this subcontract are (1) to prepare new materials based on hydrogenated amorphous silicon (a-Si:H), (2) to characterize the important defects and impurities in the bulk and at surfaces and interfaces, (3) to identify metastabilities and to determine if the metastabilities that plague devices are "intrinsic" or "extrinsic", (4) to obtain a better understanding of how defects affect device performance.

Approaches

Two major approaches are utilized both (1) to improve the understanding of metastabilities in a-Si:H, alloys based on a-Si:H, microcrystalline alloys, and devices and (2) to develop schemes to mitigate the deleterious metastabilities in these materials and devices. First, novel alloys, such as those containing sulfur or selenium, are grown and characterized. Special emphasis is placed on understanding how impurities affect the electronic properties of such alloys and of devices based on such alloys. Second, a wide array of characterization techniques is employed to study the optical and electronic properties. The optical techniques include optical absorption as measured using photo-thermal deflection spectroscopy (PDS), photoluminescence (PL), PL excitation spectroscopy, optically detected or optically pumped electron spin resonance (ESR) and other spectroscopies using a wide range of optical sources. The major magnetic resonance technique is ESR. The transport techniques are photoconductivity (PC) and the constant photocurrent method (CPM).

Research Results

The subcontract is divided into two tasks. One task is the growth of doped and undoped a-Si:H and related alloys. Alloys with concentrations of group VI elements, such as sulfur or selenium, have been found to exhibit very inefficient, n-type doping, and the potential of sulfur [1-4] and selenium [5] alloys for photovoltaic applications has been investigated. The plasma assisted chemical vapor deposition (PECVD) system has been up-graded to a three-chamber system capable of making state-of-the-art films and devices.
A second task is the characterization of a-Si:H and related alloys and devices. We have been using photoconductivity (PC) [6], photoluminescence excitation (PLE) spectroscopy, time resolved PL, optically detected magnetic resonance (ODMR), electron spin resonance (ESR) [7-9], and spin-dependent photoinduced absorption (PADMR) [10] to probe defects which produce absorption below the gap in a-Si:H. A review of some of the most recent results is available elsewhere [11].

Perhaps the most significant result of the past year is the use of second harmonic detection of ESR and optically induced ESR (LESR) in a-Si:H and related alloys. This new technique [9] provides an increase in the signal-to-noise ratios of more than three orders of magnitude and allows defects in a-Si:H to be studied at concentrations much lower than possible previously.

Electron spin resonance (ESR) and light-induced ESR (LESR) in a-Si:H have been studied for many years. In the dark there exists an ESR resonance at g = 2.0055 and a peak-to-peak linewidth of the usual derivative spectrum of ΔH_{pp} of about 7.5 G. This spectrum is attributed to a silicon dangling-bond defect. Below 40 K these dangling-bond defects are very difficult to observe because of a technical difficulty known as microwave-power saturation. For this reason we have perfected a rapid passage technique to increase the sensitivity of these measurements. To test this technique we have measured the LESR at about 40 K. In LESR two additional signals appear, a broad line at g = 2.01 with $\Delta H_{pp} \approx 20$ G and a narrow line at g = 2.004 with $\Delta H_{pp} \approx 6$ G. The broad line has been

assigned to holes trapped in the valence-band tail and the narrow line to electrons trapped in the conduction-band tail. Prior to our recent results [9] there were no detailed kinetic measurements of the low-temperature LESR in a-Si:H. The reason that detailed measurements were not performed previously is simply that the ordinary derivative detection technique does not provide sufficient signal-to-noise ratios. However, using the second-harmonic technique the saturation of the LESR (and also of the dark ESR) signal with increasing microwave power is drastically reduced. With this technique we have measured the LESR lineshapes and kinetics over a wide range of excitation intensities.

The ratio of the broad line to the narrow line is larger in the second-harmonic spectrum. This phenomenon is caused by the different saturation behaviors of the broad and narrow lines in the two detection schemes. It is not easy to get an accurate measurement of the spin density using only the second-harmonic detection, but one can accurately measure spin densities using the second-harmonic detection scheme if the signals are tied to unsaturated measurements of the signal using the ordinary detection scheme. In this way one may measure dark ESR spin densities that are well below 10^{16} cm^{-3} at low temperatures provided that the samples are thick enough so that the ESR is not dominated by spins at surface states.

Figure 1 shows that at 40 K the second-harmonic signal does not saturate appreciably with increasing microwave power even though the first-harmonic signal is very easily saturated. The magnitude of the second-harmonic signal grows roughly linearly with increasing microwave magnetic field (roughly as the square root of the microwave power). At low microwave fields the dependence is slightly super-linear while at high microwave fields the dependence becomes slightly sub-linear. This behavior is expected theoretically.

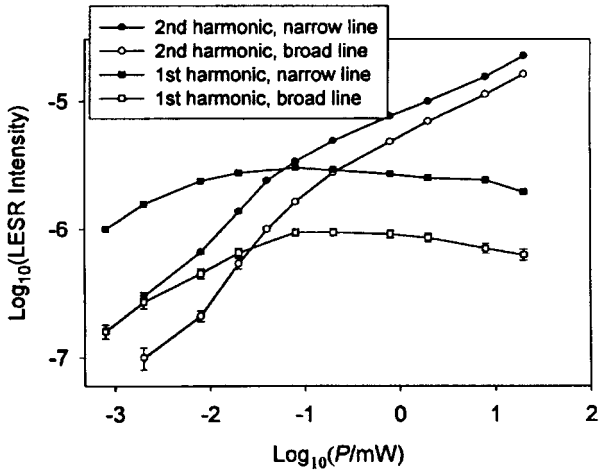

Figure 1. LESR intensity as a function of microwave power.

The increase of the narrow line with increasing microwave power is slower than the increase of the broad line, a fact that leads to the relative suppression of the narrow line. Figure 1 also shows the extensive saturation of the first harmonic signal. It is clear from Fig. 1 that at 40 K the first harmonic signal is partially saturated even at the lowest attainable microwave powers. In addition, the saturation occurs much more easily for the narrow line than for the broad line. Since saturation is always a problem at this temperature, one may easily underestimate the intensity in the narrow line using the commonly employed first-harmonic-detection scheme. There is some evidence for such an underestimate in the literature [12].

Even though it is not central to the solution of problem of eliminating the metastabilities in a-Si:H films and PV devices, whether or not there exist significant numbers of charged defects in a-Si:H is an

important question. From the defect pool model [13] it has been suggested that the density of charged dangling-bond defects is considerably greater than that of the neutral defects, even in device-quality a-Si:H. Some recent measurements also tend to confirm this suggestion [12]. Some of these conclusions have been based on the ratio of the spin densities in the broad and narrow lines of the LESR. Although the detailed reasons are not clear, it is well known that the LESR measurements only measure a fraction of the light-induced carriers in the band tails. Fast geminate recombination and short spin-spin relaxation times are clearly two important reasons why no LESR is observed for carriers trapped in shallow band-tail states. Probably only deeply trapped carriers exhibit LESR because the localization lengths decrease with increasing trapping energy. Because we do not know what energy distinguishes whether the trapped carriers yield a LESR signal, and furthermore we do not have any reason to assume that these energies are the same for trapped electrons and trapped holes, we may not expect that the spin density of the broad line must be equal to that of the narrow line, even in the absence of artifacts such as microwave saturation or of charged defects. Therefore, to postulate the existence of charged defects based solely on the LESR results is unfounded. In addition, subtle saturation effects, even in the second-harmonic-detection case, may also influence the accuracy of the decomposition into trapped electrons and trapped holes.

Conclusions

Major accomplishments of the previous year include (1) an evaluation of the potential for n-type doping of a-SiS_x:H and a-$SiSe_x$:H alloys, (2)an investigation of the optically induced metastabilities in a-SiS_x:H and a-$SiSe_x$:H alloys with regard to their potential use in photovoltaic applications, (3) an understanding of the important optically-induced metastabilities in a-Si_xN_{1-x}:H alloys, and (4) a more detailed understanding of the kinetics of light induced ESR due to carriers trapped in localized band-tail states in a-Si:H. Also of importance are preliminary measurements of the defects and metastabilities in hot-wire samples of a-Si:H and in samples of a-Si:H made under strong hydrogen dilution. The preliminary measurements on hydrogen dilution suggest that the production of neutral silicon dangling bonds is not suppressed from the standard material even though there appears to be an improvement in the stability of cells made using the hydrogen-dilution process.

The new three-chamber, load-locked PECVD deposition system is functioning and producing intrinsic and doped films of a-Si:H. Plans for the next year include the production of high quality devices using this new deposition system.

References

1. "Relaxation to Hopping Conductivity in Sulfur-Doped Hydrogenated Amorphous Silicon" (J.-H. Yoon and P. C. Taylor), J. Non-Cryst. Solids **227-230**, 385 (1998).

2. "Light-Induced Recombination Centers in Hydrogenated Amorphous Silicon-Sulfur Alloys" (J.-H. Yoon, P. C. Taylor, and Czang-Ho Lee), J. Non-Cryst. Solids **227-230**, 324 (1998).

3. "Effect of Sulfur Doping on electrical Conductivity of a-Si:H" (R. M. Mehra, Jasmina, P. C. Mathur, and P. C. Taylor), Thin Solid Films **312**, 170 (1998).

4. "Kinetics of Light Induced Defect Formation and Annealing in Hydrogenated Amorphous Silicon Alloyed with Sulfur" (B. Yan, S. L. Chen, and P. C. Taylor), MRS Symp. Proc. (1998), in press.

5. "Properties of Hydrogenated Amorphous Silicon Films Alloyed with Selenium" (S. L. Chen, J. M. Viner, and P. C. Taylor), MRS Symp. Proc. (1998), in press.

6. "Study of Photoconductivity in TBP Doped n-Type Hydrogenated Amorphous Silicon Using Argon as Carrier Gas" (R. M. Mehra, I. Kaur, P. C. Mathur, and P. C. Taylor), J. Non-Cryst. Solids **227-230**, 243 (1998).

7. "Defect Structure in Nitrogen-Rich Amorphous Silicon Nitride Films" (B. Yan, J. H. Dias da Silva, and P. C. Taylor), J. Non-Cryst. Solids **227-230**, 528 (1998).

8. "Localized Electronic States in a-Si:H as Determined from ESR and LESR" (P. C. Taylor), in *Properties of Amorphous Silicon and its Alloys*, T. Searle, ed. (INSPEC, London, 1998), p. 139.

9. "Excitation Intensity Dependence of Light-Induced Electron Spin Resonance in Hydrogenated Amorphous Silicon Films" (B. Yan and P. C. Taylor), MRS Symp. Proc. (1998), in press.

10. "Excitation Energy Dependence of Photoinduced Absorption in Intrinsic a-Si:H" (N. Schultz, Z. V. Vardeny, and P. C. Taylor), MRS Symp. Proc. (1998), in press.

11. "Photovoltaic Applications of Amorphous Silicon: The Journey from Basic Research to Development," (P. C. Taylor), Egypt. J. Phys. (1998), in press.

12. "Nonequilibrium Occupancy of Tail states and Defects in a-Si:H: Implications for Defect Structure" (G. Schumm, W. B. Jackson, and R. A. Street), Phys. Rev. **B48**, 14198 (1993).

13. "Improved Defect-Pool Model for Charged Defects in Amorphous Silicon" (M. J. Powell and S. C. Deane), Phys. Rev. **B48**, 10815 (1993).

Title: **Alternative Window Schemes for $CuInSe_2$-Based Solar Cells**

Organization: Electronic Materials Laboratory
Washington State University / Tri-Cities
Richland, Washington

Contributors: Larry C. Olsen, Principal Investigator;
F.W. Addis, Wenhua Lei and Kaushik Vaidyanathan

Objectives / Approach

The objectives of this program are: to develop alternate heterojunction partner layers for high efficiency $CuInSe_2$-based thin film solar cells; and, to improve the understanding regarding the effects of these buffer layers and related processing upon cell performance. The program is structured into three tasks: (1) MOCVD growth of non-cadmium containing window layers (or buffer layers); (2) Optimized processing of buffer layers for high efficiency solar cells; (3) Characterization of layers and devices. The general approach to these studies has consisted of utilizing substrates provided by industry and NREL, so that efforts could focus on buffer layer investigations. MOCVD growth of buffer layers is accomplished with a SPIRE 500XT reactor with added gas handling capabilities. Optimum processing parameters for candidate buffer layers have been determined by characterizing Al/X/CIS test cell structures, where X refers to a heterojunction partner. After buffer-layer growth parameters are determined, completed solar cell structures are fabricated and evaluated. A recently acquired sputtering system will allow deposition of n-ZnO for the TCO at WSU, and thus, fabrication of complete cells for process development. Efforts this past year continued to concentrate on studies of highly resistive ZnO buffer layers grown by MOCVD.

Effect Of Air Exposure On ZnO/CIS Cells

Although 12 % to 14 % cells have been fabricated with highly resistive ZnO buffer layers grown by MOCVD, an improved understanding of processing required to achieve high efficiency is still required. For example, it is found that it is beneficial to "age" i-ZnO/CIS cell structures in air for several weeks before completing the cell with a TCO and collector grid. Part of this years effort was devoted to investigating the effects of air exposure. Various aspects of these studies are discussed in the following sections.

Resistivity Of MOCVD ZnO Films

Figure 1 describes our general experience with MOCVD ZnO films grown on glass and CIS substrates. The results apply to films with nominal thicknesses of 700 Å to 800 Å. Although the time needed for films to acquire a resistivity of 10^4 ohm-cm varies, this value is consistently attained within 10 to 30 hours. The initial resistivity is apparently due to the films being oxygen-deficient. It is expected that oxygen molecules are physisorbed on the ZnO surface and in grain boundaries, and then chemisorbed to provide two oxygen atoms to occupy two oxygen vacancies, and thereby neutralize two donor states. The same process has been reported for ZnO gas sensors [1]. The film becomes resistive due to barriers formed at the grain boundaries, and possibly due to changes within grains as well since the grain sizes are only on the order of 500 to 1000 Å.

Behavior Of ZnO/CIS Cells

As described in Figure 1, experience with MOCVD ZnO buffer layers indicates that exposure of i-ZnO/CIS structures to air beyond a 30 hour period is beneficial to ultimate cell performance. Therefore, adjustment of buffer layer resistivity alone is not be sufficient to attain high efficiencies. The term test cell efficiency refers to estimated values obtained for devices fabricated with semitransparent Al contacts replacing a TCO layer. The band shown in Figure 1 that refers to efficiency is also representative of completed cell results. The effect of aging by exposure to air is further illustrated by Figure 2. Current-voltage characteristics are given in Figure 2A for a test cell formed on a i-ZnO/CIS structure designated 97XC022 and characteristics

for a completed cell, 97XC021, are given in Figure 2B. The MOCVD i-ZnO buffer layers were grown on structures 97XC021 and 97XC022 simultaneously. The CIS devices were formed on 2 cm x 2 cm substrates diced from a 10 cm x 10 cm plate provided by Siemens Solar with a cross section of CIS/Mo/Glass. Although the CIS material has a small percentage of Ga near the CIS-Mo interface, the photoresponse band edge is actually approximately 1.0 eV. Test cells were formed on 97XC022 within a few days after i-ZnO growth, while completed cells were formed on 97XC021 three weeks after buffer layer deposition. Exposure of 97XC021 to air for several weeks allowed the fabrication of cells with efficiencies greater than 11%. Cell fabrication involved: growth of a 800 Å i-ZnO buffer layer; deposition of 0.5 to 1.0 μm of n-ZnO by RF sputtering and deposition of Ni/Ag collector grid at IEC. Cells fabricated from ZnO/CIS structures immediately after buffer layer deposition and on those completed after a structure has been exposed to versus air for several weeks (aging process) differ in two significant ways. First, efficiencies differ as illustrated by cells 97XC021 and 97XC022. Secondly, dark curves translate fairly well for cells based on aged structures, whereas, cells fabricated from non-aged structures exhibit enhanced current losses under illumination. In an effort to understand these differences, J-V analyses were conducted using PC-1D to determine the behavior of device parameters and depth concentration profiles were carried out with SIMS to determine if any material changes are apparent.

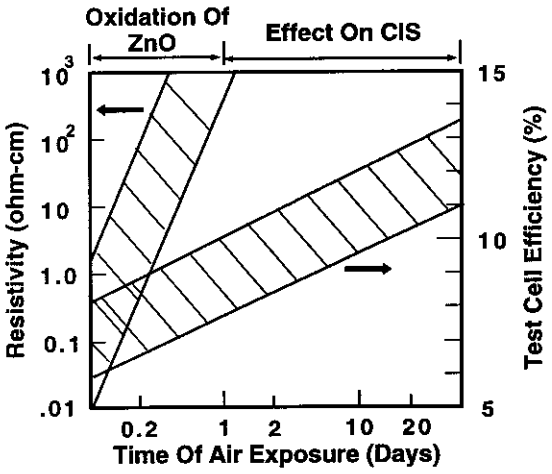

Figure 1. Resistivity for ZnO films on glass witnesses and cell efficiency versus time of air exposure

J-V Analyses Using PC-1D

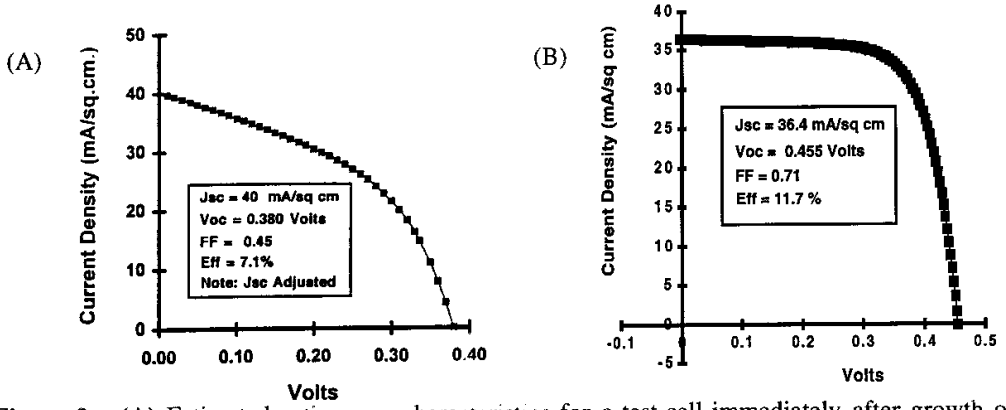

Figure 2. (A) Estimated active area characteristics for a test cell immediately after growth of ZnO buffer layer on device structure 97XC022. (B) Active area characteristics of completed cell for which ZnO buffer layer was exposed to air for three weeks prior to deposition of a TCO and collector grid.

The one dimensional code PC-1D was utilized to fit dark and illuminated data for both discussed above. Four parameters were varied in the fitting process, the dopant concentration in CIS (p_{CIS}), surface recombination velocity (S_n), electron lifetime in CIS (τ_n), and the effective shunt resistance (R_{sh}). Values of parameters for dark and illuminated curves are given in Table 1. Consider parameters for the illuminated curves of the two cells. The surface recombination velocity is essentially the same for the two cases. The other three parameters all changed significantly, however. It is interesting that τ_n and p_{CIS} are CIS properties, and even though R_{sh} involves conducting paths intersecting the ZnO-CIS interface, the conducting paths penetrate into the CIS substrate. Comparison of parameters for dark and illuminated curves in the two cases is also

Table 1. J-V Parameters Determined With PC-1D (ohm-cm^2)

		τ_n (picosec)	S_n (cm/s)	R_{sh} (ohm-cm^2)	p_{CIS} (cm^{-3})
97XC021	Dark & Illuminated	330	5E6	500	9E16
97XC022	Dark	80	7E6	500	1E16
	Illuminated	80	7E6	40	1E16

interesting. Based on these analyses, the increased current losses under illumination for cell 97XC022 are due to a light enhanced shunt conductance (or reduced shunt resistance). These results are representative of CIS cells based on MOCVD ZnO buffer layers. In summary, we find that cells based on non-aged ZnO/CIS structures exhibit a light enhanced shunt conductance, an electron lifetime on the order of 80 picoseconds, whereas cells based on aged structures are characterized by an electron lifetime on the order of 300 picoseconds and do not exhibit any significant light enhanced shunt conductance. It should also be noted that the hole concentration increases from 2E16 cm^{-3} to 9E16 cm^{-3} when comparing the non-aged and aged cells. The light-enhanced shunt conductance is discussed further below.

SIMS Depth Concentration Profiles

SIMS profiles were acquired for i-ZnO/CIS structures similar to that used for 97XC021 and 97XC022. These profiles were provided by Angus Rockett at the University of Illinois. Specifically, ZnO buffer layers were grown using a two-step approach involving growth of 100 Å at 250°C followed by growth of approximately 700Å at 100°C (2). Depth concentration profiles of zinc, oxygen, copper and selenium were obtained for structures within a few days after buffer layer growth. In addition, profiles were acquired for structures consisting of MOCVD ZnO films deposited on epitaxial CIS layers which had been grown on GaAs. Depth concentration profiles for i-ZnO grown on an epitaxial CIS substrate are given in Figure 3A. The logarithm of ion count is plotted versus sputtering time so that the nature of elemental concentrations at the interface can

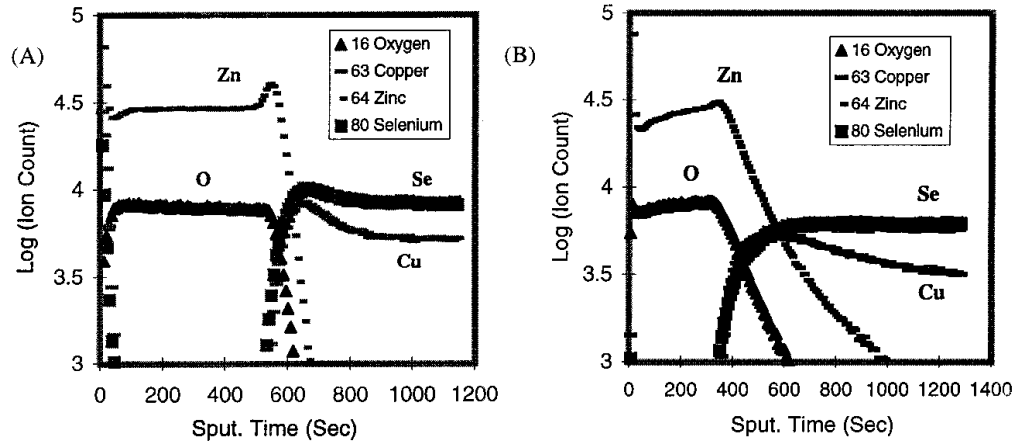

Figure 3. (A) SIMS depth concentration profiles for an i-ZnO/CIS structure with the CIS layer being an epitaxial film grown on GaAs. (B) SIMS depth concentration profiles for an i-ZnO/CIS structure with the CIS layer being the polycrystalline film of a Siemens substrate

be emphasized. The zinc and oxygen profiles at the interface are very sharp indicating that relatively little interdiffusion has occurred. Depth concentration profiles are given in Figure 3B for an i-ZnO/CIS structure consisting of MOCVD ZnO grown on Siemens polycrystalline CIS. The i-ZnO films for the epi- and polycrystalline structures were grown simultaneously. When compared with results for the epi-structure, profiles obtained for the polycrystalline sample clearly indicate that zinc and oxygen diffuse into the CIS layer. Based on a comparison of results for the epitaxial and polycrystalline CIS structures, it seems reasonable to conclude that the inward diffusion of Zn and O occurs along grain boundaries.

Based on the results for solar cell performance and depth concentration profiles, a tentative model to explain the aging effects exhibited by i-ZnO/CIS cell structures was formulated. The model consists of the following assumptions: (1) zinc and oxygen diffuse along CIS grain boundaries during growth of ZnO buffer layers by the WSU MOCVD process; (2) zinc atoms reside in copper vacancies along CIS grain boundaries creating donors, making the grain boundaries n-type and significantly reducing the electron lifetime; (3) the initial effect of oxygen is much less than zinc, either due to a smaller concentration or the particular sites occupied; (4) increased electron concentration along grain boundaries as a result of illumination leads to an enhanced junction shunt conductance; (5) air exposure of the ZnO/CIS structure results in additional oxygen along grain boundaries of CIS that can complex with Zn_{Cu} sites to neutralize the donor state; (6) the passivated grain boundaries result in increased electron lifetimes and elimination of the light induced shunt conductance. Assuming oxygen diffuses along CIS grain boundaries at ambient temperatures over a 30 day period is consistent with models for oxygen diffusion in CdS/CIS cells after a 2 minute air anneal at 200°C [2].

Studies With Siemens CIGSS Substrates

Most of our ZnO buffer layer development has been conducted with Siemens CIS material. During this past year we initiated an effort to determine a process for the graded absorber material referred to as CIGSS. This material has sulfur incorporated in the surface region such that the surface concentration is approximately CuInSeS. This effort was motivated for two reasons: higher efficiencies are possible with the CIGSS material relative to Siemens CIS; and Siemens is only producing CIGSS at this time. Several run profiles were tried for the MOCVD growth process. Best results were achieved with a procedure involving heating a substrate to 250°C in nitrogen, followed by growth at 100°C. The hydrogen carrier gas only flows during the 100°C growth step. Using this modified process, test cells were fabricated that indicated that completed cells with efficiencies in the 11 to 12 % range should be possible, and V_{oc} values should be on the order of 490 mV. After process development led to a procedure for growth of ZnO buffer layers on the CIGSS material, ZnO/CIGSS structures were sent to IEC for deposition of n-ZnO TCO layers and Ni-Ag collector grids. Although a variety of results were obtained some cells exhibited efficiencies near 11 %. The best performing cell had the following properties: Jsc = 36.1 mA/cm2, Voc = 0.486 Volts, FF = 63.6 % and Efficiency = 11.2 %. Further improvement is needed in Voc and FF. Future studies will include more work with ZnO buffer layers on CIGSS substrates.

Conclusions And Future Work

The performance of CIS cells fabricated from structures with MOCVD ZnO buffer layers improves if the i-ZnO/CIS structure is allowed to age in air for several weeks. Based on the results of J-V analyses and SIMS profiles, a model has been developed that explains the aging effects in ZnO/CIS cells fabricated with WSU ZnO buffer layers. From these studies, it is clear that it is desirable to attain stochiometric ZnO buffer layers as grown. Future investigations will focus on the use of nitrogen carrier gas instead of hydrogen, and improved control for the oxygen precursor. With the addition of a sputtering system for depositing n-ZnO TCOs, process development will involve a greater emphasis on the use of completed cells.

Acknowledgments
This work was supported by NREL Subcontracts XAF-6-15375 and XAF-8-17619. We are grateful for the guidance provided by our contract monitor Bolko Von Roedern, collaboration with Angus Rockett at the University of Illinois for SIMS studies, Kannan Ramanathan and other investigators at NREL, and William Shafarman of IEC. Finally, we are very grateful to Siemens Solar and NREL for providing CIS substrates.

References

1. P. Mitra, A. Chatterjee and H. Maiti, “ZnO Thin Film Sensor,” Materials Letters 35 (1998) p.33.
2. David Cahen and Rommel Noufi, Surface Passivation of Polycrystalline, Chalcogenide Based Photovoltaic Cells, Solar Cells 30 (1991) p. 53.

Title: **Overcoming Degradation Mechanisms in CdTe Solar Cells**

Organization: Weizmann Institute of Science, Rehovot 76100, Israel.

Contributors: D. Cahen, G. Hodes, K. Gartsman (Principal Investigators); I. Vissoly-Fisher, O. Rotlevi.

Objectives

To investigate the back ‘ ohmic’ contact to the p-CdTe with the aim of improving the stability of this contact while maintaining performance. Several strategies are involved in this study.

i) Separate back contact lifetime performance with overall cell lifetime performance.
ii) Investigate new back contact materials.
iii) Surface treatment of the CdTe to modify the contact.

Results

-a- Since starting this project in late July 1998, we have concentrated on two topics Finding experimental tools for, and conditions under which we can identify and preferably quantitate atom/ion diffusion and ion drift in CdTe films and CdS/CdTe cells, as well as correlate these with the film electronic and cell electrical characteristics. Without such tools and conditions we cannot hope to achieve the project's goals.

-b- In parallel we investigate alternative back-contact materials as well as alternative approaches to the use of existing back contacts, and with these, means for assessing the efficacy of such new methods.

While all the methods are familiar ones for our laboratories, they need to be tested with and adapted to use with the CdTe films and CdS/CdTe cells under investigation. The September '98 CdTe team meeting, as well as intensive consultations with our USF sub-contractor made clear that we will need to carry out these investigations ourselves and cannot rely on existing know-how.

-a- Due to the structure and grain size of the CdTe films that we received from USF (even before the start of the projects) we concluded that a new system for electronic materials characterization in the Scanning Electron Microscope (SEM), one mainly focussed on EBIC (Electron Beam-Induced Current) will be needed, to be operational in our JEOL 6400 SEM. As the commercial systems appeared unsatisfactory for our purposes, we built one ourselves, starting even before the official beginning of the project and mostly with other funds. This system is now operational and allows routine investigations of films, especially with view to map grain boundary versus grain interior properties. Thus we find indications for rather appreciable grain boundary recombination in as received films (Figure 1). The system uses a novel, custom-built, advanced EBIC sample holder for specimen contacting suitable for vacuum transfer, an extractable, precision micrometer-driven manipulation system for electrically contacting any place on the specimen surface. It is used for remote contacting samples during measurements and for local application of electric fields to samples.

The complete system is computerized using custom-written software for data analyses and will be enhanced shortly with a system for electron beam modulation (beam blanking) that will allow monitoring the EBIC amplitude when the frequency of the electron beam modulation is swept. An essential part of this system is the 10 MHz beam blanker that we bought (using other funds). This beam blanker arrived very recently and will be installed shortly.

In further work we explored the conditions under which we can use the transient ion drift interpretation of transient capacitance measurements, so as to distinguish ionic from electronic processes in these samples1 This work is in progress.

-b- We have started to investigate Ni-P contacts to the p-CdTe. Ni-P is a well-known electrically conducting material which can be deposited by electroless deposition. It is only recently, however, that it has been used for contacts to semiconductors 2,3. Since the deposit contains P, a known p-type dopant for CdTe, it appears a good choice as a contact material as a p^+ tunneling layer of CdTe is likely to form at the interface. Regarding the stability of the contact, the conditions of preparation of this contact on CdTe (up to 250°C for 90 mn in air) strongly suggest that it will be stable. Our investigation of this material is largely based on this latter point. The deposition procedure, at this early stage, is not reproducible. Many of the films are patchy. However we have obtained good films with contact resistance of ca. $10\Omega/cm^2$ and absolutely no change in this value after heating at 200°C for 15 hr in air (the most stringent conditions we have used up to now). This attests to the very high stability of this contact.
Based on our extensive experience with chemical solution deposition, we are optimistic that we will eventually be able to deposit these films in a reproducible manner.

Future research

The immediate future research will focus on optimization of
-a- the EBIC and TID methods for the USF (and SCI) samples and studying effects of various annealing and back contact application procedures on the EBIC and TID responses;
-b- the Ni-P deposition procedure, on understanding the chemical structure of this material and of its interface with CdTe. Accelerated and normal long-term lifetime testing will be carried out on back contact-CdTe junctions and on complete devices using this material as well as using standard contacts.

References

1. I. Lyubomirski, M. K. Rabinal, V. Lyakhovitskaya, D. Cahen. *J. Appl. Phys.*, 81, 6684 (1997)
2. B. Ghosh, S. Purakayastha, P. K. Datta, R. W. Miles, M. J. Carter, and R. Hill, Semicond. Sci. Tech., 10, 71 (1995).
3. R. W. Miles, B. Ghosh, S. Duke, J. R. Bates, M. J. Carter, P. K. Datta, and R. Hill, J. Crystal Growth 161, 148 (1996).

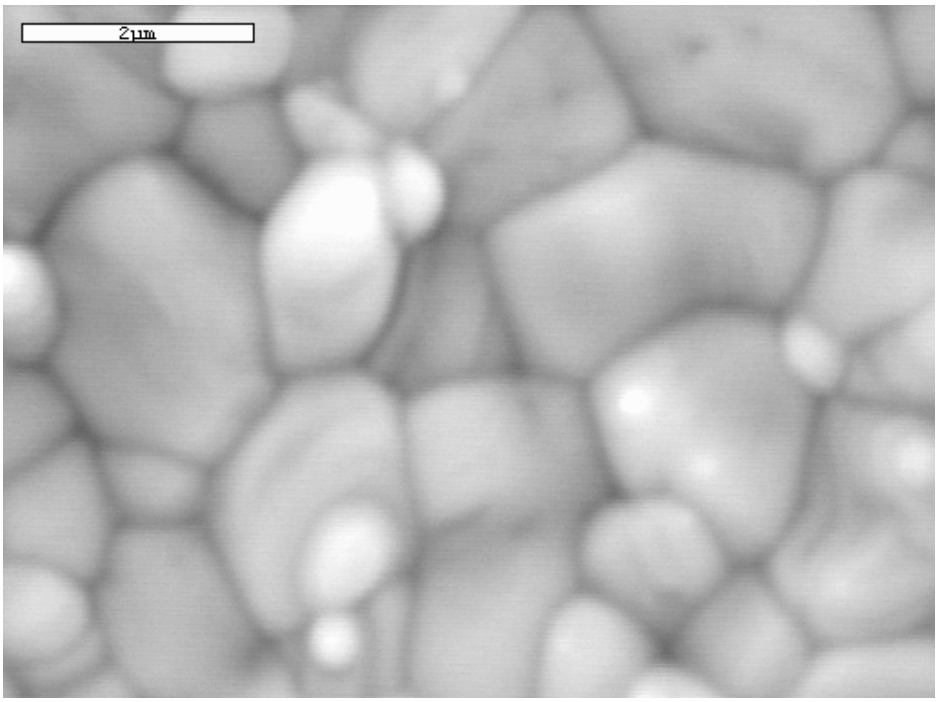

Fig.1.

EBIC image of polycrystalline semiconductor film used for solar sells: grains can be seen in the picture due to the EBIC contrast between grains and grain boundaries caused by different recombination rate (or carrier life time) inside the grains and in the vicinity of the grain boundaries.

6.0 Photovoltaic Manufacturing Technology (PVMaT) Project

6.0 PHOTOVOLTAIC MANUFACTURING TECHNOLOGY (PVMaT) PROJECT—Introduction

C. Edwin Witt (Team Leader), Richard L. Mitchell, Holly P. Thomas, Martha Symko-Davies

INTRODUCTION

The Photovoltaic Manufacturing Technology (PVMAT) Project is designed to help the U.S. PV industry improve manufacturing processes, accelerate manufacturing cost reductions for PV, improve commercial product performance, and lay the groundwork for a substantial scale-up in the capacity of U.S.-based PV manufacturing plants. PVMaT's ultimate objective is to help U.S. photovoltaic (PV) industry extend its world leadership role in PV manufacturing and the commercial development of PV modules and systems. As described in previous Annual Reports, the PVMAT Project is a government/industry research and development (R&D) partnership between the U.S. Federal government (through the U.S. Department of Energy [DOE]) and members of the U.S. PV industry.

NEW SUBCONTRACTS

NREL issued a Request for Proposals (RFP)for additional PV manufacturing R&D late in FY1997. Thirty-one (31) proposals responding to this RFP were received. In FY1998, fourteen (14) new awards were made from these respondees. The efforts are similar to previous PVMaT R&D efforts with somewhat more emphasis on specific problems amenable to manufacturing R&D solutions. The following is a list of the subcontractors and their respective R&D areas.

Company	Manufacturing R&D Area
Ascension Technology, Inc.	Manufacture of the Advanced SunSine^{TM} 325 AC Module
ASE Americas, Inc.	The EFG High Volume PV Manufacturing Line
AstroPower, Inc.	Silicon-Film^{TM} Solar Cells by a Flexible Manufacturing System
Crystal Systems, Inc.	Production of Solar Grade Silicon by Refining of Liquid Metallurgical Grade Silicon
Energy Conversion Devices, Inc.	Efficiency and Throughput Advances in Continuous Roll-to-Roll a-Si Alloy PV Manufacturing Technology
Evergreen Solar, Inc.	Continuous, Automated Manufacturing of String Ribbon Si PV Modules
Global Solar Energy, L.L.C.	Throughput Improvements for Thin-Film Based CIGS Modules
Omnion Power Engineering Corporation	Manufacturing and System Improvements for One and Two kW Inverters
PowerLight Corporation	Advanced Powerguard Manufacturing
Siemens Solar, Inc.	R&D on Siemens Cz Silicon Product Manufacturing
Solar Cells, Inc.	R&D on CdTe Product Manufacturing

Solarex	Improvements in Polycrystalline Silicon PV Module Manufacturing
Spire	Post-Lamination Manufacturing Process Automation for Photovoltaic Modules
Utility Power Group	Development of a Fully-Integrated PV System for Residential Applications

PROGRESS IN FY1998

R&D results from the FY1998 PVMaT projects which were active going into FY1998 (All of which are complete or within several months of completion as of the beginning of FY1999)are presented below. For purposes of this presentation, the five subcontracts primarily addressing module manufacturing R&D will be discussed first.

Recent accomplishments of *ASE Americas, Inc.* include construction and demonstration of prototype equipment for removing phosphorous glass from diffused wafers that can reduce acid consumption and fluoride emissions by 95%, implementation of the first phase of a Statistical Process Control program and the development of a new module diode housing. Their overall efforts have been directed toward improvements that consist of (1) a further decrease in the edge-defined film-fed growth (EFG) wafer thickness to 250 micrometers in mass production and an increase in the number of wafers produced from one crucible, (2) an increase in the electronic quality of as-grown EFG material to meet the demands for higher-efficiency solar cells, (3) an improved solar-cell fabrication technology, (4) developing a diffusion glass removal process that is environmentally safe and reduced in cost, and (5) developing an integrated interconnect, lamination, and fabrication method.

AstroPower, Inc. completed its 4A subcontract addressing the development of a low-cost manufacturing capability for Silicon-Film™ solar cells and panels by using the continuous-processing capability of the Silicon-Film™ technology. Their efforts have been to (1) eliminate wafer-sawing steps, (2) develop a high-yield, continuous manufacturing technology, and (3) increase solar-cell size. The AP225 Silicon-Film™ cell is in production, and efficiencies exceeding 12% have been measured on this 240-cm^2 cell. Small-scale devices have demonstrated efficiencies of 16.6%. Processing advances include the development of a continuous diffusion process and a continuous antireflection-coating process.

Iowa Thin Film Technologies Inc.(ITFT) is increasing the throughput of their metallization, a-Si deposition, laser-scribing, and welding processes, with the goal of reducing the overall module manufacturing costs on the ITFT production line by 68%. They have improved laser registration and substrate throughput by 30% through the development of a new position detector and alignment system and the installation of a new laser scriber, increased throughput in the printer by 70% with an active screen alignment that allows a 10-micron reproducibility, identified a water-based ink that withstands the subsequent processing temperatures, and improved the throughput of the ZnO deposition process step by 50%.

Photovoltaics International, LLC is establishing a low-cost manufacturing capability for linear concentrator modules by using their continuous-processing capability. Under this manufacturing effort, they are taking advantage of the continuous-processing capability of their lens extrusion technology. They have completed the tooling and testing of the new 20-inch lens extrusion process equipment, completed the design and initial fabrication of the receiver assembly station, completed design and prototyping of the roll-formed frame process, and completed development of the self-jigging, low $V_{oc,}$ linear concentrator module.

Siemens Solar Industries is addressing improvements in their Czochralski (Cz) silicon module manufacturing technology to reduce module cost per watt by 18%. These goals are being addressed by identifying alternative Cz module designs, material sources, and processes that lower module component costs, and by improving manufacturing process yields, reducing labor costs in Cz module manufacturing, and increasing productivity. They have implemented production of the 150-mm cell and module product line, which leverages the use of silicon by over 30% in the production of Cz solar cells; continued to improve manufacturing productivity and yield by over 10%; implemented Statistical Process Control in their diffusion and cell printing lines to improve capability and electrical yields; and implemented polysilicon preparation techniques to mitigate silicon supply variation on yields.

Next the five subcontracts addressing issues in the general category of manufacturing improvements for PV system integration will be discussed.

Ascension Technology, Inc. (ATI) completed product enhancements and established the manufacturing capability for the fully integrated "SunSine^{TM}300 AC Module." This product, rated at 250 Wac at Standard Test Conditions (STC), consists of the SunSine^{TM}300 AC inverter attached to the back of the ASE Americas, Inc., large-area PV laminate (260 to 300 Wdc). The integrated unit is UL-listed, National Electrical Code (NEC) compliant and meets Federal Communications Commission (FCC) standards for electromagnetic interference. It is sold as a complete power unit, ready for utility interconnection. Features of the SunSine^{TM}300 inverter include a plug-in connector to the PV panel for rapid "AC Module" assembly and wiring quick-connectors for rapid installation with no DC field-wiring needed. ATI recently completed a pilot production run, to ISO 9001 standards, of 109 SunSine^{TM}300 AC Modules with 100% successful operation at start-up. Over 100 units have been installed and a production run of 200 AC Modules is now in progress.

Evergreen Solar, Inc. combined several developments in module-related advancements. Based on their knowledge about the variety of polymeric materials on the market, Evergreen evaluated alternative materials to improve PV-panel manufacturing and PV-system installation. After testing and evaluation, the company identified two materials. The first is a transparent encapsulant laminated in air. This material permitted Evergreen to develop a continuous, non-vacuum lamination process for PV panels using a heated-roll method. The encapsulant has reported material costs lower than EVA-based materials currently in use. Evergreen also identified a PV-laminate backskin material. This material, used to replace Tedlar^{TM}, can also be applied as an edge sealant. This backskin material eliminates the need for a frame, as it is strong enough to protect the edges of the glass superstrate. The backskin is also highly puncture resistant, with low vapor permeability and high adhesion characteristics. The company capitalized on these multiple qualities to develop their Innovative Mounting System, where a mounting rail adheres to the back of the module for rapid, easy, panel installation in the field.

Solar Design Associates, Inc. teamed with Solarex and Advanced Energy Systems, Inc. (AESI) to improve reliability and safety and to reduce costs through pre-engineered components for standardized, low-cost PV systems. AESI completed product enhancements for their MI-250 MicroInverter, including software controls and power-line carrier monitoring. This AC inverter is UL-listed, FCC-compliant, and can be ordered in export voltage ranges. Solarex developed a low-cost, pre-engineered assembly for mounting a PV array. The standardized system combines framing and mounting the PV array and incorporates electrical interconnection, array wiring, grounding, and lightning protection into the frame. With features such as quick-connect wiring and approved, simplified grounding, PV systems can be rapidly installed at minimal cost. For example, a recent 1-kW Solarex system demonstration using thin-film modules was completely installed and operational, including the utility interconnection, in less than 4 hours.

Solar Electric Specialties (SES) completed manufacturing improvements as part of their effort to increase standardization and modularity in integrated, factory-packaged PV systems. The benefits to this approach are shorter lead times with lower materials costs, higher overall quality and system reliability, decreased management and engineering time, and lower installation labor. SES used two products, a 200 Wdc Modular Autonomous PV Power Supply (MAPPS) and a mobile 1-kW Photogenset, to establish this approach. The MAPPS product line is a stand-alone PV power system consisting of PV modules, solid-state power control systems, sealed batteries, and enclosures for the batteries and power control system.

UL-listed and FM-approved products are available with outputs ranging from 12 - 24 Vdc. The Photogenset product line combines a propane-powered generator (with an automatic oil-changer) integrated with a PV array and battery storage to provide off-grid AC power. The 1-kW mobile system used to establish the processes for this SES product line includes a fully enclosed trailer containing a 4-kW inverter, a micro-processor-based power controller with full remote communications capabilities, a 2-channel PV combiner box, and wiring protection (disconnects and over-current protection) designed to meet UL safety standards. Although the system design and component selection were based on code requirements, this product is not UL-listed, as the company was unable to obtain a UL-listed generator.

Utility Power Group, Inc. (UPGI) completed manufacturing modifications and power processing improvements for larger utility interactive (U-I) systems. Based upon their utility-scale PV demonstration installations, UPGI determined that the most important factor to reduce costs and improve reliability was to bring as much of the field installation work as possible onto the factory floor, where labor is more efficient and assembly more consistent. UPGI's approach was to address the PV modules and power conversion and control separately, and to develop factory assembly methods for each. For PV modules, UPGI established a manufacturing process for integrating PV laminates into pre-assembled, field-deployable modular panels which can be assembled into 7- to 15- kW sub-arrays. UPGI assembles laminates into Modular Panels (MPs) consisting of several Siemens frameless laminates, either Model M-55 or SP7 (depending upon the size of the system that is ordered), adhesively attached to 'C'-shaped steel mounting rails. Laminate interconnection is also accomplished on the factory floor. The pre-assembled MPs are then mounted into recyclable shipping fixtures and delivered to the field ready for placement on the ground support structures.

For their power conversion, UPGI streamlined assembly by integrating power conversion/control electronics, array-tracking control electronics, source-circuit protection hardware, and DC and AC switchgear into a single, pre-assembled unit termed an Integrated Power Processing Unit (IPPU). UPGI attaches the tracking mechanism for each sub-array to the back of the IPPU's enclosure prior to shipment to the site, so the unit arrives ready for connection at the center of each sub-array. The IPPU's 3-phase inverter is 96% efficient with less than 3% total harmonic distortion (THD) over a 25% to 100% output range. UPGI also refined the field installation methods for these systems. The company accomplished their objectives, achieving a 40% reduction in area-related balance-of-system costs and reducing net total costs of their single-axis-tracking PV systems by 23%. UPGI has deployed or contracted to place 10 systems totalling 2.5 MW.

Three subcontractors addressed manufacturing and product improvements related to PV inverters.

Advanced Energy Systems, Inc. (AESI) improved product reliability and instituted design modifications to simplify manufacturing and maintenance, and consolidated subcomponents into compact, readily serviceable units. For example, the digital inverter control and all inverter controllers (3-phase) are incorporated into a single printed circuit board. AESI also integrated power functions into a modular "PowerBlock," combining the Insulated Gate Bipolar Transistor (IGBT) power-switching subassembly, heat sink, fans, and capacitors. Another significant step was to incorporate communication, data-logging, and remote trouble-shooting capabilities into the product. AESI is demonstrating their results with a hybrid and a utility-interactive 60-kW inverter designed for fully automatic, unattended operation. The performance characteristics of the PV-wind hybrid unit include input voltages of 189 - 324 Vdc, output voltages of 3-phase 480 Vac, 60 Hz. Performance characteristics of the Utility-Interactive (U-I) unit include 95% peak efficiency, less than 5% THD, and internal circuit protection in the case of excess DC input voltages.

Omnion Power Engineering Corp. is developing a 100-kW U-I power-conversion system using a highly integrated power-switching assembly with the IGBTs laminated directly to the heat sink. The laminated power-switching assembly results in lower losses, smaller heat sinks, and reduced factory labor and assembly time. The unit's design was influenced by round-table discussions with system users, integrators, and utilities to define the most useful parameters for this product. Performance characteristics include a 93% peak inverter efficiency, a 300 - 600 Vdc input voltage window, with an operating voltage range of 252 - 308 Vac at 59-61 Hz. Omnion has emphasized reliability in this product line and will use ISO9001 qualification procedures in their design process and in manufacturing. The unit is designed for a

calculated mean-time-before-failure design goal of 40,000 hours. The product can be upgraded with optional features such as enhanced data acquisition suggested by the round-table advisors. The unit is designed to comply with applicable UL, IEEE, NEC, and FCC guidelines.

Trace Engineering streamlined their product manufacturing and improved reliability through a modular, versatile building-block inverter design for stand-alone, hybrid, or U-I applications. The building block can operate in parallel or in series for single, split- and 3-phase applications. This universal "building block" design is intended to reduce Trace Engineering's manufacturing costs while maintaining sufficient versatility and compatibility with current inverter models. Trace Engineering used a 2.5-kW unit to demonstrate their approach, and elements of this design have already been incorporated into current Trace Engineering products. In addition, Trace developed a modular, UL-listed inverter and BOS packaging system, readily expandable for a variety of applications.

It is important to put the technical progress that the U.S. PV industry is making into perspective. Based on the improvements in manufacturing processes, reductions in manufacturing costs, introduction of new products, and improvements in product performance, it would be expected that the U.S. PV industry would exhibit both a scale-up of its U.S.-based PV manufacturing capacity and a reduction in its production costs. This has indeed been the case. Data pertaining to module manufacturing cost and capacities have been collected from PVMaT participants. The most recent data, shown in the accompanying figure and collected early in FY1998, represents an update of previous projections regarding these subcontracted efforts. Data in this figure are based on each manufacturer's maximum production capacity during a given year, assuming they were to operate at maximum capacity. The "average" represents the average cost per watt of modules (weighted by each participant's capacity) produced by these twelve PVMaT industrial participants. Module cost estimates were then based on these manufacturing levels and included only those costs directly associated with the manufacturing of the modules (not marketing, administration, sales, etc.). It should be noted that data associated with any particular point in time represent a potential capability. Actual manufacturing production levels may be less (and concomitant costs higher) due to other considerations such as market conditions, available labor, etc.

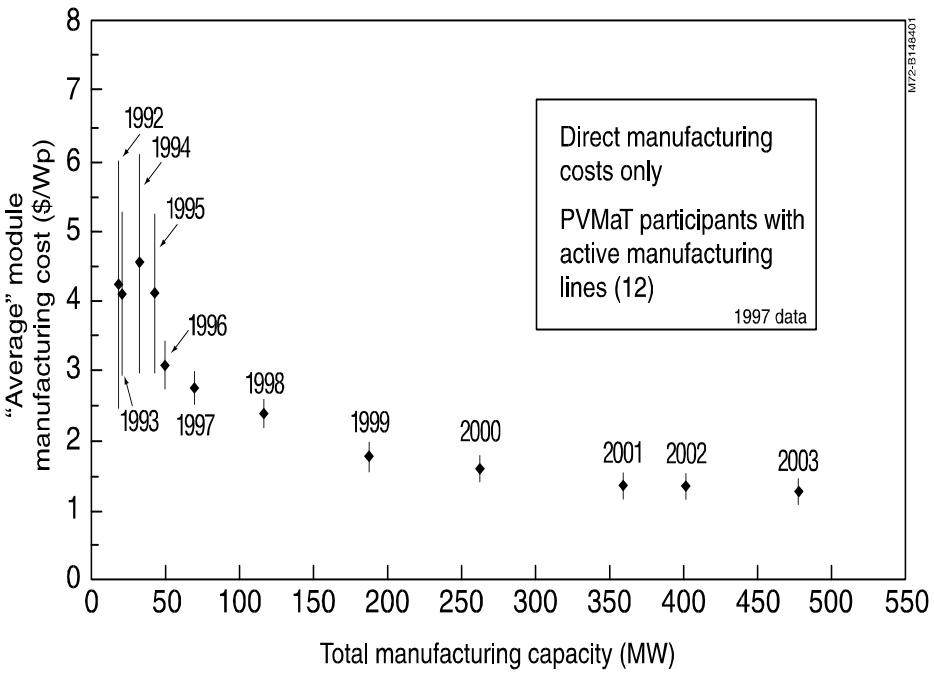

PLANS

The problems addressed by this task are proposed by the industrial participants. As such they are problems important to the manufacturers. The actual projects selected are chosen primarily by evaluators external to the government system using criteria constructed to select, in a technology neutral manner, those activities most likely to contribute to the PVMaT Project goals and objectives. The newly awarded ongoing subcontracts will continue to contribute to both the reduction of PV system costs and the improvement of PV manufacturing processes and products. Industry has generally identified this project as one of their most, if not the most, important and successful projects in the DOE Program. As such, we will continue to conduct the PVMaT Project in a manner consistent with the established industry/laboratory/government partnership by implementing multiyear subcontracts addressing industry-identified problems selected through competitive and fair processes.

Photovoltaic Manufacturing Technology (PVMaT) Subcontracts

Title: **Manufacture of an AC PV Module**

Organization: Ascension Technology, Inc., Waltham, MA and Boulder, CO.

Contributors: Dr. E. C. Kern Jr., Principal Investigator, M. C. Russell, G. A. Kern, C. P. Handleman

Research Objective

The objective of this project was to develop and establish initial production capacity for a SunSine™300 AC PV Module. Our goals in this project were to achieve UL Listing, to meet FCC Class B limits for unintentional radiators, to complete the AC module system design and development, advance the inverter design, design for manufacture, reliability, and serviceability, and to demonstrate commercialization through production and sale of 100 units. All of these project objectives were successfully met.

Approach/Background

The approach to commercializing the SunSine™300 AC PV Module included the following tasks. An Electric Utility design critique of the prospective design was conducted and used to target the product design. A third revision (Rev.3) of the inverter design was done, reducing harmonic current distortion, cost, size and efficiency. An aluminum casting was developed for packaging the inverter. Prototypes of the inverter were tested and ultimately Listed by UL. 12 PV laminates were manufactured at 300 Watts peak rating by sorting cells. Ten AC Module prototypes using the Rev.3 circuit board design were built for testing. Testing included environmental chamber testing for thermal cycling, humidity/freeze cycling, and damp heat. Testing also included outdoor performance at various sites including NREL, Sandia National Labs, and Ascension Technology, Inc. A special ac power quick-connector was developed for use with AC Modules to allow quick field connection of systems. An AC version of Ascension Technology's Listed PV Source Circuit Protector was developed. Ascension Technology's RoofJack™ mounting hardware for residential installations was improved. A Rev. 4 version of the SunSine™300 AC Module was developed based upon test results from the Rev. 3 design. This Rev. 4 version is the final version that went into Pilot Production. And finally, the resulting manufacturing and production processes were evaluated to determine strengths and weaknesses of the resulting process for use in later developments.

Significant Results

The SunSine™300 AC PV Module has received the 1998 "Best of What's New" Award by Popular Science. A pilot production run of 108 units was successfully completed in the spring of 1998. All of those units have been sold, shipped and installed at customer sites. The SunSine™300 is the first AC PV Module in the world to be Listed by Underwriters Laboratories. The SunSine™300 meets FCC Class B limits. An initial production capacity of 2,500 units per year has been established. This PVMaT 4A1 project is complete.

Conclusions

The AC Photovoltaic module is a viable approach for building grid tied PV systems. The integration of the inverter and PV laminate can be manufactured and sold with a reasonable price, high product quality and reliability. AC Photovoltaic modules provide benefits, not achievable with the standard approach to

grid tied PV systems. For example, PV array structures do not have to be co-planar to ensure maximum power tracking from individual modules. Array mismatch problems are eliminated. System reliability is increased. If one ac module fails, the rest of the ac modules in the system continue to operate. In a standard PV array, if one module fails, the entire array is disabled. The integration of the PV and the inverter is done in a controlled factory environment, leaving less work (and less chance for mistakes) in the hands of the system designer and installer. AC PV Modules require far less PV expertise to design and install systems, thus increasing the number of qualified designers and installers to a much larger base of electricians, nationwide.

Future Work

Future work will focus on cost reductions, performance enhancements such as higher power output and higher efficiency, and increased manufacturing capacity in the PVMaT 5A1 program. The PVMaT 5A1 program, "Cost Reduction and Manufacture of the SunSine™325 AC Module", began in April, 1998.

References

[1] G. A. Kern, "Interconnect Guidelines and Status of AC PV Modules in the United States", IEA PVPS Task V Workshop, Zurich, Switzerland, Sept. 1997.

[2] G. A. Kern, "SunSine300, Utility Interactive AC Module Anti-Islanding Test Results", IEEE PV Specialists Conference, Sept. 1997.

[3] C. Jennings, G. J. Chang, "AC Photovoltaic Module Magnetic Fields", IEEE PV Specialists Conference, Sept. 1997.

[4] *NREL Photovoltaic Program FY 1997 Annual Report*, NREL/BK-210-23607, (June 1998

[5] M. Dichristina (ed.), "The Best of What's New", Popular Science, December 1998, p. 77.

[6] G. Kern, "SunSine™300 Manufacture of an AC Photovoltaic Module, PVMaT 4A1 Phases I and II Final Report", Submitted to NREL for publication.

Title: **Market-Driven EFG Modules**

Organization: ASE Americas, Billerica, Massachusetts

Contributors: M. Kardauskas, principal investigator, J. Kalejs, J. Cao, S. Ebers, R. Gonsiorawski, M. Rosenblum, B. Piwczyk

Introduction

This Executive Report summarizes the progress made at ASE Americas Inc. during the last year of the three year program in Phase 4A2, which is due to end in February, 1999, and the work initiated in the PVMaT 5A2 program which commenced in August. These programs focus on the development of technology to improve photovoltaic module manufacturing processes for wafers, cells and modules, to achieve cost reductions for ASE Americas' products. These are based on polycrystalline silicon wafers produced by the **E**dge-defined **F**ilm-fed **G**rowth (EFG) technique. All tasks in PVMaT 4A2 are nearing completion. The overall goal of the program was to reduce EFG module manufacturing costs by 25%. Module cost reductions of approximately 15% are in place as a result of successes on the program to date. We expect that completion of the remainder of the tasks will let us possibly exceed the overall program goal of 25% cost reduction. This will occur if we succeed with a novel module design concept using enhanced reflection within the module to reduce the cell area required to obtained a given power output in the module. The new PVMaT 5A2 program will continue some of the development work initiated in PVMaT 4A2 in the areas of laser cutting and implementation of Statistical Process Control techniques and supporting documentation work leading to ISO9000 and ISO14000 certification. A new area of development in PVMaT 5A2 is to demonstrate pilot line equipment for growth, cutting and processing of very thin EFG wafers down to 100 μm. These wafers will be produced from EFG cylinders which will be grown with diameters up to 1 meter.

Technological Advances for PVMaT 4A2

The PVMaT 4A2 program developed improvements in wafers, cells and modules which, when fully implemented in the ASE Americas' manufacturing line, will reduce module variable costs by at least 25%, as referenced to manufacturing costs in 1995, the starting date of this program. The three areas of module manufacture where progress has been made are described next.

Wafers. Wafer variable cost accounts for about 25% of total module variable costs. In the wafer area, the work in this program has successfully developed improvements to: increase silicon feedstock utilization, extend the length of octagon tubing grown from a die, obtain better thickness uniformity of wafers, and develop higher yield processing so that thinner wafers can be handled with better yields. The work on introducing thinner wafers into manufacturing has spanned all areas of the production line from wafers through to modules. Laser cutting technology, cell processing and interconnect techniques all have been improved to allow EFG wafers down to 275 μm to be processed without yield reductions. The thinner wafer as well produces cost savings in silicon feedstock, and has resulted in improved cell efficiency. The net result is that these programs in the wafer area have contributed to about a 6% overall variable cost reduction for ASE Americas' modules.

Work in the past year of the program in the wafer area has focussed on development of new technology for improving laser cutting and wafer thickness uniformity for the wafers produced from the thinner octagons. Full implementation of 275 μm thick wafers throughout all of the production line was accomplished in 1998. We are currently finishing up work on technology improvements which have the potential to raise yields of 250 μm EFG wafers, so that they can be introduced into manufacturing with a further silicon feedstock cost savings of 8% for the wafer. Two barriers to improving yield are losses produced in laser cutting which arise from the lower fracture strength of the thinner wafer and the need to further reduce temperature nonumiformities caused by unmelted silicon in the crucible during growth. As a result of the lower fracture strength, in order to maintain yields on the thinner tubes it is necessary to reduce applied stresses on the octagon tube during the

cutting process, and to maintain a well focussed laser beam. Theoretical and experimental studies of the nozzle region of the cutting system have shown that applied stresses from the assist gas can be minimized with proper gas flow. Several laser cutting nozzles have been built and evaluated, to successfully demonstrate the concepts. Implementation in manufacturing will require improvements in the beam positioning system. These improvements are now being tested on a new R&D laser station which has been designed and set up for evaluation of new lasers and equipment for thin wafer cutting. A second area of concentration in lasers is to demonstrate increased speed cutting using new optics. This has a potential of reducing labor cost in laser cutting by 25% and overall wafer cost by 7%. Progress has been made in fully evaluating die/crucible design changes in the EFG growth system for improving thickness uniformity of the octagon, and this improvement will be transferred to manufacturing early next year. With these changes in place we will finish the program work in the wafer area with an evaluation of the performance of 250 μm thick wafers in manufacturing early next year.

Cells. Cell processing costs contribute about 25% to overall module costs. Goals were set at the beginning of the program to achieve these cost reductions through improving a number of areas of cell processing in order to raise EFG cell efficiencies in the manufacturing line, and to introduce a less costly and an environmentally beneficial advance in glass etch technology. At this point, about one-third of the cell efficiency improvements proposed at the start of the program have been implemented in the manufacturing line. Several of the improvements have been tested at the prototype level, and are ready for full evaluation in production.

Cell efficiencies have been increased as a result of: improvement of purification procedures for graphite parts used in the crystal growth furnace, from a reduction of the wafer thickness which enhanced back surface field effects in finished cells, and from reduction of impurity contamination during cell processing. These in total have contributed about 7% to a reduction in module manufacturing costs.

In the past year, we have designed and brought to the prototype stage a glass etch unit, and a front electrode fabrication system to raise the finger count from the present 32 to 40. A glass etch prototype unit was built and evaluated on the production line. These tests revealed some shortcomings and improvements were made to enhance process performance. A pilot unit was built, which is in the process of being installed and debugged for operation under full production conditions. We are completing work on additional improvements to the etch process on a section of the equipment which can be installed on a modular level to further optimize the process. The new glass etch process has significant and very important impact in the environmental area, in addition to its impact on variable costs, which are reduced by as much as 7% in the cell manufacturing area when waste disposal costs are factored in. The new process dramatically reduces fluorine ion effluent by close to two orders of magnitude for the glass etch step, and will eliminate much of the waste disposal stream in this area.

The prototype 40 finger front electrode system was tried out on the manufacturing line this year, and showed deficiencies in design which must be corrected. Expected gains in fill factor were demonstrated as a result in increase in metal coverage from the standard 32 finger configuration. We are now working on new silver inks so that finger width can be decreased to recover losses due to shadowing arising from the increase in finger coverage. A major challenge is to eliminate mechanical failures which increased in the new design. New designs have been developed and will be tested in manufacturing before the end of the program in February, 1999. An important application area will be for larger 10 cm x 15 cm area EFG solar cells, for which the increased metalization is vital to reduce series resistance and maintain cell efficiency.

We have demonstrated in the work this year that impurity contamination during cell processing was a major factor in limiting cell efficiency and preventing us from succeeding in achieving our target efficiency of 15.5% set at the beginning of the program. Although efforts have been successful to eliminate a significant part of the contamination, it still remains a concern. As a result of the shortfall in cell efficiency, the cost reduction contribution anticipated from cell efficiency increases was replaced with new objectives in the module area, with development of a new reflector module concept, described below.

To provide tools to increase cell efficiency in manufacturing, as well as for improving overall production throughput and yield, a methodology and formalism has been developed for employing Statistical Process Control (SPC). We carried out a number of Design of Experiment matrices this year to identify areas of process control which will help us stabilize and improve performance of the cell line. An SPC manual has been written and we will use it to continue to guide implementing SPC in PVMaT 5A2. A major challenge is to broaden the scope of the SPC application to include crystal growth and module fabrication.

Total cost reductions of 25% are projected for add-on variable cost in the cell area when all of the above improvements are integrated into manufacturing. In addition, we expect to continue to obtain cost savings in cell manufacturing, as well as in the wafer and module areas, as SPC implementation proceeds and is fully integrated throughout the manufacturing line in our ongoing PVMaT program over the next several years.

Modules. Add-on manufacturing costs in interconnect, lamination, wiring and module assembly account for about 50% of overall variable costs for finished modules. Projects carried out in PVMaT 4A2 have resulted in particularly significant reductions in the materials cost contributions in these areas, while higher productivity and benefits for product lifetime increases also have been achieved. We have developed new designs of diode housing, frame and module construction which in total account for about a 12% overall cost reduction in the finished module.

This year, we have finished testing and certification of a new diode housing, and it has been introduced into manufacturing. New designs for replacement of costly back glass with a soft backskin together with a replacement for the standard aluminum frame, also have been completed and are under environmental testing.

We have demonstrated new lamination cycles in order to reduce add-on costs in module labor. Overall cycle times have been reduced by about 30%, contributing to proportional increases in throughput in the lamination area. This reduces capital investment requirements in the future. These changes in lamination cycle further reduce the percentage of modules rejected for cosmetic reasons. New encapsulants also have been developed and tested under the program. This development has had two objectives. The one was to demonstrate superior performance in the field in order to allow extensions of the module warranty. In this area, we have worked on modifications of our proprietary non-EVA base encapsulant material to obtain superior performance under accelerated UV testing. This material was demonstrated to have superior performance after almost two years of field evaluation. The other objective has been to develop encapsulant formulations which will allow very thin wafers to be laminated with very high yields. We have evaluated a number of encapsulants which are liquid at room temperatures for this purpose. Our top candidate is an encapsulant which cures relatively quickly at room temperature in comparison to the conventional lamination cycle. Since the encapsulant has a viscosity near that of water at room temperature, it can be poured into a mold containing the cell strings, and thus achieve essentially 100% mechanical yield.

A new reflector module design has been proposed and demonstrated which has potential to significantly lower costs of the ASE Americas' module and push the cost savings for the PVMaT 4A2 contract to well over the overall goal of 25%. This module is constructed such that it very effectively gathers light from areas of the module not covered by solar cells. Solar cell area can be reduced by as much as 15% and still maintain a total power and energy rating for a given size module. The variable cost savings anticipated from this design innovation alone is as high as 8% of total module costs. A patent has been applied for on this design. We are still in the process of developing optimum material combination for the lowest cost product, and environmental testing. These tests will not be completed or the module go into production before the end of the PVMaT 4A2 program.

New Technology Elements in PVMaT 5A2

As noted above, technology transfer to manufacturing of improvements initiated in several areas in PVMaT 4A2, such as in lasers and SPC implementation, is to be continued in PVMaT 5A2. In addition, the scope of PVMaT 5A2 will be broadened, and a major new direction for research and development will be introduced. Foremost, is the evaluation and demonstration of a different crystal growth approach, still

based on EFG, for producing very thin tubes of wall thickness of the order of 100 μm. The material savings in solar cells of this thickness will reduce silicon used per unit of wafer produced by a factor of 3 to 4 over present levels. These EFG tubes will be cylindrical, not polygonal, in cross section. Cylinders can be grown with rotation, which evens out circumferential wall thickness variations. This EFG technology was already demonstrated for tubes of up to 15 cm diameter. The challenge in this program will be to scale up to diameters as great as 1 meter, and to produce sufficiently reproducible, high quality and regular (geometry) material in order to justify high production volumes, as well as to develop technology to fabricate thin and perhaps slightly curved wafers into modules.

One important objective in the first year of this program is to demonstrate the potential of higher productivity with cylinders. This will be accomplished by expanding the diameter of the tube to 50 cm, and raising the growth speed. The first year of this program will develop a growth system for this larger diameter cylinder, and explore the growth stability and speed limits. We anticipate productivity enhancements per growth station of a factor of between 3 and 4 over the current octagon system can be achieved, going from a current average area production rate of about 135 cm^2/min to between 450 and 500 cm^2/min. A second major objective is to demonstrate higher bulk electronic quality. This can be anticipated because major thermoelastic stress components present in the polygonal cross sectional shape are absent with the cylindrical symmetry, and we have already shown previously that the material from the EFG cylindrical format have lower dislocation densities and higher as-grown diffusion lengths. A long range goal is to expand the cylinder diameter to 1 meter and achieve productivity enhancements of a factor of six over current levels. When crystal growth is successful and thin tube growth demonstrated, we plan to develop cell processing, interconnect and encapsulation techniques applicable to thin cylinder material.

The crystal growth program is supported by tasks to develop new laser cutting technology and designs for thin cell structures in the first year. We have put programs into place to evaluate several new lasers which are available on the market. The nozzle technology developed under PVMaT 4A2 will be evaluated and its successful implementation will be very crucial to this work. Cell design and new processing approaches suited to very thin wafers are under review at this time.

Title: **Silicon-Film™ Solar Cells by a Flexible Manufacturing System**

Organization: AstroPower, Inc., Solar Park, Newark DE 19716-2000

Contributors: J.S. Culik J.A. Rand, Principal Investigators; Y. Bai, J.R. Bower, J.R. Cummings, I. Goncharovsky, R. Jonczyk, P.E. Sims, R.B. Hall and A.M. Barnett

Abstract

AstroPower is developing a manufacturing process for Silicon-Film™ solar cell production under an NREL-administered PVMaT cost-share program. Progress is reported in the development of new procedures and equipment for wet chemical processes and sheet fabrication. Future concepts and goals for the Silicon-Film™ process are also discussed.

Introduction

The Silicon-Film™ process is presently in production at a new manufacturing facility. This new facility started production in 1998 with a 9 MW nameplate capacity. The present process is based on a 240 cm^2 solar cell (AP225). Efficiencies exceeding 12% have been measured for the AP-225. Small, laboratory-scale devices have demonstrated efficiencies as high as 16.6%.

The approach and accomplishments for this reporting period focus on the concept of "flexible" solar cell manufacturing. This involves continuation of engineering efforts to generate large areas of high-quality Silicon-Film™ sheet material at high speeds and implementation of new cassette-less, in-line processing equipment for solar cell manufacture.

During this reporting period, significant progress was made in developing large-area, in-line process machines for AR coating, belt gettering, belt diffusion, hot caustic surface etching, and diffusion oxide etching. A large area, high-speed solar cell test/sort machine was designed, fabricated and commissioned for the new manufacturing facility. Large-area semi-automatic screen printers and collocators were commissioned along with 36"-wide contact firing furnaces. Further metallization improvements are planned for the next two phases of the AstroPower PVMaT effort, and a new Silicon-Film™ sheet generation machine with twice the throughput of the present machine will be constructed in 1999 based on designs established during this reporting period.

Fig. 1. Silicon-Film™ sheet material.

Approach

There are three basic development areas that are involved in moving Silicon-Film™ from the laboratory to the factory:

1. Optimization of the sheet generation process; high-speed, high quality and large areas are desired.
2. Optimization of the solar cell fabrication sequence to achieve high-efficiencies with large areas. These processes must be compatible with manufacturing and preferably be in-line and continuous rather than batch-mode.
3. Integration of these developments in an industrial setting by generating (and selling) significant quantities of solar cells.

To achieve these broad objectives, AstroPower directed 1998 PVMaT development efforts into the following specific tasks:

Task 1. In-Line Wet Processing.
Task 2. Continuous Metallization.
Task 3. New High-Throughput Sheet Machine.
Task 4. Solar Cell Efficiency and Module Cost-Reduction Improvement.

Results

In-Line Wet Processing

The goal of this task is to develop a set of production tools that are capable of processing large sheets of Silicon-Film™ material using a cassette-less in-line approach. In 1998, we achieved the following results.

- Purchased and installed an in-line Rinser-Dryer system in the new production facility. Use of this apparatus has resulted in a significant increase in throughput and quality compared to cassette-based spin-dry systems.

- Fabricated and evaluated a first-generation prototype hot caustic etching system. The results of this effort have formed the basis for a rigorous understanding of the chemistry of the NaOH-Si-H_2O-Si_xO_y system and the suitability of various wetted materials and components exposed to hot, concentrated caustic solutions. In 1999, a second generation prototype will be designed and assembled to further develop this process.

- Evaluated a number of potential in-line dilute HF "deglazing" systems for removal of diffusion oxides. We are currently in the final selection and specification process and expect to install and evaluate this system in 1999. After the evaluation process, it is expected that this machine will be directly transferred to production.

Continuous Metallization

The goal of this task is to assess technologies that are suitable for applying front and back contact metallization to Silicon-Film™ planks with the intent of handling larger and larger planks. Cutting the plank to final solar cell size will be moved further down the process sequence. In 1998, we achieved the following results.

- Installed and commissioned a number of 36-inch wide belt furnaces in both production facilities. These furnaces are used for belt-gettering, belt-diffusion, and front and back metallization process steps. These significantly wider belt furnaces have greatly increased throughput in all of these processes.

- Installed and commissioned semi-automatic screen printers with furnace belt load collocators that are matched to the 36-inch wide belt furnaces.

- Investigated new ink formulations.

- Investigated new types of screens.

- Designed metallization patterns for the "family" of proposed Silicon-Film™-based products.

- Evaluated and assessed potential metallization technologies.

New High-Throughput Sheet Machine

The goal of this task is to design and fabricate a Silicon-Film™ machine with a 2.4 m/min sheet generation speed. During 1998 the modular approach used to design and develop the existing production Silicon-Film™ machine was used as the foundation for designing a new higher-capacity system which meets the production rate and final product cost goals. Higher sheet speeds have been investigated to define process parameter issues. These preliminary experiments enabled the collection of data which will be employed to design the length of the process zones and machine components required to achieve the desired material quality in terms of morphology and performance. Practical limitations to maximum sheet speed were evaluated and, at present, none were found. Limitations considered included material quality, sheet morphology, material uniformity, production capacity, power requirements, and manageability of machine size. The new Silicon-Film™ machine will be constructed and commissioned in 1999.

Solar Cell Efficiency and Module Cost-Reduction Improvement

The goal of this task is to investigate process and characterization techniques to increase solar cell efficiency and lower module costs. In 1998, we achieved the following results.

- Developed an in-line AR coating system capable of coating large-area Silicon-Film™ solar cells.

- Evaluated the RF-PCD technique as a contactless material quality assessment tool. These results indicate that the RF-PCD technique is predictive of short-circuit current for devices with junctions. In 1999, we will continue to investigate the RF-PCD and other potential techniques with the goal of predicting the performance of as-grown Silicon-Film™ sheet material.

- Developed and improved continuous in-line gettering and diffusion processes to improve the diffusion length, current generation, fill factor and efficiency of Silicon-Film™ AP225 solar cells.

- Designed a new junction box for all AstroPower module products. This junction box is in the process of being UL approved. Identified higher current (over 10 A) bypass diodes. These diodes are in the process of being qualified.

- Installed and commissioned a Spire stringer-tabber to further mechanize module assembly, this system was specified for application to AP225 solar cell module production. Installed and commissioned two large-area laminators, one manufactured by Spire and one by NPC.

- Designed, constructed and commissioned a new automatic solar cell tester-sorter system for AP225 solar cells. This flexible system is capable of handling and testing larger-area cells up to 8" (AP400).

Summary

AstroPower is developing a new manufacturing system for Silicon-Film™ solar cell production. The present process is based on the AP-225, a 240 cm^2 solar cell. Optimization of the solar cell fabrication sequence has been utilized to achieve high-efficiencies with large areas. For the AP-225 solar cell, efficiencies exceeding 12% have been obtained. Small, laboratory-scale devices have demonstrated efficiencies up to 16.6%.

In-line solar cell process equipment is being developed to fabricate very large area solar cells (up to 1800 cm^2). This new equipment includes an in-line hot caustic surface etch system and an in-line diffusion oxide "deglaze" machine. This in-line approach has been generalized to a "Flexible Manufacturing" solar cell production concept. Future plans call for 30 x 120 cm Silicon-Film™ planks to be processed by a single set of in-line equipment and then be subdivided into a range of solar cell sizes from 105 cm^2 to 900 cm^2 in a "Just In Time" fashion before solar cell test and module assembly.

Acknowledgments

This work was supported in part by the U.S. Department of Energy through the National Renewable Energy Laboratory (NREL) under the Photovoltaic Manufacturing Technology (PVMaT) Program.

The authors would like to acknowledge the contributions of David Ford and Emanuel DelleDonne with device fabrication, Chris Kendall, for Silicon-Film™ machine design, Joe Lesko for test equipment software development, and Rich Cole for manufacturing process development.

References

1. Y. Bai, et al., "16.6% Efficient Silicon-Film™ Polycrystalline Solar Cells," *Twenty Sixth IEEE PVSC*, Anaheim CA, Sept 29 - Oct 3, 1997.

2. J.A. Rand, et al., "Large-Area Silicon-Film™ Manufacturing under the PVMaT Program", *Twenty Sixth IEEE PVSC*, Anaheim CA, Sept 29 - Oct 3, 1997.

3. Y. Bai, et al., "Investigation of Post-Growth Treatments of Silicon-Film™", *Eighth Workshop on Crystalline Silicon Solar Cell Materials and Processes*, Copper Mountain, CO, August 17 – 19, 1998.

4. J.S. Culik, et al., "Recent Advances in Silicon-Film™ Solar Cell Manufacturing Engineering", *Eighth Workshop on Crystalline Silicon Solar Cell Materials and Processes*, Copper Mountain, CO, August 17 – 19, 1998.

Title: **Production of Solar Grade (SoG) Silicon by Refining of Liquid Metallurgical Grade (MG) Silicon**

Organization: Crystal Systems, Inc., Salem, MA

Contributors: Chandra P. Khattak, Principal Investigator, Frederick Schmid, Program Manager, Maynard B. Smith, David B. Joyce (MMT), Gene Smelik (MMT), Mark A. Wilkinson (MMT)

OBJECTIVE

The objective of the PVMaT 5A1 letter subcontract awarded to Crystal Systems, Inc. (CSI) is to produce solar grade (SoG) silicon feedstock by refining metallurgical grade (MG) silicon in the liquid state so that this material can be used as feedstock for ingot processes, such as the Heat Exchanger Method (HEM)™ , for photovoltaic applications. It is intended to continue this technology development in larger scale using thermal chemical refining techniques and reduce the impurities in MG silicon to less than 1 ppma level.

PROJECT TEAM

The project team members for this contract include Crystal Systems, Inc. (CSI), team leader; Molten Metal Technologies (MMT); GT Equipment Technologies, Inc. (GTi) and Georgia Institute of Technology (GIT).

INTRODUCTION

Nearly all the photovoltaic modules for power generation applications use crystallization silicon. The industry still relies on off-specification virgin silicon meltstock and scraps from the microelectronics industry for feedstock. When the electronics industry is in a growth mode, there is scarcity of feedstock for the photovoltaic community. At the present time, the microelectronics industry is in a downturn and there is sufficient silicon meltstock for the photovoltaics industry. Growth of the crystalline silicon photovoltaic industry will be stifled by lack of low-cost silicon when the semiconductor business is growing and consumes all the silicon it produces.

Commercially available metallurgical grade (MG) silicon costs less than $2/kg and is generally 95-99% pure, which is not high enough for use by the photovoltaics industry. High purity semiconductor-grade silicon of typically 99.9999+% purity is used as feedstock by the electronics industry. The specifications of solar-grade silicon feedstock are significantly less than the semiconductor grade silicon, but at the present time there is no commercially available SoG silicon that is not tied to the microelectronics industry. A SoG silicon feedstock that can be used by all processes involved in the photovoltaics industry contain the following impurities without degradation in performance: B = 20 ppba; P = 4 ppba; C = 1 ppma; Fe = 20 ppba. The selling price that can be tolerated is approximately $20/kg.

The present program is to pursue the processing approach used by Khattak and Schmid in 1983 [1,2] for upgrading silicon in the liquid state. It is intended to analyze the data obtained earlier in laboratory experiments and pursue the *in situ* purification of molten MG silicon to produce SoG silicon by a process that can be extended to a commercial-scale operation. The feasibility of this approach will be demonstrated in charge sizes up to 500 kg.

MG SILICON FEEDSTOCK

Samples of commercially available MG silicon were obtained from seven different suppliers worldwide. These samples have been characterized for impurity levels using inductive couple plasma (ICP) emission spectroscopy and glow discharge mass spectroscopy. The material is quite inhomogeneous when analyzed from the viewpoint of ppm level of impurities. The major impurities are Al, Fe, Ca and Ti. The range of B and P for the seven samples characterized showed 5-50 and 25-50 ppmw, respectively. In addition, there are many other elements detected. The impurity levels vary for different sources of MG silicon. The refining process for removal of boron and phosphorus will be followed by a directional solidification step to remove other impurities. In the case of B and P, it is essential that these elements be reduced to satisfactory levels during the refining step as these impurities have a high segregation coefficient and therefore are not significantly reduced by directional solidification.

THEORETICAL MODELING

Theoretical modeling was carried out to explain the earlier refining results [1,2] reported by CSI, especially related to B and P from MG silicon. The removal of B and P was evaluated using different approaches with slagging, as a vapor species, volatilization under vacuum and reactions to form another product that can be removed from molten silicon.

Equilibrium calculations show that the partitioning coefficient of B and P to the slag will be of the order of 1, which is not sufficient to explain the observed reduction in B and P. However, modeling the partitioning under non-equilibrium conditions, it was found that the partitioning coefficient will be of the order of 1,000, which will be sufficient to explain the partitioning observed.

To date, almost all refining experiments carried out for effective removal of P from MG silicon use a vacuum processing step. This includes the Kawasaki Steel approach [3], which requires a separate vacuum processing step for P removal. However, it is not clear in previous experiments carried out at CSI whether this vacuum step is necessary for P removal. The results of calculations for refining vs. time and temperature for a typical bench-scale reactor run showed that P can be removed from MG silicon. Similar data for B showed that it would not be efficiently removed by vacuum treating.

During theoretical dynamic modeling using local equilibrium and non-equilibrium conditions, reactors have been calculated for B and P removal from MG silicon. A matrix of conditions has been set up that shows that B and P can be removed from MG silicon using slagging, vaporization, treatment under vacuum and reactions to form some other compound, but each of these processes does not work to the same degree and under similar oxidation conditions for each of these elements.

EXPERIMENTAL SETUP

An experimental reactor shown in Figure 1 has been set up to carry out upgrading experiments. Several design changes have been made in order to incorporate melting under controlled atmosphere, various gases flowing through the melt, additions of water vapor to the gas flow, vacuum and directional solidification of the charge. This experimental reactor has been tested, and various refining techniques have been incorporated to achieve the desired results. This reactor is now ready to start refining experiments to collaborate the results achieved from theoretical modeling.

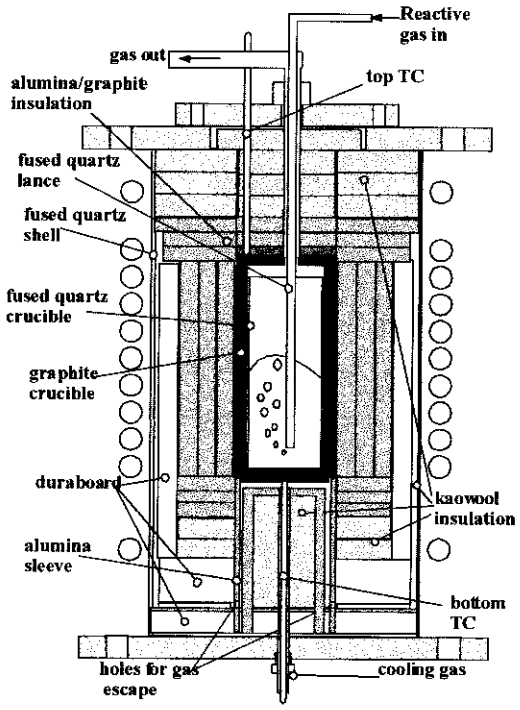

FIGURE 1. Schematic diagram of bench scale modified to allow directional solidification.

Auxiliary Heating

One of the key elements in refining elements is to develop the type of heating that is consistent with industrial procedures and allows enough time for the refining step. It was intended that an auxiliary heating source would be required to heat the molten silicon and prolong the refining step. A fused silica burner using hydrogen/oxygen as a combustible gas mixture was fabricated. The salient feature in this burner is to have ignition by external mixing to minimize chances of explosion. The gas flow of fuel such as H_2 is in the outer part of concentric tubes to ensure cooling of the fused silica at temperatures well above the melting point of silicon. Such a burner was tested in a large reactor, and it was found that it could be used as an auxiliary or primary heating source, thereby making the reactor configuration much simpler. The burner was used to melt MG silicon in the larger reactor without any degradation of the burner.

One of the design features of this burner was to use it in submerged molten silicon. During initial experiments, this burner was inserted under water and the flame continued in the submerged condition. This feature will be tested with molten silicon soon. The development of this burner will allow easy scale-up of charge sizes. It is intended that after the refining procedures are developed, this burner will be combined with the refining experiments.

SUMMARY

The present program is to pursue the earlier approach of using upgrading processing for molten metallurgical grade (MG) silicon and produce solar-grade (SoG) silicon. The feasibility of this approach will be demonstrated in charge sizes up to 500 kg and allow further extension of this approach to commercial-scale production.

Metallurgical Grade (MG) silicon feedstock samples have been analyzed for impurities. There was a wide variation in the impurity content for different samples. It is intended that refining processes will be developed for reducing these impurities, and the refining process will be followed by a directional solidification step. Boron and phosphorus impurities must be removed by refining techniques, as these have a high segregation coefficient.

Theoretical modeling has been carried out using equilibrium and non-equilibrium conditions to calculate the conditions for B and P removal from MG silicon in the molten state. A matrix of conditions involving slagging, vaporization, treatment under vacuum and reactions to form some other compound has been developed for the refining step.

An experimental reactor has been set up to confirm the theoretical models on a small-scale basis and develop experimental conditions for the refining step. A larger reactor is available for the scale up. An auxiliary burner to supply heat and other reaction products to molten silicon during the refining step has been developed and tested. This burner is capable of providing primary heat for melting as well as auxiliary heat for refining for the larger reactor. It is intended to scale up the refining process after experimental conditions for refining have been determined.

REFERENCES

[1] C.P. Khattak and F. Schmid, "Processing of MG Silicon for Photovoltaic Applications," *Proc. Symposium on Materials and New Processing Technologies for Photovoltaics* (J.A. Amick, V.K. Kaput, and J. Dietl eds.) Vol. 83-11 (Electrochem. Soc. Inc., NJ, 1983) p. 478.
[2] C.P. Khattak and F. Schmid, "Growth of Silicon Crystals by HEM for Photovoltaic Applications," invited paper at Symposium on Progress in Bulk Semiconductor Crystal Growth at Materials Research Soc. Annual Meeting, Boston, MA (1983).
[3] Sakaguchi, Y., Yuge, N., Nakamura, N., Baba, H., Hanazawa, K., Abe, M., Kato, Y., in *Proceedings of the 14th International European Photovoltaic Solar Energy Conference* held in Barcelona, Spain, Ossenbrink, H., P. Helm, H. Eimann, ed.s. Vol I, pp. 157-160.

Title: **Advanced Polymer PV System**

Organization: Evergreen Solar Inc., Waltham, MA

Contributor: J. I. Hanoka, Principal Investigator; J. Fava, R.G. Chleboski, M.A. Farber

This report summarizes the concluding work done on the last three months of a PVMaT 41 project, Contract #DE-AC36-83CH10093. The period covered is from October 1, 1997 through December 31, 1997.

Objective

The objective of this project was to develop new polymeric materials for PV modules such that module and systems costs could be reduced.

New Encapsulant

One of the key goals of this entire project was the development of a new encapsulant material. The rationale here was to find a material which could be laminated in air. This is in contrast to EVA which requires vacuum lamination. Also, we wished to develop an encapsulant which might offer a longer service life than EVA. During this three-month period, two accelerated UV light exposure tests were conducted, both for Evergreen's new encapsulant and TBEC EVA for comparison. These tests were: (1) exposure at 50^{o}C in a QUV machine under UVA lamps for bare samples of the encapsulant materials; and (2) exposure under mirror enhanced sunlight in Arizona at about 7x normal exposure intensity, with samples laminated between pieces of window glass. In the first case, the tensile strength as a function of exposure time was determined. In the second, the change in yellowness index was measured as a function of time of exposure. It should be noted that these tests have continued well beyond the three-month period of the contract end. The result of the tests then and during the period following the contract completion have been that Evergreen's new encapsulant consistently shows better UV stability than does the TBEC EVA.

For the other application of the new encapsulant, namely a non-vacuum method to laminate it, progress was also made. A prototype machine has been set up and run with as large as 60 watt modules laminated using our new encapsulant.

New Backskin and Frameless Module

Two other key goals of the project were the development of a new backskin material and its deployment in forming a frameless module.

In general, these goals were successfully met but one issue which needed to be dealt with was that of the bond strength between the backskin material and the glass superstrate. Modifications to the lamination process and the use of an accelerated test consisting of a R.T. water soak followed by freezing at –40^{o}C indicated that we were closing in on a solution to this problem.
In the use of the backskin to form a frameless module aluminum mounting components were bonded to the backskin material. Thus, tests of this bond strength were important.

In a paper presented at Anaheim at the PVSC Conference, in September 1997 [1], we reported on a thermal creep test done at 85^{o}C for 45 days with a load of 1.15 psi on a mounting component bonded to our new backskin. We extended this test using an intervening lower flex modulus material as a bonding layer by first doing it for 67 days at 85^{o}C and then for 26 days at 90^{o}C. No creep was detected—indicating an excellent bond.

Conclusions

In general, all of the objectives of the project were met. The new encapsulant appears to have a number of significant advantages over that of EVA. The new backskin material also looks very promising. Evergreen plans to introduce the frameless module based on this new backskin as a new product. A patent emerging from the work this period was filed.

References

1. Hanoka, J.I.; Kane, P.E.; Martz, J.; and Fava, J., *26th IEEE PVSC.*

Title: **Continuous, Automated Manufacturing of String Ribbon Si PV Modules**

Organization: Evergreen Solar Inc., Waltham, MA

Contributor: J. I. Hanoka, Principal Investigator; R.E. Janoch, A.M. Gabor, X. Ma, B.E. Lord, M.T. Mrowka, J. Martz, D.M. Trickett

Objective

This PVMaT 5A2 sub-contract has as its objective, the development of an automated and continuous PV manufacturing line based on Evergreen's innovative technology in all the areas of PV manufacture. This report covers the first four months of the project from June through September 1998. The project encompasses four areas: crystal growth; cell manufacturing; module lay-up; and factory layout and automation. In this initial start-up of the project, most of the work has been in the first two areas.

Crystal Growth

The focus in this area has been in reducing consumable costs, and simplifying and automating the String Ribbon growth process.

Improved Furnace Sealing

There are two principal sources of oxygen ingress in our growth furnaces. One is the top opening where the grown ribbon exits the furnace and the other is an adjacent chamber which contains the melt replenishment system. Reduction of oxygen in the system results in cleaner and more uniform growth. A better method for sealing the top opening has been designed and used on an experimental basis. Also, a new design for the chamber enclosure for the melt replenishment system allowing much better isolation from the crystal growth chamber itself has also been done. Improved furnace sealing has resulted in the cleanest looking ribbon surface we have ever grown. Consequently, we have run a small batch of about 24 cells with absolutely no etching prior to diffusion through the line and compared this group with our standard processed material which does undergo pre-diffusion etching. The efficiencies were almost identical for the two batches, particularly the fill factors. This is an encouraging first experiment.

Crucible Coatings and Carbon Dissolution

One way to retard carbon dissolution into molten silicon is through the use of SiC coated graphite crucibles. We have tried this on two separate occasions with very promising results each time. In two cases the runs lasted for significant lengths of time under 24 hour, 7 day/week growth. These are very long runs and if this is repeatable on a wider scale. This could help us in improved run lengths and lower amortized graphite parts costs. Of course, the issue of the coating cost will also have to be considered here.

New String Material

A new string material with a better CTE match to Si has been developed. A considerable amount of ribbon has been grown with it with no particular problems. Also, methods to reduce wetting of this material to the silicon so as to reduce grain boundary nucleation has been started.

One of the first possible benefits of using this new string material is an increase in run length. There are indications that the nature of this string material is such that it makes growth even easier than the prior material and prevents a growth stoppage mechanism which the earlier string material seemed to foster.

Automatic Thickness Control

A prototype which measures the ribbon thickness in-situ at three different positions across the width of the ribbon and then feeds this signal into thermal adjustments which can be done within the heated crucible has been assembled and is being debugged.

Cell Manufacturing

Evergreen has its own unique cell making process. The PVMaT work is designed to further develop and automate this cell making process. The work this period has been in the areas of high speed drying, improvements in uniformity in the diffusion process, and non-vacuum hydrogen passivation.

High Speed Drying of Front Contact and AR Coating

A somewhat novel concept for high speed drying has been prototyped and looks very promising. The conventional belt furnaces for drying are slow and cumbersome to use, so what we have developed in lieu of this is a much faster method which also requires less space. The initial results are encouraging, but much more work remains before the process is fully production worthy. The process has the potential for very high speed.

Diffusion

Three issues have been addressed here. First, there has been too wide a variability in the resulting sheet rho. This has finally been tracked down and the process considerably tightened to the point where sheet rho's of 50 Ω/Y can be done routinely and uniformly.

The second issue is that of robotic pick-up and release of cells for this process. Prior to the initiation of this PVMaT contract, a 6-axis robot system for picking up completed cells as they emerge from the metallization step was designed. This project will serve as a paradigm for the general introduction of robots into the overall handling of Evergreen's cells, especially preceding and following the diffusion step.

Thirdly, a method for continuous removal of the diffusion glass which does not require insertion of cells into plastic carriers is under development. An elastometric material which is unaffected by HF has been identified and will be utilized in this method.

Hydrogen Passivation

Non-vacuum methods of hydrogen passivation have been studied this period. Some passivation effects could be seen but the results, in general, are significantly less than that obtained with plasma nitride techniques. The reasons for this are not entirely clear but are obviously connected with introducing enough hydrogen, keeping it in the material, and then insuring that it diffuses within the bulk of the material.

Summary

In this first four months of this subcontract, substantial progress has been made in reducing consumable costs in the crystal growth area and in process improvement in the cell area.

Title: **Monolithic Amorphous Silicon Modules on Continuous Polymer Substrates**

Organization: Iowa Thin Films Technologies, Inc., Ames, IA

Contributors: F.R. Jeffrey, Principal Investigator; D. Grimmer; S. Martens, H. Shanks, and M. Noack,
Investigators

Objective

The overall goal is to develop the most cost effective PV manufacturing process possible. To this end Iowa Thin Film Technologies, Inc. has chosen a roll based manufacturing process with continuous deposition and monolithic integration. The objective of this subcontract over its three year duration is to improve overall module performance, increase the throughput of the metalization, a-Si deposition, laser-scribing and screen-printing processes, and to reduce the overall module manufacturing costs of the ITF production line by 68%.

Approach

This subcontract consists of three phases which began in July, 1995 and will be completed February 28, 1999. This report covers in-house and subcontracted research and development in FY 1998 (October 1, 1997 - September 30, 1998).

The first year activities were divided into four task efforts designed to: replace the ITF TiN layer with a less absorbing and reflection enhancing ZnO layer; design and implement a registration system for aligning the web onto the printer platen; establish new laser operating parameters to optimize the laser beam scribe speed; and develop new insulating ink printing and roll based laminating processes for the ITF production line. Second year activities were divided into five task efforts designed to: increase the throughput of the metalization, a-Si deposition, laser-scribing and printer processes; design and implement baffles for the isolation of metal deposition regions; investigation of the limits on the ZnO deposition rate; develop new machine control programs; identify new laser operating parameters to optimize the laser beam scribe speed; integrate a new, water based insulating ink into the patterning process; and automate the final process steps of busbar attachment and web cutting. The third year activities focus on task efforts designed to: increase the throughput of the metalization deposition systems; determine deposition parameters for each layer to produce the full metalization stack at a single web speed; increase the throughput in the roll-to-roll ZnO deposition system; investigate alternate feedstocks for the supply of Zn and O in the ZnO growth process; study alternative processes for the scribing and printer steps; investigate alternatives to laser operations to identify potential reductions in cost; investigate alternative methods of scribing including blade, electrochemical and ultrasonic cutting tips; study alternative methods of welding shunts in cell-interconnects including the use of electronic- or ultrasonic-spot welding techniques; reduce the cost of the polymer substrate; automate the final process steps of busbar attachment and web cutting; and establish a roll-based laminating process and decrease module assembly labor costs.

Research Results (10/1/97-9/30/98)

Increased roll-to-roll ZnO deposition system throughput: deposition parameters It has been determined that that H_2O and DEZ carrier gas flow rates, H_2O and DEZ bubbler temperatures, and deposition zone temperature and pressure significantly affect the deposition of zinc oxide (ZnO) and the transparent conducting oxide. Current near optimum ZnO deposition parameters have been established taking the following into consideration:

Gas flow rates: It was found that by increasing the DEZ carrier gas flow rate, the deposition rate decreased. This decrease was a result of the argon carrier gas flows acting as a diluent and the reaction being water starved. **H_2O and DEZ bubbler temperature:** It was found that at the optimum water bubbler temperature and argon carrier gas flow rate, there was an increase in ZnO

deposition of up to 27% over current standard operating parameters. **Deposition zone temperature and pressure**: It was determined that with an increase in temperature of approximately 15 C, there is an increase in the deposition rate of up to 20% over current operating parameters. While there was not a great dependence on pressure on the deposition rate, at significantly higher or lower pressures there was some decrease in ZnO deposition rate.

Changing the process operating parameters of the water source bubbler indicated that the vapor pick-up and transport is not 100% efficient. Although it has been found that greater water vapor flow gives improved deposition rates, the effect of the DEZ flow is larger, indicating that the reaction may be DEZ concentration limited. One way to increase the quantity of the DEZ vapor flow rate is to reduce the DEZ bubbler pressure.

It was decided that an increase in deposition rate due to the increase of each reactant indicates that the deposition rate may be diffusion limited, in that the reactants are not reaching the surface of the material effectively. The increase in delivery rate of the reactants increases the deposition rate simply by overcoming the diffusion barrier.

It has been found that an out-gassing product of the insulator ink has an effect on the nucleation of the ZnO growth on the web resulting in uneven and diminished film thickness. Printer oven temperatures and gas flow rate modifications have removed this problem.

In summary, the ZnO parameter testing has shown that:

- the H2O bubbler is not as efficient at producing water vapor as we would like to have seen a higher bubbler temperature gives better results.
- the deposition rate is diffusion limited. Moving the gas manifold closer to the surface of the web allows for better gas contact and therefore faster deposition.
- a total gas flow rate of Ar/water and Ar/DEZ to each respective manifold should be equal.
- a water vapor to DEZ vapor ratio of 2.2 to 1 near optimum.
- the state of the insulator ink bake out is important.
- the web can be deposited at 12 in/min with optimum conditions with the existing equipment.
- with the new parameters which allow for ZnO deposition at 12 inches per minute, it has been found that there is a net 25% savings of the DEZ required to coat the web.

Although optimizing the gas flow parameters and reaction chamber temperature can give the desired end result of increased throughput, good physical contact of the web with the heated platen has a marked effect. When the web moves through the chamber it ripples and makes poor thermal contact. At such time in the future when we can install a drum coater (which would guarantee good thermal contact) a much improved deposition rate can be accomplished along with much more efficient use of our reactants.

ITFT run number 522 was used to demonstrate ZnO deposition at 12 inches per minute with satisfactory results. **Current deposition rates are up 68%**. There will be even greater improvement once the new parameters have been incorporated into the process.

Step reduction in the scribing and printer processes An experimental single insulator ink print was run in which a variety of laser beam powers were used to cut an open in the TCO coating with the following results: A typical single print line thickness is around 20 μm (0.8 mil), depending on viscosity of ink printed. Laser beam powers ranging from 0.25W to 1.2W @5 kHz pulse frequency were tried. The range of 0.4W to 0.8W can produce opens in the TCO layer without totally cutting through the ink and metalization. Typically, a value in the 0.6 - 0.7W range is acceptable. Subsequent trial runs reproduced these results and a single print is now our standard increasing insulator print throughout by 100%.

Composite laminate materials Layered stacks were assembled, tested and evaluated for suitability as a possible replacement for the current encapsulation material. Test results are presented in Table 1. Evaluation criteria included durability, UV resistance, temperature cycling,

heat/humidity tests, abrasion, and cost. Each item was rated on a scale of 1-5, with 5 indicating the best performance and 1 the worst .

Table 1. Test results from composite stacks that were assembled, tested and evaluated as a viable replacement for the current encapsulation material.

Item #	Top Film	Top Adhesive	Bottom Adhesive	Bottom Film	Dura-bility	UV Resistance	Temp. Cycling	Heat/Hum-idity Soak	Resistance to Abrasion	Cost
1	1.5 mil Tefzel	18 mil EVA	18 mil EVA	1.5 mil Tefzel	5	5	5	5	5	5
2	1.5 mil Tefzel	5 mil EVA	5 mil EVA	1.5 mil Tefzel	4	5	5	5	5	5
3	1.5 mil Tefzel	5 mil EVA	5 mil EVA	1.5 mil Dartek	4	5	5	5	5	3
4	1.5 mil Tefzel	18 mil EVA	5 mil EVA	1.5 mil Dartek	4	5	5	5	5	4
5	1.5 mil Dartek	18 mil EVA	18 mil EVA	1.5 mil Dartek	5	1	5	5	2	2
6	1 mil Polyester	2 mil Poly-ethylene	2 mil Poly-ethylene	1 mil Polyester	2	2	4	4	3	1
7	3 mil Polyester	2 mil Poly-ethylene	2 mil Poly-ethylene	3 mil Polyester	3	3	5	5	3	2
8	2 mil Polyester	8 mil Poly-ethylene	8 mil Poly-ethylene	2 mil Polyester	4	4	5	5	3	3
9	2 mil Polyester	8 mil Poly-ethylene	2 mil Poly-ethylene	3 mil Polyester	4	4	5	5	3	3
10	4 mil Polyester	6 mil Poly-ethylene	6 mil Poly-ethylene	3 mil Polyester	4	4	5	5	3	3

Analysis of the data presented in Table 1 will lead to different stack selections depending on the traits desired in a composite. If the goal is to provide an alternative to the present process of vacuum lamination, then item 7 probably provides the best protection for the least cost. However, if the goal is to find a good long term, lower cost encapsulant, without compromising module performance 20 years down the road, then item 3 is the clear choice. While there is currently a need for both types of encapsulation, a “long term” encapsulation is of most immediate concern. Therefore, a potential composite laminate stack (item #3) has been selected that consists of a 1.5 mil Tefzel® top layer; a second layer of 5 mil thick Ethylene Vinyl Acetate (EVA); a third layer of the tandem thin film A-Si solar module on a polyimide substrate; a fourth layer of 5 mil EVA; and a bottom layer of 1.5 mil Dartek® (a modified nylon film with expansion coefficients similar to those of Tefzel®).

Automated busbar attachment and sheeting machines The automated busbar taping machine is fully operational, processing between 40 and 200 modules daily. Modifications to the busbar taping machine were made including the addition of a mechanical mechanical screw for

adjusting skew of the printed modules relative to the taping head; a vacuum hold down and air kiss release system was added to the busbar/taping platen; and an alignment guide for the adjustable feedstock was added for consistent start and stop points. There was some initial concern that the automated busbar taping machine would not process the rolls of PV material as delicately as rolls that were taped by hand. In order to make a comparison, several runs were split in two: the machine processed half and production workers processed the second half by hand. An analysis of yield data for "hand" taped runs compared with "machine" taped runs shown in Table 2 demonstrated dramatic results.

Table 2. Number of modules at specified current shown over the per cent of the total number of modules processed.

Module Current (mA)	<24	25-30	31-38	39	40-44	45	46	47	48	49	>50
R-T76S Hand	5 0.3%	4 0.3%	23 1.5%	8 0.5%	348 22%	109 7%	93 6%	93 6%	134 8.6%	117 7.5%	629 40.2%
R-T76S Machine	3 0.2%	6 0.3%	26 1.5%	11 1.6%	249 14.7%	71 4.2%	96 5.7%	106 6.3%	112 6.6%	94 5.6%	903 53.3%
R-542 Hand	109 6.5%	251 15%	614 36.6%	52 3.1%	274 16.3%	49 2.9%	74 4.4%	78 4.6%	67 4%	28 1.7%	80 4.7%
R542 Machine	96 5.8%	115 7%	509 31%	71 4.3%	316 19.2%	59 3.6%	73 4.4%	69 4.2%	82 5%	99 6%	155 9.4%

For the hand taped modules, run T76S yielded 1523 modules or 97.3% that were above specification (>40mA), only 40 modules or 2.6% were below specification. In comparison the machine taped run T76S yielded 1631 modules or 96.4% above specification and 46 or 3.6% of the modules that were below specification. What was most noticeable is that there was a higher percentage of modules at the preferred >40 mA specification for the machine taped portion of the run than in the hand taped portion. This was also indicated in the second run, #542. In this run, 38.78% of the hand taped modules were above specification, and 51.89% of the machine taped modules were above specification. This again indicated that the machine taped modules were not damaged any more than hand taped modules.

The same process was used for cutting out both hand taped and machine taped modules. The automated die cutting system itself performs adequately. However, a problem has been found relating to cross web registration. If the other systems in the manufacturing process produce consistent edge registration then the automated die cutting machine will cut on the appropriate lines and not in the modules. Work will continue on improving edge registration.

Conclusions

Significant progress has been made in decreasing cost and increasing throughput of the ITFT manufacturing process. Continued increased automation, selection of a new composite laminate material stack, an improved automated busbar attachment process, and a new die cutting process have contributed to a 54% manufacturing cost reduction to date.

Title: **Manufacturing and System Integration Improvements for One- and Two-Kilowatt Residential PV Inverters**

Organization: OMNION Power Engineering Corporation
2010 Energy Drive, P.O. Box 879
East Troy, WI 53120

Contributors: D. G. Porter, Principle Investigator; H. Meyer; R. H. Troyer and D. Zietlow

Objectives

The objective of this subcontract over its two-year duration is to produce two residential inverter products that are easily manufactured, and are suitable for use in rooftop residential PV applications. OMNION and its team members will evolve designs and evaluate one-kilowatt and two-kilowatt (kW) single-phase inverters for utility-interconnected applications suitable for high-volume production (5,000 units/year). The new inverters will continue to use the transformerless phase leg topology used by OMNION for its Series 2200 introduced in 1986. The input to the inverter has been modified by adding a buck-boost DC/DC converter that creates the negative half voltage. This means that the input voltage can be cut in half, from a Series 2400 introduced in 1994 input voltage of 180 to 300 to a new Series 2500 voltage range of 180 to 500. This larger input voltage span will make it easier to design a system because of the broader array voltage windows. With the Series 2400, this can be accomplished by using an auto transformer. The auto transformer solution has the problem that for an equal input voltage, the inverter rating is cut in half. This reduces the inverter efficiency and the auto transformer losses further reduce the efficiency. The new approach will result in a lighter, more efficient, lower cost solution for one-kilowatt and two-kilowatt inverters.

Approach

In Phase I, OMNION will develop a comprehensive product specification for one- and two-kilowatt inverters with input from a customer/user group. The draft product specification shall be prepared based on OMNION's under-standing of customer preferences and current technological trends. OMNION will design and build three prototypes of each one- and two-kilowatt, single-phase, photovoltaic power conversion system (PCS) design. The PCS will be demonstrated and the product specifications reviewed with the customer/user group.

During Phase II, OMNION will move from the prototyping and pilot production tasks to full production on the one-kilowatt and two-kilowatt Series 2500s. Here the design will be modified to improve the manufacturability and improve the inverter based on customer feedback. Product design documentation, including the Series 2500 Product Specification and Operation & Maintenance (O&M) Manual, will be finalized and full production will begin after resolution of pilot production problems, validation issue resolution and finalization of the manufacturing process documentation.

Results

Work on Phase I continued throughout 1998 with the collection of customer preference data and the refinement of the preliminary specification for the one- and two-kilowatt residential photovoltaic (PV) power conversion system. Design work for the new Series 2500 one- and two-kilowatt PV PCS was started late in FY98.

Phase I

Product Concept

A review of customer requirements for the new one- and two-kilowatt, single phase, residential PV PCS had previously been completed in mid 1997. From this review, a preliminary product specification was drafted in November 1997. In January 1998, work began on refining this preliminary product specification to meet perceived customer preferences. Work continued on gathering customer feedback on desired product features. In August 1998, a spreadsheet detailing the list of tasks and estimated personnel hours for the new one- and two-kilowatt residential PV PCS was completed. From this detailed task list a preliminary project schedule was developed.

Prototype Design / Build / Test

Work began in August 1998 on the conceptual design of the one- and two-kilowatt Series 2500 residential PV PCS using a new Windows® based schematic capture system recently acquired by OMNION. Several inductor designs were completed and work began on some preliminary testing of the inductor designs. Data on key components was gathered for evaluation in the design. Work gathering key component data for evaluation continued through September 1998. Design work, including software, began on a boost section for the Series 2500. Main output inductor testing also continued.

Prototype Production

In August 1998, a manufacturing review meeting was held on the Series 2500 conceptual design to facilitate engineering and production working closely together as the packaging design progresses.

Summary

Under Phase I, the following was accomplished:

- Customer preference data was collected for the new Series 2500 one- and two-kilowatt PV PCS features
- The preliminary product specification was refined based upon customer feedback and NEC requirements
- A final product specification for the Series 2500 was completed
- A detailed task list and preliminary project schedule was completed
- Design work was initiated and completed on the new Series 2500 PV PCS boost section

The next major milestones are to complete the design work on the Series 2500 boost section, begin design work on the Series 2500 main controller and DC power supplies, complete key component specifications and develop test plans. In FY99, we should have the three prototypes of each one- and two-kilowatt Series 2500 PV PCS built and tested. Once the prototypes are complete, a manufacturing review will be performed to look at methods for improving the manufacturing of the units. A draft Operations & Maintenance (O&M) Manual, final product specification and a comparison of product pricing will be prepared. With these complete, an in-house customer review will be held.

Title: **Three-Phase Power Conversion System for Utility Interconnected PV Applications**

Organization: OMNION Power Engineering Corporation
2010 Energy Drive, P.O. Box 879
East Troy, WI 53120

Contributors: D. G. Porter, Principle Investigator; H. Meyer; W. Leang and D. Zietlow

Objectives

The objective of this contract is to make advancements in three major areas of three-phase utility interconnected, photovoltaic power conversion: cost, reliability, and performance. The total manufacturing cost of a nominal 100-kilowatt power conversion system (PCS) will be reduced from approximately $0.50/watt to $0.25/watt when built in production lots of 100 units. A design goal of 40,000 hours mean time between failure (MTBF) has been established for this development. Using soft-switching technology, three performance goals have been established to, 1) improve converter efficiency from 95.5% to 96.5%, 2) meet FCC regulations for electromagnetic interference, and 3) reduce audible noise to below 60 decibels.

Approach

In Phase I of the contract, OMNION developed a comprehensive product specification with input from
a customer/user group. The draft product specification was prepared based on OMNION's understanding of customer preferences and current technological trends. OMNION designed and built a prototype 100-kilowatt, three-phase power conversion system in conjunction with Soft Switching Technologies Corp. (SST) which incorporates a soft switching resonant DC link converter. The PCS was demonstrated and the product specifications reviewed with the customer/user group.

During Phase II, OMNION finalized the revised and repackaged design for the 100-kilowatt PCS product (Series 3400). OMNION also conducted tests on modified manufacturing equipment and conduct a pre-production run of the 100-kilowatt PCS. At the conclusion of Phase II, OMNION has a production-model PCS.

Results

Significant progress has been made in FY98. Phase I was completed along with the majority of Phase II.

During the Phase II factory testing of the prototype 100 kW soft-switching PCS product (Series 3400), problems with the soft-switching PCS caused OMNION to re-evaluate the use of soft-switching technology and recommend the transition from soft-switching to hard-switching technology. With the approval of the Technical Monitoring Team, OMNION revised the Phase II approach to redesign the three-phase 100 kW soft-switching PCS product (Series 3400) as a new three-phase 100 kW hard-switching PCS product (Series 3300).

In January 1998, most of the hardware development work for the soft-switching 100 kW prototype PCS product (Series 3400) was suspended pending approval by the Technical Management Team (TMT) to pursue a new development path using hard-switching technology.

The new Phase II approach became:

- OMNION will prepare a new product specification to guide the new hard switching 100 kW prototype PCS product design and development.
- OMNION will design and build a new hard-switching prototype 100 kW, three-phase power conversion system, which will achieve the majority of the goals, defined for this project.
- OMNION will design and build a new prototype system package.
- OMNION will factory test the new hard-switching 100 kW prototype PCS product.
- OMNION will prepare an O&M Manual for the new hard-switching 100 kW prototype PCS product.
- OMNION will finalize the revised and repackaged design for the new hard-switching 100 kW PCS product.
- OMNION will also conduct tests on modified manufacturing equipment and conduct a pre-production run of the new prototype 100 kW power conversion system. At the conclusion of Phase II, OMNION will have a production model power conversion system with U.L. certification.

Phase II:

Specification Development

A list of tasks for the new hard-switched solution was completed in January 1998 and work began on developing a specification for the prototype hard-switched 100 kW PCS called the OMNION Series 3300. The task list and revised statement of work was submitted and reviewed with the TMT. Work continued in February 1998 on finalizing a list of tasks and statement of work for a hard-switched PCS solution and developing a specification for the Series 3300. The Series 3300 specification was developed following the guidelines defined in OMNION's quality program and completed in March 1998.

Prototype Design and Fabrication

Pending approval of the new development path by the TMT, OMNION continued to work off-line. In the second half of January 1998, OMNION started testing the new regulator board which was planned to be used with a Semikron Skiipack power bridge for the development of the new hard-switched 100 kW prototype PCS. Work continued in February 1998 on testing of the new regulator board and OMNION placed an order with Semikron for a Skiipack power bridge. In March 1998, work began on the Series 3300 system schematics and a preliminary one-line diagram. Work to finalize the Series 3300 schematics continued through April 1998. A Series 3300 system one-line diagram was completed, key system components were identified and key component suppliers were contacted, a preliminary bill of material was completed. Specifications for the identified key components were completed, purchase orders for key components were issued and work began on the design of the Series 3300 system package. The system bill of materials was refined in May 1998 as work continued on finalizing the Series 3300 system schematics. Receipt of some of the key components such as the Semikron Skiipack power bridge allowed significant progress to be made in the development of the system package. In June 1998,

the Series 3300 system schematics and package design were completed and the final bill of material was released to production. Work began on the printed circuit board layout for the various system circuit boards and the development of the final system package was completed.

Preproduction Power Conditioning System Development

In July 1998, production of the pre-production Series 3300 system began. With receipt of the system cabinet, significant progress had been made by the end of the month with the system 85% complete in production. Software was written for the system master control and testing of the master control board began. Production was completed on the Series 3300 in early August 1998 and the system was moved to test. Pre-energization tests were completed and at power testing began in mid August. Problems identified with the regulator control would cause the system to be de-rated by 15% if left unchanged. The decision was made to switch regulators to the optimal regulator, which allowed recovery of the 15%. A problem was also identified during testing with the system's voltage regulator, which controls the DC voltage, where the voltage regulator was, unstable at low power levels. In September 1998, the Series 3300 voltage regulator had been repaired and the testing of the pre-production system was completed. On September 30, 1998, the Series 3300 was shipped to Sandia National Laboratories for additional testing. In October 1998, a final review meeting was conducted and Sandia had begun their testing of the Series 3300. Work began on the final report.

Test Procedures and O&M Manual

In June 1998, work began to develop test procedures and a draft of an Operation & Maintenance (O&M) Manual for the Series 3300 prototype unit. The O&M manual covers safety consideration, shipping, installation, operation and trouble-shooting of the product. The Series 3300 O&M Manual was completed in October 1998 and routed internally for review prior to transmittal

Manufacturing Development

In September 1998, work began on a summary report detailing assessment results of the pre-production Series 3300 including illustrations of the manufacturing process. The manufacturing process was designed to minimize manufacturing cost while incorporating comprehensive quality control and inspection of the product.

Summary

Under Phase II, the following was accomplished:

- Performed an internal evaluation of the prototype soft-switching 100 kW PCS problems
- Submitted proposal to the PVMaT Technical Monitoring Team recommending transition from soft-switching to a hard-switching PCS
- Transition from soft-switching to hard-switching technology was completed
- A new product specification was completed to guide the new (Series 3300) hard-switching 100 kW prototype PCS design and development
- A new hard-switching 100 kW prototype PCS was designed
- A new prototype system package was designed

- Interaction with suppliers to optimize key component selections and specifications was completed for the new Series 3300
- Preparation of design documentation for the new Series 3300 was completed
- Assembly of a new hard-switching Series 3300 prototype PCS was completed
- Factory testing of the new hard-switching Series 3300 prototype PCS was completed
- Design and documentation of the manufacturing process for the new Series 3300 hard-switching 100 kW prototype PCS was completed
- Delivered the new hard-switching 100 kW prototype Series 3300 PCS to Sandia for testing
- Completed the O&M Manual for the new Series 3300 hard-switching 100 kW prototype PCS

The next major milestones are to complete the final report and complete the Sandia testing. When Sandia completes their testing of the Series 3300, OMNION will begin the U.L. listing process. Results from the testing and information from the manufacture of the pre-production PCS will be used to refine the manufacturing and test process. The refined process will be used to manufacture a production PCS.

Title: **PowerGuard Advanced Manufacturing**

Organization: PowerLight Corporation, Berkeley, CA

Contributors: T. Dinwoodie, Principal Investigator, J. Ansley, T. Kleiner, C. O'Brien, D. Shugar, M. Zucker

Objective

The objective of this subcontract over its three-year duration is to continue the advancement of the PowerLight Corporation's manufacturing of photovoltaic roofing tiles ("PowerGuard") in order to reduce cost and increase manufacturing capabilities. PowerLight will demonstrate reduced system costs and complete manufacturing improvements for PowerGuard tile fabrication capability of 16 MW/year, and stimulate US PV laminate manufacturing expansion to 2 MW/year. PowerLight will address PowerGuard system cost reduction through 1) improvements in manufacturing technology related to system (non-module) components, 2) product design enhancements, 3) increased production capacity, 4) enhanced system reliability and performance, and 5) strategic alliances to leverage PV module technical improvements and cost reduction.

Research Results

PowerLight made significant progress since this contract began in June, 1998 to the end of the fiscal year, September 30, 1998.

Task 1. Assembly Layout and Integration

Under this task, a master plan for an automated manufacturing line is being developed, fully detailing the plant layout, equipment descriptions, vendors and budgets compared with the criteria established in the Statement of Work. Production rates will be improved to 2 minutes per tile.

In this period, preliminary modifications to the manufacturing processes developed under this contract were incorporated into PowerLight's manufacturing facility in Mt. Marion, NY to carry out the manufacture of ten 6-kW sloped PowerGuard systems. These systems were fabricated under a contract with the New York Power Authority (NYPA). Preliminary improvements to the manufacturing line included savings in material and labor costs, and improved product quality.

PowerLight also developed specifications for a 3-axis CNC router for extruded polystyrene (XPS) board processing, and developed a concept for an automated coating application station. Future work will consist of developing automatic feed mechanisms, waste removal equipment, and other facility requirements.

Task 2. PV Laminate Preparation

Under this task, several automated stations will be designed and installed at the start of the manufacturing line. During this period, progress was made in identifying the requirements of an electrical harness fabrication station. Three manufacturers of electrical quick-connects were identified as possible candidates for the harness terminations. Cost, ease of use, performance, and availability of the quick-connects narrowed the list down to one manufacturer. Ten samples of these quick connects were evaluated for performance in wet megger tests and limited freeze-thaw resistance tests. Mating panel mounts for electrical boxes were evaluated for water tightness. The success of the connectors in these tests led to further research into the requirements of an automated assembly station, and a detailed cost analysis of the connectors in a typical PowerGuard system.

Future work under this task will consist of finalizing the design and installation of the electrical harness assembly station, as well as an automated station for junction box attachment, adhesive priming, and a PV laminate quality control and testing station.

Task 3. Extruded Polystyrene Processing

Under this task, PowerLight will redesign and replace the manual hot-knife cutting station with an automated router station for post processing of the XPS boards, meeting the throughput criteria described in the Statement of Work. During this period, several approaches to XPS processing were identified, including fixed routers, traveling routers, a hybrid system, hot knife, and pressurized water cutting. An experimental production station was created in the PowerLight laboratory to investigate dust collection and tolerance maintenance issues. The alternatives were evaluated by considering pollution, dust, noise, safety, throughput, cost, and flexibility in processing various board dimensions. A 3-axis CNC router was identified as the best option to meet the design requirements.

Future work will consist of finalizing the design of the dust collection system, creating CAD drawings of the automated station, and investigating potential equipment vendors.

Task 4. Automated Coating Station

Under this task, PowerLight will design and develop an automated coating station for coating the top surface of the XPS board, meeting the design requirements outlined in the Statement of Work. During this period, numerous alternatives to the current coating were identified and investigated, including a cementitious coating, plastic or metallic sheet for a roll lamination process, commercially available concrete-based boards, and elastomeric roof coatings. A cementitious coating was selected, as it was the lowest cost of the alternatives, and was the only alternative meeting established performance criteria. PowerLight took the decision to use a cementitious coating a step further by incorporating it into the manufacture of the NYPA systems. Processing issues requiring refinement were identified during this period and will be addressed in future research. This research has been initiated through consultation with experts in concrete processing.

Future work will consist of improving the cementitious mix for resistance to cracking and freeze-thaw degradation, evaluating improvements through accelerated life testing of the coating, and designing and fabricating the automated coating station.

Task 5. Automated Spacer Attachment

Under this task, PowerLight will design and implement an automated spacer attachment station to attach the spacers to the XPS board for PV laminate stand-off, meeting the throughput requirements outlined in the statement of work. During this period, alternative materials and designs were identified, including XPS, sheet metal, extruded or formed steel, and plastic. Alternate attachment mechanisms were also identified, including the use of adhesives, anchoring in concrete, and a mechanical attachment to the XPS board. Several of these options were tested for their pullout strength. The strength of the attachment by anchoring in concrete far exceeded the design criteria, and this attachment mechanism is currently the most promising.

Future work will include evaluating the weatherability of the concrete-anchored attachment through accelerated life testing, and designing and implementing an automated attachment station.

Task 6. Inverter Controller Improvements

Under this task, PowerLight will work with an identified inverter manufacturer to modify the inverter to incorporate a data acquisition system (DAS), incorporate dial-up communication capability, replace analog circuitry with digital circuitry, and eliminate non-PV related functionality currently part of the controller modification. Significant progress was made this period. Design criteria was established, and many sub-system designs were finalized, including the interface bus, high voltage signal conditioning board, communication hardware for the DAS and DAS interface, OEM memory, processor, communications boards, and modular circuitry. Several of these components have been selected and tested.

Future work will include researching compatible software, and completing the design of the inverter packaging for system integration and retrofit.

Task 7. Manufacturing Design Improvements

During this period, progress was made in the three subtasks outlined in the Statement of Work: Sloped Tile Assembly, Amorphous Silicon (a-Si) Tile Package, and Retrofit (RT) PowerCurb.

Prototypes of an improved sloped tile assembly that attempt to reduce cost, reduce shipping density, and simplify manufacturing were created and evaluated. Four prototypes were fabricated including a prototype which ships flat and "pops up" in the field, one which is shipped fixed in the slope position, a "field assembly" version (allowing the PV to be shipped separately), and a hybrid version that is partially fixed and partially assembled in the field. The hybrid version was chosen as the best interim design solution for the NYPA project. The manufacturing process and overall quality of this design were evaluated following the completion of this project, resulting in recommendations for further design modifications. Future work under this subtask will consist of continuing design iterations toward an assembly that meets the specified design requirements of shipping flat and/or assembly in the field.

Work under the a-Si Tile Packaging subtask consisted of fabricating prototype tiles with various spacer heights for field temperature measurements. Future work under this subtask will consist of selecting a tile design with the minimum possible spacer height, evaluating the performance of the XPS backerboard for resistance to temperatures seen in the chosen design, and finalizing the a-Si tile design to meet the requirements outlined in the Statement of Work.

Work under the RT PowerCurb subtask consisted of exploring alternative curb concepts for use in the NYPA project. Alternative materials were identified, including sheet metal ballast pans, plastic, and concrete. Concrete curbs were chosen as an interim design solution for the NYPA project. Numerous iterations were required in order to determine the optimum concrete formulation, and mixing, molding, and curing procedure. A means of interconnecting curb sections was developed and used in the NYPA project. The design and fabrication of the concrete curbs for the NYPA project was evaluated. Future work under this subtask will include further evaluation of alternative materials, incorporating wind tunnel performance of alternate curb designs for improved aerodynamic performance, accelerated life testing of the chosen design, and demonstration of the cost reductions described in the Statement of Work.

Task 8. Component Testing Certification and Safety

Progress was made in three of the four subtasks under this task: Environment, Health, and Safety; Wind Testing; and Underwriter's Laboratories Listing (UL).

Under the subtask Environment, Health, and Safety, PowerLight will incorporate Federal and state regulations applicable to the proposed production processes, system installation practices, and system operation, and integrate these regulations into training programs. During this period, the required compliance standards were identified, OSHA and NEPA regulations were researched and analyzed, and a summary report of federal and state regulations was completed and submitted as deliverable D-1-2.

Under the Wind Testing subtask, PowerLight will conduct wind tunnel testing on prototypes of all modifications to the PowerGuard tile system, which will result in the development of standardized engineering tables for wind loads on PowerGuard systems. During this period, a strategy was developed for wind tunnel testing through a meeting with consultants specialized in fluid dynamics, wind design standards, structural engineering. Friction coefficients of PowerGuard system components on various roof surfaces were measured for wind load analyses. Wind loads on the NYPA systems were calculated using results from current and past research results in order to calculate the necessary ballast weight for the RT PowerCurb.
First generation tables of recommended maximum wind speeds for RT arrays were created. Uplift pressure measurements on sloped tile systems were completed by a wind tunnel test facility; results contradicted prior results and the cause for this is still under investigation. Another wind testing facility was consulted to continue wind tunnel tests and evaluate the cause for the contradictions seen in the recent measurements. A test plan was developed with the wind testing facility to carry out measurement of failure velocities as a function of numerous design parameters. Testing will take place over a five-month period. Future work under this task will consist of completing the above test plan and creating a final report summarizing results. These results will lead to the generation of a final wind load design table for flat and sloped PowerGuard systems.

Under the UL subtask, the UL requirements for electrical quick-connects were determined in order to evaluate the chosen quick-connect (as described in Task 2) for PowerGuard Tiles. Future work under this task will consist of submitting modified products to UL for listing.

Task 9. Integrated Warranties
Under this task, a comprehensive system warranty for PowerGuard will be developed. Preliminary work focused on the warranty associated with the inverter. PV laminate suppliers were assessed to determine the allocation of rated watts across the life of the warranty**.**

Task 10. Assessment of Commercial Demonstrations
Under this task, PowerLight will assess the results of commercial demonstrations. During this period, an inspection checklist was created for PowerGuard systems, and a form for assessing each step of the manufacturing line was created. These forms were used to document the results of PVMaT related changes to the PowerGuard manufacturing line during the NYPA project. Future work will consist of analyzing this documentation and continuing to monitor projects that utilize improvements made under the PVMaT project.

Summary
PowerLight is fully on target in meeting its development and cost objectives under Phase I of its PVMaT contract, as defined in the contract Statement of Work. The authors wish to express their gratitude and enthusiasm for the opportunity presented by this contact to advance PowerGuard manufacturing and cost reduction.

Title: **Photovoltaic Cz Silicon Module Improvements**

Organization: Siemens Solar Industries, 4650 Adohr Lane, Camarillo, CA 93012

Contributors: Theresa L. Jester, Principal Investigator

Introduction

The objective of the DOE/NREL Photovoltaic Manufacturing Technology (PVMaT) subcontract with Siemens Solar Industries (SSI) is to continue the advancement of module design and manufacturing methods at SSI in order to achieve an 18% reduction in module cost per watt at the end of three phases of work, with each phase lasting a year. Phase I of this subcontract began in November 1995, Phase II in November 1996, and Phae III in November 1997. The approaches for reaching this cost reduction goal are to analyze existing module cost structure and explore new module configurations which address the highest cost components, investigate the reduction of labor and improvement of yield, and to implement statistical process control (SPC) in module manufacturing. Additional publications are referenced.

Module Cost Analysis and Design

A first step toward reducing the cost per watt at the module level is to gain a thorough understanding of the present factors which dominate cost. The frame and junction box contributions are significant portions of the module assembly cost. During phase III of the PVMat program, SSI has developed a low cost frame and junction box. The module design is shown in Figure 1.

Yield and Productivity Improvements

Manufacturing yield is a powerful driver of the manufacturing cost of modules. Over the first two years of the program, many gains were achieved in improving line yields, from wafering through module assembly. The third year or current year of the program has focused on the improvement of crystal growth yields. Figures 2 and 3 show the improvement over time of crystal yields for different types of grower machines. As crystal growth costs are over 30% of the finished module cost it is important that the yield be continuously improved and maintained at a high level. Figure 2 shows the yield gain this year for the 103 mm product, Figure 3 shows the yield gain over the same time period for the 125 mm product. This gain contributes over 5% absolute to the 18% cost reduction plan.

Manufacturing Systems to Improve Module Reliability

In addition to receiving ISO 9001 certification during 1996, Siemens Solar is committed to deployment of statistical process control throughout the manufacturing process. The diffusion process has been a focus for this effort and has been highly successful. The process is fully capable statistically. Figure 4 shows the statistics for the sheet resistance measurements made on every run over a specified time in the diffusion process. The statistical analysis shows the process to have a numerical capability exceeding one which indicates it is very stable and predictable. Siemens is implementing this approach of statistical control throughout the fab.

Summary

Cost drivers for Cz Si solar cell modules have been identified. Large cell modules are in production as well as low cost framing and junction box designs. Yield improvement exceed 15% in every product line from crystal growth through module assembly. The use of statistical process control is implemented in all critical processes. The goal of 18% cost reduction is in process of being achieved through this program.

Acknowledgments

Many people have contributed to the work under this contract. Thanks are due especially to Rick Mitchell, NREL technical monitor, to Dave Bender, Ruben Balanga, Jean Hummel, Dave Jeffrey, Waltraut Klein, Greg Mihalik, Maria Tsimanis, Elena Woodard, and Ken Sandland at SSI.

References

NCPV Photovoltaics Program Review, Proceedings of the 15th Conference, Denver, CO, 1998, AIP Conference Proceedings (in press).

Eighth Workshop on on Crytalline Silicon Solar Cell Materials and Processes, Copper Mountain, CO, 1998 NREL Publications

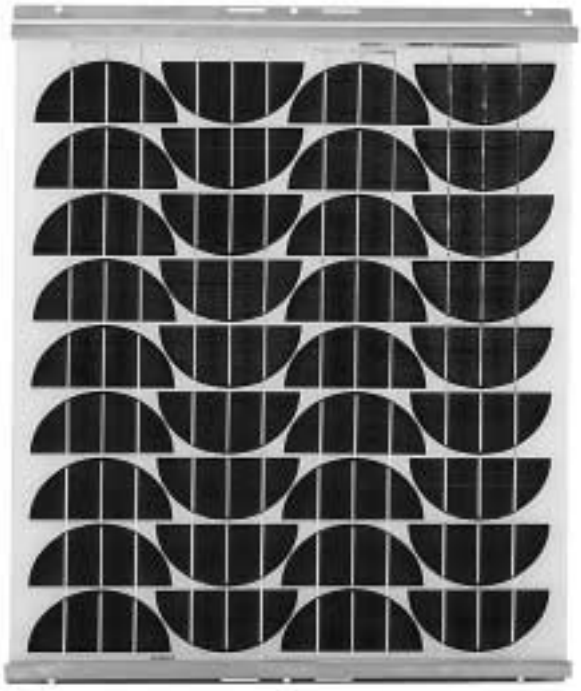

Figure 1. SR 50-Z Module

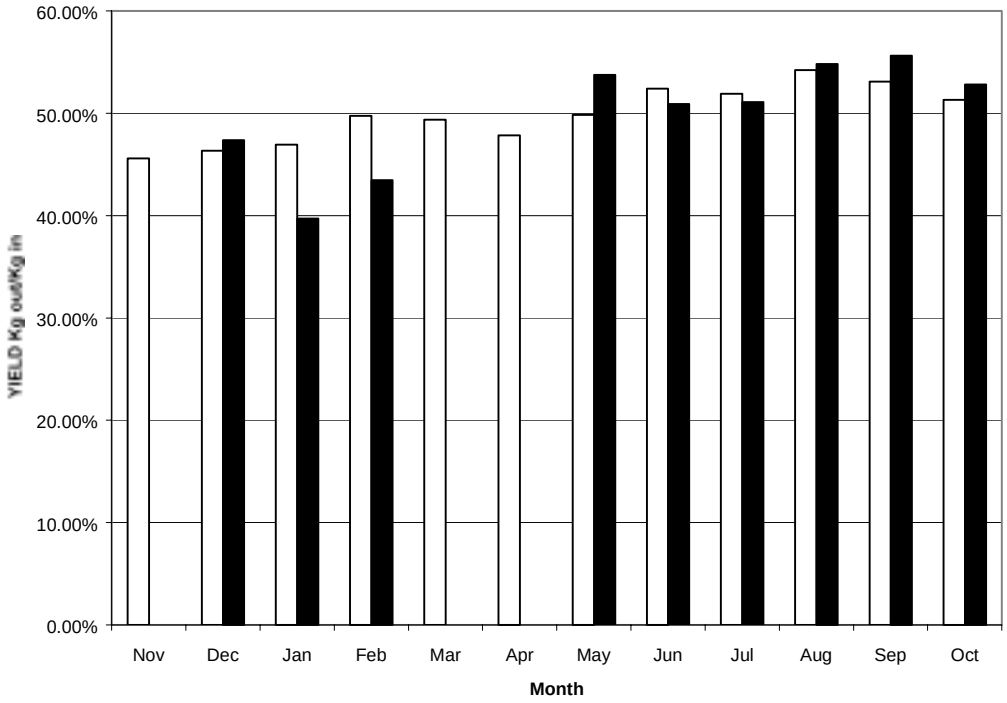

Figure 2. 103 mm Crystal Growth Yields

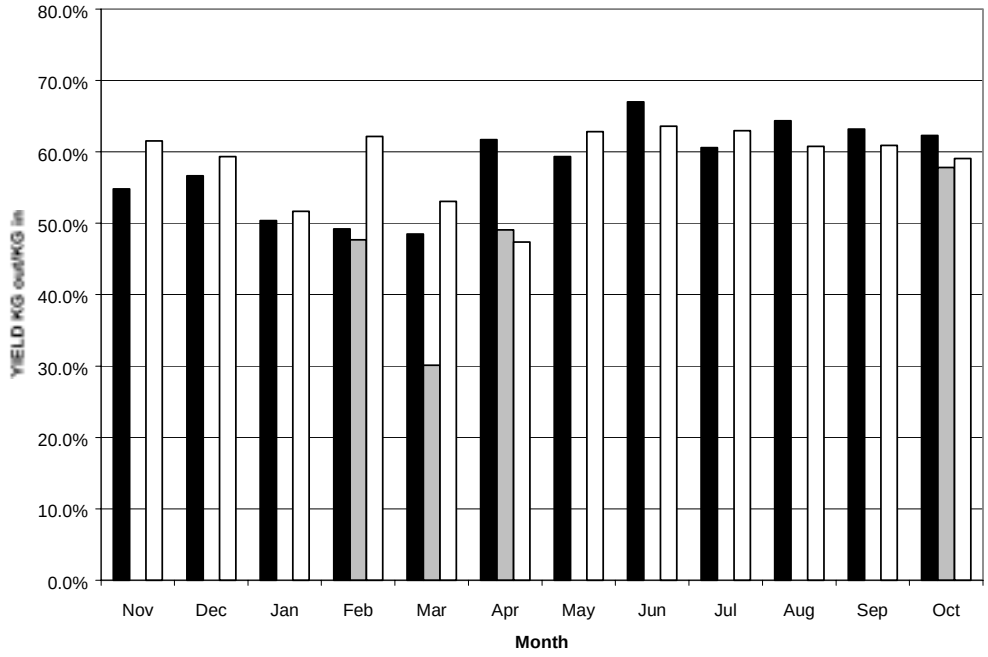

Figure 3. 125 mm Crystal Growth Yield

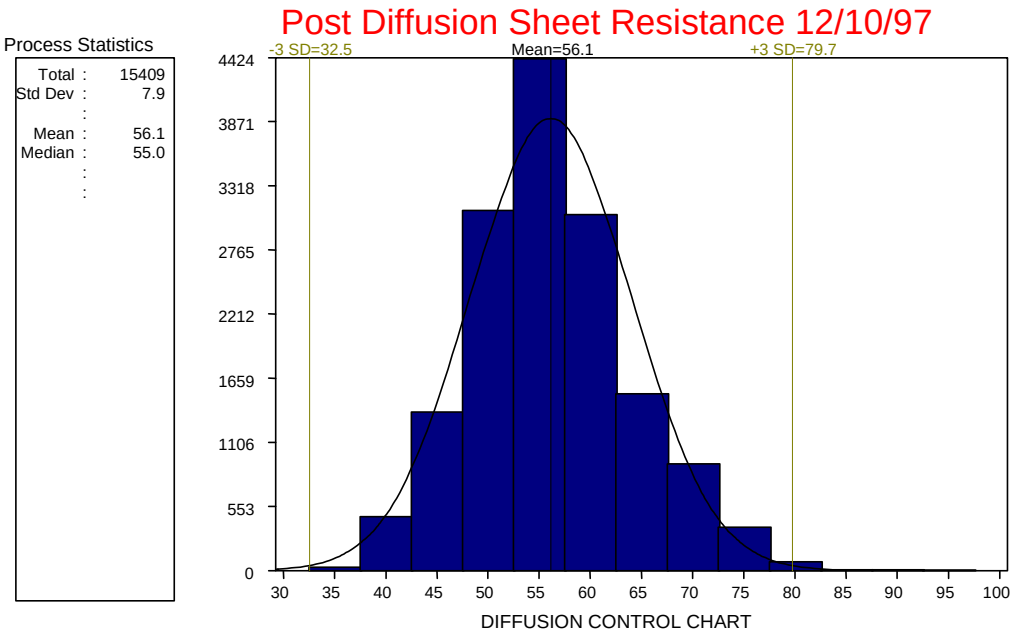

Figure 4. Diffusion Sheet Resistance Capability

Title: **Specific PVMat R&D in CdTe Product Manufacturing**

Organization: Solar Cells, Inc., Toledo, Ohio

Contributors: J. Heider, Co-Principal Investigator, A. McMaster, Co-Principal Investigator, D. Sandwisch, K. Komanyos, V. Champion, J. Bohland

Project Objectives

The objectives of Solar Cells' Phase 5A2 subcontract number ZAX-8-17647-06, Specific PVMaT R&D in CdTe Product Manufacturing, is to continue the advancement of Solar Cells, Inc. manufacturing technologies and product development. Specifically:

Lamination

Develop a high-throughput, low-cost lamination process to raise throughput from 18 modules per hour to at least 30 modules per hour while simultaneously reducing labor costs by 50% and lowering capital requirements by a factor of four.

Potting

Develop a high-throughput, low-cost potting process to increase potting line throughput by a factor of at least four, reduce labor costs by at least a factor of ten, and increase overall quality.

Laser Scribing

Develop laser scribing techniques and equipment by engaging industry experts and vendors to implement state-of-the-art techniques and automation. New scribing techniques will result in scalability to 60 modules an hour with the potential of exceeding that capacity with nominal upgrades while at the same time increasing reliability by a factor of ten and reducing capital costs by a factor of two.

Product Acceptance

Improving the acceptance of the SCI product line in existing and new markets to provide an opportunity to penetrate market segments other than those served by SCI's standard frameless, 60cm x 120cm module is an important objective of this work. Certification of SCI modules according to IEEE 1262 and UL 1703 test regimens in three successive, evolutionary steps incorporating design changes from improved product designs, manufacturing process improvements and market demands.

EHS Program Refinement

As a responsible manufacturer, SCI is dedicated to refining environmental, health and safety programs culminating in ISO 14,000 certification and implementation in year three of this work. An environmental, health and safety program that will place SCI in a leadership position relative to comparable businesses within and outside of the photovoltaic industry will be developed.

Project Approach

Manufacturing Line Improvements - Lamination

Using the support of key experts such as Automotive and Robotics Research Institute (ARRI), industrial lamination processes will be developed through vendor identification, material handling solutions and establishing parameters for integration of an improved lamination process into the SCI production line. Solar Cells, Inc. will optimize and debug the prototype laminator and make improvements before its integration on the SCI manufacturing line. Lamination preparation is included in this scope of work and includes EVA cutting and application, bus bar application, and back glass handling and application. This task is assigned to year one of the project.

Manufacturing Line Improvements - Potting

Solar Cells will develop, using the assistance of industry experts, improved potting procedures and design of associated equipment. The scope of work will include potting processes such as diode connection, mold positioning, urethane injection, and module handling. This task is assigned to year two of the project.

Manufacturing Line Improvements - Laser Scribing

Solar Cells will develop an improved scribing technique and design associated equipment, using the assistance of industry experts and equipment vendors. A thorough review of state-of-the-art laser scribing techniques and the integration of material handling solutions will result in the stated throughput, reliability, and capital equipment objectives. Solar Cells will complete testing of the improved high-throughput scribing system , including process and material handling components, on its module production line. This task is assigned to year three of the project.

Product Acceptance

The project scope of work allows for IEEE 1262 and UL 1702 module qualification testing in each of the three years of the project. The first year's test will qualify SCI's current module design while future testing will include product modifications such as junction boxes instead of pigtails, other sizes, alternative voltages, different encapsulation materials or processes or other changes based on market demand.

EHS Program Refinement

Solar Cells will continue to refine and improve its environmental, Safety and Health programs initiated during its PVMat Phase 2B subcontract. An internal review of current programs will be conducted and, again using the assistance industry experts, their status relative to industry best-demonstrated practices will be assessed. Solar Cells will complete the implementation of refinements and improvements in critical areas and establish a plan for continuous improvement. Certification under ISO 14,000 will be pursued in the last year of the work.

Project Results

Manufacturing Line Improvements - Lamination

Though this report reflects only 5 months progress of the three-year project term, concrete progress has already been achieved. Figures 1 and 2 show Solar Cells' high-throughput lamination equipment as proposed and as installed, respectively. Work continues on automated lamination preparation equipment using Automotive and Robotics Research Institute.

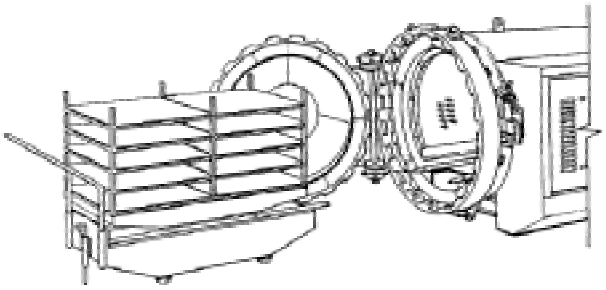

Figure 1 - Proposed High-Throughput Laminator

Figure 2 - Installed High-Throughput Laminator

Product Acceptance

Table 1 shows results of module qualification testing according to IEEE 1262 protocol as supplied by the Arizona State University Photovoltaics Testing Laboratory.

Table 1. Results of Combined Qualification Testing

Combined Qualification Testing IEEE 1262, IEC 1215, IEC 1646, PMC		**Test Dates**	**Findings**
Seq.	**Test**		
I1	Baseline visual inspection	9/2/98, 9/3/98	Pass
I1	Electrical performance (I-V)	9/14/98, 9/15/98	Pass
I2	Ground continuity		N/A
I3	Dry Electrical isolation (Dry hi-pot)	9/18/98	Pass: max. leakage current=1.43 μA Pass: min. insulation R=2500 M
I4	Wet insulation resistance	9/18/98	Pass: min. insulation R=109 M
I5	Wet Electrical isolation (Wet hi-pot)	9/18/98	Pass: max. leakage current=20.5 μA
I6	Intermediate visual inspection	9/26/98	Pass
I6	Electrical performance (I-V)	9/25/98	Pass
I7	Annealing		NA
I8	Intermediate visual inspection		NA

Combined Qualification Testing IEEE 1262, IEC 1215, IEC 1646, PMC		Test Dates	Findings
I8	Electrical performance (I-V)		NA
A1	Thermal cycle (TC200, IEEE)	In progress	
B1	Light Soak		NA
B2	UV conditioning (15 kWh/m^2)	In progress	
D1	Light soak		NA
D2	Measurement of and	9/14/98 – 9/15/98	Pass
D3	Measurement of NOCT	10/9/98	43.2°C
D4	Performance at NOCT	10/15/98	Pass
D5	Perform. at Low Irradiance	10/15/98	Pass
D6	Outdoor exposure (60 kWh/m^2)	In progress	

EHS Program Refinement

Formal compliance plans for personal protective equipment, respirator program compliance, first-aid and bloodborne pathogens training have already been completed. Additionally, a comprehensive assessment of current EHS programs has been completed and a implementation plan coinciding with PVMat objectives for safety, health and environmental programs has been completed.

Project Conclusions

Though at the beginning of the project, Solar Cells has demonstrated accomplishments in each of the three major tasks in this work; manufacturing line improvements, product readiness, and EHS program refinement. Solar Cells, using the plans developed for each project objective and employing its qualified internal staff as well as industry experts, is poised for successful project completion through diligent and intelligent work at the tasks at hand.

Readers are refereed to first quarter project deliverables for more information on the progress of lamination improvements [1], product readiness [2], and EHS program refinement [3].

References

[1] Phase I Deliverable D-1.2.1, *Summary Design of High Throughput Lamination Equipment*, October, 1998, NREL, 4 pp.

[2] Phase I Deliverable D-1.2.1, *Preliminary Module Testing Report and Testing Schedule*, October, 1998, NREL, 2 pp.

[3] Phase I Deliverable D-1.2.1, *Letter Report and Plan for Implementing EHS Improvements*, October, 1998, NREL, 5 pp.

Title: **The Development of Standardized, Low-cost AC PV Systems**

Organization: Solar Design Associates, Inc. with Solarex Corporation and Advanced Energy Systems, Inc.

Contributor: Stephen Strong

Solar Design Associates, Inc. (SDA), of Harvard, MA and Solarex Corporation, of Frederick, MD, teamed together with Advanced Energy Systems of Wilton, NH to pursue a multi-level program under PVMaT Phase 4-A1 targeted at design innovation, standardization and modularity with the goal to deliver low-cost AC PV systems to the utility-interactive market.

At the core of the PVMaT effort was the development of a reliable and cost-effective DC-to-AC micro inverter which would make the concept of a large-area ' AC PV module' practical. This inverter was to be developed based upon the prototype 250 Wp analog-control modular inverter which had been developed with support from the DOE PV:Bonus (Building Opportunities in The US for Photovoltaics) program.

When it became clear that the digital-control modular inverter would not meet the established cost and reliability goals without a good deal more work and resources, the overall PVMaT statement of work was reviewed with the goal to redirect the focus of the work to define a new set of goals which would be achievable within the framework of the PVMaT program. These new tasks were performed during FY'98 and are listed in the following table with the results described in detail below.

- Obtain UL Listing of the AC PV Module
- Achieve Compliance with Codes and Standards
- Continue Work on Inverter Cost Reduction
- Develop a Mounting System for Solarex Thin Film Modules
- Development of an Electrical Connector System for Solarex Thin Film Modules

Obtain UL Listing of the AC PV Module It was recognized that an important milestone in the commercialization of AC modules would be to take the AES modular inverter though the steps necessary to achieve fully UL Listed AC PV modules. This was to be done in as generic a way as possible so the AES inverter could be used with several manufacturer's modules and, to help pave the way for the commercialization of AC modules in general.

The AES modular inverter had already achieved UL listing. To obtain a UL listing for the AC PV module - defined as the assembly of the modular inverter and a large area PV module - required the successful completion of several UL testing sequences. These included temperature cycling, humidity cycle, rain spray and an insulation breakdown test. In addition, a mounting adhesive strength test must be completed and passed.

Fortunately, NREL agreed to provide their environmental chamber for these tests which made this work possible as the high cost of renting a commercial test chamber were beyond our resources. The AES modular inverter attached to a PV module as an ' AC PV module' did achieve UL listing as a result of this work.

Achieve Compliance with Codes and Standards It was recognized that there were a number of issues in the existing codes and standards which govern the manufacture and installation of distributed PV systems which required revision to accommodate the differing characteristics of AC modules. AES was to review the current draft UL1741 and IEEE 929 standards and work with the responsible committees to come up with practical solutions to the problems (without becoming too constrictive or product specific).

AES was then to modify the operation of their modular inverter as needed to achieve compliance with these revised codes. AES did become very involved in the assessment of existing codes and standards and their revision. This work resulted in streamlining the introduction and acceptance of AC modules.

Continue Work on Inverter Cost Reduction The manufacturing costs for the MI-250 were so high that this model is not able to compete with larger (~2-5 kW) central inverter systems. To further reduce the manufactured cost of the MI-250, AES was to pursue design refinements to achieve cost savings in the following areas: A reduced-cost power-line carrier daughter card or other suitable data communications subsystem and, cost reductions from potting vs. conformal coat, mechanical design, and general cost reduction possibilities.

AES did investigate alternate chip sets for the power-line carrier, including simpler and less capable schemes than the spread- spectrum system of Intellon. AES also worked with the NH Manufacturing Extension Program on potting vs. conformal coat, mechanical design, and general cost reduction possibilities. AES also explored other ways of reducing the cost of the MI-250 to the end user. This work resulted in a lower-cost modular inverter and also helped AES to develop their GC-1000 utility-interactive inverter.

Develop a Mounting System for Solarex Thin Film Modules During the first 18 months of this PVMaT effort, the Solarex tandem-junction thin-film product was commercialized at their new facility in Tuano, VA. In an effort to achieve the program goals for low-cost PV systems, Solarex was to develop a low cost mounting system for these new thin-film modules and obtain UL listing for the system.

Solarex did develop an integrated module / array mounting system for their thin-film product in sloped-roof applications. The system was tested and qualified to UL and ANSI Z97.1 to assure compliance with Building Codes and the NEC. It has received a UL listing.

Development of an Electrical Connector System for Thin-Film Modules In conjunction with the effort to develop an integrated mounting system for their thin-film product, Solarex also was to define and qualify a low-cost, electrical connector system. Because of the larger number of modules required in a system, a quick-connect DC connector was preferred.

Solarex did develop/select a quick-connect DC connector for their thin-film modules to be used in conjunction with their new module / array mounting system. The connector was combined with a wiring system that satisfies NEC requirements and UL listing was obtained for this connector and wiring system.

A significant result of this program is that Solarex has filed a US patent application on the new module frame and mounting system which was developed with support from PVMaT. The patent

application is US Utility Patent #09/123,724 for: “Photovoltaic Module Framing System with Integral Electrical Raceways”.

Solarex has incorporated the mounting system and quick connector into the PV-VALUE system. These systems are now commercially available. System specifications and a system installation manual have been published.

Solarex has started to manufacture this new combination framing and array mounting system. They have already begun to receive orders and a number of residential scale installations are already in place in the field.

All tasks under the revised statement of work were completed in the spring of 1998. Despite the fact that the price goals set out for the micro inverter at the onset of the program proved to be too ambitious, a number of other product developments were achieved under this program which have helped lower the costs of PV systems to the customer and moved new generations of hardware out into the marketplace.

Title: **Design, Fabrication and Certification of Advanced Modular PV Power Systems**

Organization: Solar Electric Specialties, Willits, California

Contributors: G. E. Minyard and T. J. Lambarski

Abstract

The Design, Fabrication and Certification of Advanced Modular PV Power Systems contract was completed in April 1998. It was a 2.5 year effort under a Photovoltaic Manufacturing Technology (PVMaT) cost-shared contract in Phase 4A1 for Product Driven System and Component Technologies which had the goals to improve the cost-effectiveness and manufacturing efficiency of PV end-products, optimize manufacturing and packaging methods, and generally improve balance-of-system performance, integration and manufacturing. This contract had the specific goal to reduce the installed PV system life cycle costs to the customer with the ultimate goal of increasing PV system marketability and customer acceptance.

The specific objectives of the project were to develop certified, standardized, modular, pre-engineered product lines of our main stand-alone systems, the Modular Autonomous PV Power Supply (MAPPS) and PV-Generator Hybrid System (Photogenset^{TM}). SES accomplished its essential goals and some extra goals as well. We have designed and built both a 200 W MAPPS and a 1 kW Photogenset. We have not only obtained UL Listing of the MAPPS unit, but also of a complete family of MAPPS and have also obtained approval for a MAPPS family for use in hazardous locations by Factory Mutual (FM). We have accessed the costs and level of effort involved in listing the Photogenset. The MAPPS and Photogenset have performed well in functionality testing at NREL and Sandia, respectively, and the MAPPS has been set up for permanent use at NREL. In addition to expounding on the goals, objectives and FY 1998 activities for the project, specific accomplishments and benefits are also presented in this paper.

Background

Although most PV system integration companies advertise standard product lines, most PV systems sold today are still custom designed based on general product line principles. The fact that most systems houses have system product lines attests to the need to make the specifications simple and standardized so that they can be more easily understood by the potential customer and marketed by the sales engineer. In this contract a concerted attempt was made to increase standardization and modularity as are seen in other product categories such as computers whether for consumers or commercial applications. There will always be a need for custom designs, but true cost savings and customer acceptance require that systems be more technology transparent. “Turn it on and watch it work.”

In addition, up until now no PV power systems have been certified by agencies outside the PV industry such as Underwriters Laboratories (UL) or Factory Mutual (FM). We are seeing a trend toward certification in components such as PV modules, charge controllers and inverters. More companies are getting their PV products UL or ETL Listed and FM Approved for hazardous locations. This project represents the first effort to have whole PV power systems certified.

Program Goals and Objectives

The stated goal of the Design, Fabrication and Certification of Advanced Modular PV Power Systems contract was to significantly reduce the installed PV system life cycle costs to the customer. This was part of an overall goal of improving PV system marketability and customer acceptance. In line with the philosophy presented above, SES has attempted to make this happen by developing certified, standardized, modular, pre-engineered products lines of our main stand-alone systems, the Modular Autonomous PV Power Supply (MAPPS) and PV-Generator Hybrid System (Photogenset).
The technical and cost advantages of this approach are 1) shorter production lead times, 2) higher overall quality and system reliability, 3) decreased management and engineering time, 4) lower overhead and inventory costs, and 5) lower installation labor and material costs. The marketing advantages are that the systems can be specified and described more easily by the sales engineers and the customer can more easily assess the options and choose the system he needs. A corollary to this is greater customer acceptance of the PV solution and greater confidence among lending institutions.

Discussion of Activities

The task structure of the contract called for development and fabrication of a 200 W MAPPS and a 1 kW Photogenset as the first prototypes for these respective product lines, certification of the prototypes and product lines, and functionality testing of the prototypes at NREL and Sandia. Within the charter was also room for development of new or improved components for the systems to improve performance and reliability while reducing costs or to facilitate certification.

The sizes of the prototypes were chosen for their high sales potential and manageable size and cost for fabrication and certification. The purpose of the functionality testing was to provide verification of performance and reliability and to develop test-based performance specifications.

<u>MAPPS Activities</u>
These FY 1998 activities included completion of the functionality testing at NREL and completion of the FM Approval for a line of MAPPS for use in hazardous locations. This line has enhanced incendiary safety over the basic line. The hazardous locations, as defined in Article 500 of the National Electrical Code, have environments with incendiary gases present. Following completion of the UL evaluation of the prototype MAPPS, it was modified for FM requirements and sent to them for their evaluation. During FY 1998 the evaluation was successfully completed and an initial plant inspection was performed. SES passed the initial plant inspection as well as all subsequent quarterly inspections throughout 1998.

During FY 1998 NREL completed the functionality testing of the 200 W MAPPS unit. This unit was set up and instrumented at NREL's PV Test Facility. The MAPPS was tested for 14 months. The test report from NREL indicated satisfactory performance under load with 98% availability, with the only shutdowns due to periods of inclement weather. The unit has subsequently been moved to the parking lot to serve as power for area lighting.

<u>Photogenset</u>
These FY 1998 activities included completion of a UL listing study on the Photogenset, completion of the fabrication of the 1 kW Photogenset, performance of shakedown testing prior to delivery of the unit to Sandia, and functionality testing at Sandia.

In developing the Photogenset, we attempted to make maximum use of UL Listed components; however, we were not able to obtain a UL Listed generator and accessories or a UL Listed

controller with the remote communications capabilities desired. We obtained quotes from both UL and ETL (Electrical Testing Laboratories) to assess the costs and benefits of each laboratory. We contracted with UL for a preliminary investigation to more fully assess the problems, the degree of evaluation and testing required and the cost of the listing. The results, delivered in FY 1998, indicated that a fairly extensive testing program would be required for the generator system and the controller, that there is no guarantee of Listing and that the costs between UL and ETL appear similar. We believe that additional component development and maturity is needed before the Photogenset Listing can be accomplished.

The Photogenset was tested for only one month at Sandia before having to be removed because of other commitments for its use. Therefore, a full test was not accomplished. The Photogenset performed according to specifications with the exception of an inverter failure which has subsequently been corrected.

Accomplishments and Benefits

To summarize program accomplishments, we have: 1) a UL Listed family of MAPPS with upgraded assembly process controls and installation instructions; 2) FM Approval for a family of MAPPS; 3) an understanding of certifications issues and requirements; 4) an improved, lower cost MAPPS battery enclosure; 5) a 1 kW mobile Photogenset prototype based on a multi-platform design; 6) a new microprocessor-based controller with remote communications capabilities for the Photogenset; and 7) a knowledge of what it will take to obtain UL Listing of a Photogenset.

SES has benefited from a synergy between the PVMaT contract and our normal business efforts. This synergy has resulted in some important new business and we have experienced significant sales of our UL and FM product lines. We also believe this contract has already provided, and will continue to provide, important advances in PV market penetration through lower costs, higher reliability, product standardization and product certification.

References

1. Lambarski, T.; and Minyard, G. (December 1997). *Safety Results Report for 1 kW Photogenset*, Subcontract ZAF-5-14271-07.
2. Lambarski, T; and Minyard, G. (October 1998). *Design, Fabrication and Certification of Advanced Modular PV Power Systems: Final Technical Progress Report*. NREL/SR-520-24921. 34 pp.

Title **PVMaT Improvements in the Solarex PV Module Manufacturing Technology**

Organization Solarex, A Business Unit of Amoco/Enron Solar
Frederick, Maryland 21703

Contributors J. H. Wohlgemuth, Program Manager; F. Artigliere, J. Creager, T. Corman, G. Kelly, T. Koval, M. Narayanan, M. Perry, M. Roy, S. Roncin, S. Shea , M. Susol, D. Stark, T. Tomlinson, and D. Whitehouse of Solarex; R. Fernandez and D. Vanecek of ARRI; R. Gehringer of SiNaF Products, Inc.; N. Sherman and J. Galica of STR; and G. Lucovsky of NCSU.

Introduction

During FY 1998 Solarex completed a Phase 2B PVMaT contract entitled "Cast Polycrystalline Silicon Photovoltaic Module Manufacturing Technology Improvements". This program lead to the development of and/or improvements in processes, products and equipment. The following developments from this program have been implemented in manufacturing at Solarex:

- Casting of larger ingots;
- Use of wire saws in operations;
- Addition of a back surface field to the cell process;
- Implementation of a fully automated screen printing system;
- Introduction of a larger cell (11.4 cm by 15.2 cm) into commercial production;
- Upgrade of the module assembly equipment;
- Use of a lower cost back sheet;
- Qualification of a lower cost electrical termination system; and
- Use of frameless modules in a number of PV systems.

During the course of this Phase 2B PVMaT program:

- The production volume at Solarex has tripled;
- The cost to manufacture a framed power module has been reduced by 20%; and
- The cost to manufacture the lowest cost module has been reduced by 40%.

These cost reductions occurred while the cost of silicon feedstock increased and while the factory was running at full capacity to meet increased demand. Without this PVMaT program it is likely that the consumer's cost for PV modules would have increased instead of decreasing and that less production capacity would now be in place.

During the second half of FY 1998 Solarex began work on a new Phase 5A PVMaT program entitled "PVMaT Improvements in the Solarex PV Module Manufacturing Technology". The initial efforts in this new program are described in the remainder of this summary.

Phase 5A Objectives

The objective of this program over its three year duration is to continue the advancement of Solarex PV manufacturing technologies in order to design and implement a process, which produces polycrystalline silicon PV modules that can be sold profitably for $2.00 per peak watt or

less and which increases the production capacity of the Frederick plant to at least 25 megawatts per year. Key components of this program include:

1. Developing a process to produce silicon feedstock from commercial grade H_2SiF_6;
2. Improving the control of the casting process to increase yields and improve material quality;
3. Reducing wire saw center-to-center cut distance to less than 450µm, developing a glycol-based slurry system, and developing a method to recycle silicon carbide grit;
4. Demonstrating and implementing a cost-effective, robust cell process that produces a minimum average cell efficiency of 15% and improves the cell line electrical yield;
5. Developing and qualifying an encapsulation system that can be laminated and cured in less than 6 minutes;
6. Improving product and materials handling in three specific production line process areas;
7. Improving process measurement and control to increase yield and reduce rework; and
8. Developing and implementing a brick identification system.

Approach and Accomplishments

Silicon Feedstock Development

Solarex with subcontractor support from SiNaF Products, Inc. is developing a process to produce silicon feedstock from commercial grade H_2SiF_6. Objectives during the first year include laboratory verification of the process to produce silicon from H_2SiF_6 and design of a pilot line for the production of silicon feedstock material using the H_2SiF_6/Na process.

Initial efforts involved the design and construction of equipment for and then demonstration of a laboratory process for making SiF_4 out of H_2SiF_6. A preliminary design of the sodium reduction system has been completed and a small scale prototype is being built to demonstrate the process.

Casting

The goal of this task is to improve the control of, and optimize the Solarex casting process to increase yields and improve material quality through improvements in the definition of the salient casting parameters and implementation of a new automated casting control system.

A new PC based control system was designed and implement on one group of casting stations. Once the standard process was demonstrated, this prototype unit was modified to increase the number of operating parameters that are monitored and to automatically upload this process data to the Solarex computer network.

Wire Saw

The goals of this task are to reduce the wire saw center-to-center cut distance and to reduce the cost of the wire saw process by switching to a glycol-based slurry and by recycling the silicon carbide grit. Solarex has evaluated the performance of thinner wire from several vendors and has modified one of the wire saws by reducing the center to center pitch by 25 microns. This saw has been operating for several months with this reduced center to center spacing and the thinner wire, producing wafers with a thickness equivalent to the standard process.

A centrifuge based system for recycling of the silicon carbide grit is under evaluation. Recycled grit has successfully been used in a number of wafering runs. The next step is to obtain manufacturing scale equipment and to use this equipment to establish a viable and economic recycling procedure.

Cell Process

The goals of this task are to develop, demonstrate and implement a cost-effective, robust cell process that produces a minimum average cell efficiency of 15% and improves the cell line electrical yield. Process areas to be evaluated and optimized include aluminum paste BSF, fine-line screen printing, selective emitter, PECVD silicon nitride antireflective coating (with the assistance of MV Systems and North Carolina State University).

The selective emitter process has been used to achieve a 3% improvement in average cell efficiency. Efforts in this program involve the development of a cost effective process using methods of dopant application and rapid thermal processing (RTP). During this reporting period we developed an RTP diffusion process that yields cell efficiencies that are equivalent to the standard furnace process.

During our Phase 2B PVMaT program a cost effective, aluminum paste back surface field (BSF) process was developed and a fully automated screen print line was installed. One of the issues with this BSF process was the amount of bowing that occurs when the Al paste is fired onto thin cells. Reducing the amount of Al paste results in lower cell efficiency and lower yields due to Al bead formation. To reduce the amount of BSF material required we experimented with the addition of boron to the Al paste. The boron allowed us to duplicate cell efficiency and eliminate Al bead formation with a 25% reduction in paste thickness. However the presence of boron in the paste causes the cell to bow more than the standard Al only paste, so boron addition can help to reduce material usage, but it does not help to reduce bowing.

In the Phase 2B Final report we reported on PECVD silicon nitride work performed in conjunction with the Interuniversity Micro Electronics Center (IMEC) in Belgium. IMEC processing on Solarex polycrystalline silicon wafers resulted in cells with efficiencies in excess of 16% as measured at STC. During the Phase 5A program Solarex is working with MV Systems to develop manufacturing equipment for the deposition of PECVD silicon nitride. MV Systems has successfully demonstrated the ability to deposit PECVD silicon nitride on Solarex wafers, resulting in cells with efficiencies in excess of 15%.

Faster Cure Encapsulant

Solarex with the support of Specialized Technology Resources, Inc. (STR), is developing an encapsulation system that meets the technical and reliability requirements and can be laminated and cured in less than 6 minutes in the present Solarex laminators. STR performed an information search for alternate curative technologies and higher temperature encapsulants. The analysis indicated that the EVA system was still the most promising polymeric system for use as a PV encapsulant. STR is now evaluating several candidate cure systems versus the traditional fast-cure technology (Lupersol TBEC peroxide in EVA). Preliminary results indicate that the major issue is not being able to effect a cure in a short time, but rather being able to suppress bubble formation during a rapid curing process.

Handling

This task is expected to result in the identification of improvements in Solarex's product and materials handling (including efforts in at least 3 separate areas) to increase line yield and reduce handling labor. Solarex conducted an As-Is analysis and modeling of the production process. With the assistance of the Automation and Robotics Research Institute (ARRI) of the University of Texas at Arlington the following three handling projects were selected for development.

1. Bus bar formation: Improve the method for attaching cell strings and bringing the electrical terminations out of the module.
2. Handling of slip and ceramic pieces in the ceramics area: Reduce the amount of manual handling, which has become more important as the ceramic pieces have become larger and heavier.
3. Handling in casting to include loading and unloading of casting stations: Design and develop equipment to load and unload the casting stations.

Measurement and Control

This task is expected to result in identification of improvements in process measurement and control on the Solarex production line (including efforts in at least 3 separate areas) to improve yield and reduce rework costs. ARRI has begun development work on one of the measurement and control projects. A system has been designed and is being built to monitor the doping and diffusion process. A dedicated computer will keep track of every wafer that goes through the process as well as monitoring the doping process and the resultant emitter sheet resistance on a statistical sampling of wafers.

Solarex, with support from ARRI, is working on the development of a brick identification system. This system would provide a marker on each brick that would provide a positive identification for each wafer and subsequent cell that is made from the brick. We have successfully demonstrated the technology to laser scribe the brick with a bar code label that can be read by an ordinary bar code reader. However, we have been unsuccessful at using a bar code reader to read the code on the edges of the wafers after they have been cut from the brick. Efforts are underway to evaluate optical methods for reading the bar code marks in the edges of wafers and cells.

Conclusions

The efforts on this Phase 5A program build on the successes of the Phase 2B program. Efforts to improve the casting process control, reduce wire saw costs and increase cell efficiency build on the Phase 2B accomplishments. To these efforts have been added tasks to develop a low cost, consistent supply of silicon feedstock and a rapid cure encapsulation system. Finally efforts to improve handling and measurement and control on the production line will be critical to achieving the PV program cost goals.

Publications

1. J. Wohlgemuth, et al, "Cast Polycrystalline Silicon Photovoltaic Module Manufacturing Technology Improvements", Final Subcontract Report, July, 1998
2. J. Wohlgemuth, “Cast Polycrystalline Silicon Photovoltaic Module Manufacturing Technology Improvements", Proceedings of the NCPV Program Review Meeting, September, 1998, Denver, CO

Title: **Post-Lamination Manufacturing Process Automation for Photovoltaic Modules**

Organization: Spire Corporation, Bedford, MA
Photovoltaics Division

Contributors: M.J. Nowlan, Principal Investigator; W.G. Kurth, T.D. Harmon, J.M. Murach, W.F. Breen, T.W. McCormick, S.J. Hogan

Objective

Spire Corporation is addressing the Photovoltaic Manufacturing Technology (PVMaT) project goals of PV module cost reduction and improved PV module manufacturing process technology. New cost-effective automation processes are being developed for PV module assembly after the solar cell lamination process. Four main process areas are being addressed:

- module buffer storage and handling between steps
- module edge trimming, edge sealing, and framing
- junction box installation
- testing for module performance, high voltage isolation, and ground path continuity

Currently, the majority of PV module manufacturers do not use automation for these post-lamination processes. The development and implementation of automated systems are expected to result in significant labor cost savings, improved product quality, and increased throughput. A reduction in the occurrence of repetitive stress injuries is likely to be achieved by eliminating product lifting and manual edge trimming tasks.

Approach

The automated processes under development in this program include (1) a module buffer storage system, including conveyor load/unload and module storage, (2) an integrated edge process system, combining automated edge trimming, edge sealing, and framing capabilities, (3) a junction box installation system for attaching a junction box, and (4) an integrated module test system that combines high voltage isolation testing, ground continuity testing, and module performance testing. Proof-of-concept prototype systems will be developed and evaluated with module components from several US module manufacturers. The systems will interface with a computer network for product tracking and data acquisition.

Results in FY 1998

A survey of PV module manufacturers, in both the US and foreign countries, was completed to identify current industry practices and to determine the requirements for the automated systems being developed in this program.[1] Survey data and data gathered during site visits to module manufacturers was used to define system capabilities and specifications for post-lamination automation processes.

Top-level designs were generated for a module buffer storage system and an integrated module test system. Detailed mechanical and electrical design work is underway for the buffer storage system. Process development work is in progress for module edge trimming and edge sealing.

Buffer Storage System

Six different automated buffer storage concepts were considered for transporting and storing laminates and framed modules between process steps. The vertical stacker concept was selected for detailed design and prototype fabrication, based on the simplicity of the mechanical design, the high density of storage, and the ability to use simple mobile storage carts.

The buffer storage system, shown in Figure 1, consists of a conveyor and a vertical stacker assembly that automatically stores and retrieves laminates or framed modules between process steps. The main components of the buffer system are a conveyor for transporting modules into and out of the buffer, one or more module storage carts for holding modules in vertical stacks, and a rotating pick-and-place mechanism for transporting modules from the conveyor to the cart and back. Each cart has 51 cm (20") of vertical storage depth, equivalent to 10 framed modules with a frame height of 5.1 cm (2.0") or 100 laminates with a thickness of 5.1 mm (0.20").

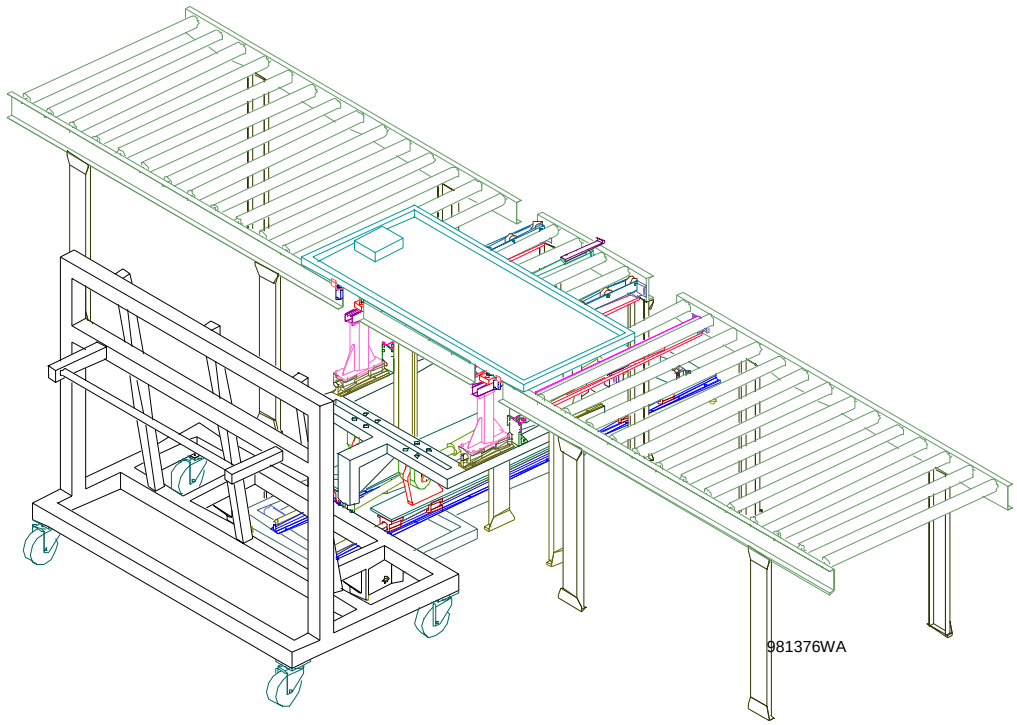

Figure 2 Automated vertical stacker buffer storage system.

Integrated Test System

A top-level design was completed for an integrated test system that combines a sun simulator for measuring module performance, a high voltage isolation tester, and a ground continuity tester. The equipment includes automation for transporting, aligning, probing, and testing modules. The system is modular, allowing the sun simulator to be separated from the high voltage isolation and ground continuity testers for process flexibility.

The integrated test system, shown in Figure 2, includes the following components:

- an in-feed conveyor with automated module alignment
- test probes and electronics for module high voltage isolation and ground path continuity tests
- a sun simulator for module performance measurements (I-V curves)
- a discharge conveyor for unloading modules
- two transport carriages that move modules from the in-feed conveyor to the sun simulator and from the simulator to the discharge conveyor

Detailed design, fabrication, and testing of the integrated test system is planned for FY 1999.

Edge Process Development

Module edge processes include edge trimming, sealing, and framing. The development of edge processes that are suitable for automation is underway at the Automation & Robotics Research Institute (ARRI), Spire's lower tier subcontractor.

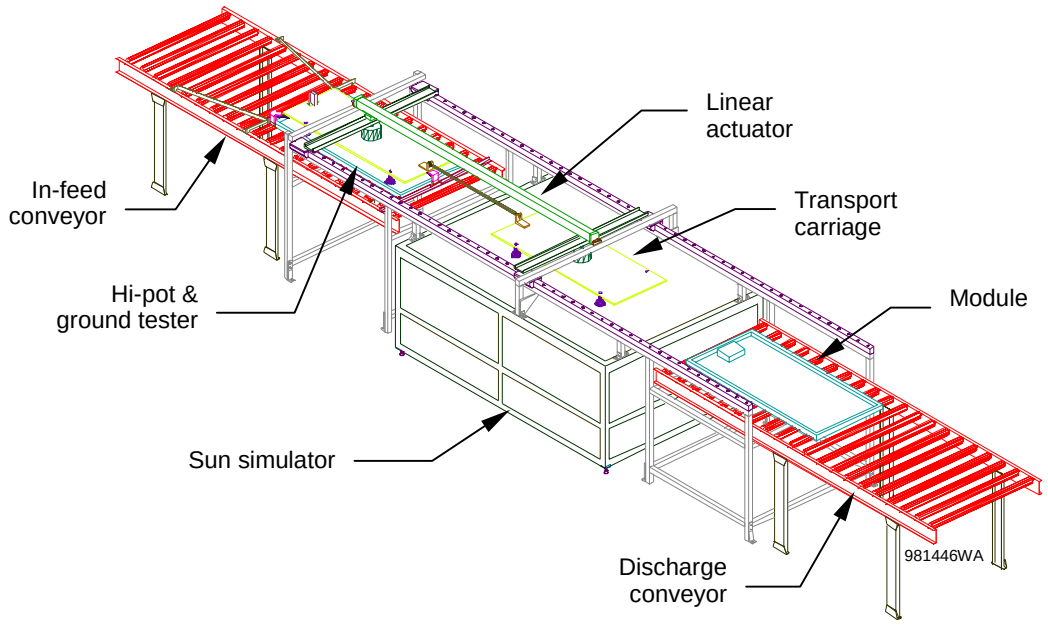

Figure 2 Integrated test system, shown with modules in 3 positions: (1) high voltage and ground tests, (2) I-V test, and (3) discharge.

Edge trimming involves cutting excess encapsulant and back cover film from module edges after lamination. Several cutting technologies are being evaluated for this application, including a spinning saw, a spinning razor, a hot knife, a hot wire, and a laser.

Module edge sealing technologies that were evaluated include applying a thick adhesive tape to the laminate edges and dispensing a bead of sealant into a frame channel. The tape method is an easy process

to implement when it is done by hand, but the material cost is relatively high. The sealant bead method has a lower materials cost but it is more difficult to implement in a manual process in terms of process consistency and labor for clean up when excess material is dispensed. Automated dispensing eliminates these problems and allows the use of lower cost materials, so the sealant bead method was selected.

Planned FY 1999 Milestones

Detailed mechanical and electrical designs will be completed and software will be developed for two prototype automation systems: module buffer storage and integrated module testing. Both systems will be fabricated, tested, and evaluated with module components from several US module manufacturers. The buffer storage system will transfer laminates or modules from a conveyor to a cart and back again, as required. The test system will align and probe modules for high voltage and ground tests, and transport laminates or modules through a sun simulator for measuring current-voltage curves. Module edge trimming, edge sealing, and framing processes that are suitable for automation will be developed and an integrated system that combines these processes will be defined.

Reference

1. M. J. Nowlan, W.G. Kurth, T.D. Harmon, T.W. McCormick, J.M. Murach, W.F. Breen, S.J. Hogan, M.R. Diver, M.I. Symko, and S.R. Rummel, "A Photovoltaic Industry Survey on Post-Lamination Module Manufacturing," *NCPV Photovoltaics Program Review; Proceedings of the 15th Conference*, Denver, CO, 1998; AIP Conference Proceedings (in press).

Title: **Advanced EVA-Based Encapsulants**

Organization: STR (formerly Springborn Laboratories, Inc.)
Enfield, Connecticut 06082

Contributors: W.H. Holley Jr., principal investigator; S. C. Agro; J.P. Galica; R.S. Yorgensen

Objectives

Yellowing of EVA-based PV encapsulants in fielded modules has been observed and well documented over the past ten to fifteen years. The purpose of this three-phase PVMaT program was to further define the problem, research possible chemical mechanisms, and then combat the yellowing phenomenon by development of advanced PV encapsulants. Findings from each phase are highlighted below.

Phase I - Further Problem Definition

This phase comprised a literature search on EVA-based encapsulant browning, survey of and site visits to installations reporting discolored encapsulant in fielded modules, and analysis of browned EVA-based encapsulant. The purpose was to better understand the parameters influencing browning and the probable chemical mechanisms involved. Findings showed that the incidence of EVA-based encapsulant browning is not limited to the modules of any one manufacturer or the encapsulant sheet provided by any one supplier.

The incidence of EVA-based encapsulant browning appears to be primarily in the West and Southwest where there is comparatively high solar insolation and higher operating temperatures.

In addition, EVA-based encapsulant browning appears to be more intense at test facilities that have a combination of high module operating temperature and high solar insolation.

Accelerated aging studies suggest that browning is not related to the EVA base resin. In particular, for one series of tests a "standard cure" A9918P encapsulant laminated between low iron glass showed significant yellowing after 17 weeks in a Xenon Arc Weather-O-Meter. While "neat" EVA resin, with no additives, showed little or no yellowing after the same exposure.

These studies also suggest that photochemistry of encapsulant browning is related to additives in the formulation, in particular Naugard P and an interaction between Lupersol 101 and Cyasorb UV-531 and not the EVA, unless the reaction products of Naugard P and Cyasorb UV-531 with Lupersol 101 are in turn involving the polymer in some way.

In a similar series of aging studies, when one additive at a time was systematically removed from A9918P, discoloration was greatly reduced. In addition, when only one additive at a time was used in Elvax 3185, discoloration was greatly diminished or eliminated. Also, when "fast cure" 15295P was substituted for A9918P in some aging samples, the rate of yellowing was reduced by a factor of approximately 2.5 after 17 weeks in the Weather-O-Meter. The reduced yellowing appears to be a result of a different chemical composition for the peroxide in 15295P, Lupersol TBEC peroxide rather than Lupersol 101, the only difference between the two types of encapsulant.

Various analyses on browned and unaged EVA-based encapsulant corroborate the findings of the laboratory aging studies. Specifically, analytical investigations by IR and Raman spectroscopy, and indirectly by TGA and XPS, show no evidence of conjugated unsaturation in the EVA polymer, which tends to discount polyene chromophores as the mechanism for encapsulant browning. However, the analyses support an interaction of additives as a cause of browning.

Notably, residual unreacted Lupersol 101 peroxide remaining after curing of A9918P significantly reduces the concentrations of stabilizing additives based on GC/FID and GC/MS. Specifically Cyasorb UV 531 concentrations suffered little reduction in concentration when a glass/encapsulant/glass laminate of A9918P without Lupersol 101 was exposed in the Weather-O-Meter for ten weeks. However, samples with the usual amount of Lupersol 101 peroxide exhibited a 40% drop in CYASORB UV-531 concentration during 12 weeks Weather-O-Meter exposure. In addition, consistent with aging studies, the latter showed significant yellowing while the former did not.

It is likely that transformation products of BHT (butylated hydroxytoluene, in the EVA resin from DuPont), Cyasorb UV 531, and nonyl phenol (from reactions of Naugard P), arising from reactions with alkoxy radicals from the photolysis of Lupersol 101 peroxide, play an important role in discoloration. As indicated before, Weather-O-Meter aging studies showed a strong correlation between color development and additive/Lupersol 101 peroxide interactions.

Phase II - Development of Stabilization Strategies

Development work, including reformulation, has resulted in four experimental encapsulants with greatly reduced browning. After 40 weeks in the Weather-O-Meter, glass/glass laminates prepared with X9903P, X9923P, X9933P and 15303P showed no visible yellowing. Yellowness index was reduced by 10 to 20 versus A9918P. Control laminates with A9918P and 15295P were a dark brown. And after 40 weeks of accelerated outdoor EMMA exposure in Phoenix at a nominal 5 U.V. suns, glass/glass laminates prepared with X9903P show no measurable yellowing.

The use of cerium oxide-containing glass, Solarphire or Solite or Solatex II greatly reduces the rate of discoloration of EVA-based A9918P and 15295P, presumably by filtering out much of the UV-B radiation (i.e., 280 to 340 nm). Thirty weeks exposure in the Weather-O-Meter of glass/15295P/glass samples with cerium-oxide containing glass produced a Yellowness Index of 5.2, undetectable by eye, and one-year exposure gave a 13 Index. By contrast, after 30 weeks exposure a 15295P control prepared with Starphire low-iron glass had a Yellowness Index of 65 and a dark brown color.

After 18 months of accelerated outdoor EMMA exposure at a nominal 5 U.V. suns, 15295P laminates prepared with cerium-containing glass had no visible color while similar samples using A9918P had almost no visible color. Versus controls, Yellowness Index was reduced by a factor of approximately 15. When samples of A9918P were evaluated with Tefzel as the superstrate, there was no discoloration during long term accelerated aging by either Weather-O-Meter or by EMMA. Presumably sufficient oxygen gets through the Tefzel to photobleach any chromophores or perhaps to inhibit their formation.

However, there was one surprise. When the experimental encapsulants were evaluated in a mini-module format, there was browning of three of the encapsulants when used under Tefzel cover film. Since there is available oxygen in these systems, we suspect, for the following reasons, that a different mechanism may be taking place than under glass superstrates: 1) Browning occurred much more rapidly than with A9918P under glass, and 2) A9918P under Tefzel showed no browning after 26 weeks which is consistent with what we observed for Tefzel/glass laminates exposed to both Weather-O-Meter and EMMA.

In our proposal for this PVMaT program, we had suggested a "family of stabilization strategies" which would be adaptable to various module constructions. While the experimental EVA-based encapsulants appear promising for modules with glass superstrates, in the case of Tefzel cover film the conventional A9918P or 15295P would be preferred.

Phase III - Full Scale Module Fabrication and Testing

The four experimental EVA-based encapsulants from Phase II were successfully prepared on a pilot scale using production equipment and the resulting sheet was used, without significant problems, by six different module producers to fabricate full-size modules. With only a couple of exceptions, curing of these modules was at a consistently high level, with average gel content greater than 83% versus a typical 80% for current EVA-based materials.

One hundred and two modules prepared with the four experimental encapsulants were subjected to IEEE 1262 qualification testing. Except for yellowing of one experimental formulation, X9933P, there was not a single failure related to the encapsulant material.

The yellowing of X9933P occurred in the modules of several manufacturers, so it was not an anomaly. However, the quality of the yellow, a bright canary yellow, was quite different from the yellowing seen in X9918P during early stages of discoloration. We suspect a different mechanism. This formulation has been dropped from serious consideration, but has been included in the modules on the two-axis tracker.

During IEEE 1262, modules were subjected to damp heat (85^{o}C/85% R.H.), thermal cycling, U.V., etc. Despite these exposures, there appeared to be little or no loss of adhesion to cells, interconnects or glass. However, on a qualitative basis, some backing film laminates showed a loss of adhesion to the encapsulant because of damp heat. These backings also developed a brown discoloration, which was traced to the adhesive/tie layer.

Finally, 36 modules, representing four different experimental encapsulants and six separate manufacturers were deployed on a two-axis tracker at the STAR facility of Arizona Public Service in Tempe. Another 12 controls modules, prepared with A9918P, were installed several months later.

These modules are being monitored and tested by personnel from the Photovoltaic Testing Laboratory of Arizona State University. After 18 months on the tracker, none of the modules has shown any discoloration or loss of power.

An expanded family of encapsulants is now commercially available in sheet form from STR for use by module manufacturers for a variety of constructions and applications. However, it is essential that module makers perform their own evaluation of these encapsulants in their module design(s) of interest.

References

W.W. Holley, S.C. Agro, (September 1998). "Advanced EVA-Based Encapsulants" Final Report, January 1993-June 1997, NREL/SR-520-25296

Title: **Development of a Fully-Integrated PV System for Residential Applications**

Organization: Utility Power Group, Los Angeles, California

Contributors: R. West, Principal Investigator; G. Fourer, W. Whalen, G. Duran, D. Metcalf, K. Mackamul and M. Stern.

Introduction

During this Phase 5A1 subcontract, Utility Power Group will address the PVMaT goals of innovative, low-cost, high-return, high-impact PV products.

UPG's approach is to solve a specific set of PV system manufacturing problems the solutions of which will immediately be passed on to the end user in the form of versatile, low cost, and high reliability roof top PV power systems. Specifically, this proposed work effort will reduce the life cycle cost of roof mounted PV power systems, improve PV power system reliability, and increase component production and system installation capacity.

Objective

The overall objective of this subcontract is to reduce the total installed cost and increase the reliability of residential roof top-mounted PV power systems. The secondary objective is to increase US system production and installation capacity. UPG is working to achieve a 30% reduction in total non-module related system costs through the development of a PV Array/Power Unit/Energy Storage Unit.

Approach

Utility Power Group (UPG) has begun to conduct parallel efforts addressing the design and testing of prototypes for each of the system elements, the PV Array, Power Unit, and Energy Storage Unit, each defined as follows:

PV Array : Includes all PV modules (either crystalline or thin-film), panels, structural support equipment and materials, dc electrical equipment and materials, and installation labor and equipment required to secure and wire the fully functional dc PV array from the roof-top to the input of the Power Unit up to 6 kWdc.

Power Unit: Includes all materials, components, and equipment required to perform all dc-ac/ac-dc power collection, conversion, and control functions from the output of the PV Array to the interconnection to utility service for power ranges from 4 - 6kW.

Energy Storage Unit: Includes a battery string, and all structural, mechanical, electrical materials and equipment required to provide a source of stored dc energy to be delivered to an input of the Power Unit. This is to be an optional "plug and play" product in which multiple units can be paralleled by the customer for additional energy storage capacity.

These efforts shall include the design, development and thorough evaluation of prototypes for each element of the integrated system, and implementing modifications as indicated in preliminary tests. A preliminary review will also be initiated with Underwriters Laboratories (UL).

PV ARRAY DEVELOPMENT

Under this task, UPG is significantly improving the current means and methods required to structurally interface PV modules to the roofs of single family residential houses and to electrically interconnect these PV modules to a power conversion unit. UPG is focusing on the design and test of a PV Array based upon the highly efficient utilization of materials and labor. Design criteria includes cost, structural integrity, electrical safety, reliability, conformance with applicable standards and building and seismic codes, and adaptability to a wide range of roof materials for both existing and retrofit roof applications.

POWER UNIT DEVELOPMENT

Under this task, UPG is designing and testing a high efficiency, low cost, high reliability prototype power conversion unit which will include all materials, components, equipment, and software required to perform all dc-ac/ac-dc power collection, conversion, and control functions between the output of the PV Array and the interconnection to the electrical grid service of single family residences. The goal of this task is to develop a Power Unit which will meet or exceed the preliminary specifications outlined in the subcontract and will conform to the draft specifications of IEEE PAR 929 and UL 1741.

ENERGY STORAGE UNIT DEVELOPMENT

Under this task, UPG is designing and testing a low cost, modular, self-contained, low maintenance, all weather, battery-based Energy Storage Unit designed to interface with the Power Unit to provide back-up electricity to supply critical household loads in the event of utility grid failure. The Energy Storage Unit will include a battery string and all structural, mechanical, and electrical materials and equipment required to provide a source of stored dc energy to be delivered to an input of the Power Unit. UPG will design this unit as a “plug and play” option in which multiple units can be easily paralleled for additional energy storage capacity or integrated with the Power Unit. The goal of this task is to develop an Energy Storage Unit which will meet or exceed the preliminary specifications outlined in the subcontract and will conform to applicable IEEE and UL Standards.

Results

UPG has made significant progress in the PV Array Structural support design, the power/control circuit design, the Power Unit electro-mechanical layout and the Energy Storage Unit electro-mechanical design.

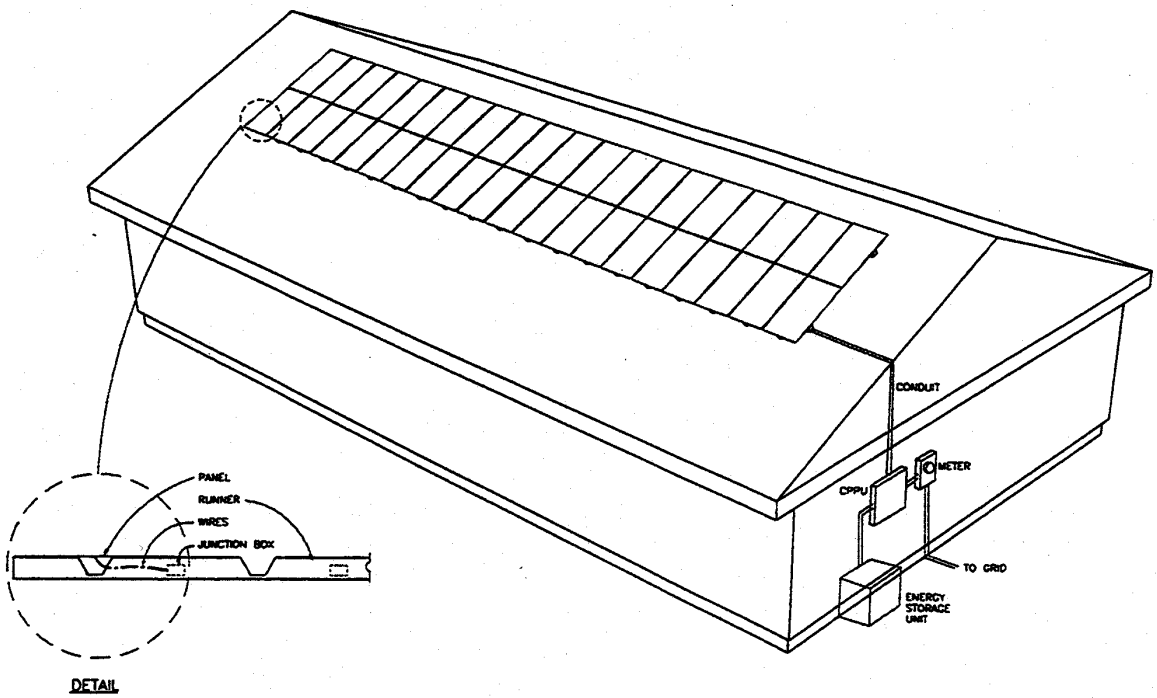

Figure 1. Residential Roof-Top Power Security System

Acknowledgment

This work was supported in part by PVMaT Phase 5A1 Subcontract No. ZAX-8-17647-02 without which the development, demonstration, and commercialization of UPG's low-cost integrated PV residential power system would not be possible.

7.0 PV Engineering and Reliability Project

7.0 PV ENGINEERING AND RELIABILITY PROJECT - Introduction

Roland L. Hulstrom

Overview and Scope

This Project's tasks and subcontracted efforts reflect a scope-of-work that includes: photovoltaic module stability/durability testing; development of environmental and accelerated tests, module failure analysis, module and system technology validation and performance testing, national and international standards and codes development, solar radiation measurements and instrumentation, and solar resource characterization. All of these project elements are critical to the successful development and commercialization of the various photovoltaic technologies. NREL's in-house and subcontracted efforts are characterized by collaborative work with the PV industry, Sandia National Laboratories, universities, and other national labs such as the National Aeronautics and Space Administration (NASA).

The PV Engineering and Reliability Project consisted of the following in-house tasks:

- **Module Testing and Technology Validation (Carl Osterwald, Task Leader)**
- **Module Accelerated Testing and Failure Analysis (John Pern, Task Leader)**
- **Photovoltaic System Performance and Standards (Dick DeBlasio, Task Leader)**
- **Photovoltaic Solar Radiometric Measurements and Evaluation (Daryl Myers, Task Leader)**
- **Solar Resource Characterization (Dave Renné, Task Leader)**

These in-house tasks were supplemented with the following subcontracts:

- The Design and Construction of a Custom-made PV Encapsulant and Solar Cell Degradation Monitor. University of Colorado at Denver, Center for Environmental Sciences, Jeffrey A. Boon, Principal Investigator
- Development of Test Methods and Procedures for Evaluation of PV Systems. NEOS Corp., Terry Schyuler, Principal Investigator
- PV Certification and Accreditation Management Support. PowerMark Corp., Steve Chalmers, Executive Director
- Management and Administration of the International Electrotechnical Commission/Technical Committee 82. Solar Energy Industries Association, Jerry Anderson, Principal Investigator
- Solar Resource Analysis from the Pacific NW Network. University of Oregon, Dr. Frank Vignola, Principal Investigator

- Combining Satellite and Surface Solar Radiation Data, SUNY/Albany, Dr. Richard Perez, Principal Investigator

- Technical Support to Solar Resource Assessments. Dr. Gene Maxwell, Principal Investigator

Objectives and Accomplishments

This project annual report contains detailed descriptions of the FY 1998 objectives, technical approaches, and results of each of the in-house and subcontracted project elements. The following paragraphs present the multi-year objectives of this project and the key accomplishments of the FY 1998.

Objectives

- Develop and implement advanced photovoltaic module and system screening, durability, reliability, and performance characterization capabilities and test methods to help advance and validate the photovoltaic technology options, devices and prototype products.

- Conduct, in collaboration with the PV industry, exploratory environmental stress and accelerated weathering tests on PV devices (mini-modules and modules) to discover and characterize failure mechanisms and/or performance stability shortcomings. Investigate, document, and help the PV industry mitigate failure mechanisms and/or performance stability shortcomings at the prototype stage of product development.

- Address PV system, subsystem, and component technical and infrastructure issues and provide solutions that accelerate PV technology readiness and commercialization. Specific objectives are to provide engineering solutions and approaches that will reduce technical barriers to commercialization and advance photovoltaic system, subsystem, and component performance, safety, and quality.

- Provide the PV industry and NREL PV research activities with appropriate, accurate radiometric data and measurements that are critical to evaluating PV device, module, and system performance. Develop and utilize solar radiation instrumentation, models and databases, as required by PV technology development and deployment.

- Develop and disseminate key information on solar energy resources to the U.S. industry and to energy planners in order to facilitate and accelerate the deployment of their technologies domestically and world-wide.

- Lead and support the PV industry's efforts to develop, maintain, and implement national and international PV module and/or system standards and codes for design, performance, safety, and quality.

Major Accomplishments

The major accomplishments for the PV Engineering and Reliability Project during FY 1998 are listed below:

- Published 34 journal articles, conference papers, and technical reports on various topics of photovoltaic engineering and reliability.

- Over 50 PV modules of various technologies were tested both indoors under controlled conditions and outdoors under prevailing conditions to help industry determine their performance and stability characteristics.

- Over 30 PV modules were tested both indoors and outdoors under accelerated environmental stress conditions to help industry determine their reliability/durability characteristics.

- Completed a "users manual" for module reliability database. The database was developed with system users and covers anomalies, failure modes, and causes of failure in PV modules and systems.

- Led the CdTe Reliability Team and completed a report on back contact screening tests.

- Planned and began implementing validation work on module energy ratings procedure. A detailed technical report on the modeling procedure will be written in FY99.

- Expanded module energy ratings testbed (PERT 2 and 3). The testbed can now measure 45 individual modules.

- Conducted materials/devices characterization, designed experiment conditions, and performed various AET studies and EVA/data analyses requested by six PV companies.

- Developed an accelerated weathering test protocol that was submitted in a 40-page summary report. The report consisted of a comprehensive documentation of literature and technical approach to reach the AWT protocol. The AWT protocol includes experimentally tested and validated operation parameters of I (irradiance), T (temperature), %RH (relative humidity), water sprays, test cycles, and duration that are considered relatively more realistic for studying degradation of materials and devices.

- Enhanced PV mini-module testing capabilities by acquiring a jar-mill for making NREL-developed EVA formulation, a PC-controlled electrochemical workstation and software.. The PC and operating software for the SPEX fluorescence spectrophotometer and the CPU and operating software for the Ci4000 weatherometers were upgraded.

- Completed interim draft PV systems performance test procedure and published as an NREL technical report, *"Interim Test Methods and Procedures for Determining the Performance of Small PV Systems,"* NREL/TP-520-25077.

- Conducted exploratory and outdoor performance testing of eight PV systems currently installed at the NREL Outdoor Test Facility (OTF) and installed six new systems for test.

- Announced the reorganization and expanded scope of the IEEE SCC21 to include Fuel Cells, Photovoltaics, Dispersed Generation, and Energy Storage.

- Conducted the annual PV Performance and Reliability workshop sponsored by NREL and SNL. This year's workshop was hosted by FSEC on November 3-5, 1998, in Cocoa Beach, Florida. More than 100 participants attended the 3-day meeting, which included more than 25 presentations. Emphasis was on the reliability of PV arrays, systems, BOS, and PVBONUS activities.

- Enhanced PV system testing capabilities by completing the validation and calibration of the small system flexible testbed and conducted small system performance characterization tests by validating newly developed test procedures.

- Reduced NREL spectral calibration uncertainty by 50%, improving NREL's ability to characterize spectral effects on PV device and module performance.

- Calibrated and characterized 49 radiometric sensors, systems, and light sources used to evaluate PV device, module, and system performance for NREL researchers and industrial partners.

- Disseminated PV related solar radiometric information in response to over 180 documented PV industry and internal NREL requests for measurements, data, sensors, solar simulator design, resource data, rating conditions, instrumentation calibration and measurement techniques.

- Continued work in using satellites for determining solar resources at any location on earth and produced a draft report on the activities.

- Upgraded Renewable Resource Data Center (RReDC) internet page to include spectral solar data, selected solar radiation and cloud cover maps, and Cooperative Network for Renewable Resource Measurements (CONFRRM) home page.

PV Engineering and Reliability Project In-House Research

Title: **Accelerated Weathering Evaluation of Materials Stability and Performance Degradation for Encapsulated PV Cells and Minimodules**

Organization: Engineering and Reliability Division, National Center for Photovoltaics (NCPV) National Renewable Energy Laboratory (NREL), Golden, CO

Contributors: F. J. Pern (Task Leader), A. W. Czanderna, S. H. Glick, D. E. King, R. Pitts

[*Abbreviated Keywords:* **AET:** Accelerated exposure test; **AWT:** Accelerated weathering test; **EVA:** Ethylene-vinyl acetate; **IS:** Impedance spectroscopy; **HFSF:** High flux solar furnace; **WOM:** Weatherometer]

Objectives

The Long-Term Task Goals are (1) to develop improved or new encapsulation materials and methods that offer greater promise for a module life expectancy of 30 years or more, (2) to establish a sound base of methodologies for cell encapsulation, testing, data analysis, and correlation that can be utilized as guidance and/or references for scalability issues by PV industries, (3) to develop and use accelerated testing methodologies to investigate material reliability problems that can affect and degrade the performance of encapsulated solar cells and minimodules, and (4) to identify, understand, and then mitigate/improve at molecular or fundamental chemical/physical levels the causes of changes in module materials that alter crucial material properties and reduce the performance and/or limit the service life of PV modules.

The Principal Purposes of this Task are (a) to develop and establish adequate accelerated exposure/weathering testing (AET/AWT) methodologies for investigating the photothermal stability of various encapsulation materials, the effects of processing methods, and their potential applications to PV modules, (b) to identify by AET/AWT deficiencies in materials, interfaces, and PV encapsulation methods, and (c) to mitigate the causes of degradation that may reduce or compromise the performance of encapsulated solar cells and minimodules for a service life in excess of 30 years.

The FY1998 Task Objectives were (1) to prepare, study, and verify experimentally improved or new encapsulation materials, designs or processing, fabrication, and construction methods that will extend module lifetime; (2) to establish and test a working AWT protocol for the reliability/durability testing of PV cells/minimodules; (3) to establish a procedural protocol for developing, processing, testing, and characterization of encapsulants and encapsulated solar cells; (4) to continue exploring the use of NREL's HFSF for AWT of module component materials; (5) to continue the study to verify IS as a non-invasive analytical method for diagnosis of materials degradation in encapsulated solar cells and minimodules; (6) to assist or collaborate with the PV industry and community by providing expert advice or AET/AWT studies; and (7) to accomplish technology transfer through presentations at professional meetings, publications of research results, and licensing of patents of the technology or materials developed.

Technical Approach

The goal of the task design is to identify and separate degradation mechanisms that may be induced by UV, temperature, humidity, materials (superstrate and substrate), and interfacial effects, resulting in undesirable changes in the optical, electrical, and mechanical properties of encapsulant, adhesion, metallic components, and solar cells. The degradation mechanisms that are identified can be used to assist in selecting new or modified materials options. The degradation mechanisms and AET results will eventually be used to project module service lifetime.

To validate the performance of NREL-developed EVA encapsulant formulations, a prior method of making target films by casting organic solutions was upgraded by using a solid state method. A jarmill was acquired, installed, and used to blend pellets of Elvax 150^{TM} base resin with new stabilizers and a curing agent. The compounded pellets were extruded into films of a specified thickness using a lab-scale mini-extruder. To verify the photothermal stability of the NREL-developed EVA formulations in comparison with the two commonly used commercial formulations (A9918 and 15295), the extruded NREL-EVA films and the commercial EVA films were laminated and cured separately. Specific curing process conditions were used to accomplish the lamination between two 1/8"-thick borosilicate glass plates. Samples of a new polyolefin-based thermoplastic pottant laminated in the same way were also provided by Evergreen Solar for parallel AET studies with the commercial EVA 15295.

The phtotothermal stability of monocrystalline and amorphous silicon (c-Si, a-Si) solar cells and the effects of various superstrates and substrates were also tested. A sample set of 24 3-cm x 3-cm c-Si cells was encapsulated with commercial EVA films between two borosilicate plates. Eight c-Si solar cells of the same size were laminated between two polymer films, Tedlar or Tefzel, with two pottant adhesives, as provided by Spire. Four a-Si minimodules were laminated with four different types of superstrate films and pottant adhesives, as provided by Iowa Thin Film.

The pottant laminates and/or c-Si/a-Si cell laminates were subjected to AET in separated groups to one of the five different AET conditions provided by using (1) a full-spectrum solar simulator (FS-SS) of ~9.0 UV suns at a black panel temperature (BPT) of ~145^{o}C, (2) an enhanced UV solar simulator (UV-SS) of ~7.5 UV suns at BPT~85^{o}C, three DSET CPS tabletop systems of ~1 UV sun at (3) 60-65^{o}C or (4) 80-85^{o}C, and (5) an oven heated at 85^{o}C. The photothermal stability of the laminates was characterized periodically by fluorescence analysis, UV-vis, color spectrophotometry, and light/dark current-voltage (I-V) measurements before, during, and after testing. Some glass/c-Si/glass laminates were additionally characterized with impedance spectroscopy (IS) analysis and scanning laser optical beam induced current (OBIC) mapping. The purpose of combining the spectrophotometric, IS, and I-V measurements was to form a basis for quantifying solar cell degradation from AET in an effort to establish a data correlation methodology for the optical and electrical results.

The design of a large-scale matrix experiment was completed with revisions to respond to the availability of materials and FTEs. To prepare for this large-scale matrix experiment, lamination process control details and spacers for various encapsulation configurations were carefully studied and fabricated. A great deal of effort was invested in the preparation of over 350 encapsulated c-Si solar cells with different superstrates, encapsulants, and substrates. A comprehensive study of present ASTM/ISO/IEEE/SAE standards for AET/AWT, climatographic data of hot-dry and hot-humid regions, and in-depth analysis of experimental results from previous EVA discoloration studies was performed over a period of two years. A matrix of operation variables was thoroughly tested on two Ci4000 weatherometers to determine system-achievable parameters (i.e., light intensity, temperature, relative humidity, and on-off cycle control) for the AWT needs. The above studies and results were used to construct the AWT Protocol, which was a Task Milestone and Deliverable.

NREL's unique HFSF was employed to perform AET for EVA laminated between two borosilicate plates with or without an embedded c-Si solar cell. The investigation of solarization of Ce-containing glasses using the HFSF, a weatherometer, and outdoor exposure was conducted to determine if the glasses would lose Ce^{3+} from the highly accelerated light exposure at controlled temperatures. The accumulated irradiance from these three exposure conditions was

correlated by using polystyrene dosimetric coupons. The samples tested with the HFSF were submerged in a cooling water flow inside a custom-built exposure chamber.

Multiple on-site visits were conducted to supervise the performance of a subcontract for fabricating a prototype, portable spectrophotometric and I-V analyzer (a degradation monitor). The purpose of the subcontract was to reduce to practice an invention disclosure (NREL IR#95-10) for such a unit.

To assist or collaborate with PV industry, we engaged in multiple discussions with several PV manufacturers (most of them were also PVMaT Program subcontractors) and made arrangements for AET studies (see above) as well as EVA encapsulation of thin film PV specimens.

Results

1. AET Studies of Encapsulation Materials and Methods (milestone met)

(a) Materials/Devices Characterization and Degradation Mechanisms. We have experimentally established the superior photothermal stability of NREL-developed EVA formulations. The results of various AET studies for the differently encapsulated c-Si solar cells and encapsulant materials were summarized and presented at the 15th NCPV PV Program Review Meeting, Sept., 1998. The results, derived from transmittance, color index, fluorescence, light and dark I-V, and impedance spectroscopic measurements, showed irregular changes in I-V parameters of c-Si and a-Si solar cells upon AET treatments that cannot be simply accounted for by optical transmittance changes. More studies will be conducted to further the investigation in the matrix experiments. **(b). Matrix Experiment.** Assisted by two part-time leased workers, more than 350 samples of differently encapsulated c-Si solar cells and other laminates have now been prepared. The experimental work was prioritized into four sets. Baseline characterization for the first sample set (AET-Set #1) was made with transmittance, color indices, dark and light I-V measurements. The initial fluorescence, adhesion strength measurements, and scanning laser OBIC will also be performed for some selected samples. The AET-Set #1 samples will be exposed in the Ci4000 weatherometers using a previously established AWT protocol. After more than a one-year delay by Atlas, we received the 150 custom-designed sample holders needed for the experiment. **(c). EVA-Browning Pattern Experiment.** Because of the non-uniform EVA browning patterns observed in (a), we have designed a new critical experiment with the following objectives: (1) to investigate the causes or mechanisms of abnormal browning patterns, to determine the effect of O_2 diffusion, (2) to determine the activation energies of EVA/Si cell photothermal degradation, and (3) to determine the upper limit of the acceleration factor from concentrated UV light intensity and elevated temperatures that can duplicate more uniform EVA browning patterns as observed on field-weathered PV modules.

2. Accelerated Weathering Test (AWT) Protocol (Milestone met)

The AWT Protocol was submitted in a 40-page summary report including14 tables and 10 figures as scheduled Task Milestone and Deliverable. The report consisted of a comprehensive documentation of literature and technical approach to reach the AWT protocol. The exposure protocol will be implemented primarily on two Atlas Ci4000 weatherometers in the AET studies of the matrix experiment samples. The test conditions need to realistically simulate natural weathering conditions. No adequate, prior AWT test standards are available in the ASTM/ISO literature for our purposes. The AWT protocol includes experimentally tested and validated operation parameters of I (irradiance), T (temperature), %RH (relative humidity), water sprays, test cycles, and duration that are considered relatively more realistic for studying degradation of materials and devices.

3. Application of the HFSF for Highly Accelerated Testing (Milestone met)

The Ce-containing glass plates were tested at 2000 suns for upto 30 h exposure. Spectral degradation on the HFSF reflector was discovered in the course of this study. After calibration, the actual exposure irradiance was determined to represent a 6 y UV equivalent. The results indicate that solarization of Ce-glass was saturated rapidly without further photochemical degradation as was suggested by industry. The results are in good agreement with those obtained in previous in-door AET studies using 5~9 UV suns in solar simulators. Experience was gained in the testing of glass/glass laminated EVA and c-Si solar cell, which indicates that considerably lower sunlight concentration (< 200 suns) are needed to avoid thermal breaking of the glass plate or c-Si solar cells. The photon doses for the various AET conditions were determined and correlated with polystyrene dosimetric coupons. The results from this study were also reported at the 15th NCPV Program Review Meeting. More experimental work as well as a new chamber design in which test samples will not be submerged in cooling water are needed to effectively utilize the potential of the HFSF.

4. Subcontract for Fabricating a Prototype Portable Spectrophotometric and I-V Analyzer

The subcontract was terminated at the end of September 1998. The subcontractor, a group at the University of Colorado at Denver, began the work in April 1996 with an 18-month performance period; the work was continued under a no-cost extension. Because of technical difficulties, the analyzer system was not completely functional as specified on the SOW. The final report and the system have not been delivered as of 12/11/98.

5. Enhanced and Upgraded Laboratory Capabilities

A jar-mill for making NREL-developed EVA formulation, a PC-controlled electrochemical workstation and software were acquired. The PC and operating software for the SPEX fluorescence spectrophotometer and the CPU and operating software for the Ci4000 weatherometers were upgraded.

6. Technology Transfer

Through NREL's Technology Transfer Office and Legal Office, we engaged in multiple meetings and discussions with several EVA and adhesive manufacturers about the potential licensing agreements for the NREL-developed EVA, which is a subject of on-going patent application. A CRADA agreement was reached with Rohm and Haas Company to study new polyacrylic polymers as potential candidate pottant. Task team members also participated in several conferences, presented a number of PV-related technical papers, and interacted extensively with PV industry or community personnel.

7. Partnership with SNL, the PV Industry, Academic Institutions, and Work-for-Others

Task members participated in a MDRC project meeting at FSEC, Cocoa, FL, at which the module reliability, EVA browning, and adhesion issues were discussed, and provided expert-advice and technical assistance (including mailing of reprints/preprints) to a number of PV manufacturers, companies, universities, and foreign research groups on EVA, encapsulation, and AET issues. The Task also initiated/submitted a Proposal for forming a PV Module Encapsulation (or Service Life) Team in an effort to build a stronger partnership with other national laboratories, the PV industry, and academic institutions. Without an increase in the FTE and funding level, the Task still promptly responded to, designed experiment conditions, and performed various AET studies and EVA/data analyses requested by several PV companies:

1. EVA gel content analysis for Solarex [PVMaT]; (completed)
2. AET for Spire's specially polymer/polymer films encapsulated c-Si cells; (completed)
3. AET for Evergreen Solar's new encapsulant [PVMaT]; (completed)
4. AET for Iowa Thin Films' a-Si minimodules; (completed)

5. EVA encapsulation of flexible $CuInSe_2$ thin film samples for ITN Energy Systems
6. Gel content/UVA analysis and AET for Russian Sovlux EVA [CRADA]; (presently on-going)

PV Task-Related Publications and Conference Presentations by Task Members in FY1998

1. A. L. Rosenthal, A. W. Czanderna, and F. J. Pern, "Performance Losses in Rooftop-Mounted PV Modules from Long-Term Environmental Exposure at Las Cruces, New Mexico." Presented at the 15th NCPV PV Program Review meeting, Sept., 1998.

2. J. R. Pitts, C. Bingham, and D. E. King, "Ultra-Accelerated Testing of PV Module Components." *ibid*.

3. A. Meier, S. H. Glick, and F. J. Pern, "Impedance Spectroscopy as a Non-Invasive Analytical Method for Monitoring Solar Cell Degradation." *Ibid.*

4. F. J. Pern and S. H. Glick, "Accelerated Exposure Tests of Encapsulated Si Solar Cells and Encapsulation Materials." *ibid*.

5. F. J. Pern, S. H. Glick, and A. W. Czanderna, "Review of the Photothermal Stability of EVA Pottants: Effects of Formulation on the Discoloration rate and Mitigation Methods." *ibid*.

6. F. J. Pern, "Degradation and Discoloration Mechanisms of EVA Copolymer for Photovoltaic Module Encapsulation," Conf. Proc. of "Polymer Stabilizers and Modifiers '98: Conference & Exhibit," March 2-4, 1998, Hilton Head Island, So. Carolina, pp. 153-168. (**Invited paper**)

7. S. H. Glick and F. J. Pern, "Studies of Browning Patterns in Laminated EVA Encapsulants under Accelerated Exposures," Abstract No. 203, Luminescence Symposium, 40th Rocky Mountain Conference on Analytical Chemistry, July 25–Aug. 1, 1998, Denver, CO.

8. D. E. King, F, J. Pern, J. R. Pitts, C. E. Bingham, and A. W. Czanderna, "Optical Changes in Cerium-Containing Glass as a Result of Accelerated Exposure Testing," Proc. 26th IEEE PVSC, 1997, pp. 1117-1120.

9. F. J. Pern and S. H. Glick, "Improved Photostability of NREL-Developed EVA Pottant Formulations for PV Module Encapsulation," Proc. 26th IEEE PVSC, 1997, pp. 1089-1092.

10. F. J. Pern, "Ethylene-Vinyl Acetate (EVA) Encapsulants for PV Modules: Degradation and Discoloration Mechanisms and Formulation Modifications for Improved Photostability," Die Angew. Makromol. Chemie, 252 (1997) 195-216. (**Invited paper** at the 19th Annual International Conference on Advances in the Stabilization and Degradation of Polymers, Luzern, Switzerland, June 9-11, 1997)

Title: **Module Testing and Technology Validation**

Organization: Engineering and Reliability Division, National Center for Photovoltaics (NCPV), National Renewable Energy Laboratory (NREL), Golden CO

Contributors: Carl Osterwald (Task Leader), Tom Basso, Joe del Cueto, Tom McMahon, Bill Marion, Jim Pruett, Dave Trudell

Objectives
The objectives of this task are to help U.S. module manufacturers develop cost-effective products with 30-year service lifetimes, and to facilitate their use in commercial PV systems. A specific goal is to characterize and improve the performance and reliability of PV modules through applied R&D efforts that are closely coupled with the needs of U.S. manufacturers.

Technical Approach
The task was to perform work in the following three areas: module testing and technology validation, module accelerated/environmental stress testing, and module failure analyses.

Considerable efforts were to be applied in developing and performing screening and exploratory tests (performance, stress, environmental) on DOE subcontract deliverables (e.g. PVMaT, Thin-Film PV Partnership), R&D prototypes, as well as commercially available modules. A concerted effort was made to complete the development and validation of new methods for rating PV modules based on energy production (energy rating) rather than on power at a specified test condition.

Module reliability/durability efforts included a variety of activities, all closely coupled with U.S. module manufacturers. Specifically, accelerated and environmental stress testing using a variety of test equipment were conducted on emerging module technologies obtained through DOE subcontract deliverables in order to identify potential performance and reliability problems. The stress testing was closely tied to and complemented by the failure analysis expertise and capabilities at NREL and SNL. In support of IEEE 1262 module qualification test standards, a long-term ultraviolet (UV) exposure test of commercial modules was initiated at NREL using five different solar and simulated UV light sources. Finally, a cooperative effort with PV system users has resulted in the assembly of a reliability database related to anomalies, failure modes, and causes of failure in modules and PV systems. An initial "user's manual" for the database was published.

A number of capabilities at NREL are used for these efforts, including real-time and accelerated outdoor exposure, indoor light-soaking and exposure, a high-voltage outdoor stress testbed, module mechanical and insulation integrity testing, and failure analysis.

Real-time outdoor exposure is performed in latitude-tilt (40°) racks at the Outdoor Test Facility (OTF). Exposure durations are measured with ultraviolet (UV) and total radiation instrumentation that are part of the Reference Meteorological and Irradiance System (RMIS). Such testing is used for several purposes, including module qualification testing such as Institute of Electrical and Electronics Engineers (IEEE) standard 1262 and long-term outdoor exposure of modules identical to those installed in arrays at the Photovoltaics for Utility Scale Applications (PVUSA) site near Davis, CA. Outdoor testing also includes the Power and Energy Ratings Testbeds (PERT), which measure complete module current-voltage (I-V) curves every 0.5 h. These results are time-integrated to obtain the daily module energy production throughout the year of a collection of commercial and prototype modules. The PERT results are used to support the module energy ratings development efforts.

A facility called the Outdoor Accelerated-weathering Test System (OATS) is used to accelerate outdoor exposure of modules in natural sunlight. This system has two 2 m × 2 m test planes on a two-axis solar tracker, with solar concentration up to 3× provided by flat rectangular mirrors. Cooling of samples can be performed by forced ambient air, and periodic spray cycles for climate

simulation are also available. The OATS facility has been in continuous operation since November 1997.

Five indoor systems are used for environmental stress testing; four of these can also provide illumination during test sequences. An Atlas XR260 Large Component Xenon Exposure System can attain 2.5-sun (2500 W) levels on modules as large as 1.5 m × 0.75 m, and a Vortek 20 kW argon arc lamp installed in a Tenney Inc. environmental chamber can also illuminate large modules. One-sun metal-halide illumination is available in an Atlas SolarClimatic 1600. Finally, two BMA Inc. environmental chambers, 0.9 m^3 and 2.2 m^3 in volume, are used for stress testing without illumination, although the larger chamber can be fitted with rows of fluorescent tubes for UV exposure testing.

The new high-voltage testbed is an outdoor stress test that applies high DC voltages between module output leads and the grounding points. The purpose is to accelerate stresses that may occur when modules are installed in larger systems, such as electric-field-induced corrosion and degradation of module insulation. Voltages of up to 3 kV and both polarities are available, and the system logs leakage currents, air temperature, and relative humidity every 2 min.

Other IEEE 1262 tests performed at the OTF include the 2400 Pa static load test; the 10,000 cycle, 1440 Pa cyclic load test; the ice ball impact test; and the mounting twist test. The static load test simulates steady wind loads on both surfaces, whereas the cyclic load test simulates dynamic wind flexing. Effects of mounting modules onto non-planar surfaces are simulated by the twist test. Electrical insulation integrity tests include dry hi-pot (0.5 – 3 kV) and insulation resistance measurements. Both of these can also be performed on modules immersed in water.

Efforts are made to ascertain the causes of visual anomalies and performance losses on modules that have undergone stress and exposure testing through failure analysis. Before-test and after-test formal visual inspections, including photography and image analysis, are made to locate and document visible changes. These are combined with nondestructive determinations of cell internal shunt and series resistances and hot spots, and with numerical analyses and modeling of current-voltage curves. If necessary, destructive analyses such as de-encapsulation (through coring or delamination) can be used to isolate problems and allow chemical composition measurements. Finally, if possible, results from failure analyses are used to recommend corrective actions and develop stress tests that reproduce failures.

As the team leader for the CdTe Reliability team of the Thin Film Partnership, we guided several aspects of this program. These included the accelerated life prediction and reliability work and the back contact screening testing. The failure mode of great concern for CdTe cells is the appearance of a non-ohmic reverse diode, and much of the team's efforts were directed at this problem.

Progress on Research Tasks

More than 40 modules of various technologies are being exposed outdoors. Data collected on these modules are used to show performance and reliability over time, and are reported to the corresponding manufacturer. The PERT facility was expanded to triple the previous capacity and can now provided real-time I-V curves for up to 45 modules. This expansion included the installation of two additional data acquisition systems; one of these allows modules with open-circuit voltages up to 240 V to be monitored. Currently, data is being collected on a total of 26 modules. The high-voltage stress test currently has four modules (two a-Si and two crystalline Si) under test at 600 Vdc and at both positive and negative polarities. 24-h per day leakage current and meteorological data are stored for analysis and development of accelerated test criteria.

NREL has sponsored a series of a-Si stability testing programs that have tried to determine the performance of modules after the initial light-induced degradation has occurred. These programs have used the Vortek argon arc light source to provide continuous illumination while the module temperatures are controlled inside an environmental chamber. The most recent of these, Light Soak 4, contained eleven modules from five manufacturers and totaled 5000 h of 1-sun exposure,

at various temperatures. An initial stabilization period of 2000 h was followed by two cycles totaling 1500 h. Each cycle consisted of 1000 h at 25°C module temperature (cold-soak) followed by 500 h at 50°C (warm-soak). The cycled light-soaking showed that performance decreases during the cold periods and increases during the warm ones. This behavior was qualitatively similar in all the modules tested, which suggests that the phenomena observed are controlled by fundamental a-Si properties. It is also consistent with annual variations observed for a-Si modules deployed in climates that have significant temperature variations between winter and summer. These results have led to the conclusion that summer-winter performance variations in a-Si modules are caused by seasonal temperature fluctuations rather than by spectral changes.

Exploratory qualification testing, similar to the IEEE 1262 sequence, was performed on a second set of prototype a-Si modules manufactured by Sovlux in Moscow, Russia, under a cooperative research agreement with Energy Conversion Devices (ECD). These 32 W modules are similar to ECD designs. Results of the testing showed dramatic improvements in reliability in the second set as compared to the first, and uncovered the inadvertent use of an incorrect backsheet material. Exploratory IEEE 1262 qualification testing was also performed on a set of light-weight polymer-substrate a-Si modules manufactured by Iowa Thin Film Technologies and some Siemens Solar 5W CIGSS modules.

The long-term UV exposure test has been initiated. Six different types of crystalline and amorphous Si commercial modules are being exposed using five methods—two indoor and three outdoor. During exposure, all modules have fixed resistive loads. The length of the test is determined by the time needed to accumulate a total UV dosage (integrated total irradiance below 400 nm) of 2000 MJ/m^2, or until failure. For this test, failure is defined as 25% of initial output power. The indoor light sources used are xenon arc in the Atlas XR260 and UVA fluorescent tubes. Real-time outdoor UV exposure is done in the latitude-tilt racks, whereas accelerated exposure uses the OATS weathering system. One OATS test plane has mirror enhancement, while the second test plane has no enhancement. Therefore, two acceleration factors are obtained. Currently, exposure totals for the five methods are: xenon, 355 MJ/m^2; UVA fluorescent tubes, 54 MJ/m^2; real-time outdoor, 254 MJ/m^2; accelerated outdoor with two-axis tracking, 325 MJ/m^2; and accelerated outdoor with mirror enhancement, 546 MJ/m^2. No modules have failed, and performance losses in the amorphous silicon modules are comparable to those expected for a-Si light-induced losses.

A total of five internal test reports detailing individual indoor and outdoor module exposure tests were written and distributed to the particular module manufacturers.

For use with the energy ratings development work, the ASTM E 1036-96 model for determining the electrical performance of PV modules was examined and improvements were made in three areas: (1) determination of temperature coefficients, (2) translation equations, and (3) accommodation for changes in fill factor. The revised model gave good agreement with measured data for the period January 1998 through June 1998 for six modules located at the OTF that represent different PV technologies. Other models in the energy rating methodology used to estimate module temperature and irradiance were also shown to give good agreement with measured values. These results were presented at the IEEE SCC21 PAR 1479 Energy Rating Working Group Meeting conducted at Winter Park, CO in July, 1998.

As the CdTe Reliability Team Leader for the Thin Film Partnership we guide the program for accelerated life prediction and reliability. A summary report for two years of progress on the CdTe Reliability Team back contact screening testing was written. This testing included using our newly developed, small laser spot, internal series resistance technique to evaluate Si, a-Si, CIS, and CdTe internal resistances. Accelerated screening tests conducted on CdTe cells with different back contact recipes were evaluated and used to calculate life predictions for these cells. Device modeling software (AMPS and PSPICE) was used to analyze device degradation behavior. Initial activation plots of time-to-failure suggest that under the worst conditions at open circuit at Edwards AFB, the expected life may be only three years for a 25% decrease in performance. The predicted decrease of 12.4 % between the end of the first summer and the end of the third summer has been recently measured establishing a correlation of AETs with field

exposure. The summary paper (with Gary Jorgensen) told how to predict the loss in module performance that was verified with field measurements performed by David King of SNL.

We diagnosed module shunt problems as an activity under the Solarex CRADA with personnel at the Toano a-Si plant. Module power and line yields had been very poor because of shunting along the tin oxide laser scribes, associated with the ZnO process used in their back contact. Solarex had a solution that helped this problem, but it slowed down the process considerably. With our help, they were able to introduce a new process that succeeded in controlling the shunt problem with minimal effect on process throughput. This collaboration with Solarex resulted in an additional passivation layer in their tandem structure.

Some special cell and module characterization techniques, glass conductivity measurements as a function of temperature, were developed to support the field wet insulation resistance tests of Chuck Whitaker (PVUSA) and the wet hi-pot stress failures observed at Solarex on a-Si modules. Different glass materials are being evaluated for bulk and surface conductivity.

Publications

C.R. Osterwald, T.S. Basso, J.A. del Cueto, T.J. McMahon, J. Pruett, and D. Trudell, "Accelerated and Environmental Module Stress Testing at NREL," Proceedings the NCPV Program Review Meeting, American Institute of Physics, 1998 (in press).

J.A. del Cueto, "Guide to the Field Performance of c-Si PV Modules," Proceedings the NCPV Program Review Meeting, American Institute of Physics, 1998 (in press).

T.S. Basso, "The NREL Outdoor Accelerated-Weathering Tracking System and Photovoltaic Module Exposure Results," Proceedings the NCPV Program Review Meeting, American Institute of Physics, 1998 (in press).

T.J. McMahon and G.J. Jorgensen, "Progress Toward a CdTe Life Prediction," Proceedings the NCPV Program Review Meeting, American Institute of Physics, 1998 (in press).

T.S. Basso, "User Manual for the Photovoltaic (PV) Technology PV Module Reliability Database," internal report distributed to NREL NCPV staff.

J.A. del Cueto, "Method for Analyzing Series Resistance and Diode Quality Factors from Field Data of Photovoltaic Modules," Solar Energy Materials and Solar Cells, v. 55, pp. 291-297, 1998.

J.A. del Cueto, "Review of the Field Performance of One Cadmium Telluride Module," Progress in Photovoltaics, 1998 (in press).

J.A. del Cueto and B. von Roedern, "Temperature-Induced Changes in the Performance of Amorphous Silicon Multi-Junction Modules in Controlled Light Soaking," Progress in Photovoltaics, 1998 (in press).

C.R. Osterwald, S. Anevsky, A.K. Barua, K. Bücher, P. Chauduri, J. Dubard, K. Emery, D. King, B. Hansen, J. Metzdorf, F. Nagamine, R. Shimokawa, Y.X. Wang, T. Wittchen, W. Zaaiman, A. Zastrow, J. Zhang, "The Results of the PEP'93 Intercomparison of Reference Cell Calibrations and Newer Technology Performance Measurements: Final Report," National Renewable Energy Laboratory Technical Report NREL/TP-520-23477, March, 1998.

Title: **Photovoltaic Solar Radiometric Measurements and Evaluation**

Organization: National Center for Photovoltaics and Center for Renewable Energy Resources, National Renewable Energy Laboratory, Golden CO

Contributors: D.R. Myers (Task Leader), T.W. Cannon, T.L. Stoffel, I.Reda,

Objectives: The task performs research, development, and engineering applications of optical and solar radiometric instrumentation and measurements to support the photovoltaic module, system, and reliability and durability activities of the National Center for Photovoltaics. The objective is to provide PV industry and NREL PV R&D activities with appropriate, accurate radiometric data and measurements identified by our customers as critical to evaluating PV device, module, and system performance.

Technical Approach: Optical and Solar radiometric measurement and data needs of the PV industry and R&D researchers are identified and addressed as needed. The task maintains core capability in broadband and spectral solar and optical radiation metrology, a suite of complex and expensive measurement equipment, and technical expertise in the fields of electrical and optical metrology, instrumentation, data analysis, atmospheric physics, and solar radiation resource assessment. Our optical radiation standards are traceable to the National Institute of Standards and Technology (NIST) spectral irradiance scale and the world Meteorological Organization (WMO) World Radiometric Reference (WRR). Expertise is maintained by technical interaction with the NIST Optical Technology Division, American Society for Testing and Materials (ASTM), Institute of Electrical and Electronic Engineers (IEEE), the Council for Optical Radiation Measurements (CORM), instrument manufacturers, and international standards bodies such as the International Standards Organization, (ISO) and *Commission International d'Eclairige* (CIE).

Results: Spectral Radiometry A major milestone for the task this year was the upgrade of the optical metrology operations to reduce the uncertainty associated with in house calibration of our suite of spectroradiometers. Post upgrade calibration measurements compared 11 National Institute of Standards and Technology (NIST) spectral irradiance standard lamps available. Deviation between NIST data and NREL measurement results averaged 1.0% (n=8) with a 2-sigma repeatability between lamps of 1.4%. The basic absolute uncertainty in NREL spectroradiometric measurements for PV applications is on the order of the assigned NIST uncertainty. Bias errors in positioning, light baffles, etc. indicated bias errors of 2% to 10% can be introduced by setup errors. Removing these sources of bias error has improved our spectral calibration by a factor of two. Revised SOP for Lab 229 to reflect upgraded operations, approved by NREL Environment Safety and Health office.

In the course of the year, we calibrated 11 spectoradiometric systems (four of our own, three belonging to NCPV tasks, and four others used in other NREL/DOE programs) supplying critical spectral irradiance information applicable to evaluating spectrally selective devices and systems.

Reference spectroradiometer systems were used to calibrate 16 ultraviolet radiometers used in PV module qualification testing, and reliability and durability testing for NREL (Reliability and Service Lifetime Team) and industry PV partners (Sandia National Laboratories, Arizona State University PV Testing Laboratory-ASU/PTL)

Spectroradiometer systems were used to measure and evaluate twelve NREL and PV Industry partner light sources and solar simulators. The NREL sources evaluated included seven in the reliability and durability area, three used for qualification testing, two industry simulators (Solarex and MV-Systems), the multi-source solar simulator developed by Bushan Sopori, (Fig 1) before and after a relocation move, and a sulfur lamp based NREL system. The UV -VIS-IR spectral reflectance of the concentrator facets and heliostat mirrors of the NREL High Flux Solar Furnace on South Table Mountain were measured, as shown in Figure 2. Spectral data as a function of position across the focal plane of a PV International concentrator module were measured which PVI will use to evaluate and fine tune cell design.

Broadband Radiometry: The traceability of the Reference Meteorological and Irradiance System (RMIS) Cavity Radiometer 29219 to the World Radiation Reference was maintained though comparison with the NREL Pyrheliometric Comparison Reference irradiance during NREL Pyrheliometric Comparisons Oct 11-16. RMIS deviations confirmed at less than 0.05% or 5 Watt/m² out of 1000, as show in a histogram of the deviations in watts/m² between the RMIS cavity and the reference irradiance shown in Figure 3.

Ten broadband (pyranometer and pyrheliometer) sensors used in NREL and ASU/PTL PV performance monitoring systems were calibrated against WMO/WRR references at the Solar Radiation Research Laboratory. We quantified a threefold improvement in pyranometer accuracy by applying zenith angle dependent calibration factors versus the single calibration factor as illustrated in Figure 4a and 4b. In 3a, the range of irradiances reported by 30 radiometers using a single calibration factor is 15 W/m² , and in 3b, by applying zenith angle dependent calibration factors, the range in reported values for the same 30 radiometers is reduced to 5 W/m² . These improvements were verified under a variety of sky conditions from overcast to clear.

Module Energy Ratings and Standard Reporting Conditions : The task participated in the 1998 PV Standards and Codes Forum, and continued to provide technical input regarding the development and validation of the NREL approach to a Module Energy Rating Methodology. We also worked closely with the Concentrator Alliance to validate a quantitative approach for establishing fair reporting conditions for evaluation of concentrator technologies against flat plate technologies. Figure 5 is a histogram of the median direct normal irradiance when plane of array global irradiance is within 50 watts/m² (+/- 25 W/m²) of 1000 W/m² for thirty sites in the southwest U.S. representative of where concentrator technology might be deployed.

Presentations/Publications/Conference Participation

National Aeronautics and Space Administration (NASA) Workshop on Validation of Satellite Remote Sensing Systems Dec 2-4, 1997, Greenbelt, MD,

Council for Optical Radiation Measurements (CORM), Annual Meeting, May 17-21 Boulder, Colorado.

5th Baseline Surface Radiation Network Science Meeting and Workshop, May 18-22. Budapest, Hungary

Gordon Research Conference on Solar Radiation and Climate, June 13-18, 1998 Plymouth, New Hampshire, ,

Photovoltaic Standards and Codes Forum July 20-23, 1998 Winter Park, Co.

1998 NREL/SNL PV Program review meeting, Sep 8-11 1998, Denver Co. Presented:
Pulse Solar Simulator Spectral Measurements at NREL
Module Energy Rating Candidate Reference Days: Criteria and Selection

Technical Contacts: The task handled over 180 documented requests for radiometric data, measurements, and technical information from the PV research and industrial community for technical information in FY 1998. A small sample of contacts includes the following:

William Bottenberg, Photovoltaics International
Ralph Romero, Solarex Thin Film Division
Dr. Hong Jeon Korea Institute of Energy Research
Dr. Nasser Taha Ahmad, University of Sharjah, United Arab Emirates
Ahmad Abu Sabha, Palestine Energy Authority, Palestine
Malek Kabariti, Jordanian National Energy Research Center, Jordan
Raphael Semiat, Rabin Desalination laboratory, Israel
Hagen Bauersachs, University of Munich , Federal Republic of Germany
Sanjay Vijayaraghavan, University of Florida
Dr. Robert Hammond, Arizona State University PV Testing Laboratory
Dr. G. Tamizhmani, Research Officer CANMET-EDRL Natural Resources Canada.
Dr. Sergio Colle, Laboratorio Energia Solar - Universidade de Santa Catarina Brazil.
Y.J. Huang Lawrence Berkley Laboratories
Michael Ross Canadian Meteorological Service
David King, Sandia National Laboratories
Jiangping Xi MV Systems, Golden Co.
Timothy Barnard ECD, Troy, MI.

Conclusions: We have provided broadband and spectral optical radiation calibrations, measurements and expertise meeting the needs of PV research, development, and industrial community. We maintain and improve the core competency and complement of instrumentation and skills to continue the meet those needs in the future.

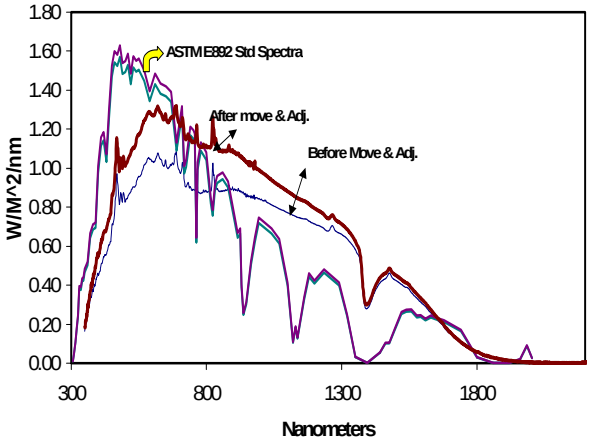

Figure 1. NREL Multi-source Simulator spectra.

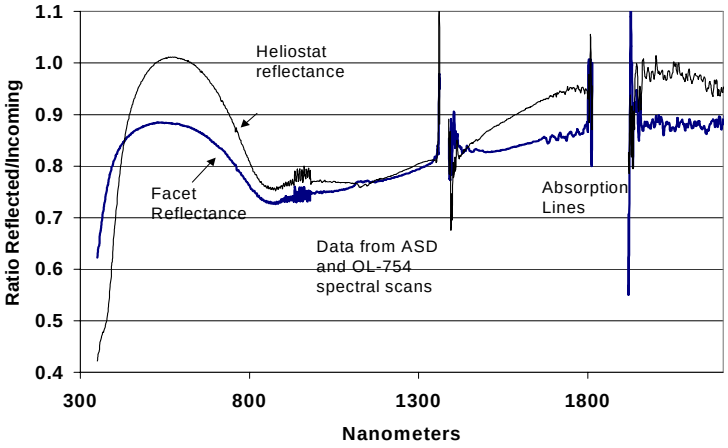

Figure 2. NREL High Flux Solar

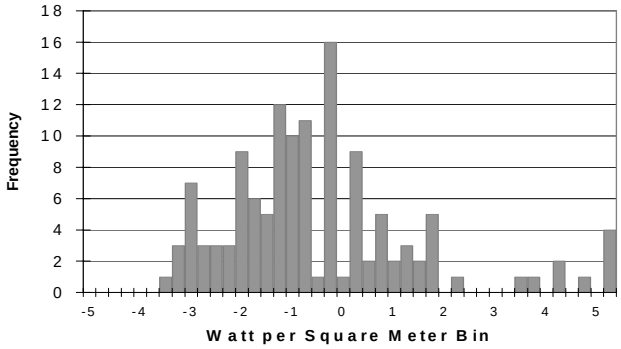

Figure 3. Histogram of deviations of RMIS cavity radiometer from WRR reference.

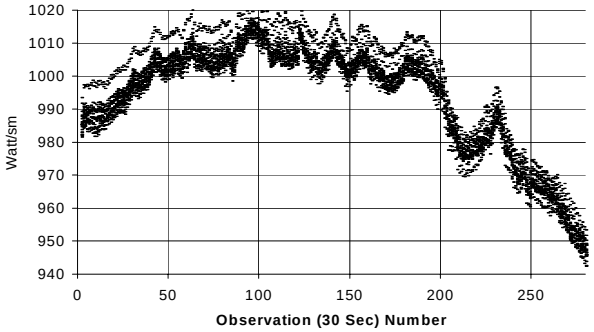

Furnace mirror spectral reflectance.

Figure 4a. Spread in Global Horizontal solar radiation for 37 radiometers with single calibration factors applied.

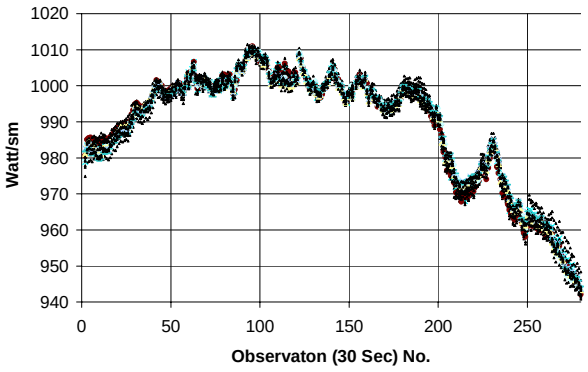

Figure 4b. Same as 4a, with zenith angle dependent calibration factors.

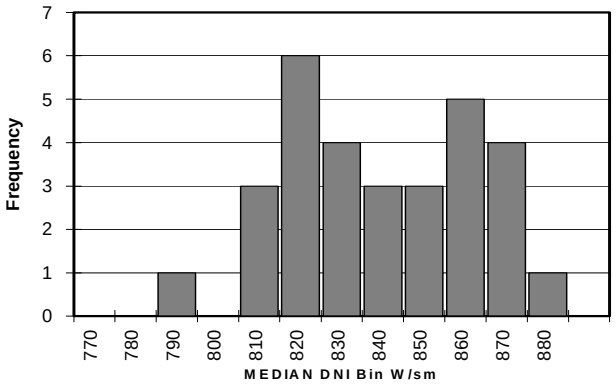

.

Figure 5. Histogram of Median Direct normal irradiance when global plane of array irradiance within 25 W/m² of 1000 W/m² for flat plate collector.

Title: **Photovoltaic System Performance and Standards**

Organization: Engineering and Reliability Division, National Center for Photovoltaics (NCPV), National Renewable Energy Laboratory (NREL), Golden, CO

Contributors: R. DeBlasio (Task Leader), R. Hansen, B. Kroposki, P. McNutt

Objectives

The overall objective of the Photovoltaic System Performance and Standards task is to address PV system, subsystem, and component technical and infrastructural issues and provide solutions that support the DOE PV Program five year plan (1996-2000) goals, and accelerates PV technology readiness and commercialization. Specific objectives are to provide engineering solutions and approaches that will reduce technical barriers to commercialization and advance photovoltaic system, subsystem, and component performance, safety, and quality.

Technical Approach

The technical approach to achieving task objectives include: (1) conducting system, subsystem, and component interface performance characterization outdoor testing and establishing standardized measurement and test procedures; (2) verifying PV system, subsystem and component development and advances through baseline outdoor performance testing, evaluation, and comparative analysis; (3) developing and documenting engineering best practices and technical guidelines for standardized system, subsystem, and component design and interface criteria and test procedures; (4) leading and supporting the development of national and international PV consensus standards and codes; (5) participating and supporting the development, implementation, and operation of domestic and international system and component certification and test facility accreditation programs; (6) facilitating information exchange and technology transfer through topical meetings, forums, and workshops; and (7) providing technical assistance and support to the domestic and international PV community for PV technology development and systems engineering and applications.

Results

The major accomplishments of this task include:

1. Validation and calibration of the small system flexible testbed and conduct small system performance characterization tests validating newly developed test procedures. Programming of the data acquisition system for the flexible testbed was completed. A calibration procedure was developed for calibrating the test bed and calibrations were completed. Testing was conducted on the following systems for validation of the flexible testbed: Two Uni-Solar lighting kit systems, SES MAPPS system, USSC telecommunication system, and a metal-halid lighting system.

2. Conducted exploratory tests of PV technology outdoor systems performance and planned for new system tests. Outdoor performance of eight PV systems continues to be monitored at the OTF. These systems include :(1) APS 1.8kW a-Si, (2) ASE 1.4kW EFG-Si, (3) SCI 1kW CdTe, (4) SSI 1kW CIS, (5) SSI 12kW Si (SERF), (6) Solarex 1kW a-Si/A-Si:Ge, (7) USSC 1.8kW a-Si/a-Si, and (8) USSC 1kW a-Si/a-Si roof shingles.

The following test reports were delivered to manufacturers and program managers:

STR98SES.001:	Report of performance of SES MAPPS System
STR98SCI.001:	Update on the SCI 1kW CdTe a-Si System
STR98SRX.001:	Update on the Solarex 1 kW a-Si/a-Si:Ge System
STR98CHI.001:	Performance data on the Chinese hybrid inverters
STR98SSI.001:	Update on Siemens 1kW CIS System
STR98USR.001:	Final Report on the United Solar Proto-type roof System
STR98SCI.002:	3-year update on SCI 1kW CdTe System
STR98SSI.002:	Final Report on Siemens 1kW CIS System
STR98USR.001:	Initial Report on United Solar 1kW triple-junction a-Si Shingle System

Installed the following new systems for long-term performance testing at the OTF:
300 W Midway concentrator tracking system

300W AC module from Ascension Technology.
USSC PV roofing shingle system
3 Uni-Solar lighting kits

3. Completed Interim draft PV Systems Performance Test Procedure. A final draft of test procedures from NEOS was received and reviewed. A draft test document "Interim Test Methods and Procedures for Determining the Performance of Small Photovoltaic Systems" was written based on the NEOS work and other sources. This document was published as an NREL technical report, *"Interim Test Methods and Procedures for Determining the Performance of Small PV Systems,"* NREL/TP-520-25077 in July 1998. The report was submitted to the IEEE SCC21 and International Electrotechnical Commission Technical Committee 82 (IEC TC82) for consideration as a consensus standard.

4. Standards and Codes Development. Two IEC TC82 Working Group meetings were conducted: (1) WG-2 on modules met at ASU on January 26-28, 1998, and addressed module testing and certification quality issues and (2) WG-3 on systems met at FSEC on February 23-25, 1998, to discuss the development of new work items for system and component testing procedures in support of the PVGAP and IECQ activities. The annual report to the IEEE Standards Board for SCC21 was submitted to the IEEE Standards office on February 23, 1998. The Standards and Codes Forum was held July 20-23, 1998, in Winter Park Colorado, at the Vintage Hotel and Conference Center. Over 40 members of the IEEE SCC21 standards committee and its working groups participated in a three-day meeting. The chairman, Dick DeBlasio, announced the reorganization and expanded scope of the SCC21. The IEEE Standards Board during its June 24, 1998, meeting approved a motion to expand the IEEE SCC21 (Standards Coordinating Committee 21 on Photovoltaics) scope for standards development and coordination to include Photovoltaics, Fuel Cells, Energy Storage, and merging the former efforts of SCC23 (Dispersed Generation) into the combined efforts of SCC21. The new title is IEEE SCC21 for Fuel Cells, Photovoltaics, Dispersed Generation, and Energy Storage. The Standards Board also reviewed actions on several SCC21 requests. IEEE 1374 on PV system safety was approved for publication, PAR 1526 on system testing was approved, PARs P937, P1013, P1145, and P1361 on PV Storage (batteries) were approved for development, and P1373 on system field testing was extended to December 1999. Ballot action requests were made for P929 (grid interconnection) and P937, P1144, and P1013 (battery installation and maintenance recommended practices). Working group meetings were held following the full committee meeting, addressing P1513 (Concentrator Qualification Tests); P1479 (Module Energy Rating); P1526 (PV System Performance Tests); P1373 (PV System Field Testing Procedures); and P937, P1013, P1144, P1145, and P1361 (Battery Storage, and Testing).

5. PV Performance and Reliability Workshop. The annual PV Performance and Reliability workshop sponsored by NREL and SNL was hosted by FSEC on November 3-5, 1998, in Cocoa Beach, Florida. More than 100 participants attended the 3 day meeting, which included more than 25 presentations. Emphasis was on the reliability of PV arrays, systems, BOS, and PVBONUS activities.

6. Accreditation and Certification Infrastructure Support. Participated and supported domestic (PowerMark) and international (PVGAP) PV accreditation and certification programs. Provided subcontract support for certification and standards development, maintaining organizational involvement, and participation in working meetings. Attended a meeting of the ECCB/NSI group regarding PVGAP in New Orleans on January 15, 1998, and provided an overview on IEC TC82 standards and development process. Outcome of meeting was preliminary assignment of the NSI (IECQ/UL) audit function to PowerMark as the agent for SEIA (PVGAP Licensee) and implementation of PVGAP in the United States through SEIA as the primary agent. A presentation on PVGAP was also given during the FSEC TC82 WG-3 meeting (February 28, 1998) regarding the need for system and component standards development. Implementation of PVGAP in Europe was also accomplished in February.

The Board of Directors meeting (July 5, 1998) officially established PVGAP, with all representatives at the meeting. It was announced that SEIA for the USA and EPIA for Europe will be the representatives for PVGAP through a master licensing agreement. A second meeting was

held on July 9, 1998, of the PVGAP Standards Committee. At that meeting, a review of IECQ quality requirements was discussed regarding PV module testing (IEC 1215, etc.) and on the proposed use of the NREL interim system tests and CENELEC component solar home tests.

The IEC TC-82 PV International Standards Development secretariat was supported (SEIA subcontract) and maintained with the establishment of new working groups in addressing the international needs for system certification test procedures. In addition to working groups for definitions, modules, systems, and storage, new working groups for certification, BOS, concentrators, and mechanical/environmental standards development were proposed for adoptions and implementation in 1998. A new IEC-TC-82 chairman (R. DeBlasio, USA) was nominated and elected by the international membership replacing Professor Y. Sekine of Japan who's term of serving was over.

Technical Assistance and Technology Transfer
Chaired IEEE SCC21 and IEC TC82 and provided leadership in system/utility interconnection, energy rating, concentrator qualification tests, and system test standards development.

Support for the International task activities included providing technical inputs on test methods and standards for international certification (World Bank) activities and testing several Chinese (Inner-Mongolian project) inverters.

Engineering and field testing support was provided by task members in support of the design and installation of the 1.2kW PV system for Earth Day Park in Washington, DC.

Technical support in reviewing statements of work was provided to PVMaT in support of the following Phase 4 and Phase 5 subcontracts: Advanced Energy Systems, Ascension Technology, Omnion, PowerLight, Photovoltaics International, Solar Electric Specialties, Trace, and Utility Power Group.

Technical Assistance was provided to the PV for Buildings task in reviewing PV systems modeling for use in the Energy-10 software.

Provided Technical Assistance to the DOE Golden Field Office (C. Power) in the design and specification of components for a PV system to light the entrance sign of the Golden Visitor's Center, in Golden CO.

Subcontracts in support of task objectives included: (1) SEIA for management and administration of the IEC TC-82 Secretariat and US Technical Advisory Group; (2) PowerMark Corp. for support in administering the accreditation and certification program activities for PV; and (3) NEOS Corp. for developing system performance test methods to be used for consensus standards development by the IEEE, IEC, PowerMark, PVGAP, and other testing bodies.

Participation and technical assistance to the PVUSA technical review committee, UPVG engineering and specification working group, PVMaT, PV Bonus, thin-film partnerships, million solar roofs, and interface for task activities with DOE, industry, and internationally were maintained and enhanced.

Presentations
A presentation on developing and validating the NREL "*Interim Test Methods and Procedures for Determining the Performance of Small Photovoltaic Systems*" was given on July 8, 1998, during the Rural Electrification Session of the 2nd World Conference on Photovoltaic Solar Energy Conversion conference.

Presentations on PV systems and applications was given at the National Western Stock Show on January 25, 1998, National Engineers Week February 23-27, 1998, IBW Local Union of Electrician in Denver on March 25.

Publications

1. *"Interim Test Methods and Procedures for Determining the Performance of Small Photovoltaic Systems"*, P. McNutt, B. Kroposki, R. Hansen, and R. DeBlasio, NREL Technical Report, NREL/TP-520-25077 July 1998
2. *"Development of Test Standards for the Performance Evaluation of Small Stand-alone PV systems"*, P. McNutt, B. Kroposki, R. Hansen, and R. DeBlasio, 2nd World Conference on Photovoltaic Solar Energy Conversion, Vienna, Austria, July 1998
3. *"Progress in Photovoltaic Balance-of-System Improvements"*, H. Thomas, B. Kroposki, P. McNutt, W. Bower, R. Bonn, and T. Hund, 2nd World Conference on Photovoltaic Solar Energy Conversion, Vienna, Austria, July 1998
4. *"Improvements in the Performance of a 1kW CIS Array"*, B. Kroposki and R. Hansen, NCPV Program Review Meeting, Denver, CO, September 1998
5. *"PV System Testing and Standards"*, R. DeBlasio, NCPV Program Review Meeting, Denver, CO, September 1998
6. *"Time Required to fully charge batteries in a Stand-Alone PV Systems Using Popular Charge Controller Types"*, P. McNutt, NCPV Program Review Meeting, Denver, CO, September 1998
7. *"PV System Standards"*, R. DeBlasio, 1998 PV Performance and Reliability Workshop, November 1998
8. *"Photovoltaic Systems, A Year 2000 Perspective"*, H. Post, M. Thomas, and R. DeBlasio, Progress in Photovoltaics, December 1998
9. *"Proceeding of the 1998 PV Performance and Reliability Workshop"*, B. Kroposki, editor

Conclusions

The development of an interim test procedure for small PV systems was a key accomplishment of the task. This document will be used throughout the domestic and international PV community for testing the performance of small PV systems. Use of this document should lead to better quality PV systems being designed. This task activity continues to provide the technical support and leadership necessary in maintaining PV program contributions to the technical side of the equation for systems certification as well as the establishment of an infrastructure that will allow U.S. PV community representation.

The task activities also focused on designing and constructing system testbeds at the OTF, conducting system and subsystem design reviews, and consolidation of best engineering and testing practices. A flexible test bed with interchangeable parts representing a variety of interface configurations was validated for performance characterization so that results can be evaluated for validation of design criteria guidelines and identification of design and performance limitations, failures (random and common mode), and enhancements. In support of these activities field testing, baseline performance comparisons and data base development and analysis of ongoing performance of experimental systems and fielded systems were conducted on a routine basis for historical validation, lessons learned, and relative advancement of system improvements and progress.

Transfer and integration of task technical information and experience to the PV community was maintained both domestically and internationally with regard to standards, codes, test method development, laboratory accreditation, product certification, and test facility development which is key to achieving PV technology quality that will assure reliability and safety. These activities combined provide the technical as well as commercial infrastructure that is essential to PV technology commercialization in reducing the institutional and technical barriers to achieving continued and long term sustainable success.

Title: **Solar Resource Characterization**

Organization: NREL Solar Resource Assessment Team, National Renewable Energy Laboratory, Golden, CO

Contributors: D. Renné (Team Leader), M. Rymes, M. Anderberg, B. Marion, R. George, L. Brady, S. Wilcox, G. Maxwell (consultant)

Objectives:

Characterizing renewable energy resources helps identify renewable energy markets, supports the efficient design of PV systems, and reduces risk and increases investor confidence in deploying renewable energy projects. Resource characterization provides the solar industry with the information necessary to perform analyses of technology performance for all types of applications.

Access to reliable information on renewable energy resources provides the U.S. industry a competitive edge in accelerating the deployment of their technologies domestically and worldwide. Hence, this project sustains a core capability established within NREL for developing and disseminating this information, and is central to the mission of the PV program.

The overriding goal of this project is to develop and disseminate key information on solar energy resources to the U.S. industry and to energy planners in order to facilitate and accelerate the deployment of their technologies domestically and worldwide. To achieve this goal, the following objectives are addressed:

- To develop accurate data bases and maintain reliable measurement activities with defined data quality;
- To develop and validate procedures for characterizing solar resource even in the absence of adequate measured data;
- To perform technology- and region-specific resource characterizations accurately, quickly, and reliably; and
- To provide a centralized, interactive source of quality assessed nonproprietary resource data and information.

To accomplish these objectives, the FY 1998 Solar Resource Characterization task consisted of three activities: 1) Measurement activities, 2) enhanced assessment method development and application, and 3) information dissemination, outreach, and training.

Measurement Activities

This subtask establishes quality data archives through ongoing measurement programs including the Cooperative Network for Renewable Resource Measurements (CONFRRM), which encompasses the Historically Black College and University (HBCU) network in the southeast U.S., and the Baseline Measurement Station at NREL's Solar Radiation Research Laboratory (SRRL) on South Table Mountain near Golden, Colorado.

There were several key accomplishments in FY 1998. One milestone was the recalibration of all the radiometers being used in the CONFRRM and HBCU stations. In addition, based on cooperative agreements that were initiated with the Florida Solar Energy Center, the Southwest Technology Development Institute, and the University of Oregon, these three sites have now become part of the CONFRRM network, bringing the total number of stations to 17. Data from all sites are being submitted to NREL and incorporated into the Renewable Resource Data Center (RReDC). We also provided small subcontracts to the 5 HBCUs that continue to participate in this measurement activity, to assure they have adequate supplies and student help to maintain the monitoring stations. An NREL technician visited each of the sites in the Spring of 1998.

We continue to work with the World Radiation Data Center in St. Petersburg, Russia, which maintains a world-wide archive of measured solar radiation collected from over 500 locations. We provide them with technical assistance in data quality assessment, and work with them to continuously add to the World Wide Web site, **http://wrdc-mgo.nrel.gov**, which is an important source of solar resource data for the solar energy industry. S. Wilcox visited the WRDC in early October, following his attendance at a Global Atmospheric Watch conference in Oslo.

Enhanced Assessment Methods Development and Application

This subtask refines and validates tools and techniques, including geo-spatial analytical tools, for estimating resources at specific locations where little or no data exist, or enhancing our understanding of the resource in the absence of adequate measured data. In FY 1998 our primary approach to this task has been to refine a model, known as the Climatological Solar Radiation (CSR) model, that uses a satellite- and surface-based cloud cover data to provide climatological solar information for any location on earth, at a spatial resolution of about 40 km. The cloud-cover data set is an assimilation of satellite- and surface-derived cloud observations that provides world-wide coverage of average cloud cover conditions. Prior to FY 1998 we had already used an earlier version of this model to develop global horizontal, direct normal, and diffuse maps of solar resources for north America. A key milestone in FY 1998 was accomplished when a draft report documenting the model and the results of several applications was completed. This report will be published in early FY 1999.

Further studies of the use of satellite imagery to provide maps at spatial scales as fine as 10 km has been continuing through our subcontractor at SUNY/Albany, Dr. Richard Perez. He is using GOES-8 and 9 imagery to test and evaluate a simple model for converting satellite pixel images to solar resource estimates. Several papers were published on this technique during FY 1998 (see "selected references", below), and the results of various evaluation studies were presented at the ASES conference in Albuquerque and a satellite meteorology conference in Paris during the spring of 1998.

We have also been exploring the various satellite-derived solar resource estimation approaches currently being used around the world, and evaluating their usefulness to the solar energy industry. We have been working closely with the NASA/Langley Research Center as they develop and refine a world-wide solar energy database structured for use by the solar energy research community, as an outcrop of their work in the World Climate Research Programme. During the summer of FY 1998 we signed a no-exchange-of-funds Interagency Agreement with NASA to strengthen our collaboration with this important program.

Because of our participation in the Paris satellite meteorology conference, and a forum on the use of satellite-derived products for the solar industry at Solar ' 98, we postponed the satellite data users workshop to 3-4 February, 1999. The workshop will be held in Golden, CO.

We also evaluated a world-wide data base known as DATSAV2, which is a compilation of three-hourly weather observations from virtually every weather station in the world, to determine its usefulness as an input to the METSTAT model for developing site-specific solar data sets that contain information on time series (such as Typical Meteorological Years) and the statistical properties of the solar resource, such as solar persistence. Based on tests of these data in Saudi Arabia, we are learning that this, too, is a useful approach for developing long-term solar resource information at many locations world-wide.

Dr. Eugene Maxwell, a long-term member of the solar resource assessment team at NREL, retired at the beginning of 1998, but remained actively involved in his modeling work as a consultant to our group. This year he published a landmark paper in the journal "Solar Energy" describing the METSTAT model that was used to develop the National Solar Radiation Data Base (see "selected publications" below).

Information Dissemination, Outreach, and Training

This subtask focuses on key additions of critical data and maps to the RReDC. During FY 1998 a vast amount of new solar data, and, in particular, spectral data, was added to the RReDC. In addition, a home page for the CONFRRM network has now been established, so that recent data from these sites can be viewed by users logging into the site. The RReDC continues to be refined to assist the user in identifying the location of virtually any published solar resource data base in the world. There was a continuing growth in the use of the RReDC by developers, researchers, and the general public during FY 1998.

An important event in FY 1998 was the availability of Technology Integration and Assessment funds, about half of which came from the PV program, which were used to make much-needed hardware and software upgrades to all of the systems and tools used for the Solar Resource Characterization task. In particular these funds were used to improve our RReDC capabilities and our Geographic Information System tools and procedures.

One additional significant accomplishment in FY 1998 was to move all of the old data files and software off of the VAX system, which was used by the Solar Radiation Resource Assessment Project for the past decade, onto Unix-based systems. This involved a substantial effort in writing new software to assure all of the codes and algorithms that resided on the VAX were preserved for future use.

Summary and Future Directions

Significant accomplishments have been made in FY 1998 in developing more refined solar resource products and in disseminating this information to the solar energy community. In addition, we have been continuing our efforts to help maintain a national solar monitoring network by supporting the CONFRRM and HBCU programs, and by linking these activities to other solar monitoring projects, such as the NOAA/ISIS network.

Our focus in FY 1999 will be to further refine our solar resource assessment techniques using satellite imagery, and to develop specific products from these data that directly assist the solar energy industry in planning for solar installations in the U.S. and abroad.

Selected References

Marion, Bill, Multi-Pyranometer Array Design and Performance Summary, *Proc. 1998 Ann. Conf., American Solar Energy Society*, Albuquerque, NM, pp. 523-528, 14-17 June, (1998).

Maxwell, E. L., METSTAT: The solar radiation model used in the production of the National Solar Radiation Data Base (NSRDB), *Solar Energy* 62(4):263-279, (1998).

Maxwell, Eugene L., Raymond L. George, and Stephen M. Wilcox, A climatological Solar Radiation Model, *Proc. 1998 Ann. Conf., American Solar Energy Society*, Albuquerque, NM, pp. 505-510, 14-17 June, (1998).

Zelenka, A., R. Perez, R. Seals, and D. Renné, Effective Accuracy of Models Converting Satellite Radiances to Hourly Surface Insolation, *Proc. 9th Conf. on Satell. Meteorol. and Oceanog.*, pp. 710-713, Paris, 25-29 May, (1998).

Zelenka, A., R. Perez, R. Seals, and D. Renné, Cogriging Surface Network and Satellite-Derived Solar Radiances: An Assessment of the Satellite-to-Irradiance Conversion Model Accuracy. *Conf. on Fusion of Earth Data*, Sophia Antipolis, France, 28-30 January, (1998).

PV Engineering and Reliability Project Subcontracts

Title: **PV Certification and Accreditation Management Support**

Organization: PowerMark Corporation

Contributors: S.M. Chalmers PE, Executive Director
Phoenix, Arizona.

Project Objective:
To support PowerMark Corporation (PMC) to manage and administer the operation of a component and module certification system and laboratory accreditation program. Administer corporate board and committee activities and liaison activities with domestic and international organizations associated with certification, accreditation, standards, codes and test methods.

Approach / Background:
The development of a domestic PV system and component certification and test facility accreditation program that is recognized, has reciprocity between other organizations and has testing conducted by accredited test facilities and products manufactured in a quality environment are key to a quality PV component and system. PowerMark Corporation, a non profit corporation, was created to implement and manage a PV module certification program based on an earlier study conducted by Arizona State University under Contract to NREL/DOE (NREL/TP-412-21291 (*Photovoltaic Module Certification / Laboratory Accreditation Criteria Development: Implementation Handbook*). The PMC Board is in the process of expanding its roll to include PV systems and components. The functions advanced by this report are: (1)Administer corporate board and committee activities. (2) Provide liaison actives with domestic and international organizations associated with PV certification, accreditation, standards, codes and test method development and validation. (3) Develop protocols for laboratory test methods based on published standards. (4) Initiate proficiency tests to compare module out put measurements between laboratories.

The objective is to provide PV manufactures with a module certification program that attests to the product's quality. The program involves the use of formal quality system criteria for the manufacturer such as ISO 9001 and a test laboratory authorized to perform testing in support of the program .The Laboratory must be accredited to ISO Guide 25 by an internationally recognized accrediting body and approved by PMC. The PV certification program is based both on U. S. and International consensus-developed standards

Status/Accomplishments:
The PowerMark Corporation (PMC) Board, Technical , Laboratory accreditation and Manufactures quality system committees have been in existence for more than two years. The Board membership was increased from 7 to 10 members and includes representation from, ASE Americas, EBARA, Siemens Solar, Solarex, United Solar Systems Corporation, Trace Engineering, Colorado Office of Energy Conservation, engineering and R&D. BP Solar has indicated an interest in joining the Board.

Two major module manufactures modules have passed the PMC testing and quality certification requirements. The PMC approved Arizona State Photovoltaic Test Laboratory (ASU/PTL) is the only accredited domestic laboratory for module testing. ASU/PTL has conducted a large number of test for US industry. Tests that otherwise would have taken longer to obtain results and would have been conducted at the only other approved Laboratory which happens to be located in European. The testing program is accredited for IEEE 1262, IEC 1215, and IEC 1646 and UL 1704 module requirements and PMC program tests.

With the advent of the PV-GAP/ IECQ program for global PV certification of components and systems several near-term activities were re-directed. PMC elected to be an active player in the PV-GAP initiative with the hope of avoiding competing programs and to participate in the potential early opportunity of establish reciprocity of certification at an international level. PMC has been identified to be the Designated Audit Body in the US for the IECQ National Supervising Inspecterate, Underwriters Laboratories (NSI/UL). And to perform the PV-GAP

administrative sublicensing of manufactures for the Solar Energy Industry Association (SEIA) who holds the Master PV-GAP license.

Six modules from three PMC manufactures were provided for proficiency testing and comparison of test ratings between laboratories. ASU/PTL,NREL, Sandia, JRC at Ispra have completed tests and comparative results were favorable and within acceptable tolerance.
The Executive Director made several presentations to various technical groups; SOLTEC '98, IEEE SCC-21, TC-82, , IEC IECQ Certification Management Committee, Electronic Component Certification Board meetings. He also represented PMC at PV-GAP / IECQ related meetings in Brussels and Vienna. He made a presentation to the California PV Alliance on PV-GAP, PMC,HUD certification and standards.

Several drafts were presented to the NSI/UL for comments addressing concepts and procedures relating to the PMC roll as Designated Audit Body for the IECQ NSI/UL.
In the absence of a function SEIA and responding to a request from the Department of Housing and Urban Development (HUD the Executive Director obtained industry review and comments on Bulletin NO. 200 HUD *Building Product Standards and Certification Program for Building Connected Photovoltaic (PV) Solar Systems*

Milestone Summary:
Broadened the industry representation on the Board and committees.

The Manufactures Quality System committee developed criteria for manufactures quality audits and the Technical committee developed information as to what is required in the way of laboratory re-testing when changes are made in a previously qualified module.

Monthly Board meetings were held. The annual meeting was at Soltec 98 in Orlando, Florida.

Two module manufactures have met PMC requirements and are awaiting final approval of their manufacturing quality system. One with an ISO 9001 system and the other with a non ISO 9001 system.

Arizona State University / Photovoltaic Testing Laboratory (ASU/PTL) completed PMC required tests on two groups modules from manufacturers. The test results have been reviewed by the Executive Director.

Established and maintained a PowerMark web site.

Proficiency test to compare laboratory module out put measurements completed.

Planned Milestones:
FY 1999: Hold monthly meetings of the PMC Board. Continue to increase component and system industry representation and participation on the Board and committees. Exert best efforts to encourage reciprocity protocols from associated certification programs. Maintain a PMC web site and answer questions. Provide representation of PMC and PV-GAP at technical and industry meetings and encourage participation and membership. Facilitate the IECQ approval of US Laboratories and manufacturers. Establish criteria with the NSI/UL for the Designated Audit Body functions and utilization of existing audit procedures and bodies for PMC/IECQ/NSI/UL use and approval. Apply for a *PV-Mark* trademark.

Major Reports and Articles Published:
Subcontract monthly reports, meeting notes, trip reports and annual report.
Promotional material describing the PMC organization and benefits of PMC certification were provided during presentations at the IEEE SCC21 and SOLTEC98 meetings.

8.0 PV Domestic Applications and Markets Project

8.0 The Domestic PV Market Development Project

John P. Thornton

The Domestic PV Applications Development Project supports the analytical, applications and market development activities of the Department of Energy's National Photovoltaic Program. The project provides a focal point for DOE activities through project development, dissemination of information, the raising of public awareness, subcontract management and technical assistance. Our work is carried out both inhouse at NREL as well as externally with and/or through a wide range of federal, state and local groups, and the photovoltaic industry. The goal of the Project is to foster wider acceptance of PV in numerous market sectors where significant penetration has not yet been attained. These sectors include the insurance and disaster mitigation industries, residential and commercial buildings, and the agricultural/ranching industry.

During FY98, we supported several major outreach activities designed specifically to raise the awareness of the general public to the present and future potential of photovoltaics and to showcase market-ready technologies.

From March through May of 1998, a photovoltaic exhibit called "Rufus' Solar Neighboorhood" was installed at the Walt Disney Epcot Center near Orlando, Florida. The exhibit remained through two major EPCOT attractions - Science Jam '98 and the Annual Flower and Garden Show. The exhibit consisted of several buildings as well as standalone displays, most of which were deesigned to be hands-on. PV modules from nearly every U.S. manufacturer were on display. Also emphasized were the importance of designing an energy-efficient building as a basis for the cost-effective use of PV, and the ability of PV to be integrated into buildings, not only to provide power, but to actually become part of the building structure or envelope. This design approach reduces the overall building structural cost, thus making photovoltaics more cost-effective.

Short lectures were given four times a day by colledge students hired by EPCOT. EPCOT staff helped the students develop their presentations. NREL staff tutored them on technical aspects of renewables and provided samples and props for their presentations. One of the most succssful of these was a PV-powered bicycle which attracted considerable attention.

According to an EPCOT survey, more than 75,000 visitors stopped at the exhibit, collected information or attended one of the 20 minute shows during the 11-week display. The last week of the exhibit coincided with the SOLTECH '98 conference, held at a nearby Disney hotel. During a special reception, SOLTECH attendees were invited to tour the display, with many of them seeing their products on display.

One of the greatest satisfactions of the EPCOT exhibit was the enthusiastic participation by PV manufacturers. Many provided special samples or produced special "runs" of products so that we could meet the tight EPCOT schedule. We also appreciated the extraordinary efforts of the EPCOT Science staff, who went far beyond contractual requirements to make the exhibit a success.

Early July witnessed the opening of the "Under the Sun" exhibit at the Smithsonian Institution's Cooper Hewitt National Design Museum in New York City. The exhibit provided a historical perspective of photovoltaics from its earliest uses in the 1950s until the present, using actual PV artifacts supplied by NREL staff, industry representatives and several PV pioneers. But the most exciting aspects of the exhibit were the glimses of how PV might be used in the 21st Century. Some of the highlights included a glass pavilion constructed of glass-encapsulated, thin-film PV modules contributed by B.P. Solar, and a tent, or tensile structure, with one kilowatt of Iowa Thin Film PV

modules laminated to the surface. The four-month long exhibit culminated in a Smithsonian-sponsored conference focused on raising the public's awareness of renewable energy.

Other outreach activities included a series of consumer workshops for potential homebuilders, and for farmers and ranchers. The workshops (and accompanying exhibits) were held on weeknights and weekends, and staffed totally by NREL volunteers. In all, nearly 700 people attended the two hour workshops, while many thousands more visited the exhibits.

During July, a meeting was convened between CEOs of about 25 major insurance companies to introduce them to the possible uses of PV to reduce casualty losses from disasters. Case studies were presented that showed the increased resistance to disasters provided by well-designed, energy-efficient buiuldings. Properly installed PV arrays provide a means for building occupants to have power in case of utility disruption and enable them to remain in their homes or businesses. Vandalism, injuries caused by gasoline generators, and business losses can be significantly greatly reduced. The CEOs were excited about the possibilities of PV and requested specific outreach activities aimed at their industry during FY99. These recommend-ations are currently being implemented.

Training in the use of portable PV generator sets was also provided to the Federal Emergency Management Agency (FEMA). In conjunction with the Federal Energy Management Program (FEMP), FEMA was furnished with eight PV gensets from different manufacturers for evaluation. These gensets were deployed during Hurricanes Georges in September 1998. NREL staff supported FEMA in Puerto Rico during these deployment efforts.

Our Project members also continued extensive support to PV-BONUS, the Million Solar Roofs Initiative, utility deregulation and the upcoming Sunrayce 99.

PV Domestic Applications and Markets Project Subcontracts

Title: **Development of the Tucson PhotoVoltaic Coalition to Promote & Support PhotoVoltaic Installations**
Community Partnership Planning, Coordination, Education, and Infrastructure Development

Organization: Learning Village Project
Tucson, Arizona

Contributors: Valerie Rauluk & David J. M. Fuller, Principal Co-Investigators, J. Beebe, R.Clayborn.

Background

The Tucson Coalition for Photovoltaics (TCPV), a public private partnership, was formed in 1997 to develop sustainable markets for PV applications in the Tucson region through stimulated demand and infrastructure support. Founding members are: Tucson Electric Power, Global Solar, City of Tucson, National Association of Home Builders Research Center (NAHB), ASETT Center of Pima Community College, Tucson Unified School District, Community of Civano, Case Enterprises, Progressive Solar, John Wesley Miller Companies, Habitat for Humanity of Tucson, Primavera Builders, and Venture Catalyst. (Additional members subsequently secured are: UniSource Energy Corporation (holding company for Tucson Electric Power and Global Solar), The Solar Store, Pima Community College, and Tucson Institute for Sustainable Communities).

TCPV serves the metropolitan community of Tucson, Arizona. Metropolitan Tucson is located in the center of the eastern third of Pima. County, Arizona. Pima County occupies an area of 9,200 square miles, and shares an approximately 120 mile-long border with the State of Sonora, Mexico. The county population of over 780,750 (1996) lives primarily (about 95%) in Metropolitan Tucson, in an area of approximately 412 square miles.

At its formation TCPV members laid out a plan to build a sustainable, viable photovoltaic industry in the Tucson metropolitan region. The plan broadly outlined a set of strategies to stimulate demand, strengthen supply, and establish the community infrastructure for widespread adoption of solar appliances.

Objective

The objective of the project was to implement key strategies and establish TCPV as a viable, sustainable partnership for the near term. The approach to achieving that objective was to

- Facilitate membership in TPVC and establish mission, objectives, and operating structure.
- Establish a Buying Cooperative for PhotoVoltaic devices for installers, developers, and contractors in the region.
- Establish relationships with funding authorities for more efficient financing of solar devices.
- Research and recommend best possible structures for a Community Energy Cooperative or Energy Service Organization, which supports widespread dissemination of PV technologies and other solar.

- Solidify the inclusion of renewable energy and sustainability criteria for programs, policies, and projects at the local government level, in particular, the City of Tucson and Pima County.

Approach

Organizational Structure

The structure and organization of TCPV were established in two ways: tactically, in the course of fulfilling installation and program commitments, and strategically, by means of reviewing best practices of other organizations, and collaboratively articulating a vision, mission, objectives and strategies for a three to five year period.

On an operational basis, the Coalition had committed to securing 35kW of photovoltaics, establishing the procedures for effective installation, and securing other resources and support to meet the commitment. The installation and project manager was asked to serve as acting chair of the organization, and in this capacity facilitated a set of operating guidelines and rules. These emerged over the course of the interaction between Coalition members, were solidified on a draft basis by the acting chair and discussed and voted on by the Coalition as a whole. The final product after nine months of interaction was a set of organization by-laws covering procedure for new members, voting, fund-raising and other operational issues. This document is available in the Final Report: Tucson Coalition for Solar, Organizational Plan, September 1998. During this process, the name of the Coalition was changed from PhotoVoltaic to Solar. The official name of the organization as of November 1998 is the Tucson Coalition for Solar.

In addition to allowing relationships and rules of operation to emerge from the give and take of fulfilling obligations, Coalition members engaged in a strategy session to identify a vision statement, mission, objectives, and key paths for progress. These statements are contained in the above-mentioned document.

Buying Cooperative

The Buying Cooperative was approached in two ways. Again, tactically by reviewing with Coalition members actively engaged in buying and selling solar devices, the emerging value of volume purchases and purchasing consolidation. In addition, a review of cooperative structures was undertaken and the key aspects of a buying cooperative relationship were established. This introduction to buying cooperative structure and outlines of issues to be discussed and reviewed with potential cooperative members is available in the Final Report: Buyers Cooperative.

Financing Relationships

The first step in establishing a relationship with local funding authorities was a telephone survey, inquiring as to the level of current involvement in financing solar devices and future interest. In addition, inquiries were made as to the interest in workshops/ seminars in solar technologies and the best way to structure these activities. The survey results were compiled and are available in the Solar Financing Final Report. A three-panel brochure was also produced for consumers listing local solar sources, phone numbers, and a summary of state of Arizona incentives. These were distributed at the Innovative Home Tour, the Fall Regional Home Show, and distributed to Coalition members involved in selling and installing solar appliances. A copy of the brochure is also contained in the Final Report.

Community Enemy Cooperatives

The cooperative organizational structure and its historical context was researched and summarized in a Final Report: Community Energy Cooperatives. The report outlines the key issues and concerns and the ways in which such issues have been addressed in various industries and over the course of the. last one hundred years. This review resulted in an outline of rights and responsibilities and can be used to begin the discussion with potential cooperative members as a first step to forming an energy cooperative. In addition, a review of current local conditions, and an assessment of the best options for piloting a cooperative program were identified.

Establish Renewable Energy Application in Local Government Policy

A basic agenda for local government was established which consisted of including solar devices in government infrastructure development, recognition of Tucson as a "Solar Capital," sales tax relief, minor outreach participation, and participation of government facilities managers in solar technical training's. This agenda was presented to Council members of the City of Tucson and Supervisors of Pima County. The City of Tucson passed official resolutions supporting all of the above, except for sales tax relief. The County has issued a letter of support and cooperation and key facilities managers have expressed willingness to investigate solar applications. Area legislators at the state and national levels were also presented with the Solar Vision for Tucson. The Vision was promoted primarily as an economic development opportunity for the region, as well as an environmental and quality of life concern. Various means were used to expand this message including presentations, newsletters, and in person activity updates.

Conclusions

In a relatively short period of time, the Coalition has secured a great deal of excitement and support for solar appliances in the metropolitan area. Key to this success has been a clearly articulated purpose with a focus on tangible results, in particular, visible applications and installations. Secondly, a rationale for the strategy was identified that crosses parties and interests: economic development. Finally, an opportunistic approach to developing and expanding the mission, keeps the mission alive for the Coalition members, local leaders and politicians, and the community at large. In conjunction with securing the time and resources to clarify the issues, generate the analysis and best practice insight, the solar conversation is deepening and widening in the community. Since the conversation is always connected to a course of action suitable to the level of awareness, solar practice has begun a pattern of incremental growth.

Areas for Continuing Research & Consideration

During the next 12 months, the Coalition will seek to build on its successes by

- Piloting a Cooperative Energy Program
- Conducting Solar Workshops for Financiers, Real Estate Agents, Appraisers and Insurers
- Increasing Coalition Members
- Increasing Technology Exchange with Local Government Facility Managers
- Increasing Solar Interest of Home Buyers
- Engaging Commercial Facilities in Solar Applications
- Including Solar Applications in Production/ Custom Home Building

Title: **Renewable Energy Applications and Economic Analysis for Electric Power**

Organization: Pacific Energy Group

Contributor**:** Tom Hoff

A Micro-Grid with PV, Fuel Cells, and Energy Efficiency

A micro-gird is an electrically isolated set of power generators that supplies all of the demand of a group of customers. This work evaluates the potential of a micro-grid composed of photovoltaics (PV), fuel cells, and energy efficiency investments and a set of residential customers. It concludes that: (1) PV, fuels cells (operated in a cogeneration mode), and energy efficiency may all be an economically attractive part of a micro-grid; (2) there is a fairly good match between supply and demand on an annual, monthly, and hourly basis; (3) fuel cells (operated in a cogeneration mode) and PV complement each other in terms of electricity supply because fuel cell electricity production peaks in the winter while PV electricity production peaks in the summer; (4) a relatively small number of customers (less than 50) can result in a reliable micro-grid; (5) customer loads that are more certain result in a smaller micro-grid; and (6) micro-grids may represent a new market for PV, fuel cells, and energy efficiency.

Reduce, Reuse, and Renew: One Possible Approach to Cut Carbon Emissions

Global climate change has become an increasingly important issue over the last several years. This issue reached a climax at the Kyoto Conference in December, 1997 where the U.S. agreed to reduce its greenhouse gas emissions to 7 percent under its 1990 levels by 2010. This paper describes how distributed resources could be part of an overall solution to achieving these reductions. It illustrates how a system composed of energy efficiency, distributed cogeneration, and distributed photovoltaics could reduce fuel consumption by 70 percent in the residential and commercial sectors. This could be a solution that makes economic sense independent of the climate change debate if implemented over the next 30 to 50 years, a timeframe which is not much worse for the climate system than achieving them in 10 years according to most analyses.

Distributed Resources: A Potentially Economically Attractive Option to Satisfy Increased Demand on Okanogan County Electric Cooperative's "Mazama Feeder" Line

Objective

When we talk about "distributed resources," we are referring to producing electricity where it will be consumed, rather than producing it at some distant facility and then transporting it over electric power lines. In this report, we use a detailed set of assumptions to evaluate the technical and economic feasibility of using distributed resources to supply the energy needs of 1,500 new homes in the Mazama Valley. The specific homes are on the Mazama Feeder—a part of Okanogan County Electric Cooperative's electric distribution system.

The three distributed resources that we consider in this report are energy-efficient appliances, cogeneration, and photovoltaics. *Energy-efficient appliances* include devices such as fluorescent lights,

high-efficiency refrigerators, and propane dryers.[1] *Cogeneration technologies* produce electricity and usable heat at the same time; for example, rather than running a generator just to produce electricity, the heat released during the generation process is captured and then used. *Photovoltaic (PV) technologies* convert sunlight directly to electricity with no moving parts.

Alternative to Feeder Upgrade

We constructed a computer model—based on the characteristics of the Mazama Feeder—that can be used to assess the technical and economic benefits of a variety of distributed resource scenarios. The distributed resource alternative that we have focused on here is the following:

(1) A moderate level of energy-efficiency appliances for each new home,
(2) Two megawatts (MW)—or 2,000,000 watts—of propane-based cogeneration, which is enough power to supply the water-heating and space-heating needs of 1,000 new homes,
(3) Propane heating (without cogeneration) to supply the water- and space-heating needs for the remaining 500 new homes, and
(4) Five-hundred kilowatts (kW)—or 500,000 watts—of photovoltaics.

Our results indicate that customer demand on the Mazama Feeder would still double even if all of the homes used propane space-heating and water-heating and energy-efficient appliances. Adding cogeneration turns the Feeder from one that distributes more electricity in the winter (a "winter peaking" feeder) to one that distributes more electricity in the summer (a "summer peaking" feeder). Using PV addresses the summer-peaking problem and brings the Feeder's peak to within the current load levels.

The Co-op would own the cogeneration, and one-third of the 1,500 new homes would each own, on average, a utility-intertied 1-kilowatt (1,000-watt) PV system.[2] Currently, the Co-op charges customers a "system access fee" to connect to the electric distribution system. However, as an incentive to encourage PV installations, the Co-op would waive the service access fee for customers who install a 1-kilowatt or larger PV system.

Conclusions

Our primary conclusion is that using distributed resources provides better economics than upgrading the Mazama Feeder to a transmission level. According to our preliminary economic analysis, this upgrade, which would enable the Feeder to carry more electricity, has a net present value (NPV)[3] of negative $1.2 million. This is based on the assumption that the entire cost of the line upgrade and new substation is incurred all at once. The alternative of providing electricity to customers locally by using distributed resources has an NPV of positive $0.2 million. By our analysis, therefore, the Co-op can save $1.4 million by using distributed resources.[4]

References

- T. E. Hoff and C. Herig, "Clean Distributed Resources in the U. S. Residential Market," Forthcoming in the IEEE Power Engineering Review (1998).

[1] While the energy efficiency appliances were focused on in this report, there is also the importance of building homes that are efficient in terms of their heat consumption regardless of the type of heating fuel used.
[2] PV panels for a 1 kW system occupy about 100 square feet. The DC electrical output is converted to AC power and connected to utility distribution system using a sine wave inverter.
[3] NPV, or net present value, is an economic evaluation approach that discounts cash flows that occur over time so that various alternatives can be compared.
[4] The costs used in this preliminary feasibility study are only estimates. These costs could change substantially when cost proposals are actually made. These costs will be known with a greater degree of certainty after an engineering study is performed.

- T. E. Hoff, H. J. Wenger, C. Herig, and R. W. Shaw, Jr., "A Micro-Grid with PV, Fuel Cells, and Energy Efficiency," Proceedings of the 1998 Annual Conference, American Solar Energy Society, Albuquerque, NM (June 1998).
- T. E. Hoff, H. J. Wenger, J. P. Weyant, and C. Herig, "Reduce, Reuse, and Renew: One Possible Approach to Cut Carbon Emissions," Forthcoming in the International Journal for Global Energy Issues.
- T. E. Hoff, H. J. Wenger, J. P. Weyant, and C. Herig, "Reducing Carbon Emissions Using Clean Distributed Resources," Proceedings of th4e 19th Annual North American Conference of the IAEE, Albuquerque, NM, October 18-21, 1998.
- *Distributed Resources: A Potentially Economically Attractive Option to Satisfy Increased Demand on Okanogan County Electric Cooperative's Mazama Feeder Line*, NREL Report, October 19, 1998.

Title: **U.S. Representation in the IEA PVPS Task 7**

Organization: Solar Design Associates
Harvard, MA 01451-0242.

Project Background

The objective of this subcontract was to represent the U.S. in the International Energy Agency (lEA) PV Power Systems (PVPS) Task 7, "Photovoltaic Power Systems in the Built Environment." U.S. involvement with this task leads to a better understanding of international PV in buildings activities and an opportunity for the U.S. to become competitive in worldwide PV in buildings industry. NREL support of this subcontract supports NREL's mission to advance the science and engineering of renewable energy technologies that will lead to facilitating commercialization of these technologies.

The IEA is an organization that promotes the collaborative research, development, and demonstration of new energy technologies between nations. IEA PVPS Task 7 is a 5-year effort involving approximately 15 countries. The objective of the task is to enhance the architectural quality, technical quality, and economic viability of PV systems in the built environment and to assess and remove non-technical barriers for their introduction as an energy-significant option. The U.S. has been involved with IEA PVPS Task 7 since its inception in the fall of 1996.

Description of Activities

The subcontractor coordinated all arrangements for the Task 7 members to hold their semi-annual meeting in conjunction with the SOLTECH98 meeting in Orlando, FL in May 1998. Approximately 30 people attended the 3-day Task 7 meeting (including subcommittee meetings). Holding the Task 7 meeting in conjunction with SOLTECH98 gave the international participants an opportunity to participate in conference sessions and meet U.S. PV industry manufactures. As a result, they became more familiar with the PV in buildings activities that are occurring in the U.S.

Task 7 includes 4 subtask areas. The subcontractor provided the level of effort for each subtask that was required by the work being completed by Task 7 during this subcontract's period of performance.

Subtask 1 – The Architectural Design

The subcontractor provided information on exemplary PV in buildings projects in the U.S. to be included in subtask documents that will be published before the conclusion of Task 7 activities. The subcontractor also provided expertise to NREL related to incorporating a PV module into the building energy computer simulation tool known as Energy-10 (under development at NREL). This activity meets the Task 7 goal to further produce design tools for architects that incorporate PV for buildings systems.

Subtask 2 – Systems Technologies
The subcontractor investigated and provided information about the current status of work in the U.S. in the following areas: 1) roof and façade integration; 2) PV in non-building structures; 3) guidelines, standardization, certifications, and safety issues; 4) hybrid elements (PV and daylighting, PV and thermal systems); 5) impact of new electrical concepts; 6) reliability evaluation; and 7) interconnection issues. The subcontractor consulted industry representatives to ensure that the information provided to Task 7 was as complete as possible.

Subtask 3 – Non-Technical Barriers
An NREL PV for Buildings Task staff member is the subtask leader for Subtask 3. The subcontractor's responsibility was to substitute as subtask leader during Task 7 meetings when the NREL staff person was not able to the meeting. This required strong communication between the subcontractor and the subtask leader and dialog between the two related to the activities occurring within the subtask.

Subtask 4 – Demonstration and Dissemination
The subcontractor encouraged U.S. industry to provide new demonstration products for the Demosite located in Lausanne, Switzerland. The subcontractor also began to work with the organizers of the next Solar Electric Buildings Conference to develop an agenda and recommend U.S. participation at the conference. The subcontractor worked with Task 7 members to present periodic workshops held in conjunction with semi-annual Task 7 meetings. The subcontractor also played a strong role in existing efforts in the U.S. to provide education to designers about Task 7 activities.

Title: **Whole-Building Design Brochure**

Organization: Solar Design Associates
Harvard, MA 01451-0242

Project Background

The objective of this subcontract is to create a brochure that defines the "whole-buildings" process and integrated building technologies including building-integrated photovoltaics (BIPV), describes the relationship between whole-buildings and BIPV, and illustrates how "whole-building" design and construction can reduce the energy use in a building. The goal of the brochure is to communicate the message that "whole-buildings" can be design and created if the components of a building are integrated properly.

The brochure encourages teams of builders, developers, architects, and engineers in the building industry to use the "whole- building" process. The "whole-building" process prioritizes and incorporates energy efficiency and renewable energy technologies throughout a building's design, construction, commissioning, and operation. The brochure includes individual technology descriptions as well as case studies that show how proper integration of these technologies reduces a buildings energy use.

Description of Activities

Background research for prospective technologies to be considered in the brochure has been completed. Research included contacting individuals and key organizations involved in this area.

Key organizations that were contacted included, but was not limited to, NREL Exemplary Buildings Program, NREL PV for Buildings Task, the Passive Solar Industries Council, the American Institute of Architects Committee on the Environment, the American Solar Energy Society, the US Green Buildings Council, and the Solar Energy Industries Association.

The following technologies have been researched and considered for use in the brochure: daylighting, advanced glazings, building envelope, integrated photovoltaic, heating and cooling strategies, active solar thermal, passive solar design, and earth-coupled heat pumps.

Potential case studies or buildings that have successfully integrated the above-mentioned technologies have been selected. Information from national and international buildings has been compiled. Candidate buildings include: The Barritt house, a “tract subdivision builder’s spec’ house in Nevada; The Lord residence, a custom designed 2,700 sq. ft. residence in Maine; The Rio Grande Botanical Gardens, a multi-faceted all-glass structure in Albuquerque NM; The Florida Solar Energy Center tract houses with unique and monitored demonstration of energy conscious whole-building design in Florida; The NREL Thermal Test Facility, Golden, CO; Tierra Concrete Home, Pueblo, CO; Konove-Ravetto Residence, Pittsboro, North Carolina; De Kleine Aarde” in Boxtel (Noord-Brabant) is the oldest national environmental education centre in The Netherlands; AVAX Headquarters, Office building, Athens; The Lisbon Multipurpose

Pavilion, Lisbon Expo` 98, Atlantico, Portugal; Forester School Lyss, Switzerland, Hall 26, Traide Fair Hannover, Germany.

The brochure outline has been developed and the technologies and case studies to be considered have been identified. The outline presents the basic structure and content of the document and follows the following structure: Goals and Objectives, Technologies and Design Strategies (thermal mass, daylighting, advanced glazings, high-integrity building envelopes, BIPV, advanced heating and cooling strategies, active solar thermal for domestic hot water, solar thermal for space hearing), and case studies. A short description for each technology has been drafted.

The brochure layout is in its conceptual design stage and will continue to develop as the technology and case study write-ups are completed. The layout will include the placement of the integrated technology descriptions, case study descriptions, photos, and other appropriate graphics. A four page summary brochure is also in the conceptual design phase and will be developed for the lay audience to provide a summary overview of whole building design and its benefits.

Title: **Photovoltaic Market Valuation and Load Matching**

Organization: tmospheric Sciences Research Center, The University at Albany, Albany, and New York

Contributors: Richard Perez, principal investigator, Howard Wenger, and Christy Herig and Marek Kmiecik

OBJECTIVES

This project was initiated in 1998. It logically follows upon the recently completed Solar Resource Utility Load Matching Assessment project [1]. Its main objectives are (1) to determine the regional distribution of the value of grid-connected commercial PV systems, and (2) to develop and test a load control methodology designed to enhance the effective capacity of photovoltaics. An additional objective of this work is to continue, as needed, investigations relevant to the effective capacity of PV, including responding to utility requests for effective capacity determination or investigating case studies relevant to the effective capacity of PV such as power outages.

RESULTS AND DISCUSSION OF ACTIVITIES COMPLETED IN FY 98

Recap on relevant past findings

- The effective capacity of PV, quantified by the Effective Load Carrying Capability (ELCC) parameter, is substantially larger than the capacity factor of PV for most US utilities.
- Effective capacity is not well correlated with the solar resource. However, a well-defined relationship exists between effective capacity and simple load shape parameters (e.g., the ratio between summer and winter peaks).
- A map showing the distribution of PV's effective capacity in the US was produced. This map shows that regions of highest capacities do not always overlap with "traditional" high solar resource regions. Regions of highest effective capacities are associated with the following factors: (1) existence of marked summer heat waves, (2) summer electric loads driven by commercial consumption and (3) small proportion of electric heating. Seasonal effective capacity maps, as well as maps quantifying other measures of PV capacity, such as the Minimum Buffer Energy Storage (MBES) were also produced. These geographical distributions were found to exhibit little year-to-year variability, with highest variability observed in Florida and the southern Atlantic seaboard. The Northeastern Atlantic seaboard, California and the Great Plains exhibited the lowest variability.
- Considering end-use loads as opposed to utility-wide loads, we found that the effective capacity of PV was consistently high for air-conditioned office buildings – ~ 65% for 5% load penetration and tracking PV.
- Distributed PV could play a substantial role in preventing heat wave-driven regional power outages.

The new results highlighted in this report include

- The mapping of the value of commercial PV installation in the US
- The assessment of PV performance during outages power outages caused by severe weather
- A brief update on the development of the PV load controller

Valuation of Commercial PV in the US: In a 1996 study, Wenger et al. [2] looked at the valuation of residential PV systems. Here we address demand-side commercial PV systems. Our focus on customer-owned PV stems from a simple economic reality: demand-side PV systems are gauged against high-value retail energy and demand rates.

We used a straightforward economic valuation approach: comparing the value of a system to its cost. The value of a system originates from energy consumption offset and demand reduction, plus fiscal and other financial incentives as applicable locally to commercial entities. Project-specific, or still intangible valuation elements such as replacement value, environmental value, or market-appeal value, are not yet considered. Economic feasibility is quantified by the PV's ***Breakeven Turnkey Cost (BTC)***. Five PV array configurations relevant to building-integrated or ground-mount designs were considered: 2-axis tracking, fixed south-facing at 30^{o} tilt, horizontal, vertical south and vertical west.

The analysis was conducted utility-by-utility, using (1) localized PV energy production [3], (2) localized PV effective capacity [4], (3) local utility commercial rates, and (4) national and statewide fiscal incentives.

A total of 143 major electric utilities, accounting for over 80% of the US capacity, were individually contacted. Energy and demand rate schedules were selected as a function of their suitability to a small-to-medium commercial operation: peak demand of the order of 100-300kW, secondary service. For most utilities, this rate was their general service-demand rate. The incentives considered in this paper include national and State tax credits, low interest

loans, accelerated depreciation, tax deductions and grants. Sales tax incentives and property tax incentives were not considered [4]. Most of the information on incentives was obtained through the Dsire database [5].

Utility specific results were gridded and mapped to generate "iso-BTC" maps for the country. An example of these maps is provided in Figure 1 for the 2-axis tracking configuration (other configurations may be found in [4]).

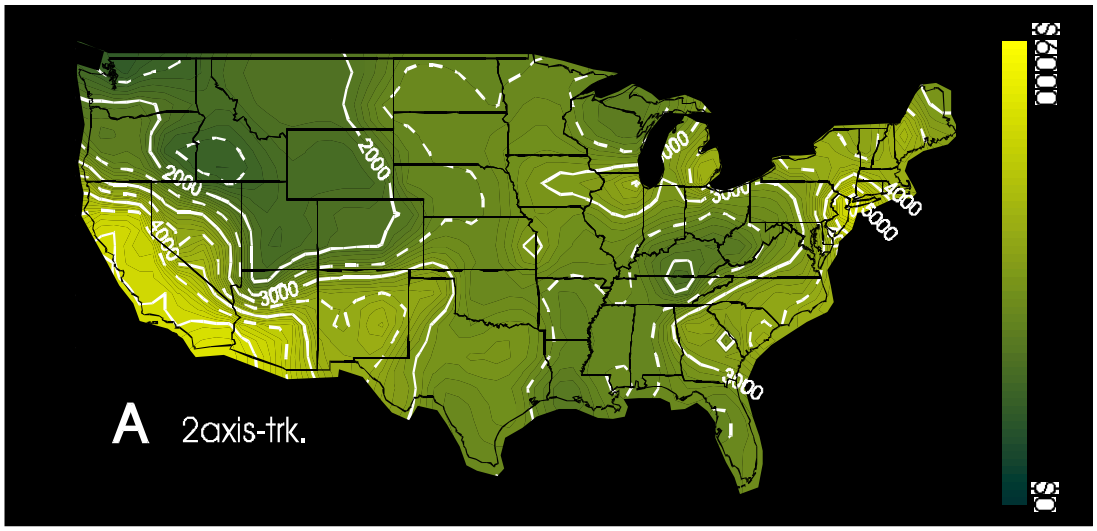

Figure 1: Geographical distribution of the break-even Turnkey PV Cost (BTC) for sun-traking demand side commercial PV systems

The highest BTCs (in excess of $11,000/kWac for a tracking system) were found in Hawaii. Within the conterminous US, the highest BTCs were found in the southwest, and the metropolitan northeastern Atlantic seaboard. These results reflect high utility rates combined with high energy production (in the southwest and Hawaii), but also high effective capacity in all three areas. Very low utility rates and low PV effective capacities account for the low northwestern and Appalachian BTCs. In the central/south region, relatively low rates tend to offset much of the observed high effective capacities, while in Florida, both low rates and modest effective capacities [3] tend to offset high energy production.

The impact of local tax incentives is apparent, but does not strongly stand-out, because states offering the most substantial incentives in the continental US -- Oregon, North Carolina and North Dakota -- also exhibit either moderate rates, or a moderate capacity/energy resource. Note that at the time this map was generated (January 1998) the new California buy-down incentive was not included.

Impact of Array Geometry: For the ideal 2-axis tracking option, BTCs range from less than $1500/kW in the northwestern US to well above $5000/kW in the lower 48 states. Going from this ideal configuration to fixed-tilt PV results in a reduction of the BTC of roughly $1000/kW at the high end, and $500 at the low end. Interestingly, going from tilted to horizontal only results in a very small additional reduction of the BTC. Vertical configurations result in a significant drop of the BTC, with maxima reaching only $2000 for both south-facing and west-facing arrays. It should be reminded however, that these apparently disappointing results for the vertical surfaces do not account for case-specific replacement value.

Details on this analysis may be found in two recent publications by the authors [4,6]. A new NREL brochure was also generated based on these findings [7].

PV performance during power outages: Last year, we reported on the massive power outage that occurred throughout the Western System Coordinating Council (WSCC) on August 10, 1996. We concluded that, had a dispersed PV resource been available throughout the WSCC service area, the events that triggered the power outage could have been minimized and the outage would probably have been avoided. In the summer of 1998 there were several cases of rolling blackout and near-outage situations in the Central US. These situations were brought on by a prolonged heat wave in the region. Looking at the photovoltaic availability during this heat wave fully confirmed our contention that a dispersed PV resource could, by providing power at times of stress on the grid, minimize the possible causes of outage such as lack of local supply and massive power transfers. Figure 2 is an illustration of the solar resource in the Dallas, TX, area, during their prolonged heat wave. Note that this resource was near its possible maximum value every single day.

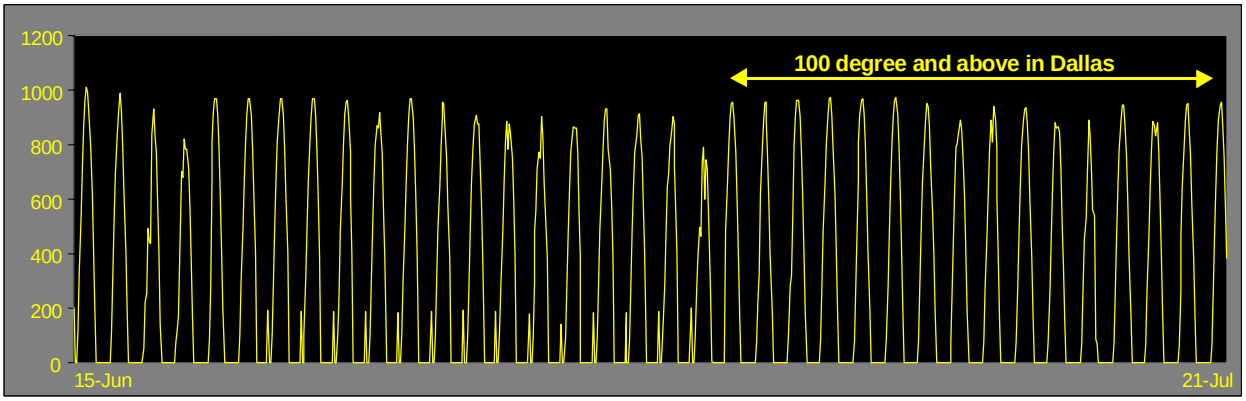

Figure 2: Global irradiance in the Dallas-Ft. Worth area during the summer 1998 heat wave

The January 1998 power outages in northern New York, Quebec, Vermont, New Hampshire and Maine, were of a different nature. While the power grid as a whole remained stable, ice storms damaged power transmission and distribution lines. Several million customers were affected by lengthy power outages. Some outages lasted for weeks.

Many of the costliest consequences of the outage could have been avoided if only a fraction of the electrical power normally available from the utility power grid had been available to customers.

- Plumbing damage (frozen pipes), exposure to cold and people evacuation to shelters resulted from the failure of heating systems. Most heating systems -- with the exception of energy inefficient electric heating systems -- require a small amount of electrical power to run.
- Food and other perishable damage resulted from the failure of refrigerating units which do not require vast amounts of electrical power
- Communication breakdown (TV, radio, computer) put people in precarious conditions and contributed to lower businesses productivity. Computer and communication equipment typically requires little electrical power.

Customer-owned grid connected photovoltaic PV systems equipped with emergency battery back-up storage could have provided the needed fraction of power and prevented much of the above collateral ice-storm damage. Reasonably sized PV systems (i.e., 1-2 kW for individual residences) would have supplied enough energy to power refrigerators, emergency lights, computer and communication equipment as well as [non-electric] heating systems. This assertion is based on a site time specific monitoring of the solar resource following the ice storm, using cloud cover data from geostationary weather satellites. A quantitative analysis of a specific point near Plattsburgh, New York (Figure 3), shows that the solar resource, although not optimal every day, was far from zero in the weeks that followed the onset of the storm on January 7-8. Regionally, the average hourly output of a 1 kW-ac PV system in the area affected by the storm would have been of the order of 120-150 Watt. Therefore, a typical 2 kW residential PV system with a 10 kWh emergency battery storage would have been able to sustain a 250-300 Watt continuous load over the two-week outage period. This is more than enough to sustain all critical loads. Meeting these critical loads would have considerably lessened the financial impact of the storm for the affected customers.

The added benefit of user-side power output reliability, demonstrated through these power outage case studies should further increase the economic attractiveness of PV to all concerned parties: end-users, the insurance industry, governments and electric power retailers. Details on this analysis may be found in [8].

Development of the Solar Load Controller: This part of the project is co-funded by the New York State Energy Research and development Authority. Its objective is to develop test and eventually commercialize a controller that could modulate end-use loads so as to maximize end-use PV effective capacity.

The load control strategy that we are developing and testing is applicable to commercial loads. It builds up on the observations that: (1) peak loads for this type of building are driven by air conditioning; (2) it would take only a small amount of reserve energy to increase the peak shaving capability of PV from a 50-60% level for fixed PV systems, up to a 80-100% range [9]. In the proposed control strategy, we replace the needed energy reserve by a

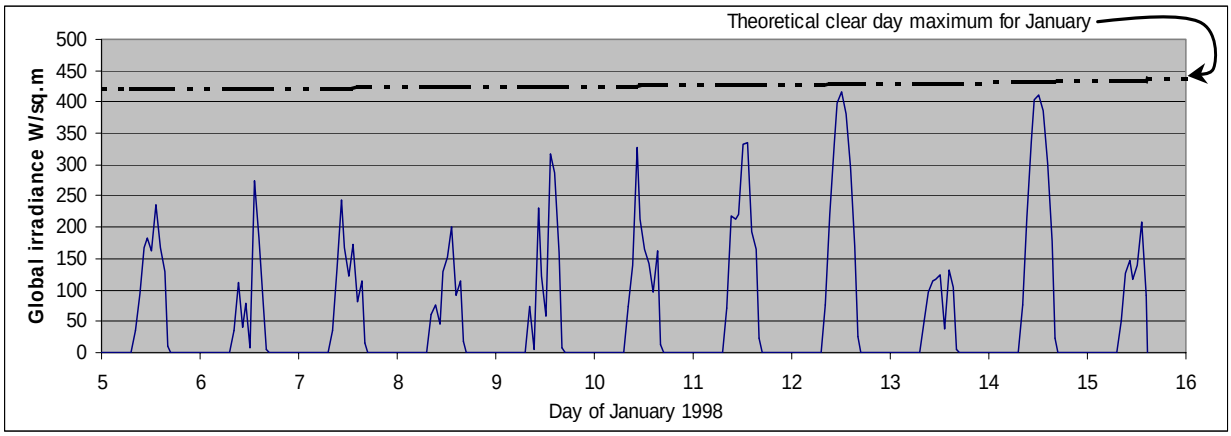

Figure 2: Global irradiance near Plattsburh, New York, following the onset of the ice storm (Jan 5)

small amount of load shedding. Load shedding is accomplished in a very simple, widely applicable and potentially "retrofit-able" fashion by acting upon the threshold setting of energy appliances. An obvious threshold setting is indoor temperature, which is highly correlated to air-conditioning demand as seen in Figure xx.

We are currently testing a prototype controller built around the Energy Management system of the CESTM building that houses our research center. This controller is programmed to override user-controlled indoor temperature settings as a function of PV availability and peak load conditions. Based on simulations using experimental building data, a gain of 20% in the demand reduction capability of PV could be achieved with minimum end-use disturbance of the order of 3-5 degree-hours offset on the worse day.

We expect to be able to report on the actual prototype testing by the summer of 1999, i.e., when the building will have experienced several air-conditioning-driven peaks.

ACKNOWLEDGMENTS: This project was undertaken as a part of NREL contract XAD-817-671-01 (Christy Herig, project manager). The load controller is co-funded by NYSERDA contract 4694-ERTER-ER-98. Satellite data acquired under NREL contract XAH-515-222-01enabled us to investigate the power outage case studies.

REFERENCE

1. Richard Perez and Robert Seals, (1997): Solar Resource utility Load matching Update. NREL PV Program FY 1996 Annual Report, pp. 455-458, NREL/BK-210-21966, NREL, Golden Colorado.
2. Howard Wenger, Christy Herig, Roger Taylor, Patrina Eiffert and Richard Perez, (1996): Niche Markets for Grid-Connected Photovoltaics. Proc. IEEE Photovoltaic Specialists Conf., Washington, DC.
3. Perez R.and R. Seals (1996): Mapping PV's Effective Capacity. Proc. UPVG mtng. (UPVG, Washington, DC)
4. Perez R., Wenger H., Herig C., (1998): Geographical Distribution of the Value of Demand-Side Commercial PV Systems in the United States. Plenary article, 2nd World PV Conference, Vienna Austria
5. DSIRE, (1998). NCSC-IREC @ http://www-solar.mck.ncsu.edu/dsire.html
6. R. Perez and H. Wenger, (1998): Final Report on PV Valuation. NREL contracts No. XAD-8-17671-01 and XAX-6-16817-01. National Renewable Energy Laboratory, Golden Co.
7. Herig, C., R. Perez and H. Wenger, (1998): Commercial Buildings and PV, a Natural Match. NREL Brochure DOE/GO-1998 NREL, Golden, CO @http://www.nrel.gov/ncpv/pdfs/pv_com_bldgs.pdf
8. Perez, R., (1998): PV Availability after the 1998 Ice Storm. Proc. Renew 98, NESEA, Greenfield, MA
9. R. Perez, (1997): Grid-Connected Photovoltaic Power: Storage Requirements to Insure 100% Peak Shaving Reliability. Proc. Energy Storage Association Annual meeting, Washington, DC

Title: **Evaluation of Photovoltaic Peak-Shaving Applications in the U.S. Buildings Sector**

Organization: Center for Energy and Environmental Policy (CEEP)
School of Urban Affairs and Public Policy
University of Delaware
Newark, Delaware 19716
TEL: (302) 831-8405 FAX: (302) 831-3098

Contributors: John Byrne, principal investigator; Young-Doo Wang, investigator; Lawrence Agbemabiese, Kyung-Jin Boo, Darren Bouton, James Kliesch, graduate students

Objectives

The Buildings sector continues to offer a sizable market for PV applications. Key utility market sectors for PV that are receiving increasing attention are peak-shaving (PS) and emergency power (EP) applications associated with the commercial buildings sector. In addition to bill savings that accrue to customers from PS uses of PV, customers can avoid unwarned interruption in electricity supply (UPS). The technology also allows utilities to avoid costly upgrading and extension of distribution system to meet increasing peak-demand.

The Center for Energy and Environmental Policy (CEEP) at the University of Delaware has been analyzing the economics of utilizing PV as a PS/EP technology. This work: 1) further refines the concept of Distributed PV-PS systems in the perspective of competitive markets; and 2) performs an extended value analysis of Building-Integrated PV-PS and PV-EP. The PV industry now faces a challenge from the electricity industry restructuring, but has an opportunity as well from major new PV initiatives in the buildings/utility sectors being promoted by the Administration. The objectives of this project during FY 1997 were:

- To perform economic and technical analyses of PV applications on commercial buildings in the U.S., using building load and other data supplied by at least three cooperating utilities;
- To assist the State of Delaware, and up to two other states upon request, in identifying high-value PV applications on public buildings;
- To identify PV value analysis refinements in light of an emerging competitive electricity market.

Tasks and Research Results

Task A: Economic and Technical Analyses of PV Applications on Commercial Buildings

CEEP has conducted economic analyses of DPS-PV for commercial buildings across several states. Specific building types and regions have been selected for load characteristics most suitable for cost-effective DPS-PV applications. The results indicate that dispatchable peak-shaving PV systems are well suited for large office buildings and fast food restaurants located in the northeastern part of the U.S. and North Carolina. The northeastern region has relatively high electric rates, and North Carolina offers a 35% renewable energy investment tax credit. The calculated benefit-cost ratios show greater than or equal to 1.00, indicating cost-effectiveness at current installed PV systems prices (excluding storage) of $8.70 per Wp.

Researchers at CEEP also analyzed the additional benefits of PV-PS systems serving as emergency back-up power. CEEP developed a methodology to integrate such additional benefits into benefit-cost analyses using PV-Planner developed by CEEP. Analysis based on this methodology was conducted across five different utility jurisdictions for both emergency lighting (EL) and uninterrupted power supply (UPS) systems, assuming three different levels of reserve battery storage (see Tables 1 and 2). A comparison of the values for each function showed that the value added by UPS to a DPV-PS system is moderately less than that added by an EL function for equal amounts of DPV-PS battery power allocated. This was due to the fact that storage cost constitutes a much smaller ratio of the total costs of conventional UPS systems. As shown in the tables, benefit-cost ratios of greater than 1.00 were identified in some selected utility districts.

Table 1. Estimated BCRs for DPV-PS (EL) in Selected Utility Jurisdictions

UTILITY	BCR w/o EL*	Low Risk	Moderate Risk	High Risk
Boston Edison	0.87	0.88 - 0.90	-0.07	1.10 - 1.28
Duke Power	0.99	1.00 - 1.01	1.09 - 1.15	1.22 - 1.39
S. California Edison	0.77	0.79 - 0.80	0.85 - 0.90	0.95 - 1.09
City of Austin Electric	0.77	0.78 - 0.79	0.85 - 0.99	0.95 - 1.09
Sacramento Muni. Util. Dist.	0.74	0.75 - 0.76	0.82 - 0.86	0.91 - 1.03

Table 2. Estimated BCRs for DPV-PS (UPS) in Selected Utility Jurisdictions

UTILITY	BCR w/o UPS*	Low Risk	Moderate Risk	High Risk
Boston Edison	0.87	0.88 - 0.88	0.92 - 0.94	0.98 - 1.03
Duke Power	0.99	1.00 - 1.00	1.04 - 1.06	1.11 - 1.15
S. California Edison	0.77	0.78 - 0.79	0.83 - 0.85	0.89 - 0.93
City of Austin Electric	0.77	0.78 - 0.78	0.81 - 0.83	0.86 - 0.89
Sacramento Muni. Util. Dist.	0.74	0.75 - 0.75	0.79 - 0.80	0.84 - 0.88

* Note: These figures include peak-shaving benefits *only.*

Task B: High-Value Photovoltaic Applications in Public Facilities

1. State Facilities

CEEP conducted a survey of State owned office buildings in Delaware to identify potential high-value PV applications. Currently, the State of Delaware owns approximately 900 facilities, most of which are located on multi-building complexes. They are scattered in three counties, New Castle, Kent, and Sussex. Facilities metered for monthly kW loads are mainly found in New Castle County where most State facilities are handled by Delmarva Power. Data availability to analyze high-value peak shaving applications is, thus, limited.

Several criteria were considered in selection of buildings for economic analysis: 1)roof-type, gable or flat; 2) independent and individual pulse meter; 3) size of building, and 4) age of building. Three State facilities equipped with the pulse meters were selected for initial analysis. Initial analysis based on the building electricity peak load pattern shows benefit-cost ratios between 0.7 and 0.8, which is consistent with previous findings by CEEP. Delaware has below-average electricity rates.

A new payback period methodology was created to fully account for the tax benefits gained by the consumer. The new analysis was adjusted to deduct the tax benefits over the first five years only, as opposed to deducting even portions of the tax benefits over the 25 year lifespan of the equipment. The net result shortens the payback period, making the PV system more attractive to the customer.

2. Cost-Effective PV Applications on Federal Buildings:

CEEP prepared preliminary screening analysis for NREL on possible cost-effective applications of PV systems for peak-shaving and emergency power in federal buildings. The report examined the economics of uninterruptible power supply (UPS) as an added value to dispatchable peak-shaving PV systems installed on specific building types. This study was conducted based on two economic feasibility guidelines used by the Federal Energy Management Program (FEMP). CEEP's report concludes that there are cost-effective opportunities, at existing module prices, for the use of these dual functions v.s. systems at federal facilities. CEEP also suggests that overseas federal buildings, where electricity prices are typically higher and/or reliability is poorer than in the contiguous U.S., should be promising sites for these systems.

Task C: Reevaluation of PS-PV system in the light of an emerging competitive electricity market.

In response to the recent development of competitive electricity markets, a number of incentive programs are being considered: portfolio standard, green pricing, system benefits charge, and buy-down financing costs of renewables. Each of these mechanisms constitutes government intervention in an otherwise biased competitive market. Such incentives will definitely create favorable environment for DPS-PV applications. CEEP is evaluating them in terms of their impacts on the near-term PV market.

CEEP has incorporated the distributed utility (DU) concept in the DPS-PV analysis. In the competitive environment in the electricity industry, DU is emerging as a key concept. Research has shown that a utility and its customers can benefit from targeted DPS-PV applications in the areas where the utility s avoided costs are high when combined by time variable. A DU analysis that evaluates localized benefits can assist utilities and regulators in their efforts to identify high-value PV applications in an emerging competitive electricity markets.

A DU approach also represents an institutional shift in which new emerging modular technologies can play a role in a new less centralized, environmentally less polluting electric utility

industry. CEEP researchers recently published a paper describing the methodology for comparing the DU approach to the conventional economic externality model in evaluating the economics of PV in a deregulated electricity market (see Letendre et al., 1998). CEEP, based on this initial study, is further working on economic and technical evaluations of DPS-PV systems in light of an emerging competitive electricity market.

References

1. Byrne, John, L. Agbemabiese, and D. Redlin. 1997. *Evaluating The Additional Value of Emergency Power Applications in Dispatchable PV Peak Shaving Systems*. Prepared for National Renewable Energy Laboratory. May. Center for Energy and Environmental Policy, University of Delaware.

2. Byrne, John, S. Letendre, L. Agbemabiese, D. Redlin and R. Nigro. 1997. Commercial Building Integrated Photovoltaics: Market and Policy Implications. *Proceedings of the 26th IEEE Photovoltaic Specialists Conference*. September. Anaheim, California.

3. Byrne, John, S. Letendre, Y. D. Wang, and C. Weinberg. 1997. *Commercializing Photovoltaics: The Importance of Capturing Distributed Benefit*. June. Albuquerque, New Mexico. ASES 1998-Forthcoming.

4. Byrne, John and Ralph Nigro. 1997. *Building Integrated Photovoltaics for Federal Facilities: Possible Cost-Effective Applications.* December.

5. Byrne, John, Y.D. Wang, and S. Letendre.1997. *Building Load Analysis of Dispatchable Peak Shaving PV System: A Regional Analysis of Technical and Economic Potential.* April. ASES Solar Energy Forum. Washington D.C.

6. Center for Energy and Environmental Policy, PV Planner: *A Spreadsheet Analytical Tool for Grid-Connected Applications.* Report submitted to the National Renewable Energy Laboratory, 1996.

9.0 International Applications and Markets Project

9.0 INTERNATIONAL PV APPLICATIONS AND TECHNICAL SUPPORT – Introduction

Jack L. Stone

During FY 1998 the International PV Applications and Technical Support Project continued to provide technical assistance for internationally focused analytical, applications, education, training, modeling, and technical feasibility studies for the DOE PV Program and the Office of Utility Technologies (now the Office of Power Technologies). The overall objective of the project is to provide technical assistance to energy decision makers in the important populous countries of the world which will lead to expanded business opportunities for the U.S. PV industry. The credibility of the U.S. government is used to facilitate the introduction of U.S. PV industry leaders to potential joint venture partners, financial organizations, and potential end users of PV systems. The following is a brief synopsis of the activities in various countries and associated support activities.

China

China received high profile attention from the Administration in FY 1998 with State visits from Jiang Zemin to the US and President Clinton to China. Renewable energy and energy efficiency took a prominent position on the agendas of these visits due to the recent emphasis on climate change issues. NREL supported DOE in the Administration preparation for these visits and recognition was given to work under the bilateral cooperation with China within the Energy Efficiency and Renewable Energy Protocol.

Progress in the bilateral cooperation between the U.S. Department of Energy and China under the Energy Efficiency and Renewable Energy Protocol agreement was substantial in FY 1998. This progress covered extensive projects and cooperative activities in the PV, wind, biomass, solar thermal, and geothermal technologies, and also included extensive business development activities and renewable energy policy studies. Two major activities in FY 1998 that involved support of the PV program included: i) extensive support of Allan Hoffman's DOE mission to China in March/April 1998, which laid the groundwork for expanded renewable energy bilateral cooperation with China in FY 1998, and ii) groundwork for the First US-China Joint Working Group Meeting on the Energy Efficiency and Renewable Energy Protocol (this meeting was held in Washington, D.C. November 4-6, but the extensive preparations occurred in FY 1998). The Working Group Meeting was the first major joint review of all protocol activities and established the work plan for FY 1999.

Important highlights of China activities in FY 1998, include: i) the "US/China Workshop on Small PV/Wind Technology Applications for Rural and Remote Development in China" conducted in Beijing During September 16-18 1998, involving 10 US companies and 20 Chinese companies, and resulting in several business development activities between US and Chinese companies, ii) completion of the installation of 300 household and school PV lighting systems in Gansu Province, and completion of a survey of these

systems after several months of operation, iii) delivery of equipment to Inner Mongolia for installation of over 200 PV/wind remote household systems in a pilot commercialization project, iv) completion of data collection for market and application characterization surveys for rural electrification options in three key provinces in Xinjiang, Qinghai, and Inner Mongolia (analysis of this data being done in FY 1999), v) completion of the background work for several reports characterizing PV business opportunities in China. The business related reports include: i) an extensive survey and interviews with over 25 companies in China representing all sectors of the PV industry, ii) preparation of a general PV technology status report for China, and iii) a provincial renewable energy business survey report of several provinces in China. All reports were completed in draft for in FY 1998 and will be published in final form early in calendar year 1999. These reports are expected to be a major resource for the US industry interested in pursuing business opportunities in China.

There were also several training and technical assistance activities in FY1998, including on-site training at NREL of four Chinese personnel, and technical assistance to China in the establishment of two regional testing and training centers in northwest China. There was also extensive assistance to numerous Chinese delegations visiting the US with training actions at NREL and assistance in making contacts with US companies. Complementary assistance to US groups was provided by our Chinese partners in the Center for Renewable Energy Development in Beijing. Major support was also provided to DOE throughout the course of FY 1998 in the routine management of four annexes under the Energy Efficiency and Renewable Energy Protocol and strategic planning for the overall Protocol.

India

The activities in India in FY 1998 continued to build on the successes of the rural electrification initiative which has been carried out as a cost shared program for the past five years. Installations of U.S. supplied PV systems were completed in the Sundarbans region of West Bengal. Eight villages were provided with three hundred home lighting systems as well as several other applications, including water pumping, community lighting systems, battery charging, vaccine refrigeration, and electrification of several youth clubs and one medical facility. The project was carried out on cooperation with the Ramakrishna Mission, a well respected humanitarian organization in the area.

An extensive before and after social and economic impact study was carried out under subcontract by the Tata Energy Research Institute which was comprised of interviews with many of the beneficiaries of the PV systems in the Sundarbans. The initiative was judged as a success based on end user satisfaction and on the fact that several thousand systems have been sold to villagers in the same region. This study was completed only within several months of the final installations, and it is planned to repeat the activity after over a year of operational experience has been accumulated.

Before the end of the fiscal year, world events overtook this project when the U.S. State Department imposed sanctions on India because of their resumption of nuclear weapons testing. As of the time of this writing a waiver of the sanctions has been requested because of the humanitarian nature of the project. Assuming approval of this request, it is planned to continue with the Ramakrishna Mission by testing technical feasibility of various commercially available thin-film product from U.S. manufacturers. In addition the systems behavior will be evaluated

from the previous installations and a lesson learned report will be generated which will benefit U.S. industry for future business in India.

Brazil

Data collection continued for the two 50 kW hybrid power systems installed under the auspices of the U.S.-Brazil cooperative program. U.S. industry continues to benefit from this past activity in the form of expanded business opportunities in the country. Brazil continues to represent an opportunity for utilization of PV systems in the many isolated communities of the country, especially in the Amazon River basin. The Brazil projects were the vanguard activities of the DOE international projects which now reach into many areas around the world. As is the case with all of the previous activities, we are in the process of transitioning all of them to sustainable programs.

Other HQ and International Support

Roger Taylor coordinated the PV International Activities with the NREL program.

The Village Power Conference detailed the opportunities to expand PV into developing countries.

Three principal agencies, UNDP, World Bank, and US-AID, continue to aggressively support renewable energy options around the world. This project continues to support these activities where appropriate.

This project continues to support DOE and NREL with visitors from many foreign countries who arrive at NREL to learn more about renewable energy and the options that are commercially available.

International Applications and Markets Project Subcontracts

Title: **Renewable Energy Business Development in China**

Organization: Center for Renewable Energy Development
Zhansimen Road
Shahe, Changping County
Beijing 102206
People's Republic of China
TEL: 011 86 10 6973-7074 FAX: 011 86 10 6973-3110

Contributors: Li Junfeng

Objectives

The overall objective of this subcontract is to promote cooperation to assist renewable energy business development in China through information exchange with the US and Chinese renewable energy industries, encouragement of business development activities between US and Chinese companies, and providing technical assistance in activities that can have an impact on renewable energy market development in China. Objectives include:

- To establish a framework for specific collaboration in order to promote renewable energy business development between the United States and the People's Republic of China, to help create market opportunities for suppliers of renewable energy products and services, and to encourage investments and other participation in renewable energy projects.

- To support the development of an extensive information base consisting of business related data from the U.S. and China for mutual exchange with renewable energy companies in both countries, detailed data collected on a province by province basis in China, technology status reports, market information, and policy status and trends. This information will be actively exchanged between the two countries.

- To proactively support the development of projects, project participation by the U.S. and China renewable energy industries, and the financing of projects by multiple sources, by: i) creating data bases for current and future projects and submitting the information in a timely manner to renewable energy industry groups in both countries, ii) providing technical assistance to multilateral development banks and agencies for support of renewable energy project development and financing, and iii) providing technical support to the Governments in both countries and to the renewable energy industry.

- To promote capacity building and the increased understanding of the renewable energy status and opportunities in both countries by promoting personnel exchanges, including individuals for training programs, companies for business development, and support of workshops.

Research Results

Business Information Development

During FY 1998, the Center for Renewable Energy Development in Beijing provided assistance to two US consultants. These two consultants had the task of developing information of use to the US and China business communities. Scott Vaupen conducted a tour of four

provinces in China to assess renewable energy markets, interview companies, generate a database for projects, and generally characterize the business and regulatory environment in those provinces. The provinces included Guangdong, Jiangxi, Jilin, and Yunnan, with an update of information for Beijing. The tour expanded upon a previous survey conducted in Inner Mongolia, Gansu, Shandong, Qinghai, Xinjiang, and Zhejiang. This survey covered all renewable energy technologies. Chris Sherring of Sherring Energy Associates conducted a survey of over 25 PV companies in China in several provinces. These PV companies covered the full range of PV business activities, including module manufacturing, balance-of-system component manufacturing, system integration and distribution.

Technology Status Reports

The Center for Renewable Energy Development prepared a draft report for the commercialization of PV Systems in China. The report characterized the status of PV development in China in terms of applications and markets, solar resource, existing system and manufacturing development, and international/domestic programs supporting PV. The report identifies barriers and new initiatives in support of further commercialization of the PV technology in China.

Professional Training

During FY 1998, four personnel received training at the National Renewable Energy Laboratory. These personnel were from the Center for Renewable Energy Development in Beijing and were sponsored by the State Economic and Trade Commission in Beijing. Two personnel on three month training assignments received training in Geographical Information System (GIS) analysis using ESRI ARC/INFO GIS software applications. These two personnel were also exposed to several analytical software applications for Life Cycle Analysis (LCA) and pursued a case study using LCA analysis. These training activities were directed toward applications involving solar and biomass resource assessment and technologies. Two additional personnel received training on US policy development for commercialization of renewable energy technologies. This information was used to generate a database and preliminary recommendations for China policy development to promote renewable energy. This work is continuing now in China to develop policy initiatives for the State Economic and Trade Commission to promote wind energy development and the use of PV for rural electrification.

Technical Assistance for Renewable Energy Financing

The Center for Renewable Energy Development in Beijing and the National Renewable Energy Laboratory in the US have collaborated in providing technical assistance to the World Bank and the United Nations Development Program. These two organizations are developing renewable energy assistance programs in China. The World Bank program will generate more than $400 million USD in funds for large-scale wind farm development and PV rural electrification projects, and the UNDP program will generate over $38 million USD in funds for PV, wind, and biomass projects. Technical assistance was also given to the State Development Planning Commission and the State Economic and Trade Commission in Beijing in the development of financing for PV and wind projects in China.

Information Clearing House

The Center for Renewable Energy Development produces bimonthly newsletters covering recent renewable energy activities in China. Information includes updates on projects,

changes in the government and new policy initiatives, updated market information, and other information. This information was distributed to the US renewable energy industry through the US Export Council for Renewable Energy and the renewable energy trade organizations, such as the Solar Energy Industries Association.

Workshop Activities

The Center for Renewable Energy Development provided support for the recent "Workshop on Small PV/Wind Technology Applications for Rural and Remote Development in China," conducted in Beijing, September 16-18, 1998. This workshop was attended by 10 US companies and over 20 Chinese companies associated mainly with PV development for rural electrification , but also including some small wind companies.

References

1. Vaupen, Scott, "Renewable Energy Markets in China: An Analysis of Renewable Energy Markets in Guangdong, Jiangxi, Jilin, and Yunnan with Updated Information from Beijing," August, 1998, in revision, to be published as NREL Report.

2. Sherring, Chris, "China PV Business and Application Evaluation," October, 1998, in revision, to be published as NREL Report.

3. Li, Junfeng, et al, "Commercialization of Solar PV Systems in China," draft report prepared January, 1999, in revision, to be published as NREL Report.

Title: **Rural Electrification Using Photovoltaics in Northwestern China**

Organization: Chinese Ministry of Agriculture
No. 11 Nongzhanguan Nanli
Beijing 100026
China
TEL: 011 86 10 6419-2610 FAX: 011 86 10 6500-2448

Contributors: Li Jingming

Objective

In February, 1995 the Secretary of the U.S. Department of Energy signed the Energy Efficiency and Renewable Energy Protocol agreement in Beijing, China with the State Science and Technology Commission. Under this protocol agreement, Annex I for "Developing Cooperative Activities in the Area of Renewable Energy under the Hundred Counties Integrated Rural Energy Development Program in China," was singed in June, 1995 by the U.S. Department of Energy and the Ministry of Agriculture. Annex I specifies projects emphasizing biomass and photovoltaics, but also including other technologies, and specifies an initial project by mutual agreement between the MOA and DOE of building an infrastructure for deploying household PV systems in rural areas of China building on the previous experience in Gansu Province in China. The emphasis of the current work is on performing a market characterization analysis of two additional provinces in Xinjiang and Qinghai in northwestern China and supporting a regional center for testing and training in Lanzhou, in Gansu Province.

The objectives of this scope-of-work are:

- To expand the use of photovoltaic renewable energy systems throughout western and northwestern China for solar home lighting, educational systems in schools, and other rural electrification applications by extending the knowledge base developed in the solar home system project which is being successfully implemented in Gansu and improving upon the technology and sustainable infrastructure development which has been conducted in Gansu.

- To perform technical and economic rural electrification options analyses in at least two additional provinces, Qinghai and Xinjiang, to compare the relative cost effectiveness of renewable energy options based on PV, wind, and PV/wind hybrid systems with conventional fossil fuel options. Levelized cost analyses will be performed based on the experience developed for similar kinds of analyses performed in Inner Mongolia.

- To characterize the market for solar home systems and other renewable applications in Qinghai and Xinjiang by examining the overall market potential, identifying the high priority areas to target for project development, and assess socio-economic factors for developing sustainable commercial markets for solar systems.

- To provide support for improving and upgrading existing facilities for the testing of rural energy systems and providing training for engineering and marketing personnel to serve as a regional facility for northwestern China.

Research Results

Rural Electrification Options Analysis in Qinghai and Xinjiang

This work is being conducted in cooperation with the Center for Energy and Environmental Policy in the University of Delaware. Based on rural electrification options analyses previously performed in Inner Mongolia extensive data templates were prepared to collect remote household and village data in five counties in each of the Provinces of Xinjiang and Qinghai. The data consisted of household statistical data for unelectrified households and households which owned renewable energy systems.

A characterization of the market for solar home systems in Qinghai and Xinjiang is being performed using the data to characterize the current development situation, evaluate the industry and assess technologies, identify areas for project development, analyze barriers, and develop sustainable implementation strategies for commercial market development.

The market characterization is taking into account the current industry situation in these provinces, including: i) current distribution of systems and overall market potential, ii) current status of industry development in the provinces, and iii) current status of technologies being deployed and needs for improvement.

The market characterization is taking into account the identification of high priority areas for development at the county and township level, including: i) resource availability, ii) current economic and environmental status, including needs and ability/willingness to pay, iii) electricity supply situation, iv) future economic and social development and v) grid development plans and costs.

The market characterization is identifying restrictions and market barriers, including: i) resource factors, ii) technology factors, iii) economic and social factors, iv) policy factors and development of policy initiatives, and v) others.

Data requested included family statistics, technical operating data on existing systems, energy usage, needs, etc. County level data and provincial data were also requested. The data is being processed to perform rural electrification options analyses to assess the technical performance and economic value based on levelized cost analysis of existing renewable options for remote and village household electrification using solar photovoltaic, small wind, and hybrid systems in comparison with conventional fossil fuel options. This survey will complement other survey work being performed in northwestern China to develop a detailed market analysis, supported by the World Bank.

During the summer of 1998 the first survey was conducted in ten counties in the two provinces and the data evaluated. It was found that additional data is required to perform an adequate statistical analysis and that data will be collected in a final survey to be conducted in March 1999. Preliminary analysis of the existing data is being performed at the University of Delaware. The analysis project will be completed in mid-1999.

Market Prospect and Development Strategies for Solar Systems in Qinghai and Xinjiang

The market characterization is contributing to an implementation strategy for promoting the sustainable commercial development of solar home system markets, including considerations related to technology status, industrial development, policies and regulations, institutional

construction, and international experience. The implementation strategy development is cooperating with the Hundred Counties Integrated Rural Energy Construction Project in China. The strategy is feeding into plans for the development of a 10,000 solar home system project in progress at the Chinese Ministry of Agriculture and is cooperating with the national solar development program incorporated in China's Brightness Program. The Ministry of Agriculture has initiated the 10,000 solar home system project by installing 3,000 systems in the two provinces in 1998.

Regional Facilities for Testing and Training

The Chinese Ministry of Agriculture is upgrading the facilities at the Lanzhou Solar Research Center of the Gansu Natural Energy Research Institute to establish a regional facility for testing solar systems for rural applications and to train rural energy technicians and marketing personnel. Functions of the facility will include product development, information exchange, personnel training, product testing and quality monitoring.

Support of the facility will include: i) upgrading some of the equipment of the facility, ii) improving the training facilities, iii) providing some of the monitoring equipment of the facility, and iv) improving communications capability. Support for increasing the institutional capacity for the widescale deployment of solar equipment will be given by the facility in the form of: i) training personnel who will become trainers at the facility, ii) developing training programs for project appraisal, management, technical service, new technologies, and domestic training, iii) assistance in developing testing procedures and establishing qualification standards, iv) compilation of training materials, and v) organizing training courses. The China side is contributing equipment and logistical support for the center. The US side is providing technical assistance by participating in training activities, to date through the Solar Electric Light Fund, and advice on equipment, test procedures, and technology.

Title: **China PV Business and Application Evaluation**

Organization: Sherring Energy Associates
3 Bellaire Drive
Princeton, NJ 08540
TEL: 609/799-8889 FAX: 609/799-5258

Contributors: Chris Sherring

Objectives

The work was performed under the Energy Efficiency and Renewable Energy Protocol agreement signed in February 1995 between the Chinese State Science and Technology Commission and the US Department of Energy. This Protocol initiated bilateral cooperation between the U.S. and the People's Republic of China for renewable energy development. Under this Protocol, Annex IV was signed between the U.S. Department of Energy and the Chinese State Economic and Trade Commission in June 1996 to establish cooperation for business development for renewable energy technologies in China. One of the activities under Annex IV is the development of business related information in China for use by the US renewable energy industry.

The overall objective of this subcontract is to perform an evaluation of the PV business sector in China and produce information that will be helpful to the US PV industry in pursuing business interests in China. The subcontractor conducted a review and assessment of related industries, technologies, markets and channels of distribution to characterize PV commercial sectors. The subcontractor identified high potential PV applications and market sectors of high growth potential. The assessment also included recommendations for facilitating useful and effective interfaces between the U.S. and Chinese renewable industries in developing photovoltaics in China and in developing mutually beneficial business relationships with each other. The objectives for this statement of work are:

- To review existing information related to PV in China, establish a liaison with the Center for Renewable Energy Development and PV experts in China, and plan an efficient review of all sectors of the PV industry in China.

- To conduct an in-country evaluation of all sectors of the PV industry, applications, and market segments China in order to collect extensive relevant information of use and benefit to the U.S. renewable energy industry and other interested parties.

- To prepare a report detailing the information obtained during the evaluation, including an evaluation of business opportunities for U.S. companies in China and recommendations for how to facilitate business interactions.

- To disseminate the findings of the evaluation to the U.S. PV industry and other interested parties.

Research Results

The subcontractor met with more than 100 PV specialists in China to perform the survey and assessment of the Chinese PV industry. He was assisted by the Center for Renewable Energy

Development in Beijing. During a 40 day tour in China, the subcontractor met with more than 22 companies associated with all sectors of the PV business community, including module and BOS manufacturers, system integrators, distributors, and representatives of the government sector. Visits were made to Beijing, Xining in Qinghai Province, Lanzhou in Gansu Province, Hangzhou and Ningbo in Zhejiang Province, Shenzhen and Foshan in Guangdong Province, Kunming in Yunnan Province, and Qinhuangdao in Hebei Province.

After either visiting or meeting with all of the indigenous PV manufacturers, most of the distributors/systems integrators and the key institutions involved in developing PV technologies and business, the following are some of the conclusions reached.

- The current PV manufacturing technology in China is significantly (5-10 years) behind that of industry leaders in the West.

- Technology updates for the Chinese PV industry are not readily available from either Provincial or National institutes who are currently being encouraged to manufacture and sell products in competition with the very industries that need their help.

- There is an overwhelming desire to collaborate with US PV industry in order to update the technology and develop the vast PV market potential, however, there is neither a clear understanding of the range of US PV companies and their technologies nor of their specific competitive strengths and weaknesses.

- The "manufacturer" of charge regulators, inverters and dc light ballasts in general by 10-50 person distributor/integrator operations with limited experience is considered to be the least reliable aspect of the PV industry.

- The larger scale, professionally designed, quality controlled, manufactured product currently being produced in China is considered too expensive by the distributors who opt to make their own. The real cost of reliability is born by the end customers.

- The emphasis on low cost systems assembled by distributor/integrators competing solely on price leads to the adoption of poor or unsuitable storage batteries resulting in short battery life.

- The PV markets are currently dominated by small (~ 10 watt), semi portable solar home systems (SHS) which are sold to widely dispersed rural customers with little or no service infrastructure.

- The limited resources of the majority of distributors do not permit the development of the critical service infrastructure required to serve the remote markets.

- The majority of existing and potential end users are ill equipped, at this stage, to make informed system choices.

- At this fragile stage of market development there is a need for a buffer between remote, ill-informed rural customer and short-term commercially motivated suppliers.

- There is a ready, cash market today for many 10's of thousands of SHS per annum.

- It is likely that most of the current small SHS that are sold to rural customers fail within a

short period (< 12 months).

- There is little quantitative data on the reliability of small systems in the remote markets.
- The very nature of the remote rural markets makes the absence of reliability data even more dangerous. No news is not necessarily good news.
- Some innovative credit mechanisms have been successfully applied to the sale of remote SHS however; there are many examples of ineffective credit programs.
- At the provincial level there is little knowledge of the critical evaluations undertaken and the experience gained in other parts of the world in adopting PV rather than grid extension as a reliable, appropriate and more cost effective way of providing electricity to remote regions.
- Making this data and experience available in the right form, to a broad range of organizations, concerned with the provision of services to remote communities should accelerate the adoption of distributed PV electrification where appropriate.
- The modest module wattage of the majority of the current PV systems sold suggests that Thin Film PV technology can be an appropriate, reliable and cost effective choice for manufacturing solar panels.
- Poor experience with indigenous thin films has stalled the adoption of arguably the most appropriate technology.

The report includes survey information on 22 specific companies contacted in this project. The report also includes an analysis of the status of PV business sectors, such as manufacturers, distributors, etc., and discusses improvements that are needed to promote improved business practices and support market expansion in China. Opportunities for participation of US companies in the China PV markets are identified in terms of companies, applications, products and expertise needed, and regional market opportunities.

Reference

Sherring, Chris, “China PV Business and Application Evaluation,” October, 1998, in revision, to be published as NREL Report

Title: **Photovoltaics for Rural Energy in Gansu Province in the People's Republic of China**

Organization: Solar Electric Light Fund
Suite 595
1775 K Street, N.W.
Washington, D.C. 20006
TEL: 202/234-7265 FAX: 202/328-9512

Contributors: Robert Freling

Objective

In February, 1995 the Secretary of the U.S. Department of Energy signed the Energy Efficiency and Renewable Energy Protocol agreement in Beijing, China with the State Science and Technology Commission. Under this protocol agreement, Annex 1 for "Developing Cooperative Activities in the Area of Renewable Energy under the Hundred Counties Integrated Rural Energy Development Program in China," was singed in June, 1995 by the U.S. Department of Energy and the Ministry of Agriculture. Annex 1 specifies projects emphasizing biomass and photovoltaics, but also including other technologies, and specifies an initial project by mutual agreement between the MOA and DOE of building an infrastructure for deploying household PV systems in rural areas of China building on the previous experience in Gansu Province in China.

The objectives of the statement of work are as noted:

- To prepare and execute a more detailed monitoring plan for the remote household solar home system project that will allow a more accurated and detailed assessment of the performance of the project in terms of system performance and success of the infrastructure building activities in the project.

- To explore the concept of a village telecommunciations system that complements the household applications of solar home systems and provides added value and services for users of small solar energy systems in China.

- To provide an interim project assessment report based on the Phase I installation of 300 household systems, considering installation, technical performance of installed systems, project financial performance, company performance, and success of the infrastructure capacity building activities associated with the project.

- To install and collect data from several data acquisition systems installed at households to monitor system performance in detail.

Research Results

An assessment of Phase I of the Gansu project was conducted by Robert Freling in June-July 1998. A total of 331 systems were installed in Phase I, including: 180 systems of 20 Watts containing US modules and batteries, 10 systems of 50 Watts for school systems containing of complete US systems, 20 USSC 22 Watt lighting kits from the US, and 126 systems of 20 Watts containing Chinese equipment that were purchased from a revolving account established for the

project. The purchase of additional systems using customer receipts in the revolving account leveraged the project by about 40%.

The subcontractor prepared a survey instrument for a mid-term assessment of the 300 installed systems in the Gansu Project. A survey company was hired in Lanzhou in Gansu Province and the survey of the 300 household and school systems was conducted in the Fall of 1998. Preliminary analysis of the survey has been performed and a more detailed analysis of survey results in progress and will be published during 1999. The survey was very effective at characterizing the rural households in Gansu receiving the systems, what the systems were used for, future plans for acquiring larger systems, income capacity of households, maintenance issues, and system failures. In general, the major issue identified was the quality of compact fluorescent lights acquired from Chinese manufacturers, which accounted for most of the maintenance requirements during the first five months after installation. There was general satisfaction with most of the systems and with the other system components. Problems were also identified which have been discussed with system vendors and installers in Gansu.

The subcontractor investigated two additional applications of PV for remote unelectrified villages. Discussions were conducted with several companies and the local government in Gansu regarding the potential for installing PV powered radio telecommunications systems in villages. Installations of phone systems in remote villages is a market that is beginning to open up in northwestern China. There have also been discussions with the provincial government regarding more advanced school systems that would incorporate satellite linkage, closed-circuit television for training, and internet-linked computers.

During the summer of 1998, five remote data acquisition systems were installed at remote households to begin collecting detailed system operating data over the course of the next year for further system analysis. This is the first time in China that this level of data is being collected at the household system level.

Title: **Evaluation of PV Systems Installed under INDO-US Collaboration Programme, Sundarbans, West Bengal**

Organization**:** Rural Energy Group
Tata Energy Research institute, New Delhi
Tata Energy and resources Institute, Washington, DC

Contributor**s:** Mr. P Venkat Ramana (Principal Investigator)
Mr. Shirish Sinha
Mr. Asim Mirza
Mr. Anand Shukla
Mr. Anil Srivastava
Mr. Pankaj Mohan
Ms. Sumana Dutta

Objectives:

The Tata Energy Research Institute (TERI), Delhi was identified by NREL as an independent agency to carry out pre and post study of the economic and social impacts of the installations of Solar PV systems (SPV) on the end users of domestic lighting systems. TERI also evaluated the implementation process of the project and the role of different agencies involved in the project implementation.

Approach:

The specific activities undertaken by this project included:

- Impact on the process of economic development
- Social-cultural impact
- Financial and economic viability of the technology in the target area, including environmental benefits
- Efficacy of the methods adopted to access the needs, and the ability or assessing willingness to pay by the end users
- Effectiveness of the institutional mechanism created for implementation, operation and maintenance, project feedback, user interface and revenue collection
- Effectiveness of the executing agency in ensuring people's participation and long term sustainability of the project
- Overall replicability of the implementation model in other areas of Sundarbans

The following table lists the PV systems installed in selected villages under the INDO-US project. Under this project, 300 domestic lighting systems, 2 battery charging stations, 1 water pump, one solar refrigeration unit, and eight institutions were provided with lighting systems.

Village	Type of PV systems	Location
Gosaba	Water pump Battery charging station Lighting system Street lighting	Rupayan (Block coordinating office of RKM)
Pakhirala	Lighting system	Weaving centre
Choota Mollakhali	Lighting system Battery charging station	Youth club
Katakhali	Domestic lighting systems Lighting system	100 households Youth club
Satyanarayanpur	Lighting system Street lighting Refrigeration unit	Health centre
Kumirmari	Domestic lighting systems Lighting system	100 households Youth club
Satjelia	Domestic lighting systems Lighting system	100 households, and Youth club
Shantigachhi	Lighting system	(Training centre)

Results:

Impact of PV system was studied by looking at the variables which could reflect the impact of the intervention. These variables include – education of the school children, entertainment and awareness, health, social and cultural changes, economic benefits, and impact of the lighting systems on the women. The following table gives the percentage of the households, which identified the impact of the PV lighting system.

Impact of PV lighting system – percentage of households

Variables	Repeat survey	Non-repeat survey
Education		
- impact on studies of school going children	88	87
Entertainment and awareness		
- TV programmes and news	44	60

Variables	Repeat survey	Non-repeat survey
Health		
- relief from eye irritation	85	89
- relief from cough and nasal problems	10	11
Social and cultural changes		
- community programmes and festivals	0	0
Economic benefits		
- increase in income	6	4
- improvement in business/occupation	44	34
Impact on women		
- household activities	46	72
- serving of food	12	15
- better light in house	33	80
- easy to use	64	84
- TV programmes (serials and cinema)	78	88
- education of children	21	22
- some economic activity (stitching, weaving, and tailoring)	19	18

Summary:

Rural lighting has positive impacts on the quality of life. In the households, people are able to work longer, education and entertainment. It can be argued that the long working hours would have negative effect especially on the women and use of TV would influence the education of the school children. Nevertheless, these are part of the process of development of the society and any intervention will have its share of negative and positive impacts. Access to electricity influences the standard of living and brings a sense of security to the household.

Title: **Evaluation of Intermediate Applications for Photovoltaics in the United States and Developing Countries**

Organization: Center for Energy and Environmental Policy (CEEP)
University of Delaware
Newark, Delaware 19716
TEL: (302) 831-8405 FAX: (302) 831-3098
Website: www.udel.edu/ceep

Contributors: John Byrne, principal investigator; Young-Doo Wang, Bo Shen, investigators; Lawrence Agbemabiese, Kyung-Jin Boo, Peng Gao, Karen Schwartz and Jihong Zhao, graduate students

Objectives

The integration of PV in peak-shaving (PS) and emergency power (EP) applications is an important component for developing a building-integrated PV market. Key utility market sectors for PV that are receiving increasing attention are PS and EP applications associated with the commercial buildings sector. The Center for Energy and Environmental Policy (CEEP) at the University of Delaware has been conducting and analyzing the economics of utilizing PV as a PS/EP technology. In addition to analyses that foster the development of near-term U.S. markets, work has been done to identify developing country opportunities for the use of PV, in conjunction with wind (in some cases) as a rural electrification technology. With the Ministry of Agriculture and the Chinese Academy of Sciences in China, CEEP is performing a least cost analysis based on the data from a technical and socioeconomic survey of several counties in the provinces of Xinjiang and Qinghai and the Inner Mongolia Autonomous Region in northwestern China.

The objectives of this research during FY 1998 were:

- To provide an economic analysis of building-integrated PV-PS and PV-EP systems in the U.S. and Korean commercial buildings sector; and
- To conduct environmental and economic evaluations of the use of PV as a rural electrification technology in western China.

Tasks and Research Results

Task A: Building-Integrated PV Applications in U.S. and Korean Commercial Buildings

CEEP undertook a technical and economic analysis of the 2.1 kW PV system located on the roof of the Cambridge, Massachusetts headquarters of the Union of Concerned Scientists (UCS) building. When this system is configured to operate as a non-dispatchable energy supply (kWh) technology (NDES-PV), the benefit-cost ratio was found to be 0.58, indicating that, at current capital and operating costs, PV offers little economic benefit to UCS. Reconfiguring the system to operate as a dispatchable peak-shaving (DPS-PV) technology enables it to serve energy management functions, primarily offering firm, peak-shaving benefits on a daily and yearly basis. The net present value of this application on the UCS building is about 7% greater than that of PV as a non-dispatchable energy supply technology. The additional cost of upgrading a building integrated PV (BIPV) energy system to perform an energy management function (about $5000) is more than offset by the value added (nearly $5700) in energy

management to the customer. A substantial share of this benefit is attributable to demand savings ($3,695) which are significantly higher than energy savings (approximately $2,850). The higher demand saving benefit is explained by the capacity charge levied on customers in large buildings. This charge is typically a much higher portion of electricity billings than energy charges. In the case of UCS, 70% of its electricity billings is for capacity.

CEEP also analyzed the economics of the UCS PV array serving an additional emergency power function. It is estimated that the payback period for a system configured in this fashion would be approximately five years. Additionally, the benefit-cost ratio of this application at the UCS site is estimated to be 1.17. These results suggest that the addition of an emergency power function (e.g., to allow orderly shutdown of computer operations) could significantly increase the value of a BIPV system. As indicated in Figure 1, the overall results of the case study indicate that the economic value of the UCS PV array would be optimized in a configuration that serves all three functions: energy supply, energy management and emergency power.

Figure 1. Comparison of Payback Periods for Three BIPV System Configurations

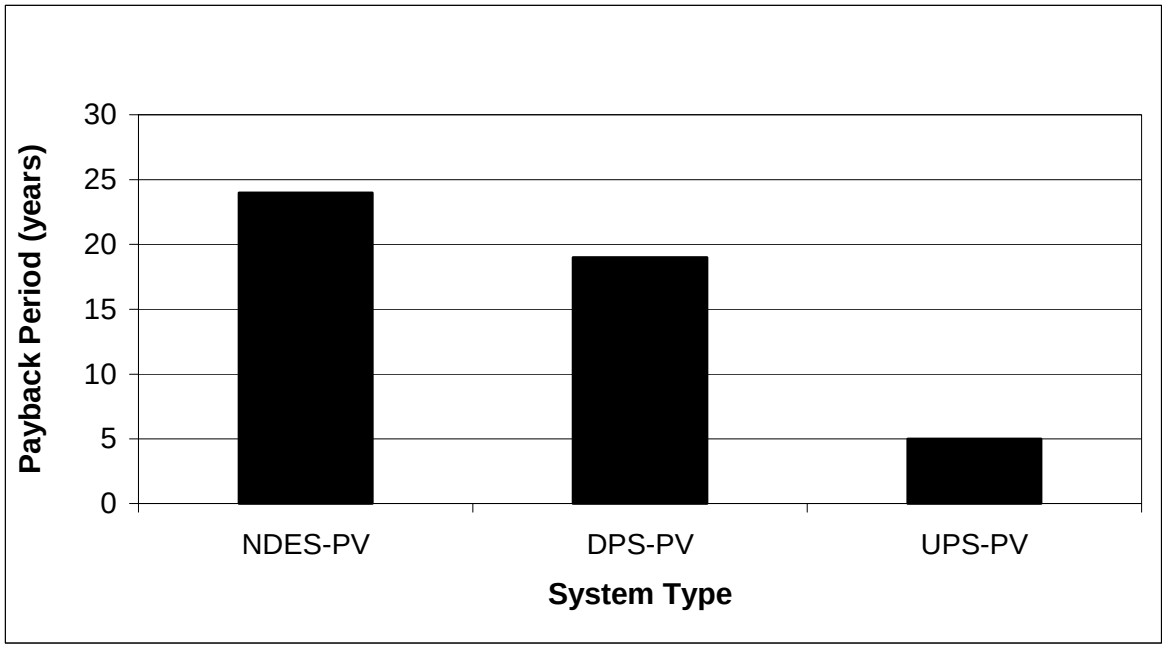

Cost-benefit analyses were also prepared for a large office building, hotel and department store in Korea. Actual building electricity loads were obtained with the assistance of the Korea Electric Power Corporation, and solar resources and temperature data were furnished by the Korea Institute of Energy Research. Staff analyzed the peak-shaving potential of a dispatchable 10 kW PV system and determined its economic value, using computer programs developed at CEEP. Findings were consistent with those found in the U.S. Accelerated depreciation tax benefits, created by the Korean government to spur investment in renewable energy, effectively offset PV s high initial capital cost, making such systems cost-effective (cost-benefit greater than 1.0) if deployed in two cities, Seoul and Taejon.

Task B. PV-PS Applications in Delaware Public Facilities

CEEP has conducted a survey of state-owned office buildings in Delaware to identify potential high-value PV applications. Currently, the State of Delaware owns approximately 900 facilities, most of which are located on multi-building complexes, scattered in three counties New Castle, Kent, and Sussex. Facilities metered for monthly kW loads are mainly found in New Castle County where most state facilities are served by Conectiv (formerly Delmarva Power and Light Company). Seven facilities (metered for monthly kW demand) were selected to provide a representative sample according to the following criteria: 1) roof-type, gable or flat; 2) size of building; and 3) age of building.

The results of CEEP s analysis show a range of benefit-cost ratios between 0.7 and 0.8. Delaware has below-average electricity rates and no incentives for PV system installations such as investment tax credits and accelerated depreciation. Without such policy incentives, additional functionality of PV applications is needed to improve benefit-cost ratios sufficiently for the technology to be cost-effective. The analysis examined the economics of uninterruptible power supply (UPS) as an added value. As shown in Table 1, the addition of a UPS function improves the benefit-cost ratio by 70-80%.

Table 1: Economics of PV-DPS System in the Selective State Facilities

	Benefit-Cost Ratio	
	W/O UPS	**W/ UPS**
WilmFam Court	0.70	1.18
Wilm Penn	0.70	1.18
Div. Stat. Serv.	0.70	1.19
DE Transit.	0.70	1.18
Emily Bissel Hosp	0.71	1.20
Gov. Bacon Health	0.72	1.21
Stockley Health	0.72	1.24

Task C. Support for PV Applications in Developing Countries

CEEP has completed a comprehensive feasibility study of off-grid renewable energy applications in China s Inner Mongolia Autonomous Region (IMAR). The study was undertaken in collaboration with the Institute of Policy and Management of the Chinese Academy of Sciences and the New Energy Office of the Inner Mongolia Government. The analysis, based on a representative sample of 41 households from IMAR, indicates that levelized cost of off-grid, household-scale wind turbine (100-300 W) and PV (20-200 W) energy systems are cost competitive with conventional gasoline gen-sets, and PV/wind hybrid systems appear to be an economic means of providing year-round electricity service while meeting the rising energy demands of households in remote villages in Inner Mongolia. The

findings of this study led the U.S. DOE and NREL to launch a demonstration project involving 300 Inner Mongolian households, cost-shared by DOE and the Chinese Government.

CEEP is currently conducting a socio-economic assessment of the short, middle, and long-term potential for household-scale wind, PV and PV/wind hybrid systems in IMAR. CEEP has developed household, county and province level survey instruments and designed a detailed sampling method for the study. Survey data on 200 Inner Mongolia herder households and social-economic information for ten counties in IMAR have been collected, in collaboration with the Institute of Policy and Management Institute of the Chinese Academy of Sciences and Inner Mongolia New Energy Office. These data are now being processed and analyzed by CEEP s research team.

CEEP is also conducting, in collaboration with the China s Ministry of Agriculture (MOA), a feasibility study of renewable energy applications in Xinjiang and Qinghai, two China s western provinces. The goals of the study are to evaluate the energy and economic performance of household-scale renewable energy systems and to identify the cost-effective renewable options for rural electrification in these provinces. A socio-economic study similar to the one in IMAR is also being carried out by CEEP.

References

1. J. Byrne, L. Agbemabiese and D. Redlin. 1997. *Evaluating the Additional Value of Emergency Power Applications in Dispatchable PV Peak Shaving Systems*. Prepared for National Renewable Energy Laboratory. May. Center for Energy and Environmental Policy, University of Delaware.
2. J. Byrne, S. Letendre, L. Agbemabiese, D. Redlin and R. Nigro. 1997. Commercial Building Integrated Photovoltaics: Market and Policy Implications. *Proceedings of the 26th IEEE Photovoltaic Specialists Conference*. September. Anaheim, California.
3. J. Byrne, S. Letendre, Y-D. Wang and C. Weinberg. 1997. Commercializing Photovoltaics: The Importance of Capturing Distributed Benefits. *Proceedings of Solar 97* (American Solar Energy Society). June. Albequergue, New Mexico.
4. J. Byrne, Y-D. Wang and S. Letendre. April 1997. Building Load Analysis of Dispatchable Peak Shaving PV System: A Regional Analysis of Technical and Economic Potential. *Proceedings of Solar 97* (American Solar Energy Society). June. Albequergue, New Mexico.
5. J. Byrne and K. Boo. 1998. *High-Value Photovoltaic Applications for Public Facilities in the State of Delaware*. Prepared for the national Renewable Energy laboratory. December. Center for Energy and Environmental Policy, University of Delaware.
6. J. Byrne, Y-D. Wang, K. Boo and J-S. Song. 1997. The Economic Viability of Dispatchable Peak Shaving PV Systems in Commercial Buildings of Korea. *Proceedings of the 1997 Solar World Congress*. Vol. 3: 294-303.
7. J. Byrne, B. Shen and W. Wallace. 1998. The Economics of Sustainable Energy for Rural Development. *Energy Policy*. Vol. 26, No. 1: 45-54.
8. J. Byrne, Y-D. Wang et al. 1997. *Sustainable Energy Options for Asia: Case Studies of China and Korea*. Prepared for Kyoto NGO Forum, held in conjunction with the Third Conference of Parties to the UN Framework Convention on Climate Change. December. Center for Energy and Environmental Policy, University of Delaware.
9. J. Byrne, B. Shen and W. Wallace. 1997. Renewable Energy for Rural Development: Case Studies of Off-Grid Wind, Photovoltaic and Hybrid Systems in Rural China. *Proceedings of the 1997 Solar World Congress*. Vol. 7: 94-103.
10. J. Byrne, S. Letendre, L. Agbemabiese, D. Bouton and J. Kliesch. 1998. *Photovoltaics as an Energy Services Technology: A Case Study of PV Sited at the Union of Concerned Scientists Headquarters*. Prepared for the Union of Concerned Scientists. Boston, Massachusetts.

Title: **Renewable Energy Business Development in China**

Organization: Xinergy
3122 9th Road North #3
Arlington, VA 22201
TEL: 703/243-9468

Contributors: Scott Vaupen

Objectives

The overall objective of this subcontract was to expand a previous project, initiated at the US Export Council for Renewable Energy, conducting a survey to develop local information on the business environment and opportunities in several Provinces in China. The work was performed under the Energy Efficiency and Renewable Energy Protocol agreement signed in February 1995 between the Chinese State Science and Technology Commission and the US Department of Energy. This Protocol initiated bilateral cooperation between the U.S. and the People's Republic of China for renewable energy development. Under this Protocol, Annex IV was signed between the U.S. Department of Energy and the Chinese State Economic and Trade Commission in June 1996 to establish cooperation for business development for renewable energy technologies in China. One of the activities under Annex IV is a provincial tour for developing business related information in China for use by the US renewable energy industry.

Objectives of the subcontract included working with the cooperation of the Center for Renewable Energy Development in Beijing to develop information in up to four new provinces in China. Information will include but not be limited to: i) specific project information, especially projects that are open for international bidding, ii) general business environment in a specific province, including regulatory environment, general market information, etc., iii) summaries of Chinese companies and other business groups that are interested in doing business with US companies, and iv) prospects for specific technologies in a given provinces. The focus is on photovoltaic technologies, but the information survey also seeks opportunities for other technologies as well.

The work included one trip to China and with the assistance of CRED and visits to four provinces to collect relevant information. CRED scheduled meetings in the provinces and coordinated information collection. Scott Vaupen at Xinergy prepared a final document based on a preliminary report. The report will be distributed to the US renewable industry trade organizations in Washington, D.C. and to interested renewable energy companies in the United States.

Research Results

In January 1997 previous work conducted in cooperation with the US Export Council for Renewable Energy resulted in a report covering the central government in Beijing and the Provinces of Gansu, Xinjiang, Qinghai, Inner Mongolia, Shandong, and Zhejiang. During 1998, an additional tour was made including the Provinces of Guangdong, Jiangxi, Jilin, and Yunnan, with updates of central government activities.

Some of the issues covered in the report, include:

- Listing of government contacts by key agencies and functions.

- Information on government policies and regulations, incentives for renewable energy development, (including tax, tariff, and loan incentives), new legislation, and ownership issues.

- Competitive environment, including the activities of other countries in developing renewable energy markets in China.

- A discussion of potential obstacles related to financing, approval processes, currency convertibility, lack of incentives for renewables, restrictions on investment returns, and legal issues.

In the discussions for Provinces which are covered in this report, topics include general overview, local contacts, legal environment, regulations and incentives related to renewable energy, the competitive environment, technology overviews, and profiles of renewable energy companies. Also discussed are project opportunities open for international competition,, interests of local companies in developing business relationships with US companies, and other factors which impact renewable energy development.

Reference

Vaupen, Scott, "Renewable Energy Markets in China: An Analysis of Renewable Energy Markets in Guangdong, Jiangxi, Jilin, and Yunnan with Updated Information from Beijing," August, 1998, in revision, to be published as NREL Report.

10.0 Sandia National Laboratory Projects

Sandia National Laboratories In-House Research

Title: **Crystalline Silicon Device Research**

Organization: Photovoltaic System Components Department
Sandia National Laboratories, Albuquerque, New Mexico

Contributors: D.S. Ruby (P.I.), D.D. Smith, M.D. Bode, B.L. Silva, J.W. Tingley, B.R. Hansen, J.M. Moore

Introduction

The objective of this research is to improve commercial photovoltaic crystalline-silicon (c-Si) module performance (cost, efficiency, and reliability) through development of improved device structures and processes. This task emphasizes research activities with near-term impact that are identified collaboratively with major c-Si manufacturers. This task also supports a world-class photovoltaic device characterization laboratory. An internally funded R&D program at Sandia assists the development of the self-aligned selective-emitter cell, plasma texturization process, and simplified module assembly using back-contact c-Si solar cells.

Task 1. Self-aligned Selective-emitter (SASE) Cell. (Milestone: Demonstrate improved self-aligned selective-emitter cells).

"Selective emitter" refers to an optimized emitter profile where the emitter (carrier-collection junction on the front surface of a solar cell) is heavily doped beneath the contacts for low contact resistance and recombination, and lightly doped between the contacts for high current collection. We are developing a potentially low-cost process for fabricating selective-emitter solar cells that requires only a single emitter diffusion and no alignments. We continued optimization of our self-aligned selective-emitter process during the past year. Standard commercial screen-printed gridlines were used to mask a plasma-etchback of the emitter. A subsequent PECVD-nitride deposition provided good surface and bulk passivation and an antireflection coating. We used full-size multicrystalline silicon (mc-Si) cells processed in a commercial production line and performed a statistically designed multiparameter experiment to optimize the use of a hydrogenation treatment to increase performance. We obtained an improvement of 0.8% absolute in efficiency when the self-aligned emitter etchback was combined with an optimized 3-step PECVD-nitride surface passivation and hydrogenation treatment.

The SASE process was improved by using statistical experiments, more complete emitter etchback, and lower absorbance nitride films to achieve nearly a full percentage point efficiency increase over the standard production line process. The use of an optimum-duration, NH3-plasma hydrogenation treatment was found to be crucial to the increased performance. As the data in Figure 1 show, the fill factor and open-circuit voltage increase for durations up to 10 minutes, and then decrease due to higher non-ideal diode recombination, probably due to accumulated plasma-induced damage.

This SASE process has been developed in collaboration with Solarex. Future work with both Siemens and Evergreen is also planned.

Task 2. Emitter-Wrap-Through (EWT) Cell Development. (Milestone: Assemble monolithic module using 17% EWT cells, and work with at least two U.S. companies on project).

Back-contact c-Si solar cells are of interest because they potentially have higher efficiency (no grid obscuration) and simpler module assembly when compared to conventional front-contact solar cells. Sandia is developing a back-contact cell ("emitter wrap-through – EWT") where the emitter is wrapped from the front surface to the back surface through laser-drilled holes. This cell structure can potentially be implemented with low-cost, high-throughput processing.

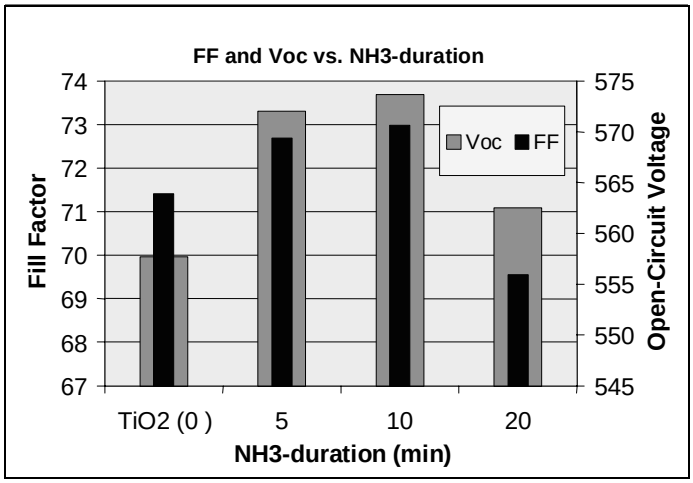

Figure 1. Voc and FF peak at NH3-plasma hydrogenation durations of 10 minutes.

Significant improvements in EWT cell performance were achieved, including the demonstration of a 17.5% efficiency in a 40-cm^2 solar cell. This device used evaporated metal grids and photolithographic patterning. A limitation in the past with this device was a low fill factor caused by an apparent shunt near the maximum-power point. In FY98 this cause was isolated as an edge effect due to excessive voltage drop along the front junction. The cell drilling and scribing patterns were redesigned to minimize this effect. This has resulted in a fill factor of 78%, as measured on a recent device. Other recent improvements include improved front and rear surface passivation.

Recent work has also indicated that the wrap-through holes introduce no defects that degrade cell performance. Laser scanning of finished cells has shown no decrease in photoresponse in the vicinity of the holes. In Figure 2, a laser scan of the front of a finished EWT cell is shown at 980 nm. The hole spacing is 1 mm and the dark regions associated with the holes are no larger than their diameter of 70 microns. The dark stripes show enhanced carrier recombination over the regions used to make p-type contact on the back surface.

A concentrator cell version of the EWT cell is also under development in a Work-for-Others project. This cell will require further refinement of the processing due to the finer geometries required for higher current operation under concentrated illumination. Preliminary work has uncovered yield issues associated with the finer geometries, which are currently being resolved.

Task 3. Streamlined Module Assembly using Back-Contact Cells. (Milestone: Examine new electrical attachment materials for new crystalline-silicon module assembly using back-contact cells, and perform cost analysis of new module assembly process).

Researchers at Sandia are examining the entire photovoltaic module production process, with a goal of optimizing the cell and module design concurrently for lower cost. This approach finds that considerable cost in the module assembly is due to the use of solar cells with contacts on both surfaces. Sandia is therefore developing silicon solar cells with both contacts on the back surface, and developing new module assembly concepts using back-contact solar cells. Our preliminary studies estimate that cost reductions of 25% compared to current designs are possible with the new approach. Our preliminary work has demonstrated an 11%-efficient module using back-contact cells and one-step assembly process using conductive epoxies for the electrical-attachment material.

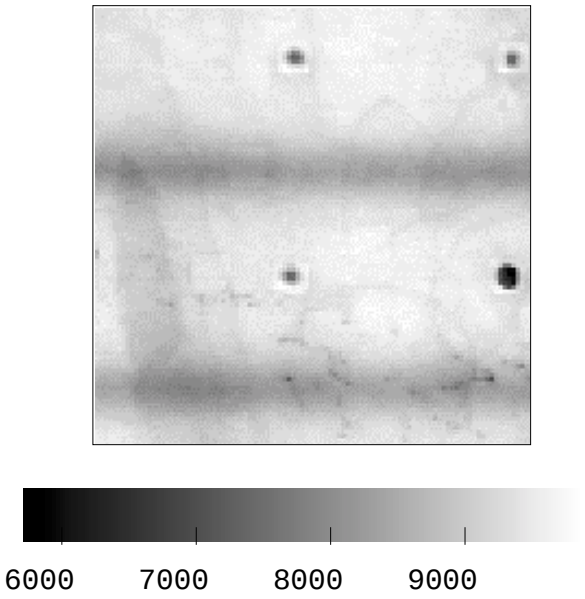

Figure 2. Laser scan of EWT cell at 980 nm.

Work during the past year emphasized development of a single-step module assembly process using low-temperature solders for the electrical-attachment material. Solder potentially has improved reliability, better conductivity, and lower cost compared to conductive epoxies, but a low-temperature version is required for compatibility with the other module materials (such as ethylene vinyl acetate). A module was successfully assembled in a single step with two different low-temperature solders. This work was performed in collaboration with Evergreen Solar, ASE Americas, and Iowa Thin-Films.

Task 4: Investigate Self-doping Metallizations. (Milestone: Demonstrate back-surface field (BSF) cells with new metallization, and submit patent disclosure).

New metal compositions will be studied which have the potential to form self-aligned selective-emitters and back-surface fields using low-cost deposition and simple firing conditions. This project will be closely coordinated with Georgia Institute of Technology and an industrial collaborator (EBARA Solar).

We have acquired sputtering targets (B-, Ga, and P-doped Ag) to test our new metallization concept of a self-doping metallization using a doped Ag-Si eutectic. In the meantime, we tested an Al-doped Ag-alloy process for forming a back-surface field (BSF) cell. The Al and Ag were deposited by evaporation, and the alloy was performed in a tube furnace. We also alloyed pure-Ag to test contamination of the bulk. We believed that alloying Ag should not be detrimental to silicon due to the extremely low solid solubility of Ag in Si and its relatively low recombination activity. However, both the non-doped and Al-doped Ag-alloyed cells had very poor bulk diffusion lengths. The problem is believed to be due to other metallic contaminants in the evaporated Ag, which is only 99.99% pure. A more pure Ag evaporation source has been acquired to test this hypothesis.

Additional Activities

Plasma texturization.
The quality of the best mc-Si wafers has increased to the point where mc-Si cell performance is approaching that of single-crystal silicon solar cells, with the major difference due to the inability to texture mc-Si using the standard wet chemical etches. This task has examined reactive ion etching (RIE) for texturing entire wafers in a single process step.

Plasma texturing was shown to reduce reflectance significantly while removing only the heavily diffused portion of the emitter region. As a result, texturing could be included as part of the emitter etchback step in the SASE process (Task 1). To perform the texturing, the emitter surface is first covered with a low-temperature oxide, whose normal randomly distributed pinholes and defects act as an etch mask for the silicon below. Hemispherical reflectance using a PECVD-oxide mask is shown in Figure 3.

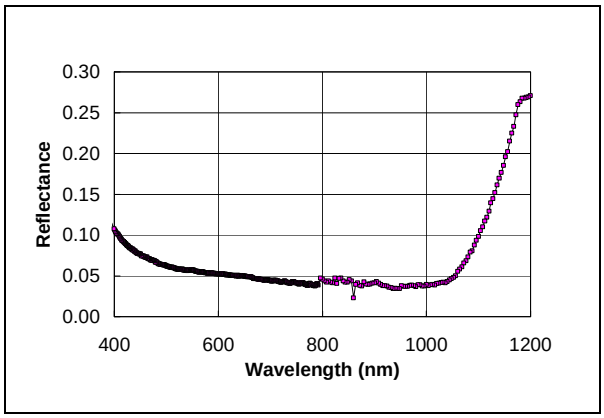

Figure 3. Hemispherical reflectance for a c-Si sample without ARC and textured using PECVD-oxide mask. Only the most heavily doped part of the emitter was removed, implying that this texturing could be done after an emitter diffusion as part of the SASE process.

The broadband, low-reflectance surface is indicative of the submicron texture obtained, which functions like a graded refractive-index surface. This produces a lower reflectance minimum than the value of 9% expected from a double-bounce off of micrometer-sized pyramids, and also a lower integrated reflectance than a single-layer ARC.

Solar-grade Silicon
Polysilicon feedstock is a critical issue for the continued rapid expansion of c-Si PV industry. A small project to examine solar-grade polysilicon feedstock production was initiated. Thermochemical calculations were used to examine the chemical basis of liquid silicon refining. These calculations identified a promising method for removing boron from silicon melts. Several experiments at the Liquid Metal Processing Laboratory at Sandia were initiated. These experiments involve examining refining of liquid silicon by reactive gas blowing.

CRADA with ASE Americas
In a CRADA with ASE Americas, we helped evaluate contamination from belt-furnace materials and characterize a new optical structure for their modules. We also updated a spreadsheet for optimization of grids and provided a metallurgical analysis of their solder bonds. These particular experiments assisted ASE in evaluating their current processes and proposed process upgrades, in optimizing the design of their solar cells, and in developing a new module product.

Title: Energy Storage for Photovoltaics

Organization: Sandia National Laboratories
Photovoltaic System Applications Department
Albuquerque, New Mexico

Contributors: T. Hund and M. Brown (Sandia); J. Dunlop (FSEC)

Battery Evaluations for Hybrid Photovoltaic Systems

Sandia and the Florida Solar Energy Center (FSEC) are now using their extensive experience with small stand-alone photovoltaic battery testing to address new work related to photovoltaic-hybrid battery testing. Photovoltaic-hybrids represent a relatively large group of renewable energy power systems with multiple power sources that vary considerably with respect to system design, size, load characteristics, and possible battery management strategies. Preliminary test results at Sandia indicate that both flooded and valve-regulated lead-acid (VRLA) batteries can quickly lose capacity in a photovoltaic-hybrid environment. This premature capacity loss stems primarily from an operational mode known as deficit-charge cycling. Deficit-charge cycling occurs when a discharged battery is not fully recharged after each discharge. This is a common occurrence that results from cost-reduction practices, themselves a result of the high cost of sizing the photovoltaic array to fully recharge the battery or the added engine/generator runtime required to finish-charge the battery. Work at Sandia is now focusing on identifying the minimum hybrid battery-charging requirements to prevent premature capacity loss resulting in a shortened battery cycle-life. The goal is to minimize operation and life-cycle costs in photovoltaic-hybrid systems. A photovoltaic array and/or engine/generator can charge batteries in photovoltaic-hybrid systems in a variety of configurations. Multiple power sources provide more system design flexibility and improved availability, but they also increase complexity. With complexity come more uncertainties with respect to system design and management of that design. Since there can be a wide variation of power contributed by the photovoltaic array or other power sources, it is possible to design photovoltaic-hybrid systems that are almost totally dependent on the engine/generator for battery charging or systems that are essentially stand-alone photovoltaic systems with the engine/generator used only as an emergency power source. Battery-charging requirements and the necessary controls will vary considerably as the dependence on the engine/generator varies. Batteries in photovoltaic-hybrids may also be subjected to more abusive conditions than in stand-alone photovoltaic systems if the system design does not provide the necessary controls. An engine/generator does not guarantee proper battery charging. With this in mind, laboratory testing is now under way to identify appropriate deficit-charge cycle periods, finish-charge ("equalization") times, regulation voltages, and time intervals between finish-charges ("equalization") for flooded and VRLA deep-cycle batteries. It should be noted that battery equalization in photovoltaic-hybrid systems is frequently used interchangeably with battery finish-charge. Equalization is a distinct process that begins at the end of the finish-charge for the express purpose of bringing all cells in a battery string to equal voltage or capacity.

Preliminary Test Results

Traditional lead-acid battery cycle test results to rate photovoltaic battery performance can be significantly skewed toward the positive by using high charge/discharge rates. Most battery testing by battery manufacturers and others, including Sandia, has used test procedures that more rapidly cycle the battery than it would normally see in a photovoltaic-hybrid system. The more rapid 10-hr or less cycle rates commonly used by most laboratories are not typically characteristic of photovoltaic-hybrids. Photovoltaic-hybrids will more commonly see charge and discharge rates of 20 to 100 hours. Cycling at the slower rates promotes hard sulfation and premature capacity loss due to the extended time spent in a discharged condition and the resulting deeper cycles. Thus battery recovery at low rates can be much more difficult and cycle-life can be less than expected. Therefore, the test results reported here may not

be consistent with either manufacturers' or other laboratory testing, since those tests are generally performed at high rates and the tests reported on here were performed at lower rates. It is always important that the test procedure duplicate the battery application as closely as possible because of these performance differences.

Test results at Sandia's Photovoltaic System Applications Department have shown that the deficit-charge cycle time and full recovery requirements are significantly different for flooded (vented) and VRLA batteries; therefore, it is critical to understand the specific charging requirements of the battery used in the photovoltaic-hybrid system. Vented batteries that spend more than a few days in a deficit-charge condition will begin to suffer from electrolyte stratification. Stratification makes recharge more difficult by prematurely raising battery voltage during recharge. This condition falsely indicates a higher battery state-of-charge than is actually present. In addition to stratification in vented batteries, the charge efficiency of both vented and VRLA batteries needs to be accounted for by charging more amp-hours (Ah) into the battery than were removed during each cycle. The Ah overcharge requirement for a fully discharged vented battery is usually between 120 and 130%. VRLA batteries usually require between 105 and 112% overcharge. The combination of renewable energy power sources and engine/generator battery charging must meet the overcharge requirement to compensate for the losses in battery charging. Because charge efficiency is a non-linear inverse function of battery state-of-charge, with efficiency being very high at low states-of-charge and less than 50% at high states-of-charge, generic overcharge statements should be tempered with the knowledge that battery charge efficiency is highly dependent on the battery depth-of-discharge regularly experienced.

In all cases, photovoltaic-hybrids need to be designed to minimize deficit-charge cycling while still minimizing engine/generator run time. This can be accomplished by using appropriate regulation voltages and providing no more than the minimum required finish-charge intervals. If the photovoltaic and/or engine/generator charge controller regulation voltage is too low, or the time at regulation voltage is too short, then the required battery overcharge cannot be achieved effectively with either the photo-voltaics or engine/generator. Proper battery management requires a photovoltaic or engine/ generator charge controller with an appropriate photovoltaic regulation voltage, adequate time at regulation voltage, and a temperature compensated regulation voltage. A key element in achieving this is an engine/ generator battery charge-control strategy that provides a bulk charge function that initiates on low voltage and terminates on voltage and time, and an automatic battery finish-charge at set intervals from one to four weeks for specified finish-charge times and voltages.

As an example of this work, two VRLA batteries, one gelled electrolyte and one absorbed glass mat, are being tested in the laboratory to identify appropriate deficit-charge intervals and finish-charge requirements. Follow-up field tests will be conducted to further validate the findings. However, since these preliminary results are important they are being released at this time. Laboratory testing at a 24-hr charge and 35-hr discharge rate to 1.98 Vpc (11.88 volts), a ~65% depth of discharge, has shown that both Batteries A and B can lose capacity quickly after short periods in deficit-charge cycling. As shown in Graphs 1 and 2, Battery A lost 19% and Battery B lost 27 % of its available capacity to 1.98 Vpc after three 30-day deficit-charge cycle intervals. In both cases the battery was bulk charged to 2.35 Vpc (14.1 volts) from 1.98 Vpc (11.88 volts) every 1.5-days, then finish-charged at 2.35 Vpc (14.1 volts) for 12-hours every 30-days.

Graph 1 below showing premature available capacity loss to 1.98 Vpc after each finish-charge indicates that Battery A lost 0.31, 0.19, 0.06, and –0.30% per cycle for the third 30-, 15-, 7.5- and 1.5-day deficit-charge interval. Battery B initially lost 2% per cycle after the first 3-cycle 5-day deficit charge interval. After the second and third deficit charge intervals, the capacity loss stabilized to between 0.68 and 0.41%

per cycle for all deficit charge intervals including the 1.5-day interval. The graph indicates that both batteries do experience less capacity loss with each succeeding deficit charge interval and this may eventually result in a stable capacity, but not without significant initial capacity loss. Battery A clearly demonstrates a capacity gain with the 1.5-day deficit-charge interval to only a small capacity loss (-0.3 to 0.06%/cycle) with the 7.5-day deficit charge interval. Battery B, with a much higher capacity loss rate at all deficit charge intervals (~0.41%/cycle), does not clearly show a reduction in capacity loss due to more frequent finish-charges at less than 15-day intervals.

Graph 2 below showing the percent of initial capacity as a function of the number of finish-charge intervals indicates that after the third 30-day deficit-charge interval Batteries A and B quickly lost capacity to 81% and 73% of their original value. With more frequent finish-charges of 15, 7.5, and 1.5 days, Batteries A/B measured 95/88, 99/94, and 104/92% of their initial capacity. Battery A shows that it can almost maintain or even gain capacity with 7.5- to 1.5-day finish-charges, but Battery B consistently lost capacity at all finish-charge intervals, indicating that it had an insufficient finish charge. The above test results are important in defining battery charging requirements and predicting expected cycle-life for the above test conditions. The test results indicate that battery performance would probably be significantly better for Battery A if finish-charged every week. The clear performance improvement for weekly finish-charges is not apparent for Battery B, but at finish-charge intervals of 15 days vs. 30 days the capacity loss is significantly less. It is generally accepted that less capacity loss will promote improved battery cycle-life. Certainly the traditional thinking that either no finish-charges were required or that 30-day intervals between finish-charges ("equalization") were acceptable for all VRLA batteries has been shown to be incorrect for photovoltaic-hybrid applications using a similar cycle.

Summary

Battery management in photovoltaic-hybrid systems needs to follow a few simple rules even though the system design can vary considerably. If the system designer provides the photovoltaic battery with its basic charging needs on a regular basis, then the traditional photovoltaic battery problem of premature capacity loss and early cycle-life failure can be minimized. Maintaining photovoltaic batteries in a healthy condition in many cases will more than double cycle-life and thus increase reliability, thereby significantly reducing overall life-cycle costs. Unfortunately, all the information required to do this is not always available. Sandia's photovoltaic balance-of-system group is working with battery manufacturers to provide the missing information.

Proper Battery Charging of Photovoltaic-Hybrids

Any photovoltaic-hybrid battery-management strategy should limit the number of days the battery spends in a deficit-charge condition and should provide a means for full recovery of that battery on a regular basis.

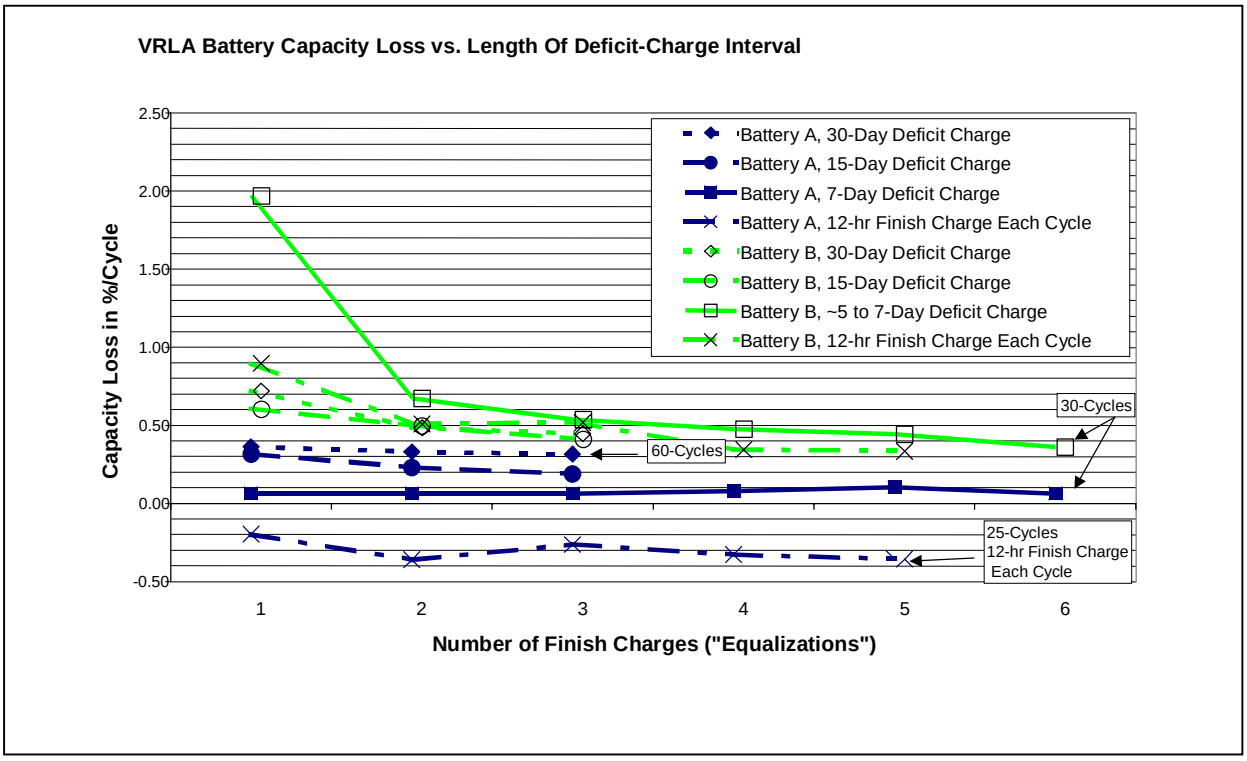
VRLA Battery Capacity Loss vs. Length Of Deficit-Charge Interval
Capacity Loss in %/Cycle
2.50
2.00
1.50
1.00
0.50
0.00
-0.50
1
2
3
4
5
6
Number of Finish Charges ("Equalizations")
Battery A, 30-Day Deficit Charge
Battery A, 15-Day Deficit Charge
Battery A, 7-Day Deficit Charge
Battery A, 12-hr Finish Charge Each Cycle
Battery B, 30-Day Deficit Charge
Battery B, 15-Day Deficit Charge
Battery B, ~5 to 7-Day Deficit Charge
Battery B, 12-hr Finish Charge Each Cycle
30-Cycles
60-Cycles
25-Cycles
12-hr Finish Charge
Each Cycle

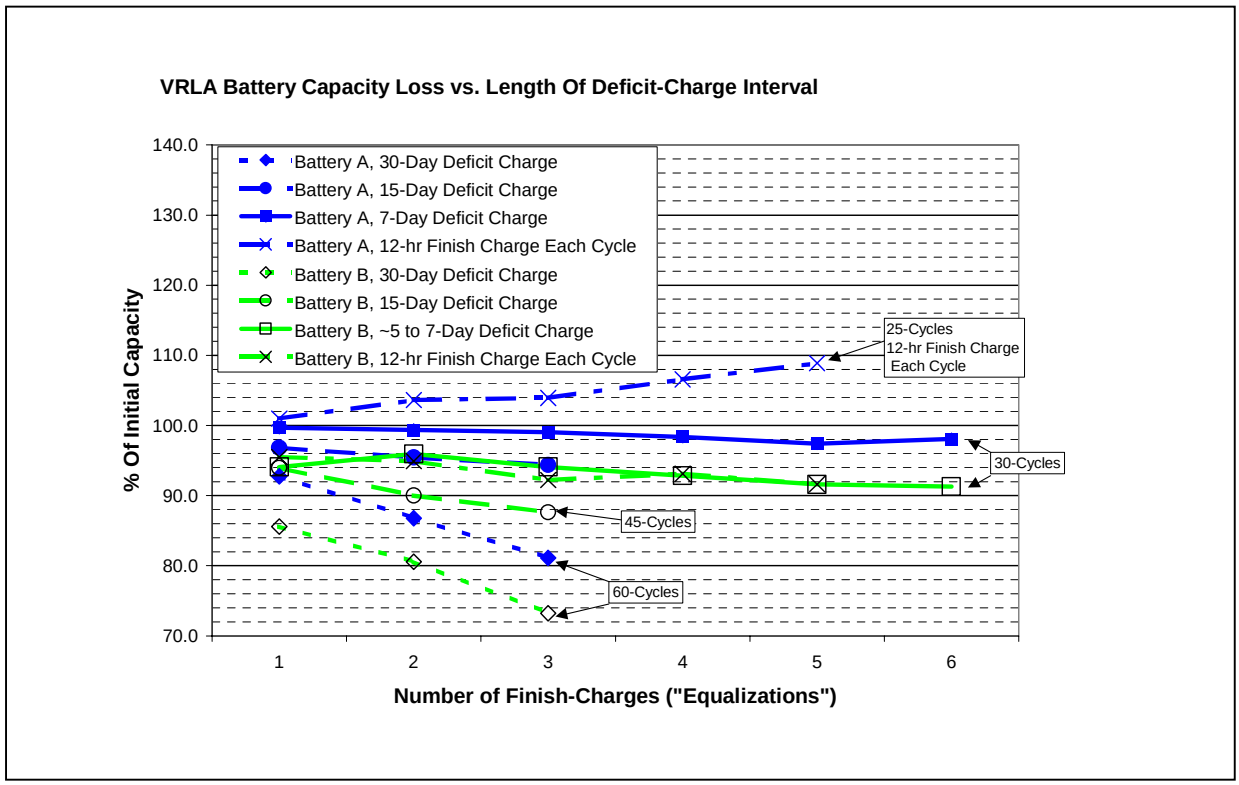
VRLA Battery Capacity Loss vs. Length Of Deficit-Charge Interval
% Of Initial Capacity
140.0
130.0
120.0
110.0
100.0
90.0
80.0
70.0
1
2
3
4
5
6
Number of Finish-Charges ("Equalizations")
Battery A, 30-Day Deficit Charge
Battery A, 15-Day Deficit Charge
Battery A, 7-Day Deficit Charge
Battery A, 12-hr Finish Charge Each Cycle
Battery B, 30-Day Deficit Charge
Battery B, 15-Day Deficit Charge
Battery B, ~5 to 7-Day Deficit Charge
Battery B, 12-hr Finish Charge Each Cycle
25-Cycles
12-hr Finish Charge
Each Cycle
30-Cycles
45-Cycles
60-Cycles

Title: **Industry Guided Module Durability Research**

Organization: Sandia National Laboratories, Albuquerque, New Mexico

Contributors: M. A. Quintana, D. King, J. Kratochvil, D. Ellibee, B. Hansen, J. Moore

Objectives

The objective of the Module Durability Research Cooperative (MDRC) is to improve durability of commercial PV modules. This work is highly collaborative with manufacturers often participating in the research and sometimes cost sharing the expense. To date, the MDRC has performed research in collaboration with Solarex, Spire, STR, ASE Americas, AstroPower, USSC, and Siemens. Tentative plans call for collaborations with additional manufacturers including Solar Cells Inc. and Evergreen.

Technical Approach

The technical approach for conducting MDRC studies has been to (1) collaboratively identify module durability issues, (2) examine the underlying physical mechanisms associated with these module durability issues, and (3) feed back the resultant information to positively influence the reliability of future products. This is accomplished by utilizing expertise and resources available at Sandia, NREL, Southwest Technology Development Institute, and Florida Solar Energy Center. This year, MDRC activities have examined issues related to:

1. Adhesion of EVA encapsulant to the glass and cell surfaces
2. Physical characteristics of field-aged EVA
3. Integrity of as-manufactured and field-aged solder-joints
4. Adhesion of metallization to cell surfaces
5. Etching of glass surfaces during accelerated aging tests
6. Fracture characteristics of tempered glass
7. Optical characteristics of new and field-aged glass
8. Surface characteristics of cells
9. Soldering process optimization in manufacturing
10. Module performance changes due to solder-joint degradation
11. Thermal characteristics resulting from solder-joint degradation

Wherever possible, established techniques are used to perform analyses. For example, measuring optical characteristics of glass is straightforward, but measuring optical characteristics of field-aged glass from photovoltaic modules provides a challenge because of the difficulty with extracting a suitable tempered-glass sample to test on a spectrophotometer. Similarly, surface analysis of cells is easily done with Auger Electron Spectroscopy or other surface-analysis techniques. However, extracting a cell sample for surface analysis from a field-aged module was not a trivial matter prior to the inception of the MDRC.

Other analysis techniques have been developed in order to satisfy the demand for information. One of the most important techniques developed is the module dark I-V test procedure. Based on the established cell dark I-V tests, this technique allows easy measurement of module series resistance, which is an important parameter for characterizing degradation in module performance due to field aging. Another technique that has generated interest is the extraction of cell samples and the concurrent measurement of adhesion characteristics at the cell-EVA interface. This technique has provided insight as to how EVA adhesion degrades as a function of time in different climates.

Results

Failure Analysis of Fractured Glass: During FY98 the MDRC performed a detailed analysis of several failed photovoltaic modules with shattered glass from a single system fielded at the New York Power

Authority Yonkers Wastewater Treatment Facility. Initially there was a concern that there might be a module materials problem that could affect all module manufacturers. The photovoltaic array was inspected and the origin of each fracture was identified as a mechanically damaged spot on the top surface of the tempered-glass sheet of the module. Origin points ranged from very pronounced points with finely fractured glass that indicated definite impact to very subtle impact points not visible to the human eye. All fractures followed a classic pattern of radial crack lines emanating from a point with random cross dicing. More importantly, it was found that multiple modules had been impacted (pitted glass) but not shattered. Failure analysis was undertaken to determine how the damage had been produced and to determine if other factors had contributed to the failure. Figure 1 shows an example of a cross-section taken from the Yonkers system. *Mist and hackle*, visible features created when glass is fractured, help analyze failures. These features, which resemble tiny bubbles and filaments, are typically found in the central plane of the glass except where an impact has occurred. Figure 1 shows a distinct shift in the location of the *mist and hackle* away from the impact point. This, along with evidence that there was no shift of the *mist and hackle* at 2 cm from the impact point, suggests that failure occurred as a result of indentation of the upper compressive layer at a distinct point. In addition, lack of shift of the *mist and hackle* beyond 2 cm also indicates that no bending stress was incurred during the failure.

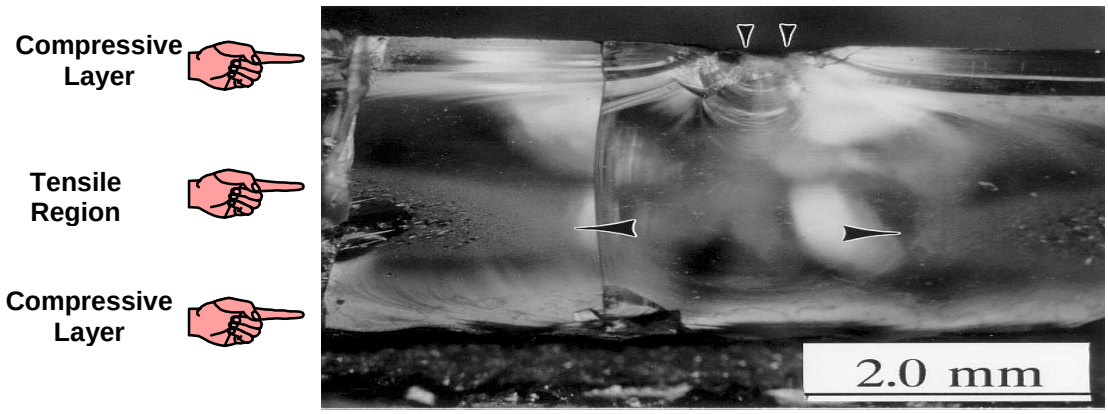

Figure 1. Cross-section of fractured glass showing impact point (top arrows), mist and hackle (center arrows) and tensile region and compressive layers.

Small size of the damage zones at the origin of the failures, and lack of evidence of other contributory stresses, were consistent with a scenario in which rooftop pebbles at the facility were lifted in windstorms and impacted the module surfaces. Transport of the gravel off the roof and onto an adjacent canopy top suggested wind speeds in the range of 6.1-12.4 m/s. It was not intuitively obvious that pebbles roughly 2-6 grams propelled to this velocity could fracture the glass. Qualification tests determined that the glass could withstand much larger masses at much greater velocities. Impact tests were performed using stones from the Yonkers roof propelled to similar velocities using Sandia's Hail Gun. Failures occurred using stones in the 3-4 gram range at velocities $\geq$ 12.7 m/s, verifying the initial hypothesis. Impact damage was the primary factor in the failure of the modules. This information has provided users and manufacturers additional requirements for system designs, a potential failure mode, and data for determining warranty issues. Life-cycle predictions of photovoltaics must include information regarding applications.

Infrared Thermography and Dark I-V Tests: During this period infrared (IR) and dark I-V tests were performed on 31 randomly selected modules from the manufacturing line of a single manufacturer. The objective of this effort was to gain a statistical understanding of the series resistance, saturation current, shunt resistance, and diode factor for a sixteen-month sampling and to develop confidence in the use of Sandia's Module Dark I-V tester. Infrared imaging was used to survey modules prior to dark I-V tests to

look for hot spots that could be attributed to poor solder-joints. Results have led to improvements in the module dark I-V tester allowing greater accuracy in measurements. Dark I-V provided a more sensitive measurement of the baseline series resistance of new crystalline-silicon modules than conventional light I-V tests. The sensitivity of this technique was examined by adding precision resistors to a test module. The technique was able to discern the types of changes in series resistance that is expected for field-aged modules. Manufacturers are investigating this procedure as a new process control technique.

IR thermography provides a snapshot of the temperature distribution on a module during normal operation. Figure 2 shows thermal scans of front surface of two different modules. Scans were performed indoors under dark conditions to eliminate light-induced effects. A power supply is used to circulate constant current through the module. The module on the left has relatively uniform thermal distribution, with no significant difference in the areas where the ribbons are located. On the right is a field-aged module from a different manufacturer. This module was known to have significant solder-joint degradation, which is exhibited in the IR thermographs as regions with distinctively different coloration ("hot spots"). These hot spots are typically near ribbons and degraded solder joints. This is another technique being investigated as a manufacturing quality-control test.

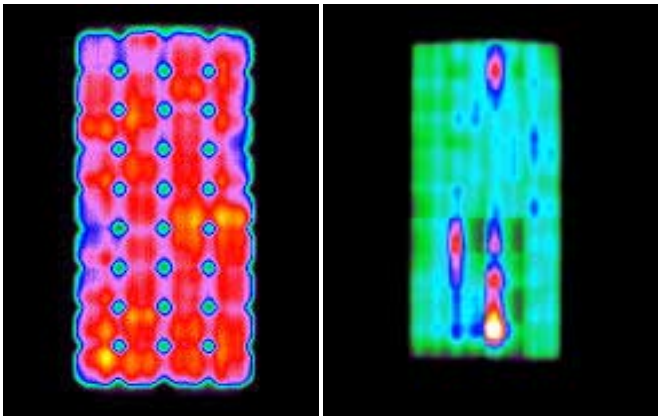

Figure 2. IR thermograph of two different modules.

Solder-Joint Characterization: Degradation of solder joints is a primary cause of increased series resistance in modules. Increased series resistance causes a decrease in fill factor that reduces electrical output. During this period Sandia characterized solder joints from three different manufacturers. Solder joints are examined after sample joints are extracted from a cell or a module. Each sample is then potted in a clear epoxy. After a series of grinding and polishing steps the cross-section of the joint is examined under a high power microscope and photographed. Previous studies identified characteristics of poor or failed joints. These include dewetting, voids, cracks, and solder coarsening. One or more of these characteristics were seen in all of the studies performed this fiscal year. We have also identified other characteristics that may contribute to the degradation of joints. Specifically, there is concern about the relative strength of the solder joint versus the strength of the metallization-to-silicon bond. Another problem observed this year is a discrepancy in the volume of solder on pre-tinned ribbons versus the volume of solder required to form a continuous joint. All of these issues have significant impact on manufacturing processes and on module durability. Exhibited from top to bottom are the copper, solder, cell metallization, a gap (black) caused by a silicon/metallization bond failure, silicon cell, irregular rear-contact metallization with voids, irregular gaps where solder-joining should occur, solder, and copper. Note the difference in thickness and uniformity of top and bottom metallization. Note also the thickness of the solder on the bottom relative to the volume required to form a joint. Finally, except for small voids, the relatively uniform top solder-joint may be representative of an optimum joint. Different solder treatments, metallization processes, soldering process variables, and soldering machines all contribute to the difficulty in defining an optimum process. Impetus to move to environmentally friendly

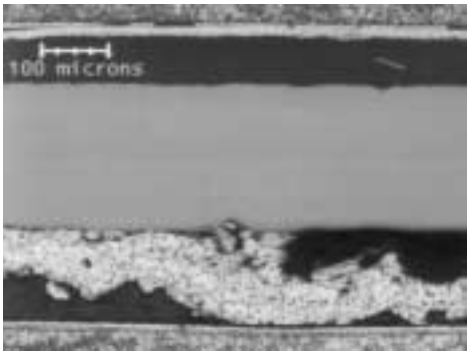

Fig. 3. Solder-joint Cross Section.

processes and materials further complicates the direction that manufacturers must take to improve durability of the product

Module Long Term Exposure: During FY 98 the Module Long-Term Exposure (MLTE) task was initiated. The objective of this task is to examine subtle module degradation mechanisms by conducting a structured and controlled long-term (minimum of five years) outdoor exposure of commercially available modules in cooperation with module manufacturers. Manufacturers participate by submitting a group of modules for outdoor exposure. Modules are concurrently being exposed to a hot and humid climate at FSEC and to a hot and dry climate at SWTDI. Thus far Siemens (crystalline and CIGS modules), USSC, and ASE Americas are participating. Solarex, Astropower, and Solar Cells Inc. are expected to begin participation in FY99. Participants have submitted 12 similar modules for the study. All modules underwent baseline testing at Sandia, including visual inspection, dark I-V, thermal imaging (IR), electric performance and thermal performance tests. Two control modules were kept in indoor storage at Sandia and five modules were sent to FSEC and SWTDI. Four of the five modules sent to each site were mounted outdoors in identical configurations (under load) and one module was stored indoors as an additional control. Modules are inspected and I-V curves are being taken on a monthly basis. If field failures occur, modules will be set to the manufacturer, Sandia, or NREL for failure analysis.

Publications

M. A. Quintana. "A Study of Shattered Glass," presented at PV Module Durability and Long-Term Exposure Symposium.

D. L. King, B. R. Hansen, J. A. Kratochvil, M. A. Quintana. "Dark Current-Voltage Measurements on Photovoltaic Modules as a Diagnostic or Manufacturing Tool**,"** *IEEE PV Specialists Conference*, September 29-October 3, 1997.

M. A. Quintana, et al. Technical-Briefs (6) on coring glass-glass modules, cutting tempered glass, solder-joint studies, adhesion of field-aged encapsulant, and analysis of tempered-glass fractures.

D. L. King, M. A. Quintana, J. A. Kratochvil, D. E. Ellibee, and B. R. Hansen. "Photovoltaic Module Performance and Durability Following Long-Term Field Exposure**,"** FY98 NCPV Program Review

N. G. Dhere, K. S. Gadre, and A. M. Deshpande. "Durability of Photovoltaic Modules," *Proc. 14th European Photovoltaic Solar Energy Conference*, Barcelona, Spain, (1997), pp. 256-259.

N. G. Dhere, M. E. Wollam, and K. S. Gadre. "Correlation Between Surface Carbon Concentration and Adhesive Strength At The Si Cell/Eva Interface In A PV Module," *Proc. 26th IEEE Photovoltaic Specialists' Conference*, (1997), pp. 1217-1220.

N. G. Dhere and K. S. Gadre. "Comparison of Mechanical Properties of EVA Encapsulant in New and Field-Deployed PV Modules," *Proc. 2nd World Photovoltaic Solar Energy Conf.*, Vienna, Austria, July 6-10, 1998.

N. G. Dhere and K. S. Gadre. "Tensile Testing of EVA in PV Modules," *Proc. Int. Solar Energy Conf. Solar Engineering 1998*, ASME 1998, Albuquerque, New Mexico, (1998), pp. 491-497.

N. G. Dhere, et al. "Quality Control of PV Module Manufacture Using Adhesion Measurement at Si-Cell/Encapsulant Interface," Sandia Tech Brief 22, July 1998.

N. G. Dhere, et al**. "**Statistical Error Analysis of Adhesional Strength Measurements," Sandia Tech Brief 23, July 1998.

N. G. Dhere, et al. "Review of ASTM Standard on Plastics Relevant for PV Module Encapsulants," Sandia Tech Brief 24, July 1998.

N. G. Dhere, M. A. Quintana, and D. L. King. P*roceedings MDRC/MLTE Workshop*, Feb. 1998.

Title: **Module/Array Performance Testing and Modeling**

Organization: Sandia National Laboratories, Albuquerque, New Mexico

Contributors: David King (Task Leader), Jay Kratochvil, William Boyson, Michael Quintana, Barry Hansen

Objectives

The objective of this task is to apply measurement and modeling capabilities available at Sandia to characterize the electrical, thermal, and optical behavior of photovoltaic modules and arrays. These efforts are tailored to, and conducted in close cooperation with, module manufacturers, system designers/integrators, system owners, and organizations that establish photovoltaic testing standards.

Technical Approach

The technical activities associated with this task can be described in three categories: (1) development and application of improved outdoor test methods for module performance, (2) development and validation of improved field testing procedures for photovoltaic array performance characterization (rating), and (3) the incorporation of improved testing and modeling procedures in both consensus standards and the software used for system design and sizing.

Upon industry request, comprehensive outdoor tests are conducted that provide a combination of specific module performance characteristics not available elsewhere. Improved outdoor test methods are continually being developed that meet the needs of an industry with very diverse testing requirements. The information gained from the testing provides not only traditional performance "calibrations" at ASTM Standard Reporting Conditions but also module parameters required for system engin-eering (design, sizing, rating). Specific tests provide module temperature coefficients, direct measurements of the influences of solar spectral variation and solar angle-of-incidence on performance, module thermal time constants, thermal "hot-spot" behavior in reverse-bias. Complementary dark current-voltage measure-ments conducted indoors provide physical parameters (series resistance, shunt resistance, saturation currents, diode factor) required for electrical modeling of cell circuits, as well as a functionality test of incorporated bypass diodes. In many cases, individual cell measurements in Sandia's Photovoltaic Device Measurement Laboratory are also used to confirm performance characteristics observed in outdoor module testing.

Figure 1 Sandia's computer-controlled solar tracker is used to characterize dozens of modules annually.

The development and improvement of field testing procedures for arrays involves adapting our outdoor module measurement procedures to large photovoltaic arrays. By doing so, a significant improvement in the accuracy and utility of performance characterizations (ratings) of large arrays has been obtained. During the last two years, improved array testing procedures have been successfully demonstrated for virtually all photovoltaic technologies: crystalline and multi-crystalline silicon, EFG silicon, Silicon-

Film, amorphous silicon (single, tandem, and triple-junction), cadmium telluride, and linear-focus concentrators. Our new methods and models are being evaluated and applied by several organizations including Endecon/PVUSA, UPVG, SWTDI, Ascension, and NIST, and are contributing to the evolution of new field testing standards by organizations such as IEEE and IEC. Additional work will still be required through standards committees to formalize the thermal models used to relate module (cell) operating temperature to environmental parameters (ambient temperature, wind speed, wind direction, solar irradiance) and mounting configurations (open rack, roof mounted, building integrated, solar trackers). Some of these additional thermal issues were addressed this year through contracted research with Endecon Engineering at the PVUSA site.

Other activities related to improved field testing procedures involved efforts to improve the accuracy of devices used for array performance testing, in particular the pyranometers widely used by the industry for measuring solar irradiance. Inaccuracy in solar irradiance measurements has been perhaps the biggest factor contributing to uncertainty in array ratings. New calibration and correction procedures have been developed for both thermopile based (Eppley) pyranometers and the inexpensive but prolific silicon-photodiode based pyranometers (LI-COR and now Kipp & Zonen). Similar to techniques used for modules, the new procedures developed at Sandia compensate for angle-of-incidence, temperature, and solar spectral influences during irradiance measurements. This work has been coordinated with NREL (Myers) and the pyranometer manufacturers (LI-COR, Kipp & Zonen, and Eppley).

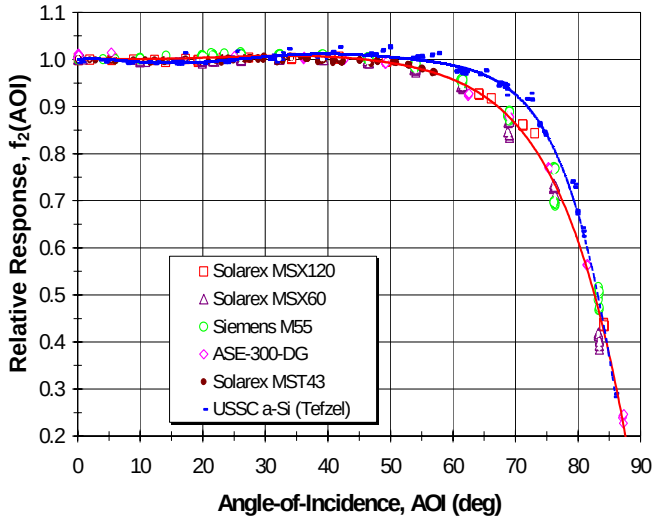

Figure 2 Unique outdoor test procedure has been used to quantify the influence of solar angle-of-incidence on commercial module performance.

Results

During FY98, outdoor characterization of more than one hundred commercial modules at Sandia resulted in nearly a dozen test reports to module manufacturers and users, including Solarex, Siemens, AstroPower, USSC, ASE Americas, Matrix Solar, Solar Cells Inc., PowerLight, Applied Power Corporation, SMUD, PVUSA, Idaho Power, Real Goods Corporation, GenSun, and Solar Energy Systems. Comprehensive baseline testing of 56 commercial modules was completed for module manufacturers currently participating in the Module Long-Term Exposure program at the Florida Solar Energy Center (FSEC) and the Southwest Technology Development Institute (SWTDI). At the request of module manufacturers and commercial users, carefully controlled measurements of the "stabilization" trends in commercially available amorphous silicon modules from USSC, Solarex, and EPV were conducted requiring multiple measurements on multiple modules over a 6- to 12-month period. Results from these stabilization tests were presented at the NREL Amorphous-Silicon Team Meeting at Copper Mountain. Our outdoor module calibrations, in conjunction with calibrations at NREL and at ESTI in Europe, also provided the traceability required for accreditation of commercial module testing organizations such as PowerMark and the Photovoltaic Testing Laboratory at Arizona State University (ASU/PTL).

During FY98, new array testing and analysis methods were applied during field characterization of five large photovoltaic arrays/systems and documented in test reports and conference proceedings. These field

characterizations included a 75-kW Solarex mc-Si array at Mt. Home AFB, a 100-kW ASE Americas EFG-Si array at San Clemente Island, a GenSun portable hybrid system with ASE array, a Solar Energy Systems portable hybrid system with Siemens c-Si array, and a 100-kW roof-integrated ASE Americas array by PowerLight. Sandia's field testing procedures were enhanced by a new method developed for modeling photovoltaic array performance for all outdoor operating conditions.

Figure 3. New array performance characterization methods were applied to a roof-integrated PowerLight system with 100-kW array of modules from ASE Americas.

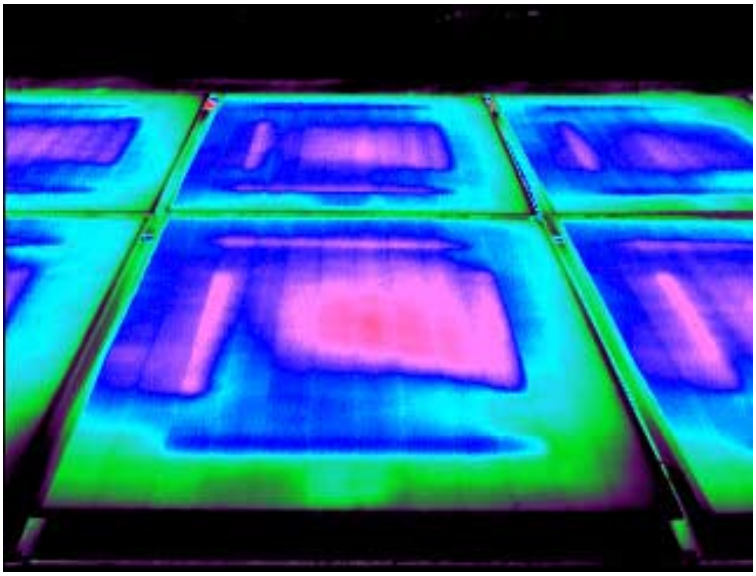

Figure 4. Module temperature distributions in roof-integrated PowerLight array measured in-situ using infrared (IR) imaging camera.

This new array performance modeling procedure also provided a more accurate means for calculating annual energy production from PV systems. Using detailed module parameters, the new model was used to calculate the estimated "annual ac-energy production" for five different photovoltaic technologies proposed for a 5-megawatt grid-tied system for the Public Service Company of New Mexico. The same modeling procedure was used to estimate the monthly ac-energy production from a 100-kW roof-integrated system by PowerLight in Hawaii. A field investigation of the thermal behavior (operating temperature) of the roof-integrated system was also conducted in order to improve the accuracy of the system performance model. Our efforts next year will involve the incorporation of elements of the new model in the evolving IEEE standard for determining a "module energy rating."

In a related activity, commercial vendors of system design software have expressed an interest in incorporating improved array performance algorithms in their products. Collaboration is in progress with the developers of the following software programs: PV-DesignPro, Nsol! , PVGrid, PVDesigner, and PVCAD.

Publications

1. King, D.L., Kratochvil, J. A, and Boyson, W. E. "Field Experience with a New Performance Characterization Procedure for Photovoltaic Arrays," *2nd World Conference and Exhibition on PV Solar Energy Conversion*, Vienna, July 1998.
2. King, D.L., Boyson, W.E., and Hansen, B.R. "Improved Accuracy for Low-Cost Irradiance Sensors," *2nd World Conference and Exhibition on PV Solar Energy Conversion*, Vienna, July 1998.
3. King, D. L., Kratochvil, J. A., and Boyson, W. E. "Measuring Solar Spectral and Angle-of-Incidence Effects on PV Modules and Solar Irradiance Sensors," *26th IEEE PVSC*, 1997, pp.1113-1116.
4. King, D. L., Kratochvil, J. A., and Boyson, W. E. "Temperature Coefficients for PV Modules and Arrays: Measurement Methods, Difficulties, and Results," *26th IEEE PVSC*, 1997, pp.1183-1186.
5. Whitaker, C. M., et. al. "Application and Validation of a New PV Performance Characterization Method," ," *26th IEEE PVSC*, 1997, pp.1253-1256.
6. King, D. L. and Myers, D. R. "Silicon-Photodiode Pyranometers: Operational Characteristics, Historical Experiences, and New Calibration Method," 26th IEEE PVSC, 1997, pp.1285-1288.
7. Wiles, J. C. and King, D.L. "Blocking Diodes and Fuses in Low-Voltage PV Systems," *26th IEEE PVSC*, 1997, pp.1105-1108.
8. King, D. L., Hansen, B. R., Kratochvil, J. A., and Quintana, M.A. **"**Dark Current-Voltage Measurements on Photovoltaic Modules as a Diagnostic or Manufacturing Tool;" *26th IEEE PVSC*, 1997, pp.1125-1128.
9. King, D. L., Kratochvil, J. A., Boyson, W. E., and Gee, J. M. "Performance Characterization of Commercial a-Si Modules," NCPV Amorphous-Silicon Workshop, Copper Mountain, August 1998.

Title: **PV Power Processing Program**

Organization: Sandia National Laboratories
Photovoltaic System Applications Department
Albuquerque, New Mexico

Contributors: R. Bonn, J. Ginn, S. Gonzalez

The Sandia balance-of-system (BOS) program concentrates on power electronics and the application of batteries in photovoltaic systems. The goals of the program are to advance the reliability of photovoltaic electronic components to the levels achieved by more mature products; reduce the life-cycle cost of photovoltaic systems; remove barriers to implementing photovoltaics; and assist component manufacturers and system integrators with the development of more reliable, cost-effective systems. The program includes both contracts with industry and laboratory evaluations. The in-house laboratory evaluations supplement the capability of photovoltaic component manufacturers by providing a test-bed that includes extensive measurement capability and realistic reproduction of equipment in field conditions, including complex loads, photovoltaic arrays, engine/generators, and batteries. Further testing support is obtained from laboratories at the Southeast and Southwest Region Experiment Stations and private labs. Benchmarking of products is conducted to obtain product information. Contracts with the photovoltaic industry focus on improving system reliability and reducing life-cycle cost, including the development of quality programs, HALT™ (highly accelerated lifetime testing), quality audits at the contractors' facilities, and some product development. Information about the BOS work at Sandia is available on Sandia's WEB site (www.sandia.gov/pv).

Figure 1. Sandia National Laboratories' Inverter Test Facility

Islanding of Multiple Grid-Tied Inverters

A section of a utility system containing both load and generation that has been disconnected from the rest of the utility is called an island. Utilities currently require photovoltaic inverters to disconnect when they are in an island because of reasons related to safety, protection of loads, and utility operation. During the summer of 1997, Sandia conducted a series of tests to investigate islanding of multiple inverters on a single 120-V ac circuit. It was found that for $Power_{generation}/Power_{load}$ ratios in the range of .8 to 1.2, the inverters frequently islanded for more than the 2 seconds (times > 30 seconds were observed) within which some utilities require the inverter to shut down. It was also observed that the presence of a transformer in the islanded circuit resulted in shorter islanding times (disconnect times of < .5 seconds) because the transformer required a nonlinear magnetizing current that most inverters could not supply. Conclusions drawn from these tests were that (1) multiple inverters on a single 120-V ac circuit were not disconnecting quickly enough; (2) the presence of a distribution transformer resulted in quicker disconnect; (3) future tests should include other than purely resistive loads, so that worst-case islanding

conditions could be determined; and (4) the use of multiple inverters utilizing different anti-islanding techniques increased islanding times. Sandia initiated a working group composed of U.S. inverter manufacturers to address these issues and sponsored the development of a new approach through Ascension Technology, Inc. to prevent islanding. This method has been developed and tested; the results, titled "Results of Sandia National Laboratories Grid-Tied Inverter Testing" are on the Sandia WEB page, www.sandia.gov/pv, and were presented at the 2nd World Conference and Exhibition on Photovoltaic Solar Conversion in Vienna in 1998. The salient points of this work are the definition of a non-islanding inverter, an acceptable design to develop a non-islanding inverter, and the identification of a resonant RLC circuit as being a "worst case" test for islanding. A non-islanding inverter is defined as an inverter that does not island when the inverter output frequency is within the defined operating frequency and voltage ranges, and the Q (quality factor) of a connected resonant RLC load is less than 2.5. Typically in the U.S., the acceptable frequency range is from 59.5 to 60.5 Hz and the voltage range is from 106 V ac to 127 V ac. If the frequency is outside the defined frequency range, the RLC circuit can have any Q. The value of Q = 2.5 was selected because the input from utility engineers on the IEEE P929 (Recommended Practice for Utility Interface of Photovoltaic Systems) working group indicated that higher values of Q were unlikely on a utility distribution line.

A further requirement is that all inverters in parallel with the non-islanding inverter be also non-islanding and that no synchronous generators be present. A method for designing an anti-islanding inverter that

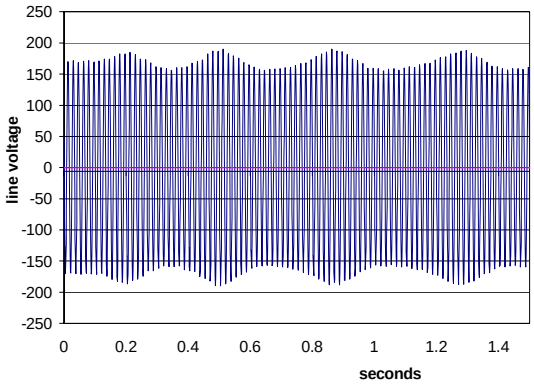

Figure 2. Islanding of a Single Inverter Worst Case Load, RLC Circuit, Q = 7.7

includes combined passive and active techniques was included in the Vienna paper. The passive methods are over/under frequency and over/under voltage. The active methods are defined as SFS (Sandia frequency shift) and SVS (Sandia voltage shift). For the inverter developed during the course of this project, all of these methods were required to prevent islanding in a resonant RLC circuit with a Q of 2.5. Loads other than the RLC circuit disconnected very rapidly with the exception of an induction motor. Although the case with the induction motor did not disconnect as rapidly as the cases in which the loads were not tuned to 60-Hz, the motor load was slightly easier to disconnect from than a resonant RLC circuit with a high Q.

When manufacturers develop new grid-tied inverters, it is inconvenient to require a multiple inverter test to verify non-islanding inverters. Furthermore, Underwriters Laboratories, which plans to perform anti-islanding tests as part of its UL1741 inverter test procedure, desires a single inverter test. Therefore, Sandia is currently working on the development of a single inverter test that identifies an "islanding" inverter. In addition, Sandia is preparing a report that documents a procedure for evaluating multiple

inverters. When IEEE P929 becomes a standard, it is likely that a single inverter UL test will be required and that Sandia's multiple inverter work will be referenced. Utilities feeling uncomfortable with the UL single-inverter test may either conduct their own multiple inverter tests or refer to Sandia's multiple-inverter evaluations. Work in 1999 will include multiple-inverter testing of several new inverters, each of which will be evaluated alone and with other inverters. At this time, it appears that any inverter that will island in the multiple-inverter scenario will also island by itself with a high Q resonant RLC load. This is demonstrated by the waveform above, where the utility disconnects at .1 second and the inverter runs on indefinitely.

Development of a New Hybrid 30-kW Power-Processing Unit

Some large hybrid power-processing units (PPUs) have experienced reliability problems, which may be attributed to their unique, site-specific designs. With that in mind, a specification was developed jointly between Sandia and Trace Technologies for a replicable design of a 30-kW hybrid power processor as a first step toward standardization. The PPU was to be tested at Sandia and provided to Arizona Public Service (APS) for use in its STAR facility. At STAR, it is to be integrated with a bank of tubular gel batteries of a new type that has been developed jointly by Yuasa and Sandia's battery group specifically for hybrid applications. The objectives of the project were to assist in the development of reliable photovoltaic-hybrid power-processing products with widespread applications; to provide APS with a useful tool for its application-driven research; and to enhance understanding of hybrid power-processing issues. Many of the observed problems in past installations resulted from the approach to site development. That approach assumed that the PPUs existed for the intended application, but then defined a specification that required a new product, and, consequently, fielded an untried prototype. The preferred approach, used in this development, includes the following steps: (1) define system requirements for a wide range of applications; (2) define inverter specification for a universal design; (3) build and evaluate an alpha unit; (4) field the unit at a test site; and, finally, (5) go to the production stage. The key point is that development and evaluation be completed prior to field deployment. The objective is to prevent deployment of a new, under-tested, prototype in a field installation. This product is now being deployed at other sites.

Testing: During the course of testing at Sandia, several issues were identified. All were addressed by Trace Technologies in a cooperative, cost-sharing effort. The major modifications involved primarily the control system and were made in response to suggestions by Sandia and APS personnel. These modifications have an impact on system reliability, generator compatibility, battery maintenance, and/or user satisfaction. They should make the PPU more universally applicable and less site-specific so that it can be applied in various sites with minimal field interaction required from the design engineer.

Lessons Learned: Reliability is a critical concern of APS. From the perspective of a utility, the number of conditions that could result in a loss of load should be minimized. A second lesson is that if ac current limiting is used to protect the PPU, then voltage sags are inevitable when large loads are applied. To minimize such sags, a reduced-voltage starter should be considered for motors that are a significant fraction of the PPU rating. Installation of such relatively inexpensive equipment can enhance performance significantly and should be considered a routine part of site load management when installing a photovoltaic-hybrid system. Site loads should be assessed for their sensitivity to disturbances and, if necessary, protected with an uninterruptible power supply. Selection of an undersized or poorly regulated engine/generator can undermine system performance. Engine/generators for PV-hybrid systems should include modern electronic (isochrynous) governors and should be rated for the maximum "expected" site load.

Accelerated lifetime testing of photovoltaic electronics: Highly accelerated lifetime testing (HALT™) is an effective tool for increasing reliability. By identifying latent problems, HALT™ lowers the failure rate from that typically associated with new products to that of a mature product. This evaluation stresses products beyond design specifications, establishes destruct limits, determines the root cause for failures and corrects problems before a product is fielded. Sandia is acting as a facilitator between the photovoltaic manufacturers and highly accelerated test laboratories (such as QualMark), which provide this testing. A typical test on a small inverter or charge controller costs $11,000, takes 200 hours for a humidity test and about 30 hours for vibration, temperature, and electrical stresses. Products in the development stage are targeted for HALT™ testing.

Quality and Reliability Contracts: Sandia has initiated contracts with selected companies to install quality programs at the contractor facilities that can lead to ISO 9000 certification. These programs are leading to more robust balance-of-system components.

Quality audits at contractor facilities: In lieu of funding full-scale quality programs at the contractors' facilities, a quality audit can be provided by Sandia. The quality audit consists of a visit by a quality inspector who then provides a written list of problem areas and suggested improvements. Quality audits are provided to qualified contractors who request them.

Sandia's Testing/Benchmarking Activities

- Filling a continuing need, the evaluation laboratory at Sandia supports PVMaT, photovoltaic manufacturers, and the photovoltaic industry. It includes instrumentation, loads, and power sources that may be beyond the means of balance-of-system manufacturers. Evaluations are provided free of cost to most U.S. manufacturers of photovoltaic components. As well as supporting the development of new products, the laboratory facilities benchmark existing products. These evaluations include:
- Evaluations of small, grid-tied inverters for islanding, power quality, and response to power disturbances, including voltage sags, surges, and EMI pulses while the inverters are connected in parallel with other inverters.
- Benchmarking evaluations of inverters that identify inverter problems or result in a report posted on the WEB. These are products that are generally not the result of a government contract and are available to the public for purchase. The tests of four such inverters in the past year resulted in redesign of the inverters and no report for the WEB. One evaluation of a product led to a WEB report.
- Evaluations of PVMaT hardware. When delivered to Sandia, PVMaT prototypes undergo a rigorous characterization. This is generally the first real evaluation of these prototypes, and design changes invariably result from this evaluation. Correcting problems and retest are essential elements in the development of any new product. Frequently, however, the contract is near its end and the contractor has not allotted funding for more product changes.
- Prototypes and other developmental photovoltaic balance-of-system hardware. These evaluations typically result from a manufacturer's request.

Sandia National Laboratories Subcontracts

Title: **Module Durability and Module Long-Term Exposure**

Organization: Florida Solar Energy Center, Cocoa, Florida

Contributors: Neelkanth G. Dhere, Principal Investigator; Kaustubh S. Gadre, Nachiket R. Raravikar, Piyush S. Jamkhandi, Shashank R. Kulkarni

Objective

The objective of the project is to identify and correct the mechanisms that affect module durability in collaboration with Sandia National Laboratories, National Renewable Energy Laboratory (NREL), and US photovoltaic (PV) module manufacturers. This work is sponsored and directed by Sandia as a part of the Module Durability Research Cooperative (MDRC). Thus far, FSEC's Module Durability and Module Long-Term Exposure (MLTE) project has performed research in collaboration with Siemens Solar Industries, Solarex, STR, ASE Americas, and United Solar Systems Corporation. Studies are being planned with additional manufacturers including Evergreen, AstroPower, and Solar Cells Inc.

Technical Approach

Adhesional strength measurements and morphology and composition analysis were employed as tools to demonstrate a quality control technique for manufacture of PV modules. A test plan with mutual goals was developed in consultation with the PV manufacturer and Sandia. Adhesion and surface morphology tests were conducted on 31 unframed PV modules randomly selected periodically from the assembly line over a period of about 16 months. Statistical error in the measurement of adhesional strength on the encapsulant was estimated in order to assess the reliability of the data and consequently the feasibility of the technique for industry wide use as a process quality control tool.

In a second study, elemental compositions and adhesional strength at the silicon-cell/EVA interface of samples extracted from a module deployed in the hot and humid Florida climate were studied. The module had been fabricated by a major PV manufacturer using slow-cure EVA.

A structured and controlled long-term outdoor exposure of commercially available modules was initiated during this fiscal year. Modules are exposed to the hot and humid climate of Florida in cooperation with Sandia and module manufacturers.

Results

Quality Control of PV Modules and Statistical Error Analysis

A total of 31 new crystalline-silicon PV modules were analyzed. Performance characterization of the modules was carried out at Sandia. Modules were then shipped to FSEC and examined under normal and ultraviolet light. Halos were observed under UV illumination in the bus line region of few modules. Usually four cells from each module were selected for sample extraction. Initially 40 samples were extracted from four cells of each module. The number was increased to 56 samples in order to improve the statistical averages in the bus line and middle regions. Additional samples were extracted around the bus lines of cells in the regions that showed the halos.

Average torque values necessary to twist off samples and the corresponding adhesive strengths were compiled. The bus lines stuck to the EVA on some samples in the bus line regions of three modules. Variation in the measured values of adhesional strength was in the 15-20% range. Statistical error was estimated in the measurement of adhesional strength on the encapsulant. It was found that experimental error introduced by sample chipping and non-circular sample shapes was caused by erratic application of

the torque and use of blunt tools during sample extraction. The error was reduced by use of sharp tools and through steady gradual torque application by raising the milling table in minute increments during sample extraction. The remaining major source of error was found to be in the measurement of the sample diameter. Error in the adhesive strength measurements introduced by assuming an ideal or inside diameter of the tool versus accurate measurement with a vernier caliper and vernier caliper attached to cross hair movement of an optical microscope was estimated to be <5%. Moreover, the actual error will be considerably lower if the same diameter measurement method is used consistently. Hence differences over 5% in adhesional strength can be ascribed to changes in the module manufacturing process. A reduction in the values of shear strength was accompanied by an increased spread in the values obtained at different locations on a given module.

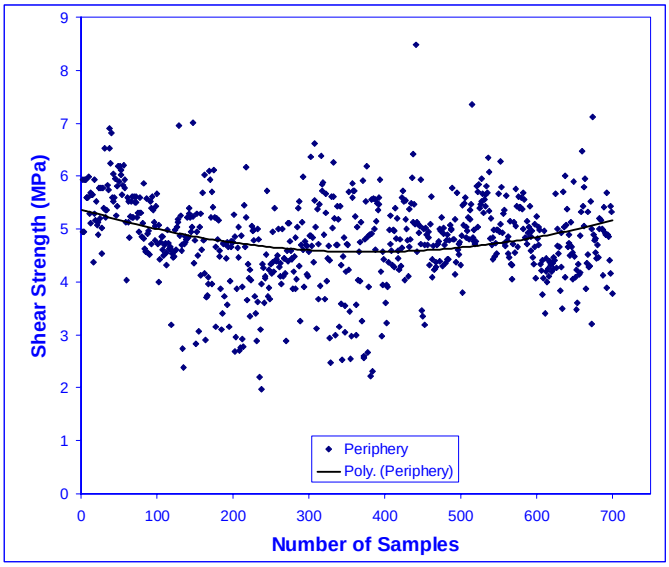

Figure 1. Adhesive strength of samples extracted from periphery region of cells of all modules.

This indicates that part of the reduction may be caused by variation of process parameters from one region to another. Modules were graded based on their average shear strengths for all the three regions viz. periphery, bus and middle as having excellent, good, moderate and low adhesive shear strengths. Figure 1 shows the variation of adhesive strength at the cell/EVA interface respectively in the periphery region during the course of this study. Mostly good to excellent shear strength was observed for the modules. A continuous spell of low to moderate average shear strength was observed for nine modules close to the middle of the test period. This may have been caused by the problems due to a transition from one model to another. Detailed extraction data has been supplied to Sandia and the PV manufacturer with a recommendation to investigate the reasons for low strengths.

Surface Analysis and Adhesional Strength Measurement

Samples were extracted from a module manufactured by a major US manufacturer using slow-cure EVA and deployed in the hot and humid climate at Cocoa, Florida. The average adhesive shear strength of the samples was lower by ~75% compared to that of samples from new modules. Auger Electron Spectroscopy (AES) was performed on the surface of a sample from one cell. The following energies and the atomic concentrations of elements were found: Si, 94 eV, ~0 at. %, P, 112 eV, 2.3 at. %, carbon, C, 270 eV, 26.6 at. %, Ti, at 385 eV, 13.9 at. %, Sn at 430 eV, 1.2 at. %, O, at 512 eV, 44.7, and Na at 990 eV, 11.3 at. % (Figure 2). An AES depth profile showed peaks of the anti-reflection coating elements titanium and oxygen and then a gradual decline beyond depths of 825 Å. Beyond the anti-reflection coating of TiO_x, the concentration of silicon increased continuously with increasing depth. Oxygen concentration was high at the surface. Surface

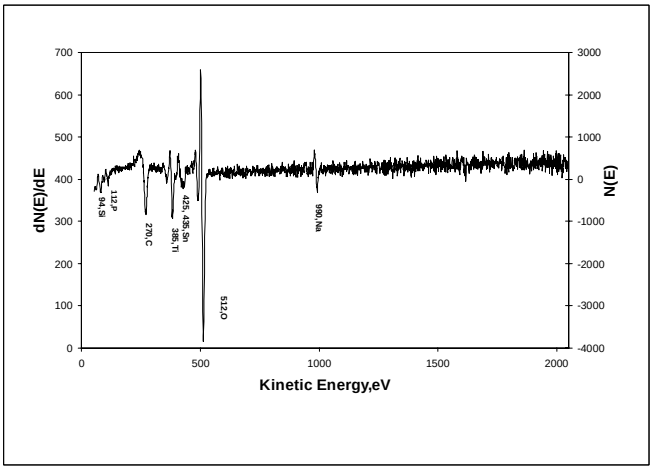

Figure 2. AES survey of a sample from cell (peripheral area) of a module deployed in a hot and humid climate.

concentrations of impurities phosphorous, sodium and tin were also high. Concentrations of carbon, sodium, phosphorous, and tin fell rapidly with increasing depth.

Compared to samples from new modules, all the samples from field deployed modules showed low adhesive strengths as well as low surface concentrations of carbon and high concentrations of phosphorous and sodium. Earlier, a good correlation was observed between the adhesive strength and surface concentration of carbon. Low carbon concentration, which indicated less EVA clinging to the cell surface, always resulted in low adhesive strengths. The reduction in the adhesive strength may be attributed to the precipitation of reaction products such as sodium phosphates and hydro-phosphates on the silicon cell surface reducing the sites for a bond between the silicon and EVA.

Initial high concentrations of impurities viz. sodium, phosphorous, and tin and an initial high concentration of oxygen point to a formation of a corrosive compounds, possible attack of the grid lines and solder, and spread of corrosion products containing tin on the cell surface. It is interesting to note that corrosion has occurred prior to delamination. Similar results were observed with the modules of two other major PV manufacturers.

Module Long-Term Exposure

Five modules each fabricated by Siemens (crystalline and CIGS modules), USSC, and ASE Americas were received from Sandia. Modules were carefully inspected and photographed. Four modules from each set have been mounted outdoors in identical configurations and one module was stored indoors as a control. Field-deployed modules and the control module are inspected and I-V curves are being taken on a monthly basis. This study is expected produce valuable information on module performance over a prolonged period.

1st MDRC/MLTE Symposium

The first PV Module Durability and Long-Term Exposure Symposium was organized at FSEC February 17-18, 1998. It was attended by 27 professionals from the US PV Industry, Sandia, NREL, and FSEC.

Publications

1. N. G. Dhere and K. S. Gadre, "Comparison of Mechanical Properties of EVA Encapsulant in New and Field-Deployed PV Modules," *Proc. 2nd World Photovoltaic Solar Energy Conf.* Vienna, Austria, July 6-10, 1998.
2. N. G. Dhere, et al., "Adhesion Measurement and Analysis at Cell/Encapsulant Interface as Quality Control Tools during PV Module Manufacture", *Proc. NCPV Program Review Meeting*, Denver, Colorado, Sept. 1998.
3. N. G. Dhere and K. S. Gadre, "Tensile Testing of EVA in PV Modules", *Proc. Int. Solar Energy Conf. Solar Engineering 1998*, ASME 1998, Albuquerque, New Mexico, (1998), pp. 491-497.
4. N. G. Dhere, M. E. Wollam, and K. S. Gadre, "Correlation Between Surface Carbon Concentration and Adhesive Strength at the Si Cell/Eva Interface in a PV Module", *Proc. 26th IEEE Photovoltaic Specialists' Conference*, Anaheim, California, (1997), pp. 1217-1220.
5. N. G. Dhere, K. S. Gadre, and A. M. Deshpande, "Durability Of Photovoltaic Modules", *Proc. 14th European Photovoltaic Solar Energy Conference*, Barcelona, Spain, (1997), pp. 256-259.
6. N. G. Dhere, "PV Module Technologies, Durability Concerns, Semiconductor Packages, Common Goals and Strategies", *Proc. PV Module Durability and Long-Term Exposure Symp.*, FSEC, February 17-18, 1998.
7. N. G. Dhere and K. S. Gadre, "Sample Extraction: Adhesion Measurements at Si/EVA Interface and Study of Mechanical Properties of EVA," *Proc. PV Module Durability and Long-Term Exposure Symp*., FSEC, Feb. 17-18, 1998.

8. N. G. Dhere, “Morphology and Surface Analysis of the c-Si cell/EVA Interface in New and Field-deployed PV Modules” *Proc. PV Module Durability and Long-Term Exposure Symp*., FSEC, February 17-18, 1998.
9. N. G. Dhere, K. S. Gadre, and N. Raravikar, “Quality Control,” *Proc. PV Module Durability and Long-Term Exposure Symp*., FSEC, February 17-18, 1998.
10. N. G. Dhere, K. S. Gadre, and K. W. Lynn, “Review of ASTM Standards Relevant to Encapsulants: Quality Control,” *Proc. PV Module Durability and Long-Term Exposure Symp*., FSEC, February 17-18, 1998.
11. *Proc. PV Module Durability and Long-Term Exposure Symp.,* FSEC, Feb. 17-18, 1998.
12. N. G. Dhere, et al., “Quality Control of PV Module Manufacture Using Adhesion Measurement at Si-Cell/Encapsulant Interface”, Sandia Tech Brief 22, 1998.
13. N. G. Dhere, et al., “Statistical Error Analysis of Adhesional Strength Measurements”, Sandia Tech Brief 23, 1998.
14. N. G. Dhere, et al., “Review of ASTM Standard on Plastics Relevant for PV Module Encapsulants”, Sandia Tech Brief 24, 1998.
15. N. G. Dhere, et al., “Study of Solarex c-Si Module deployed in Hot and Humid Climate” Sandia Tech Brief 25, 1998.

Title: **Photovoltaic System Performance and Engineering**

Organizations: Photovoltaic Systems Assistance Center
Sandia National Laboratories, Albuquerque, New Mexico
Florida Solar Energy Center, Cocoa, Florida
Southwest Technology Development Institute, Las Cruces, New Mexico

Contributors: H. Post, W. Bower, R. Chapman, R. Hill, A. Maish, J. Stevens, M. Thomas, J. Ventre (FSEC), S. Durand (FSEC), A. Rosenthal (SWTDI), J. Wiles (SWTDI)

Objectives

This project supports the National PV Program by using our systems engineering expertise to focus on the following major objectives:

- make sure that systems work as expected
- make sure that systems meet customers' needs, and
- work with the PV industry to identify approaches to reduce the life-cycle cost of PV systems.

The primary focus for this project is the near-term time frame reflecting system applicability, design, component integration, installation, and performance.

Technical Approach

This project provides system level technical assistance and information to the PV community through the Photovoltaic Systems Assistance Center (PVSAC); validates the performance, safety, reliability, and cost of systems and components of fielded systems; and integrates new hardware and designs for PV applications. The project is a fully integrated team effort consisting of Sandia, Southwest Technology Development Institute (SWTDI), and the Florida Solar Energy Center (FSEC).

Results

Specific results were achieved for a number of systems' activities including safety, performance, design, education and training, economic analyses, federal agency assistance, and state programs.

System Safety – Sandia has taken the lead in providing PV input into the development of the National Electrical Code (NEC) for the past several cycles. A total of 57 recommended changes that will enhance the safety of PV installations were submitted and approved for inclusion in the 1999 NEC. In addition, Code Corner, a regular section in *Home Power* magazine, which addresses the NEC for PV, has been authored through the PVSAC for the last two years.

System Performance – Monthly performance reports for fielded systems at Pinnacles National Monument, Rogers Peak, Dangling Rope, Santa Cruz Island, and Desert Studies were prepared. These reports serve as a database for system life-cycle cost analyses. In addition, an assessment on the side-by-side comparison of super energy efficient housing with and without PV was completed. The report documents the load compatibility with PV generation and opportunities for as much as an 84 percent residential load

reduction through higher efficiencies (1). The cost of house modifications, however, needs to be reduced by 50 percent for PV to be economically feasible.

System Design – Working with system reliability databases from several hundred SMUD and EPA systems, an initial assessment of PV system reliability was made (2). The continuing maintenance costs for these systems, however, vary by over an order of magnitude, from approximately $0.01/kWh to $0.10/kWh. These results emphasize the continuing need to develop a qualified database to assess PV reliability. A report on hurricane-resistant housing design for disaster mitigation was prepared (3). The report documents a collaborative effort with industry to identify components and system integration needs.

Education and Training – To support the Million Solar Roofs Initiative, both FSEC and SWTDI have established education and training centers to familiarize program partners with PV systems. These centers provided eight workshops on PV to various utilities, developers, and government agencies leading to active team participation in UPVG-funded projects at Lakeland, Florida and Tucson, Arizona. The IEA Task V meeting covering distributed PV interconnection was hosted by Sandia in September 1998. Although this was planned as the final meeting for this task group, the activity was extended by IEA for another three years. The Europeans are far ahead of the US in distributed generation because of heavily subsidized government programs. To promote PV with the general public and maintain a continuing communications channel with industry and others in the PV community, Sandia developed a nationally recognized website www.sandia.gov/pv that provides both technical and non-technical information. The website ranks among Sandia's ten most frequently accessed sites.

System Economic Analyses – To address the issue of true system life-cycle cost, we completed comprehensive performance and economic assessment reports on three large (>10kW) hybrid PV systems at Pinnacles National Monument, Rogers Peak, and Dangling Rope (4,5,6). All three systems are performing as expected, although none would satisfy a simple 10-year payback on the PV investment. Of particular importance for these systems is the value of the recurring cost as a fraction of the overall net present value of the life-cycle cost. While recurring maintenance costs are limited to about 5 percent, the overall recurring costs (maintenance plus capital replacement) run as high as 25 percent.

Federal Agency Assistance – The PVSAC *Renew the Government* partnerships with the National Park Service, the Bureau of Land Management, and the USDA Forest Service were completed with the installation of 122 systems accounting for 313 kW of PV at agency sites around the US (7). Our assistance to these agencies included field assessment, conceptual design, specification development, design review, and procurement assistance. As part of this effort, we collaborated with the Bureau of Land Management to develop packaged procurements using standardized specifications for 10 water pumping systems and 5 small facility power systems with the goals of reduced cost, simplified operation and maintenance, and a sustainable procurement process. In addition, the systems team conducted system assessments at 8 sites, as well as project assessments at another 8 sites, to expand our partner familiarity with PV and to help assure that the systems work as expected. The lessons learned through our federal agency assistance activities are summarized in Table I.

State Program – Pilot PV projects in seven states (Colorado, Maryland, Missouri, Montana, New Mexico, Oregon, and Wisconsin) were completed. These projects were developed in collaboration with state utilities and/or agencies that have limited experience with PV with the purpose of increased familiarization with PV systems and system opportunities. The lessons learned in the project development work are currently being documented (8).

Table I. Lessons Learned to Increase Agency use of Photovoltaic Systems

- Determine what you need before you procure it.
- A project advocate for photovoltaics use must exist in the agency and must be in a position to affect decisions.
- A system should be adequately specified before it is procured, and the agency should be directly involved.
- The procurement of standardized photovoltaic systems through standardized specifications and standardized processes greatly benefits the agency.
- Packaged procurements of standardized systems for multiple agency sites through a centralized office have proven successful.
- Human presence, such as a site host with a photovoltaic power system, is an effective way to prevent theft and other vandalism at a remote site.
- The cost of battery replacement in photovoltaic systems must be included in planning for future maintenance costs for the system.
- Successful projects are those that are based on best value, such as environmental concerns, energy security, educational opportunities, lowest user investment, and lowest life-cycle costs.
- Viable photovoltaic projects are typically for remote applications where the cost of photovoltaics is compared against other remote power options.
- Energy savings cannot be used to justify the photovoltaic project costs.

Conclusions

These efforts directly address the commercialization of PV systems by using PV program expertise to assist both the industry and the user community to achieve the highest probability of success that systems work as expected. Cost and lack of familiarity have been identified as the primary barriers to increased use of PV systems. We will continue to address these issues. The completion of the *Renew the Government* partnerships and the resulting 122 systems, which provided hands-on experience to agency personnel in the design, procurement, installation, and operation of PV systems, is a major accomplishment for the PVSAC. The success of the activity and the importance of the work were acknowledged by leadership awards this year from the National Park Service, the Bureau of Land Management, and the Interstate Renewable Energy Council to PVSAC team members. The need for quality field data to develop information on reliability, maintenance cost, and life-cycle system cost has never been greater. A number of accomplishments addressed these issues during this year, including the initial assessment of system reliability, economic assessments of hybrid systems, and continued evaluation of fielded systems. More effort to resolve these issues is needed.

References

1. Parker, D. *The Impact of PV on Energy-Efficient Housing*. FSEC-CR-1019-98. Florida Solar Energy Center, July 1998.
2. Maish, A. "Defining Requirements for Improved PV System Reliability," *Proceedings of the 1998 Photovoltaic Performance and Reliability Workshop,* Cocoa Beach, Florida, November 1998.

3. Rosenthal, A., S. Durand, M. Thomas, and H. Post. "Economic Analysis of PV Hybrid Power System: Pinnacles National Monument," *Proceedings of the 26th IEEE PVSC*, Anaheim, California, October 1997.
4. Rosenthal, A., S. Durand, M. Thomas, and H. Post. "Economics and Performance of PV Hybrid Power Systems: Three Case Studies," *Proceedings of ASES Solar 98 Conference*, Albuquerque, New Mexico, June 1998.
5. "Dangling Rope Marina: A Photovoltaic-Hybrid Power System," *Quarterly Highlights of Sandia's Photovoltaic Program*, Volume 1, 1998.
6. Post, H., M. Thomas, T. Duncan, P. Fleming, and A. Dziobek. *Renew the Government – Summary of Projects and Lessons Learned.* SAND98-1943, Sandia National Laboratories, October 1998.
7. Hill, R. *PV in the States: Summary of Projects and Lessons Learned* (to be published, 1999).

Title: **University Center of Excellence for Photovoltaics Research and Education**

Organization: School of Electrical and Computer Engineering
Georgia Institute of Technology, Atlanta, Georgia

Contributors: A. Rohatgi, Director; S. Narasimha, P. Doshi , A. Ebong, V. Yelundur, T. Krygowski, S. Kamra and A. Ristow

The overall objective of this program is threefold: First, to develop rapid and low-cost manufacturable processes that can improve yield, throughput, and performance of silicon photovoltaic devices; second, to design and fabricate high efficiency solar cells on promising low-cost photovoltaic materials; and third, to improve the fundamental understanding of advanced photovoltaics devices. In this report several rapid and potentially low-cost technologies are developed and applied toward the fabrication of high efficiency silicon solar cells.

Fundamental Understanding and Development of Screen-Printing Metallization for Mono-crystalline Si Solar Cells

One of the most difficult aspects of large-scale solar cell production is forming low-cost, high-quality front contacts. Screen-printing (SP) offers a simple, cost-effective contact method that is consistent with the requirements for high-volume manufacturing. The current problem with SP, however, is that the throughput gains are attained at the expense of device performance. Literature shows considerable scatter in the fill factor values of SP solar cells. In addition there are no clear guidelines for achieving high fill factors. Therefore, a methodology for optimizing SP metallization is developed, recognizing the fact that fill factor can be degraded by gridline resistance, contact resistance, and contact-formation-induced junction leakage and shunting. The first step in this methodology involves measuring metal resistivity as a function of firing temperature. For the Ag paste #3349 used in this study, metal resistivity decreased with increase in firing temperature and for a firing time of 30 sec, it went below 3 μ-ohm-cm for firing temperature above 700^{o}C. Model calculations indicated that 3 μ-ohm-cm was sufficient to achieve fill factor in excess of 0.78. The next step involved measuring shunt resistance as a function of firing temperature, which showed that for 30 sec firing time, firing temperature should not exceed 730^{o}C to maintain Rsh in excess of 1 kΩ-cm^{2}. The third step involved tailoring the junction depth for 730^{o}C/30 min firing cycle in order to minimize junction leakage current (J_{02}). It was found that ~0.5 μm deep junction with a sheet resistance of ~40 ohms/sq was required to maintain J_{02} value below 10^{-8} A/cm^{2} along with acceptable shunt resistance. Finally, a 400^{o}C/10 min forming gas anneal was required to reduce the series resistance to about 0.5 ohm-cm^{2}. Systematic optimization of the firing cycle and junction depth, coupled with a post contact forming gas anneal, resulted in fill factors in excess of 0.78 on monocrystalline silicon. Preliminary results on multicrystalline silicon cells indicate that firing cycle and junction depth may need to be optimized for each multicrystalline silicon material due to the possible role of defects in causing junction shunting underneath the gridlines. Shorter firing times in conjunction with higher firing temperatures are being investigated for mc-Si cells.

Comparison of Front and Back Surface Passivation Schemes for Silicon Solar Cells

A comprehensive and systematic investigation of low-cost surface passivation technologies was conducted for achieving high-performance silicon devices such as solar cells. Most commercial solar cells today lack adequate surface passivation, while laboratory cells use conventional furnace oxides (CFO) for high-quality surface passivation involving an expensive and lengthy high-temperature step. This investigation tries to bridge the gap between commercial and laboratory cells by providing fast, low-

cost methods for effective surface passivation. This research demonstrates for the first time the efficacy of TiO_2, thin (<10 nm) RTO, and PECVD SiN individually and in combination for (phosphorus diffused) emitter and (undiffused) back surface passivation. The effects of emitter sheet resistance, surface texture, and three different SiN depositions (two direct PECVD systems and one remote plasma system) were investigated. The impact of post-growth/deposition treatments such as forming gas anneal (FGA) and firing of screen-printed contacts was also examined. This study reveals that the optimum passivation scheme consisting of a thin RTO with a SiN cap and 730°C screen-printed contact firing anneal can (a) reduce the emitter saturation current density, J_{oe}, by a factor >15 for a 90 Ω/sq emitter, (b) reduce J_{oe} by a factor of >3 for a 40 Ω/sq emitter, and (c) reduce S_{back} below 20 cm/s on 1.3 Ωcm p-Si. (Fig. 1) Furthermore, this double-layer RTO+SiN passivation is relatively independent of the deposition conditions (direct or remote) of the SiN film and is more stable under heat treatment than SiN or RTO alone. Critical to achieving low *S* by the RTO/PECVD SiN stack is the use of a short, moderate temperature anneal (in this study 730°C for 30 seconds) after the stack formation. This thermal treatment is believed to enhance the release and delivery of atomic hydrogen from the SiN film to the $Si\text{-}SiO_2$ interface, thereby reducing the density of interface traps at the silicon surface. Compatibility with this post-deposition anneal makes the stack passivation scheme attractive for cost-effective solar cell production where a similar anneal is required to form screen-printed contacts. Model calculations are also performed to show that the RTO+SiN surface passivation scheme may lead to greater than 17% efficient thin screen-printed cells even with a low bulk lifetime of 20 μs.

An Optimized Rapid Aluminum Back Surface Field Technique for Silicon Solar Cells

Screen-printing and rapid thermal annealing have been combined to achieve an aluminum-alloyed back surface field (Al-BSF) that lowers the effective back surface recombination velocity (S_{eff}) to approximately 200 cm/s for solar cells formed on 2.3 Ω-cm Si. Analysis and characterization of the BSF structures show that this formation process satisfies the two main requirements for achieving low S_{eff}: (1) deep p^+ regions and (2) uniform junctions. Screen-printing is ideally suited for fast deposition of thick Al films which, upon alloying, result in deep BSF regions. Use of a rapid alloying treatment is shown to significantly improve the BSF junction uniformity, reduce $S_{eff,}$ and increase $V_{oc.}$ (Fig. 2) The Al-BSFs formed by screen-printing and rapid alloying have been integrated into both laboratory and industrial-type fabrication sequences to achieve solar cell efficiencies in excess of 19.0% and 17.0%, respectively, on planar 2.3 Ω-cm float zone Si. For both process sequences, these cell efficiencies are 1-2% (absolute) higher than analogous cells made with un-optimized Al-BSFs or highly recombinative rear surfaces.

Development of High Efficiency String Ribbon Silicon Solar Cells

Research was also conducted to achieve high efficiency cells on multicrystalline silicon materials. In this report, the effect of impurity gettering and defect passivation by hydrogenation was examined on 100 μm thick string ribbon silicon material from Evergreen Solar. The first 100 μm thick fully screen-printed cell with a beltline diffused emitter (BLP) of 45 Ω/ produced efficiencies as high as 10.9%. The main loss components of the screen-printed devices were in the blue response and low shunt resistance. The shunt resistance of screen-printed devices was increased from 200 $\Omega\text{-cm}^2$ to over 5000 $\Omega\text{-cm}^2$ by implementing a spike in the contact firing profile. An increase in the red response resulted in cells that were spike fired and may be due to enhanced bulk hydrogenation from the SiN film. Cell efficiencies as high as 14.9% were achieved on 250 μm substrates using beltline processing and screen-printing. (Fig. 3)

A Novel Processing Technology for High-Efficiency Silicon Solar Cells

A novel simultaneous boron and phosphorus diffusion technique is presented to produce simple, high efficiency $n^+ pp^+$ silicon solar cells in one thermal cycle. This technique uses boron and phosphorus spin-

on dopant films to fabricate limited solid doping sources out of dummy silicon wafers. This approach results in the delivery of a fixed dose of P_2O_5 or B_2O_3 to the diffused sample. The resulting diffusion glass is extremely thin (~60 Å) which allows for the *in-situ* growth of a passivating thermal oxide without increasing the solar cell reflectance. J_o measurements show that the *in-situ* oxide passivation for a light boron and phosphorus diffusion provides excellent passivation properties, resulting in J_o values in the 100 fA/cm^2 range. Measurements of the bulk minority carrier lifetime show that by fabricating separate boron solid sources, trace impurities in the spin-on dopant film are not transported to the diffused sample. This filtering action is shown to result in bulk lifetimes in excess of 1 ms for silicon doped indirectly from the source wafers, but gives much lower lifetimes (~6 µs) for the wafers on which the boron spin-on film was directly applied. This process was validated by fabricating *in-situ* oxide passivated, n^+pp^+ solar cells in one high temperature cycle incorporating several high efficiency features including surface texturing and a Back Side Reflector (BSR), resulting in confirmed efficiencies in the 19-21% range. (Fig. 4)

Integration of Rapid Process Technologies for High Efficiency Silicon Solar Cells

Finally, the rapid and potentially low-cost processes are integrated to form high efficiency devices. RTP solar cell efficiencies of 17% and >19% are achieved on monocrystalline silicon with screen printed and photolithography contact, respectively. Rapidly formed screen printed cells in a commercial beltline machine also resulted in 17% efficient cells on monocrystalline silicon and 14.9% efficient cells on multicrystalline string ribbon material. Table 1 summarizes the gradual progression of rapid thermal technologies being developed at Georgia Tech. This research has the potential of transforming 300-400 µm thick 12-15% efficient industrial cells today to 100-200 µm thick >17% efficient cells in the near future.

Table 1. Progression of Rapid Processing Technologies Developed at Georgia Tech

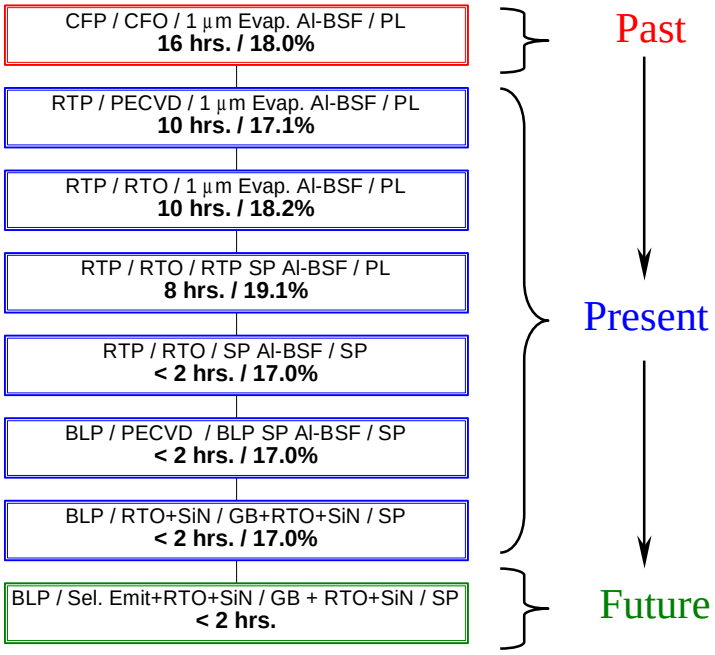

CFP = Conventional Furnace Processing
RTP = Rapid Thermal Processing
BLP = Belt Line Processing (with Lamps)
PL = Photolithography; SP = Screen Printing
GB = Grided Back (SP Contacts)

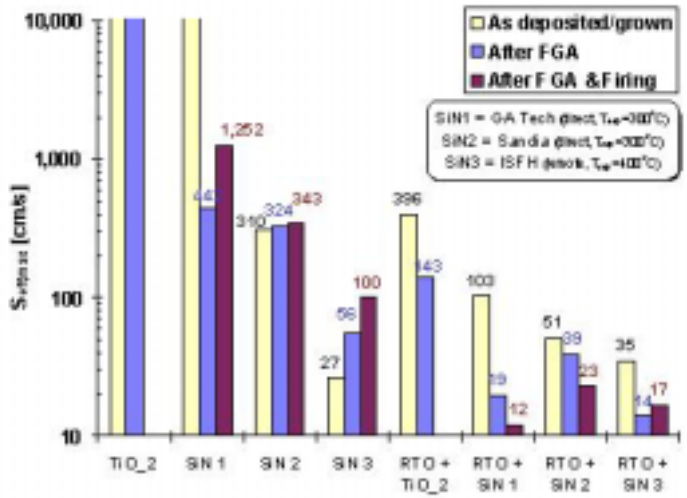

Fig.1. Library of back surface passivation schemes.

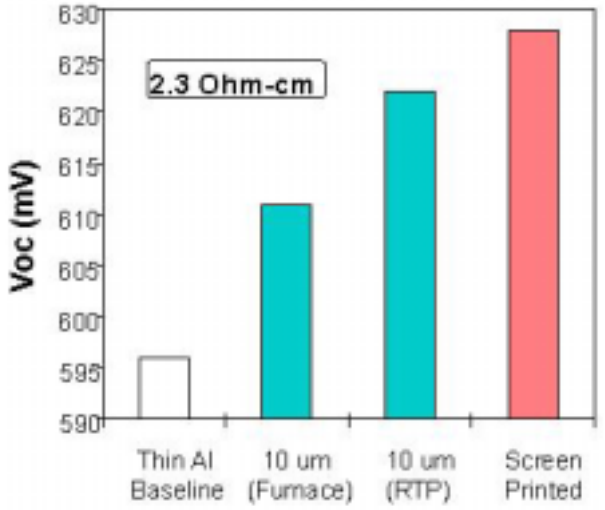

Fig.2. Effect of different Al-BSF processes on V_{oc}.

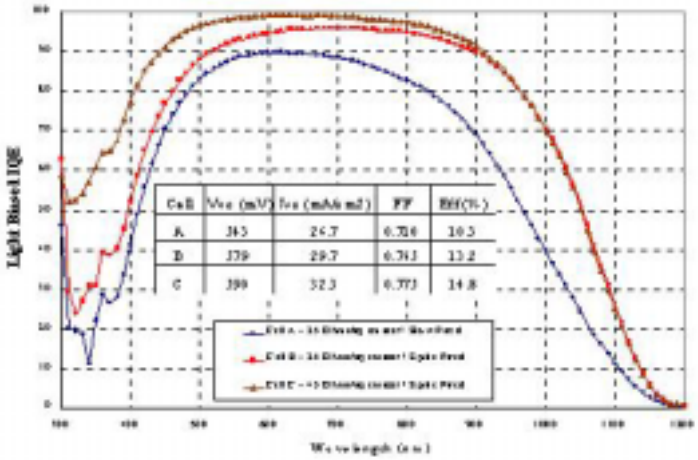

Cell	Voc (mV)	Jsc (mA/cm2)	FF	Eff(%)
A	383	29.7	0.726	20.5
B	379	29.7	0.713	20.2
C	399	32.3	0.723	24.8

Fig.3. Comparison of screen-printed String Ribbon cells: A - 25 Ohms/sq emitter and slow fired contacts, B - 25 Ohms/sq emitter and spike fired contacts, C - 45 Ohms/sq emitter and spike fired contacts.

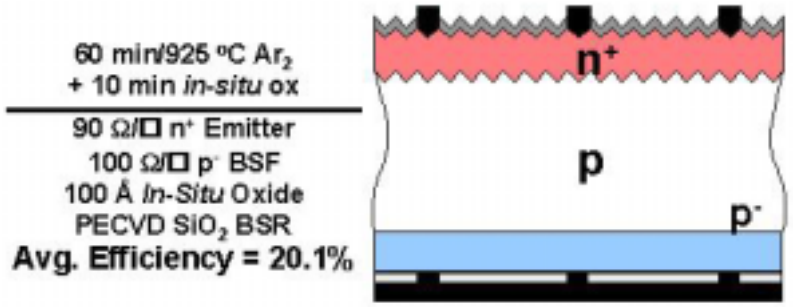

Fig.4. High-efficiency STAR II cells.

11.0 List of Active NREL Subcontracts

11.0 LIST OF ACTIVE NREL SUBCONTRACTS FOR FY 1998

Contractor, Principal Investigator, Address	Work Title (Research Activity)	Contract Number	FY 1998 Funding ($K)	Start/ End Dates
PV FUNDAMENTAL AND EXPLORATORY RESEARCH PROJECT **Crystalline Silicon** **Bhushan Sopori**				
Cornell Univerity D. Ast Ithica, NY 14853-1501	Low Cost Glass and Glass-Ceramics Substrates for Thin film Silicon Solar Cells	XAF-8-17607-06	105	2/98 12/00
Duke University T. Tan Durham, NC 27708	Investigation of Gettering Mechanisms in Crystalline Silicon	XAF-7-17607-01	30	7//97 3/00
Georgia Institute of Technology A. Rohatgi Atlanta, GA 30332	High Efficiency Solar Cell Fabrication on Commercial Silicon Substrates	XAF-8-17607-05	140	2/98 2/01
Lehigh University M. Stavola Bethlehem, PA 18015	Hydrogen-Defect Interactions Relevant to Si Solar-Cell Fabrication Studied by Vibrational Spectroscopy	XCE-8-18684-01	29.9	8/98 7/99
Massachusetts Institute of Technology L. Kimerling Cambridge, MA 02139	Role of Point Defects and Impurities in Processing and Performance of Crystalline Silicon Solar Cells	XD-2-11004-4	35	7/92 12/98
North Carolina State University G. Rozgonyi Raleigh, NC 27695	Characterization and Ti Gettering of PV Substrates	XAF-8-17607-03	105	1/98 1/01
Texas Tech. University S. Eistreicher Lubbock, TX 79409	Theoretical Analysis of Hydrogen-Vacancy-Impurity Formation and Dissociation	XAX-5-15230-01	49.9	6/95 6/99
University of California at Berkeley E. Weber Berkeley, CA 94720	Impurity Precipitation, Dissolution, and Gettering in PV Silicon	XAF-8-17607-04	140	1/98 1/01
University of South Florida S. Ostapenko Tampa, FL 33620	Optimization of Gettering Processes for PV Silicon	XD-2-11004-5	30	1/98 6/99

NREL Subcontracts for FY 1998				
Contractor, Principal Investigator, Address	**Work Title (Research Activity)**	**Contract Number**	**FY 1998 Funding ($K)**	**Start/ End Dates**
PV FUNDAMENTAL AND EXPLORATORY RESEARCH PROJECT **Exploratory Materials and Devices** **R. McConnell**				
California Institute of Technology H. Atwater Pasadena, CA 91125	Novel Low-Temperature Substrate Technology for Compound Semiconductor Solar Cells on Low-Cost Substrates	XAL-4-13357-01	0	7/94 12/97
Johns Hopkins University P. Searson Baltimore, MD 21218	Solar Energy Conversion at Dye-Sensitized Nanostructured Electrodes Fabricated by Sol-Gel Processing	XAD-3-12114-04	0	7/93 4/98
Research Triangle Institute R. Venkatasubramanian Research Triangle Park, NC 27709	High-Efficiency GaAs Solar Cells on Polycrystalline Ge Substrates	YAL-4-13357-03	0	8/94 12/97
University of California at Los Angeles E. Yablonovitch Los Angeles, CA 90095	Ultra-Efficient Epitaxial Liftoff Solar Cells Exploiting Optical Confinement in the Wave Limit	XAL-4-13357-02	80	7/94 7/98
University of Illinois at Urbana-Champaign A. Rockett Urbana, IL 61820-6242	Fundamental Studies of the Effect of Crystal Defects on $CuInSe_2$ Heterojunction Behavior	XAD-3-12114-1	0	6/93 6/98
University of South Florida D. Morel Tampa, FL 33620	Heterojunction Development and Optimization in Thin-Film Compound Semiconductor Cells	XAD-3-12114-3	0	5/93 5/98
University of Utah P. Taylor Salt Lake City, UT 84112	Electronic Process in Thin-Film PV Materials	XAD-3-12114-02	0	4/93 12/98

NREL Subcontracts for FY 1998				
Contractor, Principal Investigator, Address	**Work Title (Research Activity)**	**Contract Number**	**FY 1998 Funding ($K)**	**Start/ End Dates**
PV FUNDAMENTAL AND EXPLORATORY RESEARCH PROJECT **Historically Black Colleges and Universities (HBCU)** **R. McConnell**				
Central State University C.W. Fuller Wilberforce, OH 45384	HBCU PV Research Associates Program	XAX-5-15021-04	16.9	10/95 10/98
Clark Atlanta University G. Grams Atlanta, GA 30314	HBCU PV Research Associates Program	XCR-6-15327-01	0	10/95 4/98
Clark Atlanta University G. Grams Atlanta, GA 30314	HBCU PV Research Associates Program	XAX-5-15021-02	60.4	9/95 9/98
Mississippi Valley State Univ. B. Balam Itta Bena, MS 38941	HBCU PV Research Associates Program	XAX-5-15021-06	33.7	10/95 10/99
Southern University P. Bhattacharya Baton Rouge, LA 70813	HBCU PV Research Associates Program	XAX-5-15021-05	15.5	9/95 9/98
Texas Southern University J. Hill Houston, TX 77004	HBCU PV Research Associates Program	XAX-5-15021-03	17	10/95 10/98
THIN-FILM PV PARTNERSHIP PROJECT **K. Zweibel**				
Astropower, Inc. J. Rand Newark, DE 19716	Monolithically Interconnected, Silicon-Film Modules	ZAK-8-17619-01	744	11/97 11/00
BP Solar D. Cunningham Fairfield, CA 94533	Apollo Thin-Film Process Development	ZAK-8-17619-27	151.4	5/98 5/01
Colorado School of Mines D. Williamson Golden, CO 80401	Microstructure of a-Si-Based Solar Cell Materials by Small-Angle X-Ray Scattering	XAN-4-13318-04	0	4/94 6/98

NREL Subcontracts for FY 1998				
Contractor, Principal Investigator, Address	**Work Title (Research Activity)**	**Contract Number**	**FY 1998 Funding ($K)**	**Start/ End Dates**
Colorado School of Mines D. Williamson Golden, CO 80401	Nanostructure of a-Si:H and Related Alloys by Small-Angle Scattering of Neutrons and X-rays	XAK-8-17619-31	37	5/98 7/01
Colorado School of Mines J. Trefny Golden, CO 80401	Process of Development and Basic Studies of Electrochemically Deposited CdTe-Based Solar Cells	XAK-8-17619-28	251.4	5/98 4/01
Colorado School of Mines J. Trefny Golden, CO 80401	Process of Electrochemically Deposited CdTe-Based Solar Cells	XAF-5-14142-11	127.8	4/95 6/98
Colorado State University J. Sites Fort Collins, CO 80525	Device Physics of Thin-Film Polycrystalline Cells and Modules	XAX-4-14000-01	0	12/93 3/98
Colorado State University J. Sites Fort Collins, CO 80525	Device Physics of Thin-Film Polycrystalline Solar Cells	XAK-8-17619-07	140.3	01/98 01/01
Daystar Technologies J. Tuttle Denver, CO 80209	Development of a Thin-Film Based Microconcentrator Photovoltaic Technology	ZAK-8-17619-25	38.4	5/98 4/99
Energy Conversion Devices X. Deng Troy, MI 48084	Development of High, Stable-Efficiency Triple-Junction a:Si Alloy Solar Cells	ZAN-4-13318-11	48	7/94 2/98
Energy Conversion Devices S. Jones Troy, MI 48084	Use of Very High Frequency Plasmas to Prepare a-Si:H-Based Triple-Junction Solar Cells at High Deposition Rates	ZAK-8-17619-18	235	3/98 5/01

NREL Subcontracts for FY 1998				
Contractor, Principal Investigator, Address	**Work Title (Research Activity)**	**Contract Number**	**FY 1998 Funding ($K)**	**Start/ End Dates**
Energy Photovoltaics A. Delahoy Princeton, NJ 08543	Thin-Film CIGS Photovoltaic Technology	ZAF-5-14142-04	0	1/95 1/98
Energy Photovoltaics A. Delahoy Princeton, NJ 08543	Thin-Film CIGS Photovoltaic Technology	ZAK-8-17619-21	510.5	4/98 4/01
Florida Solar Energy Center N. Dhere Cocoa, FL 32922	CdTe Module Testing and Study of Transients and Irreversible Effects in CdTe Thin-Film Solar Cells	XCR-6-16773-01	5	5/96 11/98
Florida Solar Energy Center N. Dhere Cocoa, FL 32922	$CuIn_{1-x}Ga_xSe_2$ Thin Film Solar Cells	XAK-8-17619-12	31.7	02/98 02/01
Global Solar Energy J. Britt Tucson, AZ 85747	Process Development of Large Area, Thin-Film CIGS-Based PV Modules	ZAK-8-17619-04	503.3	2/98 2/01
Harvard University R. Gordon Cambridge, MA 02138	Optimization of Transparent and Reflecting Electrodes for a-Si Solar Cells	XAN-4-13318-05	39.5	5/94 5/98
Harvard University R. Gordon Cambridge, MA 02138	Optimization of Transparent and Reflecting Electrodes for Solar Cells	XAK-8-17619-26	86	4/98 4/01
Iowa State University V. Dalal Ames, IA 50011	Comprehensive Research on Stability and Performance on a-Si:H and Alloys	XAN-4-13318-08	65	5/94 7/98
Iowa State University V. Dalal Ames, IA 50011	Research on Improved Amorphous Silicon and Alloy Materials and Devices Prepared using ECR Plasma Techniques	XAK-8-17619-30	70	7/98 7/01
ISET V. Kapur Inglewood, CA 90301	Application of CIS to High-Efficiency PV Module Fabrication	ZAF-5-14142-07	189	4/95 6/98

NREL Subcontracts for FY 1998				
Contractor, Principal Investigator, Address	**Work Title (Research Activity)**	**Contract Number**	**FY 1998 Funding ($K)**	**Start/ End Dates**
ISET V. Kapur Inglewood, CA 90301	CIS-Type PV Device Fabrication by Novel Technique	ZAK-8-17619-10	350	6/98 6/01
ITN Energy Systems P. Meyers Wheat Ridge, CO 80033	Atmospheric Pressure CVD of CdTe for High Efficiency Thin-Film PV Devices	ZAK-8-17619-03	198.3	1/98 1/01
Materials Research Group I. Eisgruber Wheat Ridge, CO 80033	In-Situ Sensors for Process Control of $CuInGaSe_2$	ZAK-8-17619-08	90	2/98 2/01
MV Systems A. Madan Golden, CO 80401	High Efficiency, Stable Hot Wire CVD Prepared Amorphous and Polycrystalline Silicon Film Solar Cells	XAK-8-17619-16	175	4/98 4/01
National Institute of Standards and Technology A. Gallagher Boulder, CO 80303	Atomic-Scale Characterization of a-Si:H Films and Devices	DAD-4-14084-01	50	12/94 3/98
National Institute of Standards and Technology A. Gallagher Boulder, CO 80303	Characterization of Small Particle Formation in the Preparation of Amorphous Silicon Solar Cells and Determination of the Electric Field Profile in Solar Cells using Scanning Tunneling Microscopy	DAD-8-18653-01	60	7/98 7/01
Pennsylvania State University R. Collins University Park, PA 16802	Wide-Band-Gap Solar Cells with High Stabilized Performance	XAN-4-13318-03	65	7/94 3/98
Pennsylvania State University R. Collins University Park, PA 16802	Stable a-Si:H-Based Multijunction Solar Cells with Guidance from Real Time Optics	XAF-8-17619-22	175	3/98 9/01
Pennsylvania State University S. Fonash University Park, PA	Modeling of Wide-Bandgap CIS-Based Solar Cells	XAK-8-17619-35	0	10/98 10/01

NREL Subcontracts for FY 1998				
Contractor, Principal Investigator, Address	**Work Title (Research Activity)**	**Contract Number**	**FY 1998 Funding ($K)**	**Start/ End Dates**
Purdue University J. Gray West Lafayette, IN 47907	Computer Modeling Support for $CuInSe_2$ and CdTe Solar Cells	XAK-8-17619-36	0	11/98 11/01
Siemens Solar Industries D. Tarrant Camarillo, CA 93011	CIS-Based Thin Film PV Technology	ZAF-5-14142-03	1,076.3	8/95 12/98
Solar Cells, Inc. G. Dorer Toledo, OH 43607	Technology Support for Initiation of High-Throughput Processing of Thin-Film CdTe PV Modules	ZAF-5-14142-05	1032.5	3/95 3/98
Solar Cells, Inc. G. Dorer Toledo, OH 43607	Technology Support for Initiation of High-Throughput Processing of Thin-Film CdTe PV Modules	ZAK-8-17619-17	460	4/98 4/01
Solarex, a Business Unit of Amoco/Enron Solar R. Arya Toano, VA 23168	Research on Amorphous Silicon Cells and Modules	ZAK-8-17619-02	655	3/98 5/01
Syracuse University E. Schiff Syracuse, NY 13244	Research on High-Bandgap Materials and Amorphous-Silicon-Based Solar Cells	XAN-4-13318-06	27.5	5/94 1/98
Syracuse University E. Schiff Syracuse, NY 13244	Electroabsorption and Transport Measurements and Modeling Research in Amorphous-Silicon-Based Solar Cells	XAK-8-17619-23	75	3/98 3/01
United Solar Systems Corporation S. Guha Troy, MI 48084	High-Efficiency Triple-Junction Amorphous Silicon Alloy PV Technology	ZAK-8-17619-09	892	3/98 3/01

NREL Subcontracts for FY 1998				
Contractor, Principal Investigator, Address	**Work Title (Research Activity)**	**Contract Number**	**FY 1998 Funding ($K)**	**Start/ End Dates**
University of California at Los Angeles R. Braunstein Los Angeles, CA 90024	Photocharge Transport and Recombination Measurements in Amorphous Silicon Films and Solar Cells by Photoconductive Frequency Mixing	XAN-4-13318-10	7.5	5/94 4/98
University of California at Los Angeles R. Braunstein Los Angeles, CA 90024	Photocharge Transport and Recombination Measurements in Amorphous Silicon Films and Solar Cells by Photoconductive Frequency Mixing	XAK-8-17619-24	25	4/98 7/01
University of Delaware-IEC R. Birkmire Newark, DE 19716	Optimization of Processing and Modeling Issues for Thin-Film Solar Cell Devices	XAK-7-17609-01	1,010.5	2/97 9/98
University of Delaware-IEC R. Birkmire Newark, DE 19716	Optimization of Processing and Modeling Issues for Thin-Film Solar Cell Devices	XAK-8-17619-33	150	8/98 10/01
University of Florida T. Anderson Gainesville, FL 32611	Processing of $CuInSe_2$-Based Solar Cells: Characterization of Deposition Processes in Terms of Chemical Reaction Analyses	XAF-5-14142-10	200.6	5/95 12/98
University of Florida T. Anderson Gainesville, FL 32611	Future CIS Manufacturing Technology Development	XAK-8-17619-32	105	7/98 7/01
University of Illinois A. Rockett Urbana, IL	Properties of Wide-Gap Chalcopyrite Semiconductors for Photovoltaic Applications	XAK-8-17619-34	16	7/98 7/01

NREL Subcontracts for FY 1998				
Contractor, Principal Investigator, Address	**Work Title (Research Activity)**	**Contract Number**	**FY 1998 Funding ($K)**	**Start/ End Dates**
University of North Carolina D. Han Chapel Hill, NC 27514	Search for Factors Determining the Photodegradation in High-Efficiency a-Si:H-Based Solar Cells	XAK-8-17619-11	101.3	1/98 1/01
University of Oregon D. Cohen Eugene, OR 97403	Identifying Electronic Properties Relevant to Improving Stability in a-Si:H-Based Cells and Overall Performance in a-SiGe:H-Based Cells	XAN-4-13318-07	33	4/94 1/98
University of Oregon D. Cohen Eugene, OR 97403	Identifying Electronic Properties Relevant to Improving Stability in a-Si:H-Based Cells and Overall Performance in a-SiGe:H-Based Cells	XAF-8-17619-05	97.6	1/98 1/02
University of South Florida D. Morel Tampa, FL 33620	Advanced Processing of CdTe and Cu(In,Ga)Se_2-Based Solar Cells	XAF-5-14142-09	188.5	4/95 5/98
University of South Florida D. Morel Tampa, FL 33620	Advanced Processing Technology for CdTe and High Bandgap CIGS Solar Cells	ZAF-8-17619-29	172.5	5/98 7/01
University of Toledo A. Compaan Toledo, OH 43606	High-Efficiency Thin-Film Cadmium-Telluride-Based Solar Cells	ZAX-4-14013-01	0	1/94 3/98
University of Toledo A. Compaan Toledo, OH 43606	High-Efficiency Thin-Film Cadmium-Telluride- and Amorphous Silicon-Based Solar Cells	ZAF-8-17619-14	253.5	3/98 3/01
University of Utah C. Taylor Salt Lake City, UT	Characterization of Amorphous Silicon thin Films and PV Devices	XAK-8-17619-13	63.4	1/98 1/01
Washington State University L. Olsen Richland, WA	Alternative Window Schemes for $CuInSe_2$-Based Solar Cells	XAF-6-15375-01	0	11/95 12/97

NREL Subcontracts for FY 1998				
Contractor, Principal Investigator, Address	**Work Title (Research Activity)**	**Contract Number**	**FY 1998 Funding ($K)**	**Start/ End Dates**
Washington State University L. Olsen Richland, WA	Alternative Window Schemes for $CuInSe_2$-Based Solar Cells	XAF-8-17619-06	138.7	12/97 12/00
Weizmann Institute of Science D. Cahen Rehovot, Israel	Identifying and Overcoming Degradation Mechanisms in CdTe Solar Cells	AAK-8-17619-15	34	8/98 7/01
PHOTOVOLTAIC MANUFACTURING TECHNOLOGY (PVMAT) PROJECT **E. Witt**				
Advanced Energy Systems, Inc. R. Wills Wilton, NH	Next Generation Three-Phase Inverter	ZAF-5-14271-10	135.7 plus WE 53.2	9/95 5/98
Ascension Technology, Inc. E. Kern Waltham, MA 01773	Cost Reduction and Manufacture of the SunSine™325 AC Module	ZAX-8-17647-03	144.3	4/98 6/00
Ascension Technology, Inc. E. Kern Waltham, MA 01773	Manufacture of an AC Photovoltaic Module	ZAF-5-14271-05	31.3	7/95 6/98
ASE Americas J. Kalejs Billerica, MA 01821	Cost Reductions in High Volume EFG PV Module Manufacturing Line	ZAX-8-17647-10	486	7/98 10/01
ASE Americas M. Kardauskas Billerica, MA 01821	Market Driven EFG Modules	ZAF-6-14271-13	368	12/95 5/99
AstroPower, Inc. J. Rand Newark, DE 19711	Large-Area Silicon-Film Panels and Solar Cells	ZAF-5-14271-03	195.7	6/95 2/98
AstroPower, Inc. J. Rand Newark, DE 19711	Silicon-Film Solar Cells by a Flexible Manufacturing System	ZAX-8-17647-01	874.7	4/98 6/01

NREL Subcontracts for FY 1998				
Contractor, Principal Investigator, Address	**Work Title (Research Activity)**	**Contract Number**	**FY 1998 Funding ($K)**	**Start/ End Dates**
Crystal Systems C.P. Khattak Salem, MA 01970	Production of Solar Grade Silicon by Refining of Liquid Metallurgical Grade Silicon	ZAX-8-17647-13	143.5	6/98 8/00
Energy Conversion Devices M. Izu Troy, MI 48084	Efficiency and Throughput Advances in Continuous 'Roll-to-Roll a-Si Alloy Manufacturing Technology	ZAX-8-17647-09	572	6/98 8/01
Evergreen Solar, Inc. J. Hanoka Waltham, MA 02154	Advanced Polymer PV System	ZAF-5-14271-09	0	9/95 2/98
Evergreen Solar, Inc. J. Hanoka Waltham, MA 02154	Continuous, Automated Manufacturing of String Ribbon Silicon PV Modules	ZAX-8-17647-07	363.5	5/98 5/01
Global Solar S. Wiedeman Tucson, AZ 85747	Manufacturing Cost and Throughput Improvements for CIGS based Thin Film PV Modules	ZAX-8-17647-11	489	7/98 9/01
Iowa Thin Film Technology F. Jeffrey Ames, IA 50010	Monolithic a-Si Modules on Continuous Polymer Substrates	ZAF-5-14271-04	605.6	7/95 2/99
Omnion Power Engineer Corp. D. Porter East Troy, WI 53120	Manufacturing and System Integration Improvements for One- and Two-Kilowatt Residential PV Inverters	ZAX-8-17647-08	96	7/98 6/00
Omnion Power Engineer Corp. D. Porter East Troy, WI 53120	Three-Phase Power Conversion System for Utility Interconnected PV Applications	ZAF-5-14271-02	142.1	9/96 12/98
Photovoltaics International, LLC W. Bottenberg Sunnyvale, CA 94086	Manufacturing of the PVI PowerGrid	ZAF-6-14271-11	956.4	10/95 2/99

NREL Subcontracts for FY 1998				
Contractor, Principal Investigator, Address	**Work Title (Research Activity)**	**Contract Number**	**FY 1998 Funding ($K)**	**Start/ End Dates**
PowerLight Corporation T. Dinwoodie Berkeley, CA 94710	Power-Guard® Advanced Manufacturing	ZAX-8-17647-12	275	6/98 6/00
Siemens Solar Industries T. Jester Camarillo, CA 93011	Photovoltaic Cz Silicon Module Improvements	ZAF-6-14271-12	864	11/95 1/99
Siemens Solar Industries T. Jester Camarillo, CA 93011	Specific R&D Problems in Product Manufacturing	ZAX-8-17647-14	626	6/98 8/01
Solar Cells, Inc. D. Sandwisch Toledo, OH 43607	High-Throughput Manufacturing of Thin-Film CdTe PV Modules	ZAI-4-11294-02	290.2	11/93 3/99
Solar Cells, Inc. D. Sandwisch Toledo, OH 43607	Specific PVMaT R&D in CdTe Product Manufacturing	ZAX-8-17647-06	682	5/98 7/01
Solar Design Associates S. Strong Harvard, MA 01451	Development of Standardized, Low-Cost AC PV Systems	ZAF-5-14271-01	58.5	9/95 6/98
Solar Electric Specialties Company G. Minyard Willits, CA 95450	Design, Fabrication, and Certification of Advanced Modular PV Power Systems	ZAF-5-14271-07	0	9/95 6/98
Solarex Corporation J. Wohlgemuth Frederick, MD 21754	Improvements in Polycrystalline Silicon PV Module Manufacturing Technology	ZAX-8-17647-05	561	5/98 7/01
Spire Corporation M. Nowlan Bedford, MA 01730-2396	Post-Lamination Manufacturing Process Automation for Photovoltaic Modules	ZAX-8-17647-04	454.6	4/98 6/01
STR (Springborn Testing and Research) W. Holley Enfield, CT 06082	Advanced Development of PV Encapsulants	ZAG-3-11219-02	0	12/92 3/97

NREL Subcontracts for FY 1998				
Contractor, Principal Investigator, Address	**Work Title (Research Activity)**	**Contract Number**	**FY 1998 Funding ($K)**	**Start/ End Dates**
Trace Engineering C. Freitas Arlington, WA 98223	2-kW DC to AC Power Inverter Module for PV Applications	ZAF-4-14271-08	0	9/95 5/98
Utility Power Group R. West Chatsworth, CA 91311	Development of a Fully-Integrated PV System for Residential Applications	ZAX-8-17647-02	237.9	3/98 7/00
PV ENGINEERING AND RELIABILITY PROJECT **R. Hulstrom**				
NEOS Corporation T. Schuyler Lakewood, CO	Development of Test Methods and Procedures for Evaluation of PV Systems	AAD-7-17628-01	0	5/97 5/98
Powermark Corporation S. Chalmers Phoenix, AZ	PV Certification and Accreditation Management Support	AAX-7-16821-01	0	11/96 11/98
Solar Energy Industries Assoc. J. Anderson Washington, DC	Management and Administration of the IEC/TC82	ACU-7-17605-01	0	4/97 4/99
University of Colorado at Denver J. Boon Denver, CO	Prototype Portable Custom-Made PV Encapsulant and Solar Cell Degradation Monitor (A Spectrophotometric Analyzer)	XAX-6-14454-01	0	3/96 9/97
PV DOMESTIC APPLICATIONS AND MARKETS PROJECT **J. Thornton**				
Ann Deering, Consultant Ann Deering New York, NY	Photovoltaic Technology, Application, and Market Analysis Support	CCE-8-18659-01	18	4/98 7/98

NREL Subcontracts for FY 1998				
Contractor, Principal Investigator, Address	**Work Title (Research Activity)**	**Contract Number**	**FY 1998 Funding ($K)**	**Start/ End Dates**
City of Albuquerque Development Services Division K. Kalender Albuquerque, NM 87104	Million Solar Roofs Community Partnership Planning, Coordination, Education, and Infrastructure Development for the City of Albuquerque	RBW 8-18667-01	25	6/98 6/99
The Greater Flagstaff Economic Development Council K. Poirier Flagstaff, AZ 86001-7302	Community Education, Outreach and Value Identification for the Greater Flagstaff Area	RBW 8-18672-01	15	6/98 6/99
Hawaii Electric Light Company S. Burns Hilo, HI 96720	Million Solar Roofs Community Partnership Planning for the Island of Hawaii	RBW 8-18664-01	25	6/98 6/99
Interstate Renewable Energy Council (IREC) V. Maistitis Latham, NY 12110-1156	Solar Policy Forums	ACU-7-1682301	10	6/97 8/98
Learning Village Project V. Rauluk and D. Fuller Tucson, AZ 85733	Development of the Tucson Photovoltaic Coalition to Promote & Support Photovoltaic Installations	RBW 8-18685-01	25	6/98 6/99
McNeil Technologies K. DeGroat Springfield, VA 22150	Photovoltaic Technology, Application, and Market Analysis Support	AAK-6-16784-01	93.3	6/96 12/98
New Resources Group D. Eberle Freeman, MO 64746	Sunrayce 99 Management	AAX-8-18646-01	157.1	12/97 12/98
Pacific Energy Group H. Wenger Walnut Creek, CA 94596	Renewable Energy Applications and Economic Analysis for Electric Power	AAX-5-15330-01	85	8/95 12/98
Solar Design Associates S. Strong Harvard, MA 01451-0242	Photovoltaic Power Systems in the Built Environment	AAR-8-18620-01	49.2	2/98 9/98

NREL Subcontracts for FY 1998				
Contractor, Principal Investigator, Address	**Work Title (Research Activity)**	**Contract Number**	**FY 1998 Funding ($K)**	**Start/ End Dates**
Solar Design Associates S. Strong Harvard, MA 01451-0242	Whole Buildings Design Brochure	ADC-8-18451-01	25	8/98 5/99
SUNY at Albany R. Perez Albany, NY 12205	Solar Resource Utility Load-Matching Assessment	XAR-1-11168-1	60	9/91 1/98
University of Delaware J. Byrne Newark, DE 19616	Evaluation of Photovoltaic Peak-Shaving Applications in the U.S. Buildings Sector	XAX-8-17678-01	38	12/97 12/98
Washington State University Energy Program M. Nelsen Olympia, WA 98504-3165	Coordination and Development of the Washington 5,000 Solar Rooftops by 2005 Collaborative	AAX-8-18640-01	25	6/98 6/99
Wortman Engineering D. Wortman Longmont, CO 80501	Renewable Energy and Energy Efficiency Technologies in Building Codes and Standards	AAA-8-18450-01	34.3	6/98 9/98
PV INTERNATIONAL APPLICATIONS AND MARKETS PROJECT **J. Stone**				
Center for Renewable Energy Development J. Li Beijing, China	Renewable Energy Business Development in China	AAX-8-17679-01	39.9	2/98 2/99
Chinese Ministry of Agriculture J. Li Beijing, China	Renewable Energy Business Development in China	AAX-8-17680-01	50	12/97 6/99

NREL Subcontracts for FY 1998				
Contractor, Principal Investigator, Address	**Work Title (Research Activity)**	**Contract Number**	**FY 1998 Funding ($K)**	**Start/ End Dates**
Princeton Economic Research, Inc. D. Ancona Rockville, MD 20852	U.S. China Progress Report on the Protocol for Cooperation in the Fields of Energy Efficiency and Renewable Energy Technology Development and Utilization	AAA-8-18689-01	60	8/98 11/98
Sherring Energy Associates C. Sherring Princeton, NJ 08540-7824	China PV Business and Application Evaluation	AAA-8-18688-01	57.5	8/98 10/98
Solar Electric Light Fund R. Freling Washington, DC 20006	Photovoltaics for Rural Energy in Gansu Province in the People's Republic of China	AAX-6-15376-01	60	12/95 2/99
Tata Energy and Resources Institute P. Venkat Ramana Arlington, VA 22209	Evaluation of SPV Systems Installed under INDO-US Collaboration Programme, Sundarbans, West Bengal	AAD-6-16780-01	0	7/96 3/98
University of Delaware J. Byrne Newark, DE 19616	Evaluation of Intermediate Applications for Photovoltaics in the United States and Developing Countries	XCU-7-16806-01	22.6	6/97 1/99
Xinergy Resources S. Vaupen Arlington, VA	Renewable Energy Business Development in China	AAX-8-18676-01	18	6/98 10/98

12.0 NCPV FY 1998 Bibliography

12.0 NCPV FY 1998 BIBLIOGRAPHY

Abulfotuh, F. A.; Balcioglu, A.; Wangensteen, T.; Moutinho, H. R.; Hassoon, F.; Al-Douri, A.; Alnajjar, A.; Kazmerski, L. L. **Study of the Defect Levels, Electrooptics, and Interface Properties of Polycrystalline CdTe and CdS Thin Films and Their Junction.** *Conference Record of the Twenty-Sixth IEEE Photovoltaic Specialists Conference, 29 September–3 October 1997, Anaheim, California.* New York: Institute of Electrical and Electronics Engineers; 1997; pp. 451-454.
Note: For preprint version, including full text online document, see NREL/CP-530-23522.

Ahrenkiel, R. K.; Ahrenkiel, S. P.; Al-Jassim, M. M.; Venkatasubramanian, R. **Electronic and Mechanical Properties of Ge Films Grown on Glass Substrates.** *Conference Record of the Twenty-Sixth IEEE Photovoltaic Specialists Conference, 29 September–3 October 1997, Anaheim, California.* New York: Institute of Electrical and Electronics Engineers; 1997; pp. 527-529.
Note: For preprint version, including full text online documents, see NREL/CP-530-22974.

Ahrenkiel, R. K.; Johnston, S. **Contactless Measurement of Recombination Lifetime in Photovoltaic Materials.** *Solar Energy Materials and Solar Cells.* 1998; 55; pp. 59-73.

Ahrenkiel, R. K.; Johnston, S. **Contactless Measurement of Recombination Lifetime in Photovoltaic Materials.** *Conference Record of the Twenty-Sixth IEEE Photovoltaic Specialists Conference, 29 September–3 October 1997, Anaheim, California.* New York: Institute of Electrical and Electronics Engineers; 1997; pp. 119-122.
Note: For preprint version, including full text online document, see NREL/CP-530-22958.

Ahrenkiel, R. K.; Levi, D. H.; Johnston, S.; Song, W.; Mao, D.; Fischer, A. **Photoconductive Lifetime of CdS Used in Thin-Film Solar Cells.** *Conference Record of the Twenty-Sixth IEEE Photovoltaic Specialists Conference, 29 September–3 October 1997, Anaheim, California.* New York: Institute of Electrical and Electronics Engineers; 1997; pp. 535-538.
Note: For preprint version, including full text online document, see NREL/CP-530-22950.

Ahrenkiel, S. P.; Ahrenkiel, R. K.; Arent, D. J. **Domain Structure and Transient Photoconductivity in Ordered $Ga_{0.47}In_{0.53}As$ Epitaxial Films.** Moss, S. C., et al., eds. *Thin Films--Structure and Morphology: Proceedings of the Materials Research Society Symposium, 2-6 December 1996, Boston, Massachusetts.* Materials Research Society Symposium Proceedings, Vol. 441. Pittsburgh, PA: Materials Research Society; 1997; pp. 133-138.

Albin, D.; Rose, D.; Dhere, R.; Levi, D.; Woods, L.; Swartzlander, A.; Sheldon, P. **Comparison Study of Close-Spaced Sublimated and Chemical Bath Deposited CdS Films: Effects on CdTe Solar Cells.** *Conference Record of the Twenty-Sixth IEEE Photovoltaic Specialists Conference, 29 September–3 October 1997, Anaheim, California.* New York: Institute of Electrical and Electronics Engineers; 1997; pp. 367-370.
Note: For preprint version, including full text online document, see NREL/CP-520-22949.

Aldrich, D. J.; Jones, K. M.; Govindarajan, S.; Moore, J. J.; Ohno, T. R. **Microstructure of Molybdenum Disilicide-Silicon Carbide Nanocomposite Thin Films.** *Journal of the American Ceramic Society.* June 1998; 81(6); pp. 1471-1476.

Bai, Y.; Ford, D. H.; Rand, J. A.; Hall, R. B.; Barnett, A. M. **16.6% Efficient Silicon-Film™ Polycrystalline Silicon Solar Cells.** *Conference Record of the Twenty-Sixth IEEE Photovoltaic Specialists Conference, 29 September–3 October 1997, Anaheim, California.* New York: Institute of Electrical and Electronics Engineers; 1997; pp. 35-38.
Note: Work performed by AstroPower, Inc., Newark, Delaware.

Banerjee, A.; Yang, J.; Guha, S. **Improved Amorphous Silicon Alloy Solar Cells for Module Fabrication.** Wagner, S. et al., eds. *Amorphous and Microcrystalline Silicon Technology 1997: Proceedings of the Materials Research Society Symposium, 31 March–4 April 1997, San Francisco, California.* Materials Research Society Symposium Proceedings, Vol. 467. Pittsburgh, PA: Materials Research Society; 1997; pp. 711-716.
Note: Work performed by United Solar Systems Corp., Troy, Michigan.

Bechinger, C.; Gregg, B. A. **Development of a New Self-Powered Electrochromic Device for Light Modulation Without External Power Supply.** *Solar Energy Materials and Solar Cells.* 1998; 54; pp. 405-410.

Bhattacharya, R. N.; Granata, J. E.; Batchelor, W.; Hasoon, F.; Wiesner, H.; Ramanathan, K.; Keane, J.; Noufi, R. N.; Sites, J. R. **$CuIn_{1-x}Ga_xSe_2$-Based Photovoltaic Cells from Electrodeposited Precursor.** Lampert, C. M., et al., eds. *Optical Materials Technology for Energy Efficiency and Solar Energy Conversion XV: Proceedings from the SPIE Annual Meeting, 28-29 July 1997, San Diego, California.* SPIE Proceedings, Vol. 3138. Bellingham, WA: Society of Photo-Optical Instrumentation Engineers; 1997; pp. 90-95.

Birkmire, R. W. **Recent Progress and Critical Issues in Thin Film Polycrystalline Solar Cells and Modules.** *Conference Record of the Twenty-Sixth IEEE Photovoltaic Specialists Conference, 29 September–3 October 1997, Anaheim, California.* New York: Institute of Electrical and Electronics Engineers; 1997; pp. 295-300.
Note: Work performed by University of Delaware, Newark, Delaware.

Biswas, R.; Li, Q.; Yoon, Y.; Branz, H. M. **Dangling-Bond Levels and Structure Relaxation in Hydrogenated Amorphous Silicon.** *Physical Review. B, Condensed Matter.* 15 October 1997-I; 56(15); pp. 9197-9200.

Bower, W.; Thomas, H.; Kroposki, B.; Bonn, R.; Hund, T. **Balance-of-System Improvements for Photovoltaic Applications Resulting from the PVMaT Phase 4A1 Program.** *Conference Record of the Twenty-Sixth IEEE Photovoltaic Specialists Conference, 29 September–3 October 1997, Anaheim, California.* New York: Institute of Electrical and Electronics Engineers; 1997; pp. 1093-1096.
Note: Work performed by Sandia National Laboratories, Albuquerque, New Mexico.

Branz, H. M.; Adler, D.; Silver, M. **Theory of Sweep-out Experiments: A New Spectroscopy for the Electronic Density of States in Doped Hydrogenated Amorphous Silicon Films.** Matyas, M.; Kocka, J.; Velicky, B. eds. *Journal of Non-Crystalline Solids: Proceedings of the 12th International Conference on Amorphous and Liquid Semiconductors.* 1987; 97/98; pp. 655-658.

Branz, H. M.; Fan, S.; Flint, J. H.; Adler, D.; Haggerty, J. S. **Doping of Hydrogenated Amorphous Silicon Films Prepared by Laser-Induced Chemical Vapor Deposition.** von Gutfield, R. J.; Greene, J. E.; Schlossberg, H. eds. *Beam-Induced Chemical Processes.* Pittsburgh, PA: Materials Research Society; 1985; pp. 105-107.

Branz, H. M.; Silver, M. **Charged Dangling Bonds: Key to Electronic Transport, Recombination and Metastability in Hydrogenated Amorphous Silicon.** Paesler, M.; Agarwal, S. C.; Zallen, R. eds. *Journal of Non-Crystalline Solids: Proceedings of the Thirteenth International Conference on Amorphous and Liquid Semiconductors, 21-25 August 1989, Asheville, North Carolina.* 1989; 114; pp. 639-641.

Britt, J. S.; Delahoy, A. E.; Kiss, Z. J. **Pilot Production of CIGS Photovoltaic Modules.** *Conference Record of the Twenty-Sixth IEEE Photovoltaic Specialists Conference, 29 September–3 October 1997, Anaheim, California.* New York: Institute of Electrical and Electronics Engineers; 1997; pp. 335-338.
Note: Work performed by Energy Photovoltaics, Inc., Princeton, New Jersey.

Brown, H. **FLC Innovators: Olson, Kurtz, Kibbler, Kramer, and Friedman, National Renewable Energy Laboratory.** *The FLC Newslink.* January 1998; p. 6.

Bulovic, V.; Burrows, P. E.; Garbuzov, D. Z.; Thompson, M. E.; Tsekoun, A. G.; Forrest, S. R. **Photovoltaic Cells Based on Vacuum Deposited Molecular Organic Thin Films.** McConnell, R. D. , ed. *Future Generation Photovoltaic Technologies: Proceedings of the First NREL Conference, 22-26 March 1997, Denver, Colorado.* AIP Conference Proceedings No. 404. Woodbury, NY: American Institute of Physics; 1997; pp. 235-242.
Note: Work performed by Princeton University, Princeton, New Jersey; Sarnoff Corporation, Princeton, New Jersey; and University of Southern California, LosAngeles, California.

Byrne, J.; Shen, B.; Wallace, W. **Economics of Sustainable Energy for Rural Development: A Study of Renewable Energy in Rural China.** *Energy Policy.* 1998; 26(1); pp. 45-54.

Calixto, M. E.; Bhattacharya, R. N.; Sebastian, P. J.; Fernandez, A. M.; Gamboa, S. A.; Noufi, R. N. **Cu(In,Ga)Se_2-Based Photovoltaic Structure by Electrodeposition and Processing.** *Solar Energy Materials and Solar Cells.* 1998; 55; pp. 23-29.

Carlson, D. E. **High-Volume Manufacturing Issues: Toxicity, Materials Supply, Yield Management, and Marketing.** McConnell, R. D.,. ed. *Future Generation Photovoltaic Technologies: Proceedings of the First NREL Conference, 22-26 March 1997, Denver, Colorado.* AIP Conference Proceedings No. 404. Woodbury, NY: American Institute of Physics; 1997; pp. 11-19.
Note: Work performed by Solarex, Newtown, Pennsylvania.

Carlson, D. E.; Rajan, K.; Bradley, D. **Irreversible Light-Induced Degradation in Amorphous Silicon Solar Cells.** *Conference Record of the Twenty-Sixth IEEE Photovoltaic Specialists Conference, 29 September–3 October1997, Anaheim, California.* New York: Institute of Electrical and Electronics Engineers; 1997; pp. 595-598.
Note: Work performed by Solarex Corporation, Newtown, Pennsylvania.

Chen, C. C.; Zhong, F.; Cohen, J. D.; Yang, J. C.; Guha, S. **Significance of Charged Defects in Understanding the Light-Induced Degradation of Hydrogenated Amorphous Silicon-Germanium Alloys.** Wagner, S. et al., eds. *Amorphous and Microcrystalline Silicon Technology 1997: Proceedings of the Materials Research Society Symposium, 31 March–4 April 1997, San Francisco, California.* Materials Research Society Symposium Proceedings, Vol. 467. Pittsburgh, PA: Materials Research Society; 1997; pp. 55-60.
Note: Work performed by University of Oregon, Eugene, Oregon and United Solar Systems Corp., Troy, Michigan.

Ciszek, T. F., Inventor. **Substrate for Thin Silicon Solar Cells.** U.S. Patent No. 5,785,769. July 1998; 6 pp.
Note: Assignee: Midwest Research Institute, Kansas City, Missouri.

Ciszek, T. F.; Wang, T. H. **Growth and Properties of Silicon Filaments for Photovoltaic Applications.** *Conference Record of the Twenty-Sixth IEEE Photovoltaic Specialists Conference, 29 September–3 October 1997, Anaheim, California.* New York: Institute of Electrical and Electronics Engineers; 1997; pp. 103-106.
Note: For preprint version, including full text online document, see NREL/CP-450-22927.

Ciszek, T. F.; Wang, T. H.; Doolittle, W. A.; Rohatgi, A. **Minority-Carrier Lifetime Degradation in Silicon Co-Doped with Iron and Gallium.** *Conference Record of the Twenty-Sixth IEEE Photovoltaic Specialists Conference, 29 September–3 October 1997, Anaheim, California.* New York: Institute of Electrical and Electronics Engineers; 1997; pp. 59-62.
Note: For preprint version, including full text online document, see NREL/CP-450-22926.

Conboy, J. C.; Olson, E. J. C.; Adams, D. M.; Kerimo, J.; Zaban, A.; Gregg, B. A.; Barbara, P. F. **Impact of Solvent Vapor Annealing on the Morphology and Photophysics of Molecular Semiconductor Thin Films.** *Journal of Physical Chemistry B.* 1998; 102; pp. 4516-4525.

Contreras, M. A.; Egaas, B.; Dippo, P.; Webb, J.; Granata, J.; Ramanathan, K.; Asher, S.; Swartzlander, A.; Noufi, R. **On The Role of Na and Modifications to Cu(In,Ga)Se_2 Absorber Materials Using Thin-MF (M=Na, K, Cs) Precursor Layers.** *Conference Record of the Twenty-Sixth IEEE Photovoltaic Specialists Conference, 29 September–3 October 1997, Anaheim, California.* New York: Institute of Electrical and Electronics Engineers; 1997; pp. 359-362.
Note: For preprint version, including full text online document, see NREL/CP-520-22945.

Contreras, M. A.; Wiesner, H.; Tuttle, J.; Ramanathan, K.; Noufi, R. **Issues on the Chalcopyrite/Defect-Chalcopyrite Junction Model for High-Efficiency Cu(In,Ga)Se_2 Solar Cells.** *Solar Energy Materials and Solar Cells.* December 1997; 49(1-4); pp. 239-247.

Coutts, T. J.; Allman, C. S.; Benner, J. P., eds. **Thermophotovoltaic Generation of Electricity: Third NREL Conference, May 1997, Colorado Springs, Colorado.** AIP Conference Proceedings No. 401. Woodbury, NY: American Institute of Physics; 1997; 605 pp.

Coutts, T.; Fitzgerald, M. **Thermophotovoltaics: The Potential for Power.** *Physics World.* August 1998; 11; pp. 49-52.

Crandall, R. S.; Liu, X.; Iwaniczko, E. **Recent Developments in Hot Wire Amorphous Silicon.** *Journal of Non-Crystalline Solids.* 1998; 227-230; pp. 23-28.

Crandall, R. S.; Mahan, A. H.; Iwaniczko, E.; Jones, K. M.; Liu, X.; White, B. E.; Pohl, R. O. **New Results on the Microstructure of Amorphous Silicon as Observed by Internal Friction.** Wagner, S. et al., eds. *Amorphous and Microcrystalline Silicon Technology 1997: Proceedings of the Materials Research Society Symposium, 31 March–4 April 1997, San Francisco, California.* Materials Research Society Symposium Proceedings, Vol. 467. Pittsburgh, PA: Materials Research Society; 1997; pp. 191-196.

Dake, L. S.; Lad, R. J. **Ultrathin Al Overlayers on Cleaned and K-Covered TiO_2(110) Surfaces.** *Surface Science Spectra.* 1998; 4(3); pp. 232-245.

Dalal, V. L.; Maxson, T.; Hahn, K. **Properties of a-Si:H and a-(Si, Ge):H Solar Cells Prepared Using ECR Deposition Techniques.** *Conference Record of the Twenty-Sixth IEEE Photovoltaic Specialists Conference, 29 September–3 October 1997, Anaheim, California.* New York: Institute of Electrical and Electronics Engineers; 1997; pp. 695-698.
Note: Work performed by Iowa State University, Ames, Iowa.

Dalal, V. L.; Maxson, T.; Girvan, R.; Haroon, S. **Stability of Single and Tandem Junction a-Si:H Solar Cells Grown Using the ECR Process.** Wagner, S. et al., eds. *Amorphous and Microcrystalline Silicon Technology 1997: Proceedings of the Materials Research Society Symposium, 31 March–4 April 1997, San Francisco, California.* Materials Research Society Symposium Proceedings, Vol. 467. Pittsburgh, PA: Materials Research Society; 1997; pp. 813-817.
Note: Work performed by Iowa State University, Ames, Iowa.

Dangling Rope Marina: A Photovoltaic-Hybrid Power System, *Quarterly Highlights of Sandia's Photovoltaic Program*, Sandia National Laboratories, Volume 1, 1998.

Deb, S. K.; Ferrere, S.; Frank, A. J.; Gregg, B. A.; Huang, S. Y.; Nozik, A. J.; Schlichthorl, G.; Zaban, A. **Photochemical Solar Cells Based on Dye-Sensitization of Nanocrystalline TiO_2.** *Conference Record of the Twenty-Sixth IEEE Photovoltaic Specialists Conference, 29 September–3 October 1887, Anaheim, California.* New York: Institute of Electrical and Electronics Engineers; 1997; pp. 507-510.
Note: For preprint version, including full text online document, see NREL/CP-450-22953.

del Cueto, J. A.; McMahon, T. J. **Performance of Single-Junction a-Si Modules Under Varying Conditions in the Field.** *Conference Record of the Twenty-Sixth IEEE Photovoltaic Specialists Conference, 29 September–3 October 1997, Anaheim, California.* New York: Institute of Electrical and Electronics Engineers; 1997; pp. 1205-1208.
Note: For preprint version, including full text online document, see NREL/CP-510-22920.

Deng, X.; Jones, S. J.; Liu, T.; Izu, I.; Ovshinsky, S. R. **Improved mu-c-Si p-Layer and a-Si i-Layer Materials using VHF Plasma Deposition.** *Conference Record of the Twenty-Sixth IEEE Photovoltaic Specialists Conference, 29 September–3 October 1997, Anaheim, California.* New York: Institute of Electrical and Electronics Engineers; 1997; pp. 591-594.
Note: Work performed by Energy Conversion Devices, Inc., Troy, Michigan.

Deng, X.; Jones, S. J.; Liu, T.; Izu, M.; Ovshinsky, S. R.; Hoffman, K. **VHF Plasma Deposition of mu zeta-Si p-Layer Materials.** Wagner, S. et al., eds. *Amorphous and Microcrystalline Silicon Technology 1997: Proceedings of the Materials Research Society Symposium, 31 March–4 April 1997, San Francisco, California.* Materials Research Society Symposium Proceedings, Vol. 467. Pittsburgh, PA: Materials Research Society; 1997; pp.795-806.
Note: Work performed by Energy Conversion Devices, Inc., Troy, Michigan and United Solar Systems Corp, Troy, Michigan.

Dhere, N. G. **Appropriate Materials and Preparation Techniques for Polycrystalline-Thin-Film Thermophotovoltaic Cells.** Coutts, T. J.; Allman, C. S.; Benner, J. P. ,. eds. *Thermophotovoltaic Generation of Electricity: Third NREL Conference, May 1997, Colorado Springs, Colorado.* AIP ConferenceProceedings No. 401. Woodbury, NY: American Institute of Physics; 1997; pp. 423-442.

Dhere, R.; Rose, D.; Albin, D.; Asher, S.; Al-Jassim, M.; Cheong, H.; Swartzlander, A.; Moutinho, H.; Coutts, T.; Ribelin, R.; Sheldon, P. **Influence of CdS/CdTe Interface Properties on the Device Properties.** *Conference Record of the Twenty-Sixth IEEE Photovoltaic Specialists Conference, 29 September–3 October 1997, Anaheim, California.* New York: Institute of Electrical and Electronics Engineers; 1997; pp. 435-438.
Note: For preprint version, including full text online document, see NREL/CP-520-22947.

Dong, S.; Tang, Y.; Liebe, J.; Braunstein, R.; Crandall, R. S.; Nelson, B. P.; Mahan, A. H. **Transport Properties of Intrinsic Hydrogenated Amorphous Silicon Produced by the Hot-Wire Technique Investigated by the Photomixing Technique.** *Journal of Applied Physics.* 15 July 1997; 82(2); pp. 702-707.

Durand, S. **Center for Renewable Energy for Utilities (CREU**), Southwest Technology Development Institute, August 1997.

Durand, S., A. Rosenthal, and D. King. **The Impact of Peak-Power Tracking on PV Array Utilization in Battery Charging Applications**, *26th IEEE PV Specialists Conference*, Anaheim, California, September 29-October 3, 1997.

Ellis, A. **Test Report: Sacramento Municipal Utility District Photovoltaic Systems at Rancho Seco and the Hedge Sites**, Southwest Technology Development Institute, Las Cruces, New Mexico, October 1998.

Eisgruber, I.; Matson, R.; McMahon, T. J. **Automated Screening for Severe Shunting Defects in Encapsulated Series-Connected Modules.** *Conference Record of the Twenty-Sixth IEEE Photovoltaic Specialists Conference, 29 September–3 October 1997, Anaheim, California.* New York: Institute of Electrical and Electronics Engineers; 1997; pp. 727-730.

Erickson, K.; Dalal, V. L.; Chumanov, G. **Growth of Micro-Crystalline Si:H and (Si,Ge):H on Polyimide Substrates Using ECR Deposition Techniques.** Wagner, S. et al., eds. *Amorphous and Microcrystalline Silicon Technology 1997: Proceedings of the Materials Research Society Symposium, 31 March–4 April 1997, San Francisco, California.* Materials Research Society Symposium Proceedings, Vol. 467. Pittsburgh, PA: Materials Research Society; 1997; pp. 409-413.
Note: Work performed by Iowa State University, Ames, Iowa.

Federal Participation in Million Solar Roofs. What's New in Federal Energy Management: Program Overview (Fact sheet). March 1998; 2 pp. DOE/GO-10098-516.

Ferekides, C.; Marinskiy, D.; Morel, D. L. **CdS: Characterization and Recent Advances in CdTe Solar Cell Performance.** *Conference Record of the Twenty-Sixth IEEE Photovoltaic Specialists Conference, 29 September–3 October 1997, Anaheim, California.* New York: Institute of Electrical and Electronics Engineers; 1997; pp. 339-342.
Note: Work performed by University of South Florida, Tampa, Florida.

Ferekides, C.; Poorsala, U.; Morel, D. L. **Effect of SnO_2 Roughness on the Properties of CdTe/CdS Solar Cells.** *Conference Record of the Twenty-Sixth IEEE Photovoltaic Specialists Conference, 29 September–3 October 1997, Anaheim, California.* New York: Institute of Electrical and Electronics Engineers; 1997; pp.427-430.
Note: Work performed by University of South Florida, Tampa, Florida.

Ferekides, C. S.; Viswanathan, V.; Morel, D. L. **RF Sputtered Back Contacts for CdTe/CdS Thin Film Solar Cells.** *Conference Record of the Twenty-Sixth IEEE Photovoltaic Specialists Conference, 29 September–3 October 1997, Anaheim, California.* New York: Institute of Electrical and Electronics Engineers; 1997; pp. 423-426.
Note: Work performed by University of South Florida, Tampa, Florida.

Fernandez, A. M.; Calixto, M. E.; Sebastian, P. J.; Gamboa, S. A.; Hermann, A. M.; Noufi, R. N. **Electrodeposited and Selenized ($CuInSe_2$)(CIS) Thin Films for Photovoltaic Applications.** *Solar Energy Materials and Solar Cells.* 1998; 52; pp. 423-431.

Ferrere, S.; Gregg, B. A. **Dye Sensitized Solar Cells for Water Splitting and Fundamental Studies.** *Proceedings of the Twenty-First DOE Solar Photochemistry Research Conference, 7-11 June 1997, Copper Mountain, Colorado.* NREL/CP-520-22068. 1997; p. 114.

Field, H. **Solar Cell Spectral Response Measurement Errors Related to Spectral Band Width and Chopped Light Waveform.** *Conference Record of the Twenty-Sixth IEEE Photovoltaic Specialists Conference, 29 September–3 October 1997, Anaheim, California.* New York: Institute of Electrical and Electronics Engineers; 1997; pp. 471-474.
Note: For preprint version, including full text online document, see NREL/CP-530-22969.

Fischer, A.; Feng, Z.; Bykov, E.; Contreras-Puente, G.; Compaan, A.; Castillo-Alvarado, F.; Avendano, J.; Mason, A. **Optical Phonons in Laser-Deposited CdS_xTe_{1-x} Films.** *Applied Physics Letters.* 16 June 1997; 70(24); pp. 3239-3241.

Ford, D. H.; Rand, J. A.; Barnett, A. M.; DelleDonne, E. J.; Ingram, A. E.; Hall, R. B. **Development of Light-Trapped, Interconnected, Silicon-Film Modules.** *Conference Record of the Twenty-Sixth IEEE Photovoltaic Specialists Conference, 29 September–3 October 1997, Anaheim, California.* New York: Institute of Electrical and Electronics Engineers; 1997; pp. 631-634.
Note: Work performed by AstroPower, Inc., Newark, Delaware.

Frank, A. J.; Gregg, B. A.; Gratzel, M.; Nozik, A. J.; Zaban, A.; Ferrere, S.; Schlichthorl, G.; Huang, S. Y. **Photochemical Solar Cells Based on Dye-Sensitization of Nanocrystalline TiO_2.** McConnell, R. D., ed. *Future Generation Photovoltaic Technologies: Proceedings of the First NREL Conference, 22-26 March 1997, Denver, Colorado.* AIP Conference Proceedings No. 404. Woodbury, NY: American Institute of Physics; 1997; pp. 145-153.

Fujiwara, H.; Koh, J. K.; Lee, Y.; Wronski, C. R.; Collins, R. W. **Real Time Spectroscopic Ellipsometry Studies of the Top Junctions of a-Si:H-Based Solar Cells.** *Conference Record of the Twenty-Sixth IEEE Photovoltaic Specialists Conference, 29 September–3 October 1997, Anaheim, California.* New York: Institute of Electrical and Electronics Engineers; 1997; pp. 599-602.
Note: Work performed by Pennsylvania State University, University Park, Pennsylvania.

Gee, J. M.; Sopori, B. L. **Effect of Gettering on Areal Inhomogeneities in Large-Area Multicrystalline-Silicon Solar Cells.** *Conference Record of the Twenty-Sixth IEEE Photovoltaic Specialists Conference, 29 September-3 October 1997, Anaheim, California.* New York: Institute of Electrical and Electronics Engineers; 1997; pp. 155-158.

Gessert, T. A.; Sheldon, P.; Li, X.; Dunlavy, D.; Niles, D.; Sasala, R.; Albright, S.; Zadler, B. **Studies of ZnTe Back Contacts to CdS/CdTe Solar Cells.** *Conference Record of the Twenty-Sixth IEEE Photovoltaic Specialists Conference, 29 September–3 October 1997, Anaheim, California.* New York: Institute of Electrical and Electronics Engineers; 1997; pp. 419-422.
Note: For preprint version, including full text online document, see NREL/CP-520-22983.

Gillespie, T. J.; Lanning, B. R.; Marshall, C. H.; Contreras, M. **Large-Area Copper Indium Diselenide (CIS) Process, Control and Manufacturing.** *Conference Record of the Twenty-Sixth IEEE Photovoltaic Specialists Conference, 29 September–3 October 1997, Anaheim, California.* New York: Institute of Electrical and Electronics Engineers; 1997; pp. 403-406.
Note: Work performed by Lockheed Martin Astronautics, Denver, Colorado.

Gillespie, T. J.; Miles, W. A.; del Cueto, J. A. **Reactive Magnetron Sputtering of Transparent and Conductive Zinc Oxide Films Deposited at High Rates onto CIS/CIGS Photovoltaic Devices.** *Conference Record of the Twenty-Sixth IEEE Photovoltaic Specialists Conference, 29 September–3 October 1997, Anaheim, California.* New York: Institute of Electrical and Electronics Engineers; 1997; pp. 487-490.
Note: Work performed by Lockheed Martin Astronautics, Denver, Colorado.

Ginley, D. S.; Perkins, J. D.; McGraw, J. M.; Parilla, P. A. **$LiCoO_2$ Thin Films Grown by Pulsed Laser Deposition on Low Cost Substrates.** Ginley, D. S., et al., eds. *Materials for Electrochemical Energy Storage and Conversion II --Batteries, Capacitors and Fuel Cells: Proceedings of the Materials Research Society Symposium, 1-5 December 1997, Boston, Massachusetts.* Materials Research Society Symposium Proceedings, Vol. 496. Warrendale, PA: Materials Research Society; 1998; pp. 293-302.

Granata, J. E.; Sites, J. R.; Asher, S.; Matson, R. J. **Quantitive Incorporation of Sodium in $CuInSe_2$ and $Cu(In,Ga)Se_2$ Photovoltaic Devices.** *Conference Record of the Twenty-Sixth IEEE Photovoltaic Specialists Conference, 29 September–3 October 1997, Anaheim, California.* New York: Institute of Electrical and Electronics Engineers; 1997; pp. 387-390.
Note: Work performed by Colorado State University, Fort Collins, Colorado and National Renewable Energy Laboratory, Golden, Colorado.

Green, M. A.; Emery, K.; Bucher, K.; King, D. L.; Igari, S. **Solar Cell Efficiency Tables (Version 10).** *Progress in Photovoltaics: Research and Applications.* July-August 1997; 5(4); pp. 265-268.

Guha, S.; Yang, J.; Banerjee, A.; Hoffman, K.; Sugiyama, S.; Call, J.; Jones, S. J.; Deng, X.; Doehler, J.; Izu, M.; Ovshinsky, H. C. **Triple-Junction Amorphous Silicon Alloy PV Manufacturing Plant of 5 MW Annual Capacity.** *Conference Record of the Twenty-Sixth IEEE Photovoltaic Specialists Conference, 29 September–3 October 1997, Anaheim, California.* New York: Institute of Electrical and Electronics Engineers; 1997; pp. 607-610.
Note: Work performed by United Solar Systems Corp, Troy, Michigan and Energy Conversion Devices, Inc.,Troy, Michigan.

Han, D.; Wang, K.; Yeh, C.; Yang, L.; Deng, X.; von Roedern, B. **Luminescence in Amorphous Silicon p-i-n Diodes under Double-Injection Dispersive-Transport-Controlled Recombination.** *Physical Review. B, Condensed Matter.* 15 June 1997; 55(23); pp. 15,619-15, 629.

Han, D.; Yeh, C.; Wang, K.; Wang, Q. **Internal Electric Field Profile in Thin Film Hydrogenated Amorphous Silicon Diodes Studied by the Transient-Null-Current Method.** Wagner, S. et al., eds. *Amorphous and Microcrystalline Silicon Technology 1997: Proceedings of the Materials Research Society Symposium, 31 March–4 April 1997, San Francisco, California.* Materials Research Society Symposium Proceedings, Vol. 467. Pittsburgh, PA: Materials Research Society; 1997; pp. 729-734.
Note: Work performed by University of North Carolina, Chapel Hill, North Carolina and March Instruments, Concord, California.

Hanna, M. C.; Lu, Z.; Nozik, A. J. **Hot Carrier Solar Cells.** McConnell, R. D., ed. *Future Generation Photovoltaic Technologies: Proceedings of the First NREL Conference, 22-26 March 1997, Denver, Colorado.* AIP Conference Proceedings No. 404. Woodbury, NY: American Institute of Physics; 1997; pp. 309-316.

Hanoka, J. I.; Kane, P. E.; Martz, J.; Fava, J. **Low Cost Module and Mounting Systems Developed Through Evergreen Solar's PVMaT Program.** *Conference Record of the Twenty-Sixth IEEE Photovoltaic Specialists Conference, 29 September–3 October 1997, Anaheim, California.* New York: Institute of Electrical and Electronics Engineers; 1997; pp. 1081-1092.
Note: Work performed by Evergreen Solar, Inc., Waltham, Massachusetts.

Hasoon, F. S.; Al-Jassim, M. M.; Swartzlander, A.; Sheldon, P.; Al-Douri, A. A. J.; Alnajjar, A. A. **Morphology of CdS Thin Films Deposited on SnO_2-Coated Glass Substrates.** *Conference Record of the Twenty-Sixth IEEE Photovoltaic Specialists Conference, 29 September–3 October 1997, Anaheim, California.* New York: Institute of Electrical and Electronics Engineers; 1997; pp. 543-546.
Note: For preprint version, including full text online document, see NREL/CP-530-23580.

Hegedus, S. S.; Albright, S.; Jeffrey, F.; McMahon, T. J.; Wiedeman, S. **Substrates, Contacts and Monolithic Integration.** *Progress in Photovoltaics: Research and Applications.* Papers from the 25th Anniversary Symposium of the Institute of Energy Conversion, 1-2 May 1997, Newark, Delaware. September-October 1997; 5(5); pp. 365-370.

Hegedus, S. S.; Buchanan, W. A.; Eser, E. **Improving Performance of Superstrate p-i-n a-Si Solar Cells by Optimization of n/TCO/Metal Back Contacts.** *Conference Record of the Twenty-Sixth IEEE Photovoltaic Specialists Conference, 29 September–3 October 1997, Anaheim, California.* New York: Institute of Electrical and Electronics Engineers; 1997; pp. 603-606.
Note: Work performed by University of Delaware, Newark, Delaware.

Herdt, G. C.; King, D. E.; Czanderna, A. W. **Penetration of Deposited Au, Cu, and Ag Overlayers through Alkanethiol Self-Assembled Monolayers on Gold or Silver.** *Zeitschrift fur Physikalische Chemie.* 163-196; 202; pp. 163-196.

Herig, C.; Stevens, J.; Wenger, H.; Hoff, T.; Furseth, D. **QuickScreen Software for Distributed PV Evaluation.** *Proceedings of the Annual Utility PV Experience Exhibition & Conference, 15-18 October 1996, Lakewood, Colorado.* Report to Utilities on Results from TEAM-UP Ventures and Other Photovoltaic Commercialization Activities. Washington, DC: Utility PhotoVoltaic Group; 1997; pp. 145-153.

Hester, S.; DeBlasio, R.; Stevens, J. **PV Interconnection Report.** (Viewgraphs from oral presentation). *Proceedings of the Annual Utility PV Experience Exhibition & Conference, 15-18 October 1996, Lakewood, Colorado.* Report to Utilities on Results from TEAM-UP Ventures and Other Photovoltaic Commercialization Activities. Washington, DC: Utility PhotoVoltaic Group; 1997; pp. 327-340.

Hoff, T. E.; Wenger, H. J.; Herig, C.; Shaw, R. W. ,. Jr. **Micro-Grid with PV, Fuel Cells, and Energy Efficiency.** Campbell-Howe, R.; Cortez, T.; Wilkins-Crowder, B. eds. *Proceedings of the 1998 American Solar Energy SocietyAnnual Conference, 14-17 June 1998, Albuquerque, New Mexico.* Boulder, CO: American Solar Energy Society; 1998; pp. 225-230.

Jagannathen, B.; Wallace, R. L.; Anderson, W. A.; Ahrenkeil, R. N. **Amorphous and Microcrystalline Silicon by ECR-CVD using Highly Dilute Silane Mixtures.** *Conference Record of the Twenty-Sixth IEEE Photovoltaic Specialists Conference, 29 September–3 October 1997, Anaheim, California.* New York: Institute of Electrical and Electronics Engineers; 1997; pp. 675-678.
Note: Work performed by State University of New York, Amherst, New YorkEvergreen Solar, Waltham, Massachusetts.

Jiang, L.; Schiff, E. A.; Finger, F.; Hapke, P.; Koynov, S.; Schwarz, R.; Wyrsch, N.; Shah, A.; Yang, J.; Guha, S. **Electroabsorption Spectra of Hydrogenated Amorphous and Microcrystalline Silicon.** Wagner, S. et al., eds. *Amorphous and Microcrystalline Silicon Technology 1997: Proceedings of the Materials Research Society Symposium, 31 March–4 April 1997, San Francisco, California.* Materials Research Society Symposium Proceedings, Vol. 467. Pittsburgh, PA: Materials Research Society; 1997; pp. 295-300.
Note: Work performed by Syracuse University, Syracuse, New York; Forschungszentrum Juelich GmbH, Juelich, Germany; University of Munich, Garching, Germany; University de Neuchatel, Neuchatel, Switzerland; and United Solar Systems Corp., Troy, Michigan.

Jiao, L.; Semoushikina, S.; Lee, Y.; Wronski, C. R. **Selfconsistent Analysis of Mobility-Lifetime Products and Subgap Absorption on Different PECVD A-Si:H Films.** Wagner, S. et al., eds. *Amorphous and Microcrystalline Silicon Technology 1997: Proceedings of the Materials Research Society Symposium, 31 March–4 April 1997, San Francisco, California.* Materials Research Society Symposium Proceedings, Vol. 467. Pittsburgh, PA: Materials Research Society; 1997; pp. 233-238.
Note: Work peerformed by Pennsylvania State University, University Park, Pennsylvania.

Jones, E. D.; Kalejs, J.; Noufi, R.; Sopori, B., eds. **Thin-Film Structures for Photovoltaics: Proceedings of the Materials Research Society Symposium, 2-5 December 1997, Boston, Massachusetts.** Materials Research Society Symposium Proceedings, Vol. 485. 1998; 323 pp.

Jones, K. M.; Al-Jassim, M. M.; Moutinho, H. R.; Dhere, R.; Sheldon, P. **Improved Sample Preparation Procedures for Analytical Studies of Polycrystalline CdTe Thin Films.** *Proceedings of the Annual Microbeam Analysis Society Conference, 29 August 1995, Breckenridge, Colorado.* 1995; pp. 139-140.

Kadirgan, F.; Mao, D.; Balcioglu, A.; McCandless, B. E.; Song, W.; Ohno, T. R.; Trefny, J. U. **Electrodeposited CdS Thin Films and Their Application in CdS/CdTe Solar Cells.** *Conference Record of the Twenty-Sixth IEEE Photovoltaic Specialists Conference, 29 September–3 October 1997, Anaheim, California.* New York: Institute of Electrical and Electronics Engineers; 1997; pp. 443-445.
Note: Work performed by Colorado School of Mines, Golden, ColoradoIstanbul Technical University, Istanbul, TurkeyTUBITAK, Kocaeli, TurkeyUniversity of Delaware, Newark, Delaware.

Kazmerski, L. L. **Measurements and Characterization in Photovoltaics: Lessons Learned for TPV.** Coutts, T. J.; Allman, C. S.; Benner, J. P. ,. eds. *Thermophotovoltaic Generation of Electricity: Third NREL Conference, May 1997, Colorado Springs, Colorado.* AIP Conference Proceedings No. 401. Woodbury, NY: American Institute of Physics; 1997; pp. 549-558.

Kazmerski, L. L. **Photovoltaics: A Review of Cell and Module Technologies.** *Renewable and Sustainable Energy Reviews.* March 1997; 1(1/2); pp. 71-170.

Kern, G. A. **SunSine300, Utility Interactive AC Module Anti-Islanding Test Results.** *Conference Record of the Twenty-Sixth IEEE Photovoltaic Specialists Conference, 29 September–3 October 1997, Anaheim, California.* New York: Institute of Electrical and Electronics Engineers; 1997; pp. 1265-1268.
Note: Work performed by Ascension Technology, Inc., Boulder, Colorado.

Keyes, B. M.; Hasoon, F.; Dippo, P.; Balcioglu, A.; Abulfotuh, F. **Influence of Na on the Electro-Optical Properties of Cu(In,Ga)Se_2.** *Conference Record of the Twenty-Sixth IEEE Photovoltaic Specialists Conference, 29 September–3 October 1997, Anaheim, California.* New York: Institute of Electrical and Electronics Engineers; 1997; pp. 479-482.
Note: For preprint version, including full text online document, see NREL/CP-530-22963.

King, D. L.; Myers, D. R. **Silicon-Photodiode Pyranometers: Operational Characteristics, Historical Experiences, and New Calibration Procedures.** *Conference Record of the Twenty-Sixth IEEE Photovoltaic Specialists Conference, 29 September–3 October 1997, Anaheim, California.* 1997; pp. 1285-1288.

King, D. E.; Pern, F. J.; Pitts, J. R.; Bingham, C. E.; Czanderna, A. W. **Optical Changes in Cerium-Containing Glass as a Result of Accelerated Exposure Testing.** *Conference Record of the Twenty-Sixth IEEE Photovoltaic Specialists Conference, 29 September–3 October 1997, Anaheim, California.* 1997; pp. 1117-1120.
Note: For preprint version, including full text online document, see NREL/CP-510-22954.

Koh, J.; Fujiwara, H.; Wronski, C. R.; Collins, R. W. **Structural and Optical Properties of a-Si:H/Mu zeta-Si:H:B Junctions in the a-Si:H-Based n-i-p Solar Cell Configuration.** Wagner, S. et al., eds. *Amorphous and Microcrystalline Silicon Technology 1997: Proceedings of the Materials Research Society Symposium, 31 March–4 April 1997, San Francisco, California.* Materials Research Society Symposium Proceedings, Vol. 467. Pittsburgh, PA: Materials Research Society; 1997; pp. 705-710.
Note: Work performed by Pennsylvania State University, University Park, Pennsylvania.

Koshka, Y.; Ostapenko, S.; Cao, J.; Kalejs, J. P. **Relationship Between Room Temperature Photoluminescence and Electronic Quality in Multicrystalline Silicon.** *Conference Record of the Twenty-Sixth IEEE Photovoltaic Specialists Conference, 29 September–3 October 1997, Anaheim, California.* New York: Institute of Electrical and Electronics Engineers; 1997; pp. 115-118.
Note: Work performed by University of South Florida, Tampa, Florida and ASE Americas, Inc., Billerica, Massachusetts.

Kroposki, B.; Hansen, R. **Technical Evaluation of Four Amorphous Silicon Systems at NREL.** *Conference Record of the Twenty-Sixth IEEE Photovoltaic Specialists Conference, 29 September–3 October 1997, Anaheim, California.* New York: Institute of Electrical and Electronics Engineers; 1997; pp. 1357-1360.
Note: For preprint version, including full text online document, see NREL/CP-510-22919.

Kurtz, S. R.; Myers, D.; Olson, J. M. **Projected Performance of Three-and Four-Junction Devices Using GaAs and GaInP.** *Conference Record of the Twenty-Sixth IEEE Photovoltaic Specialists Conference, 29 September–3 October 1997, Anaheim, California.* New York: Institute of Electrical and Electronics Engineers; 1997; pp. 875-878.
Note: For preprint version, including online full-text document, see NREL/CP-520-22925.

Kurtz, S. R.; Olson, J. M.; Friedman, D. J.; Reedy, R. **Effect of Front-Surface Doping on Back-Surface Passivation in $Ga_{0.5}In_{0.5}P$ Cells.** *Conference Record of the Twenty-Sixth IEEE Photovoltaic Specialists Conference, 29 September–3 October 1997, Anaheim, California.* New York: Institute of Electrical and Electronics Engineers; 1997; pp. 819-822.
Note: For preprint version, including full text online document, see NREL/CP-510-22943.

Kwon, D.; Cohen, J. D.; Garcia, R. **AFM Study of the Effect of Growth Method and Conditions on the Microstructure of A-Si:H.** Wagner, S. et al., eds. *Amorphous and Microcrystalline Silicon Technology 1997: Proceedings of the Materials Research Society Symposium, 31 March–4 April 1997, San Francisco, California.* Materials Research Society Symposium Proceedings, Vol. 467. Pittsburgh, PA: Materials Research Society; 1997; pp.567-566.
Note: Work performed by University of Oregon, Eugene, Oregon and Instituto de Microelectronica de Madrid, Tres Cantos, Spain.

Lee, Y.; Ferlauto, A. S.; Wronski, C. R. **Contributions of Bulk, Interface and Built-In Potential to the Open Circuit Voltage of a-Si:H Solar Cells.** *Conference Record of the Twenty-Sixth IEEE Photovoltaic Specialists Conference, 29 September–3 October 1997, Anaheim, California.* New York: Institute of Electrical and Electronics Engineers; 1997; pp. 683-686.
Note: Work performed by Pennsylvania State University, University Park, Pennsylvania.

Lee, Y.; Jiao, L.; Koh, J.; Fujiwara, H.; Lu, Z.; Collins, R. W.; Wronski, C. R. **Impact of Hydrogen Dilution on the Properties and Light Induced Changes of a-Si:H Based Materials and Solar Cells.** Wagner, S. et al., eds. *Amorphous and Microcrystalline Silicon Technology 1997: Proceedings of the Materials Research Society Symposium, 31 March–4 April 1997, San Francisco, California.* Materials Research Society Symposium Proceedings, Vol. 467. Pittsburgh, PA: Materials Research Society; 1997; pp. 747-752.
Note: Work performed by Pennsylvania State University, University Park, Pennsylvania.

Levi, D. H.; Woods, L. M.; Albin, D. S.; Gessert, T. A.; Niles, D. W.; Swartzlander, A.; Rose, D. H.; Ahrenkiel, R. K.; Sheldon, P. **Back Contact Effects on Junction Photoluminescence in CdTe/CdS Solar Cells.** *Conference Record of the Twenty-Sixth IEEE Photovoltaic Specialists Conference, 29 September–3 October 1997, Anaheim, California.* New York: Institute of Electrical and Electronics Engineers; 1997; pp. 351-354.
Note: For preprint version, including full text online document, see NREL/CP-530-22971.

Levi, D. H.; Woods, L. M.; Albin, D. S.; Gessert. T. A.; Niles, D. W.; Swartzlander, A.; Rose, D. H.; Ahrenkiel, R. K.; Sheldon, P. **Effects of Back Contact Treatments on Junction Photoluminescence in CdTe/CdS Solar Cells.** Jones, E. D., et al., eds. *Thin-Film Structures for Photovoltaics: Proceedings of the Materials Research Society Symposium, 2-5 December 1997, Boston, Massachusetts.* Materials Research Society Symposium Proceedings, Vol. 485. Warrendale, PA: Materials Research Society; 1998; pp. 209-214.

Liu, X.; Pohl, R. O.; Asher, S.; Crandall, R. S. **Contamination of Silicon During Ion-Implantation and Annealing.** *Journal of Non-Crystalline Solids.* 1998; 227-230; pp. 407-410.

Liu, X.; White, B. E. ,. Jr; Pohl, R. O.; Iwanizcko, E.; Jones, K. M.; Mahan, A. H.; Nelson, B. N.; Crandall, R. S.; Veprek, S. **Amorphous Solid without Low Energy Excitations.** *Physical Review Letters.* 9 June 1997; 78(23); pp. 4418-4421.

Mahan, A. H.; Molenbrock, E. C.; Nelson, B. P., Inventors. **Deposition of Device Quality, Low Hydrogen Content, Amorphous Silicon Films by Hot Filament Technique Using "Safe"Silicon Source Gas.** U.S. Patent No. 5,776,819. July 1998; 15 pp.
Note: Assignee: Midwest Research Institute, Kansas City, Missouri.

Mahan, A. H.; Williamson, D. L.; Furtak, T. E. **Observation of Improved Structural Ordering in Low H Content, Hot Wire Deposited a-Si:H.** Wagner, S. et al., eds. *Amorphous and Microcrystalline Silicon Technology 1997: Proceedings of the Materials Research Society Symposium, 31 March–4 April 1997, San Francisco, California.* Materials Research Society Symposium Proceedings, Vol. 467. Pittsburgh, PA: Materials Research Society; 1997; pp. 657-662.

Marudachalam, M.; Birkmire, R. W.; Hichri, H.; Schultz, J. M.; Swartzlander, A.; Al-Jassim, M. M. **Phases, Morphology, and Diffusion in $CuInxGa_{1-x}Se_2$ Thin Films.** *Journal of Applied Physics.* 15 September 1997; 82(6); pp. 2896-2905.

Mascarenhas, A.; Zhang, Y.; Millunchick, J. M.; Twesten, R. D.; Jones, E. D. **Lateral Superlattice Solar Cells.** McConnell, R. D., ed. *Future Generation Photovoltaic Technologies: Proceedings of the First NREL Conference,22-26 March 1997, Denver, Colorado.* AIP Conference Proceedings No. 404. Woodbury, NY: American Institute of Physics; 1997; pp. 303-308.

Matulionis, I.; Nakade, S.; Compaan, A. D. **Wavelength and Pulse Duration Effects in Laser Scribing of Thin Films.** *Conference Record of the Twenty-Sixth IEEE Photovoltaic Specialists Conference, 29 September–3 October 1997, Anaheim, California.* New York: Institute of Electrical and Electronics Engineers; 1997; pp. 491-494.
Note: Work performed by University of Toledo, Toledo, Ohio.

McCandless, B. E.; Birkmire, R. W. **$CdTe_{1-x}S_x$ Absorber Layers for Thin-Film CdTe/CdS Solar Cells.** *Conference Record of the Twenty-Sixth IEEE Photovoltaic Specialists Conference, 29 September–3 October 1997, Anaheim, California.* New York: Institute of Electrical and Electronics Engineers; 1997; pp. 307-312.
Note: Work performed by University of Delaware, Newark, Delaware.

McMahon, T. J.; von Roedern, B. **Effect of Light Intensity on Current Collection in Thin-Film Solar Cells.** *Conference Record of the Twenty-Sixth IEEE Photovoltaic Specialists Conference, 29 September–3 October 1997, Anaheim, California.* New York: Institute of Electrical and Electronics Engineers; 1997; pp. 375-378.
Note: For preprint version, including full text online document, see NREL/CP-520-22921.

Meyer, G. J. **Electron Transfer in Sensitized TiO_2 Photoelectrochemical Cells.** McConnell, R. D., ed. *Future Generation Photovoltaic Technologies: Proceedings of the First NREL Conference, 22-26 March 1997, Denver, Colorado.* AIP Conference Proceedings No. 404. Woodbury, NY: American Institute of Physics; 1997; pp. 137-143.
Note: Work performed by John Hopkins University, Baltimore, Maryland.

Mitchell, R. L.; Witt, C. E.; Thomas, H. P.; Ruby, D. S.; King, R.; Aldrich, C. C. **Progress Update on the U.S. Photovoltaic Manufacturing Technology Project.** *Conference Record of the Twenty-Sixth IEEE Photovoltaic Specialists Conference, 29 September–3 October 1997, Anaheim, California.* New York: Institute of Electrical and Electronics Engineers; 1997; pp. 1073-1076.
Note: For preprint version, including full text online document, see NREL/CP-520-22962.

Moore, J. T.; Wang, T. H.; Heben, M. J.; Douglas, K.; Ciszek, T. F. **Fused-Salt Electrodeposition of Thin-Layer Silicon.** *Conference Record of the Twenty-Sixth IEEE Photovoltaic Specialists Conference, 29 September–3 October 1997, Anaheim, California.* New York: Institute of Electrical and Electronics Engineers; 1997; pp. 775-778.
Note: For preprint version, including full text online document, see NREL/CP-450-22928.

Moutinho, H. R.; Al-Jassim, M. M.; Abulfotuh, F. A.; Levi, D. H.; Dippo, P. C.; Dhere, R. G.; Kazmerski, L. L. **Studies of Recrystallization of CdTe Thin Films After $CdCl_2$ Treatment.** *Conference Record of the Twenty-Sixth IEEE Photovoltaic Specialists Conference, 29 September–3 October 1997, Anaheim, California.* New York: Institute of Electrical and Electronics Engineers; 1997; pp. 431-434.
Note: For preprint version, including full text online document, see NREL/CP-523-22944.

Mueller, C. H.; Galt, D.; Treece, R. E.; Rivkin, T. V.; Webb, J. D.; Moutinho, H. R.; Dalberth, M.; Rogers, C. T. **Infrared Characterization of $SrTiO_3$ Thin Films Using Attenuated Total Reflectance.** *IEEE Transactions on Applied Superconductivity.* June 1997; 7(2); pp. 1628-1631.

Mueller, C. H.; Treece, R. E.; Rivkin, T. V.; Miranda, F. A.; Moutinho, H. R.; Swartzlander-Franz, A.; Dalberth, M.; Rogers, C. T. **Tunable $SrTiO_3$ Varactors Using Parallel Plate and Interdigital Structures.** *IEEE Transactions on Applied Superconductivity.* June 1997; 7(2); pp. 3512-3515.

Muljadi, E. **PV Water Pumping with a Peak-Power Tracker Using a Simple Six-Step Square-Wave Inverter.** *IEEE Transactions on Industry Applications.* May/June 1997; 33(3); pp. 714-721.

Muljadi, E.; Taylor, R. W., Inventors. **Apparatus and Method for Maximizing Power Delivered by a Photovoltaic Array.** U.S. Patent No. 5,747,967. May 1998; 31pp.
Note: Assignee: Midwest Research Institute, Kansas City, Missouri.

Narasimha, S.; Rohatgi, A. **Optimized Aluminum Back Surface Field Techniques for Silicon Solar Cells.** *Conference Record of the Twenty-Sixth IEEE Photovoltaic Specialists Conference, 29 September–3 October 1997, Anaheim, California.* New York: Institute of Electrical and Electronics Engineers; 1997; pp. 63-66.
Note: Work performed by Georgia Institute of Technology, Atlanta, Georgia.

Nelson, A. J.; Levi, D. **Novel Method for Growing CdS on CdTe Surfaces for Passivation of Surface States and Heterojunction Formation.** *Journal of Vacuum Science and Technology. A, Vacuum, Surfaces, and Films.* May/June 1997; 15(3); pp. 1119-1123.

Nurdjaja, I.; Schiff, E. A. **Photocapacitance and Hole Drift Mobility Measurements in Hydrogenated Amorphous Silicon (a-Si:H).** Wagner, S. et al., eds. *Amorphous and Microcrystalline Silicon Technology 1997: Proceedings of the Materials Research Society Symposium, 31 March–4 April 1997, San Francisco, California.* Materials Research Society Symposium Proceedings, Vol. 467. Pittsburgh, PA: Materials Research Society; 1997; pp. 723-728.
Note: Work performed by Syracuse University, Syracuse, New York.

Olsen, L. C.; Lei, W.; Addis, F. W.; Shafarman, W. N.; Contreras, M. A.; Ramanathan, K. **High Efficiency CIGS and CIS Cells with CVD ZnO Buffer Layers.** *Conference Record of the Twenty-Sixth IEEE Photovoltaic Specialists Conference, 29 September–3 October 1997, Anaheim, California.* New York: Institute of Electrical and Electronics Engineers; 1997; pp. 363-366.

Olson, J. M.; Friedman, D. J. **High Efficiency III-V Solar Cells.** *Compound Semiconductor.* November/December 1996; 2(6); pp. 27-29.

Olson, J. M.; Kurtz, S. R.; Friedman, D. J.; Bertness, K. **High Efficiency, Multijunction GaInP/GaAs Solar Cells.** Shur, M. S.; Suris, R. A. ,. eds. *Compound Semiconductors 1996: Proceedings of the Twenty-Third International Symposium on Compound Semiconductors, 23-37 September 1996, St. Petersburg, Russia.* Institute of Physics Conference Series No. 155. Bristol, UK: Institute of Physics Publishing; 1997; pp. 419-424.

O'Regan, B.; Schwartz, D. T. **Solid State Photoelectrochemical Cells Based on Dye Sensitization.** McConnell, R. D., ed. *Future Generation Photovoltaic Technologies: Proceedings of the First NREL Conference, 22-26 March1997, Denver, Colorado.* AIP Conference Proceedings No. 404. Woodbury, NY: American Institute of Physics; 1997; pp. 129-136.
Note: Work performed by University of Washington, Seattle, Washington.

Osterwald, C. R.; Anevsky, S.; Barua, A. K.; Chaudhuri, P.; Dubard, J.; Emery, K.; Hansen, B.; King, D.; Metzdorf, J.; Nagamine, F.; Shimokawa, R.; Wang, Y. X.; Wittchen, T.; Zaaiman, W.; Zastrow, A.; Zhang, J. **World Photovoltaic Scale: An International Reference Cell Calibration Program.** *Conference Record of the Twenty-Sixth IEEE Photovoltaic Specialists Conference, 29 September–3 October 1997, Anaheim, California.* New York: Institute of Electrical and Electronics Engineers; 1997; pp. 1209-1212.
Note: For preprint version, including full text online document, see NREL/CP-510-22942.

Parilla, P. A.; McGraw, J. M.; Schulz, D. L.; Wendelin, J.; Bhattacharya, R. N.; Blaugher, R. D.; Ginley, D. S.; Voigt, J. A.; Roth, E. P. **Development of Buffer Layers for High Quality Tl-Pb-Sr-Ba-Ca-Cu-O Thick Films on Flexible Metal Substrates.** *IEEE Transactions on Applied Superconductivity.* Proceedings of the 1996 Applied Superconductivity Conference, 25-30 August 1996, Pittsburgh, Pennsylvania. 2 June 1997; 7(2); pp. 1969-1972.

Perez, R.; Wenger, H.; Herig, C. **Valuation of Demand-Side Commercial PV Systems in the United States.** Campbell-Howe, R.; Cortez, T.; Wilkins-Crowder, B. *Proceedings of the 1998 American Solar Energy Society annual Conference, 14-17 June 1998, Albuquerque, New Mexico.* Boulder, CO: American Solar Energy Society; 1998; pp. 219-224.

Perkins, J. D.; Fu, M. L.; Trickett, D. M.; McGraw, J. M.; Ciszek, T. F.; Parilla, P. A.; Rogers, C. T.; Ginley, D. S. **Raman Scattering in $LiCoO_2$ Single Crystals and Thin Films.** Ginley, D. S., et al., eds. *Materials for Electrochemical Energy Storage and Conversion II --Batteries, Capacitors and Fuel Cells: Proceedings of the Materials Research Society Symposium, 1-5 December 1997, Boston, Massachusetts.* Materials Research Society Symposium Proceedings, Vol. 496. Warrendale, PA: Materials Research Society; 1998; pp. 329-334.

Petkov, M. P.; Marek, T.; Asoka-Kumar, P.; Lynn, K. G.; Crandall, R. S.; Mahan, A. H. **Investigation of Hydrogenized Amorphous Si Structures with Doppler Broadening Positron Annihilation Techniques.** *Applied Physics Letters.* 6 July 1998; 73(1); pp. 99-101.

Philips, J. E.; Titus, J.; Hofman, D. **Determining the Voltage Dependence of the Light Generated Current in $CuInSe_2$-Based Solar Cells Using I-V Measurements Made at Different Light Intensities.** *Conference Record of the Twenty-Sixth IEEE Photovoltaic Specialists Conference, 29 September–3 October 1997, Anaheim, California.* New York: Institute of Electrical and Electronics Engineers; 1997; pp. 463-466.
Note: Work performed by University of Delaware, Newark, Delaware.

Ramanathan, K.; Bhattacharya, R. N.; Granata, J.; Webb, J.; Niles, D.; Contreras, M. A.; Wiesner, H.; Hanson, F. S.; Noufi, R. **Advances in the CIS Research at NREL.** *Conference Record of the Twenty-Sixth IEEE Photovoltaic Specialists Conference, 29 September–3 October 1997, Anaheim, California.* New York: Institute of Electrical and Electronics Engineers; 1997; pp. 319-322.
Note: For preprint version, including full text online document, see NREL/CP-520-22946.

Ramanathan, K.; Noufi, R.; Granata, J.; Webb, J.; Keane, J. **Prospects for In Situ Junction Formation in $CuInSe_2$ Based Solar Cells.** *Solar Energy Materials and Solar Cells.* 1998; 55; pp. 15-22.

Ramanathan, K.; Wiesner, H.; Asher, S.; Niles, D.; Webb, J.; Keane, J.; Noufi, R. **Study of the $CdS/CuIn(Ga)Se_2$ Interface in Thin Film Solar Cells.** Jones, E. D., et al., eds. *Thin-Film Structures for Photovoltaics: Proceedings of the Materials Research Society Symposium, 2-5 December 1997, Boston, Massachusetts.* Materials Research Society Symposium Proceedings, Vol. 485. Warrendale, PA: Materials Research Society; 1998; pp. 121-126.

Rand, J. A.; Bai, Y.; Checchi, J. C.; Culik, J. S.; Ford, D. H.; Kendall, C. L.; Sims, P. E.; Hall, R. B.; Barnett, A. M. **Large-Area Silicon-Film™ Manufacturing under the PVMaT Program.** *Conference Record of the Twenty-Sixth IEEE Photovoltaic Specialists Conference, 29 September–3 October 1997, Anaheim, California.* New York: Institute of Electrical and Electronics Engineers; 1997; pp. 1169-1172.
Note: Work performed by AstroPower, Inc., Newark, Delaware.

Remes, Z.; Vanecek, M.; Torres, P.; Kroll, U.; Mahan, A. H.; Crandall, R. S. **Optical Determination of the Mass Density of Amorphous and Microcrystalline Silicon Layers with Different Hydrogen Contents.** *Journal of Non-Crystalline Solids.* 1998; 227-230; pp. 876-879.

Remes, Z.; Vanecek, M.; Mahan, A. H.; Crandall, R. S. **Silicon Network Relaxation in Amorphous Hydrogenated Silicon.** *Physical Review. B, Condensed Matter.* 15 November 1997-II; 56(20); pp. R12,710-R12,713.

Riker, G. M.; Al-Jassim, M. M.; Hasoon, F. S. **Characterization of Chemical Bath Deposited CdS on Single Crystal InP Substrates.** Jones, E. D., et al., eds. *Thin-Film Structures for Photovoltaics: Proceedings of the Materials Research Society Symposium, 2-5 December 1997, Boston, Massachusetts.* Materials Research Society Symposium Proceedings, Vol. 485. Warrendale, PA: Materials Research Society; 1998; pp. 285-290.

Risser, V. **Phillies Bridge Farm [Gardiner, New York] PV/Hybrid System Data Evaluation Report**, (prepared for SunWize Technologies, Inc.), Southwest Technology Development Institute, Las Cruces, New Mexico, June 1998.

Risser, V. **Maintaining Large Photovoltaic Power Systems: Concepts and Costs**, (System Lifetime Report), Southwest Technology Development Institute, Las Cruces, New Mexico, November 1998.

Rockett, A.; Birkmire, R.; Morel, D.; Fonash, S.; Hou, J. Y.; Marudachalam, M.; D'Amico, J.; Panse, P.; Zafar, S.; Schroeder, D. J. **Next Generation CIGS for Solar Cells.** McConnell, R. D., ed. *Future Generation Photovoltaic Technologies: Proceedings of the First NREL Conference, 22-26 March 1997, Denver, Colorado.* AIP Conference Proceedings No. 404. Woodbury, NY: American Institute of Physics; 1997; pp. 403-410.
Note: Work performed by University of Illinois, University of Delaware, University of South Florida, and University of Pennsylvania.

Rose, D. H. **Effect of Oxygen on CdTe-Absorber Solar Cells Deposited by Close-Spaced Sublimation.** Ph.D. Thesis. 1997; 212 pp.
Note: A thesis submitted to the Faculty of the Graduate School of the University of Colorado in partial fulfillment of the requirement for the degree of Doctor of Philosophy, Department of Electrical and Computer Engineering.

Rosenthal, A., S. Durand, M. Thomas, and H. Post. **Economic Analysis of PV Hybrid Power System: Pinnacles National Monument**, *26th IEEE PV Specialists Conference*, Anaheim, California, September 29-October 3, 1997.

Rosenthal, A., S. Durand, M. Thomas, and H. Post. **Economics and Performance of PV Hybrid Power Systems: Three Case Studies**, Solar 98 Renewable Energy for the Americas Conference, June 13, 1998, Albuquerque, New Mexico.

Rosenthal, A. **Performance and Economics of the PV Hybrid Power System at Dangling Rope Marina, Utah**, 1998 NCPV Annual Program Review, Denver, Colorado.

Rosenthal, A., A. Czanderna, F. Pern. **Performance Losses in Roof-Top Mounted PV Modules from Long-Term Environmental Exposure at Las Cruces, NM**, 1998 NCPV Annual Program Review, Denver, Colorado.

Rosenthal, A. **Rogers Peak PV Hybrid Power System Performance and Economic Summary**, Sandia National Laboratories, Photovoltaic Systems Assistance Center, February 1998.

Rosenwaks, Y.; Li, X.; Coutts, T. J. **Characterization of Heat-Treated ITO/InP Solar Cells.** *Journal of Vacuum Science and Technology. A, Vacuum, Surfaces, and Films.* July/August 1997; 15(4); pp. 2354-2358.

Schlichthorl, G.; Huang, S. Y.; Sprague, J.; Frank, A. J. **Band Edge Movement and Recombination Kinetics in Dye-Sensitized Nanocrystalline TiO_2 Solar Cells: A Study by Intensity Modulated Photovoltage Spectroscopy.** *Journal of Physical Chemistry B.* 1997; 101(41); pp. 8141-8155.

Schultz, N.; Vardeny, Z. V.; Taylor, P. C. **Spin Dependent Photoinduced Absorption in A-Si:H.** Wagner, S. et al., eds. *Amorphous and Microcrystalline Silicon Technology 1997: Proceedings of the Materials Research Society Symposium, 31 March–4 April 1997, San Francisco, California.* Materials Research Society Symposium Proceedings, Vol. 467. Pittsburgh, PA: Materials Research Society; 1997; pp. 179-183.
Note: Work performed by University of Utah, Salt Lake City, Utah.

Schulz, D. L.; Curtis, C. J.; Cram, A.; Alleman, J. L.; Mason, A.; Matson, R. J.; Perkins, J. D.; Ginley, D. S. **CIGS Films via Nanoparticle Spray Deposition: Attempts at Densifying a Porous Precursor.** *Conference Record ofthe Twenty-Sixth IEEE Photovoltaic Specialists Conference, 29 September–3 October 1997, Anaheim, California.* New York: Institute of Electrical and Electronics Engineers; 1997; pp. 483-486.
Note: For preprint version, including full text online document, see NREL/CP-520-22959.

Schulz, D. L.; Curtis, C. J.; Flitton, R. A.; Wiesner, H.; Keane, J.; Matson, R. J.; Jones, K. M.; Parilla, P. A.; Noufi, R.; Ginley, D. S. **Cu-In-Ga-Se Nanoparticle Colloids as Spray Deposition Precursors for $Cu(In,Ga)Se_2$ Solar Cell Materials.** *Journal of Electronic Materials.* May 1998; 27(5); pp. 433-437.

Schulz, D. L.; Pehnt, M.; Curtis, C. J.; Ginley, D. S. **Spray Deposition of CdTe Thin Films Using Nanoparticle Precursors.** *Metastable, Mechanically Alloyed and Nanocrystalline Materials: Proceedings of the International Symposium, 24-28 July 1995, Quebec City, Canada.* Materials Science Forum Vols. 225-227. Switzerland: Transtec Publications; 1996; pp. 169-174.

Schulz, D. L.; Pehnt, M.; Curtis, C. J.; Ginley, D. S. **Spray Deposition of CdTe Thin Films Using Nanoparticle Precursors.** *Materials Science Forum.* Proceedings of the Metastable, Mechanically Alloyed and Nanocrystalline Materials International Symposium, 24-28 July 1995, Quebec City, Canada. 19961996; 225-227; pp. 169-174.

Schuyler, T.; Kroposki, B. **Development of Test Methods and Procedures for Evaluation of PV Systems.** *Workshop Handbook from the 1997 Photovoltaic Performance and Reliability Workshop, 5-6 August 1997.* 1997; 5 pp.

Schwerdtfeger, C. R.; Ciszek, T. F.; Noufi, R. **High-Pressure, Liquid-Encapsulated Directional Solidification of Copper-Deficient Copper Indium Selenides.** *Crystal Growth of Novel Electronic Materials: Proceedings of the 97th Annual Meeting of the American Ceramic Society, 1-3 May 1995, Cincinnati, Ohio.* Westerville, OH: American Ceramic Society; 1995; pp. 95-103.

Shafarman, W. N.; Birkmire, R. W.; Marsillac, S.; Marudachalam, M.; Orbey, N.; Russell, R. W. F. **Effect of Reduced Deposition Temperature, Time, and Thickness on Cu(InGa)Se_2 Films and Devices.** *Conference Record of the Twenty-Sixth IEEE Photovoltaic Specialists Conference, 29 September–3 October 1997, Anaheim, California.* New York: Institute of Electrical and Electronics Engineers; 1997; pp. 331-334.
Note: Work performed by University of Delaware, Newark, Delaware.

Sites, J. R.; Granata, J. E.; Hiltner, J. F. **Losses Due to Polycrystallinity in Thin-Film Solar Cells.** *Solar Energy Materials and Solar Cells.* 1998; 55; pp. 43-50.
Note: Work performed by Colorado State University, Fort Collins, Colorado.

Sites, J.; Rand, J.; Kazmerski, L. L.; Phillips, J. E. **Device and Materials Characterization in Manufacturing.** *Progress in Photovoltaics: Research and Applications.* Papers from the 25th Anniversary Symposium of the Institute of Energy Conversion, 1-2 May 1997, Newark, Delaware. September/October 1998; 5(5); pp. 371-378.

Sopori, B. **Optics Software Models Photovoltaic Light Trapping.** *Laser Focus World.* February 1998; 34(2); pp. 159-161.

Sopori, B. L. **Using Photonic Effects in Optical Processing for Silicon Device Fabrication.** Ravindra, N. M.; Singh, R. K. ,. eds. *Transient Thermal Processing Techniques in Electronic Materials.* Proceedings of a Symposium Sponsored by the Thin Films & Interfaces Committee of the Electronic, Magnetic and Photonic Materials Division of TMS, 4-8 February 1996, Anaheim, California. Warrendale, PA: The Minerals, Metals and Materials Society; 1996; pp. 17-20.

Sopori, B. L.; Allen, L. C.; Marshall, C.; Murphy, R. C.; Marshall, T. **System for Characterizing Semiconductor Materials and Photovoltaic Devices through Calibration.** U.S. Patent No. 5, 757,474. May 1998; 50 pp.
Note: Assignee: Midwest Research Institute, Kansas City, Missouri.

Sopori, B.; Symko, M. I.; Reedy, R.; Jones, K.; Matson, R. **Mechanism(s) of Hydrogen Diffusion in Silicon Solar Cells During Forming Gas Anneal.** *Conference Record of the Twenty-Sixth IEEE Photovoltaic Specialists Conference, 29 September–3 October 1997, Anaheim, California.* New York: Institute of Electrical and Electronics Engineers; 1997; pp. 25-30.
Note: For preprint version, including full text online document, see NREL/CP-520-23578.

Southwest Technology Development Institute. **Natural Bridges National Monument Photovoltaic Array Test Report**, January 1998, Las Cruces, New Mexico.

Stanbery, B. J.; Lambers, E. S.; Amderson, T. J. **XPS Studies of Sodium Compound Formation and Surface Segregation in CIGS Thin Films.** *Conference Record of the Twenty-Sixth IEEE Photovoltaic Specialists Conference, 29September–3 October 1997, Anaheim, California.* New York: Institute of Electrical and Electronics Engineers; 1997; pp. 499-502.
Note: Work performed by University of Florida, Gainesville, Florida.

Starrs, T.; Wenger, H.; Brooks, B.; Herig, C. **Barriers and Solutions for Connecting PV to the Grid.** Campbell-Howe, R.; Cortez, T.; Wilkins-Crowder, B. eds. *Proceedings of the 1998 American Solar Energy Society Annual Conference, 14-17 June 1998, Albuquerque, New Mexico.* Boulder, CO: American Solar Energy Society; 1998; pp. 205-210.

Stephen, J. T.; Rutland, J. M.; Han, D.; Wu, Y. **NMR Investigation of H Cluster Configurations in A-Si:H.** Wagner, S. et al., eds. *Amorphous and Microcrystalline Silicon Technology 1997: Proceedings of the Materials Research Society Symposium, 31 March–4 April 1997, San Francisco, California.* Materials Research Society Symposium Proceedings, Vol. 467. Pittsburgh, PA: Materials Research Society; 1997; pp. 159-164.
Note: Work performed by University of North Carolina, Chapel Hill, North Carolina.

Stone, J. L.; Ullal, H. S.; Sastry, E. V. R. **Indo-U.S. Cooperative Photovoltaic Project.** *Conference Record of the Twenty-Sixth IEEE Photovoltaic Specialists Conference, 29 September–3 October 1997, Anaheim, California.* New York: Institute of Electrical and Electronics Engineers; 1997; pp. 1273-1275.
Note: For preprint version, including full text online document, see NREL/CP-520-22932.

Sugiyama, S.; Yang, J.; Guha, S. **Improved Stability Against Light-Exposure in Deuterated Amorphous Silicon Alloy Solar Cells.** Wagner, S. et al., eds. *Amorphous and Microcrystalline Silicon Technology 1997: Proceedings of the Materials Research Society Symposium, 31 March–4 April 1997, San Francisco, California.* Materials Research Society Symposium Proceedings, Vol. 467. Pittsburgh, PA: Materials Research Society; 1997; pp. 49-54.
Note: Work performed by United Solar Systems Corp., Troy, Michigan.

Sundaram, V. S.; Saban, S. B.; Morgan, M. D.; Horne, W. E.; Evans, B. D.; Ketterl, J. R.; Morosini, M. B. Z.; Patel, N. B.; Field, H. **GaSb Based Ternary and Quaternary Diffused Junction Devices for TPV Applications.** Coutts, T. J.; Allman, C. S.; Benner, J. P., eds. *Thermophotovoltaic Generation of Electricity: Third NREL Conference, May 1997, Colorado Springs, Colorado.* AIP Conference Proceedings No. 401. Woodbury, NY: American Institute of Physics; 1997; pp. 105-115.

Surek, T. **Progress in Photovoltaics: From the Laboratory to the Marketplace.** *Proceedings of the Twenty-First DOE Solar Photochemistry Research Conference, 7-11 June 1997, Copper Mountain, Colorado.* NREL/CP-520-22968. 1997; p. 21.

Tanenbaum, D. M.; Laracuente, A. L.; Gallagher, A. **Surface Roughening During Plasma-Enhanced Chemical-Vapor Deposition of Hydrogenated Amorphous Silicon on Crystal Silicon Substrates.** *Physical Review. B, Condensed Matter.* 15 August 1997-I; 56(7); pp. 4243-4250.
Note: Work performed by JILA, National Institute of Standards and Technology, and University of Colorado, Boulder, Colorado.

Tang, J.; Mao, D.; Ohno, T. R.; Kaydanov, V.; Trefny, J. U. **Properties of ZnTe:Cu Thin Films and CdS/CdTe/ZnTe Solar Cells.** *Conference Record of the Twenty-Sixth IEEE Photovoltaic Specialists Conference, 29 September -3 October 1997, Anaheim, California.* New York: Institute of Electrical and Electronics Engineers; 1997; pp. 439-442.
Note: Work performed by Colorado School of Mines, Golden, Colorado.

Thomas, M.; DeBlasio, R. **Challengine Performance and Reliability Demagoguery.** *Workshop Handbook from the 1997 Photovoltaic Performance and Reliability Workshop, 5-6 August 1997.* 1997; 4 pp.

Tuttle, J. R.; Cole, E. D.; Berens, T. A.; Alleman, J.; Keane, J. **Thin-Film Filament-Based Solar Cells and Modules.** McConnell, R. D., ed. *Future Generation Photovoltaic Technologies: Proceedings of the First NREL Conference, 22-26 March 1997, Denver, Colorado.* AIP Conference Proceedings No.404. Woodbury, NY: American Institute of Physics; 1997; pp. 243-250.

Ullal, H. S.; Zweibel, K.; von Roedern, B. G. **Current Status of Polycrystalline Thin-Film PV Technologies.** *Conference Record of the Twenty-Sixth IEEE Photovoltaic Specialists Conference, 29 September–3 October 1997,Anaheim, California.* New York: Institute of Electrical and Electronics Engineers; 1997; pp. 301-305.
Note: For preprint version, including full text online document, see NREL/CP-520-22922.

Unold, T.; Mahan, A. H. **ESR Studies on Hot Wire Amorphous Silicon.** Wagner, S. et al., eds. *Amorphous and Microcrystalline Silicon Technology 1997: Proceedings of the Materials Research Society Symposium, 31 March–4 April 1997, San Francisco, California.* Materials Research Society Symposium Proceedings, Vol. 467. Pittsburgh, PA: Materials Research Society; 1997; pp. 663-668.

Unold, T.; Reedy, R. C.; Mahan, A. H. **Defects in Hot-Wire Deposited Amorphous Silicon: Results from Electron Spin Resonance.** *Journal of Non-Crystalline Solids.* 1998; 227-230; pp. 362-366.

Venkatasubramanian, R.; O'Quinn, B. C.; Siivola, E.; Keyes, B.; Ahrenkiel, R. **20% (AM1.5) Efficiency GaAs Solar Cells on Sub-mm Grain-Size Poly-Ge and its Transition to Low Cost Substrates.** *Conference Record of the Twenty-Sixth IEEE Photovoltaic Specialists Conference, 29 September–3 October 1997, Anaheim, California.* New York: Institute of Electrical and Electronics Engineers; 1997; pp. 811-814.
Note: Work performed by Research Triangle Institute, Research Triangle Park, North Carolina.

Venkatasubramanian, R.; Siivola, E.; O'Quinn, B.; Keyes, B.; Ahrenkiel, R. **Pathways to High-Efficiency GaAs Solar Cells on Low-Cost Substrates.** McConnell, R. D., ed. *Future Generation Photovoltaic Technologies: Proceedings of the First NREL Conference, 22-26 March 1997, Denver, Colorado.* AIP Conference Proceedings No. 404. Woodbury, NY: American Institute of Physics; 1997; pp. 411-418.

Wallace, W. L.; Tsuo, Y. S. **Photovoltaics for Rural Electrification in the People's Republic of China.** *Conference Record of the Twenty-Sixth IEEE Photovoltaic Specialists Conference, 29 September–3 October 1997, Anaheim, California.* New York: Institute of Electrical and Electronics Engineers; 1997; pp. 1277-1280.
Note: For preprint version, including full text online document, see NREL/CP-520-22970.

Wang, Q.; Crandall, R. S.; Han, D. **Effects of Hydrogen Dilution on Voc in a-Si:H pin Solar Cells.** Wagner, S. et al., eds. *Amorphous and Microcrystalline Silicon Technology 1997: Proceedings of the Materials Research Society Symposium, 31 March–4 April 1997, San Francisco, California.* Materials Research Society Symposium Proceedings, Vol. 467. Pittsburgh, PA: Materials Research Society; 1997; pp. 753-758.

Wangensteen, T. L.; Wanlass, M. W.; Carapella, J. J.; Moutinho, H. R.; Mason, A. R.; Webb, J. D.; Abulfotuh, F. A. **Optical Characterization of Epitaxial $Ga_xIn_{1-x}As$ Suitable for Thermophotovoltaic (TPV) Converters.** *Conference Record of the Twenty-Sixth IEEE Photovoltaic Specialists Conference, 29 September–3 October 1997, Anaheim, California.* New York: Institute of Electrical and Electronics Engineers; 1997; pp. 967-970.
Note: For preprint version, including full text online documents, see NREL/CP-530-22975.

Warner, C. L. **Photovoltaic Technology Developments.** *Building Energy: Proceedings of 3 Conferences (1st International Solar Electric Buildings, Renew '96, and 12th Annual Quality Building Conference), 4-6 March 1996, Boston, Massachusetts.* 1996; Vol. 2: pp. 19-22. 1996.

Webb, J. D.; Rose, D. H.; Niles, D. W.; Swartzlander, A.; Al-Jassim, M. M. **FTIR, EPMA, Auger, and XPS Analysis of Impurity Precipitates in CdS Films.** *Conference Record of the Twenty-Sixth IEEE Photovoltaic Specialists Conference, 29 September–3 October 1997, Anaheim, California.* New York: Institute of Electrical and Electronics engineers; 1997; pp. 399-402.
Note: For preprint version, including full text online document, see NREL/CP-530-22966.

Wickboldt, P.; Pang, D.; Paul, W.; Chen, J. H.; Chen, C. C.; Cohen, J. D. **Ambipolar Phototransport (mu tau e=mu tau h) Observed as an Intrinsic Property of A-SiGe:H.** Wagner, S. et al , . eds. *Amorphous and Microcrystalline Silicon Technology 1997: Proceedings of the Materials Research Society Symposium, 31 March–4 April 1997, San Francisco, California.* Materials Research Society Symposium Proceedings, Vol. 467. Pittsburgh, PA: Materials Research Society; 1997; pp. 263-268.
Note: Work performed by Harvard University, Cambridge, Massachusetts, Boston College, Boston, Massachusetts, University of Oregon, Eugene, Oregon, and Lawrence Livermore National Laboratory, Livermore, California.

Wiles, J. **Protecting Photovoltaic Modules from Reverse Currents**, Southwest Technology Development Institute, Las Cruces, New Mexico (prepared for ASES 1998 Conference, Albuquerque, New Mexico).

Wiles, J. **Protecting PV Modules from Reverse Currents**, Solar 98 Renewable Energy for the Americas Conference, June 13, 1998, Albuquerque, New Mexico.

Wiles, J. **Photovoltaic Power Systems and the National Electrical Code: A Presentation for Electrical Inspectors, Electrical Contractors, and PV Professionals**, (presented to the City of Tucson and Pima County Electrical Inspectors), June 1998.

Wiles, J. and W. Bower. **Designing and Installing PV Systems that Meet the National Electrical Code**, Solar 98 Renewable Energy for the Americas Conference, June 13, 1998, Albuquerque, New Mexico.

Wiles, J. (co-chair) and S. Chalmers (co-chair), *IEEE Guide for Terrestrial Photovoltaic Power System Safety (IEEE Std. 1374-1998*), IEEE Standards Coordinating Committee 21, Institute of Electrical and Electronics Engineers, Inc., New York, New York, September 30, 1998.

Wiles, J. and D. King. **Blocking Diodes and Fuses in Low-Voltage PV Systems**, *26th IEEE PV Specialists Conference*, Anaheim, California, September 29-October 3, 1997.

Wiles, J. and S. Stoll. **Initial Test Report with Performance Data from August 1997 through March 1998: SunWize Energy Corporation 1200 Watt Hybrid PV Power System**, Southwest Technology Development Institute, Las Cruces, New Mexico, June 1998.

Wohlgemuth, J. H.; Whitehouse, D.; Koval, T.; Creager, J.; Artigliere, F.; Tomlinson, T.; Cliber, J.; Buckman, A.; Perry, M.; Narayanan, S.; Shea, S.; Roy, M.; Kelly, G.; Brisson, M.; Dominguez, R.; Conway, M. **Progress in Solarex's Crystalline Silicon PVMaT Program.** *Conference Record of the Twenty-Sixth IEEE Photovoltaic Specialists Conference, 29 September–3 October 1997, Anaheim, California.* New York: Institute of Electrical and Electronics Engineers; 1997; pp. 1055-1060.
Note: Work performed by Solarex Corporation, Frederick, Maryland.

Workshop Handbook from the 1997 Photovoltaic Performance and Reliability Workshop, 5-6 August 1997. 1997; 57 pp.
Note: Sponsored by Sandia National Laboratories and the National Renewable Energy Laboratory.

Wronski, C. R.; Lu, Z.; Jiao, L.; Lee, Y. **Approach to Selfconsistent Analysis of a-Si:H Material and P-I-N Solar Cell Properties.** *Conference Record of the Twenty-Sixth IEEE Photovoltaic Specialists Conference, 29 September–3 October 1997, Anaheim, California.* New York: Institute of Electrical and Electronics Engineers; 1997; pp. 587-590.
Note: Work performed by Pennsylvania State University, University Park, Pennsylvania.

Wu, X.; Sheldon, P.; Coutts. T. J.; Rose, D. H.; Moutinho, H. R. **Application of Cd_2SnO_4 Transparent Conducting Oxides in CdS/CdTe Thin-Film Devices.** *Conference Record of the Twenty-Sixth IEEE Photovoltaic Specialists Conference, 29 September–3 October 1997, Anaheim, California.* New York: Institute of Electrical and Electronics Engineers; 1997; pp. 347-350.
Note: For preprint version, including full text online document, see NREL/CP-520-22941.

Yan, B.; Taylor, P. C. **Electron Spin Resonance of Hydrogenated Amorphous Silicon Alloyed with Sulfur.** Wagner, S. et al., eds. *Amorphous and Microcrystalline Silicon Technology 1997: Proceedings of the Materials Research Society Symposium, 31 March–4 April 1997, San Francisco, California.* Materials Research Society Symposium Proceedings, Vol. 467. Pittsburgh, PA: Materials Research Society; 1997; pp. 103-108.
Note: Work performed by University of Utah, Salt Lake City, Utah.

Yang, J.; Baneerjee, A.; Guha, S. **Amorphous Silicon Alloy Triple-Junction Solar Cell with 14.6% initial and 13.0% Stable Efficiencies.** Wagner, S. et al., eds. *Amorphous and Microcrystalline Silicon Technology 1997: Proceedings of the Materials Research Society Symposium, 31 March–4 April 1997, San Francisco, California.* Materials Research Society Symposium Proceedings, Vol. 467. Pittsburgh, PA: Materials Research Society; 1997; pp. 693-698.
Note: Work performed by United Solar Systems Corporation, Troy, Michigan.

Yang, J.; Banerjee, A.; Glatfelter, T.; Sugiyama, S.; Guha, S. **Recent Progress in Amorphous Silicon Alloy Leading to 13% Stable Cell Efficiency.** *Conference Record of the Twenty-Sixth IEEE Photovoltaic Specialists Conference, 29 September–3 October 1997, Anaheim, California.* New York: Institute of Electrical and Electronics Engineers; 1997; pp. 563-568.
Note: Work performed by United Solar Systems Corp., Troy, Michigan.

Yoon, J. H.; Taylor, P. C.; Yan, B.; Lee, C. H. **Light Induced Effects in A-Si:H Films Alloyed with Sulfur.** Wagner, S. et al., eds. *Amorphous and Microcrystalline Silicon Technology 1997: Proceedings of the Materials Research Society Symposium, 31 March–4 April 1997, San Francisco, California.* Materials Research Society Symposium Proceedings, Vol. 467. Pittsburgh, PA: Materials Research Society; 1997; pp. 97-102.
Note: Work performed by University of Utah, Salt Lake City, Utah and College of Natural Sciences, Chunchon, Korea.

Zafar, S.; Sankaranarayana, H.; Jayapalan, A.; Narayanaswamy, R.; Ferekides, C. S.; Morel, D. L. **Use of Ga in Two-Step Processing to Optimize the Electronic Properties of $CuIn_xGa_{1-x}Se_2$ Solar Cells.** *Conference Record of the Twenty-Sixth IEEE Photovoltaic Specialists Conference, 29 September–3 October 1997, Anaheim, California.* New York: Institute of Electrical and Electronics Engineers; 1997; pp. 379-382.
Note: Work performed by University of South Florida, Tampa, Florida.

Zunger, A.; Zhang, S. B.; Wei, S. H. **Revisiting the Defect Physics in $CuInSe_2$ and $CuGaSe_2$.** *Conference Record of the Twenty-Sixth IEEE Photovoltaic Specialists Conference, 29 September–3 October 1997, Anaheim, California.* New York: Institute of Electrical and Electronics Engineers; 1997; pp. 313-318.
Note: For preprint version, including full text online document, see NREL/CP-450-23581.

REPORT DOCUMENTATION PAGE

Form Approved
OMB NO. 0704-0188

1. AGENCY USE ONLY (Leave blank)	2. REPORT DATE	3. REPORT TYPE AND DATES COVERED
	June 1999	Annual Report

4. TITLE AND SUBTITLE
NCPV FY 1998 Annual Report

5. FUNDING NUMBERS
C:
TA: PV901102

6. AUTHOR(S)
R.D. McConnell, PV Communications Leader; A. Hansen, Communications Coordinator

7. PERFORMING ORGANIZATION NAME(S) AND ADDRESS(ES)

8. PERFORMING ORGANIZATION REPORT NUMBER

9. SPONSORING/MONITORING AGENCY NAME(S) AND ADDRESS(ES)
National Renewable Energy Laboratory
1617 Cole Blvd.
Golden, CO 80401-3393

10. SPONSORING/MONITORING AGENCY REPORT NUMBER
NREL/BK-210-25626

11. SUPPLEMENTARY NOTES
NREL Technical Monitor: N/A

12a. DISTRIBUTION/AVAILABILITY STATEMENT
National Technical Information Service
U.S. Department of Commerce
5285 Port Royal Road
Springfield, VA 22161

12b. DISTRIBUTION CODE

13. ABSTRACT *(Maximum 200 words)*

This report summarizes the in-house and subcontracted research and development (R&D) activities under the National Center for Photovoltaics (NCPV) from October 1, 1997, through September 30, 1998 (FY 1998). The NCPV is part of the U.S. Department of Energy's (DOE's) National Photovoltaics Program, as described in the DOE *National Photovoltaics Program Plan for 1996-2000*. The mission of the DOE National Photovoltaics Program is to make PV a significant part of the domestic economy—as an industry and an energy resource. The two primary goals of the national program are to (1) maintain the U.S. industry's world leadership in research and technology development and (2) help the U.S. industry remain a major, profitable force in the world market. The NCPV provides leadership and support to the national program toward achieving its mission and goals.

14. SUBJECT TERMS
photovoltaics ; National Center for Photovolataics ; NCPV ; crystalline silicon ; high-efficiency materials and devices ; measurements and characterization ; exploratory materials and devices ; Historically Black Colleges and Universities ; HBCU ; thin films ; Photovoltaic Manufacturing Technology ; PVMaT ; modules ; systems ; applications ; market development

15. NUMBER OF PAGES
572

16. PRICE CODE

17. SECURITY CLASSIFICATION OF REPORT	18. SECURITY CLASSIFICATION OF THIS PAGE	19. SECURITY CLASSIFICATION OF ABSTRACT	20. LIMITATION OF ABSTRACT
Unclassified	Unclassified	Unclassified	UL

NSN 7540-01-280-5500

Standard Form 298 (Rev. 2-89)
Prescribed by ANSI Std. Z39-18
298-102